"SYNTHESIS AND BIOPHYSICAL STUDIES OF PYRROLIDINYL DNA ANALOGUES CONTAINING AMIDE, OXYAMIDE AND CARBAMATE LINKAGES"

MEENA

NATIONAL CHEMICAL LABORATORY

PUNE 411 008

AUGUST 2002

"SYNTHESIS AND BIOPHYSICAL STUDIES OF PYRROLIDINYL DNA ANALOGUES CONTAINING AMIDE, OXYAMIDE AND CARBAMATE LINKAGES"

Thesis submitted to the
University of Pune for the degree of
Doctor of Philosophy in Chemistry

By

MEENA

Division of Organic Chemistry (Synthesis)
National Chemical Laboratory
Pune 411 008

August 2002

CERTIFICATE

This is to certify that the work presented in the thesis entitled **"SYNTHESIS AND BIOPHYSICAL STUDIES OF PYRROLIDINYL DNA ANALOGUES CONTAINING AMIDE, OXYAMIDE AND CARBAMATE LINKAGES"**, submitted by Meena, was carried out by the candidate at the National Chemical Laboratory Pune, under my supervision. Such materials as obtained from other sources have been duly acknowledged in the thesis.

August 2002

(**K. N. Ganesh**)
Research Guide
Head, Division of Organic Chemistry (Synthesis)
National Chemical Laboratory
Pune 411 008

CANDIDATE'S DECLARATION

I hereby declare that the thesis entitled **"SYNTHESIS AND BIOPHYSICAL STUDIES OF PYRROLIDINYL DNA ANALOGUES CONTAINING AMIDE, OXYAMIDE AND CARBAMATE LINKAGES"**, submitted for the degree of Doctor of Philosophy in Chemistry to the University of Pune, has not been submitted by me to any other university or institution. This work was carried out at the National Chemical Laboratory, Pune, India.

National Chemical Laboratory **(Meena)**
Pune 411 008
August 2002

Acknowledgement

First and foremost, I wish to thank Dr. K. N. Ganesh, my supervisor, for the confidence he had in me which allowed me near total freedom in pursuing avenues which I thought were interesting. His undying enthusiasm for science and unwavering support is always a source of inspiration.

I am indebted to my respectable teachers Dr. M. S. Batra, Dr. J. S. Gandhi and Dr. S. K. Pushkarna who continuously provided me the encouragement and motivation.

I owe much to Dr. V. A. Kumar who never failed to stop by and discuss interesting results. She truly helped shape and improve my thinking. Without her boundless love and support, I would not have been able to complete this work.

The most important people to thank are my family. My father was the nicest and most giving person. I hope that someday I can be more like him. My mother for her unconditional love and support for all things I do. I always wonder how she could have been so selfless for so many years and wonder how I can repay her for all she has done for me. My sister Neelam deserves special thanks. Her love and support kept me going through the lean times.

The KNG group has been my family for past five years. During this time, all members past and present have helped me, inspired me and entertained me. I was glad to be a member of such a diverse and lively group.

My sincere thanks go to Mrs. Anita Gunjal for all her help in carrying out DNA synthesis and Mrs. M. V. Mane and Mrs. S. S. Kunte for carrying out HPLC analysis.

I benefited immensely from my senior colleagues. I thank, in no particular order, Sanjayan, Rajeev, Gopal, Vasant, Leena, Anand, Gangamani, Pradeep, Vipul, Nagamani, Ramesh, Moneesha and Vallabh.

I acknowledge my junior colleagues Pallavi, Dinesh, Nagendra, Govind, Raman, Praveen, Umashankar and Gourishankar for always willing to help and for making the lab a pleasant and productive place.

I also thank Pawar, Bhumkar and Sunil their assistance.

I acknowledge The Council of Scientific and Industrial Research, New Delhi for providing me financial support. I am grateful to the Director, NCL, for giving me the opportunity to work in this institute.

No account of my time at NCL would be complete without a mention of friends at New Hostel and G. J. Hostel. I would like to thank Bindu, Prakash, Nagesh, Sivappa, Rachna, Sulatha, Meena, A., Priya, Aslam, Anuradha and Aparna for their great company and excellent lunch table conversations.

Contents

PUBLICATIONS

1. **Synthesis and Evaluation of Prolyl Carbamate Nucleic acids (PrCNA).** Meena, V. A. Kumar, K. N. Ganesh, *Nuceosides, Nucleotides and Nucleic Acids* **2001**, *20*, 1193-1196.

2. **Pyrrolidine Nucleic Acids: DNA/PNA Oligomers With 2-hydroxy/aminoethyl-4-(thymin-1-yl)pyrrolidine-N-acetic acid.** V. A. Kumar, P. S. Pallan, Meena, Krishna N. Ganesh, *Org. Lett*. **2001**, *3*, 1269-1272.

3. **Synthesis of Prolyl Carbamate Nucleic Acids (PrCNA): Uncharged and Chiral Nucleic Acid Analogues.** Meena, Vaijayanti A. Kumar, Krishna N. Ganesh. Poster presented at *5th International Bioorganic Symposium* **1999** at Pune, India.

4. **Chimeric Antisense Oligonucleotides**. Meena, Vaijayanti A. Kumar, Krishna N. Ganesh. Poster presented at *7th National Bioorganic Symposium* **2001** at Amritsar, India.

5. **Effect of Stereochemistry on the DNA Binding Abilities of Pyrrolidine Nucleic Acids: Synthesis and DNA Complementation Studies of 2*S*/2*R*-aminoethyl-4*S*/4*R*-(thymin-1-yl)-pyrrolidine-N-acetyl PNAs.** Meena, Vaijayanti A. Kumar, K. N. Ganesh (Manuscript under preparation).

6. **Oxyamides of 2*S*,4*S*-oxyamino-proline induce β-turn: Evidence from NMR, Circular Dichroism and X-ray crystallography.** Meena, Gangadharan J. Sanjayan, K. N. Ganesh (communicated).

Abstract

SYNTHESIS AND BIOPHYSICAL STUDIES OF PYRROLIDINYL DNA ANALOGUES CONTAINING AMIDE, OXYAMIDE AND CARBAMATE LINKAGES

CHAPTER 1: Introduction

Modified oligonucleotides are used as antisense and antigene inhibitors of gene expression. The formation of the duplex would prevent or substantially reduce the expression of disease related proteins by inhibiting the translation of mRNA. For synthetic oligonucleotides, the antisense strategy is convincing from a mechanical point of view. However, these oligonucleotides are rapidly cleaved by the action of nucleases that primarily hydrolyze the phosphodiester of the internucleoside backbone. Furthermore, the ability of the negatively charged DNA to cross phospholipid cell membrane is poor. Hence structural modifications are needed to enable oligonucleotides to be used as antisense therapeutic agents in biological systems and also to understand the structural changes that they introduce in the oligonucleotides incorporating them.

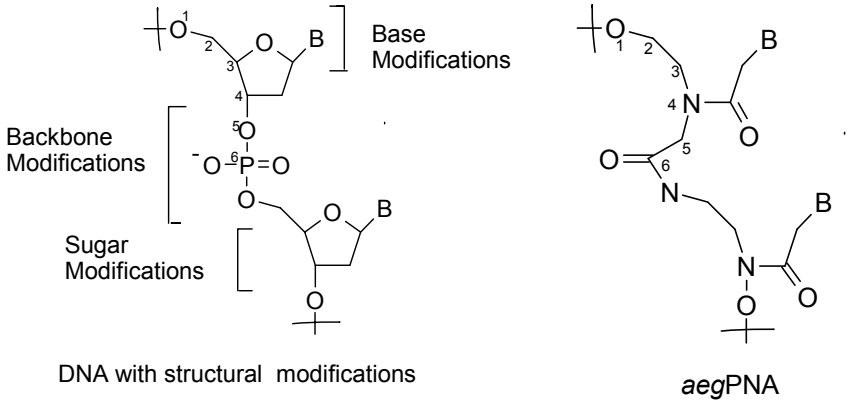

Figure 1.

The structural changes include the modifications in nucleobase, phosphodiester linkage and/or the sugar moiety (Figure 1). The first generation of antisense oligonucleotides was based on backbone modifications in which the phosphodiester bond is replaced by phosphorous containing linkages such as phosphorothioate, methylphosphonates, phosphoroamidates etc. The second generation of oligonucleotides involves backbone linkages that do not contain phosphorous. In these, phosphate linkages are replaced by neutral functionalities and particularly important are the analogues that are less susceptible to degradation by nucleases, activate RNase H, cross cell membrane due to their enhanced lipophilicity, and encounter diminished charge-charge repulsion on binding to complementary strands.

The replacement of a natural nucleotide by a chemically modified congener within a certain sequence gives rise to fundamental changes in the double and triple helix forming properties. The improvement of oligonucleotide properties by modifying the base moieties is of limited application due to their involvement in *Watson*-C*rick* hydrogen bonding with the complementary strand; base modification should not interfere with this property for specific recognition.

Early literature has demonstrated that large structural changes in sugar portion are tolerated as witnessed by the successful binding of carbamate linked morpholine based oligonucleosides complementary to DNA and RNA. One more class of DNA analogues with little similarity to natural oligonucleotides but having interesting and potentially useful bioactivities is aminoethyl glycyl polyamide nucleic acids (*aeg*PNAs) (Figure 1). This chapter reviews the first and second generation of antisense oligonucleotides and nonsugar chiral and achiral backbones, in particular the peptide nucleic acid based systems.

CHAPTER 2: Pyrrolidinyl Peptide Nucleic Acids

Introduction of chirality and conformational restraint in the achiral aminoethylglycyl PNA (*aeg*PNA) with the intention of preorganizing the PNA structure compatible for binding with target DNA/RNA and to discriminate the parallel/antiparallel binding modes has been partially successful. Recently, in our laboratory, synthesis of neutral prolyl nucleic acids and *aep*PNAs having chirality with conformational constrain and positive charge in the backbone was achieved (Figure 2). Prolyl nucleic acids were derived by linking the α-carbon of the glycyl backbone to the β''-carbon of the ethylene segment. *aep*PNAs which formed highly stable PNA:DNA complexes were derived by linking α-carbon of the glycyl backbone to the β'-carbon of the side chain. In this chapter, the cationic, chiral PNA generated by linking α"-carbon of the

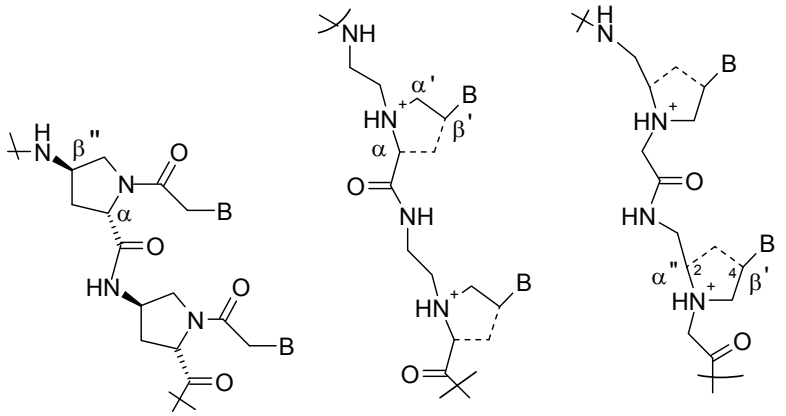

Prolyl nucleic acids aep-PNA pyrrolidine PNA

Figure 2.

Scheme 1a

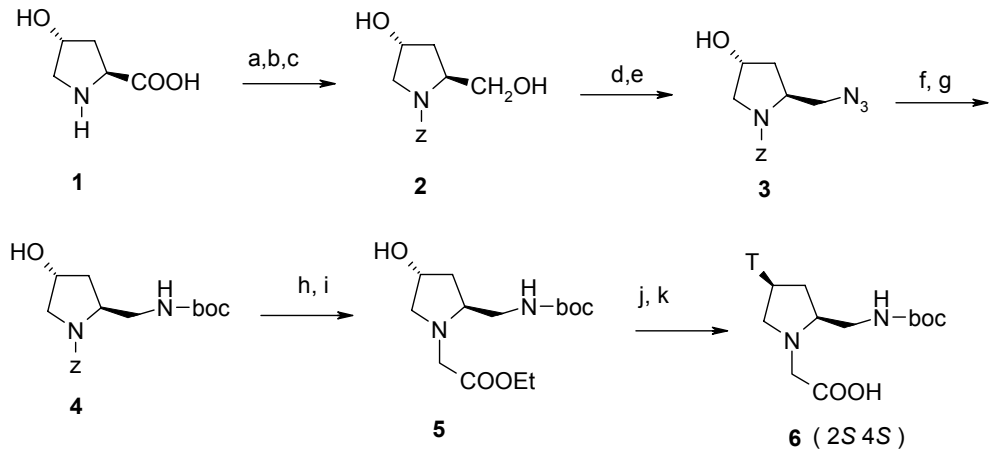

1 **2** **3** **4** **5** **6** (2*S* 4*S*)

Scheme 1b

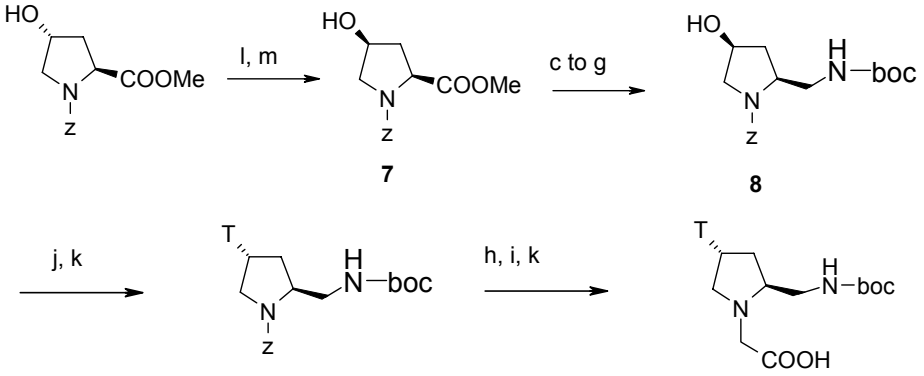

7 **8** **9** **10** (2*S* 4*R*)

Scheme 2a

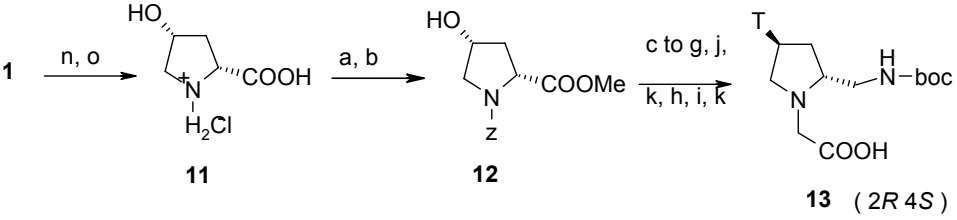

11 **12** **13** (2*R* 4*S*)

Scheme 2b

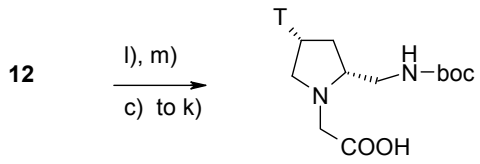

14 (2*R* 4*R*)

(a) ZCl, $NaHCO_3/H_2O$ b) $SOCl_2$, MeOH c) $LiBH_4$/THF d) TsCl/Py e) NaN_3/DMF f) Raney Ni/H_2 g) $BocN_3$/DMSO, Et_3N h) Pd/C, H_2 i) $BrCH_2COOEt$, KF/Celite j) N3-Bz Thymine, DEAD, PPh_3 k) NaOH/aqMeOH l) C_6H_5COOH, DEAD, PPh_3 m) NaOMe/MeOH n) Acetic anhydride, acetic acid, reflux o) 4N HCL, reflux

ethylenediamine backbone segment to the β'-carbon of the side chain, termed pyrrolidine DNA, is described. All four pyrrolidine PNA diastereomers namely (2*S*,*4S*), (2*S*,4*R*), (2*R*,4*S*) and (2*R*,4*R*) have been synthesized following the routes mentioned in scheme 1a, 1b, 2a and 2b and their site-specific incorporation in *aeg*PNA oligomer has been carried out.

Table 1. PNA and DNA sequences

Entry	Sequences
S1	H-T T T T T T T T-NH-β-alanine-OH
S2	H-T T T T T T T t-NH-β-alanine-OH
S3	H-T T T T t T T t-NH-β-alanine-OH
S4	H-T T T T T T T **t**-NH-β-alanine-OH
S5	H-T T T T **t** T T **t**-NH-β-alanine-OH
S6	H-T T T T T T T **T**-NH-β-alanine-OH
S7	H-T T T T **T** T T **T**-NH-β-alanine-OH
S8	H-T T T T T T T ***T***-NH-β-alanine-OH
S9	H-T T T T ***T*** T T ***T***-NH-β-alanine-OH
S10	5'-G C A A A A A A A A C G-3'

T denotes *aeg*PNA monomer, t represents (2*S*,4*S*), **t** representing (2*R*,4*R*), **T** indicating (2*S*,4*R*) and ***T*** symbolizes (2*R*,4*S*) configurations for thymine monomer.

The binding studies of all the oligomers mentioned in Table 1 are carried out using UV-Tm experiments.

CHAPTER 3: Pyrrolidinyl Carbamate Nucleic Acids

Literature reports depict that carbamate linked nucleic acids are more stable towards enzymes as compared to the unmodified oligomers. Further, cytosine containing oligomers with carbamate internucleoside linkage exhibited binding to $p(dG)_6$ with higher Tm (+6.3 ^{o}C/mod). Being uncharged, these oligomers are also expected to penetrate the cell membrane. This chapter describes the extension of the backbone in prolyl PNA by extra atoms replacing amide linkage by carbamate linkage to give *proly*CNAs (Figure 3).

The activated monomers of thymine and cytosine were prepared from trans-L-hydroxy proline in the following steps (Scheme 3). Ring nitrogen was protected as benzylcarbamate followed by esterification to obtain **1** in 93% yield. 4-hydroxy group was converted to the 4S-azide in two steps: mesylation and azidation to get **2**. Selective hydrogenation of azide group in **2** in the presence of Z-group with Raney Ni/H_2 followed by protection of resulting amine as t-Boc

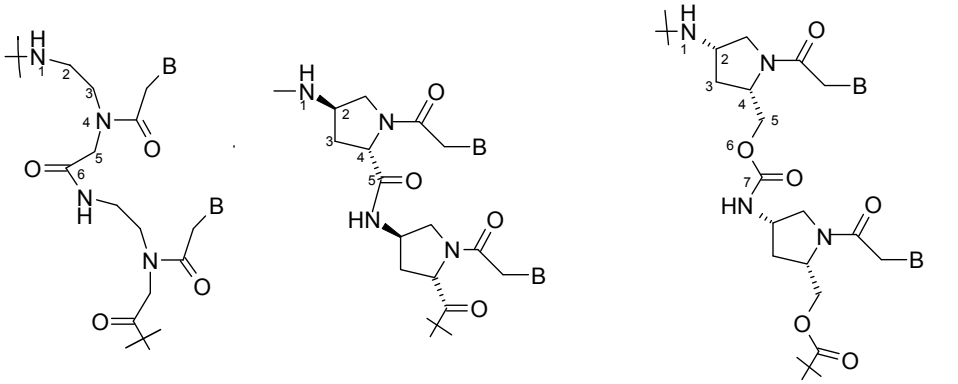

Figure 3.

carbazate gave **3**. $LiBH_4$ assisted reduction of the methyl ester in compound **3** gave boc protected amino alcohol **4** in excellent yields. The benzyloxycarbonyl deprotection in **4** was achieved by hydrogenation in the presence of Pd/C catalyst, and the resulting amine was separately coupled with thymine acetic acid and Cbz protected cytosine acetic acid using DCC/HOBt in DMF to achieve **5a** and **5b** respectively. The primary alcohol in **5a** and **5b** were converted to their corresponding carbonates **6a** and **6b** by reacting with *p*-nitrophenyl

Scheme 3

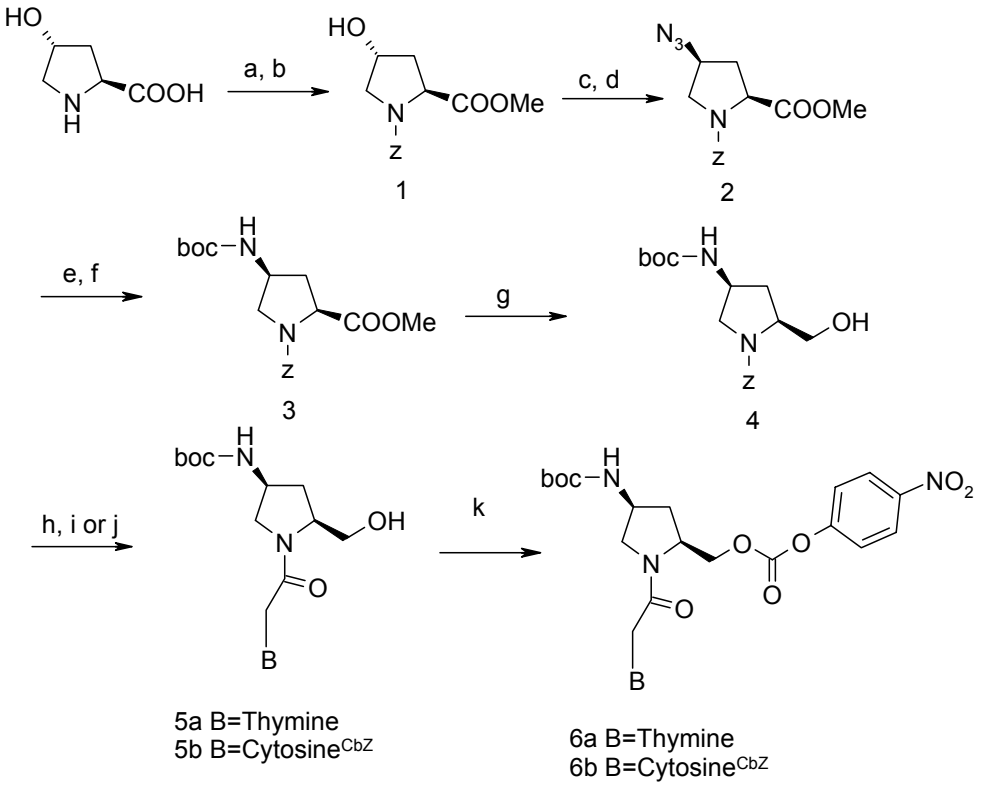

a) ZCl, $NaHCO_3/H_2O$ b) $SOCl_2$, MeOH c) MsCl/Py d) NaN_3/DMF e) Raney Ni/H_2 f) $BocN_3$/DMSO, Et_3N g) $LiBH_4$/THF h) Pd/C, H_2 i) Thyminyl acetic acid, DCC, HOBt j) Cbz-cytosine acetic acid, DCC, HOBt k) p-nitrophenylchloroformate, py

chloroformate. All the intermediates were characterized by ^{1}H, ^{13}C and FAB MS. For the purpose of standardizing the cleavage conditions of carbamate linked oligomer, carbamate linked thymine dimer **7** was prepared in solution. The activated monomer synthons along with standard *aeg*PNA monomers were used to prepare oligomers **8 - 14** (on solid support) using standard protocols (Table 2). The oligomers **8 – 14** were cleaved from the support using TFMSA/TFA method used for the cleavage of peptides.

Table 2. PrCNA, PNA and DNA sequences #

Entry	Sequences
7	H-T* T –OH
8	H- T* T* T* -(β-ala)-OH
9	H-T T T T T T T T- (β-ala)-OH
10	H-T T T T T T T* T- (β-ala)-OH
11	H-T T T T* T T T T- (β-ala)-OH
12	H-T* T T T T T T T- (β-ala)-OH
13	H-T* T* T* T* T* T* T* T* -(β-ala)-OH
14	H-T* C* T* C* T* T* T* T* -(β-ala)-OH
15	5'-G C A A A A A A A A C G-3'
16	5'- A A A A A G A G A -3'

 # * denotes carbamate linkage. T and C represent thymine and cytosine pyrrolidinyl monomer respectively.

Table 3. Tm values of PrCNA/PNA:DNA complexes

Complexes	**$(9)_2$:15**	**$(10)_2$:15**	**$(11)_2$:15**	**$(12)_2$:15**	**$(13)_2$:15**	**$(14)_2$:16**
Tm ^{o}C	44.5	31.5	---	44	-----	-----
% Hyperchromicity	18.2	18.4	6.8	22.2	7.1	9.3

The oligomers **8** – **14** were purified by FPLC and their homogeneity was established by MALDI – TOF mass spectrometry. Binding of the oligomers **9**–**14** with complementary DNA sequences has been studied and the UV-Tm values are shown in Table 3.

CHAPTER 4: Oxyamide Prolyl Nucleic acids

In the work reported previously from this laboratory, conformational constraint on PNA structure was introduced by bridging the α-carbon of glycyl unit with β''-carbon of aminoethyl unit (prolyl nucleic acids). *trans*-4-Hydroxy-L-proline was used for making PNA monomers and it was found that homooligomers of prolyl peptide nucleic acids did not bind to DNA. This suggested that extra strain introduced into the backbone with proline ring might have changed

the internucleobase distance in *prolyl*PNA, which is not compatible for binding with the DNA. Therefore, it was thought of extending the backbone by one oxygen atom by making Oxyamide nucleic acids (Figure 4). To prepare oxyamide-linked nucleic acids the masked oxyamine moiety

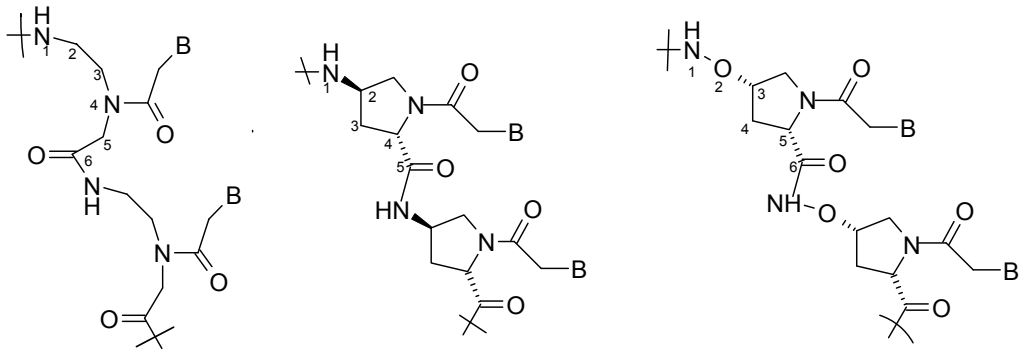

aegPNA Prolyl nucleic acids Oxyamide prolyl nucleic acids

Figure 4.

carrying free carboxylic group was required. Attempts were made towards the preparation of the monomer carrying nucleobase at ring nitrogen via acetyl linker, which failed to provide the required monomer. Finally the orthogonally protected monomer **6** was prepared as shown in scheme 4 which could be used as such for the solid phase synthesis of peptides and the nucleobase was attached to the ring nitrogen on support.

Synthesis of monomer 6

trans-4-Hydroxy-L-proline was protected as carboxy ethyl ester and N-t-butyl carbamate to obtain **2**. The alcohol **2** was converted to the aminoxy alcohol in two steps using N-hydroxyphthalimide as a nucleophile through the corresponding O-phthalimido derivative **3** via Mitsunobu reaction leading to inversion at C-4 followed by removal of phthaloyl group with hydrazine hydrate giving **4** in overall yield 50%. The aminoxy alcohol **4** was protected as flourenylmethyl carbamate using FmocCl in Dioxane:water. Hydrolysis of ester in **5** using NaOH/aq. MeOH led to 20-30% of Fmoc cleavage. Hence using dry ice as buffer it was reprotected in situ with Fmoc succinimide. The other routes for the preparation of **6** with improved yields were also discovered. The structural effects of incorporating this monomer into mixed *aeg*PNA sequence on the stabilities of derived PNA: DNA hybrid is studied.

During the deprotection of phaloyl group in compound **3**, one unusual side product was always formed. This side product was systematically characterized using NMR and X-ray crystallography.

Scheme 4

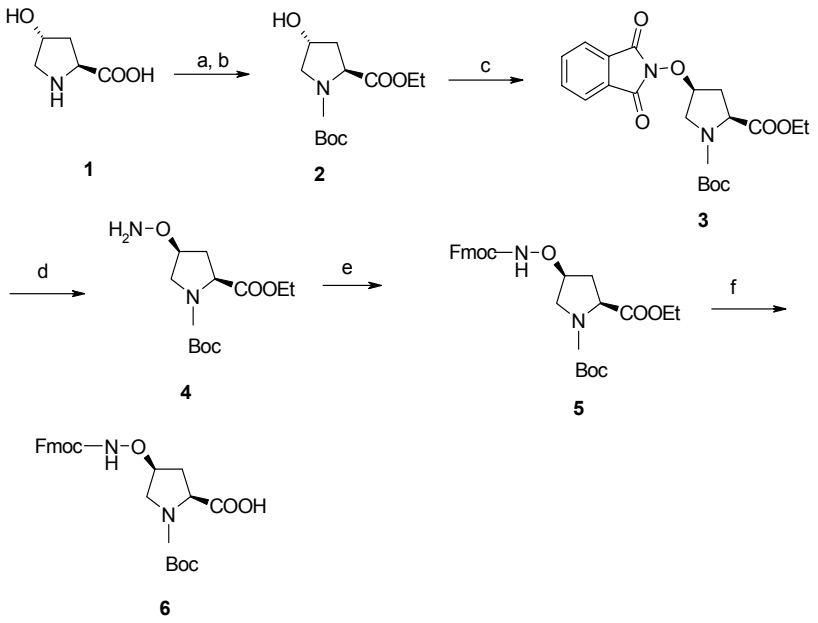

1 **2** **3** **4** **5** **6**

a) $SOCl_2$/MeOH b) $BocN_3$, Et_3N, c) PhthNOH, PPh_3, DEAD d) 90% $NH_2.NH_2$, CH_2Cl_2:EtOH e) FmocCl, DIPEA, Dioxane:water f) NaOH/H_2O , dry ice, Fmoc succinimide

(2*S*,4*S*)-oxyamino proline was also explored for the synthesis of β-turn mimetic. Addition NMR and crystal structure analysis of the tripeptide showed that (2*S*,4*S*) 4-amino proline induces N-O turn.

CHAPTER 5: Pyrrolidine Based Chimeric Antisense Nucleic Acids

The combination of PNA and DNA to form PNA-DNA chimera which in addition to excellent binding, with complementary DNA/RNA can also have useful biological roles such as primers for DNA polymerases. In this regard in our laboratory, (2*R* 4*R*) 2-hydroxy-4-thymin-1-yl-pyrrolidine acetic acid unit was used to make PNA-DNA chimera and was incorporated in DNA sequences at selected positions and it was found to destabilise the derived DNA/DNA-PNAchimera duplexes and triplexes. Since amide linkage is shorter than phosphodiester linkage, replacement of the phosphodiester linkage with amide linkage should include the

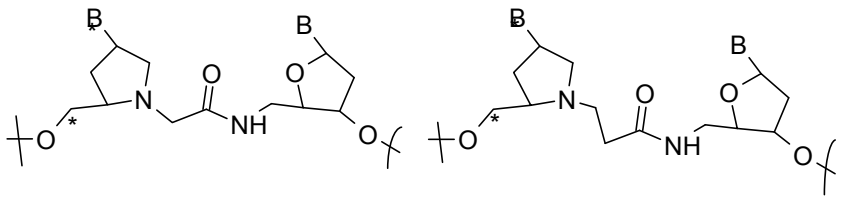

PNA-DNA chimera

PNA-DNA chimera with one extra carbon atom in the backbone

Figure 5.

insertion of an extra atom in the backbone (Figure 5). With this idea, study of PNA-DNA chimera where pyrrolidine unit has one extra carbon atom in the backbone as compared to phosphodiester linkage was attempted. This chapter gives the synthesis of building block used for chimera, synthesis of DNAs with chimeric unit at selected positions and their binding studies.

Synthesis of dimeric block for PNA:DNA chimera (Scheme 5)

The (*2R 4S*) N-protected proline methyl ester **1** was subjected to alkylation with N3-benzoylthymine at C-4 under Mitsunobu conditions to obtain **2**. The reduction of **2** with excess of $LiBH_4$ afforded the alcohol **3** with simultaneous removal of N3-benzoyl of thymine. The

Scheme 5

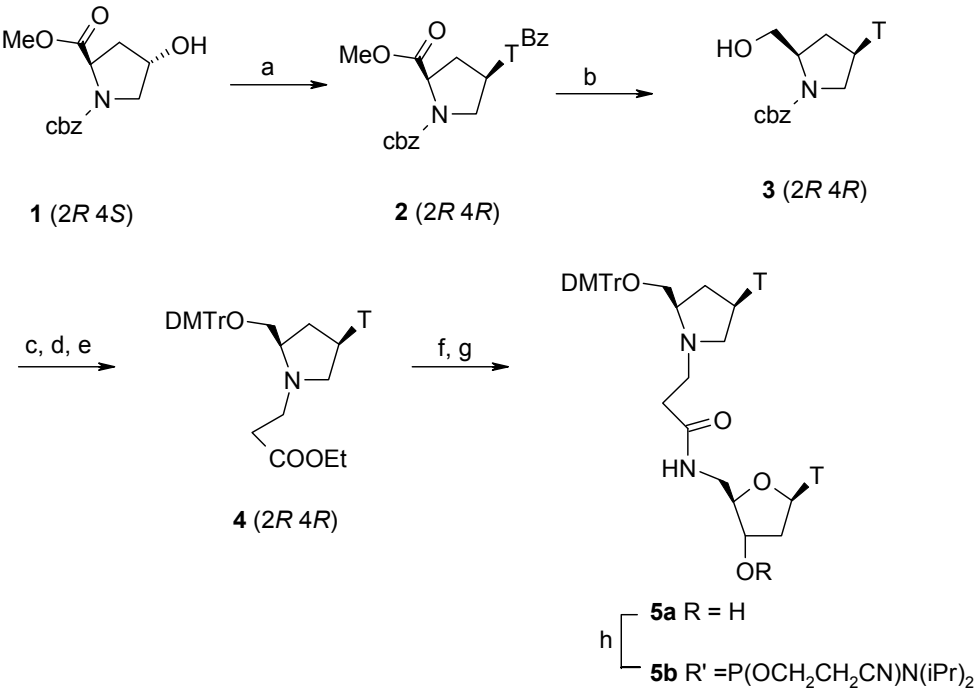

a) N3-Bz-thymine, DEAD, PPh_3, Benzene b) $LiBH_4$/THF c) DMTrCl, Py d) Pd/C, H_2 e) ethylacrylate, MeOH f) NaOH/aq MeOH g) 3'-O-acetyl-5'-aminodeoxythymidine, TBTU, DIPEA, HOBt h) tetrazole, $P(OCH_2CH_2)(N(ipr)_2)$

primary hydroxyl function in **3** was protected as dimethoxytrityl ether followed by deprotection of pyrrolidine ring nitrogen by hydrogenation over Pd-C. Subsequent alkylation via Michael type reaction using ethylacrylate gave DMTr protected ester **4.** Hydrolysis with 1M NaOH/aq MeOH and TBTU-HOBt mediated condensation of acid with 3'-O-acetyl- 5'-amino-deoxythymidine gave the dimer unit **5a** with simultaneous deprotection of 3'-acetyl group which upon phosphitylation gave protected dimer monomer unit **5b.**

DNA-PNA chimeras

The phosphoramidite **5b** was used for incorporation of the dimer block into oligonucleotides **2** and **5** at the desired position in control DNA **1** and **4** by automated solid

phase DNA synthesis using phenoxyacetyl protected regular amidites on Gene assembler plus synthesizer. The oligomers were cleaved from solid support by treatment with aqueous ammonia at room temperature to obtain zwitterionic PNA: DNA chimeras**.** The purity of the oligomers was established by RP-HPLC after gel filtration. The chimeric oligonucleotides **2** and **5** were individually hybridized with complementary DNA strand **5** and **6** respectively for duplex studies and with the duplex 7:8 for triplex studies and the Tm of the resulting complexes was determined by the temperature dependent change in UV absorbance.

Table 4. DNA and chimeric DNA sequences

Entry	Sequence
1	TTC TTC TTC TTT TCT TTT
2	TTC TTC TTC **t*T**T TCT TTT
3	AAA AGA AAA GAA GAA GAA
4	CTT GTA CTT TTC CGG TTT
5	CTT GTA CT**t*T**TC CGG TTT
6	AAA CGG GAA AAG TAC AAG
7	TCC AAG AAG AAG AAA AGA AAA TAT
8	ATA TTT TCT TTT CTT CTT CTT GGA

t*T = pyrrolidinamide dimer block

The Tm data for the duplexes and triplexes revealed that the chimeric DNA having five atom amide based linker formed stable triplxes compared to the corresponding four atom linker.

ABBREVIATIONS

β-ala	β-alanine
A	Adenine
aeg	Aminoethylglycine
aep	Aminoethylprolyl
ala	Alanine
ap	Antiparallel
C	Cytosine
Cbz	Benzyloxycarbonyl
CD	Circular Dichroism
dA	2'-Deoxyadenosine
dC	2'-Deoxycytidine
DCC	Dicyclohexylcarbodiimide
DCM	Dichloromethane
DCU	Dicyclohexyl urea
dG	2'-Deoxyguanosine
DIAD	Diisopropylazodicarboxylate
DIPCDI	Diisopropylcarbodiimide
DIPEA	Diisopropylethylamine
DMF	N, N-dimethylformamide
DNA	2'-deoxynucleic acid
ds	Double stranded DNA
eda	Ethylenediamine
EDTA	Ethylenediaminetetraacetic acid
FAB	Fast Atom Bombardment
Fmoc	9-Fluorenylmethoxycarbonyl
FPLC	Fast Protein Liquid Chromatography
g	gram
G	Guanine
gly	Glycine
h	hours
his	Histidine
HOBt	1-Hydroxybenzotriazole

HPLC	High Performance Liquid Chromatography
Hz	Hertz
IR	Infra Red
MALDI-TOF	Matrix Assisted Laser Desorption Ionization – Time of Flight
MF	Merrifield Resin
mg	milligram
MHz	Megahertz
μM	micromolar
ml	milliliter
mM	millimolar
mmol	millimoles
MS	Mass Spectrometry / Mass Spectrum
N	Normal
nm	nanometer
NMR	Nuclear Magnetic Resonance
p	Parallel
PCR	Polymerase Chain Reaction
PPh_3	Triphenylphosphine
PNA	Peptide Nucleic Acid
Pro	Proline
R	Rectus
RNA	Ribonucleic acid
r.t.	room temperature
S	Sinister
ss	Single strand / single stranded
T	Thymine
t-Boc	tert-Butoxycarbonyl
TEA	Triethylamine
TFA	Trifluoroacetic acid
TFMSA	Trifluoromethanesulfonic acid
THF	Tetrahydrofuran
UV-Vis	Ultraviolet-Visible

Chapter 1

Introduction

1.1 DNA Structure

Nucleic acids (DNA, RNA) are the most important of all biopolymers. DNA is the basic hereditary material in all cells and contains all the information necessary to make proteins. DNA is a linear polymer that is made up of nucleotide units. Each nucleotide unit consists of a base, a deoxyribose sugar, and a phosphate. There are four bases: adenine (A), thymine (T), guanine (G), and cytosine (C) and each base is connected to a sugar via a ß glycosyl linkage (Figure 1). The nucleoside units are connected via the O3' and O5' atoms forming phosphodiester linkages. The mutual recognition of A by T and C by G uses hydrogen-bonds to establish the fidelity of DNA (Watson & Crick, 1953).

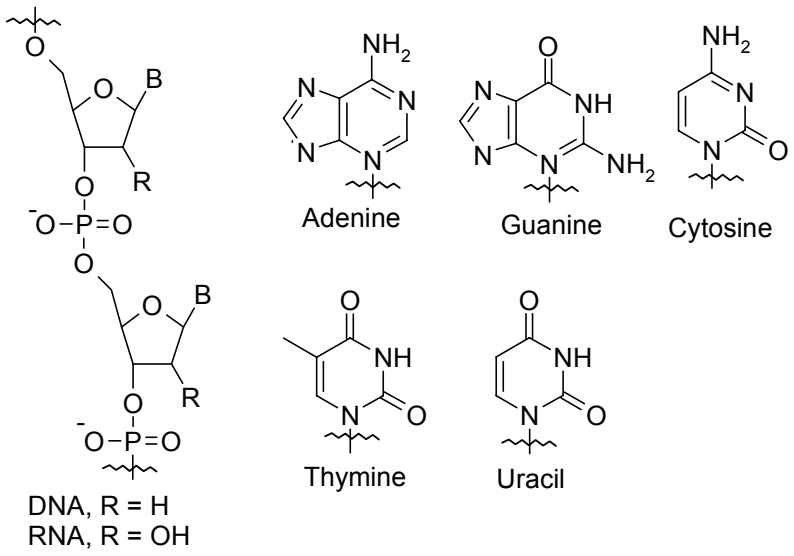

Figure 1. Chemical structure of DNA/RNA and Nucleobases.

RNA contains ribose rather than deoxyribose sugars and the base composition is: guanine, adenine, cytosine and uracil. The four base pair combinations in DNA A:T, T:A, C:G and G:C are geometrically isomorphous, and when linked through the sugar phosphate backbone lead to the classical antiparallel double- helical structure for DNA in which the two strands held together by hydrogen bonds are twisted around each other to form a right-handed helix (Figure 2). The backbones of the two strands cross each other at the edge of the base pairs, giving rise to major and minor grooves in a double- stranded helix. From a functional point of view the grooves play key roles, as the most specific interactions of the DNA duplex with other species such as proteins, drugs, water and metal ions take place in these grooves (Saenger, 1984). Among the three basic components of DNA- sugar, phosphate and heterocyclic bases – the sugar

and phosphate provide centers for non-sequence specific hydrophobic and electrostatic interactions respectively, while the heterocyclic bases are responsible for sequence-specific hydrogen bonding interactions in the major and minor grooves. Many molecules use combinations of the above modes to generate high sequence specificity in DNA recognition.

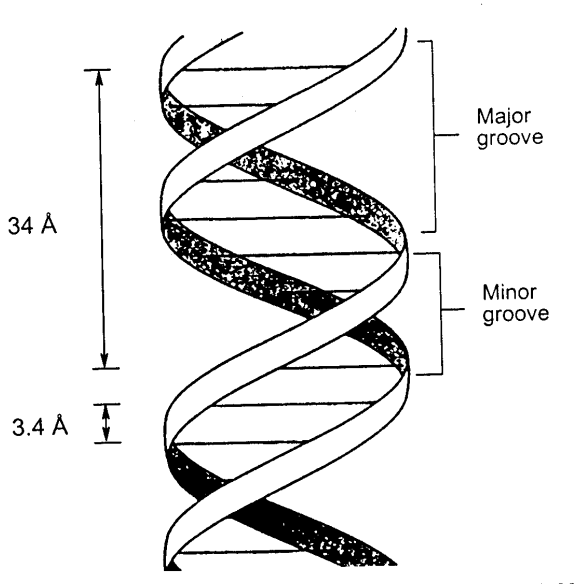

Figure 2. The ribbon model of B DNA. The two ribbons represent the sugar phosphate backbone and the horizontal lines the base pairs, the rise per base-pair 3.4 Å is also shown

Hydrogen bonding

The N-H groups of the bases are potent hydrogen donors, while the sp^2-hybridised electron pairs on the oxygens of the base C=O groups and on the ring nitrogens are much better hydrogen bonding acceptors than are the oxygens of either the phosphate or the pentose. The hydrogen bonds so formed are largely ionic in character. In Watson-Crick pairing, there are two hydrogen bonds in an A:T base pair and three in a C:G base pair (Figure 3).

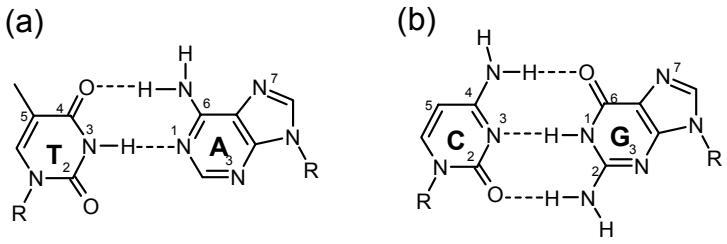

Figure 3. Watson-Crick hydrogen-bonding scheme for (a) T:A and (b) C:G base pairs

While Watson-Crick base pairing is the dominant pattern between the nucleobases, other significant pairings are Hoogsteen (HG) (Hoogsteen, 1963) and Wobble (Crick, 1966; Soll *et al.*, 1966) base pairs (Figure 4). Hoogsteen base pairing is not isomorphous with Watson-Crick base pairing and has importance in triple helix formation. In Wobble base pairing, a single purine is able to recognize a noncomplementary pyrimidine (e.g. GU, where U=Uracil). Wobble base pairs have

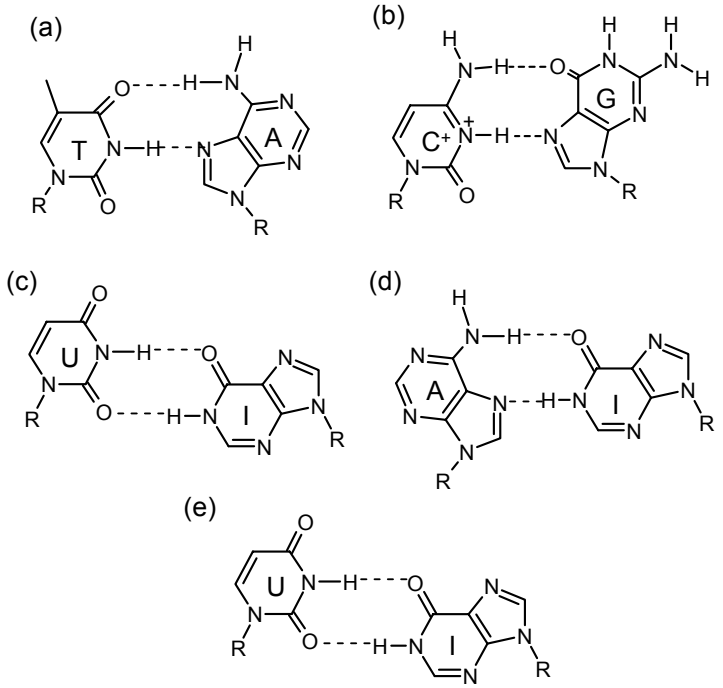

Figure 4. (a and b) Hoogsteen and (c-e) wobble base-pairing schemes. I= inosine

importance in the interaction of messenger RNA (mRNA) with transfer RNA (tRNA) on the ribosome during protein synthesis (codon-anticodon interactions). Several mismatched base pairs and anomalous hydrogen bonding patterns have been seen in X-ray studies of synthetic oligodeoxynucleotides (Seeman *et al.*, 1976; Kennard *et al.*,1989).

Sugar pucker

The furanose rings are twisted out of plane in order to minimize non-bonded interactions between substituents. This puckering is described by identifying the major displacement of carbons-2' and –3' from the median plane of $C^{1'}$-$O^{4'}$-$C^{4'}$. From several crystal structure studies of nucleotides and substituted nucleotides, two major sugar-puckers have been recognized – C2'-*endo* and C3'-*endo*. The deoxy sugars prefer C2'-*endo* while ribo sugars prefer C3'-*endo* sugar puckering. If the *endo*-displacement of C-

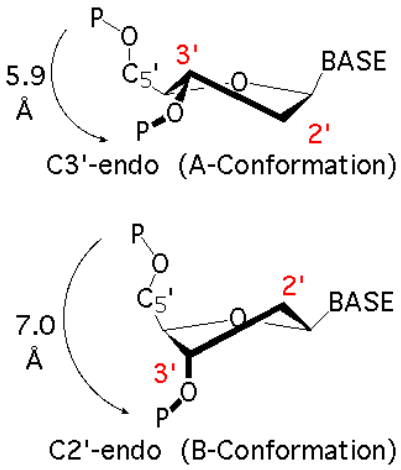

Figure 5. Structures of C2'-endo and C3'-endo preferred sugar puckers.

2' is greater than the *exo*-displacement of C-3' the conformation is called C2'-*endo* (Figure 5). The *endo*-face of the furanose is on the same side as C5' and the base; the *exo* face is on the opposite face to the base. In solution, the C2'-endo and C3'-endo conformations are in rapid equilibrium and are separated by an energy of less than 20 kJ mol^{-1}. The average position of the equilibrium is influenced by (i) the preference of electronegative substituents at C2' and C3' for axial orientation, (ii) the orientation of base (C2'-endo gives syn) and (iii) the intrastrand hydrogen bonding from O2' in one RNA residue to O4' in the next, which favors C3'-endo-pucker.

Syn-anti conformation

The plane of the bases is almost perpendicular to that of the sugars. This allows the bases to occupy either of two principal orientations. The *anti*-conformer has the smaller atom H-6 (Py) or H-8 (Pu) above the sugar ring while the *syn*-conformer has the larger atom O-2 (Py) or N-3 (Pu) in that position. Pyrimidines occupy a narrow range of *anti*-conformations while purines are found in a wider range of *anti*-conformations (Figure 6).

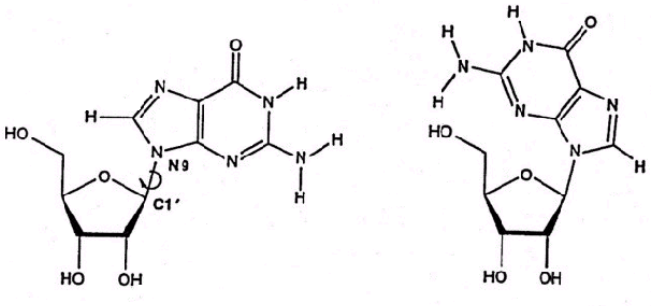

Figure 6. *Anti* and *Syn* conformations of the glycosidic bond in purine.

DNA Secondary structures

The results of fiber and single crystal x-ray diffraction studies have shown that DNA can have several conformations (Figure 7). The most common of these is called B-DNA. B-DNA is a right-handed double helix with a wide major-groove and a narrow minor-groove where the bases are perpendicular to the helical axis. DNA can also be

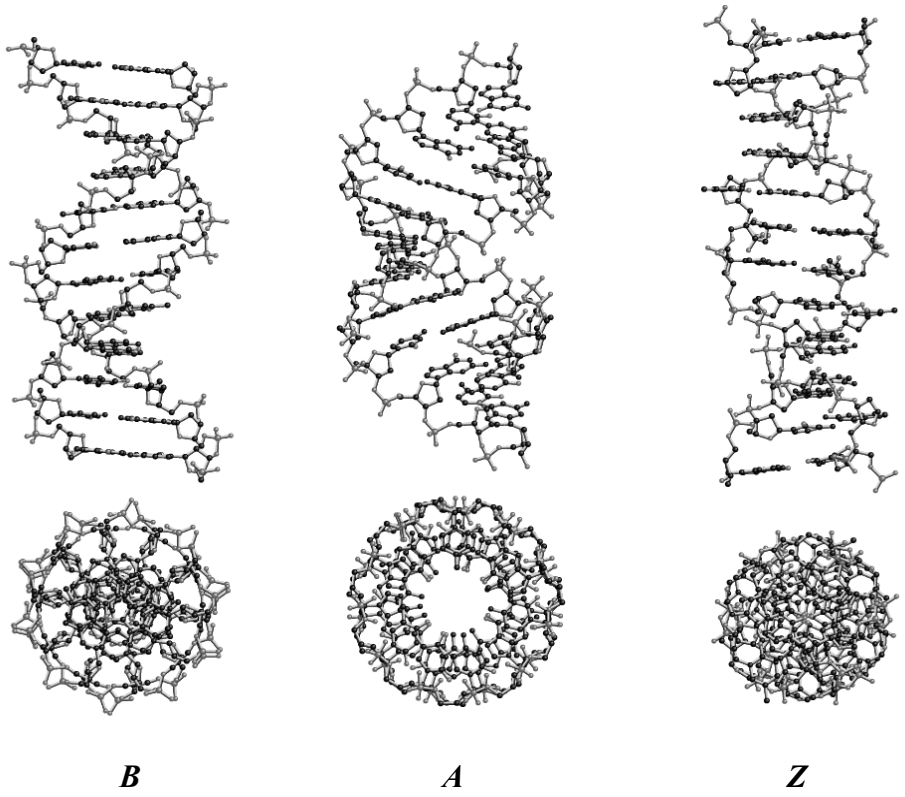

Figure 7 Top: Molecular models of B, A and Z form DNA. Bottom: views along the helical axis.

found in the A-form, another right-handed helix, in which the major-groove is very deep and the minor-groove is quite shallow. At low humidity and high salt, the favored form is highly crystalline A-DNA while at high humidity and low salt, the dominant structure is B-DNA. In both A and B forms of DNA the Watson-Crick base pairing is maintained by an anti glycosidic conformation. The sugar conformation however, is different in both forms with the B form showing C2'-*endo* puckered sugar and the A form DNA exhibiting C3'-*endo* sugar-pucker. A very unusual form of DNA-duplex is the left-handed Z-DNA. This conformation of DNA is stabilized by high concentrations of $MgCl_2$, NaCl and ethanol, and is favored for alternating G:C/G:C sequences. Z-DNA has characteristic zig-zag phosphate backbone and the Watson-Crick base pairing is achieved by purines

adopting *syn* glycosidic conformation with C3'-*endo* sugar-pucker. (Wang, 1981). Z-DNA forms excellent crystals. The features of major DNA conformations are summarized in Table 1.

RNA can form double stranded duplexes. These duplexes are in the A conformation because of the presence of 2'-OH which results in C3'-*endo* sugar-pucker thus precluding the B conformation. More commonly, RNA is single stranded and can form complex and unusual shapes such as stem and bubble structures, which occur due to the chain folding into itself (intramolecular base pairing). An example of RNA structures is tRNA, which is the key molecule involved in the translation of genetic information to proteins. tRNA contains about 70 bases that are folded such that there are base paired stems and open loops. The overall shape of the completely folded tRNA is L shaped.

Table 1 Salient features of major DNA conformations

Structure type	Conditions	Helix type	Residues per turn	Sugar pucker	Glycosidic torsion	Groove width (Å)	
						Major	Minor
B-DNA	Dilute aqueous solutions	Right-handed	10	C2'-endo	*anti*	5.7	11.7
A-DNA	Low humidity and high salt	Right-handed	11	C3'-endo	*anti*	11.0	2.7
Z-DNA	High salt and alternating G,C sequences	Left-handed	12	C2'-*endo* in pyrimidines and C3'-*endo* in purines	*anti* in pyrimidines and *syn* in purines	2.0	8.8

Molecular Recognition in the Major and Minor Grooves of Duplex DNA

The major and the minor grooves of DNA differ significantly in their electrostatic potential, hydrogen bonding character (Seeman *et al.*, 1976), steric effects, hydration (Saenger *et al.*, 1986) and dielectric strength (Jin & Breslauer 1988; Barawkar & Ganesh, 1995). AT and TA base pairs can accept additional hydrogen bonds from ligands bound in the major groove via the C4 carbonyl of T and N7 of A, while in the minor groove hydrogen bonding occurs through the C2 carbonyl of T and N3 of A (Figure 8). The only hydrogen bond donor in the major groove for the AT base pair is the N6 amino group of A, while none exists in the minor groove. For CG and GC duplexes, the H- bond acceptors in the major groove are N7 and O6 for G and in the minor groove are O2 of C and N3 of G. The hydrogen bond donor in the major groove for CG is the N4 amino of C and in the minor groove, the N2 amino of G.

The salient outcome of this pattern of hydrogen bond donors and acceptors in the grooves is that the binding molecules can discriminate the AT base pair from CG efficiently from the major groove side but not so well in the minor groove (Seeman *et al.*, 1976). Two further features of molecular discriminations are noteworthy. In AT and TA base pairs, the C5 methyl of T offers substantial hydrophobic recognition in the major groove which is absent for CG and GC base pairs. However, in the CG and GC duplexes, the N2 amino of G presents a steric block to hydrogen bond formation at N3 of G and the C2 carbonyl of C in the minor groove. It is possible to distinguish AT from TA and CG from GC in the major groove since the horizontally ordered array of hydrogen-bonding sites and hydrophobic centers differ among the four pairs (Figure 8).

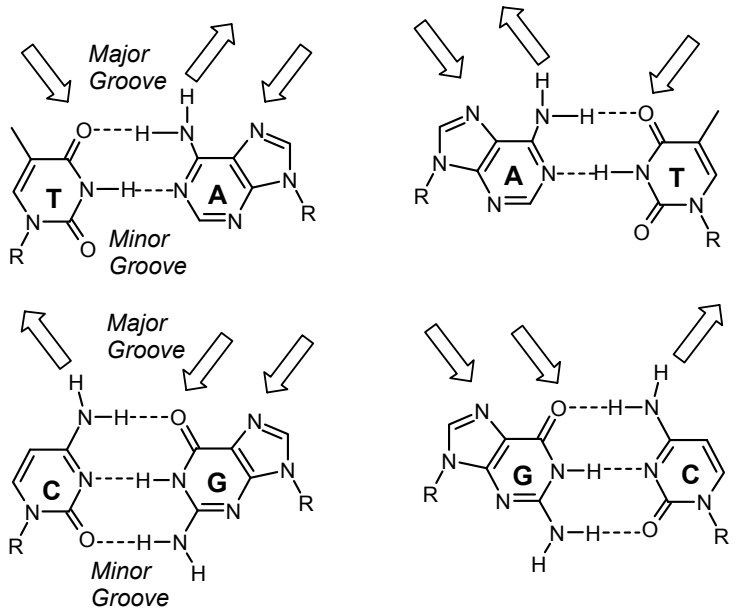

Figure 8: Hydrogen bond donor and acceptor sites in the major groove of duplex DNA at (a) TA (b) AT (c) CG and (d) GC base pairs. Arrows pointing to the atoms indicate acceptor sites; arrows pointing away from the atoms indicate donor sites.

The negative electrostatic potential due to phosphate charges is greater in the AT minor groove than in GC- rich regions, and this provides an additional important source for AT- specific minor groove recognition (Saenger *et al.*, 1986).

1.2 Oligonucleotides As Therapeutic Agents

For curing a disease, nothing would be more gratifying than discovering a "magic bullet"- a drug able to reverse the illness without producing side effects. For most of the 20th century, researchers hoping to find magic bullets thought in terms of

the agents that are able to combine with the active sites of proteins that contribute to disease. By filling these active sites, which differ from one protein to another, the drugs would presumably inhibit the activity of the targeted proteins but would not interfere with needed ones.

There are natural rules that determine how a given sequence of amino acid chains directs its chain into discrete conformation. Yet, given the amino acid sequence of a protein of unknown structure and function, it is still not possible to predict reliably or even to understand how the sequence of the amino acids determines the spatial organization of the chain.

The rules, through which the sequence determines the folding represents an undeciphered aspect of the genetic code, the need to break this part of the code is increasingly urgent. The ability to design proteins from scratch will require an understanding of what the sequence determinants of folding and assembly are. Furthermore, designing a drug against a protein target requires the knowledge of binding sites and binding forces. Although recent advances in X-ray crystallography, NMR and computer modeling of proteins have accelerated the drug design process, this method lacks generality. Designing a drug against a protein target requires a specific understanding of the protein.

In contrast, the nucleotide sequence in RNA and DNA is universal and this generality is very appealing from the drug-design point of view. In principle one can design a drug that, like nucleic acids, is repetitive in its primary structure and binds sequence specifically to these drug targets. In order for the sequence specific recognition to happen, such a drug should contain nucleobases, which are fundamental units of nucleic acid recognition. Two innovative strategies are being tested for inhibiting the production of disease related proteins using such sequence specific DNA fragments as gene expression inhibitors (Figure 9).

(I) The triplex approach, also called *antigene strategy*, aims to stall production of an unwanted protein by selectively inhibiting transcription of gene. In this method, oligonucleotides target the major groove of DNA where it winds around the double-helical DNA to form a triplex.

(II) The antisense strategy (Wagner, 1994) aims to selectively impede translation. The sequence of the bases along a messenger RNA molecule spells out the series of amino acids that must be stung together to make a protein. To obtain a molecule that can bind to the sense strand, one must construct a string of nucleotides having the complementary “antisense,” sequence.

The nucleic acid binding agents receiving the most study are complementary DNA oligomers, which can be designed to recognize a unique site on a chosen gene or its RNA transcripts. These agents have the potential to achieve the specificity required of a magic bullet.

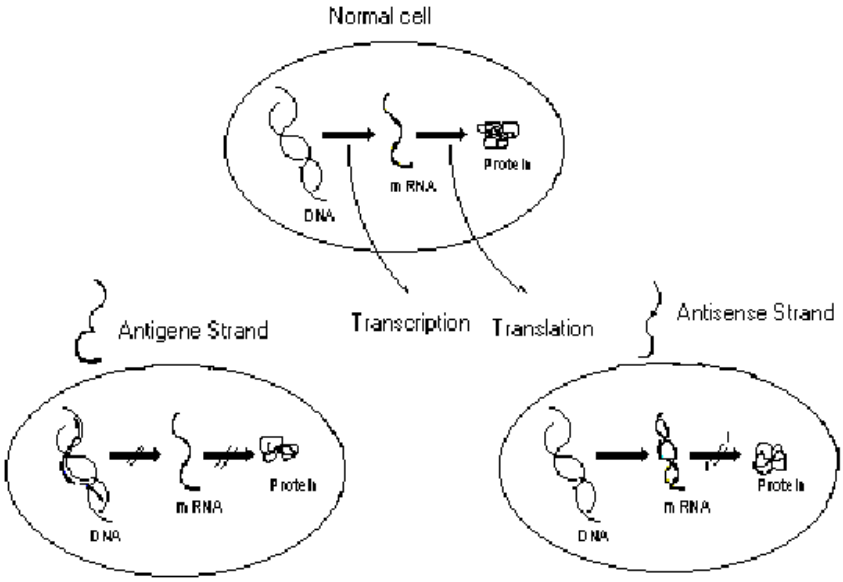

Figure 9. Principle of action of antigene and antisense oligonucleotides.

Zamecnik and Stephenson, 1978 were the first to propose the use of synthetic oligonucleotide analogues as a new class of potential therapeutic agents that could be rationally designed to specifically inhibit the synthesis of chosen target proteins. They showed that replication of Rous sarcoma virus (RSV) can be inhibited by a synthetic 13mer oligonucleotide complementary to a specific mRNA of RSV. Apparently, the tridecamer and its counterpart with blocked 3'- and 5'-hydroxyl termini enter the chick fibroblast cells, hybridize with the terminal reiterated sequences at the 3' and 5' ends of the 35 S RNA, and interfere with one or more steps involved in viral production and cell transformation.

Ribonuclease H mediated antisense effects

Ribonuclease H is an endoribonuclease that specifically degrades the RNA strand in a RNA-DNA hybrid (Liebhaber *et al.*, 1984; Shakin & Liebhaber, 1986). RNase H is involved in generating the antisense effects of ODNs in cell free systems and microinjected cells by inhibiting protein synthesis (Walder & Walder, 1988; Giles *et al.*, 1995). The oligonucleotide itself is not cleaved and is free to bind to another RNA molecule. Thus, essentially, a catalytic cleavage reaction can be obtained in which a

few oligodeoxyribonucleotides (antisense agents) can give rise to cleavage of a large number of RNA molecules. For these reasons, the ability to form hybrids with mRNA that are substrates for RNase H may hence be considered as an important feature in the design of antisense oligonucleotide analogues.

The antisense oligonucleotide approach has two advantages over conventional drugs; (1) the mRNA of the disease target has a defined sequence, and (2) the antisense oligonucleotide interacts with the target gene by Watson-Crick base pairing, providing specificity and affinity. The use of antisense oligonucleotides to regulate specific gene expression allows one to apply the principles learned from working with one gene target to an indefinite number of genes, thereby providing therapies for many diseases. With recent breakthroughs in genetic engineering technologies, such as the completion of human genome sequencing, the speed at which the nucleotide sequence of genes can be determined has far outstripped the rate at which the protein products can be isolated and characterized. This has encouraging consequences for researchers to focus their efforts towards the development of nucleic acid based drugs with therapeutic potential. With the recent FDA approval of Vitravene (or Formivirsen), for the treatment of cytomegalovirus (CMV) induced retinitis in AIDS patients, the first drug based on antisense principle, the technology has achieved an important milestone. Nevertheless, the technology is still in its infancy. Although the basic questions have been addressed, there are still many more questions to be answered.

1.3 Spectroscopic Methods For Studying DNA Complexes

The ability of synthetic oligonucleotide analogues to bindto complementary DNA/RNA sequences needs to be tested for.

1.3.1 UV Spectroscopy

The two strands of a DNA helix readily come apart when hydrogen bonds between its paired bases are disrupted. This can be accomplished by heating a solution of DNA (also called DNA-melting) or by adding acid or alkali to ionize its bases. The melting temperature (Tm) is defined as the temperature at which the duplex and the single strands exist in equal proportion (50% each). DNA double helix, in which the two strands are held together by several reinforcing bonds, is a highly cooperative structure. The double helix is stabilized by the stacking of bases as well as by base pairing. Hydrogen bonding contributes in the order of 5-15 kcal/mol/base pair to the stability of the nucleic acid helix (electronic or intrinsic energy). This contribution is

selective, i.e., there is a preferential stability of the Watson-Crick guanosine-cytosine (G-C) pair relative to all other pairs. Stacking interactions contribute approximately the same amount as H bonding (Rein *et al.*, 1978). The DNA melting is readily monitored by measuring its absorbance at a wavelength of 260 nm. A plot of absorbance against the temperature of measurement gives a sigmoidal curve in the case of duplexes and the midpoint of the transition gives the Tm. In case of triplexes, the first dissociation leads to the duplex (Watson-Crick duplex) and the third strand (Hoogsteen strand), followed by the duplex dissociation at higher temperature into two single strands. The DNA triplex melting shows a characteristic double sigmoid transition with separate melting temperature (Tm) for each transition. The lower melting temperature corresponds to the triplex⇔duplex transition while the second transition gives the Tm of the duplex⇔single strand (Figure 10).

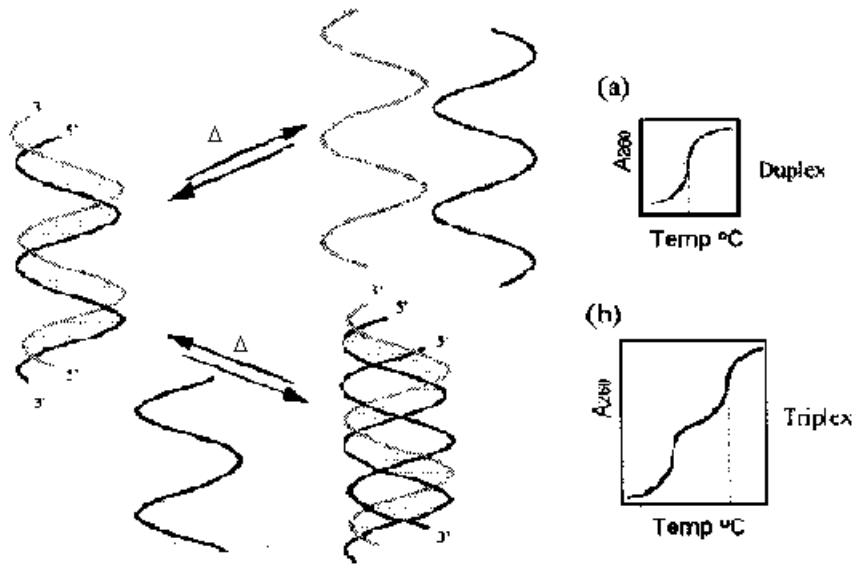

Figure 10. Schematic representation of thermal dissociation of DNA double and triple helices. Mid point of the transition corresponds to the melting temperature (Tm).

When two polynucleotide species combine to form a helical complex there is a decrease in the optical density of the absorption band. The magnitude of this decrease can be used as a quantitative measure of the extent of the complex formation and a means of measuring the stoichiometry of binding by using the method of continuous variation.

The melting temperature of a DNA duplex molecule depends markedly on its base composition (Tong & Leung, 1977) with the sequences rich in G:C base pairs having a higher Tm than those with high A:T base pair content. In fact, the Tm of DNA

from many species varies linearly with G:C content rising from 77°C to 100°C as the fraction of G:C pairs rises from 20% to 78%. G:C pair is more stable than A:T pair, as the former base pair is held together by three hydrogen bonds while the latter has only two hydrogen bonds. In addition, adjacent G:C base pairs interact more strongly with one another than do adjacent A:T base pairs. Hence in a long DNA-double helix with both AT and GC rich tracts, the AT-rich regions are the first to melt. The separated complementary strands of DNA spontaneously reassociate to form a double helix when the temperature is lowered below the Tm. This renaturation process is called annealing.

UV spectroscopy to study DNA-drug interactions

DNA binding molecules regulate mechanisms central to cellular function, including DNA replication and gene expression. Many small molecules that mimic or block these processes offer potential therapeutic agents. The characterization of their binding modes is critical to the understanding of the function of such molecules and is usually investigated through spectroscopic measurements. There are three major classes of binding modes: intercalation, groove binding and covalent crosslinking. In the presence of DNA binding agents, the Tm shifts to a higher or a lower temperature depending upon the stabilization or destabilisation induced by the ligand. An understanding of how the complexation affects both the structural and mechanical properties of DNA is an important step towards understanding the functional mechanisms of the binding agents, and may also provide a key to more rational drug design.

1.3.2 Circular Dichroism (CD) Spectroscopy

Circular dichroism (CD) is a spectroscopic method, which depends on the fact that certain molecules interact differently with right and left circularly polarized light. Circularly polarized light is chiral, that is, occurs in two non-superimposable forms, which are mirror images of one another. To discriminate between the two chiral forms of light, a molecule must be chiral, which includes a vast majority of biological molecules.

CD is measured as the difference in absorbance of right- and left- circularly polarized light as a function of wavelength. Each type obeys the Lambert-Beer law so that the difference in extinction coefficients (left - right) at a given wavelength is equal to the difference in absorbance divided by the product of the pathlength and the concentration. The most commonly used units in current literature are mean residue

ellipticity (degree cm^2 $dmol^{-1}$) and the difference in molar extinction coefficients called the molar circular dichroism or delta epsilon (liter mol^{-1} cm^{-1}). The molar ellipticity [theta] is related to the difference in extinction coefficients by [theta] = 3298(delta epsilon). Here [theta] has the standard units of degrees cm^2 $dmol^{-1}$ and the molar ellipticity has the units degrees deciliters mol^{-1} $decimeter^{-1}$.

The chromophores that are responsible for the intrinsic CD of nucleic acids are the purine and pyrimidine bases (Callis, 1983; Ho, Pui. 1990). These nucleobases themselves are achiral, but their presence in a chiral environment such as double helix affects their transition moments resulting in highly conformation specific CD spectra. Thus, this technique has been used extensively for following conformational transitions in DNA, such as denaturation and transitions from B→A and B→Z DNA (Gray, 1995; Sprecher *et al.*, 1979). The CD of DNA also depends on the ionic strength and, to some extent, on the nature of the salt (Baase & Johnson, 1979). In general, an increase in salt concentration leads to a decrease in the positive 275 nm band with little change in the 245 nm band. The salt dependence of DNA CD was correlated with changes in the helix-winding angle (the angle between neighboring bases) deduced from measurements of super-helical density in closed circular DNA (Anderson & Bauer, W). The CD at 275 nm is highly sensitive to the winding angle (Sprecher *et al.*, 1979). On going from dilute salt to 3.0 M CsCl, for example, the 275 nm band is nearly abolished.

The vacuum-UV CD spectrum of nucleic acids is a reliable diagnostic of the sense of the helix, with right-handed helices (A and B-forms) giving a positive couplet centered near 180 nm and left-handed helices (Z-form) giving a negative couplet centered near 190 nm (Riazance*et al.*, 1985). In the near-UV CD most right-handed RNA and DNA duplexes have a positive long wavelength band.

1.4 Chemical Modifications

The ability of unmodified oligonucleotide strand to cross the anionic phospholipid cell membrane is poor because it carries a negative charge on each phosphate group. Further, the oligomers that manage to enter cells would rapidly be cleaved by cellular nucleases that cleave foreign DNA. To address these drawbacks, a great deal of effort has been directed towards the synthesis of DNA analogues.

Major advances in the design, synthesis and evaluation have led to two classes of modified oligonucleotides (Figure 11). In the first class, the phosphodiester component of the backbone of 2'-deoxyribo-oligonucleotides has been modified in

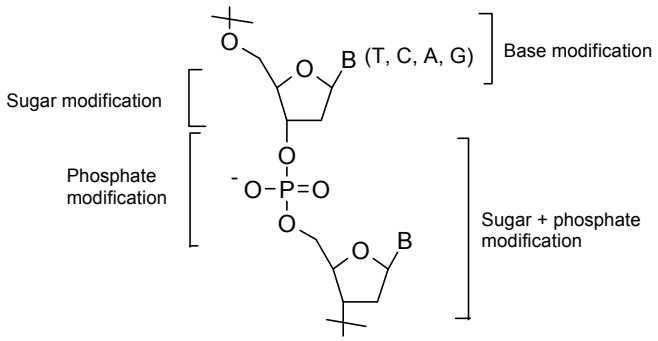

Figure 11. Possible chemical modifications in DNA.

several ways. In the second group, both the sugar and phosphate groups are replaced by amino acids. In addition to the phosphodiester backbone modification, several chemical modifications of the sugar moiety (Uhlmann & Peyman, 1990; Milligan, *et al.*, 1993) as well as the nucleobases (Wagner *et al.*, 1993; Ganesh *et al.*, 1996) have also been attempted. The pentose ribose sugar has been replaced by a hexose (Eschenmoser & Loewenthal, 1992; Augustyns *et al.*, 1992) or carbocycles (Perbost *et al.*, 1989) and these have failed to show any co-operative binding with natural DNA .

1.4.1 Alternative Phosphate Containing Linkages

The most extensively studied analogues are those containing modified phosphate linkages (Figure 12). These comprise phosphorothioates (1), oligonucleoside methylphosphonates (2), alkylphosphonamidates (3)

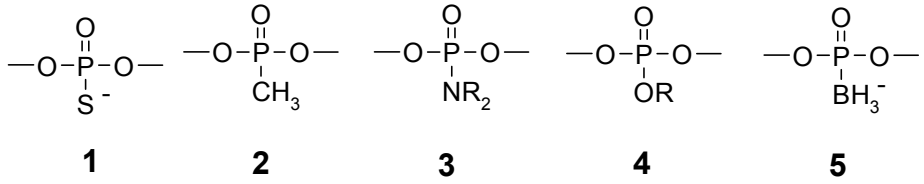

Figure 12. Oligonucleotides with modified phosphate internucleotide linkages.

alkylphosphotriesters (4), and boranophosphate DNA (5). In all these cases, the tetrahedral phosphorous atom is chiral which results in a pair of diastereomers per linkage. Consequently, an oligomer having *n* non-ionic, inter-nucleotide linkages will consist of a mixture of 2^n isomers. The application of modified oligonucleotides requires stereospecific synthesis at each coupling step, which has not been achieved satisfactorily, except in case of phosphorothioates.

The phosphorothioates (PS-oligos)

These comprise a sulfur-for oxygen substitution at phosphorus, and the linkage thus retains a formal negative charge, which is however reduced compared to the phosphodiester homologue. PS-oligos are easily synthesized on a commercial DNA synthesizer, albeit as a mixture of diastereomers at the phosphorus atom, and are resistant to nuclease cleavage, although less so than other modified oligomers (Wagner, 1995). The non-stereocontrolled method of synthesis gives mixture of diastereomers and this heterogeneity is responsible for the concomitant lowering of the melting temperature value. Stec & Zon (1984a,b) synthesised P-chiral analogues of oligonucleotides, which were used for biological studies on antisense targets inside living cells. PS oligomers can act as substrates to RNase H and these first generation antisense agents have been extensively tested in various human clinical trials against numerous targets. The very first antisense agent approved by FDA (Vitravene) is also based on PS-oligos. However, these oligomers have a tendency to induce non-specific effects, through binding to extracellular and cellular proteins (Stein, 1995) as well as cleavage of non-target mRNAs that are only partially complementary (Summerton *et al.*, 1997). Due to the ease of their synthesis, PS-oligos are invariably used against new antisense targets and have become a reference by which most other backbone modified oligos, with therapeutic pretensions, are measured.

The methylphosphonates

In methylphosphonate oligos, a methyl group replaces one of the non-bridging oxygen atoms of the phosphodiester group (Figure 13) rendering the phosphorus atom chiral. This linkage is uncharged and gives rise to nucleotides that are less water-soluble than their phosphate counterpart. Methylphosphonates are easily synthesized

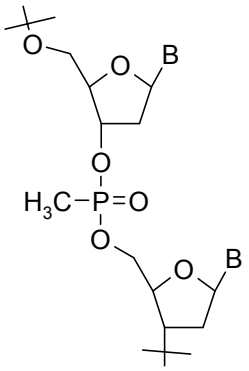

Figure 13. Structure of Methylphosphonate.

as diastereomers by standard solid phase synthetic protocols from readily available methylphosphoramidites. The pioneering work of Miller *et al.* (1979) has shown that the methylphosphonates, (also known by the name MATAGE-NES, masking tape for gene expression) can enter cells and are very stable with respect to cellular nucleases.

Although oligodeoxyribonucleoside methylphosphonates form stable duplexes with single stranded DNA, hybrids formed with complementary RNA of the same nucleotide sequenece generally have lower stability (Kean *et al.*, 1995). The reduction in Tm has been ascribed to the presence of mixed diastereomers. The stabilities of methylphosphonate-DNA duplexes are not significantly affected by changes in ionic strength, whereas those of oligodeoxyribonucleotide-DNA duplexes decrease when ionic strength is decreased. This effect is attributed to the lack of charge repulsion between the non-ionic methylphosphonate linkages in the oligonucleoside methylphosphonate and the negatively charged PO linkages of the complementary target strand. In addition to poor aqueous solubility, methylphosphonates cannot induce RNase H activity. For these reasons this modification is less useful than phosphorothioate oligos in biological studies.

The phosphonamidates

They include negatively charged, achiral N3'→P5' phosphonamidate linkage with a bridging 3'-amino group (Figure 14a) (Gryaznov & Chen, 1994, Gryaznov *et al.*, 1995), the oppositely oriented P3'→ N5' phosphonamidates (Barsky *et al.*, 1997) as

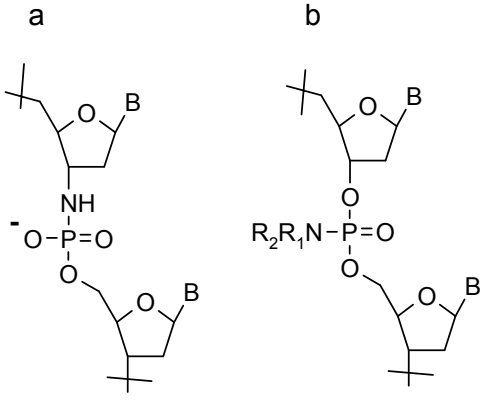

(i) R_1=H, R_2=CH_3
(ii) R_1=H, R_2=$(CH_2)_2OMe$
(iii) R_1, R_2=CH_3
(iv) R_1, R_2=$(CH_2CH_2)_2O$
(v) R_1=H, R_2=$(CH_2)_2N(CH_2CH_2)_2O$
(vi) R_1=H, R_2=$CH_2CH_2NMe_2$

Figure 14. Structure of Phosphonamidates

well as the neutral, but chiral phosphonamidates with non-bridging amino groups (Peyrottes *et al.*, 1996, Endo & Komiyama, 1996) (Figure 14b). Of these the N3'→P5' phosphonamidates developed by Gryaznov and coworkers have superior biophysical properties and greatest promise for therapeutic and other applications. In addition to superior qualities for binding to single and double stranded nucleic acid targets, uniformly modified N3'→P5'phosphonamidates are stable to nucleases (e.g. snake venom phosphodiesterase (SVPD) and alkaline phosphatase), and are resistant to hydrolysis in human plasma for up to 8hrs (Gryaznov *et al.*, 1996). The single stranded phosphonamidate oligos do not bind to cellular proteins as was observed with PS-oligos. However, unlike PS-oligos, N3'→P5' modified oligos are unable to activate RNase H when bound to complementary RNA (Heidenreich *et al.*, 1997). Despite this, N3'→P5' phosphonamidate oligomers have shown potent antisense activity in cell culture and *in vivo* (Skorski *et al.*, 1997). Finally, N3'→P5' phosphonamidate oligos were shown to be amongst the best inhibitors of HIV-1 reverse transcription *in vitro*, compared with a series of other promising antisense oligomers.

The oligonucleotide phosphonamidates of the type (i)-(iv) (Figure 14b) exhibit poor hybridization characteristics (Δ Tm/mod for NHR= -0.1 to –2.3^{o}C, at pH 7.2) (Froehler *et al.*, 1988; Letsinger *et al.*, 1988). Oligonucleotides of the type (v) form weak duplexes at neutral pH but form duplexes with higher stability under acidic conditions (pH 5.6) due to the protonation of the terminal amine. Type (vi) oligos hybridize to DNA targets at both neutral and acidic pH. The hybridization of oligonucleotides consisting of alternating phosphonamidate type (vi)/phosphodiester linkages to RNA targets is similar to the corresponding interactions with normal DNA (Jung *et al.*, 1994). The Tm of these complexes is independent of the ionic strength of the buffer, in contrast to the behavior of wild-type oligonucleotides with DNA or RNA targets, which show a strong Tm increase with increasing salt concentration.

Phosphate triesters

Oligonucleotide phosphate esters lack the usual negative charge present on oxygen in the oligonucleotides (Figure 15). The phosphotriester when R=Et, forms substantially less stable self-complementary duplexes compared to wild type (Summers *et al.*, 1986). A single modification on a self-complementary sequence (which had a backbone modification in each strand of the duplex) resulted in a Tm decrease of –4^{o}C and –11^{o}C, depending on whether the S_p or R_p diastereomer was used. This destabilizing effect is surprising, since the reduction or removal of the negative charge of the backbone as in thiophosphonates (Figure 12a) and

methylphosphonates (Figure 13) should result in increased duplex or triplex stability. Nevertheless, these modifications result in the decreased stability of their complexes with complementary nucleic acids at physiological ionic strength (Froehler *et.al.*, 1988). No stereoselective synthetic approaches are available for phosphate triesters and the chirality problem of the phosphorus also persists in this case.

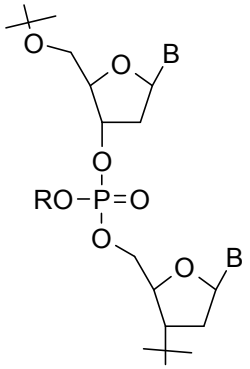

Figure 15. Structure of phosphate ester.

Boranophosphate DNA

These are derived by replacing one of the non-bridging oxygen atoms in the phosphodiester group of DNA with borane (BH_3) (Sood *et al.*, 1990; Spielvogel *et al.*, 1991; Sergueev *et al.*, 1998) (Figure 16). The boranephosphate diester is isoelectronic with phosphodiesters, isosteric with the methylphosphonate group and is chiral. These negatively charged oligos are highly water soluble, but more lipophilic than DNA. NMR and CD studies show that replacing the phosphodiester group in dinucleotides with the boranephosphate diester results in only a slight change in conformational

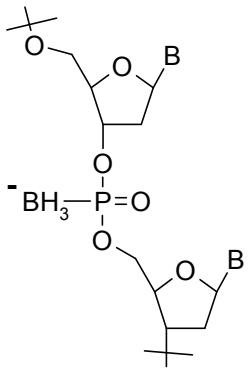

Figure 16. Structure of boranophosphate DNA.

characteristics, such as sugar pucker, acyclic torsional angles and base stacking (Li H. *et al.*, 1997). Boranophosphate DNA is considerably more stable to various nuclease enzymes than native DNA and overall more stable than phosphorothioate DNA (Sergueev & Shaw, 1998). The discovery that boranophosphate DNA can activate *E. coli* RNase H and induce cleavage of RNA (Higson *et al.*, 1998; Rait & Shaw, 1999) is both interesting and encouraging.

1.4.2 Phosphate-Free Backbones

Of all the backbone modifications, those involving the replacement of the phosphodiester group with neutral linkers, outnumber the rest. Initially it was supposed that these lipophilic oligos might increase the efficiency of passage into the cells, decrease the electrostatic repulsion with target nucleic acids and therefore improve affinity. Whilst the former has not been shown to be the case, affinity can be improved with neutral linkages, provided that the linkage is pre-organized into the correct conformation for binding and is favorably hydrated in the duplex state.

In the light of chirality problems associated with phosphorus containing backbones, alternative neutral, achiral internucleoside linkages have been investigated (De Mesmaeker *et al.*, 1995) (Figure 17). De Mesmaeker and co-workers have

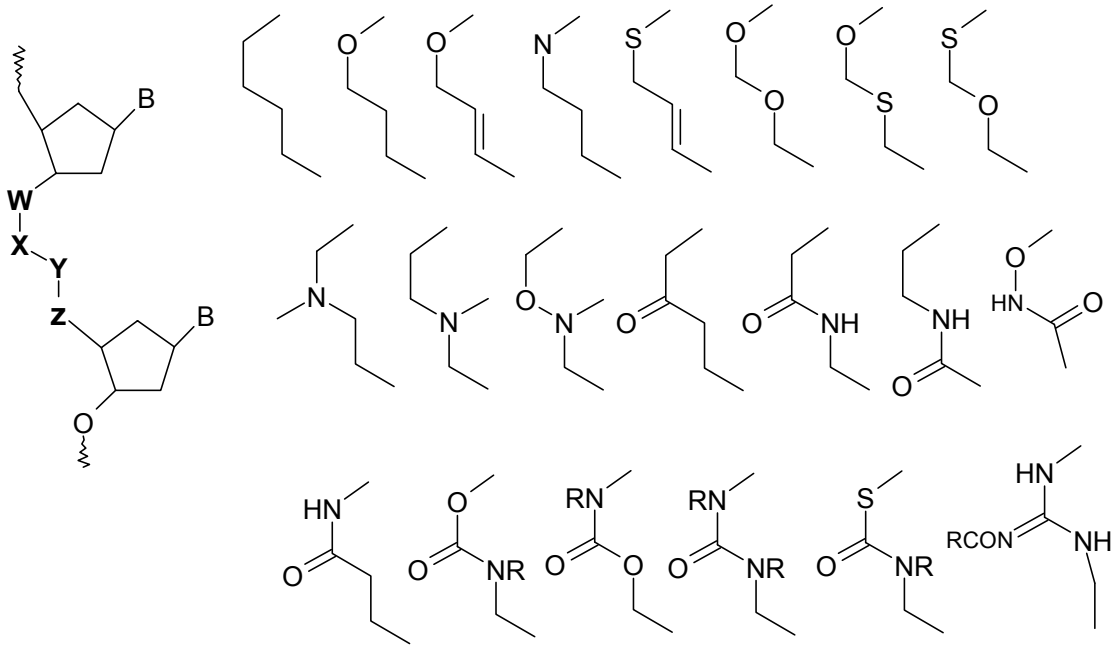

Figure 17. Nonphosphorus backbone replacements

synthesized neutral dinucleotide analogues with many different linkers including ureas, carbamates, amides, alkyl and alkenyl chains. These dinucleotide analogues were then incorporated into several DNA sequences using a block synthesis approach with modified dinucleotide phosphoramidites, resulting in chimeric backbones with alternating phosphodiester and modified linkages and the influence of the modifications was tested on the stability of the duplexes formed between the oligodeoxyribonucleotides and their complementary RNA strands. Of all the modifications investigated, the two isomeric amides; 3'-$CH_2CONHCH_2$-5' and 3'-$CH_2NHCOCH_2$-5' (Figure 17), lead to a slightly increased or a similar binding affinity compared to the wild type for an RNA target.. Interestingly, the affinity for complementary DNA is somewhat lower for these amide chimeras. It is argued that restricted rotation about the amide bond, with a preference for the *trans* isomer, preorganises these two backbones into a conformation resembling A-type duplexes.

1.4.3 Backbones Containing Sulfonyl Groups

A number of modifications have been introduced involving replacement of the PO_2^- group of native oligos with neutral isosteric and isoelectronic SO_2 groups. These include dimethylene sulfones, sulfonamides, sulfonates, 5'-N-sulfamates, 3'-N-sulfamates and sulfamides (Figure 18). In most of these cases duplex stability is diminished significantly, with the exception of the sulfamates. The most destabilizing is

dimethylene sulfone	X=Y=CH_2
sulfonamides	X=NH; Y= CH_2
sulfonates	X=O; Y= CH_2
5'-N-sulfamates	X=NH; Y= NH
3'-N-sulfamates	X=NH; Y=NH
sulfamides	X=Y=NH

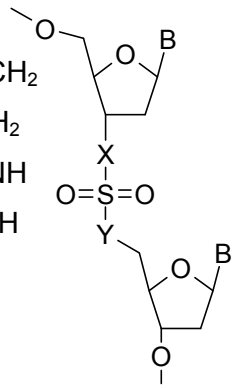

Figure 18. Structures of sulfonyl containing oligos

the dimethylene sulfone group, which results in a dramatic drop in Tm of duplexes with both DNA and RNA (Δ Tm/mod -15 ^oC).

1.4.4 Analysis Of Nonphosphorus Backbones

The above section presented various backbone modifications according to their influence on the Tm of the corresponding duplexes formed with an RNA (or DNA) strand. For an evaluation of the stabilizing or destabilizing effect of given modification on the duplex structure, various backbone replacements are divided into three groups according to the degree of rigidity introduced by the modification.

In the first group, four atoms are present in the backbone (Urea, thiocarbamate, carbamate, guanidine, sulfamate). Because of the conjugation of lone pairs of electrons from nitrogen and oxygen atoms with a carbonyl (or imine) group, three atoms are maintained in the same plane. As a consequence, a rather severe destabilization of the duplexes was observed when these modifications were introduced into DNA strand. The same arguments pertain to the relatively short and rigid backbone of oxyamide linked oligomers (Burgess *et al.*, 1994) (Figure 19). In this case, only three atoms separate the two sugar units and rotation around the N-CO and the O-N bonds is restricted. In the thiocarbamate derivative, greater ease of rotation around the S-CO

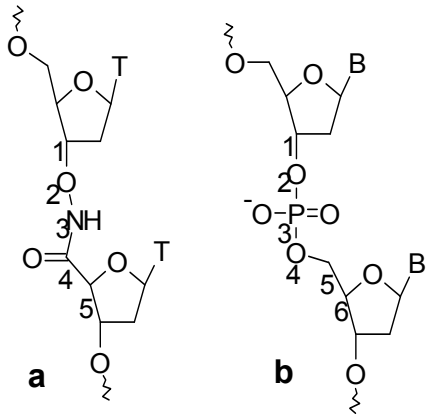

Figure 19. a) 5'-O-NH-CO-3' linked oligomer b) DNA

bond compared to the N-O bond of urea and the greater C-S bond length was assumed to make the backbone more flexible, allowing to reach a geometry compatible with an A-type double helix. In fact, the thiocarbamate backbone is almost as destabilizing as the urea analogue, but replacement of the carbonyl group in the carbamate by an SO_2 moiety in the sulfamate derivative has been argued to have a beneficial effect on the Tm value of the duplex.

The second group of modifications (amide, hydroxylamine, thioformacetal, formacetal, allyl ether, ether; Figure 20), introduce less pronounced conformational restrictions. Molecular modeling studies on duplex structures containing amide at

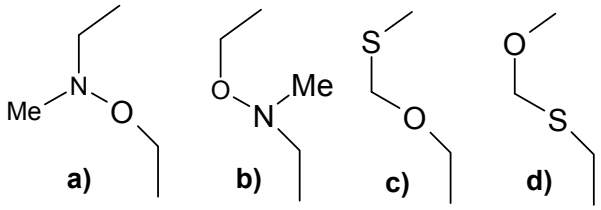

Figure 20. Structural isomers of hydroxylamine (a,b) and thioformacetal (c,d)

various positions in the linkage suggest that the upper (i.e. amide bond closest to the 5' end of the oligonucleotide) sugar moiety adopts a 3'-endo conformation, whereas the lower (i.e. amide bond closest to the 3' end of the oligonucleotide) sugar unit puckers between the 2'-and 3'-endo conformations. The geometry adopted by the amide modification is also found in crystal structure of A-DNA (De Mesmaeker *et al.*, 1994). Because of the low electronegativity of the CH_2-CO-NH residue in the upper sugar, it adopts 3'-endo conformation. The backbone is therefore shorter compared to that in which upper sugar adopts 2'-endo conformation. The shorter backbone would be more favorable for the formation of A-type duplex with RNA. The same effect is probably responsible for the higher Tm value obtained for 3'-thioformacetal (c) compared with 5'-thioformacetal (d). The low electronegativity of the sulfur atom would favor a 3'-endo conformation of the upper sugar unit. Interestingly, an increase in the size of the substituents on the nitrogen atom does not substantially destabilize the duplexes, when the amide group is located in the middle of the backbone. This could be useful if the properties of the oligonucleotides have to be improved. An elongation of the amide backbone by one atom decreases the thermal stability of the duplex with DNA (Chur *et al.*, 1993). This probably arises from the elongated backbone having a lower degree of preorganization in the geometry required for optimal incorporation in the duplex.

The stability results of hydroxylamine, thioformacetal and formacetal modified backbones can be discussed based on strereoelectronic effects (Jones *et al.*, 1993; Metteuci *et al.*, 1990). In the hydroxylamine derivative, the lowest energy conformation is obtained when the repulsion between lone pairs on both heteroatoms is minimized. In thioformacetal and formacetal types, the lowest energy conformation arises from the anomeric affect. Significant difference between structural isomers of hydroxylamine (Figure 20a,b) as well as between thioformacetal (Figure 20c,d) was observed. Modification types (a) and (c) stabilize the duplex, whereas the corresponding inverted structure isomer types (b) and (d) strongly destabilize the double helix. These results

indicate clearly that factors other than the geometry of the backbone also play an important role in helix stability.

In the third group of modifications (ketone, ether, thioether and amine), the backbone has a high degree of conformational freedom (Figure 21). Consequently, much lower Tms were obtained for the corresponding duplexes because of an increased negative entropy contribution to the hybridization process. The results show

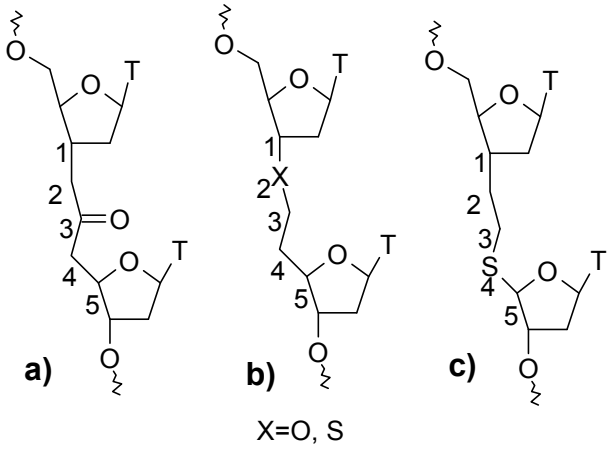

Figure 21. Linkages with conformational freedom;.a) ketone b) and c) thioether DNA

that duplex stability is enhanced by modifications in which there is restricted conformational freedom about the middle of the backbone. This preorganization can be achieved by restricted rotation around an amide or hydroxylamine bond or by taking advantage of anomeric affect. The extent to which the sugars pucker and the distance between the sugars are important parameters in gaining the desired thermal stability of the duplexes. New backbone types displaying this type of preorganization have been identified, which increase the binding affinity of an oligonucleotide for its RNA complement. The improved association with the target is an extremely important achievement. Resistance towards endo- and exonucleases was most pronounced in the alternating phosphodiester modified backbones. It has been observed that phosphodiester linkages located between two amide bonds seem to be very resistant to enzymatic degradation (Lebreton *et al.*, 1994).

1.4.5 Non-(Sugar-Phosphate) Backbones

1.4.5a. Morpholino Nucleosides

Summerton *et al.* (1997) prepared novel oligonucleotide analogues from ribonucleotide-derived morpholine units, linked by carbamate groups (Figure 22a).

Cytosine hexamer with stereoregular backbone was prepared in solution phase and was shown to bind to *poly*(G) with very high affinity. Solubility characteristics of the resulting oligomer have been improved by terminal conjugation with polyethylene glycol (Summerton & Weller, 1997). Fully modified morpholino oligomers where nucleosides are linked by phosphorodiamidate groups are shown to be more effective antisense agents than iso-sequential PS-oligos in cell-free systems and in various cultural cells (Figure 22b). This is attributed to the fact that morpholino oligos, unlike PS-oligos, do

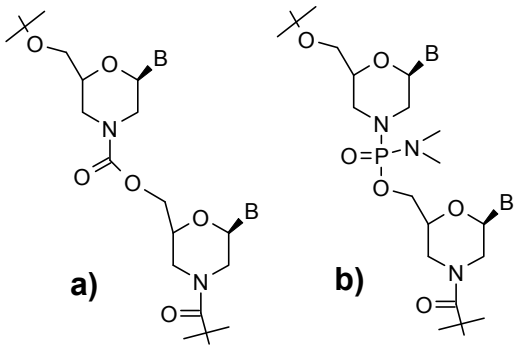

Figure 22. Morpholino derivatives linked by a) carbamate b) phosphorodiamidate

not bind to non-specific proteins and are much more sequence specific in their binding to DNA. In one notable study, morpholino oligos were shown to be more effective than PS-oligos as sequence specific antisense inhibitors of tumor necrosis factor-α (TNF-α) in mouse macrophages, despite poor uptake into these cells (Taylor *et al.*, 1996, 1998).

1.4.5b. Peptide Nucleic Acids

Nielsen *et al.* (1991) designed a DNA analog, *peptide nucleic acid* (PNA), in which the backbone is structurally homomorphous with the deoxyribose backbone and consists of N-(2-aminoethyl)glycine units to which the nucleobases are attached (Figure 23). PNAs containing all four natural nucleobases hybridize to complementary oligonucleotides obeying the Watson-Crick base-pairing rules, and PNA is a true DNA

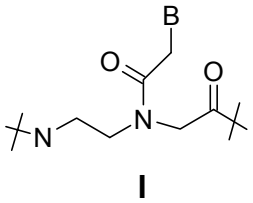

I

Figure 23. Chemical Structure of PNA.

mimic in terms of base-pair recognition. Excellent RNA and DNA hybridization properties and biophysical stability, combined with convenient solid phase peptide synthesis, have made PNA a highly interesting lead for gene pharmaceutical drugs.

Antisense properties of duplex- and triplex- forming PNAs

Knudsen & Nielsen, (1996) studied the potential of peptide nucleic acids (PNAs) as specific inhibitors of translation. PNAs with a mixed purine/pyrimidine sequence form duplexes, whereas homopyrimidine PNAs form $(PNA)_2$/RNA triplexes with complementary sequences of RNA. Neither of these PNA/RNA structures are substrates for RNase H. Translation experiments showed that a 15mer duplex-forming RNA blocked translation in a dose-dependent manner when the target was 5'-proximal to the AUG start codon on the RNA, whereas similar 10-, 15- or 20mer PNAs had no effect when targeted towards sequences in the coding region. Triplex-forming 10mer PNAs were efficient and specific antisense agents with a target overlapping the AUG start codon and caused arrest of ribosome elongation with a target positioned in the coding region of the mRNA. Furthermore, translation could be blocked with a 6mer bisPNA or with a clamp PNA, forming partly a triplex, partly a duplex, with its target sequence in the coding region of the mRNA. Moreover, PNAs are stable against nuclease and protease cleavage.

A unique property of PNAs is their ability to displace one strand of a DNA double helix to form strand invasion complexes, which is an additional attribute for their application as antisense/antigene agents. Such strand invasion process is inefficient or absent in DNA or any other DNA analogues studied so far. The strand invasion by PNA (Figure 24) is dictated by the formation of triple helical structures *via* Watson-Crick and

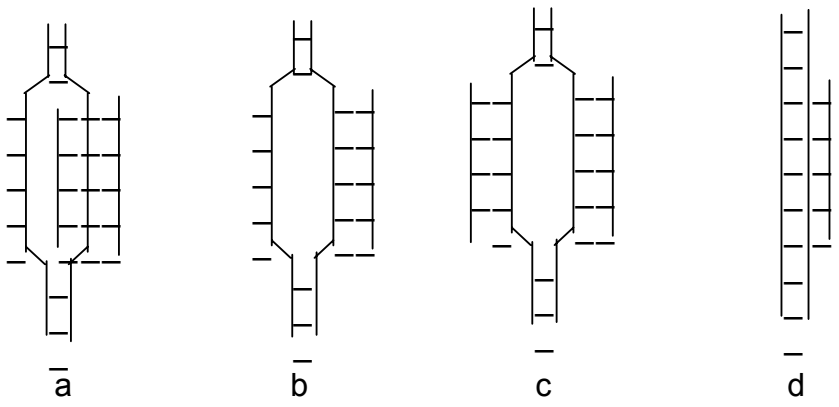

Figure 24. a. Triplex invasion **b.** Duplex invasion **c.** Double duplex invasion **d.** Third strand binding forming a PNA:DNA_2 complex.

Hoogsteen binding modes and is by far confined to the polypyrimidine PNA oligomers, which form PNA_2:DNA triplexes.

The relatively high binding affinity of PNAs towards the natural oligonucleotides is attributed to the lack of electrostatic repulsion between the uncharged PNA backbone and the negatively charged sugar-phosphate backbone of DNA and RNA. PNA being acyclic, single-stranded PNA is conformationally flexible in its aminoethyl, glycyl segments as well as in the nucleobase carrying acetyl linker arm.

Peptide Nucleic Acid forms DNA-like double helix

Although the importance of the nucleobases in the DNA double helix is well understood, the evolutionary significance of the deoxyribose phosphate backbone and the contribution of this chemical entity to the overall helical structure and stability of the double helix are not so clear. Wittung *et al.* (1994) by the use of CD spectroscopy, showed that two complementary PNA strands could hybridize to one another to form a helical duplex. Since PNA has achiral backbone, a lysine residue was attached to the C-terminus and there was found seeding of preferred chirality that was induced by the presence of an L- (or D-) lysine residue. These results indicate that a (deoxy) ribose phosphate backbone is not an essential requirement for the formation of double helical DNA-like structures in solution.

Crystal structure of a peptide nucleic acid (PNA) duplex

The crystal structure of a PNA duplex, which was reported very recently by Rasmussen *et. al*. (1997), revealed both a right- and a left-handed helix in the unit cell. The helices are wide (28 Å), large pitched (18 bp) with the base pairs perpendicular to the helix axis, thereby demonstrating that PNA besides adapting to oligonucleotide partners also has unique structure by itself.

Chemical Modifications of PNA

The structure of classical PNA monomer has been subjected to a variety of rational modifications with the aim of understanding the structure activity relations in this class of DNA mimics as well as obtaining PNA oligomers with specifically improved properties for various applications within medicine, diagnostics, molecular biology etc. (Figure 25). The limitations of PNA include low aqueous solubility, ambiguity in DNA binding orientation and poor membrane permeability. Structurally, the analogues can be derived from ethylenediamine or glycine sector of the monomer, linker to the nucleobase, the nucleobase itself or a combination of the above. The strategic rationale behind the modifications (Dueholm *et al.*, 1997) are (i) introduction of chirality

into the achiral PNA backbone to influence the orientation selectivity in complementary DNA binding, (ii) rigidification of PNA backbone via conformational constraint to pre-organize the PNA structure and to entropically drive the duplex formation, (iii) introduction of cationic functional groups directly in the PNA backbone, in a side chain substitution or at the N or C terminus of PNA, (iv) to modulate nucleobase pairing either by modification of the linker or the nucleobase itself and (v) conjugation with 'transfer' molecules for effective penetration into cells. In addition to improving the PNA structure for therapeutics, several modifications are directed towards their applications in diagnostics.

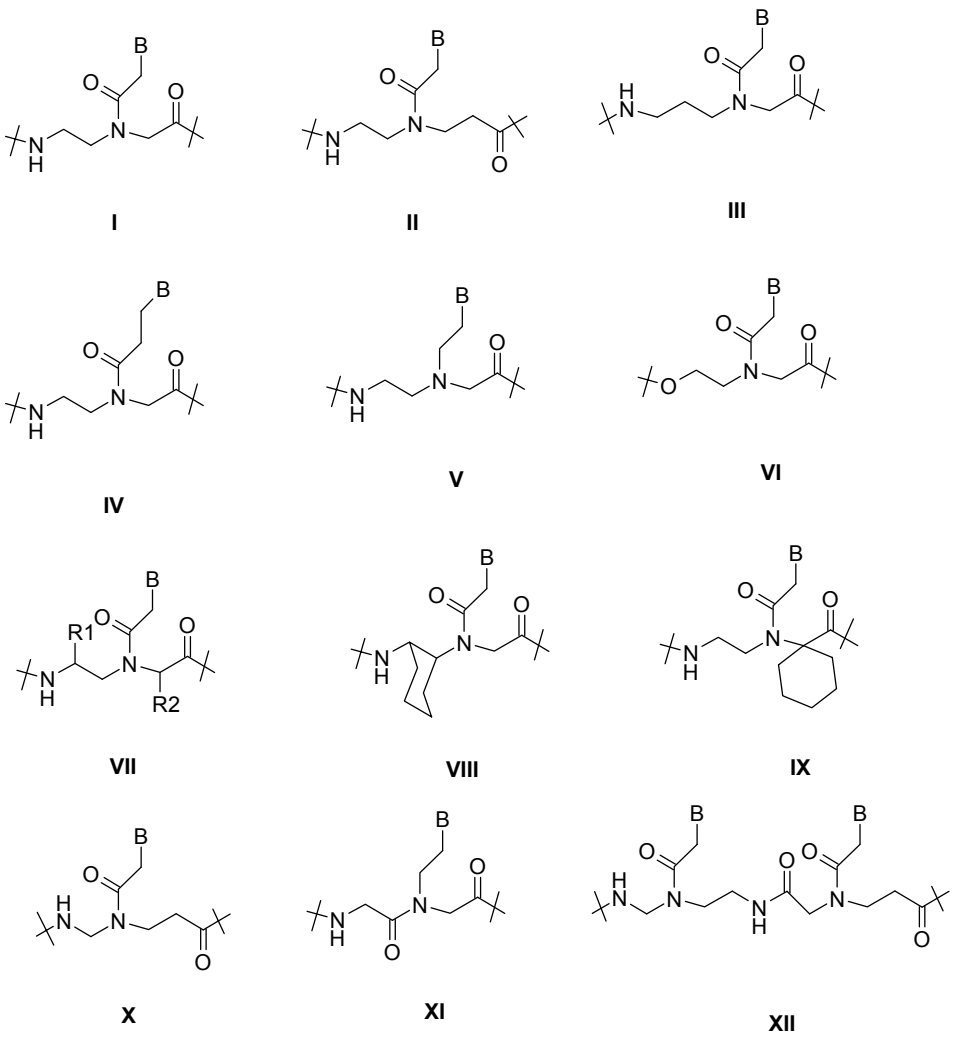

Figure 25. Chemical modifications of PNA

The earliest and the simplest of the modifications involved extension of the PNA structure I with a methylene group individually in each of the structural sub-units:

aminoethyl (Hyrup *et al.*, 1993), glycine (Hyrup *et al.*, 1994) and the acetyl linker of the PNA monomer. These resulted in PNAs with N-(2-aminoethyl)-β-alanine II and N-(3-aminopropyl)glycine III backbone and ethylene carbonyl linked nucleobase IV. However, these modifications resulted in a significant lowering of Tm of the derived PNA:DNA hybrids. The deleterious consequences of such subtle changes to PNA structure suggested the high structural organization to which the original PNA structure is inherently tuned for interaction with DNA. The replacement of the tertiary amide carbonyl by a methylene group leading to a flexible, cationic tertiary amine monomer V resulted in a large destabilization of the PNA:DNA hybrids (Hyrup *et al.*, 1996). The necessity of such a pseudo rigid amide group pointed to the importance of controlled flexibility in the backbone.

Further rigidification of the PNA has been attempted by the introduction of alkyl substituents, individually or simultaneously, in the aminoethyl or glycine (Dueholm *et al.* 1994; Haaima *et al.*, 1996 and Puschl *et al.*, 1998) segments or in both (VII). Suitable substitutions may also lead to generation of cyclic structures with 1,2-cyclohexylamino (VIII) and spirocyclohexyl (IX) rings in monomers (Lagriffoule *et al.*, 1997; Maison *et al.*, 1999). While PNAs that bear (*S*,*S*) cyclohexyl ring in the aminoethyl part hybridize with complementary DNA similar to the unmodified PNA, those derived from (*R*,*R*) lacked such a property. A number of modifications generated by substitution of glycine component by other α-amino acids, leading to chiral PNA VII (R_1=H) having hydrophobic, hydrophilic or charged α-substituents have been reported (Haaima *et al.*, 1996). Another type of modification involved interchange of CO and NH groups on the peptide linkages leading to X (Krotz *et al.*, 1995a,b, 1998) peptoid XI (Almarsson & Bruice, 1993) and heterodimeric XII analogues. In all these systems, except for heterodimer analogue, these exhibited a lower potency for duplex formation with complementary DNA/RNA suggesting that in addition to geometric factors, other subtle requirements such as hydration and dipole-dipole interactions, etc. influencing the microenvironment of the backbone, may be involved in affecting efficient PNA: DNA hybridization.

1.5. Present Work

The above resume outlines the utility of chemically modified DNA analogues for their application in antisence therapeutics. In view of this, the major work in the thesis is focused on understanding the criteria for the design of oligomers with altered backbones. The flexible and semi-rigid polyamide linkages are emphasized which are

best suited to adapt to solid phase synthetic methodologies, at the same time satisfying the necessary physical requirements for optimum binding to form a duplex or triplex. A novel approach is described which takes advantage of the established solid phase chemistry in the synthesis of oligonucleosides with various neutral backbones.

Chapter 2

Introduction of chirality in *aeg*PNA backbone may enable it to discriminate between the parallel and antiparallel modes of binding with complementary DNA strand. Furthermore, the introduction of positive charge in the backbone may also help to increase the water solubility of oligomers at neutral pH. This chapter first describes the synthesis of a novel modified *pyrrolidinyl*PNA that was envisaged to confer conformational constraint on the relatively flexible PNA backbone. The modification

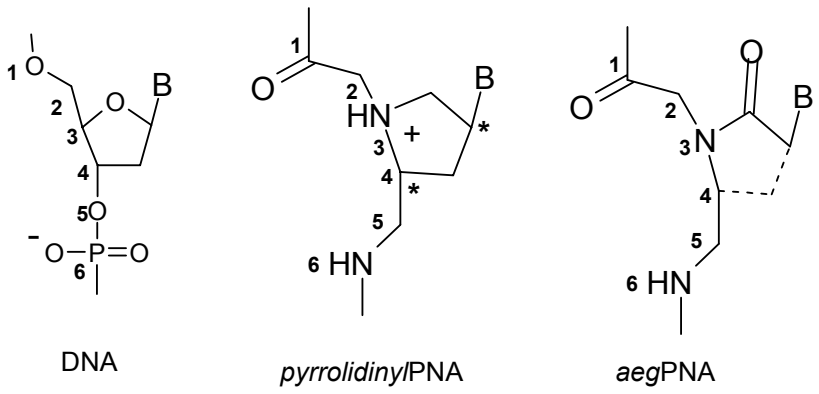

DNA *pyrrolidinyl*PNA *aeg*PNA

derived by linking ethylenediamine segment in PNA to the side chain introduces two chiral centers per unit in addition to a positive charge. Synthesis of all four diastreomers of pyrrolidine-based analogues starting from *trans*-4-Hydroxy-L-proline, a naturally occurring amino acid, was carried out followed by their incorporation in *aeg*PNA and their DNA binding studies.

Chapter 3

Non-ionic oligonucleotide analogues are totally resistant to nuclease hydrolysis, which makes them an attractive candidate for therapeutic use. *prolyl peptide nucleic acids* with stereoregular backbones based on partial substitution of *trans/cis*-4-Hydroxy-L/D-prolyl units destabilized PNA:DNA hybrids. To extend the backbone with more number of atoms while still retaining the stereogenic centers, peptide linkage was replaced with carbamate linkage. Early literature shows that carbamate linked nucleic acids as compared to the unmodified ones are more stable towards enzymes and being uncharged they are expected to permeate the cell membrane. In view of this,

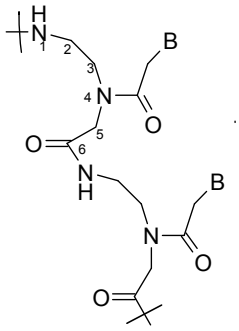

aegPNA

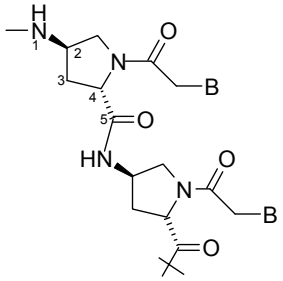

Prolyl nucleic acids

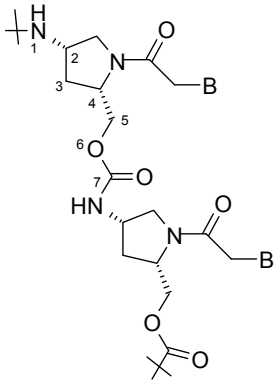

Carbamate linked pyrrolidinyl nucleic acids

(2*S*,4*S*)-pyrrolidine monomers having thymine and cytosine nucleobases were synthesized. Carbamate/peptide mixed sequences and homooligomers with carbamate linkage were prepared and DNA binding studies were carried out using UV-Tm experiments.

Chapter 4

The possibility of extending the backbone of *prolyl peptide nucleic acids* was further explored by incorporating an oxygen atom in the backbone-giving rise to an oxy-

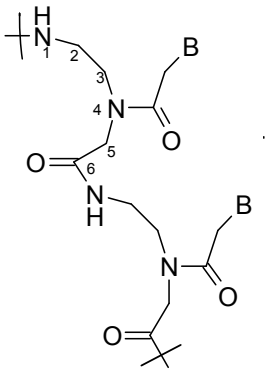

*aeg*PNA

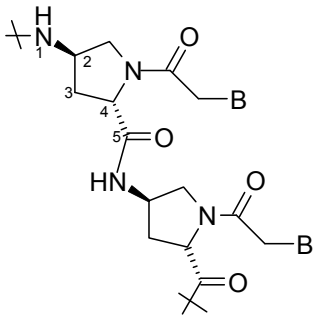

Prolyl Nucleic Acids

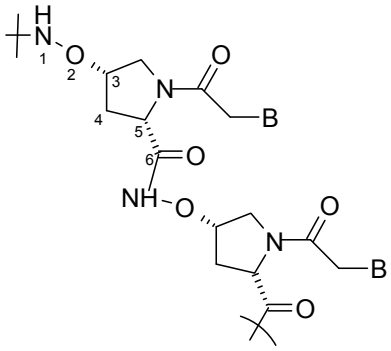

Oxyamide prolyl Nucleic Acids

amide backbone. Oxy-amide linked oligomers are also expected to have higher solubility in water as compared to *aeg*PNA. This chapter describes the synthesis of orthogonally protected monomer required for synthesis of *oxy-amide linked* oligomer and incorporation of the monomer in *aeg* PNA followed by its binding studies with DNA.

Chapter 5

The combination of PNA and DNA to form PNA/DNA chimera results in new structures, which in addition to excellent binding can also have biological role such as primer for DNA polymerases. In this chapter the synthesis of phosphoramidite of amide linked sugar/proline dimer is described. It also describes incorporation of dimer in DNA

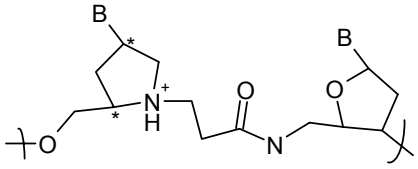

PNA-DNA chimera

sequences at selected positions and their binding studies. This chimera introduces a positive charge per modification in the oligomers, and having an amide linkage in the backbone it is expected to be stable towards enzyme degradation.

Chapter 2

Pyrrolidinyl Peptide Nucleic Acids

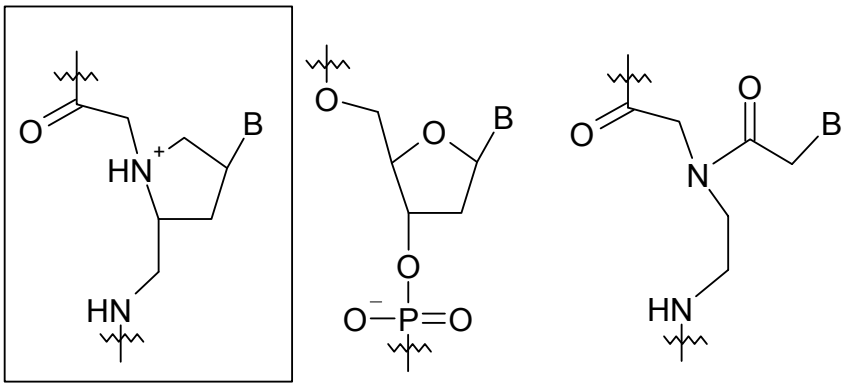

*pyrrolidinyl*PNA DNA *aeg*PNA

2.1 Introduction

The previous chapter has described various structurally modified oligonucleotide analogues, some of which have been found to show significant increase in RNA binding affinity and/or nuclease resistance than the corresponding oligonucleotides. While most of the resulting analogues still closely display many of the structural features characteristic of the deoxyribose-phosphate backbone of DNA (e.g. five membered ring structures and/or limited number of unmodified phosphodiester linkages as part of the overall modified backbone), the discovery of peptide nucleic acids (PNA) demonstrates that even more rigorous changes in DNA structure do not automatically abrogate binding to complementary RNA or DNA with high affinity and specificity. The PNA facts: (a) polyamide based nucleic acid analogues are intrinsically insensitive to degradation by nucleolytic enzymes, (b) polyamides are synthetically more accessible than many types of modified oligonucleotides and (c) their favorable RNA- and DNA-binding properties, have led to the design of other polyamide based structures.

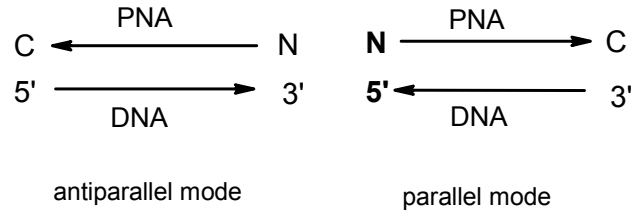

Figure 1. Parallel and antiparallel modes of PNA-DNA binding

PNAs obey Watson-Crick base pairing rules when binding to complementary DNA/RNA, but the orientation of the strands is ambiguous. In antiparallel mode, the PNA *N*-terminus is oriented towards the 3'- end and the *C*-terminus, towards the 5'- end of the complementary DNA/RNA oligonucleotide (Figure 1). In the parallel mode of binding, PNA *N*-terminus is oriented towards the 5'- end of DNA and the *C*-terminus against the 3'- end of the complementary oligonucleotide. PNAs can form duplexes with DNA in both parallel and antiparallel orientations (Wittung *et al.*, 1994), the antiparallel mode slightly preferred over the parallel one (Egholm *et al.*, 1993).

2.2 Bridged PNA Structures

Preliminary reports so far suggest that the sterically allowed constriction of the PNA backbone may improve its tendency to hybridize with DNA, but this strongly depends on the stereochemistry of the residue used. For example, the PNAs based

partially on (2*S*,4*R*)-4-aminoproline (Jordan *et al.*, 1997a,b) or all *S*,*S*-cyclohexyl-bridged (Lagriffoull, *et al.*, 1997) aminoethyl PNA backbones have a tendency to hybridize with DNA similar to that of unmodified PNA (Figure 2). In a sharp contrast,

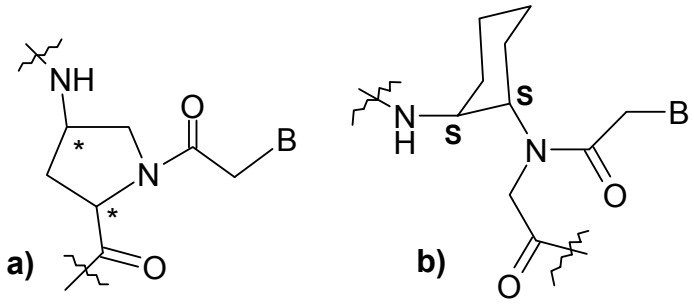

Figure 2. a) *aminoprolyl* PNA b) *S*,*S*-cyclohexyl-derived PNA

the hybridization of PNAs with fully *R*,*R*-cyclohexyl derived or partially (2*S*,4*S*)-4-aminoproline, (2*R*,4*S*)-4-aminoproline backbones significantly decrease the binding properties as compared to the unmodified achiral PNA. However, inclusion of even a single (2*S*,4*R*) 4-aminoproline into a PNA sequence, either at *N*-terminus or in the interior, leads to stabilization of the PNA-DNA hybrid, as studied by circular dichroism spectroscopy (Gangamani, *et al.*, 1999). Thermodynamic calculations of enthalpic and entropic contributions to the hybridization energy show that, in case of *S*,*S*-cyclohexyl-derived PNAs, upon hybridization a significant reduction of entropy loss is accompanied by a decrease in enthalpic gain, therefore it may be presumed that the constraining of backbone flexibility leads to a low energy conformation different from the conformation preferred for the formation of a stable PNA-DNA complex.

Introduction of chemical bridges in *aeg*PNA to get cyclic structures may help in constraining the backbone and thus achieving orientation selective binding by virtue of chirality in the backbone. Structural pre-organization of PNA may trigger a shift in the equilibrium towards the desired hybrid form because of the reduced entropy loss upon

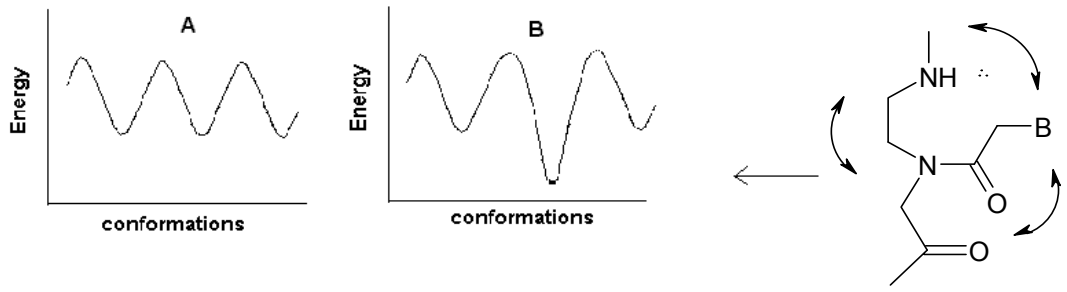

Figure 3. Energy level diagram of A) Molecules with flexible structure B) Molecules with conformational constraint derived form *aeg*PNA.

complex formation, provided the enthalpic contributions remain unaffected. This may be achieved if the conformational freedom in *aeg*PNA is curtailed by bridging the aminoethyl, or glycyl acetyl linker arms (Figure 3) leading to cyclic analogues that may have structures pre-organized for efficient recognition of complementary DNA *via* hydrogen bonding.

Such a structural pre-organization approach using additional conformational constraint has been extremely successful in case of various DNA analogues. The prominent examples (Figure 4) are conformationally *locked nucleic acids* (LNA)

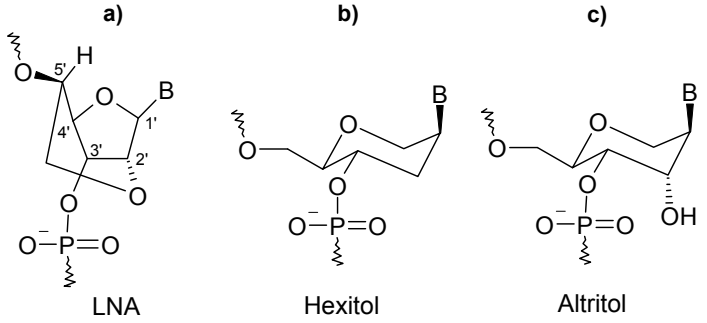

Figure 4. a) Locked 3'-*endo* conformation b) & c) frozen 3'-*endo* conformation.

(Wengel, 1999), conformationally frozen hexitol (Lescrinier *et al.*, 2000) and altritol nucleic acids (Allart *et al.*, 1999) that are pre-organized with 3'-*endo* sugar conformation that is prevalent in highly stable DNA-RNA duplexes. LNAs exhibit unprecedented binding affinity towards complementary DNA/RNA and are stable to 3'-exonuclease degradation, and show better water solubility. The furanose ring in LNA monomer, being a part of dioxabicyclo [2,2,1] heptane skeleton, is locked in an N-type conformation (C3'-*endo*). Such conformational or structural preorganization of the furanose ring is an important factor for the exceptional binding affinity of these modifications.

2.2.1. PNA with Five-Membered Nitrogen Heterocycles

Many researchers have exploited *trans*-4-hydroxy-L-proline, a naturally occurring amino acid (Robinson & Greenstein, 1952; Gangamani *et al.*, 1996) to synthesize a wide variety of chiral, constrained and structurally pre-organized PNAs (Figure 5). Depending on the construction strategy and the presence or absence of the tertiary amine group in the monomers, the modifications lead to either positively charged or neutral cyclic PNA analogues.

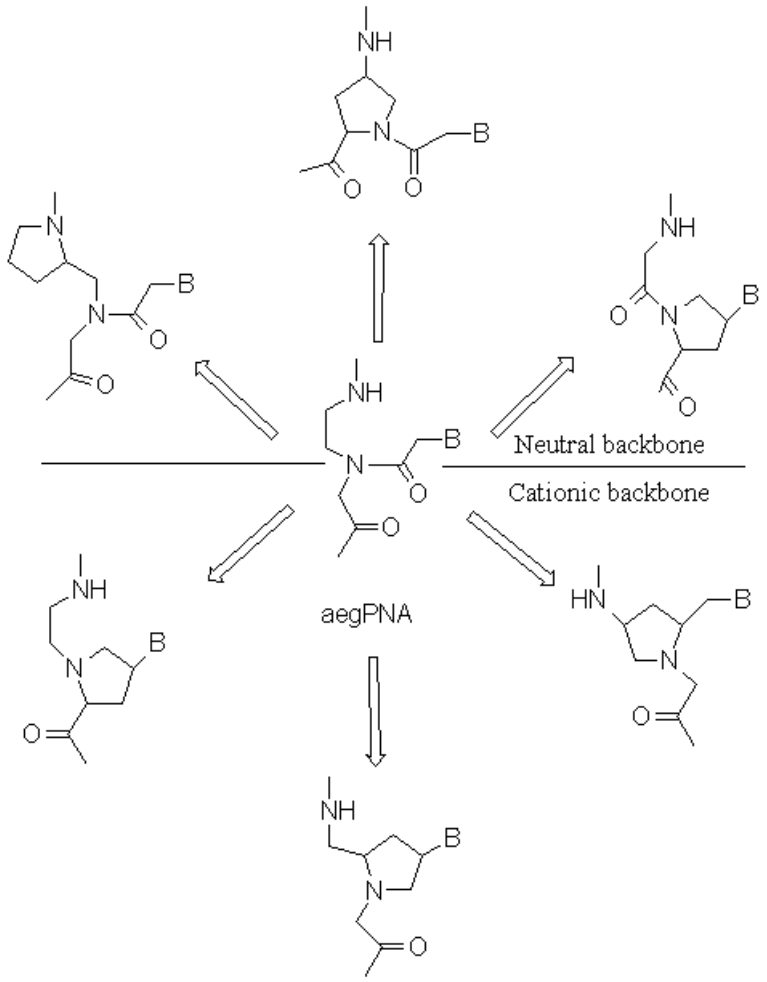

Figure 5. PNA analogues with five-membered pyrrolidine rings.

Aminoprolyl PNA

Introduction of a methylene bridge between the β-carbon atom of the aminoethyl segment and the α"-carbon atom of the glycine segment of the *aeg*PNA led to 4-*aminoprolyl*PNA, simultaneously introducing two chiral centers (Figure 6.) (Gangamani *et al.*, 1996). All the four-diastereomeric monomers were synthesized and were incorporated into PNA oligomers. However, the introduction of single chiral (2*R*,4*S*) and (2*S*,4*R*)-prolylPNA monomer in the PNA oligomers at *N*-terminus showed very interesting CD profiles and discrimination between parallel and antiparallel modes of binding towards the target DNA sequences. The homochiral *aminoprolyl*PNAs with thymine monomers did not bind to the target sequences (Gangamani *et al.*, 1999 a,b). Perhaps the bridged structure of the monomers imparted high rigidity to the oligomers, making them structurally incompatible with the geometry of DNA for effective nucleobase recognition. An alternating *aeg*PNA/(2*S*,4*R*)-*aminoprolyl*PNA backbone

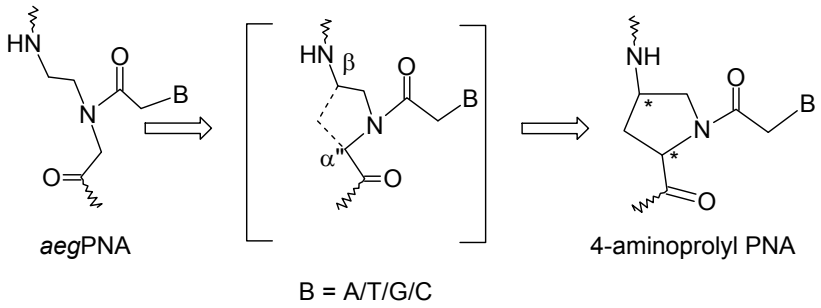

Figure 6. Prolyl PNA with α''-β methylene bridge.

was shown to bind to the target sequences with higher affinity as compared to the oligomers of pure *aeg*PNA (Jordan *et al.*, 1997). Another modification of *prolyl*PNA was derived from the replacement of the amide linkage by the phosphate diester linkage

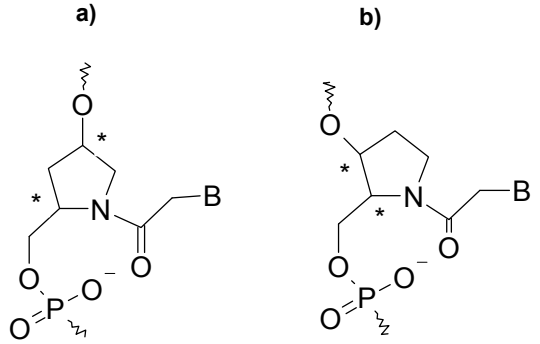

Figure 7. a) 4-hydroxy prolinol Nucleic acid b) 3-hydroxy prolinol Nucleic acid.

(Figure 7). However, no additional advantage was observed by the usage of either 4-hydroxy (Verheijen *et al.*, 2000) or 3-hydroxy prolinol (Ceulemans, G., *et al.* 1997) derivatives in the backbone.

Prolyl-Glycyl PNA

In another interesting modification, the (2*S*,4*R*)-4-hydroxyproline was exploited for the synthesis of a novel chiral PNA. A methylene bridge was inserted between the α''- carbon atom of glycine unit and the β'-carbon atom of the nucleobase linker of the *aeg*PNA (Lowe & Vilaivan, 1997 a,b) (Figure 8). The tertiary amide bond in the backbone between proline and glycine units replaced the aminoethylglycyl backbone and the nucleobase was directly attached to the proline ring by alkylation through the 4-hydroxy function. The backbone so obtained consisted of alternating proline-glycine units, which led to undesired rotameric populations. The oligomers with such a

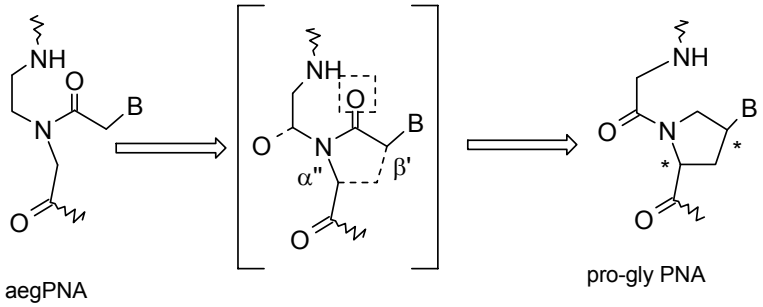

Figure 8. Prolyl-glycyl PNA with α"-β' methylene bridge.

backbone were found to be too rigid to bind to the target sequences. Nevertheless, unlike their 4-aminoproline counterparts, the sequences with alternating *aeg*PNA/proline-glycine PNA units showed reduced binding to the target sequences (Jordan *et al.*, 1997).

Aminoethylprolyl PNA (aepPNA)

The elimination of the tertiary amide group in the backbone of the above analogue leads to *aminoethyl prolyl* PNA (Figure 9, D'Costa *et al.*, 1999). In these

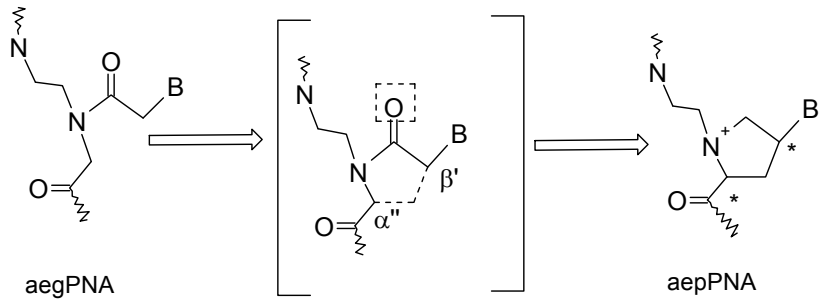

Figure 9. Aminoethylprolyl PNA with a α"-β' methylene bridge.

analogues, the flexibility of the aminoethyl segment of the *aeg*PNA was retained unlike prolyl-glycine PNA. The nucleobase attachment to the pyrrolidine ring was fixed by virtue of the chirality of C-4 carbon thus omitting the possibility of any rotameric populations arising from the side chain as in *aeg*PNA. The oligomers of both (2*S*,4*S*) and (2*R*,4*S*) strereochemistries with the nucleobase thymine showed very strong binding towards the target sequences - without compromising the sequence-specificity. The stereochemistry at C-2 center did not exert any significant effect on the binding ability of the homooligomer sequences. The *aep*PNA units carrying individual nucleobases; adenine, thymine, cytosine and guanine in a mixed purine/pyrimidine sequence exerted nucleobase-dependent binding efficacies and orientation selectivities

towards target oligomers (D'Costa *et al.*, 2001). Interestingly, a thymine *aep*PNA homo-oligomer having (2*R*,4*R*) stereochemistry, showed significant stabilization of the complexes with target *poly*RNA (Vilaivan *et al.*, 2000).

Pyrrolidinone PNA

A methylene bridge inserted between the α-carbon atom of the aminoethyl segment and the β'-carbon atom of the acetyl linker to the nucleobase of *aeg*PNA (Figure 10) (Puschl *et al.*, 2001) leads to pyrrolidinone PNAs. The bridge as in *aep*PNA

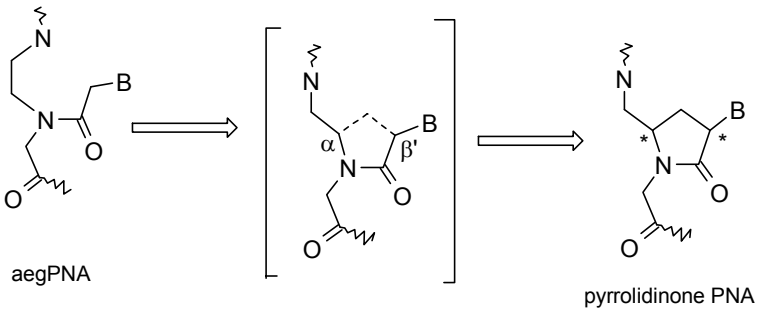

Figure 10. Pyrrolidinone PNA with α-β' methylene bridge.

prevented the rotation around the C-N bond of the acetyl segment connecting the nucleobase residue and pre-organized PNA in a rotameric conformation prevailing in complexes of PNA with nucleic acids as studied earlier. The synthesis of all the four diastereomers of adenin-9-yl-*pyrrrolidinone*PNA was accomplished from D/L-pyroglutamic acid in an eighteen-step synthesis. The hybridization properties of PNA decamers containing this analogue were investigated with complementary DNA, RNA and PNA strands. The (3*S*,5*R*) isomer was shown to have the highest affinity towards RNA when compared to DNA. The fully modified decamer bound to rU_{10} with a small decrease in the binding efficiency relative to *aeg*PNA.

Proline-β-Amino Acid PNA

The conformational strain in the alternating proline-glycine backbone was released or tuned by replacing the β-amino acid residue with different β-amino acid spacers having appropriate rigidity (Figure 11) (Vilaivan *et al.*, 2001). Novel *pyrrolidinyl*PNAs comprising alternate sequences of nucleobase-modified D-proline and either L/D-aminopyrrolidine-2-carboxylic acid, (1*R*,2*S*)-2-aminocyclopentane carboxylic acid or β-alanine were synthesized. Gel mobility-shift assay revealed that only the homothymine PNA oligomer bearing D-aminopyrrolidine-2-carboxylic acid spacer could

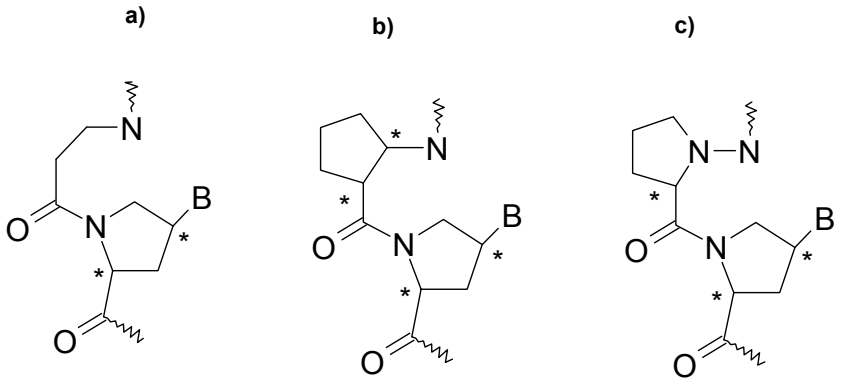

Figure 11. a) Prolyl-βalaninyl PNA b) prolyl-2-aminocyclopetane carboxylic acid PNA c) prolyl-D/L-aminopyrrolidine carboxylic acid PNA

bind to its DNA target. The cyclic nature and the stereochemistry of the β-amino acid in the backbone exhibited important contributions for effective binding to the target oligomers. The constraint in the backbone geometry thus seems to be an important feature for the structural mimics of DNA.

2.3 Rationale and Objective of The Present Work

To achieve structural preorganization, taking advantage of the above mentioned features; chirality, conformational constrain and positive charge were simultaneously introduced in the backbone by bridging the β'-carbon atom of the acetyl linker in *aeg*PNA to the α-carbon of the ethylene segment (Figure 12). The attractive feature of this modification is that it has the same number of atoms in the backbone as are there in phosphodiester and *aeg* backbone. To delineate the binding preferences of different stereochemically divergent pyrrolidine PNAs, synthesis of all possible diastereomers of

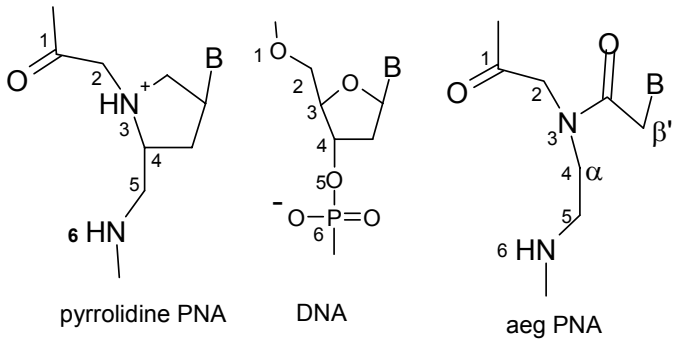

Figure 12.Comparison of backbones in pyrrolidine PNA, DNA and *aeg*PNA.

I (Figure 13) and the systematic complexation studies of these PNA analogues with DNA is required.

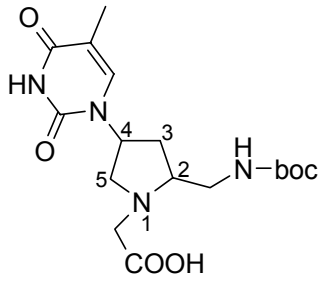

I

a) 2*S*,4*S* **b)** 2*S*,4*R*
c) 2*R*,4*R* **d)** 2*R*,4*S*

Figure 13. The monomer required for oligomer preparation

The objective of this chapter is to:

(i) Synthesize 2*R*/*S*-(*tert*-butoxycarbonyaminomethyl)-4*R*/*S*-(thymin-1-yl) pyrrolidin-1-yl acetic acid.

(ii) Incorporate these building blocks in *aeg*PNA.

(iii) Purification of heterooligomeric PNAs by HPLC.

(iv) The binding studies of the purified *pyrrolidinyl*PNA analogues with complementary DNA.

2.3.1 Synthesis of [(2*S*,4*S*)-2-(*tert*-butoxycarbonyaminomethy)-4-(thymin-1-yl) pyrrolidin-1-yl]acetic acid (9)

(2*S*,4*R*)-4-hydroxyproline (*trans*-4-hydroxy-L-proline) is a versatile synthon. It is the most abundant of the three naturally occurring diastereomers (Remuzon, P., 1996), is commercially available and is inexpensive. With its two chiral centers at C-2 and C-4, *trans*-4-hydroxy-L-proline is a material of choice to access multifunctionallized pyrrolidine rings. Thus, the synthesis of (2*S*,4*S*) monomer was achieved in eight steps starting from naturally occurring *trans*-4-hydroxy-L-proline (Scheme 2.1a). The N1-Cbz protected compound **1** was obtained in quantitative yield by reacting *trans*-4-hydroxy-L-proline with benzylchloroformate in water in the presence of $NaHCO_3$ as a base (Williams & Rapoport, 1994). Compound **1** was converted to its methylester **2** using MeOH/$SOCl_2$ and TEA (Rueger & Benn, 1982). The Cbz group is acid sensitive and thus the addition of TEA is essential to neutralize the HCl liberated during the reaction.

Scheme 2.1a.

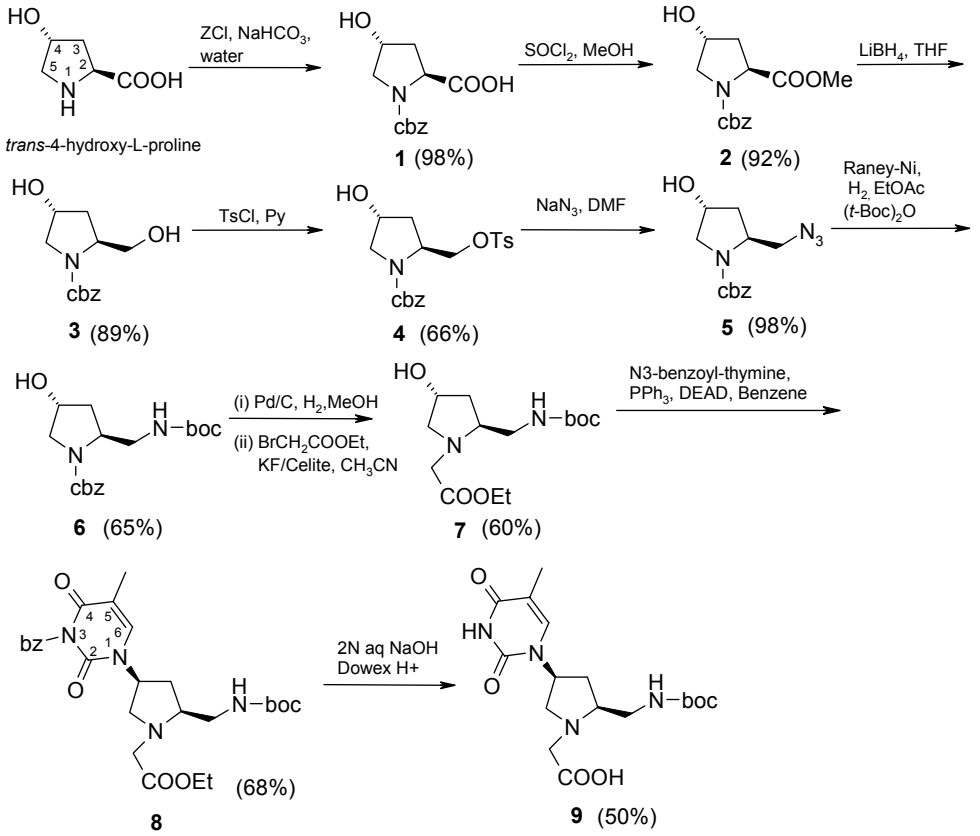

Using $LiBH_4$/THF the methyl ester functionality in **2** was selectively reduced, without affecting the Cbz group, to yield the diol **3**. However after prolonged reduction times, a partial removal of Cbz group was observed leading to a drop in the yield. Thus, the reaction mixture was continually monitored and a reaction time of 3-½ h was found to be optimal. A complete reduction of the ester was confirmed by the disappearance of a peak at δ 3.8-3.4 (methyl ester) and the appearance of a multiplet at δ 3.9-3.4 corresponding to the CH_2OH group in the ^1H NMR spectrum. The reduction of ester also resulted in loss of multiplicity of aromatic peaks. Taking advantage of the higher reactivity of primary hydroxyl (2*S*-hydroxymethyl) as compared to the secondary 4*R*-OH a selective tosylation of the primary –OH (2*S*-hydroxymethyl) in the diol **3** was achieved by reacting with 1 eq. of freshly crystallized *p*-TsCl in pyridine to obtain the monotosylate **4** (66%) which in its ^1H NMR spectrum showed signals in the aromatic region integrating for 10H (Ar<u>H</u>, tosyl). Some amount of ditosylate (5-10%) was also formed in this reaction and was removed by column chromatography. The C2-tosylate compound **4** was treated with NaN_3 in DMF at 70°C to give the azido compound **5**. A characteristic peak appearing at 2106 cm^{-1} in the IR spectrum of **5** and the

disappearance of aromatic signals corresponding to the tosylate group confirmed the formation of azide. Selective hydrogenation of -N_3 to –NH_2 in the presence of N1-Cbz, and its simultaneous protection with *t*-Boc was achieved by subjecting compound **5** to pressure hydrogenation for 1 ½ hr in the presence of Raney-Ni/ di-*tert*-butyldicarbonate to give compound **6** in 65% yield. Longer reaction times were found to result in partial removal of N1-Cbz and the formation of corresponding di-*t*-Boc compound was also observed. It is essential to remove (*t*-Boc)$_2$O completely from the reaction mixture by column chromatography before proceeding to free the N1; otherwise, the former would react with the N1 amine to give the di-*t*-Boc product. In the ^{1}H NMR of **6,** a peak for 9H appeared at δ 1.5 (*t*-Boc) accompanied by an upfield shift of C2 methylene protons. Upon catalytic hydrogenatioin of compound **6** with Pd-C/H_2 to remove Cbz at N1, followed by alkylation of the amine with ethylbromoacetate in presence of KF-Celite, compound **7** was obtained in 60% yield. ^{1}H NMR of **7** showed a quartet and a triplet at δ 4.2 (CH_2) and δ 1.27 (CH_3) respectively accompanied by the complete disapperance of peaks in the aromatic region.

One-step conversion of 4-OH in **7** to the corresponding thymin-1-yl derivative with an inversion of configuration can be achieved under Mitsunobu conditions. As the reactivities of N1 and N3 of thymine are comparable towards alkylation, this reaction results in both N1-alklated and N1,N3-dialkylated products. Hence, N3 of thymine was first protected as benzoyl (Rabinowitz & Gurin, 1953) - the synthesis of which is shown

Scheme 2.1b.

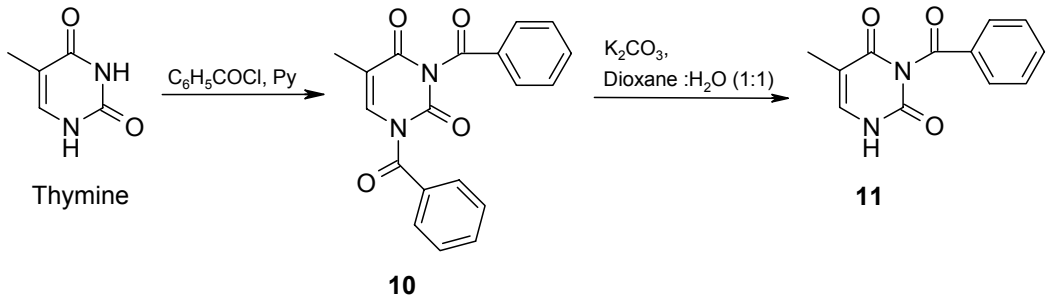

in Scheme 2.1b. N1,N3-di-benzoyl derivative **10** of thymine was prepared by treating thymine with more than 2 eq. of benzoylchloride in pyridine. The treatment of N1,N3-dibenzoyl derivative **10** with K_2CO_3 (0.25 N) in 1:1 mixture of dioxane:water for 5h under carefully controlled conditions resulted in selective hydrolysis of N3-benzolyl group in **10** to yield the N1-benzoyl compound **11**.

Mitsunobu reaction of compound **7** with DEAD, Ph_3P in benzene, and N3-benzoyl-thymine **11** as a nucleophile, gave compound **8** with an inversion of configuration at C4. ^{1}H NMR of **8** showed a peak at δ 8.15 (Thy-H6) and 2.01 (Thy-CH_3) characteristic of thymine. The retention of peaks in aromatic region (m 7.9-7.43) integrating for five protons, indicated that benzoyl group on thymine was intact during Mitsunobu reaction. During this work, it was observed that DIAD often delivered inferior yields in Mitsunobu reactions especially while using poor nucleophiles such as N3-benzoyl-thymine. Simultaneous removal of the ethyl ester protection and the N3-benzoyl group on thymine in compound **8** was achieved by saponification with 2N aq. NaOH/MeOH. The sodium salt so obtained was neutralized with a cation-exchange resin (Dowex-H^+) by careful acidification of the reaction mixture to pH 5 and subsequent washing of the aqueous layer with DCM to remove benzoic acid. The overall yield (50%) in this saponification-neutralization procedure was low, presumably due to partial absorption of the basic *tert*-amine to the acidic cation-exchanger. An efficient protocol to obtain free *tert*-amino acid **9** in quantitative yields is yet to be optimized.

2.3.2 Synthesis of [(2*R*,4*R*)-2-(*tert*-butoxycarbonyaminomethy)-4-(thymin-1-yl) pyrrolidin-1-yl]acetic acid (22)

The (2*R*,4*R*) monomer **22** was prepared in eleven steps starting from *trans*-4-hydroxy-L-proline as outlined in Scheme 2.2. First, the epimerization at C2 (Baker *et al.* 1981) position was achieved by refluxing *trans*-4-hydroxy-L-proline with Ac_2O/AcOH followed by continued refluxing with 4N HCl to obtain (2*R*,4*R*)-4-hydroxyproline hydrochloride **12**. The purity of the diastereomer was confirmed from ^{13}C NMR, which showed singlets at δ 55.5 (C4) and (C2). The synthesis of compounds **13** to **18** was accomplished using the same protocol as described previously for compounds **3**–**9** and the identity of all the compounds was established by standard spectroscopic data. The **i**nversion of the C4-OH group in *trans*-4-hydroxy-L-proline is described in literature via lactone (Papaioannou *et al.* 1990), formate intermediate (Seki and Matsumoto 1995) and by nucleophilic displacement of a 4*S*-*O*-tosylate with hot NaOH solution or with tetraethylammoniumacetate (Baker *et al.*, 1981). In the present work, an alternative method was explored for the inversion of C4-OH in which compound **18** was treated with benzoic acid under Mitsunobu conditions to afford the 4*S*-*O*-benzoate **19** in 79% yield. Upon benzoyl protection, an expected downfield shift of multiplet (C4-H) at δ 5.4-5.31 from 4.35-4.25 in **19** was observed. Earlier, a similar method has been used (Peterson & Robert, 1991) where inverting-esterification is done with acetic acid under

Mitsunobu conditions followed by solvolysis, to invert the configuration at C-3 in pyrrolidinone PNA (Puschl *et al.* 2001). Unexpectedly, ethanolysis of compound **19** could not be achieved using K_2CO_3 or Et_3N as base. Even after 30 hrs of heating at 50°C in Na/EtOH gave very poor yield (30%) of 4*S*-OH compound **20** with ~20% of the unreacted starting material recovered in column purification. Optical rotation for compound **20** was found to be exactly opposite to its enantiomer **7** (Scheme 2.1a). Subjecting the compound **20** to Mitsunobu conditions using N3-benzoyl thymine, (2*R*,4*R*) (*tert*-butoxycarbonyaminomethy)-4-(N3-Bz-thymin-1-yl) pyrrolidin-1-yl] ethyl acetate **21** was obtained in 70% yield, which on saponification provided (2*R*,4*R*) free acid monomer **22**. The optical rotation of the compound **21** closely matched with its enantiomer **8**.

Scheme 2.2.

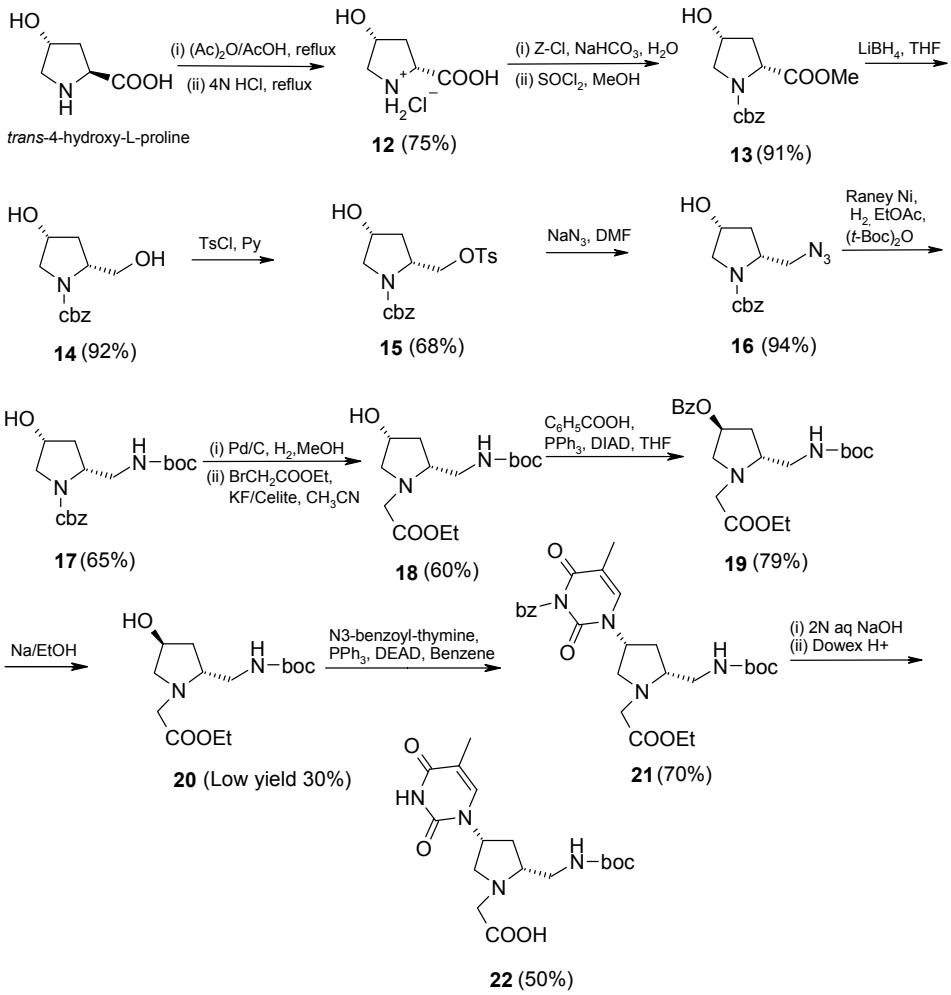

Though this method gave high stereospecificity, to improve the yields, an alternative route (Scheme 2.3) was sought for the preparation of (2*R*,4*R*) monomer **22**. The inversion at C-4 was attempted on intermediate **17**, with the idea that removal of 4-*O*-benzoate can be facilitated under hydrolytic conditions rather than solvolysis. The benzoate derivative **23** was prepared via Mitsunobu reaction, which after alkaline hydrolysis furnished 4*S*-OH compound **24** in excellent yields. After deprotection of Cbz

Scheme 2.3.

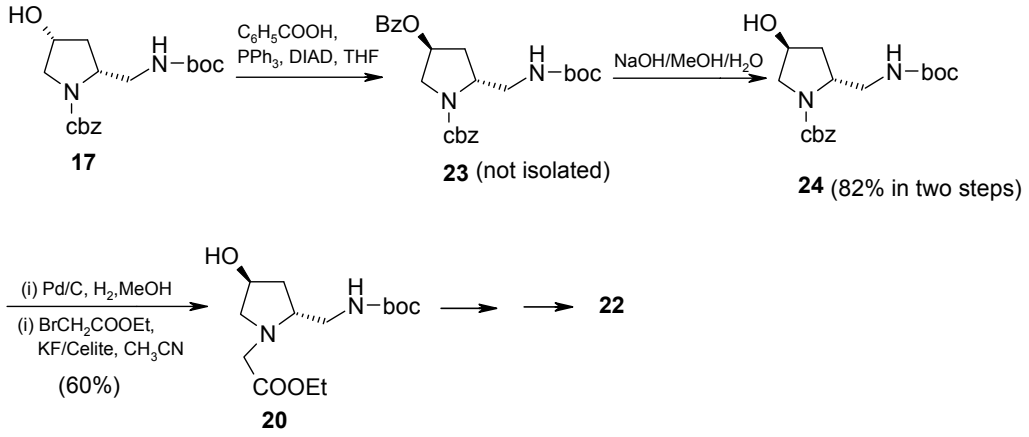

group in **24** using 10% Pd-C/H_2 followed by alkylation with ethylbromoacetate afforded compound **20** in 60% yield, which can be converted to the target **22**, after two steps as mentioned in scheme 2.2. Thus the overall yields for the synthesis of (2*R*,4*R*) monomer preparation were improved drastically, using scheme 2.3.

2.3.3 Synthesis of [(2*S*,4*R*)-2-(*tert*-butoxycarbonyaminomethy)-4-(thymin-1-yl) pyrrolidin-1-yl]acetic acid (42)

In a recently published method for the preparation of (2*R*,4*S*) adenine monomer (Puschl *et al.* 2000), intermediate **7** was used to couple the nucleobase at C-4 position via mesyl derivative. In another report (Ying *et al.*, 2001), the S_N2 substitution of the 4-*O*-Ts group in (2*S*,4*R*)-4-hydroxy-N1-(*t*-Boc-aminoethyl)proline by thymine was reported with 42% yield.

Introduction of thymine in the present work was planned using a similar intermediate **26** (Scheme 2.4a). Compound **7** was converted to its benzoyl derivative **25a**, which upon solvolysis using NaOMe/MeOH furnished (2*S*,4*S*) compound **26** in very good (90%) overall yield. It may be noted that the yields of the solvolysis of (2*R*,4*S*) benzoyl derivative were modest (30%) (Scheme 2.2). Surprisingly compound **26** gave only 5% of the desired (2*S*,4*R*) monomer **27** when reacted with N3-benzoyl thymine under Mitsunobu conditions.

Use of PPh_3-DEAD Mitsunobu inversion on compound **8** using methyl *p*-toluenesulfonate as nucleophile gave the 4*S*-O-tosylate **25b** (Scheme 2.4b). It has been demonstrated (Dormoy, 1982; Dormoy & Castro, 1986) that application of this methodology proceeds with an inversion of configuration. In the present case however,

Scheme 2.4a.

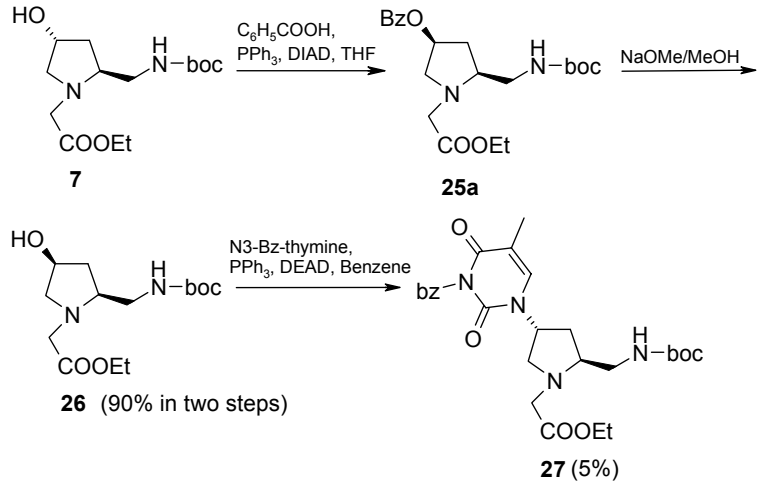

Scheme 2.4b.

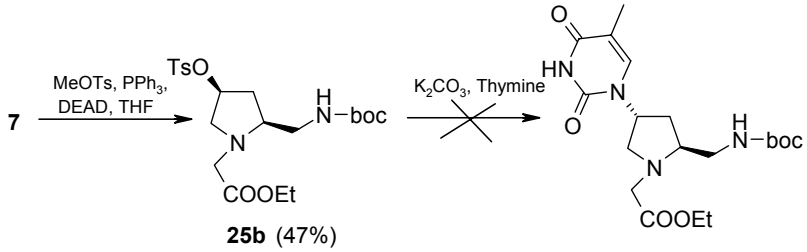

attempts to displace the tosylate with thymine as a nucleophile resulted in either recovery or, at higher temperatures, a decomposition of the starting material.

At this point, it was decided to introduce thymine with inversion of configuration at C-4 center from the beginning as reported by Hickman *et al.* (2000) for the synthesis of (2*R*,4*R*) thymine monomer (Scheme 2.5). A Mitsunobu reaction on compound **3** with benzoic acid as nucleophile yielded the benzoyl derivative **28** with an inversion of configuration at C-4. Though this material was difficult to separate from the diisopropylhydrazide dicarboxylate formed during the reaction, purification could be achieved after the solvolysis using Na/MeOH to give the 4*S*-OH compound **29** in 90% overall yield. A second Mitsunobu reaction with N3-benzoyl thymine as nucleophile yielded the (2*S*,4*R*)-thymine-1-yl derivative **30** in 70% yield. Treatment of **30** with two equivalents of $LiBH_4$ in THF reduced the methyl ester along with simultaneous deprotection of N3-benzoyl on thymine to give compound **31** in excellent yields.

Scheme 2.5.

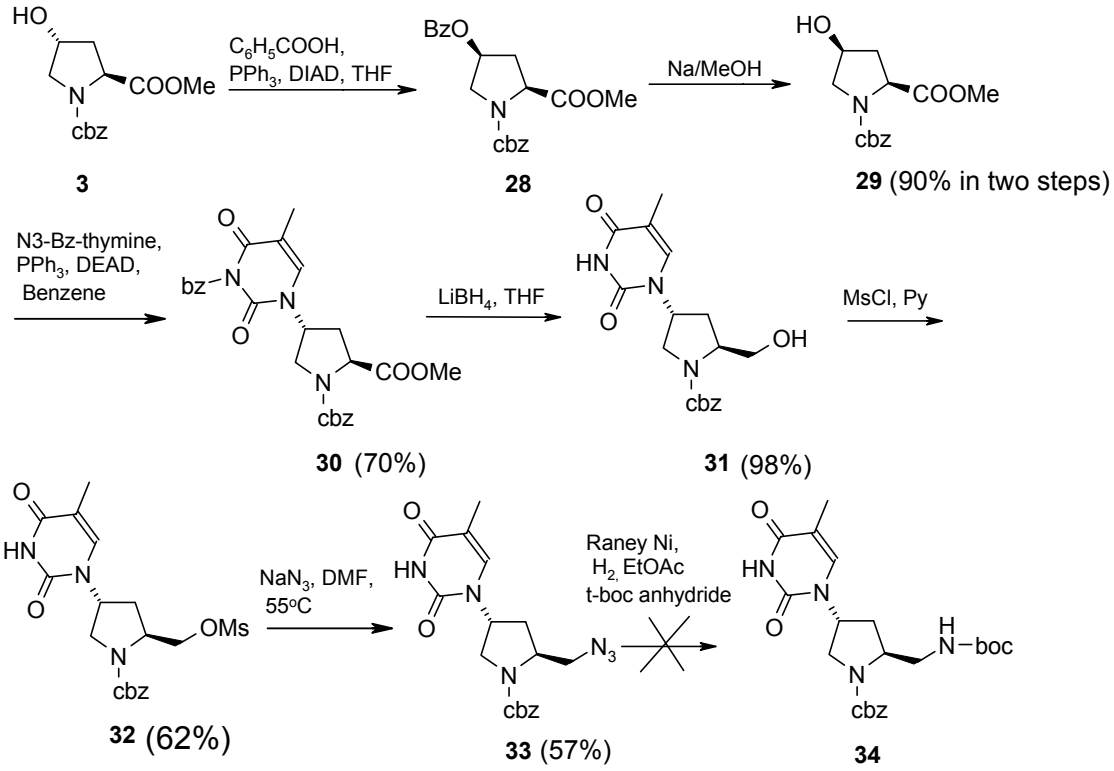

Successive mesylation and azidonation with NaN_3 gave **32** and **33** respectively. The reduction of the resulting azido group in compound **33** could not be accomplished with Raney Nickel even after prolonged hydrogenation. As the catalytic hydrogenation is a surface reaction, it is possible that in compound **33** with (2*S*,4*R*) configuration, there is a steric hindrance from the thymine group due to which N_3 group is not exposed to the catalyst. Now a third route was designed to achieve monomer with (2*S*,4*R*) configuration where the C-2 & C-4 centers were functionalized prior to N1-alkylation (Scheme 2.6). The ester group of (2*S*,4*S*) N1-benzyloxycarbonyl-hydroxyproline methyl ester was reduced with $LiBH_4$ to yield (2*S*,4*S)* diol **35**. This diol was further converted to monoazide **37** via montosylate **36** and the azide was subsequently hydrogenated using Raney Nickel followed by *t*-Boc protection in one-pot procedure giving **38**. When N1-benzyloxycarbonyl on **38** was deprotected using Pd-C/H_2, a complete migration of N3-benzoyl group was observed resulting in N1-benzoyl product **40**. In order to circumvent this difficulty, the reaction sequence was modified with benzoyl deprotection preceding the reduction (Scheme 2.7). Alkaline hydrolysis of **39** gave **34** in quantitative yield. Complete N1 deprotection of **34** was achieved by treatment with 50% Pd/C under H_2 pressure (80psi) to furnish free amine, which upon N1 deprotection followed by

alkylation gave the desired compound **41**. Basic hydrolysis of **41** and neutralization of the resulting solution with cation exchange resin (Dowex H+) afforded **42** in 68%yield.

Scheme 2.6.

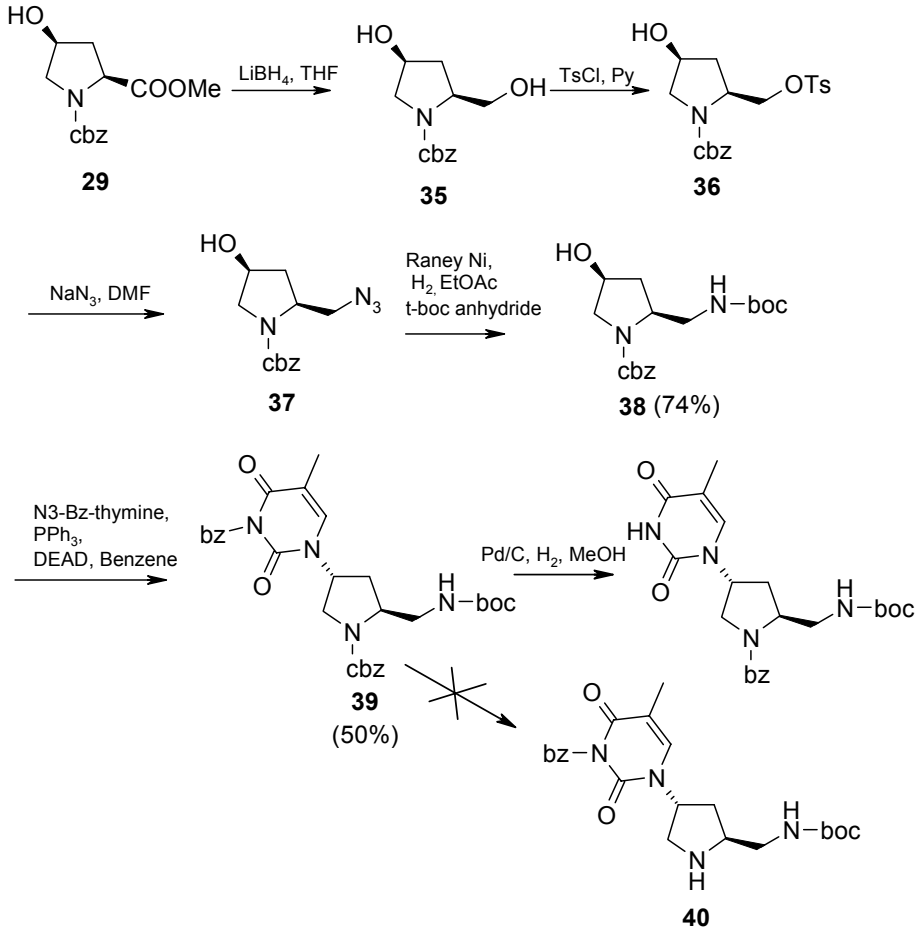

Scheme 2.7.

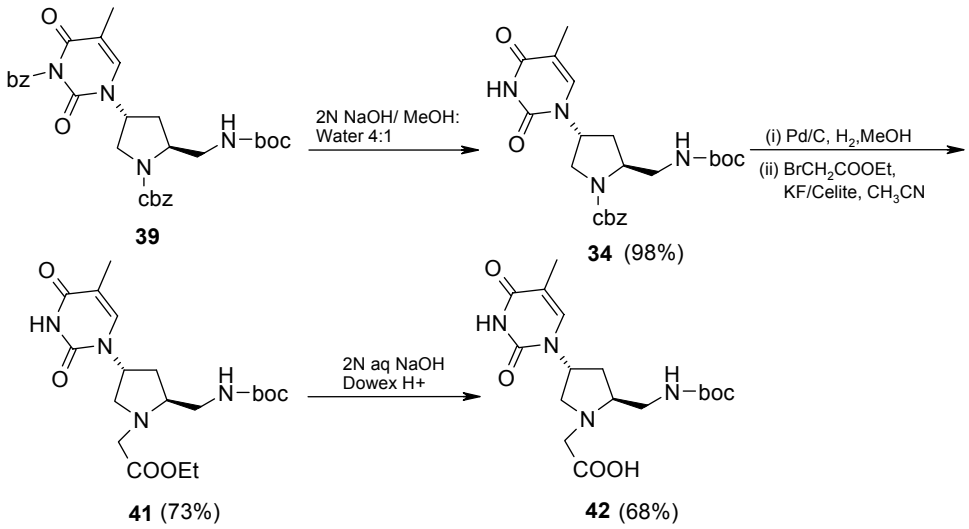

Optimised scheme for the synthesis of (2*S*,4*R*) monomer

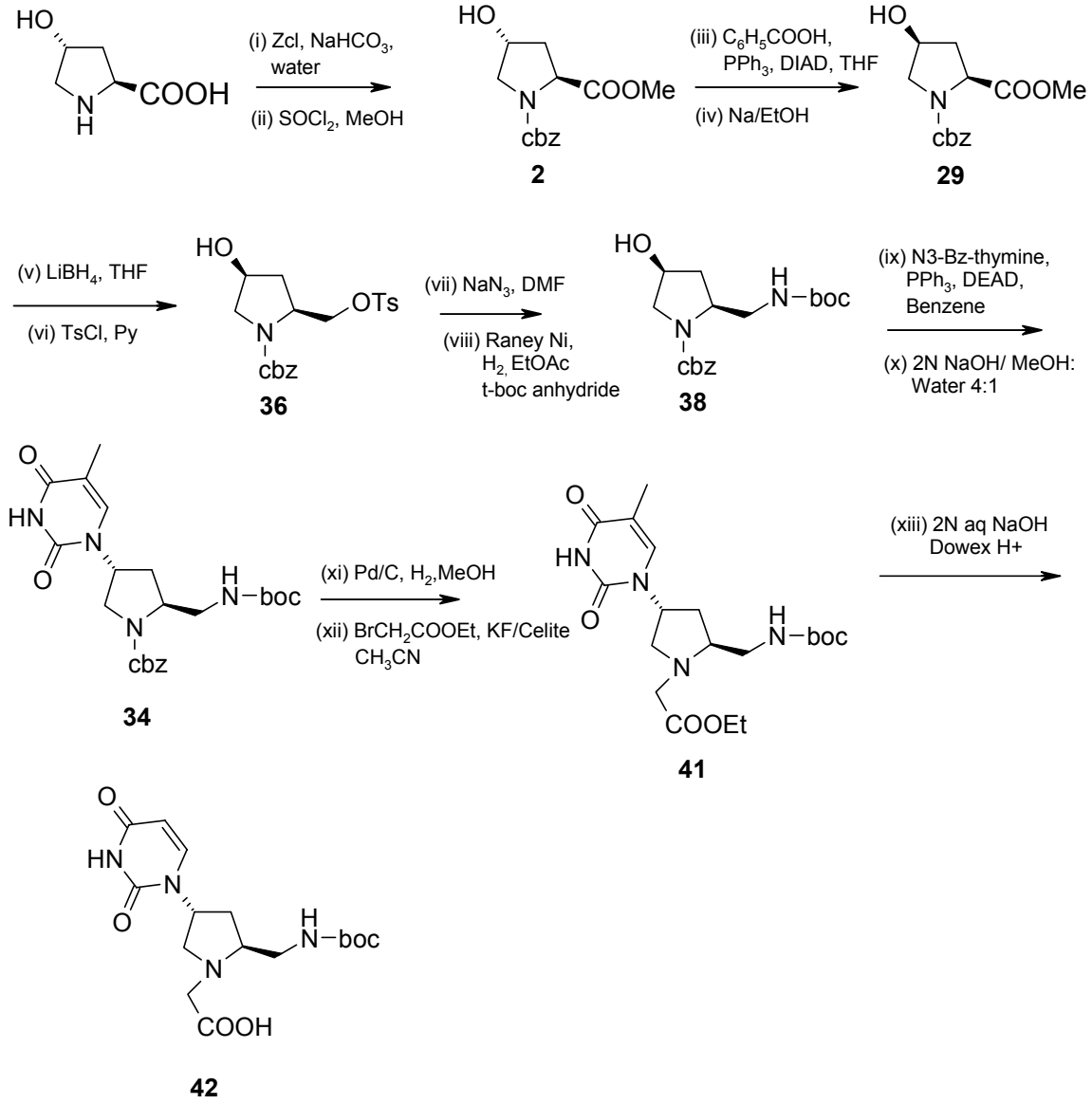

2.3.4 Synthesis of [(2*R*,4*S*)-2-(*tert*-butoxycarbonyaminomethy)-4-(thymin-1-yl) pyrrolidin-1-yl]acetic acid (46)

Likewise the synthesis of (2*R*,4*S*) monomer was achieved from intermediate **16** (Scheme 2.8) using the same sequence of steps as employed for (2*S*,4*R*) monomer. Coupling of the N3-benzoyl thymine with **16** proceeded well to yield 70% of **43** derivative. Cleavage of benzoyl group with aq. NaOH/MeOH provided **44**, which was subjected to catalytic hydrogenation followed by alkylation to furnish **45** in 70% yield. After saponification and neutralisation of **45**, compound **46** was obtained in 65% yield. The enantiomeric purity of **45** (α^{27}_D= 9.75 in $CHCl_3$) was assessed by comparing its optical rotation with that of its enantiomer **42** (α^{27}_D= -9.7 in $CHCl_3$).

Scheme 2.8.

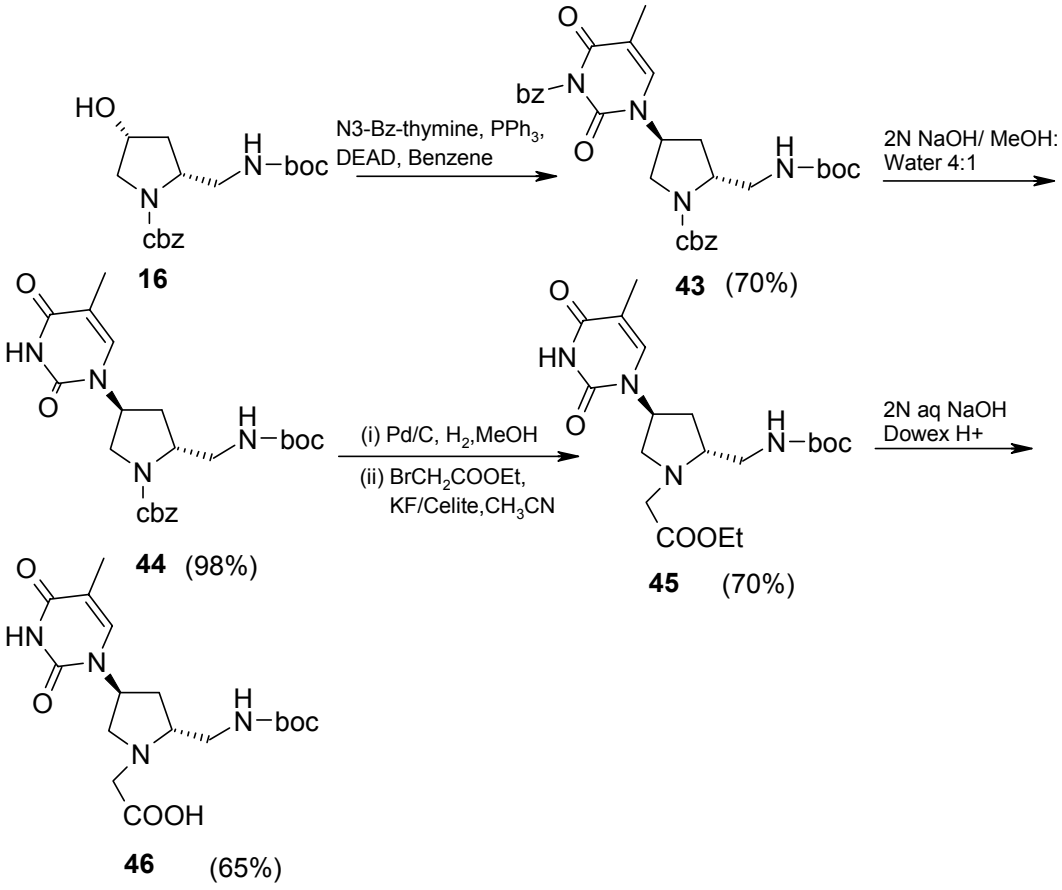

2.4 Synthesis of *aeg*PNA Monomers

The synthesis was carried out as reported in literature (Egholm *et al.*, 1992) starting from the readily available 1,2-diaminoethane (Scheme 2.9a). The mono-protected derivative **47** was prepared by treating a large excess 1,2-diaminoethane with *t*-butyloxycarbonylazide in dioxan:water under high dilution conditions. In this reaction a small amount of di-*t*-Boc derivative was also obtained, but being insoluble in water, was removed by filtration. The N1-*t*-Boc-1,2-diaminoethane was then subjected to *N*-alkylation using equimolar amount of ethylbromoacetate and KF-Celite in dry CH_3CN. The use of KF-Celite (Ando & Yamawaki, 1979) was found to be advantageous over conventional bases such as K_2CO_3, both in terms of product-yield and ease of work-up. The compound **48** was not stable for longer times. The aminoethylglycine **48** thus obtained was treated with chloroacetylchloride in aqueous

Scheme 2.9a

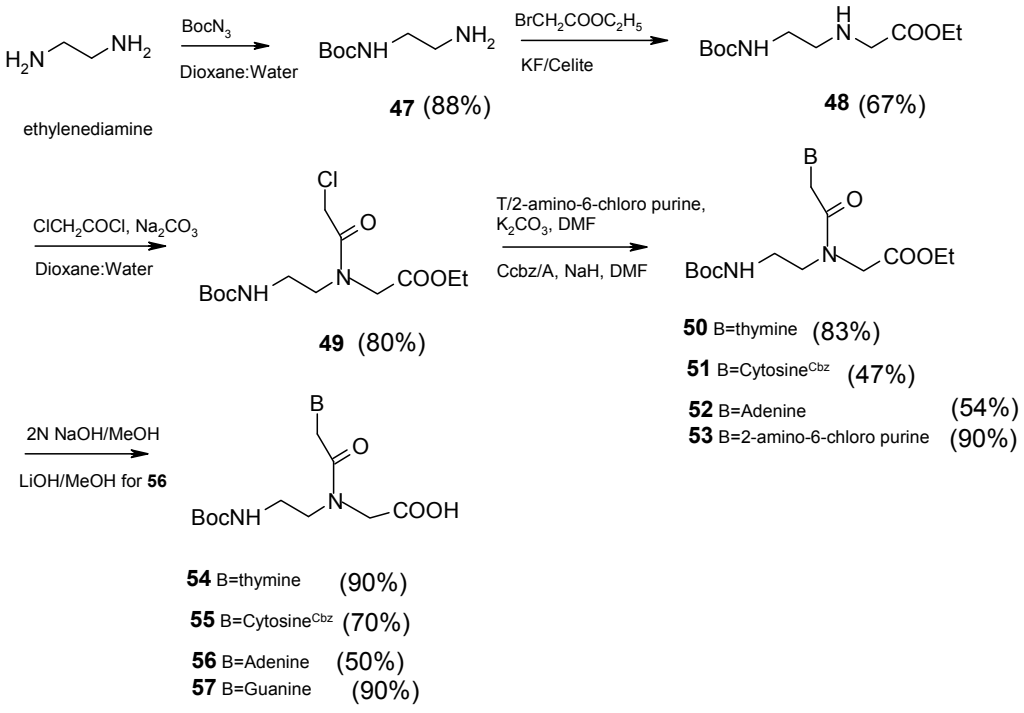

Scheme 2.9b

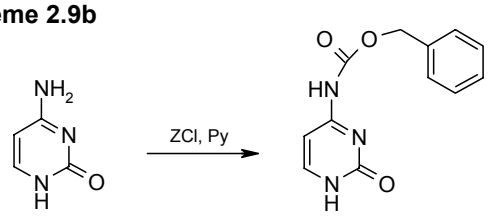

dioxane with Na_2CO_3 as a base to yield the chloro derivative **49** in good yield. Chloroacetyl chloride was distilled under vacuum from a mixture of chloroacetic acid and benzoyl chloride at 70°C. The ethyl *N*-(*t*-Boc-aminoethyl)-*N*-(chloroacetyl)-glycinate **49** was used as a common intermediate for the preparation of all the PNA monomers. Alkylation of the ethyl *N*-(*t*-Boc-aminoethyl)-*N*-(chloroacetyl)-glycinate with thymine and cytosine is regiospecific on the glycinate amine. Thymine was reacted with ethyl *N*-(*t*-Boc-aminoethyl)-*N*-(chloroacetyl)-glycinate using K_2CO_3 as a base to obtain the *N*-(*t*-Boc- aminoethylglycyl)-thymine ethyl ester **50** in high yield. In the case of cytosine, the exocyclic-amine N^4 was protected with Cbz (Scheme 2.9b) to obtain **58**, which was used for alkylation employing NaH as the base to provide the N1-substituted product **51**. Adenine was treated with NaH in DMF to give sodium adenylide, which was then reacted with ethyl *N*-(*t*-Boc-aminoethyl)-*N*-(chloroacetyl)-glycinate to obtain *N*-(*t*-Boc-aminoethylglycyl)-adenine ethyl ester **52** in moderate yield. The alkylation of 2-amino-6-chloropurine with ethyl *N*-(*t*-Boc-aminoethyl)-N-(chloroacetyl)-glycinate was facile with K_2CO_3 as the base and yielded the corresponding N-(*t*-Boc-aminoethylglycyl)-(2-amino-6-chloropurine)-ethyl ester **53** in excellent yield. All compounds exhibited ^1H and ^{13}C NMR spectra consistent with the reported data (Egholm *et al.*, 1992). The ethyl esters except Cytosine were hydrolyzed in the presence of NaOH to give the corresponding acids (**54** - **57**), which were used for solid phase synthesis. Cytosine monomer is more susceptible to Cbz deprotection in basic conditions, so in this case LiOH was used for hydrolysis. The need for the exocyclic amino group protection for adenine and guanine was eliminated, as they were found to be unreactive under the conditions used for peptide coupling.

2.5 pK_a Determination of N1 Nitrogen in *pyrrolidinyl*PNA Monomers

The pK_a of an ionizable group is the pH at which there are equal amounts of protonated and unprotonated species. At a pH below the pK_a value, a group will be mainly protonated, while at a pH above the pK_a, a group will be mainly non-protonated. The carboxyl and the amino groups have very different pK_a values which depend on the temperature, ionic strength, and the microenvironment of the ionizable group. pK_a of an ionizable group can be determined by monitoring the pH of a solution as equivalents of a base, such as NaOH, are added. In this titration curve, the pH values correspond to the inflection point

The pyrrolidinyl monomers carry a tertiary amino group that can be protonated, and a pH titration experiment was carried out with the two diastreomers (2*R*,4*R*) **22** and

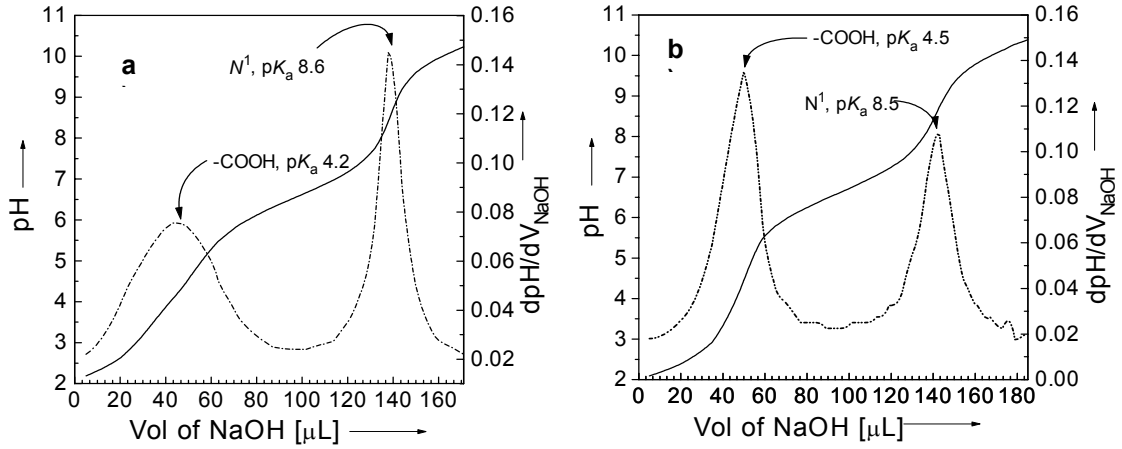

Figure 14. pH titration and its first derivative curve of *pyrrolidinyl*PNA monomers a) (2*R*,4*R*) and b) (2*R*,4*S*).

(2*R*,4*S*) **46** to determine the exact pK_a of the pyrrolidine ring nitrogen atom. A plot of pH versus volume of NaOH added gave two transitions; the first one corresponding to the carboxylic acid and the second corresponding to the pyrrolidine ring nitrogen (Figure 14). pK_a of the tertiary amine in both the diastereomers was found to be around 8.5 which indicates that at pH 7, ~97% of the monomer is likely to be in the protonated form.

2.6 Peptide Synthesis: General Principles

Peptide synthesis can be carried out either by solution phase or by solid phase methods. In the first method, an N^{α}-protected amino acid is coupled to the *C*-terminal amino acid with a carboxyl protection (Figure 15). The coupling reactions are performed by *in situ* activation of the carboxylic acid using condensing reagents such as dicyclohexylcarbodiimide (DCC). The activation step of the DCC mediated coupling reaction is the formation of the *O*-acylisourea of the carboxylic acid with DCC, which is favoured in a nonpolar solvent such as DCM. The *O*-acylisourea intermediate can react directly with the amines to form the desired amide or react further with carboxylic acid to yield the symmetric anhydride or with another agent such as 1-hydroxybenzotriazole (HOBt) to form a secondary acylating agent. In these reactions, HOBt acts both as a catalyst and as a racemization-suppressing agent. Alternatively, preactivated amino acid esters with pentafluorophenyl (pfp) or 3-Hydroxy-1,2,3-benzotriazin-4(3H)-one (DHBt) may be used. The solution phase method however, requires a tedious

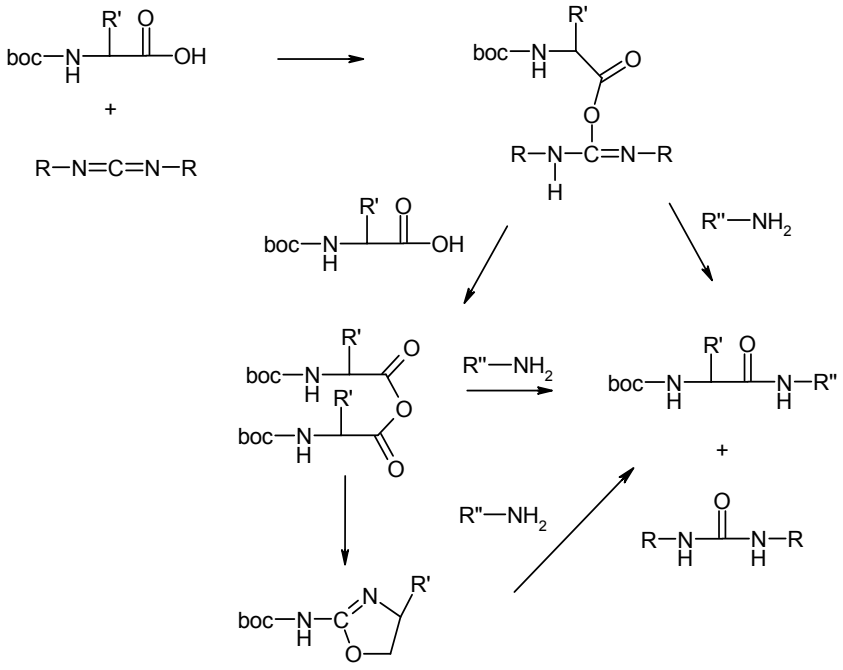

Figure 15. Peptide synthesis in solution

separation step after each coupling reaction, thus preventing usage of large excess of the carboxylic acid component.

In contrast, the solid phase method devised by Merrifield (1963), offers great advantages (Figure 16). In this method, the *C*-terminal amino acid is linked to an insoluble matrix such as polystyrene beads, which also acts as a permanent protection for the carboxylic acid. The next N^{α}-protected amino acid is coupled to the resin bound

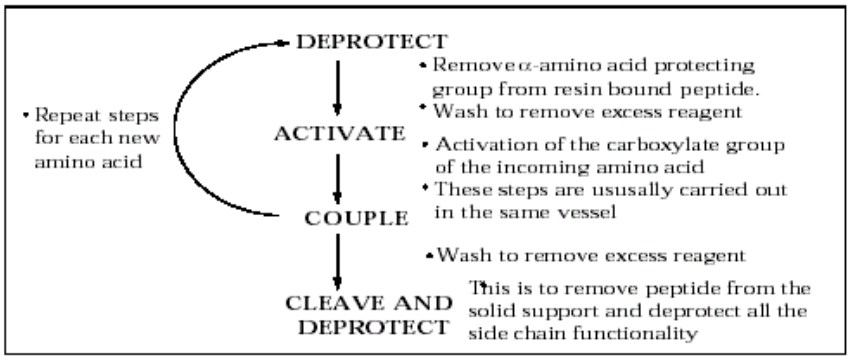

Figure 16. Steps in Solid phase peptide synthesis.

amino acid either by using an active pfp or DHBt ester or by *in situ* activation with carbodiimide reagent. The excess amino acid is washed out and the deprotection and coupling reactions are repeated until the desired peptide is achieved. The need to purify intermediates at every step is obviated. Finally, the resin bound peptide and the

side chain protecting groups are cleaved in one step. The advantages of the solid phase synthesis are: (i) all the reactions are performed in a single vessel minimizing the loss due to transfer, (ii) large excess of the carboxylic acid component can be used resulting in high coupling efficiency, (iii) excess reagents can be removed by simple filtration and washing steps and (iv) the method is amenable to automation and semimicro manipulation.

Currently, two chemistries are available for the routine synthesis of peptides by solid phase method. First method involves the use of *t*-butoxycarbonyl (*t*-Boc) group as N^{α}-protection that is removed by mildly acidic conditions such as 50% TFA in DCM. The reactive side chains of amino acids are protected with groups that are stable to *t*-Boc deprotecting conditions and removable under strongly acidic conditions using HF in dimethylsufide or TFMSA in TFA. Alternatively a base labile protecting group strategy is used involving fluorenylmethyloxycarbonyl (Fmoc) group for N^{α}-protection, which is stable to acidic conditions but can be cleaved efficiently with a secondary base such as piperidine. Coupled with mild acid sensitive side chain protection, this method offers a second strategy for the SPPS. In both chemistries the linker group that joins the peptide to the resin is chosen such that the side chain protecting group and the linker are cleaved in one step at the end of the peptide synthesis.

Common methods used to cleave benzyl ester bound peptides, as is the case with peptide synthesis on Merrifield-resin (chloromethylated-DVB-cross-linked polystyrene), are: (i) hydrogenolysis and (ii) ammonolysis. A peptide linked to styrene-DVB-copolymer via benzyl ester is cleaved by treatment with $Pd(OAc)_2$ in DMF or THF and subsequent hydrogenolysis at 40°C and 60 psi. $Pd(OAc)_2$ *in situ* gets reduced to Pd black, which catalyzes the hydrogenolysis of peptide benzyl ester bonds (Schlatter *et al.*,1977). In the second method peptide built on Merrifield resin is amidated with NH_3/MeOH. In this case some partial transesterification of the benzyl ester with MeOH gives rise to *C*-terminal methyl ester of the peptide, which subsequently is amidated with NH_3 to give the peptide-*C*-terminal amide (Wright *et al.*, 1980). In another method, a peptide-*C*-terminal amide is synthesised by treatment of the peptide bound to Wang-resin (*p*-benzyloxybenzyl alcohol resin) or Tentagel resin (where PEG spacer is attached to the polystyrene backbone via a benzyl ether linkage) with ammonium chrloride under ambient conditions to yield peptide-C-terminal amides (Barn *et al.*, 1996).

2.7 Synthesis of Oligomers

SPPS protocols can be easily applied to the synthesis of oligomeric PNAs from the *C*-terminus to the *N*-terminus. For this, the monomeric units must have their amino functions protected with either *t*-Boc or Fmoc and their carboxylic acid functions free. The Fmoc protection strategy has a drawback in PNA synthesis since a small amount of acyl migration from the tertiary amide to the free amine has been observed during Fmoc deprotection with piperidine (Erickson & Merrifield, 1976). Hence, in the present work, *t*-Boc-protection strategy was selected and the synthesis of all the four stereoisomers of N1-*t*-Boc protected *pyrrolidinyl*PNA T monomers has been described in the previous sections. Merrifield resin (Chlormethylstyrene-1%divinylbenzene resin) was selected as the solid polymeric matrix on which the oligomers were built and the monomers were coupled by *in situ* activation with HBTU/HOBt (Dueholm *et al.*, 1994).

In the systhesis of all the oligomers β-alanine ($H_2N(CH_2)_2COOH$) was selected as the *C*-terminal spacer-amino acid. Being achiral, it would not interfere with the chirality-induced structural properties of the pyrrolidinyl monomeric units that bear two chiral centers each. Its contribution to the hydrophobicity of PNA is also negligible since it has only a short alkyl chain. *N*-*t*-Boc-β-alanine was linked to the resin by a benzyl ester linkage *via* the formation of its cesium salt (Gisin, 1970). *t*-Boc deprotection was first carried out on the resin loaded with first residue. The amine content on the resin was then determined by the picrate assay (Merrifield & Stewart, 1966; Erickson & Merrifield, 1976) and found to be 0.68mmol/g. Loading was suitably lowered to approximately 0.3mmol/g by partial acetylation by using calculated amount of acetic anhydride and the $–NH_2$ on the resin was again estimated before starting synthesis.

The PNA oligomers were synthesized using repetitive cycles (Figure 17), each comprising the following steps:

(i) Deprotection of the N-*t*-Boc- group using 50% TFA in CH_2Cl_2.

(ii) Neutralization of the trifloroacetate salt of amine with diisopropylethyl amine (DIPEA) to liberate the free amine.

(iii) Coupling of the free amine with the free carboxylic acid group of the incoming monomer (3 to 4 equivalents). The coupling reaction was carried out in DMF & NMP mixture with HBTU as coupling reagent in the presence of DIPEA and HOBt as catalysts. The deprotection of the *N*-*t*-Boc protecting group and the coupling reaction were monitored by Kaiser's test (Kaiser *et al.*, 1970). The *t*-Boc-deprotection step leads to a positive Kaiser's test, wherein the resin beads as well as the solution are blue in color

(Rheumann's purple). On the other hand, upon completion of the coupling reaction, the Kaiser's test is negative, the resin beads remaining colorless.

(iv) Capping of the unreacted amino groups using Ac_2O/Pyridine in CH_2Cl_2, in case coupling does not go to completion.

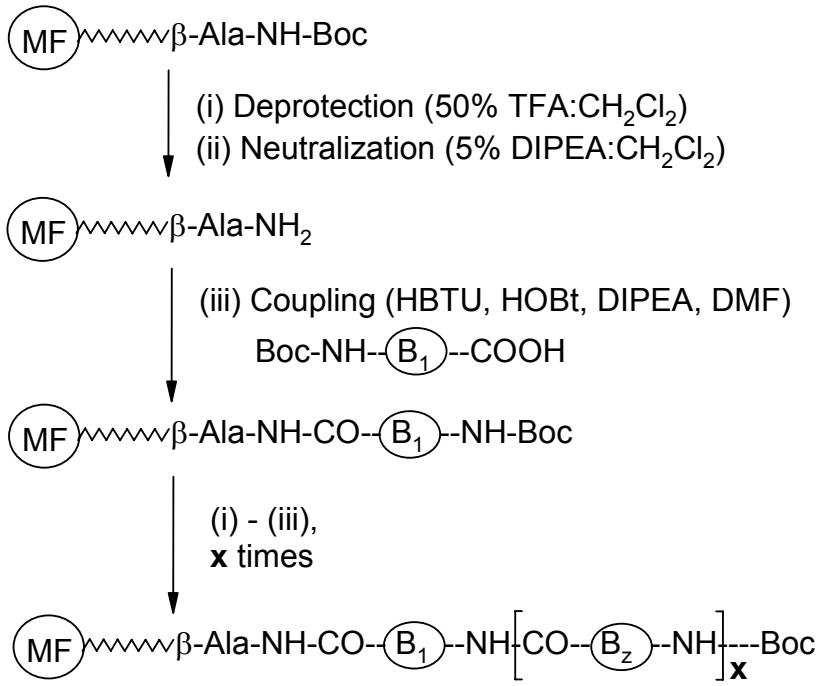

Figure 17. Scheme representing the solid phase peptide synthesis using the *t*-Boc-protection strategy

2.7.1 Synthesis of *aeg*PNA and *pyrrolidinyl*PNA Oligomers

Various oligomers synthesized in the present study are shown in Table1. The unmodified *aeg*PNA homooligomer T_8 (**S1**) was synthesized using *t*-Boc protected *aeg*PNA monomer (**51**). This was used as the control sequence for comparing the properties of *pyrrolidinyl*PNA oligomers. The synthesis of the oligomers (**S1**-**S9**) incorporating the chiral, conformationally constrained monomers at specific positions in the *aeg*PNA oligomers was achieved by following the *t*-Boc chemistry protocol of SPPS.

2.7.2 Cleavage of The PNA Oligomers from The Solid Support

The cleavage of peptides from the Merrifield resin by strong acids like trifluoromethane sulphonic acid (TFMSA)-in the presence of trifluoroacetic acid (TFA) yields peptides with free carboxylic acids at their *C*-termini (Fields & Fields, 1991). The

Table 1. PNA and DNA sequences used in the present chapter.

Entry	Sequences
S1	H-T T T T T T T T-NH-β-alanine-OH
S2	H-T T T T T T T t-NH-β-alanine-OH
S3	H-T T T T t T T t-NH-β-alanine-OH
S4	H-T T T T T T T **t**-NH-β-alanine-OH
S5	H-T T T T **t** T T **t**-NH-β-alanine-OH
S6	H-T T T T T T T **T**-NH-β-alanine-OH
S7	H-T T T T **T** T T **T**-NH-β-alanine-OH
S8	H-T T T T T T T ***T***-NH-β-alanine-OH
S9	H-T T T T ***T*** T T ***T***-NH-β-alanine-OH
S10	5'-G C A A A A A A A A C G-3'

T denotes *aeg*PNA monomer, t represents (2*S*,4*S*), **t** representing (2*R*,4*R*), **T** indicating (2*S*,4*R*) and ***T*** symbolizes (2*R*,4*S*) configurations for thymine monomer.

synthesized PNA oligomers were cleaved from the resin using this procedure to obtain sequences bearing *β*-alanine at their *C*-termini. After cleavage reaction, the peptide was precipitated from methanol with dry diethylether.

2.7.3 Purification of The PNA Oligomers

The cleaved oligomers were subjected to initial gel filtration to remove low molecular weight impurities. These were subsequently purified by reverse phase HPLC on a semi-preparative C4 RP column. The purity of the oligomers was ascertained by RP-18 HPLC and their structural integrity was confirmed by MALDI-TOF mass spectroscopic analysis. Some representative HPLC profiles and mass spectra are shown in Figures 18, 19 and 20.

2.7.4 Synthesis of Complementary Oligonucleotides

The oligodeoxynucleotide **S10** complementary to the PNA sequences was synthesized in the 3' $\rightarrow$ 5' direction on a *controlled pore glass* (CPG) solid support on a

Pharmacia Gene Assembler Plus DNA synthesizer using the standard β-cyanoethyl phosphoramidite chemistry (Gait 1984; Agrawal, 1993). The oligomer was cleaved from the support by treatment with aqueous ammonia and was de-salted by gel filtration. The purity of the DNA oligomer **S10** as ascertained by RP HPLC on a C18 column was more than 98% and was used without further purification in the biophysical studies.

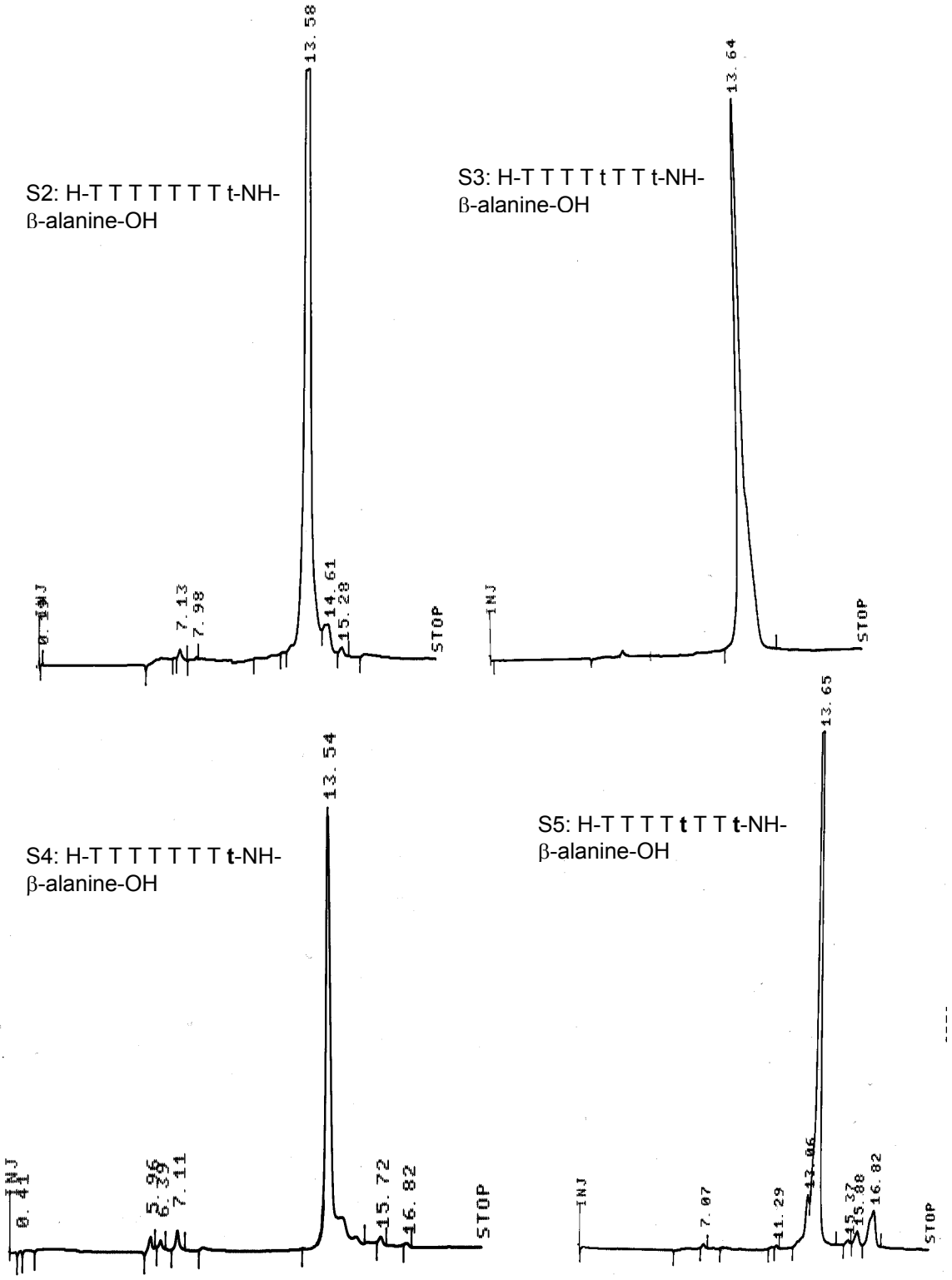

Figure 18. HPLC profiles of oligmers: S2, S3, S4, S5.
For HPLC conditions, see experimental section.

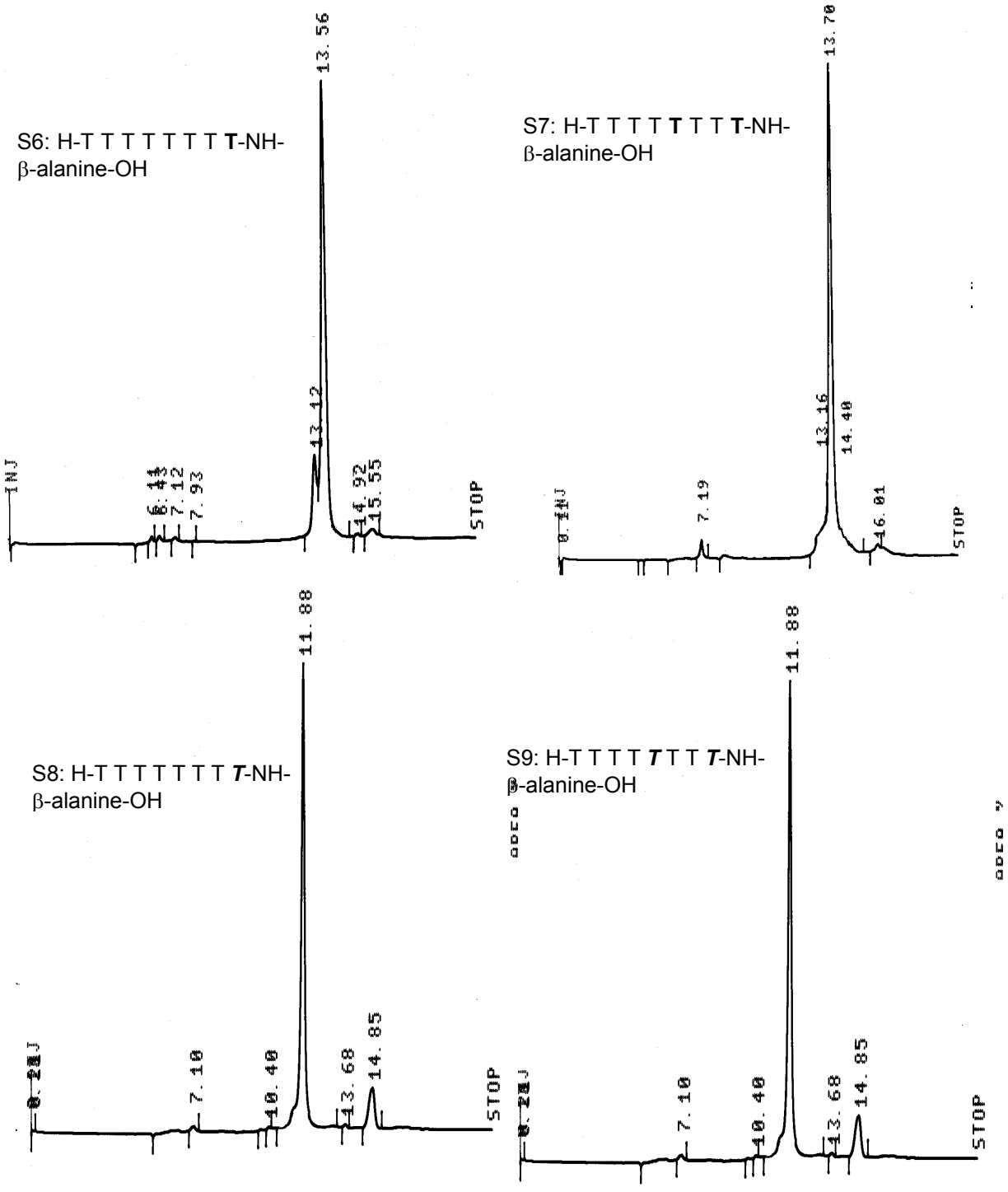

Figure 19. HPLC profiles of oligomers: S6, S7, S8, S9. For HPLC conditions, see experimental section.

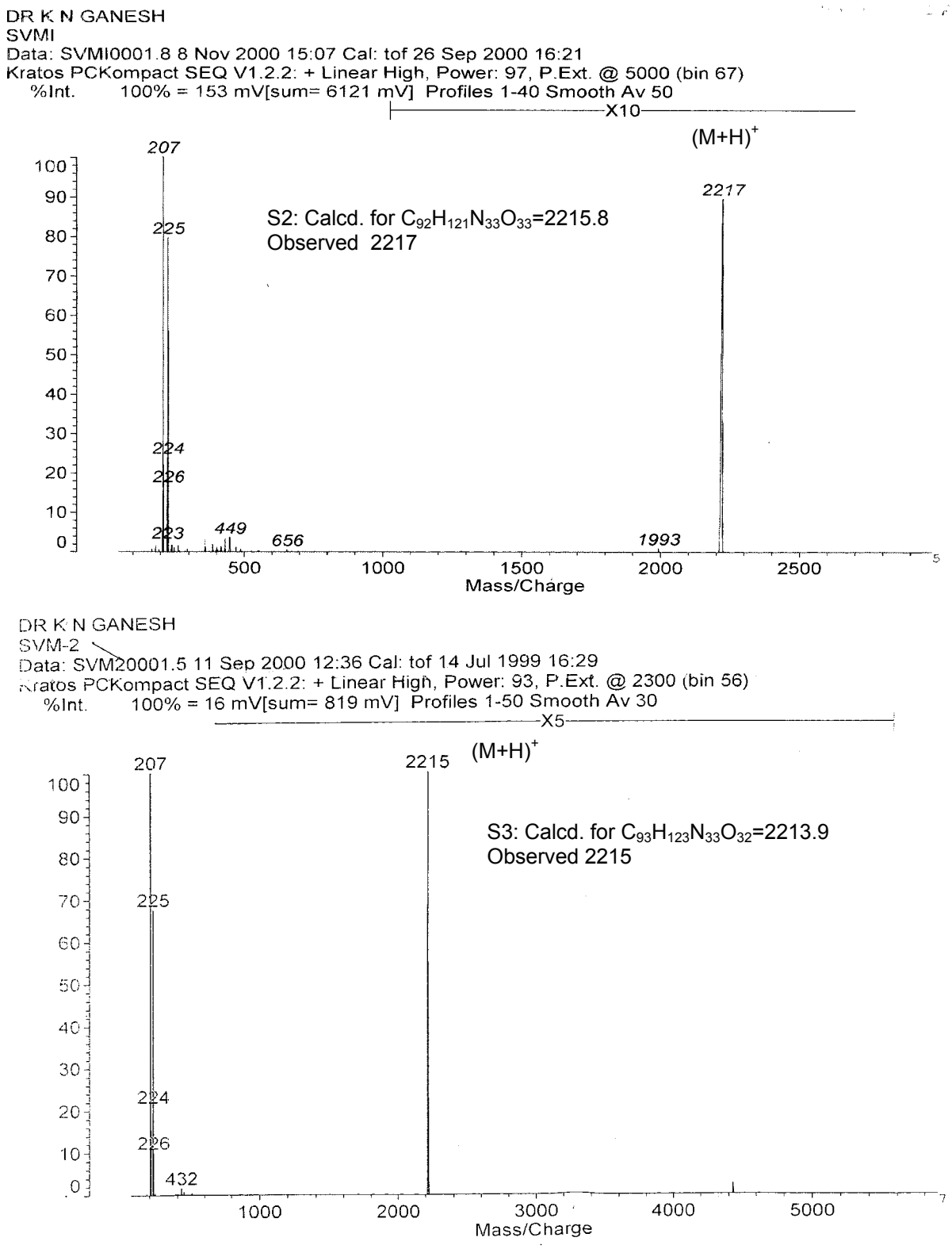

Figure 20. MALDI-TOF mass spectra of PNA sequences S2 and S3.

2.8 Biophysical Studies of *pyrrolidinyl*PNA:DNA Complexes

To investigate the binding ability of *pyrrolidinyl*PNA towards complementary DNA, first the stoichiometry of the *pyrrolidinyl*PNA:DNA was determined using Job's method (Job, 1928). The UV-melting studies were carried out with all the synthesized oligomers and the Tm data was compared with the reference *aeg*PNA T_8. The CD spectra of the single strands and the complexes were recorded.

2.8.1. Binding Stoichiometry: CD and UV Mixing curves

*aeg*PNA is inherently achiral. However, upon complexation with complementary DNA/RNA, it is rendered chiral andcontributes to the total CD of the complex. Chirality can also be induced into the achiral PNA strand by linking chiral moieties like amino acids (Egholm *et al.*, 1993) peptides (Koch *et al.*, 1995) or oligonucleotides (Petersen *et al.*, 1995, 1996; Uhlmann *et al.*, 1998) to the PNA termini. PNA has also been rendered chiral by the incorporation of chiral amino acids in its backbone (Haaima *et al.*, 1996; Lowe *et al.*, 1997).

Ultraviolet absorption and circular dichroism (CD) measurements are extremely useful in the study of duplexes and triplexes. These techniques can be used to monitor mixtures of complementary oligomer sequences and characterize the resulting structures. The stoichiometry of the paired strands may be obtained from the mixing curves, in which the optical property at a given wavelength is plotted as a function of the mole fraction of each strand (Job, 1928; Cantor & Schimmel, 1980), and from isodichroic and isoabsorptive points. The combination of absorption and CD spectra provides unambiguous determination of the complex formation and strand stoichiometry than is provided by absorption spectra alone.

Various stoichiometric mixtures of **S10** and **S6** were made with relative molar ratios of (**S10**:**S6**) strands of 9:1, 8:2, 7:3, 6:4, 5:5, 4:6, 3:7, 2:8, 1:9, all at the same strand concentration 2μM in sodium phosphate buffer (10mM, pH 7.3). The samples with the individual strands were annealed and the CD spectra were recorded.

Figure 21 shows the CD spectra of the various mixtures. The curve (i) is the spectrum of the single strand DNA **S10** that is a polypurine sequence with CG clamps on both ends. It displays one strong +ve band at 217nm and one broad +ve band in the region of 260-285nm. It also shows two negative bands at 205 and 249nm with two crossover points at 239 and 261nm. The curve (xi) is the spectrum of *pyrrolidinyl*PNA **S6** containing only pyrimidines. The intensity of the spectrum is negligible in the whole range of 200-320. The curves (ii) to (x) show the spectra of the mixtures of **S10**:**S6** with

the molar concentrations ranging from 9:1 to 1:9. As the concentration of **S6** strand increases in the mixture, the –ve band at 249 for curve (i) shifts slightly to lower wavelength accompanied by a progressive decrease in the intensities of the three bands at 205, 217 and 249nm.

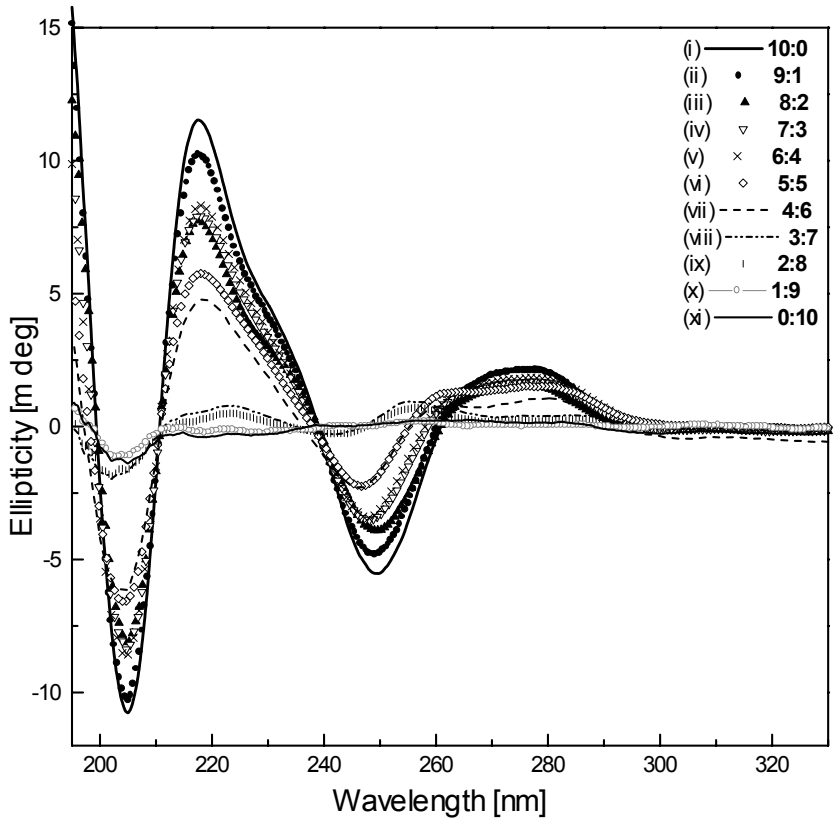

Figure 21. CD mixing spectra of **S10**: **S6** in molar ratios 10:0, 9:1, 8:2, 7:3, 6:4, 5:5, 4:6, 3:7, 2:8, 1:9, 0:10 in 10mM sodium phosphate buffer (pH= 7.3).

If the mixtures of the two strands had consisted simply of the two noninteracting strands, the spectra of the mixtures (ii to x), would be a simple addition spectra with all bands lying within the envelope formed by the curve (i) and curve (xi). Further, the spectra of the mixtures would have been spaced proportionally between the spectra of the individual strands without any isodichroic points (wavelength of the equal CD magnitude). Moreover, any isodichroic points () for the individual strands would have

The enlarged CD spectra in Figure 22 shows that CD spectra fall into two families as seen from two sets of isodichroic points. Spectra of the samples containing 60% or more of **S6** (vii-x) had isodichroic points at 260 and 236 nm. CD spectra of the samples with 50% or less of **S6** (ii-vi) had isodichroic points at 265 and 240.5 nm. The calculated (arithmetic addition of CD of single stands in that molar ratio), observed and

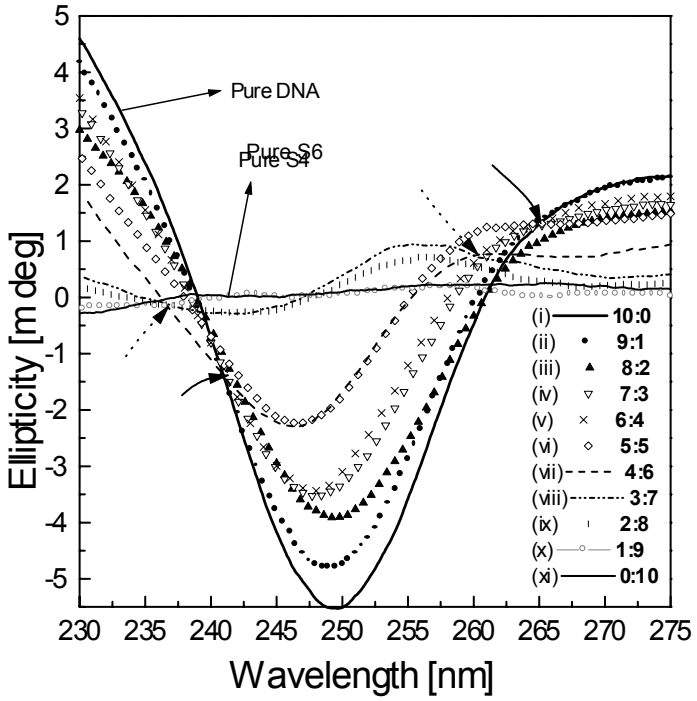

Figure 22. Expanded CD spectra of molar mixtures of **S10:S6**; Solid arrows indicate isodichroic points for mixtures 10:0-5:5, where as the dotted arrows indicate isodichroic points for the mixtures 4:6-1: 9.

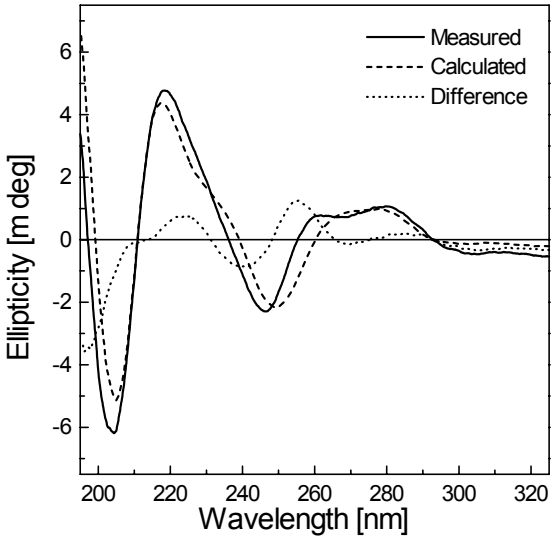

Figure 23. Measured, calculated (60% of θ for S6 + 40% of θ for S10) and the difference CD spectra of 6:4 mixture of S6 and S10 at 15 °C in 10mM phosphate buffer (pH 7.3).

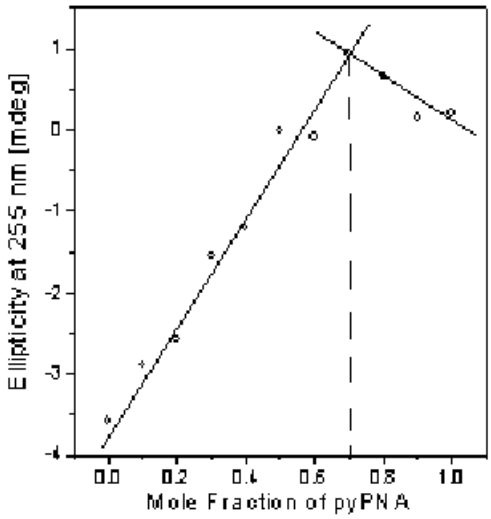

Figure 24. CD mixing curve for S6 and S10 mixtures in the molar proportions of 0:100, 10:90, 20:80, 30:70, 40:60, 50:50, 60:40, 70:30, 80:20, 90:10. Solution conditions (10mM sodium phosphate buffer, pH 7.3).

the difference CD spectra for all the mixtures were compared for all molar ratios and 60:40 molar solution of **S6**:**S10**. deviated most from the average of the spectra of the

individual strands at wavelengths 230 and 255nm (Figure 23). CD values at such wavelengths were therefore especially useful for plotting mixing curves. The mixing curve in Figure 24 was plotted using the CD data at 255 nm from the spectra in Figure 22. The mixing curve indicated the formation of the triplex structure at 66:33 stoichiometry of *pyrrolidinyl*PNA:DNA.

Absorbance spectra were also recorded for the mixtures of **S10**:**S6** in different proportions used for mixing curve to check their $\lambda_{max.}$ Figure 25 shows the change in λ_{max} observed for the mixtures of S6 and S10 in different proportions. There was a drastic shift in the λ_{max} value when the concentration of the **S6** in the mixture increased form 60 to 70%, which further supports the presence of *pyrrolidinyl*PNA_2:DNA complex in the mixture.

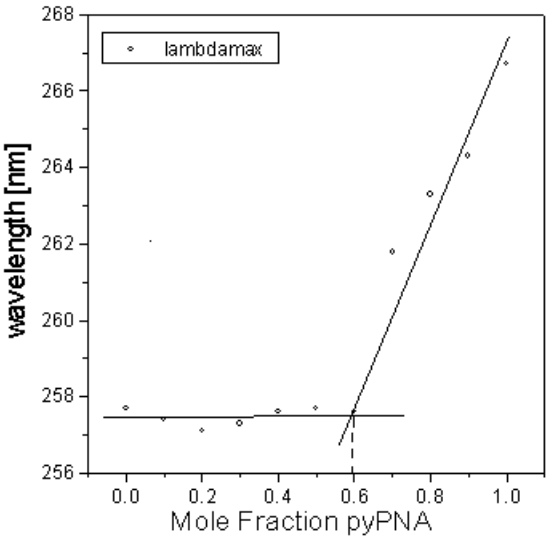

Figure 25. λ_{max} of S6 and S10 mixtures in the molar proportions of 0:100, 10:90, 20:80, 30:70, 40:60, 50:50, 60:40, 70:30, 80:20, 90:10. Solution conditions (10mM sodium phosphate buffer, pH 7.3)

2.8.2. CD Spectroscopy of *pyrrolidinyl*PNA:DNA Complexes

As described in the previous section, the *pyrrolidinyl*PNA single strands (**S2**-**S9**) exhibited very low induced CD. Two representative CD spectra of **S3** with two (2*S*,4*S*) units, one at the *C*-terminal and one in the middle, and **S5** with two (2*R*,4*R*) units, one *C*-terminal and one in the middle, are shown in Figure 26. The CD spectra of these enantiomeric sequences were nearly mirror images of each other.

Figure 27 shows the CD spectra of the complexes of **S2** and **S6** with the complementary DNA **S10**. These spectra exhibit positive maxima at 257, 277, and 285

nm, a negative minimum at 244 nm, and cross-over points at 232 and 247 nm. A positive band in the region of 255 to 260 nm as seen in the CD spectra of the complexes which is characteristic of the *poly*(dA) $[PNA\text{-}T_8]_2$ complex (Kim *et al.*, 1993) further confirms that *pyrrolidinyl*PNA **S2** and **S6** bind to DNA **S10** in 2:1 stoichiometry i.e. *pyrrolidinyl*PNA_2:DNA.

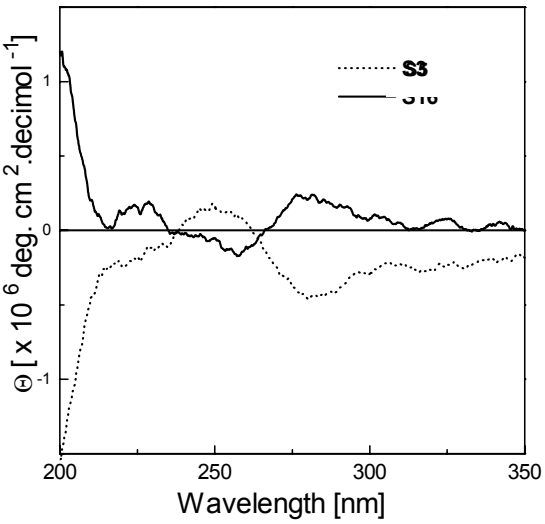

Figure 26. CD spectra of (------) **S3** single strand and (——) **S5** single strand.

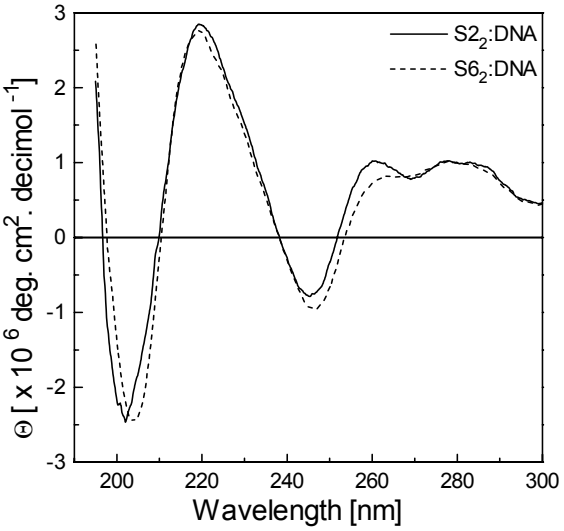

Figure 27. CD spectra of (——)**$S2_2$:DNA** complex and (------) **$S6_2$:DNA** complex.

2.8.3 UV-Melting Studies of *aeg*PNA:DNA and *pyrrolidinyl*PNA:DNA Complexes

DNA double helix is highly cooperative structure, held together by many reinforcing bonds and is also stabilized by the stacking interactions between the heterocyclic bases. When two polynucleotide species combine to form a helical complex there is a decrease in the optical density of the absorption band. This change (hypochromicity) can be used as measure of extent of complex formation in the mixture. The hypochromicity in the ultraviolet region arises as a consequence of the alterations in the stacking of purine and pyrimidines bases (Rein *et al.*, 1978). The melting temperature is measured by observing the change in absorbance at 260nm as a function of temperature. As the complex denatures, the absorbance of the solution increases, due to unstacking of the bases in the oligomer strands. Unlike in DNA triplexes, where two types of transitions are usually observed; the first low temperature transition corresponding to the melting of the third strand, whereas the second high temperature transition corresponding to melting of the duplex, PNA triplexes are known to show only one transition corresponding to the dissociation of triplex to single strands.

The UV-Tm data of the synthesized PNA oligomers with complementary DNA sequences was examined. Homopyrimidine thymine PNA sequences bind to the complementary homopurine DNA sequence forming PNA_2:DNA triplexes and melting of this triplex shows only one transition corresponding to the melting of triplex to single strands in a single step (Nielsen *et al.*, 1994; Egholm *et al.*, 1992a,b). Since, the incorporation of *pyrrolidinyl*PNA unit in the *aeg*PNA does not affect the stoichiometry of its complex formed with complementary DNA strand, the DNA-binding affinities of sequences **S2**-**S9** were measured with relative molar ratio of *pyrrolidinyl*PNA to DNA taken as 2:1.

The stabilities of PNA:DNA complexes differed depending upon the

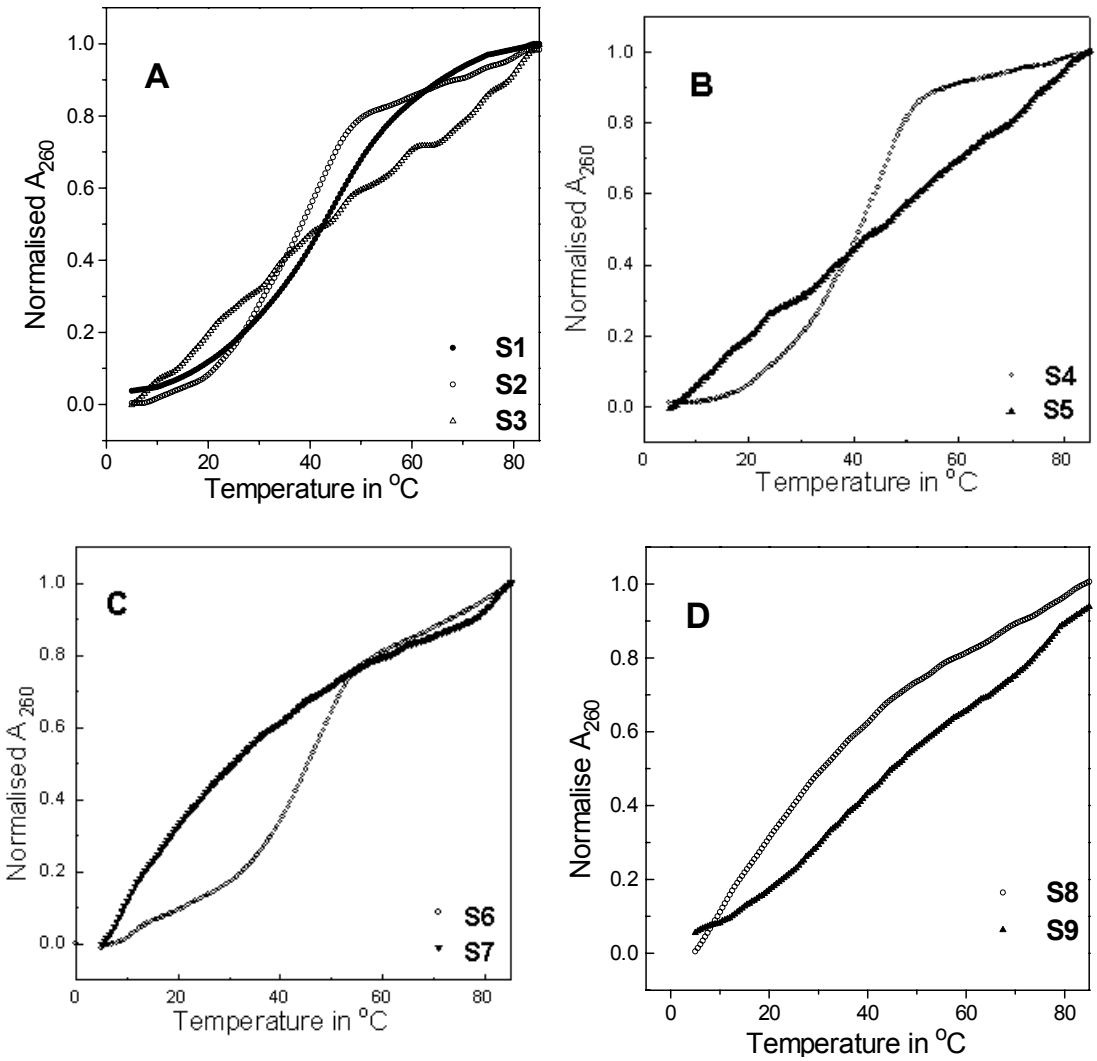

Figure 28. UV-Tm plots of PNA_2:DNA complexes A) S1:S10, S2:S10, S3:S10 B) S4:S10, S5:S10 C) S6:S10, S7:S10 D) S8:S10, S9:S10.

stereochemistry, position and the number of the modified units introduced in *aeg*PNA (**S1**) (Table 2). UV-melting profiles of all the sequences (**S1**-**S9**) are shown in Figure 28. The sigmoidal melting transitions for the DNA complexes formed with **S2**, **S4** and

Table 2. UV-Tm (^{o}C) PNA:DNA complexes

Entry	**PNA:DNA**	**Tm**	**ΔTm**	**% Hyperchromicity**
1	S1:S10	43.5	------	10.6
2	S2:S10	37.0	-6.5	15.6
3	S3:S10	------	----	4.7
4	S4:S10	44	+0.5	23.5
5	S5:S10	------	------	7.6
6	S6:S10	46.5	+3.0	19.3
7	S7:S10	-----	-------	12.4
8	S8:S10	------	-------	7.6
9	S9:S10	------	--------	5.8

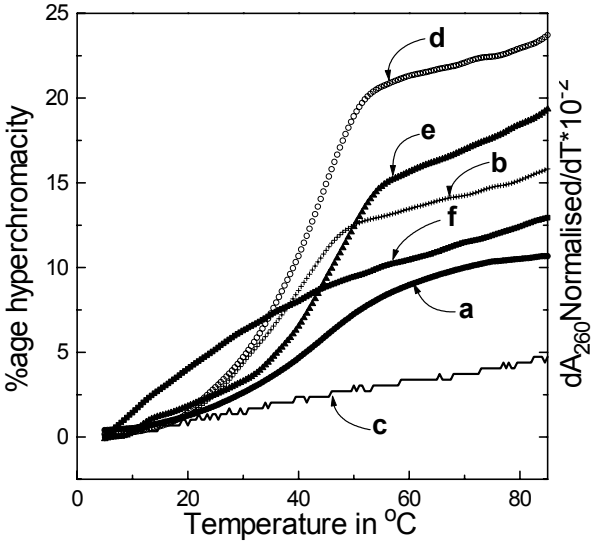

Figure 29. UV melting plots of PNA_2: DNA complexes a) S1:S10, b) S2:S10, c) S3:S10, d) S4:S10, e) S6:S10, f) S8:S10.

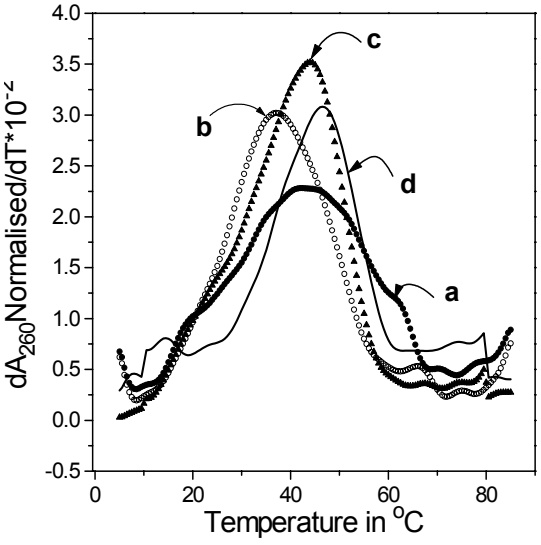

Figure 30. First Derivative curves of normalized A_{260} for a) S1:S10, b) S2:S10, c) S4:S10, d) S6:S10.

S6 oligomers were sharp compared to *aeg*PNA_2:DNA complex (**S1$_2$**:**S10**). The Tm data observed for the *pyrrolidinyl*PNA:DNA complexes is summarised in Table 2. The complex of the *pyrrolidinyl*PNA **S2** (2*S*,4*S*) with DNA **S10** showed 6.5°C destabilization as compared to the reference *aeg*PNA:DNA complex. When two modifications (**S3**, one

at *C*-terminal and one in the middle of the sequence) with the same stereochemistry were introduced the oligomer did not show any binding toward DNA Oligomer. Sequence **S4** with one (2*R*,4*R*)-*pyrrolidinyl*PNA unit at the*C*-termius showed a Tm of 44°C indicating 0.5°C stabilization compared to **S1**. Surprisingly **S5** with two (2*R*,4*R*)-

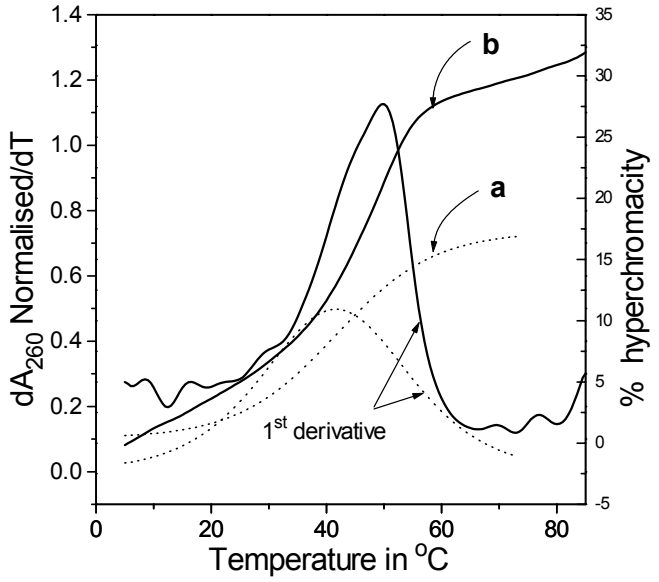

Figure 31. UV melting curves of PNA_2:DNA and their first derivative a) S1:S10 , b) S6:S10.

*pyrrolidinyl*PNA units did not bind to DNA. One unit of (2*S*,4*R*)-*pyrolidinyl*PNA unit at the *C*-terminal (**S6**) stabilized the triplex by 3°C. The sequence **S7** where two (2*S*,4*R*)-*pyrrolidinyl*PNA units are introduced in *aeg*PNA , again did not bind to DNA. DNA complexes **S8** and **S9**, with one and two *pyrrolidinyl*PNA units respectively of (2*R*,4*S*) did not show any sigmoidal transition upon heating.

One interesting feature observed in the melting transitions of *pyrrolidinyl*PNA:DNA complexes was that the percentage hyperchromicity during the melting process was higher compared to *aeg*PNA:DNA complexes. The percentage hyperchromicity data in Table 2 and absorbance profile Vs temperature plots in Figure 30 depict that even the sequence **S2**, which shows less Tm (-6.5°C) exhibits more change (15.6%) in absorbance compared to the reference (10.6%). The **S4** sequence with one (2*R*,4R)-*pyrrolidinyl*PNA unit at the *C*-terminus shows very large change in absorbance (23.5%) despite of only a small change in the Tm (+0.5°C). The sequence **S6** that is stabilizing by 3°C also has considerable increase in the hyperchromicity. Since, hypochromicity is directly proportional to the extent of base stacking, it can be

concluded that the introduction of one (2*R*,4*R*)-*pyrrolidinyl*PNA unit at the *C*-terminus has enhanced the base stacking without affecting the strength of hydrogen bonding of the complex. In the complex **S6$_2$**:**S10** having the (2*S*,4*R*)-*pyrrolidinyl*PNA unit at the *C*-terminus also led to the stabilisation of the complex as well as enhancement in base stacking.

Table 3. Tm data values of PNA_2:DNA complexes at different concentrations

Complex	PNA strand concentration			
	2μmol		3μmol	
	Tm in ^oC	%Hyperchromacity	Tm in ^oC	%Hyperchromacity
$S1_2$:DNA	43.5	10.6	46(+2.5)	16.7(+6.1)
$S2_2$:DNA	39.5	17.5	40(+0.5)	22(+4.5)
$S6_2$:DNA	46.5	19.3	50(+3.5)	31.8(+12.5)

The small width of the first derivative curves of the melting profiles for *pyrrolidinyl*PNA:DNA complexes, shown in Figure 31 indicates sharp melting of the complexes as compared to to *aeg*PNA:DNA complexes (broad transition).

Tm measurements for the DNA complexes with individual **S1**, **S2** and **S6** were also carried out at different concentrations. When the strand concentration of **S1** was increased from 2μM to 3μM (keeping the stoichiometry as *pyrrolidinyl*PNA:DNA 2:1) the increase in Tm was 2.5^0C and for the same increase in concentration of strand **S6** the rise in Tm was 3.5 ^{o}C. There was negligible change (+0.5^{o}C) in Tm of **S2$_2$**:**S10** upon increment of strand concentration. At 3μM strand concentration the percentage hyperchromacity for **S6$_2$**:**S10** was twice that for reference **S1$_2$**:**S10**. The increased change in hyperchromicity at higher concentration is perhaps due to the shift in equilibrium the double strand. The hyperchromicity change (19.3 to 31.8%) showed by **S6$_2$**:**S10** with concentration suggest an increased association constant.

The overall results indicate that the stereoconfiguration of the pyrrolidine ring significantly affects the binding abilities of *pyrrolidine*PNA to DNA. It is observed that the incorporation of a single modified unit can bring changes in resulting PNA, which may be favorable or unfavorable for DNA binding. It can also be inferred form the above melting data that the 2*S* configuration is more favorable than 2*R*. Further for the same stereochemistry at C2-centre, changes in C4 configuration significantly contribute towards the ring pucker and hence to the thermal stabilities of the triplexes as seen

from the Tm data for **S2** [Tm=39.5°C ΔTm= -4 with one unit; (2*S*,4*S*)] and **S6** [Tm=46.5°C ΔTm=+3 with one unit; (2*S*,4*R*)].

2.9 Crystal Structure of Compound 20: The Pyrrolidine Ring Conformation

Amongst four isomers studied here The (2*R*,4*S*) stereochemistry was found to be more favorable. The crystal structure of its enantiomeric key intermediate: Ethyl[(2*R*,4*S*)-2-{(tert-butoxycarbonyl)aminomethyl}-4-hydroxypyrrolidin-1-yl]acetate **20** was studied. An X-ray crystal structure of compound **20** shows that the pyrrolidine ring closely resembles the ribose sugar in ring-pucker. An X-ray crystal structure of (2*R*,4*S*)-N-(1-benzyl-4-methyl-3-pyrrolidinyl)-5-chloro-2-methoxy-4-(methylaminobenzamide)-hydrochloride containing protonated pyrrolidine ring which is stereoelectronically identical to the pyrrolidine ring in compound **20** also exhibited the preferred Northern (*N*) conformation of uridine in crystalline state (Furuya *et al.*, 1986;

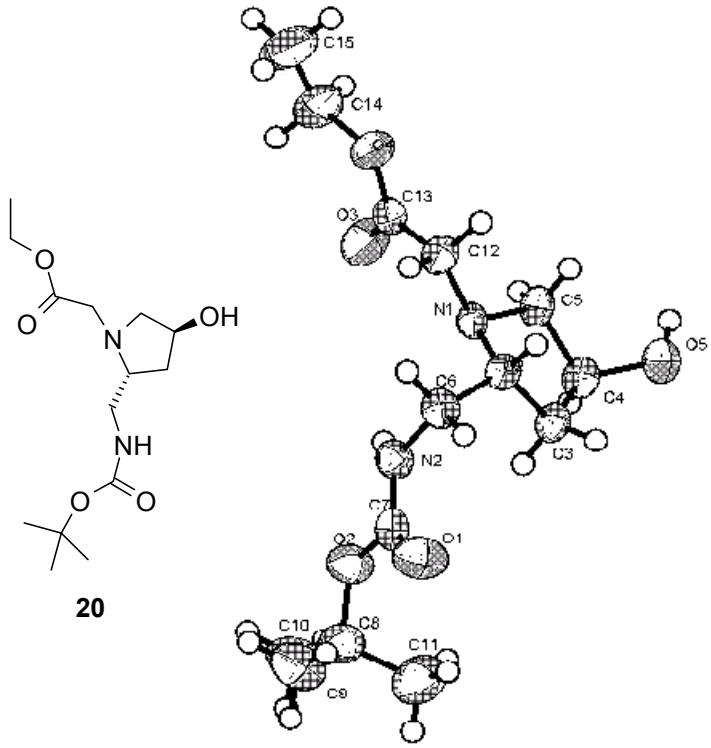

20

Figure 32. Crystal structure and chemical structure of compound **20**: Ethyl[(2*R*,4*S*)-2-{(*tert*-butoxycarbonyl)aminomethyl}-4-hydroxypyrrolidin-1-yl]acetate

Green *et al.*, 1975).

While this work was in progress, two reports appeared in the literature in which oligomers containing (2*R*,4*R*) (Hickman *et al.*, 2000) and (2*R*,4*S*) (Puschl *et al.*, 2000) configurations of the pyrrolidine unit were explored for DNA/RNA binding studies. A pentamer of thymine with streoregular backbone with (2*R*,4*R*) configuration was found to stabilize DNA as well as RNA complexes. In the case of (2*R*,4*S*)-*pyrrolidinyl*PNA, a stereoregular decamer bearing adenine nucleobase was found to stabilise the duplex with dT_8 as compared to *aeg*PNA.

Table 4. Crystal data and structure refinement for compound **20**

Empirical formula C14 H27 N2 O5
Formula weight 303.38
Temperature 293(2) K
Wavelength 0.71073 A
Crystal system, space group ORTHORHOMBIC, P212121
Unit cell dimensions a = 5.964(3) A alpha = 90 deg. b = 10.027(5) A beta = 90 deg. c = 27.935(14) A gamma = 90 deg.
Volume 1670.6(14) A^3 Z, Calculated density 4, 1.206 Mg/m^3
Absorption coefficient 0.091 mm^-1 F(000) 660
Crystal size 1.44 x 0.94 x 0.79 mm Theta range for data collection 2.16 to 25.00 deg. Limiting indices -4<=h<=7, -11<=k<=11, -30<=l<=33 Reflections collected / unique 7399 / 2837 [R(int) = 0.0575] Completeness to theta = 25.00 98.4 % Max. And min. transmission 0.9320 and 0.8806
Refinement method Full-matrix least-squares on F^2 Data / restraints / parameters 2837 / 0 / 199 Goodness-of-fit on F^2 1.127 Final R indices [I>2sigma(I)] R1 = 0.0734, wR2 = 0.1721 R indices (all data) R1 = 0.0983, wR2 = 0.1837 Absolute structure parameter -2(3) Largest diff. peak and hole 0.287 and -0.329 e.A^-3 _

2.10 Conclusions

A novel class of modified nucleic acids with a pyrrolidine amide backbone has been introduced. All four stereoisomers of the pyrrolidine unit have been synthesized and were introduced in *aeg*PNA backbone using solid phase synthesis protocol. It is found that the stereochemistry of the *pyrrolidinyl*PNA unit introduced into the *aeg*PNA greatly affects the stability of the complexes formed with DNA. Even one pyrrolidine unit can induce the conformational changes in the oligomer.

From the UV-thermal denaturation data, it appears that (2*S*,4*R*) and (2*R*,4*R*)-pyrrolidinyl units bring in favorable changes in the *aeg*PNA in terms of thermal stability and increased base stacking.

Unlike *aeg*PNA no precipitation for *pyrrolidinyl*PNAs was observed on prolonged storage or during melting experiments, which indicates that *pyrrolidinyl*PNAs have better water solubility as compared to *aeg*PNA.

These results have implications for choosing the right stereochemistry of the pyrrolidinyl unit for incorporation into *aeg*PNA-T backbone. The effect of this unit in mixed sequences (purine+pyrimidine) needs to be explored. The (2*R*,4*S*) strereochemistry employed in the present work with thymine as the nucleobase destabilsed the triplex with DNA whereas the same stereochemistry pocessing an adenine (stereoregular backbone) stabilsed the duplex with DNA. Thus the nucleobase specificity of the modification needs to be verified by the synthesis of the sequences with modified units in homo as well as mixed base sequences. A recent report by Pushi *et al.* (2000) has shown that the introduction of one modified (2*R* 4*S*)-*pyrrolidinyl*PNA unit with adenine as nucleobase in the *aeg*PNA backbone destabilises its complex with DNA but a streoregular backbone with the same configuration and nucleobase gave very stable *pyrrolidinyl*PNA:DNA complexes.

In the light of this it is necessary to study the effect of (2*S*,4*R*)-*pyrrolidinyl*PNA unit which is found to be suitable from the UV-Tm studies as well as form X-ray crystal data, on streoregular backbone. An important feature responsible for the dependence of thermal stability of the *pyrrolidinyl*PNA:DNA complexes seems to be the stereochemistry of the pyrrolidine ring and the nucleobase type. The conformation the pyrrolidine ring that is dependent on the relative stereochemisties of C-2 and C-4 substituents and the electronegativity of the substituents appear to dictate the conformation of the oligomers and their ability to bind to target DNA.

2.11. Experimental Section

General Remarks

The chemicals used were of laboratory or analytical grade. All the solvents used were purified according to the literature procedures (Perrin, 1989). Reactions were monitored by TLC. Usual work-up implies sequential washing of the organic extract with water and brine followed by drying over anhydrous sodium sulphate and evaporation under vacuum.

Column chromatography was performed for purification of compounds on 100-200 mesh silica gel (Loba Chemie, India). TLCs were carried out on pre-coated silica gel GF_{254} sheets (Merck 5554). TLCs were run in either dichloromethane with an appropriate quantity of methanol or in petroleum ether with an appropriate quantity of added ethyl acetate for most of the compounds. Free acids were chromatographed on TLC using a solvent system of MeOH:DCM:CH_3COOH 20:80:0.1. The TLCs were visualized with UV light and/ or by spraying with Ninhydrin reagent after *t*-Boc-deprotection (exposing to HCl vapors) and heating.

The ^1H and ^{13}C NMR spectra were recorded on a 200 MHz Bruker ACF 200 spectrometer fitted with an Aspect 3000 computer and all the chemical shifts are referred to internal TMS for ^1H and chloroform-d for ^{13}C. The chemical shifts are quoted in δ (ppm) scale. In compounds that bear a tertiary amide group, splitting of NMR signals was observed due to the presence of rotamers. In such cases, the major isomer is designated as 'major' and the minor isomer as 'minor'.

Optical rotations were measured on a Bellingham Stanley Ltd. ADP 220 polarimeter and CD spectra were recorded on a JASCO J715 spectropolarimeter. FAB-Mass spectra were recorded on a Finnigan-Matt mass spectrometer, while MALDI-TOF spectra were obtained from a KRATOS PCKompact instrument.

For the enantiomers, the repetition of ^1H and ^{13}C NMR data is avoided here and only optical rotation is reported.

(2S,4R)-N1-(benzyloxycarbonyl)-4-hydroxyproline **1**

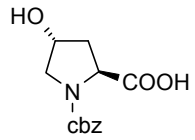

1

trans-4-Hydroxy-L-proline (5g, 38mmol) was dissolved in 20 ml of water and to it $NaHCO_3$ (8g 95mmol) was slowly added while stirring. To this mixture, benzychloroformate (5.7ml 50% solution in toluene, 45.7mmol) was added in one portion and the mixture was stirred For 8 hrs. Toluene was removed under vacuum and the mixture was diluted with 25 of water, extracted with ether (2 x 25ml). Ethereal layers were discarded; the aqueous layer was brought to pH 2 with Conc. HCl and extracted with ethyl acetate (5 x 25ml). The organic washings were pooled together, washed with water and brine. Ethyl acetate layer was dried over anhy. Na_2SO_4 and concentrated to dryness to obtain 10 g (37.6mmol %Yield 98) of compound **2** (Rf =0.3, MeOH:EtOAc 5:95)

^{1}H (CDCl$_3$) δ 7.4-7.15 (m 5H $C_6\underline{H}_5$), 6.6-6.3 (bs 1H O$\underline{H}$), 5.1 (m OC$\underline{H}_2$), 4.5-4.35 (m 2H C4$\underline{H}$, C2$\underline{H}$), 3.65-3.5 (m 2H C5$\underline{H}$), 2.4-2.2 (m 1H C3$\underline{H}$), 22-2.0 (m 1H C3'$\underline{H}$) (Williams & Rapoport, 1994*)*

(2S,4R)-N1-(benzyloxycarbonyl)-4-hydroxyproline-methylester **2**

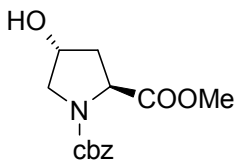

2

Compound **1** (10g, 37.6mmol) was taken in 120ml dry methanol and triethylamine (13ml 94mmol) was added into it. Under dry conditions thionyl chloride (3.3ml, 45.1mmol) was added drop wise into the continuously stirred reaction mixture while keeping the flask in ice bath. After the addition was over, it was stirred further overnight. Evaporated the solvent completely, dissolved the residue in ethyl acetate and washed it with water (3 x 50ml) and then with brine. Ethyl acetate layer was dried over anhy. Sodium sulphate and concentrated to dryness to obtain **3** (9.7g, yield=92%, Rf=0.5, EtOAc:Petroleum ether 5:5. $[\alpha]^{27}_D$=4.96

^{1}H (CDCl$_3$) δ 7.45-7.2 (m 5H $C_6\underline{H}_5$), 5.2-4.8 (m 2H OC$\underline{H}_2$), 4.6-4.4 (m 2H C4$\underline{H}$), 3.8-3.4 (m 6H OC$\underline{H}_3$ two rotamers, C5$\underline{H}$, C2$\underline{H}$), 2.4-2.2 (m 1H C3$\underline{H}$), 2.1-2.95 (m 1H C3'$\underline{H}$)

^{13}C NMR (CDCl$_3$) δ 173.0,172.9 ($\underline{C}OOCH_3$), 154.7, 154.4 (N$\underline{C}$OO), 136.0, 135.8 (Ar), 128.1, 127.7 127.4 (Ar), 69.3, 68.6 (O$\underline{C}H_3$), 66.9 (OC$\underline{H}_2$), 57.7, 57.4 ($\underline{C}$4), 54.7, 54.2 ($\underline{C}$5), 52.0, 51.7 ($\underline{C}$2), 38.7, 37.9 ($\underline{C}$3) (Rueger & Benn, 1982)

(*2S,4R*)*-N1-(benzyloxycarbonyl)-4-hydroxy-2-(hydroxymethyl)-pyrrolidine* **3**

The methyl ester **2** (9.7g, 34.6mmol) was dissolved in dry THF (200ml) and reaction flask was chilled to 0^{o}C. Lithium borohydride (1.1g, 51.9mmol) was then added to it in

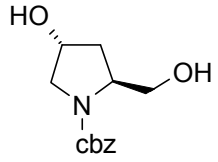

3

two portions. After stirring for 3.5 hrs under nitrogen atmosphere, the solution was made acidic with saturated solution of ammonium chloride. The THF was evaporated under vacuum and water was added to the residue. The resulting solution was washed three times with ethyl acetate and the organic washings were pooled, washed with water followed by brine. The solution was dried over anhy. Na_2SO_4 and concentrated to afford **3** (7.8g, yield=89%, Rf= 0.3, EtOAc:Petroleum ether 5:5).

^{1}H (CDCl$_3$) δ 7.4 (s 5H $C_6\underline{H}_5$), 5.2-5.75 (bs 1H C4-O$\underline{H}$, exchangeable), 4.4 (bs 1H $CH_2O\underline{H}$, exchangeable), 4.2 (m 1H C4$\underline{H}$), 3.9-3.4 (m 5H $C\underline{H}_2OH$, C2$\underline{H}$, C5$\underline{H}$), 2.15-1.9 (m 1H C3$\underline{H}$), 1.9-1.65 (m 1H C3'$\underline{H}$)

(2S,4R)-N1-benzyloxycarbonyl-4-hydroxy-2-(p- toluenesulfonyloxymethyl)pyrrolidine **4**

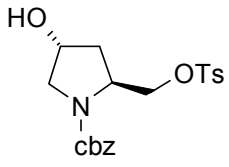

4

The diol **3** (7.8g, 31mmol) crude from the previous reduction step was evaporated twice from dry pyridine, and was dissolved in pyridine (150ml). Freshly crystallized p-toluenesulfonylchloride (6.5g, 34.1mmol) was taken separately in pyridine (100ml) in a dropping funnel and was added drop wise to the chilled reaction mixture over a period of 1hr. After stirring the mixture for 7-8hrs, pyridine was removed under vacuum. Water was added to the residue, extracted with ethyl acetate (3X50ml). All organic washings were pooled together, washed with water and then with brine. The organic layer dried over anhy. Na_2SO_4 was concentrated to obtain crude tosylate (14g) which was purified by column chromatography to get the monotosylate **4** (8.3g, yield=66%, Rf=0.36 EtOAc:Petroleum ether 5:5) and 2,4-ditosylate (5-10%).

^{1}H (CDCl$_3$) (compound 4) δ 7.80-7.76 (d 2H J=7.82Hz Ts), 7.39 (s 5H $OCH_2C_6\underline{H}_5$), 7.25-7.21 (d 2H J=7.82Hz Ts), 5.9 (s 2H CO$\underline{O}CH_2$), 5.17-4.89 (m 2H C4$\underline{H}$, O$\underline{H}$), 4.54-4.38 (m 2H $C\underline{H}_2OTs$), 4.18 (s 3H $OC\underline{H}_3$), 3.17-3.29 (m 2H C5H), 2.47 (s 3H $OC\underline{H}_3$), 2.43-2.06 (m 3H, C2, C3$\underline{H}$)

(2S,4R)-N1-benzyloxycarbonyl-2-(azidomethyl)-4-hydroxypyrrolidine **5**

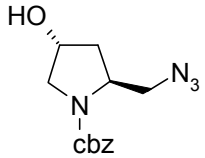

5

Monotosylate **4** (8.3g, 20.4mmol) was taken in dry DMF (75ml) and sodium azide (10.6g, 0.16mol) was added into it. The reaction mixture was heated at 55^{o}C with stirring for 6hrs. The solvent was removed under vacuum, the residue was taken in water and extracted with ethyl acetate (3X50ml). The pooled organic extracts were washed with water and brine and then dried. Ethyl acetate layer was concentrated to get azide **5**. (5.3g, yield=94%, Rf=0.6, EtOAc:Petroleum ether 5:5)

IR (neat) cm^{-1} 3016, 2360, 2106, 1697, 1419 **(m/z)=**276 (Calcd for $C_{13}H_{16}N_4O_3$: 276.1)

^{1}H NMR ($CDCl_3$) δ 7.31 (s 5H $C_6\underline{H}_5$), 5.09 (s 2H $OC\underline{H}_2$), 4.45-3.97 (m 2H C2<u>H</u>, C4<u>H</u>), 3.85-3.07 (C5<u>H</u>, $C\underline{H}_2N_3$, O<u>H</u>), 2.02-1.95 (m 2H C3<u>H</u>)

^{13}C NMR ($CDCl_3$) δ 162.5 (N<u>C</u>O), 136.2 (Ar), 128.1, 127.5, 127.2 (Ar), 68.8, 68.4 (<u>C</u>4), 67, 66.6 ($O\underline{C}H_2$), 55.6 (<u>C</u>2), 55.2, 54.8 ($\underline{C}H_2N_3$), 53.2, 51.9 (<u>C</u>5), 37.5, 36.9 (<u>C</u>3)

(2S,4R)-N-benzyloxycarbonyl 2-(tert-butoxycarbonylaminomethyl)-4-hydroxypyrrolidine **6**

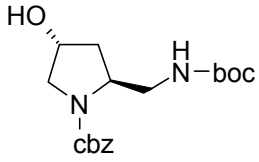

6

Compound **5** (5.3g, 19.1mmol) was taken in dry EtOAc (20ml) in 500 ml hydrogenation flask and di-tert-butyldicarbonate (5.9g, 21mmol) was added into it. Raney Ni (2ml, suspension in ethanol) was separately washed thoroughly with EtOAc and was added to the hydrogenation flask. Subjected it to hydrogenation at 40-psi pressure for 1.5hrs. The catalyst was filtered and washed with methanol/EtOAc mixture. The filtrate was concentrated under vacuum to crude protected amine. Purification using column chromatography afforded **6** (6.5g, yield=65%, Rf=0.6, EtOAc:Petroleum ether 5:5) $[\alpha]^{27}_D$= -11.6

^{1}H ($CDCl_3$) δ 7.45 (s 5H $C_6\underline{H}_5$), 5.5 (bs 1H N<u>H</u> exchangeable), 5.2 (s 2H, $COOC\underline{H}_2$), 4.75 (bs 1/2 H CHO<u>H</u> exchangeable), 4.45 (m 1H, C4<u>H</u>), 4.2-4.0 (m 1H C5<u>H</u>), 3.75-3.15 (m C5'<u>H</u>, $C\underline{H}_2NH$), 2.45-2.2 (m 1H C2<u>H</u>), 2.2-1.7 (m C3<u>H</u>), 1.5 (s 9H $C(C\underline{H}_3)_3$)

Ethyl ((2S,4R)-2-(tert-butoxycarbonylaminomethyl)-4-hydroxypyrrolidin-1-yl)acetate **7**

4R-N-benzyloxycarbonyl-2-tert-butoxycarbonyamino-hydroxypyrrolidine (6.5g, 18.5mmol) **6** was taken in methanol (20ml) in 500 ml hydrogenation flask and Pd/C (0.65g, 10% Pd-C) was added into it. The flask was kept under 60-psi H_2 pressure for 8hrs in a Parr hydrogenation apparatus. The catalyst was filtered through Celite and solvent was removed using vacuum to get yellow solid. The product thus obtained was dissolved in dry CH_3CN (50 ml) to which was added KF/Celite (8g, 3.7mmol). The reaction mixture was heated the in an oil bath at 60^{o}C and ethylbromoacetate (3ml, 28mmol) was added into it. After stirring the reaction mixture for 2hrs, the Celite was filtered and the filtrate was concentrated. The residue was applied to a silica gel column to isolate pure **7** (3.4g, yield=60%, Rf=0.3, EtOAc:Pet.ether 1:1). $[\alpha]^{27}_D$= -50

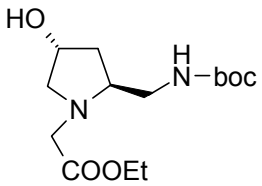

7

^{1}H (CDCl$_3$) δ 5.0 (bs 1H CH_2NH), 4.35-4.2 (m 1H C4H), 4.2(q 4H J=7.08 HzCOOCH_2CH_3), 3.53.3.41(m 3H CH_2NH, C5H)), 3.38-3.16 (m 2.5H NCH_2COO, OH), 3.0 (m 1H), 3.06-2.98 (m 1H C5'H) 2.69-2.64 (m 1H C2H) 1.93-1.7 (m 2H C3H), 1.43 (s 9H C(CH_3)$_3$), 1.27 (t 3H J=7.08 OCH_2CH_3)

m/z=302 (calcd for $C_{14}H_{26}N_2O_5$: 302.18)

IR (CHCl$_3$) cm^{-1} 3402, 3325, 2923, 2854, 1712, 1520, 1458

mp = 58°C

Ethyl [(2R, 4S)-2-(tert-butoxycarbonyaminomethy)-4-(N^3-benzoyl-thymin-1-yl) pyrrolidin-1-yl]acetate **8**

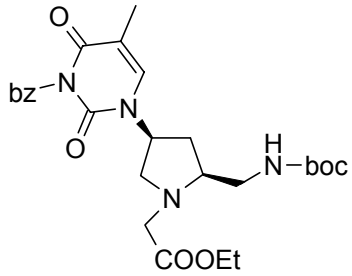

8

A solution of **7** (3.4g, 11.2mmol), N3-benzoyl-thymine (5.1g, 22.4mmol) and PPh_3 (5.87g, 22.4mmol) in freshly dried THF (20ml) was stirred at 0°C and DEAD (3.5ml, 22.4mmol) was added drop wise. The temperature was maintained at 0°C during addition. After stirring for 4hrs, the solvent was evaporated and the residue was purified by silica gel column chromatography to obtain **8** as a pale yellow foam (3.8g, yield=68%, Rf=0.4, EtOAc:Pet.ether 1:1) $[\alpha]^{27}_D$= -7.5

1H (CDCl$_3$) δ 8.15 (s 1H Thy H6), 8-7.4 (m 5H C_6H_5), 5.14 (bs 1H CH_2NHCO), 4.98 (m 1H C4H), 4.35-4.1 (q 2H J=7.33Hz OCH_2CH_3), 3.7-3.5 (m 1H C5H), 3.5-3.0 (m 4H OCH_2, NHCH_2), 2.9-2.5 (m 2H C5'H, C2H), 2.1 (s 3H Thy CH_3), 1.93-1.79 (m 1H C3H), 1.72-1.59 (m 1H C3'H), 1.45 (s 9H C(CH_3)$_3$), 1.25 (t 3H J=7.33Hz OCH_2CH_3)

^{13}C NMR (CDCl$_3$) δ 170.8 (COOCH_2CH_3), 169.1 (CONH), 162.6 (Thy 4CO), 156.2 (Thy 2CO), 149.7 (C_6H_5CO), 137.9 (Thy C6), 134.7 (Thy C5), 131.5, 130.1, 128.9 (Ar), 110.6 (Ar), 79.2 (C(CH_3)$_3$), 62.4 (C4), 60.7 (OCH_2), 58.8 (N^{1}CH_2CO), 52.8 (CH_2NHCO), 51.7 (C2) , 39.7 (C5), 35.7 (C3), 28.1 (C(CH_3)$_3$), 13.9 (OCH_2CH_3), 12.5 (Thy CH_3).

FAB-MASS: 514 $(M+H)^+$ (calcd. for $C_{26}H_{33}N_4O_7$=513.2)

[(2R,4S)-2-(tert-butoxycarbonyaminomethy)-4-(thymin-1-yl) pyrrolidin-1-yl]acetic acid **9**

Compound **8** (3.8g, 7.57mmol) was dissolved in 2N NaOH in methanol: water (4:1, 20ml) and stirred for 10hrs. The solution was adjusted to pH 2 by addition of cation exchange resin (Dowex H+). The methanol was evaporated and water (10ml) was added. Benzoic acid was removed by washing the aqueous layer with EtOAc. The

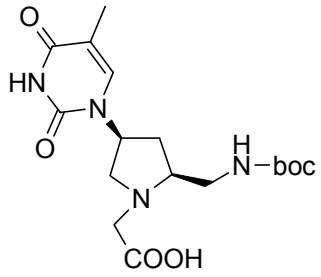

9

aqueous layer was dried completely by coevaporating it with toluene (2X20ml) to obtain **9** as white solid (1.3g, yield=50%, Rf=0.3, MeOH:DCM 2:8).

^{1}H NMR (D_2O) δ 7.5 (s 1H Thy H6), 4.8 (m, 1H, C4H), 4.1-3.5 (m, 2H C5H), 3.6-3.3 (m 5H, CH_2NH, CH_2CO, C2H), 2.8-2.6 (m 1H C3H), 2.4-1.9 (1H C3'H), 1.9 (s 3H Thy CH_3), 1.5 (s 9H $C(CH_3)_3$)).

^{13}C NMR (D_2O) δ 170.9 (CH_2COOH), 167.5 (CO ThyC4), 159.2 (NHCOO), 144.2 (CO ThyC2), 144.2 (C6 Thy), 111.5 (C5 Thy), 82.5 ($C(CH_3)_3$), 68.3 (C4), 60.3 (CH_2COO), 59.2 (C2), 56.0 (CH_2NH), 38.4 (C5), 32.7 (C3), 28.5 ($C(CH_3)_3$), 12.3 (CH_3 Thy).

FAB-MS 383 $(M+H)^+$, 405 $(M+Na)^+$ (Calcd for $C_{17}H_{26}N_4O_6$: 382.18)

N3-benzoylthmine **11**(Cruickshank *et a*l., 1984)

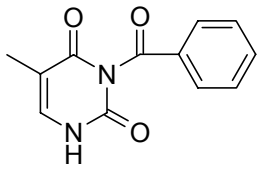

11

To a stirred solution of thymine (5.0g, 40mmol) in dry acetonitrile (50ml) and dry pyridine (10ml) in an ice-bath, benzoyl chloride (10ml, 88mmol), was added dropwise. Stirring was continued at room temperature overnight, when dibenzoyl thymine (**10**) was found to be present. The pyridine was evaporated to obtain a crude yellow solid which was stirred with 0.25M K_2CO_3 in dioxane:water (75ml, 1:1) for 5h, which gave a suspension. The suspension was filtered and the solid was washed with ice-cold water and ether. The precipitates were first air dried and then dried under vacuum to obtain monobenzoylated product (7.5g, yield=82% Rf=0.3 EtOAc).

(2R,4R)-4-hydroxy-1-methylpyrrolidine-2-carboxylic acid **12** (Baker *et al*., 1981)

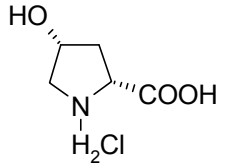

12

A solution of acetic anhydride (102ml, 1mol) in glacial acetic acid (300ml) was heated to 50°C and 2*S*,4*R*-Hydroxy-L-proline (24.7g, 18.9mol) was added in one portion. The heating was continued until the reflux temperature was reached and the solution was held at reflux for 5.5h. The mixture was cooled and the solvent was removed under vacuum giving thick oil. The oil was dissolved in 2N HCl 350ml and was refluxed for 3hrs. The solution was treated with charcoal while hot and then filtered through Celite. Upon concentrating the solution by rotary evaporation, white needles were formed and collected by suction filtration. The needles were dried

under reduced pressure to give **12** (24g, yield=75%). The filtrate was concentrated to give another 4g (12%) of *allo*-4-hydroxy-D-proline hydrochloride. mp 161-163^{o}C

^{1}H NMR (D_2O, external Me_4Si) δ 2.3-3.0(m, 2H), 3.5 (d, 2H, J=2.5 Hz), 4.4-4.8 (m 2H)

^{13}C (D_2O) δ 174.0 (COO), 72.0 (C5), 61.5 (C3), 56.0 (C4), 40.2 (C2)

(2R,4R)-1-(benzyloxycarbonyl)-4-hydroxypyrrolidine-1-methylcarboxylate **13**

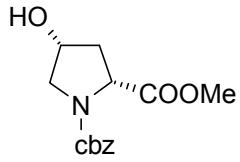

13

allo-4-hydroxy-D-proline **12** (12.7g, 76mmol) was dissolved in water (40ml), to which $NaHCO_3$ (22.3g, 0.27mol) was slowly added while stirring. To this mixture, benzychloroformate (31ml, 50% soln. in toluene, 91mmol) was added in one portion and the mixture was stirred for 8 hrs. Toluene was removed under vacuum and the mixture was diluted with 25 of water and extracted with ether (2 x 25ml). The ethereal layers were discarded and the aqueous layer was brought to pH 2 with conc. HCl and extracted with ethyl acetate (5 x 25ml). The organic washings were pooled together, washed with water, brine, dried over anhy. Na_2SO_4 and concentrated to dryness to obtain N1 benzyloxycarbonyl protected hydroxyproline (19.5g, yield=98%, Rf=0.3, MeOH:EtOAc 5:95), which was converted to its respective methyl ester by procedure as mentioned in the preparation of compound **2** to get **13** (18.8g, yield=91%). $[\alpha]^{27}_{D}$= 5.3

^{1}H ($CDCl_3$) δ 7.7-7.6 (d 5H C_6H_5), 5.3-4.9 (m 2H CH_2), 4.6-4.2 (m 2H C4H, C2H), 3.9-3.25 (m 6H CH_3, C5H, C5'H, OH), 2.5-2.25 (m 1H, C3H), 2.5-2 (m 1H C3'H)

(2R,4R)-1-(benzyloxycarbonyl)-4-hydroxy-2-(hydroxymethyl)-pyrrolidine **14**

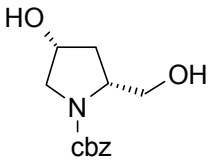

14

Starting form compound **13**, method of preparing **14** was same as followed for the synthesis of compound **3.** (Yield=92%, Rf=0.5, EtOAc:Pet. ether 5:5)

1H ($CDCl_3$) δ 7.5-7.1 (s 5H C_6H_5), 5.4-5.0 (m 3H $OCH_2C_6H_5$, CH_2OH), 4.45-25 (C4H) , 4.25-4.0 (m 3H CH_2OH, C4-OH), 3.5 (m 3H C5H, C2H), 2.5-2.25 (m 1H C3H), 2.0-1.75 (m 1H C3'H)

(2R,4R)-1-benzyloxycarbonyl-4-hydroxy-2-(p-toluenesulfonyloxy methyl)pyrrolidine **15**

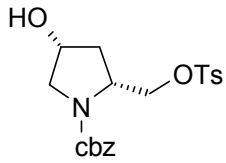

15

Starting from compound **14,** the procedure for the synthesis of compound **4** was followed (Yield=68%, Rf=0.34 EtOAc:Petroleum ether 5:5)

^{1}H ($CDCl_3$) δ 7.9-7.6 (m 2H Ts), 7.5-7.2 (m 7H C_6H_5, Ts), 5.0 (m 2H $COOCH_2$), 4.5-4.0 (m 4H CH_2, C5H, C5'H), 3.75-3.5 (m 1H

C4), 3.5-3.3 (m 1H C2H), 2.8-2.5 (m 1H C3H), 2.45 (s 3H OCH_3), 2.2 (m 1H C3'H).

(2R,4R)-N1-benzyloxycarbonyl-2-(azidomethyl)-4-hydroxypyrrolidine **16**

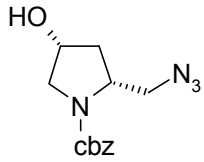

16

This compound was prepared from **15** according to the same procedure as **5.** (Yield=94%, Rf=0.55, EtOAc:Petroleum ether 5:5)

^{1}H ($CDCl_3$) δ 7.6-7.4 (m 5H C_6H_5), 5.35-5 (m 2H OCH_2), 4.6-3.9 (m 3H C4H, C5H, C5'H), 3.9-3.4 (m 4H CH_2, OH, C2H), 2.4-1.90 (m 2H C3H, C3'H)

IR (neat) cm^{-1} 3321, 2947, 2102, 1697, 1681, 1666, 1415, 1099.

(2R,4R)-N1-benzyloxycarbonyl 2-(tert-butoxycarbonylaminomethyl)-4-hydroxypyrrolidine **17**

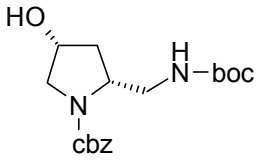

17

The method of preparation is same as followed for the synthesis of compound **6**. (Yield=65%, Rf=0.62, EtOAc:Petroleum ether 5:5)

^{1}H ($CDCl_3$) δ 7.5-7.25 (m 5H C_6H_5), 5.6 (bs 1H NH), 5.2-5.1 (m 2H $C_6H_5OCH_2$), 4.5 (m 1H C4H), 4.3-3.9 (m C5H C5'H), 3.7-3.4 (m 3H CH_2 NH Boc), C2H), 3.2 (bs 1H OH), 2.2-1.9 (m 2H C3H, C3'H), 1.4 (s 9H $C(CH_3)_3$)

Ethyl [(2R,4R)-2-{(tert-butoxycarbonyl)aminomethyl}-4-hydroxypyrrolidin-1-yl)acetate **18**

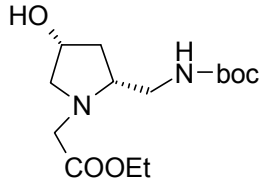

18

The procedure followed for the preparation was same as for compound 7. (Yield=60%, Rf=0.32, EtOAc:Pet.ether 1:1)

1H ($CDCl_3$) δ 5.4 (bs 1H NH), 4.35-4.25 (m 1H C4H), 4.25-4.1 (q 2H OCH_2CH_3), 3.55-3.25 (m 3H CH_2COOEt, C2), 3.25-3 (m 2H CH_2NH), 3-2.9 (m 1H C5), 2.85-2.7 (m 1H C5'), 2.45-2.2 (m 2H C3H, C3'H), 1.4 (s 9H $C(CH_3)_3$), 1.4-1.2 (t-3H OCH_2CH_3).

^{13}C ($CDCl_3$) δ 170.9 ($COOCH_2$), 156.2 (NHCOO), 78.5 ($C\{CH3\}_3$), 69.6 (C4), 62.1 (OCH_2CH_3), 60.9 (C2), 60.1 (NCH_2CO), 53.1 (CH_2NH), 41.7 (C5), 37.9 (C3), 28.1 ($C\{CH_3\}_3$), 13.8 (OCH_2CH_3)

(2R,4R)-2-[(tert-butoxycarbonyl)aminomethyl]-1-(ethoxycarbonylmethyl) pyrrolidin-4-yl-benzoate **19**

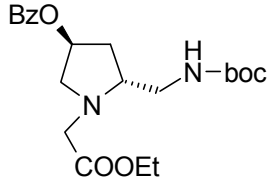

19

To a mixture of **18** (5g, 16.5mmol), benzoic acid (2.2g, 18.1mmol) and PPh_3 (4.8g, 18.1mmol) in freshly dried THF,

DIAD (3.6ml, 18.1mmol) was added dropwise while maintaining the temperature at 0°C. After stirring the reaction for 4hrs, solvent was evaporated under vacuum and residue was purified by column chromatography to obtain pure product 18. (5.3 g, yield=79%, Rf=0.6 EtOAc:Pet. ether 3:7)

^{1}H (CDCl$_3$) δ 8.01-7.96 (m 2H Ar), 7.58-7.51 (m 1H Ar), 7.45-7.37 (m 2H Ar), 5.4-5.31 (m 1H, C4H), 5.2-5.18 (bs 1H NHCO), 4.20-4.09 (q 2H J=7.32 OCH_2CH_3), 2.1-2.03 (m 2H C3H), 1.42 (s 9H $C(CH_3)_3$), 1.28-1.21 (t 3H J= 7.32Hz OCH_2CH_3)

Ethyl[(2R,4S)-2-{(tert-butoxycarbonyl)aminomethyl}-4-hydroxypyrrolidin-1-yl]acetate **20**

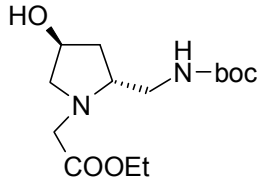

20

Compound **19** (1.06g, 2.61mmol) was taken in absolute ethanol and after the addition of a few pieces of sodium metal (~50mg) into it, the mixture was stirred at room temperature for 1h. The mixture was further heated at 50°C for 30 hrs under nitrogen atmosphere. Aqueous $KHSO_4$ was added to neutralize the base and the mixture was concentrated under *vacuo*. The residue was taken in EtOAc and was washed with water and brine. The organic layer was dried over anhy. $NaSO_4$ and concentrated. The crude residue was purified by column chromatography to obtain **20** in moderate yield (0.2g, yield=30%, Rf=0.3, EtOAc:Pet.ether 1:1) and the unreacted starting material (0.2g, yield=19%). $[\alpha]^{27}_D$= 50

Ethyl [(2R, 4R)-2-(tert-butoxycarbonyaminomethy)-4-(N3-benzoyl-thymin-1-yl) pyrrolidin-1-yl]acetate **21**

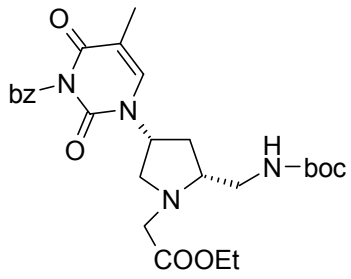

21

Compound **19** on Mitsunobu reaction using same conditions as used for the preparation **8** gave **21**. (Yield=70%, Rf=0.4, EtOAc:Pet.ether 1:1)

$[\alpha]^{27}_D$= 7.5 mp = 44°C

[(2R,4R)-2-(tert-butoxycarbonyaminomethy)-4-(thymin-1-yl) pyrrolidin-1-yl]acetic acid **22**

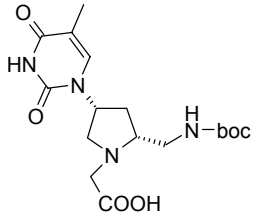

22

Starting from compound **21**, the method of preparation is same as for compound **9.** (Yield=50%, Rf=0.3, MeOH:DCM 2:8) mp = 94°C

(2R,4S)-N-benzyloxycarbonyl-2-(tert-butoxycarbonylaminomethyl) pyrrolidin-4-yl-benzoate **23**

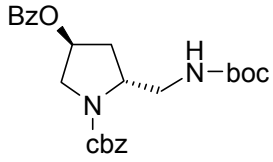

23

Using Mitsunobu conditions as followed for the synthesis of compound **19**, compound **17** was converted to **23.** The crude compound was dissolved in diethyl ether and petroleum ether was added into it to remove PPh_3O byproduct. The crystalline PPh_3O was filtered and the filtrate was concentrated under vacuum to obtain crude **23**. This crude product was used without further purification.

(Rf=0.5 EtOAc:Pet.ether 4:6)

(2R,4S)-N-benzyloxycarbonyl-2-(ter-butoxycarbonylaminomethyl)-4-hydroxy-pyrrolidine **24**

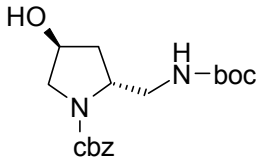

Compound **19** (2g, 4.4mmol) was taken in 2N NaOH in water:Methanol mixture (1:1, 20ml) and the reaction was stirred for 5h. The solvent was evaporated under *vacuo*. The residue was taken in EtOAc, washed with water and brine. Organic layer was then dried over anhy. Na_2SO_4 and concentrated to obtain compound **24** (1.5g, overall yield of benzoylation and hydrolysis=82%, Rf=0.5 EtOAc:Pet.ether 5:5). $[\alpha]^{27}_D$=50 ($CHCl_3$)

(2S,4S)-2-[(tert-butoxycarbonyl)aminomethyl]- 1-(ethoxycarbonylmethyl) pyrrolidin-4-yl-benzoate **25a**

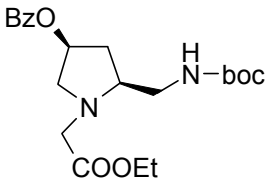

25a

Compound **7** obtained in scheme 2.1a was used for synthesizing **25** and the method of preparation was same as followed for compound **19**. The byproduct PPh_3O was removed by precipitation with diethyl ether and petroleum ether and the crude compound was used as such for the next step without further purification (Rf=0.45, EtOAc:Pet.ether 1:1).

(2S,4S)-2-[(tert-butoxycarbonyl)aminomethyl]- 1-(ethoxycarbonylmethyl) pyrrolidin-4-yl-O-tosylate **25b**

To a solution of compound **7** (1g, 3.3mmol) and PPh_3 (1.3g, 4.96mmol) in dry THF (10ml), methyl tosylate (0.75ml, 4.96mmol) was added slowly. The mixture was cooled in ice bath and DEAD (0.77ml, 4.96) was added dropwise with constant stirring. After

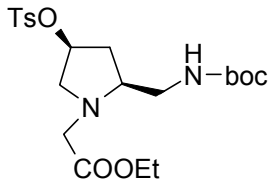

25b

3h, THF was removed under vacuum and the residue was purified by silica gel column chromatography to obtain (0.7g, yield=47%, Rf=0.3 EtOAc).

^{1}H (CDCl$_3$) δ 7.8 (d 2H Ar J=8.3Hz), 7.32 (d 2H Ar J=8.3Hz), 5.2-4.96 (m 2H C4H, NH), 4.15 (q 2H OCH_2CH_3 J=7.33Hz), 3.48-3.17 (m 5H C5H, N1-CH_2, C2H), 3.08-2.9 (m 2H CH_2NH), 2.44 (s 3H OCH_3), 2.35-2.18 (m 1H C3H), 1.86-1.75 (m 1H C3'H), 1.44 (s 9H $C(CH_3)_3$), 1.25 (t 3H OCH_2CH_3 J=7.33Hz)

(2S,4S)-2-[(tert-butoxycarbonyl)aminomethyl]- 1-(ethoxycarbonylmethyl) pyrrolidin-4-yl-benzoate **26**

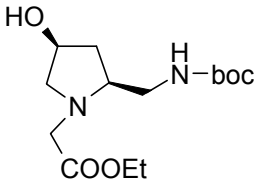

26

Solvolysis of compound **25a** to obtain **26,** was achieved using the procedure as followed for synthesis of **20** form **19** (overall yield of benzoylation and solvolysis=90%, Rf=0.45, EtOAc:Pet.ether 5:5).

1-benzyl 2-methyl (2S,4S)-4-(benzoyloxy)pyrrolidine-1,2-dicarboxylate **28**

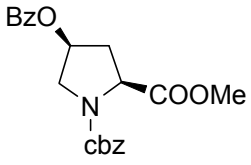

28

Starting from compound **2**, synthesis of **28** was achieved by following the same method as for compound **19.**
(Yield=80%, Rf=0.45, EtOAc:Pet.ether 3:7)
^{1}H (CDCl$_3$) δ 8-7.5 (m 5H C_6H_5 Bz), 7.5-7.1 (s 5H C_6H_5 Cbz), 5.2 (m 3H OCH_2, C4H), 4.7-4.45 (m 1H C2H), 4-3.6 (m 2H C5H), 3.74-3.53 (2s 3H major, minor $COOCH_3$), 2.5-2.1 (m 2H C3H)

(2S,4S)-1-(benzyloxycarbonyl)-4-hydroxypyrrolidine-1-methylcarboxylate **29**

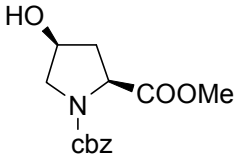

29

After subjecting the compound **28** to methanolysis conditions as followed in the preparation of compound **20**, desired product was obtained in 90% yield. (Rf=0.45, EtOAc:Pet.ether 5:5). $[\alpha]^{27}_D$= -5.3
^{1}H (CDCl$_3$) δ 7.33, 7.3 (2s 5H major, minor C_6H_5), 5.26-4.99 (m 2H OCH_2), 4.45, 4.35 (m 2H C4H, C2H), 3.76, 3.59 (2s 3H $COOCH_3$), 3.67-3.52 (m 2H C5H), 2.32-2.25 (m 1H C3H), 2.24-2.02 (m 1H C3'H)
^{13}C NMR (CDCl$_3$) δ 174.1, 174.0 ($COOCH_3$), 154.8, 154.3 (NCO), 136.2, 128.2, 127.8, 127.6 (C_6H_5), 70.4, 69.4 ($COOCH_3$), 67.1 (OCH_2), 57.9, 57.6 (C4), 55.3, 55.1 (C5), 52.5, 52.3 (C2), 38.5, 37.6 (C3)

(2S,4R)-1-(benzyloxycarbonyl)-4-[N3-benzoylthymin-1-yl]pyrrolidine-1-methylcarboxylate **30**

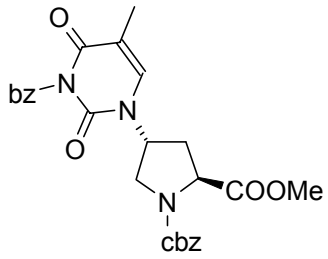

The method of preparation of **30** from compound **29** was same as followed for synthesis of compound **8.**

(Rf=0.4, EtOAc:Pet.ether 4:6)

^{1}H (CDCl$_3$) δ 8.0-7.3 (m 11H ArH, H6-Thy), 5.4-5.1 (m 3H C4H, OCH_2), 4.6-4.4 (m 1H C5H), 4.15-3.9 (m 1H C5'H), 3.9-3.6 (m 4H OCH_3, C2H), 2.3-2.1 (m 2H C3H, C3'H), 2.0 (s 3H CH_3-Thy).

(2S,4R)-1-(benzyloxycarbonyl)-4-(thymin-1-yl)-2-(hydroxymethyl)-pyrrolidine **31**

Compound **30** (3.5g, 7.12mmol) was taken in dry THF (50ml) and cooled to 0-5^{o}C in an ice bath. $LiBH_4$ (320mg, 14.2mmol) was added into it in two portions in 30 min. The reaction mixture was stirred for 7hrs, and solvent was evaporated in vacuum. The residue was extracted with MeOH:EtOAc mixture (5X20ml, 2:8) and the organic layer was dried under vacuum. The crude residue was further purified by column chromatography to obtain pure **31** (2.5g, yield=98%, Rf=0.3, MeOH:EtOAc 5:95)

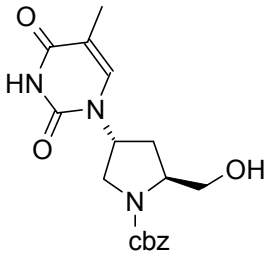

31

^{1}H (CDCl$_3$) δ 9.69 (s 1H Thy NH), 7.32 (s 5H C_6H_5), 5.05 (m 3H C4H, $OCH_2C_6H_5$), 4.15 (bs 1H OH), 3.84-3.19 (m 5H C5H, C5'H, CH_2OH, C2H), 2.2-2.0 (m 2H C3H, C3'H)

IR (CHCl$_3$) cm^{-1} 3018, 2399, 1689, 1419, 1215 $[\alpha]^{27}_D$= -47

(2S,4R)-1-benzyloxycarbonyl-4-(thymin-1-yl)-2-(p-toluenesulfonyloxy methyl)pyrrolidine **32**

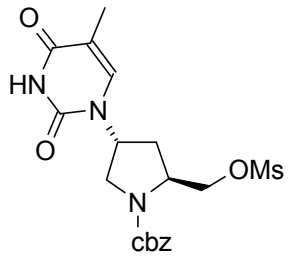

32

Compound **31** (2.7g, 7.5mmol) was taken in dry pyridine (25ml) and mesylchloride (0.64ml, 8.27mmol) was added dropwise into it while maintaining the reaction temperature 0^{o}C during addition. Reaction mixture was stirred at 0^{o}C for 1h and then was kept in refrigerator overnight. Pyridine was evaporated under vacuum, and residue was purified by column chromatography to afford pure **32** (2g, Yield=62%, Rf=0.35, MeOH:EtOAc 5:95)

(2S,4R)-1-benzyloxycarbonyl-4-(thymin-1-yl)-2-(azidomethyl)pyrrolidine **33**

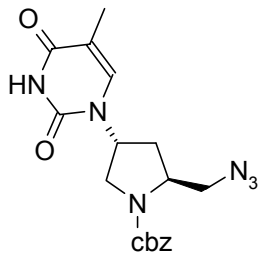

33

The mesyl **32** (2g, 4.57mmol) was taken in dry DMF 920ml) and NaN_3 (2.37g, 36.6mmol) was added into it. The mixture was heated at 70°C for 7h and the solvent was evaporated under vacuum. Water (10ml) was added to the residue and was extracted with EtOAc (5X25ml). Organic layer was then washed with water, brine, dried over anhy. $NaSO_4$ and concentrated to get azide **33** (1g, 57%, Rf=0.4, MeOH:EtOAc 5:95) $[\alpha]^{27}_D$= -32

^{1}H (CDCl$_3$) δ 10.39 (bs 1H NH-Thy), 7.27 (s 5H C_6H_5), 6.93 (s 1H H6-Thy), 5.1 (s 2H OCH_2), 5 (m 1H C4H), 4.18 (m 1H C5H), 3.76-3.35 (m 2H C5'H, C2H), 2.23 (m 2H C3H), 1.98 (s 2H CH_2N_3), 1.79 (s 3H CH_3-Thy)

IR (neat) cm^{-1} 3018, 2108, 1691, 1215

(2S,4R)-N-benzyloxycarbonyl-2-(tert-butoxycarbonylaminomethyl)-4-(thymin-1-yl)pyrrolidine **34**

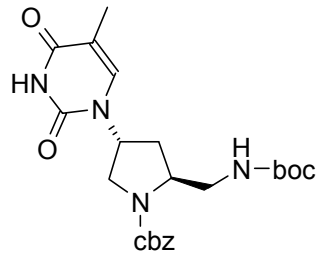

34

Compound **39** (3g, 5.33mmol) was taken in 2N NaOH solution Methanol:water (50mL, 4:1) and was stirred for 9h. Methanol was evaporated and water (20ml) was added into it. The aqueous layer was washed with EtOAc (3X50mL) and all organic layers were pooled together, washed with water and brine. EtOAc layer was dried over anhy. $NaSO_4$ and concentrated under *vacuo* to get **34** (2.4g, yield=98%, Rf=0.3, MeOH:$CHCl_3$ 1:99). $[\alpha]^{27}_D$= -9.96 mp = 81°C

^{1}H NMR (CDCl$_3$) δ (bd 1H NH-Thy), 7.33 (s5H C_6H_5), 6.87 (s 1H H6-Thy), 5.27-5.01 (m 3H NH-Boc, CH_2Ph), 4.2 (m 1H C4H), 3.83-3.30 (m CH_2NH, C5H, C5'H), 2.31-2.16 (m 2H C2H, C3H), 2-1.75 (m 4H C3'H, CH_3-Thy), 1.42 (s 9H, $C(CH_3)_3$)

(2S,4S)-N1-(benzyloxycarbonyl)-4-hydroxy-2-(hydroxymethyl)-pyrrolidine **35**

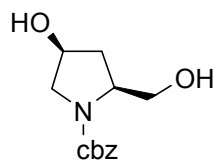

The methyl ester in compound **29** was reduced using the same procedure as followed the preparation of compound **3.**

(Yield=90%, Rf=0.5, EtOAc:Pet. ether 4:5)

(2S,4S)-N-benzyloxycarbonyl 2-[(tert-butoxycarbonyl)aminomethyl]-4-hydroxypyrrolidine **38**

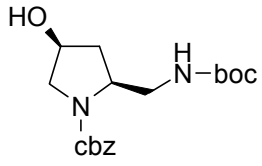

38

Compound **37** (3g, 10.8mmol) was taken in methanol (15ml), and Raney Nickel (1.5 ml, suspension in water) was added into it. This slurry was subjected to hydrogenation at pressure 40psi for 1.5h, filtered through Celite and solvent was evaporated to obtain dry free amine 92.7g). *t*-Boc azide (1.85ml, 12.9 mmol), Et_3N(1.9ml, 14.0 mmol) and DMSO (20 ml) were added into it. The reaction mixure was heated at 50^oC for 9h and then allowed to cool. This mixture was poured in a beaker containing ice water (150ml) and the precipitates thus formed were extracted with diethylether (5X50ml). All organic layers pooled together were washed with water, brine, and dried over anhy. Na_2SO_4. The ether layer was concentrated to dryness under vacuum to achieve *t*-Boc protected amine **38** (2.93g, 73.8%, Rf=0.55, EtOAc:Petroleum ether 5:5).

^{1}H NMR ($CDCl_3$) δ 7.33 (s 5H $C_6\underline{H}_5$), 5.67 (bs 1H N$\underline{H}$), 5.12 (s 2H O$C\underline{H}_2$), 4.42 (m 1H C4$\underline{H}$), 4.17-3.88 (m 2H C5$\underline{H}$), 3.72-3.15 (m 4H $C\underline{H}_2$NH, C2$\underline{H}$, O$\underline{H}$), 1.41 (s 9H C($C\underline{H}_3$)$_3$)

^{13}C NMR ($CDCl_3$) δ 156.84 (N$\underline{C}$O), 155.4 (NH$\underline{C}$O), 136.4, 128.2, 127.7, 127.5 (Ar), 69.87 ($\underline{C}(CH_3)_3$), 68.81 (O$\underline{C}H_2$), 57.3, 57.26 ($\underline{C}$4), 55.3 ($\underline{C}$2), 55.09 ($\underline{C}$5), 44.06 ($\underline{C}H_2$NH), 36.75, 36.23 ($\underline{C}$3), 20.5 ($C(\underline{C}H_3)_3$)

$[\alpha]^{27}_D$= -.0.47

(2S,4R)-N-benzyloxycarbonyl 2-[(tert-butoxycarbonyl)aminomethyl]-4-(N3-benzoylthymin-1-yl)pyrrolidine **39**

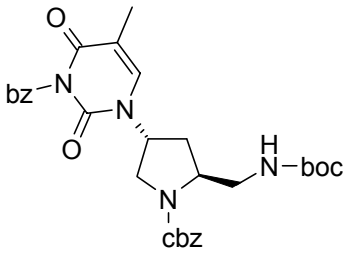

39

Compound **38** was subjected to Mitsunobu conditions using the same method as followed for the preparation of **8,** which afforded compound **39** (yield=50%, Rf=0.32, MeOH:DCM 1:99)

^{1}H NMR ($CDCl_3$) δ 7.9-7.45 (m 5H $C_6\underline{H}_5$ Bz), 7.35 (s 5H $C_6\underline{H}_5$ Cbz), 6.96 (s 1H $\underline{H}$6-Thy), 5.16 (s, bs 3H O$C\underline{H}_2$, N$\underline{H}$), 4.24-4.1 (C4$\underline{H}$), 3.87-3.73 (m 2H C5$\underline{H}$), 3.48-3.24 (m 2H $C\underline{H}_2$NH), 2.26 (m 2H C2$\underline{H}$, C3$\underline{H}$), 2.03-1.79 (m 4H $C\underline{H}_3$-Thy, C3'$\underline{H}$), 1.41 (s 9H C($C\underline{H}_3$)$_3$)

Ethyl [(2S,4R)-2-(tert-butoxycarbonyaminomethy)-4-(thymin-1-yl) pyrrolidin-1-yl]acetate **41**

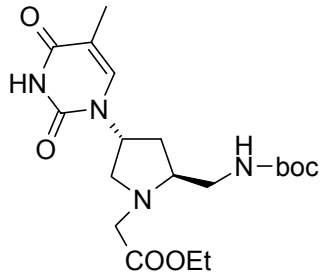

41

Compound **34** (2g, 4.36mmol) and Pd-C (1g) was taken methanol (20 ml) in 500ml hydrogenation flask and acetic acid (0.5ml) was added into it. The reaction mixture was hydrogenated at 60-psi pressure for 20 h. The solvents were removed and DIPEA (1ml) was added into it. The mixture was dried under *vacuo* and CH_3CN (20mL), KF-Celite (1.8g, 15.2mmol) and ethylbromoacetate (0.6 ml, 5.24mmol) were added to it. After stirring at room temperature overnight, the reaction mixture was filtered over celite and the filtrate was evaporated to dryness. The residue was purified by chromatography (100-200 mesh silica) using MeOH/DCM system to obtain pure product 41 (1.34g, yield=73%, Rf = 0.2, MeOH:DCM 7:93) $[\alpha]^{27}_{D}$= -9.75 mp = 112.5 ^{o}C

[(2S,4R)-2-(tert-butoxycarbonyaminomethy)-4-(thymin-1-yl)pyrrolidin-1-yl]acetic acid **42**

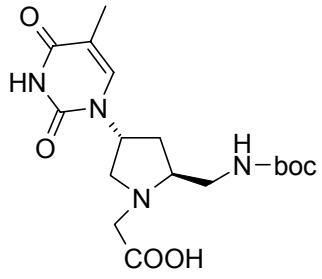

42

Ester **41** (o.5g 1.2mmol) was dissolved in methanol (3ml) and NaOH aq. solution (2N, 3ml) was added into it. The mixture stirred for 30min and methanol was evaporated under vacuum. Cation exchange resin (Dowex H+) was added to the aq. solution to bring pH~5. The resin was filtered and the filtrate was evaporated to dryness and coevaporated with toluene 92X20ml) to get white foam 42 (0.31g, yield=68%, Rf=0.42 MeOH:DCM 2:8) mp = 138 ^{o}C

(2R,4S)-N-benzyloxycarbonyl 2-[(tert-butoxycarbonyl)aminomethyl]-4-(N3-benzoylthymin-1-yl)pyrrolidine **43**

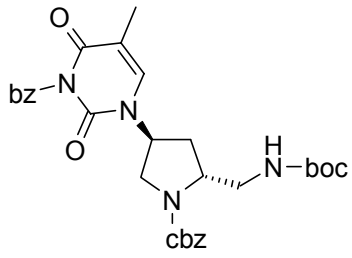

43

Compound **16** was subjected to Mitsunobu conditions using the same method as followed for the preparation of compound **8** to obtain **43** (yield=70%, Rf=0.32, MeOH:DCM 1:99).

N1-(tert-Boc)-1,2-diaminoethane **47**

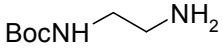

47

1,2-diaminoethane (20g, 0.33mol) was taken in dioxane:water (1:1, 500ml) and cooled in an ice-bath. *tert*-Boc-azide (6ml, 41mmol) in dioxane (50ml) was slowly added with stirring. The mixture was stirred for 8h and the resulting solution was concentrated to 100ml. The N1,N2-di-Boc derivative not being soluble in water, precipitated, and it was removed by filtration. The corresponding N1-mono-Boc derivative was obtained by repeated extraction from the filtrate in ethyl acetate. The removal of solvents yielded the mono-*tert*-Boc-diaminoethane **47** (5.9g, 88%). Rf=0.25 (DCM: MeOH: NH_4OH 89:10:1)

^{1}H NMR ($CDCl_3$) δ: 5.21 (br s 1H N<u>H</u>CO), 3.32 (t 2H J=8 Hz CONHC<u>H_2</u>), 2.54 (t 2H J=8 Hz C<u>H_2</u>NH_2), 1.42 (s 9H C(C<u>H_3</u>)$_3$).

Ethyl N-(2-tert-Boc-aminoethyl)-glycinate **48**

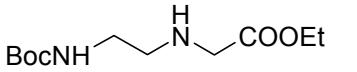

48

The *N1*-(tert-Boc)-1,2-diaminoethane **47** (5.8g, 36.2mmol) in acetonitrile (100ml) was stirred at 60^{o}C temperature in the presence of KF-Celite (15g, 129mmol). Then ethylbromoacetate (3.6ml, 32.6mmol) was added into it After stirring the mixture for 1.5h, solid was separated by filtration and the filtrate was evaporated to obtain the crude ethyl *N*-(2-tert-Boc-aminoethyl)-glycinate, which was purified by column chromatography to get **48** (5.3g, yield=67%, Rf=0.3, EtOAc) as a light yellow oil.

^{1}H NMR ($CDCl_3$) δ: 5.02 (bs 1H CON<u>H</u>), 4.22 (q 2H J=8Hz OC<u>H_2</u>CH_3), 3.35 (s 2H NHC<u>H_2</u>), 3.20 (t 2H J=6Hz CONHC<u>H_2</u>), 2.76 (t 2H J=6Hz C<u>H_2</u>$NHCH_2$), 1.46 (s 9H C(C<u>H_3</u>)$_3$), 1.28 (t 3H J=8Hz OCH_2C<u>H_3</u>).

Ethyl N-(tert-Boc-aminoethyl)-N-(chloroacetyl)-glycinate **49**

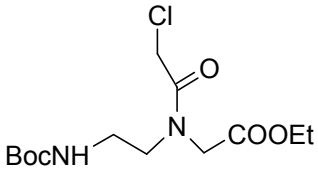

49

The ethyl *N*-(2-Boc-aminoethyl)-glycinate **48** (4.0g, 16.2mmol) was taken in 10% Na_2CO_3 soln. (12g, 113mmol) in water:dioxane (1:1) and cooled in an ice bath. Chloroacetyl chloride (6.5ml, 81mmol) was added with vigorous stirring. PH~9 was maintained during the reaction with addition of more Na_2CO_3. After 15 min., the reaction mixture was concentrated to remove the dioxane. The product was extracted from the aqueous layer with dichloromethane and was purified by column chromatography to obtain the ethyl *N*-

(tert-Boc-aminoethyl)-*N*-(chloroacetyl)-glycinate **49** as a colorless oil in good yield (4.2g, yield=80%, Rf=0.3, EtOAc:Pet.ether 2:8).

^{1}H NMR ($CDCl_3$) δ: 5.5 (bs 1H NH), 4.35-4.2 (q 2H J=8Hz $OC\underline{H}_2CH_3$), 4.2 (s 2H $C\underline{H}_2Cl$), 4.00 (s 2H $NC\underline{H}_2COO$), 3.53 (m 2H $C\underline{H}_2NCO$), 3.28 (q 2H J=8Hz $NHC\underline{H}_2CH_2$), 1.46 (s 9H $C(C\underline{H}_3)_3$), 1.23 (t 3H J=8Hz $OCH_2C\underline{H}_3$).

N-(tert-Boc-aminoethylglycyl)-thymine ethyl ester **50**

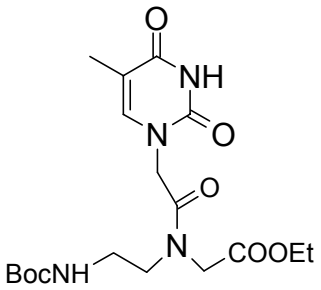

50

Ethyl *N*-(*tert*-Boc-aminoethyl)-*N*-(chloroacetyl)-glycinate **49** (1.0g, 3.1mmol) was stirred with anhydrous K_2CO_3 (0.47g, 3.4mmol) in DMF with thymine (0.41g, 3.25mmol) at 70°C for 5-6 hrs. DMF was evaporated from reaction mixture and crude oil was purified by column chromatography to obtain **50 (**1g, yield=83%, Rf=0.2 MeOH:DCM 5:95)

^{1}H NMR ($CDCl_3$) δ 9.00 (bs 1H Thy-N$\underline{H}$), 7.05 (min) & 6.98 (maj) (s 1H Thy-$\underline{H}$6), 5.65 (maj) & 5.05 (min) (br s 1H N$\underline{H}$COO), 4.58 (maj) & 4.44 (min) (s 1H Thy-$C\underline{H}_2$), 4.25 (m 2H $OC\underline{H}_2$), 3.55 (m 2H $C\underline{H}_2NCO$), 3.36 (m 2H $NHC\underline{H}_2$), 1.95 (s 3H Thy-$C\underline{H}_3$), 1.48 (s 9H $C(C\underline{H}_3)_3$), 1.28 (m 3H $OCH_2C\underline{H}_3$).

N-(tert-Boc-aminoethylglycyl)-(N^4-benzyloxycarbonyl cytosine)ethyl ester **52**

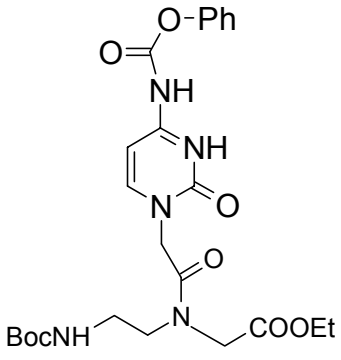

52

To a suspension of N^4-benzyloxycarbonyl cytosine **58** (1.3g, 6.52mmol) in DMF (20ml) at 75°C, NaH (0.16g, 6.83mmol) was added slowly and stirred for 30 min. When the formation of sodium salt of nucleobase was complete which is indicated by ceased effervescence, solution of ethyl *N*-(*tert*-Boc-aminoethyl)-*N*-(chloroacetyl)-glycinate **49** (2.0g, 6.2mmol) in DMF (10ml) was added. After stirring it for another 1h at 75°C, DMF was removed under *vacuo* and crude solid was purified by column chromatography to obtain the cytosine monomer, *N*-(Boc-aminoethylglycyl)-(N^4-benzyloxycarbonyl cytosine)ethyl ester **52**, in moderate yield (1.42g, yield=47% Rf=0.3 MeOH:DCM 5:95)

^{1}H NMR ($CDCl_3$) δ: 7.65 (d 1H Cyt-H6 J=8Hz), 7.35 (s 5H Ar), 7.25 (d 1H C-H5 J=8Hz), 5.70 (br s 1H NH), 5.20 (s 2H Ar-$C\underline{H}_2$), 4.71 (maj) & 4.22 (min) (bs 2H Cyt-CH_2), 4.15 (q, 2H $OC\underline{H}_2CH_3$), 4.05 (s, 2H $NC\underline{H}_2COO$), 3.56 (m 2H $NC\underline{H}_2$), 3.32 (m 2H $NHC\underline{H}_2CH_2$), 1.48 (s 9H $C(C\underline{H}_3)_3$), 1.25 (t 3H $OCH_2C\underline{H}_3$).

N-(tert-Boc-aminoethylglycyl)-adenine ethyl ester **53**

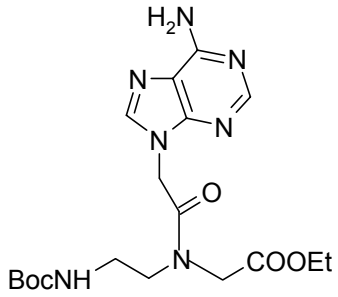

53

This compound was prepared from adenine and the common precursor **49** as described for **52** (yield=54%, Rf=0.2, MeOH:DCM 5:95)

^{1}H NMR ($CDCl_3$) δ: 8.32 (s 1H), 7.95 (min) & 7.90 (maj) (s 1H), 5.93 (maj) & 5.80 (min) (bs 2H), 5.13 (maj) & 4.95 (min), 4.22 (min) & 4.05 (maj) (s 2H), 4.20 (m 2H), 3.65 (maj) & 3.55 (min) (m 2H), 3.40 (maj) & 3.50 (min) (m 2H), 1.42 (s 9H), 1.25 (m 3H).

N-(Boc-aminoethylglycyl)-2-amino-6-chloropurine ethyl ester **54**

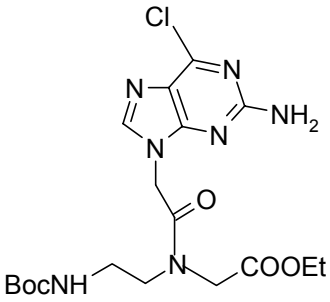

54

This compound was prepared from 2-amino-6-chloropurine and the common precursor **49** as described for **51** (Yield=90%, Rf=0.25, MeOH:DCM 5:95)

^{1}H NMR ($CDCl_3$) δ: 7.89 (min) & 7.85 (maj) (s 1H), 7.30 (s 1H), 5.80 (bs 1H, N*H*), 5.18 (bs 2H), 5.02 (maj) & 4.85 (min) (s 2H), 4.18 (min) & 4.05 (maj) (s 2H), 3.65 (maj) & 3.16 (min) (m 2H), 3.42 (maj) and 3.28 (min) (m 2H), 1.50 (s 9H), 1.26 (m 3H).

N^4-Benzyloxycarbony cytosine **58**

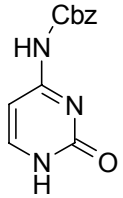

58

Over a period of about 15min, 50% soln of benzyloxycarbonyl chloride in toluene (12.3ml, 36mmol) was added dropwise to a suspension of cytosine (2g, 18mmol) in dry pyridine (100ml) at 0^{o}C underanhydrous conditions. The solution then was stirred vigorously for 20hrs, after which the pyridine suspension was evaporated to dryness, in vacuum. To the reaction mixture, an Ice cold water (20ml) followed by 2N HCl was added to reach pH~2. The resulting white precipitate was filtered off, washed with water and partially dried by air suction. The still-wet precipitate was boiled with absolute ethanol (50ml) for 10 min, cooled to 0^{o}C, filtered, washed thoroughly with ether, and dried in vacuum to obtain of **2** (2.7g, yield= 61%, Rf=0.3, MeOH:DCM 1:9, mp=256^{o}C)

^{1}H NMR (DMSO-d6) δ: 7.71-7.67 (d 1H J=7.32hz C6H-Cyt), 7.28 (s 5H C_6H_5 Cbz), 6.84-6.6 (d 1H J=7.32) C5H-Cyt), 5.02 (s 2H OCH_2)

m/z=245 (calcd for $C_{12}H_{11}N_3O_3$ 245.2)

General method for hydrolysis of carboxy esters

The ethyl esters (**50**-**53**) were hydrolyzed using 2N aqueous NaOH (5ml) in methanol (5ml), except in the case of cytosine monomer where mild base LiOH was used. The resulting salt was neutralized with cation exchange resin (Dowex H+) till the pH of the solution was 5.The resin was removed by filtration and the filtrate was concentrated to obtain the resulting tert-Boc-protected acid (**54**-**57**) in excellent yield (>85%).

pK_a determination

20 mg of each monomer (**22** and **46**) was taken separately in one ml of deionised water and made the pH ~2 with few μl of 2NHCl. NaOH solution of approximately ten times the concentration of the monomer, was prepared which was added to the monomer solution in small amounts (2 μl) with constant stirring. pH was recorded after each addition.

Functionalization of the Merrifield Resin (Gisin, 1970)

N-*tert*-butoxycarbony-β-alanine (1g, 5.29mmol) was dissolved in methanol and was neutralized with saturated aqueous solution of exactly 1 equivalent cesium carbonate (0.86g, 2.6mmol) (Hodges & Merrifield, 1975). Ethanol was evaporated under vacuum and co evaporated with toluene (four times) to get dry salt (1.7g). Merrifield resin (3g, 2.1mmol/g) and the cesium salt (1.7g, 5.29mmol) were added in dry DMF (40ml) and the slurry was stirred (not vigorously) at 60 ^{o}C for 36hrs. The reaction mixture was filtered in a sintered funnel, washed thoroughly with DMF, followed by DMF: Water (9:1 v/v), DMF and ethanol. It was dried under vacuum over P_2O_5 to obtain functionalised resin (3.26g).

Picric Acid Estimation of functionalised resin

The procedure for estimation of the loading value of the resin was carried out with 5mg of the resin and comprised the following steps:

The resin was swollen in dry CH_2Cl_2 for at least 30min. The CH_2Cl_2 was drained off and a 50% solution of TFA in CH_2Cl_2 was added (1ml x 2), 10 min each. After washing thoroughly with CH_2Cl_2, the TFA salt was neutralized with a 5% solution of DIPEA in CH_2Cl_2 (1ml x 2, 2 min each). The free amine was treated with a 0.1M picric acid solution in CH_2Cl_2 (2ml x 2, 3min each). The excess picric acid was washed away with CH_2Cl_2. The adsorbed picric acid was displaced form the resin by adding a solution of

5% DIPEA in CH_2Cl_2. The eluant was collected and the volume was made up to 10 ml with CH_2Cl_2 in a volumetric flask. The absorbance was recorded at 358nm in ethanol and the concentration of the amine groups on the resin was calculated using the molar extinction coefficient of picric acid 14,500 $cm^{-1}M^{-1}$ at 358 nm.

Kaiser Test

Kaiser's test was used to monitor the t-Boc-deprotection and amide coupling steps in the solid phase peptide synthesis. Three solutions were used, viz. (1) Ninhydrin (5.0 g) dissolved in ethanol (100 ml), (2) Phenol (80 g dissolved in ethanol (20 ml) and (3) KCN: 2 ml of a 0.001M aqueous solution of KCN in 98 ml pyridine).

To a few beads of the resin to be tested taken in a test tube, were added 3-4 drops of each of the three solutions described above. The tube was heated at 100 ^oC for ~2min, and the color of the beads was noted. A blue color on the beads, which slowly comes in solution, indicated successful deprotection, while colorless beads and the solution confirmed the completion of the amide coupling reaction. The blank solution should remain yellow.

Cleavage of the PNA from the Resin

The resin (20mg) was stirred with thioanisole (38μl) and 1,2-ethanedithiol (13μl) in an ice bath for ten minutes. TFA (250μl) was added, and after equilibration for ten minutes, TFMSA (29μl) was added slowly. The reaction mixture was stirred at for 1.5h room temperature, filtered and concentrated in *vacuo*. The product was precipitated with dry ether from methanol and the precipitate was dissolved in water (200μl) and loaded over Sephadex G25 column. 0.5ml fractions were collected and the presence of oligomer was detected by measuring the absorbance at 260nm. The fractions containing the oligomer were freeze-dried and the purity of the fractions was assessed by analytical RP-18 HPLC

HPLC (High Performance Liquid Chromatography) purification of oligomers

Peptide purifications were performed on a Waters DELTAPAK –RP4 (30 X 0.78 cm, 15μm) semi-preparative column attached to a Hewlett Packard 1050 HPLC system equipped with an auto sampler and Jasco-UV970 variable-wavelength detector. An isocratic elution method with 10% CH_3CN in 0.1% TFA/H_2O was used with flow rate 1.5ml/min. and the eluant was monitored at 260nm. The purity of the oligomers was further assessed by RP-18 analytical HPLC column (25x0.2cm, 5μm) with gradient

elution: A→ 50% B in 30min, A=0.1% TFA in H_2O, B=0.1% TFA in CH_3CN:H_2O 1:1 with flow rate 1ml/min. Representative HPLC profiles and mass spectra are shown in (Figure 14 and 15) and (Figure 16) respectively.

MALDI-TOF Mass spectrometry

The structural integrity of the oligomers was verified by MALDI-TOF mass spectrometry (Bulter *et al.*, 1996). Several matrices are reported in the literature like sinapinic acid (3,5-dimethoxy-4-hydroxycinnamic acid), CHCA (α-cyano-4-hydroxycinnamic acid) and DHB (2,5-dihydroxybenzoic acid), of these, sinapinic acid was found to give the best results.

Binding stoichiometry

Nine mixtures were made with molar ratios of the strands of 9:1, 8:2, 7:3, 6:4, 5:5, 4:6, 3:7, 2:8, 1:9. Together with samples of the individual strands, this gave eleven samples, all of the same strand concentration (2μM) in Sodium phosphate buffer (10 mM, pH 7.3). The samples, including the individual strands, are heated to 85^o in water bath for 2.0 min., allowed to cool to room temperature and then cooled further to 15^o. CD spectra for all the eleven samples were recorded at 15^{o}C with wavelength range 190-350 nm with scan speed-100nm/min, accumulation-6, response time-4sec, bandwidth-1nm and sensitivity-10mdeg. CD cell used for the studies was of 10mm path length. Base line was subtracted from all the CD spectra.

UV-Tm Experiments

The melting experiments were carried out in 10mM phosphate buffer. PNA/*Pyrrolodinyl*PNA with complementary oligonucleotide each at a strand concentration with concentration 2μM and and 1μM respectively based on UV absorbance calculated using molar extinction coefficient at 260nm, A=15.4, C=7.3, G=11.7, T=8.8 $cm^2/\mu M$, were mixed, heated to 80^{o}C for 2min., cooled to room temperature and kept in refrigerator at 4^{o}C overnight. The A_{260} at various temperatures were recorded using perkin Elmer 15 UV/VIS spectrophotometer, equipped with variable temperature probe, Julabo water circulator with a heating rate of 0.5^{o}C/min. over the range of 5-85^{o}C. Nitrogen gas was flushed in the spectrophotometer chamber to prevent the condensation of water at low temperature. Microcal Origin software was used for data analysis.

Appendix I

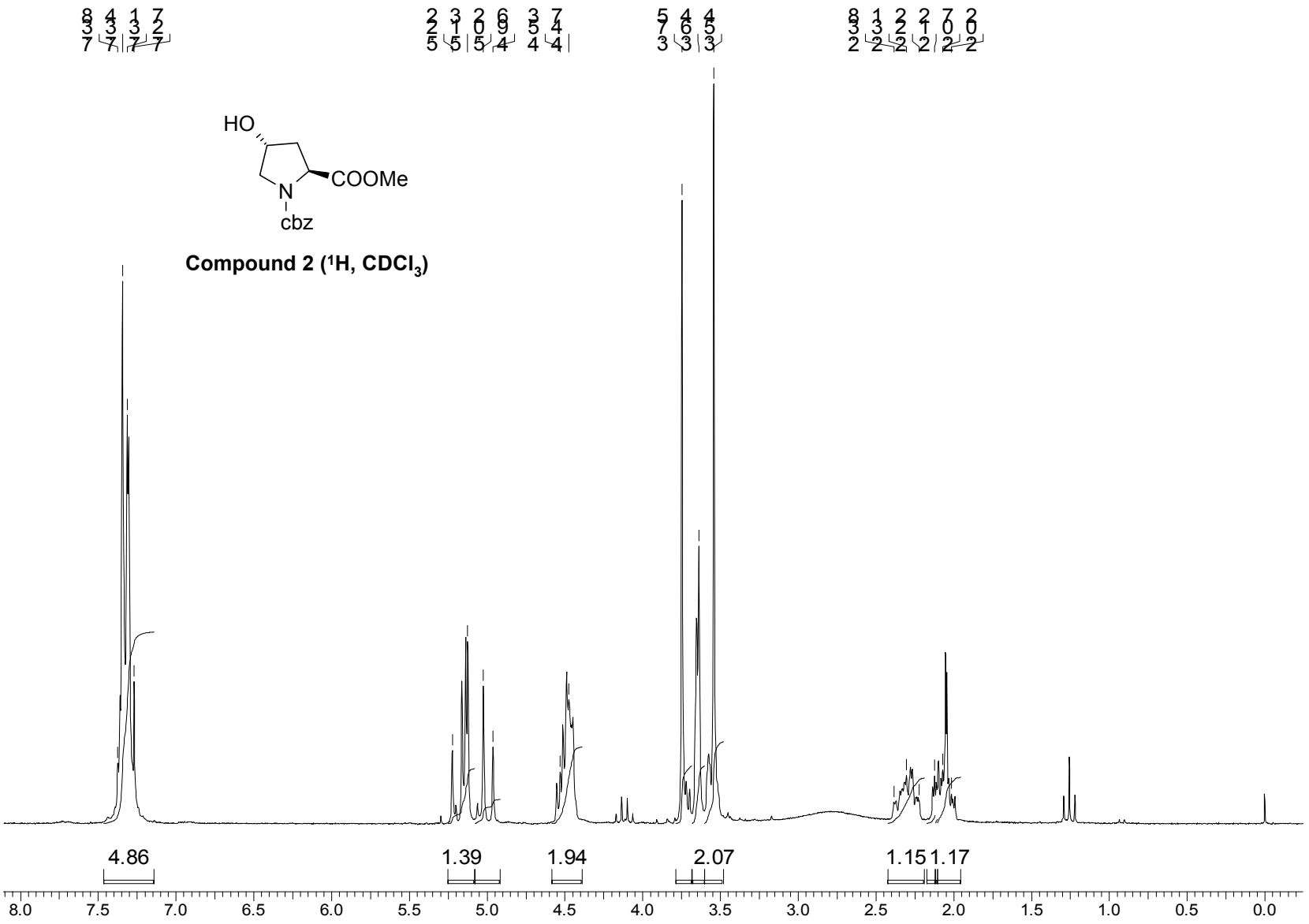

Compound 2 (^{1}H, $CDCl_3$)

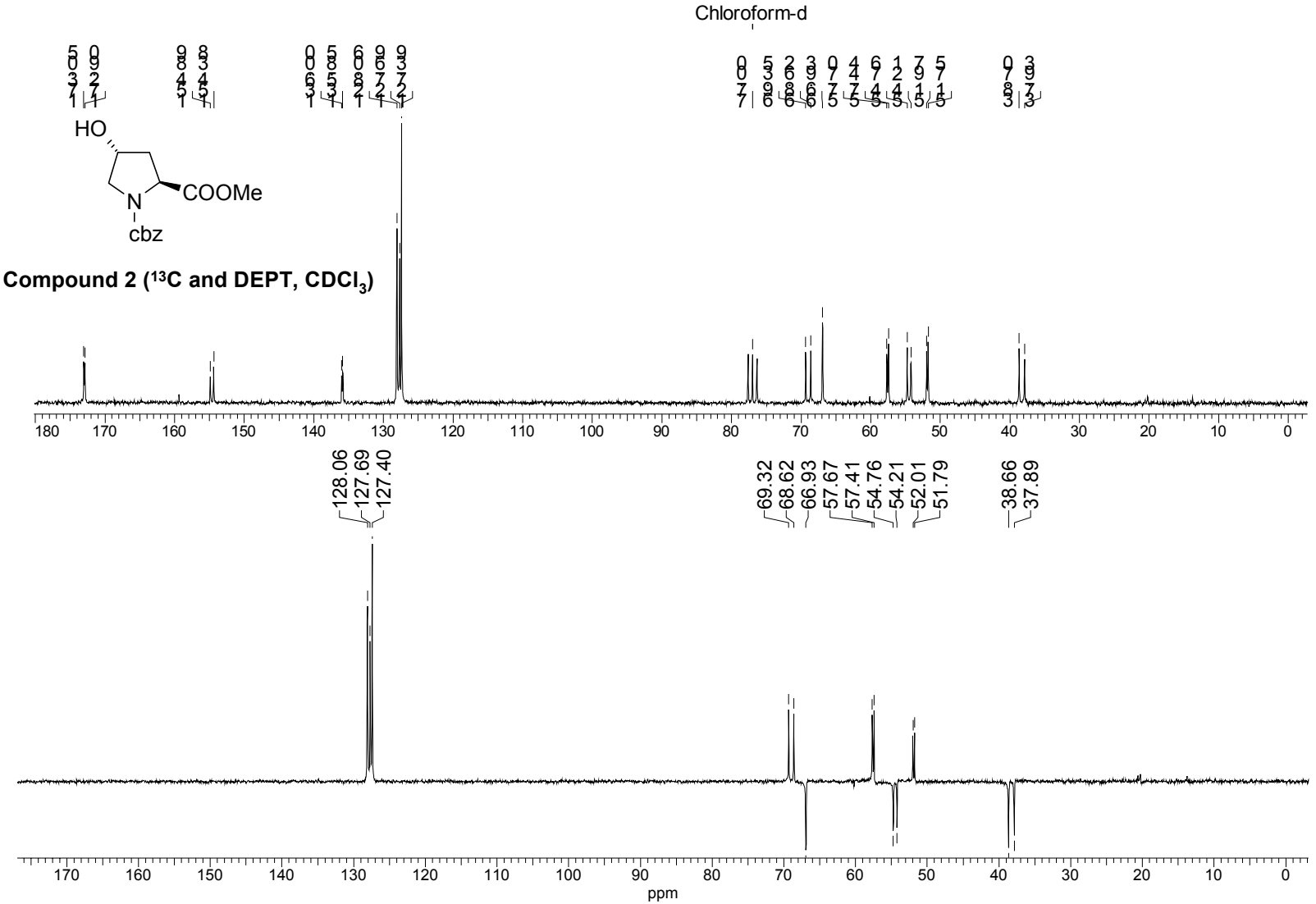
Chloroform-d
HO
COOMe
N
cbz
Compound 2 (13C and DEPT, CDCl3)
128.06
127.69
127.40
69.32
68.62
66.93
57.67
57.41
54.76
54.21
52.01
51.79
38.66
37.89
ppm

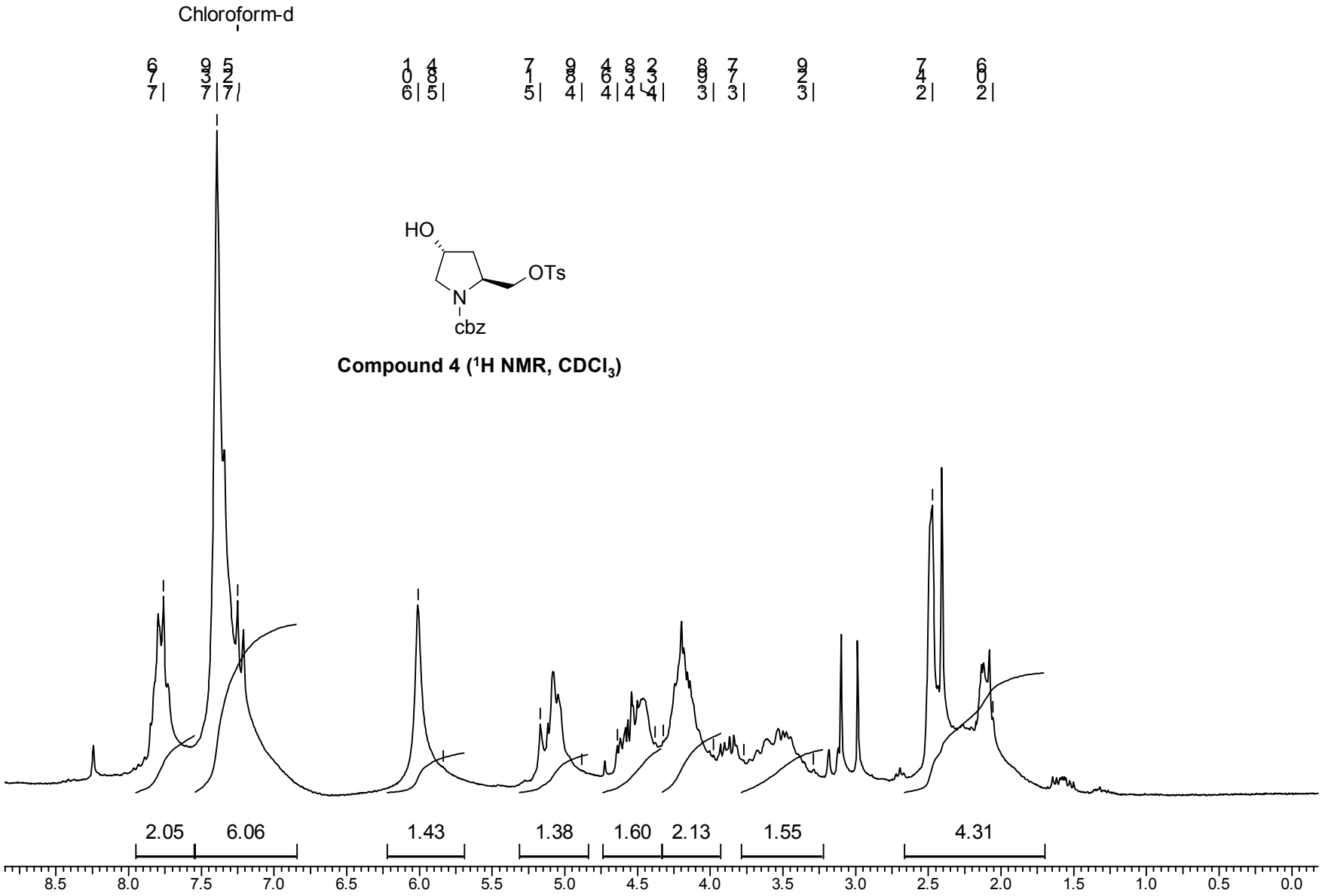

Compound 4 (^{1}H NMR, $CDCl_3$)

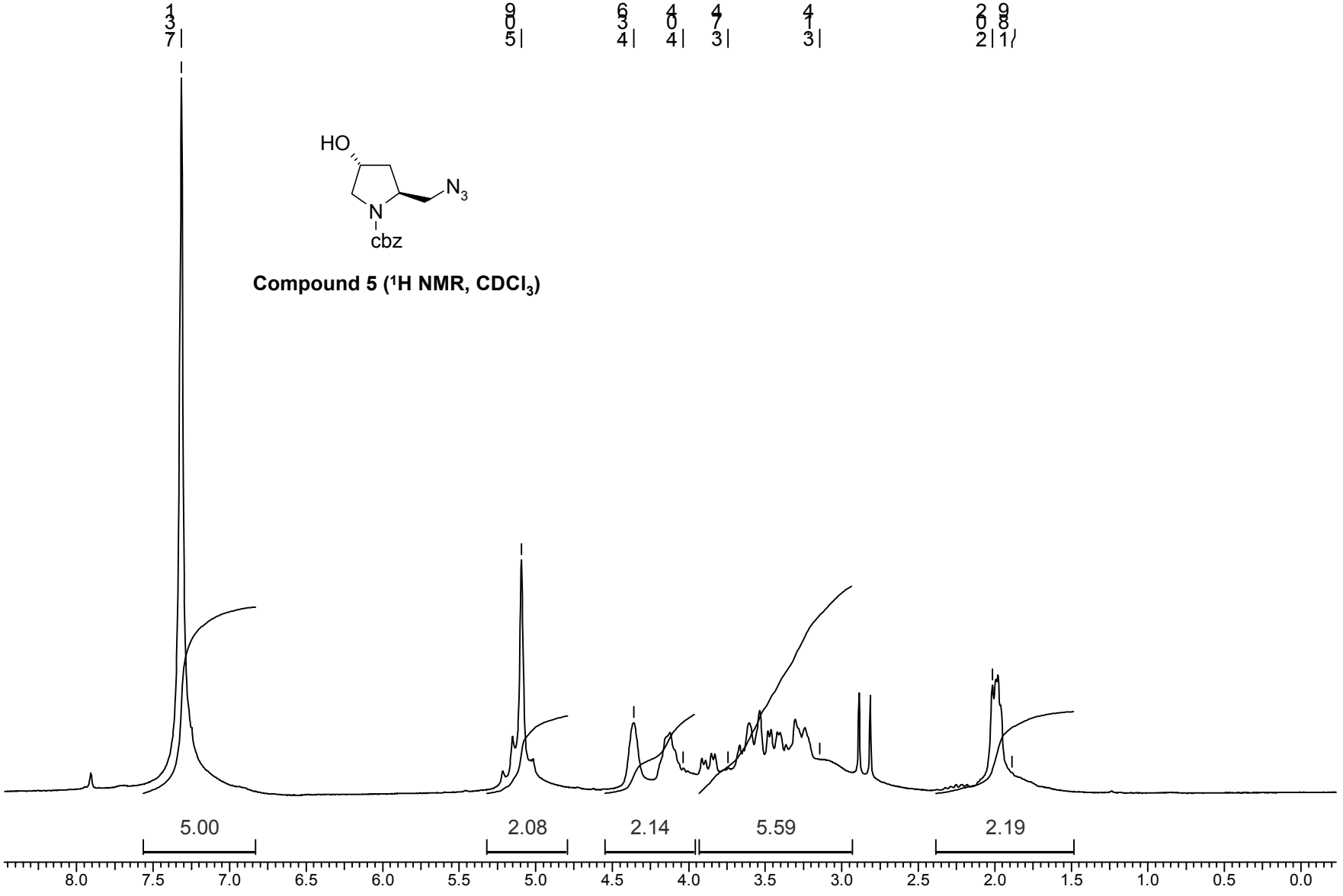

Compound 5 (^{1}H NMR, $CDCl_3$)

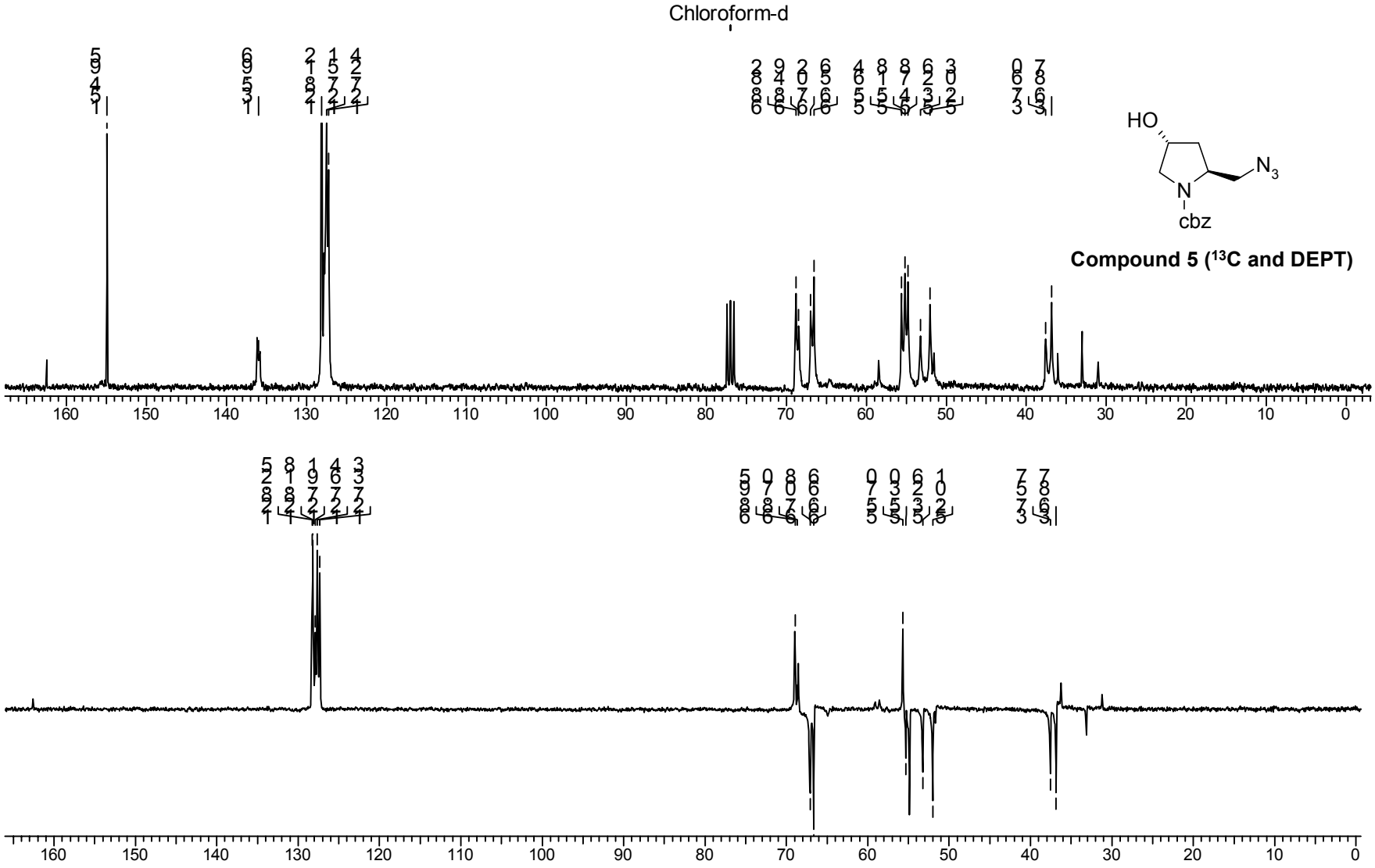
Chloroform-d
HO
N3
N
cbz
Compound 5 (13C and DEPT)

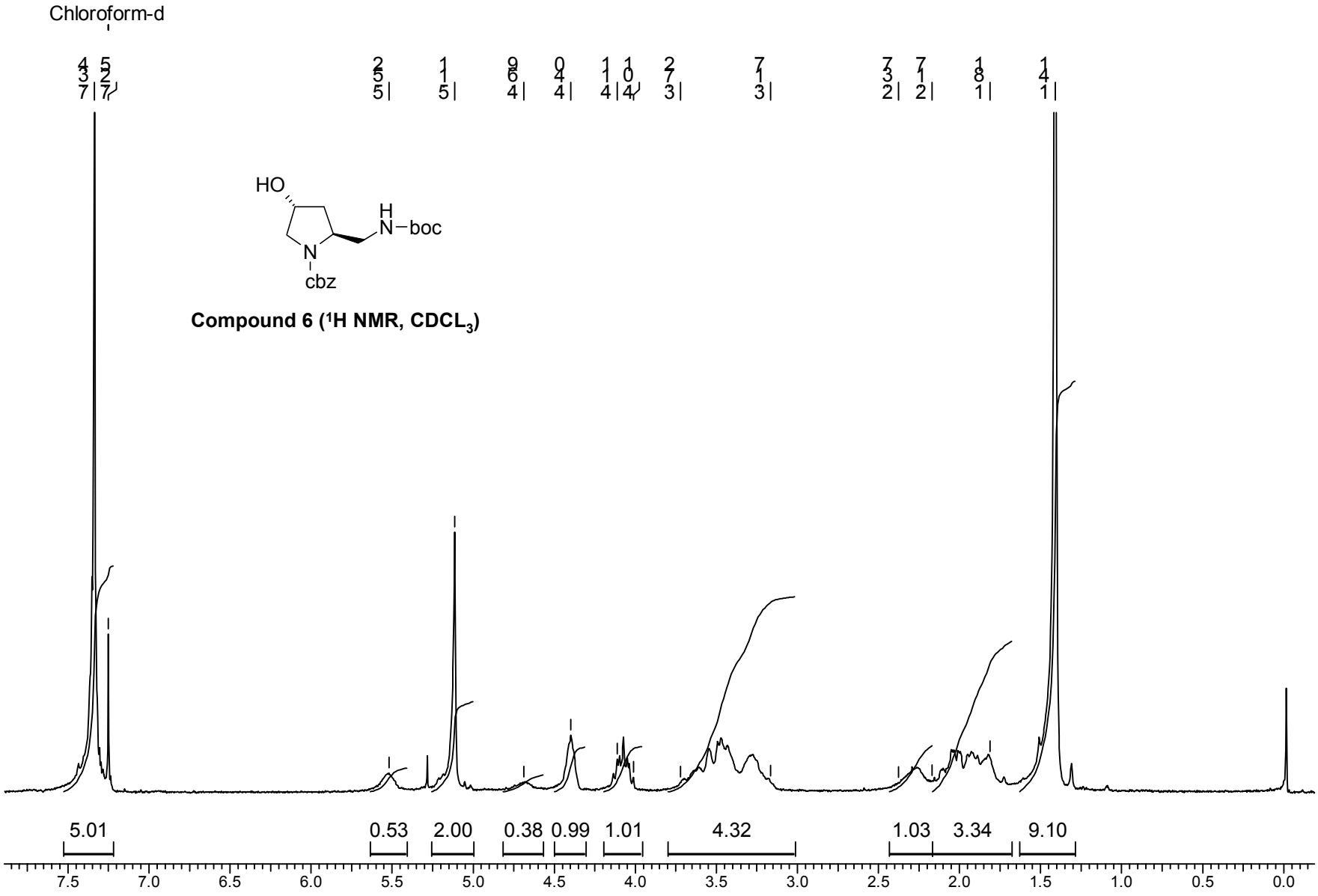

Compound 6 (^{1}H NMR, $CDCL_3$)

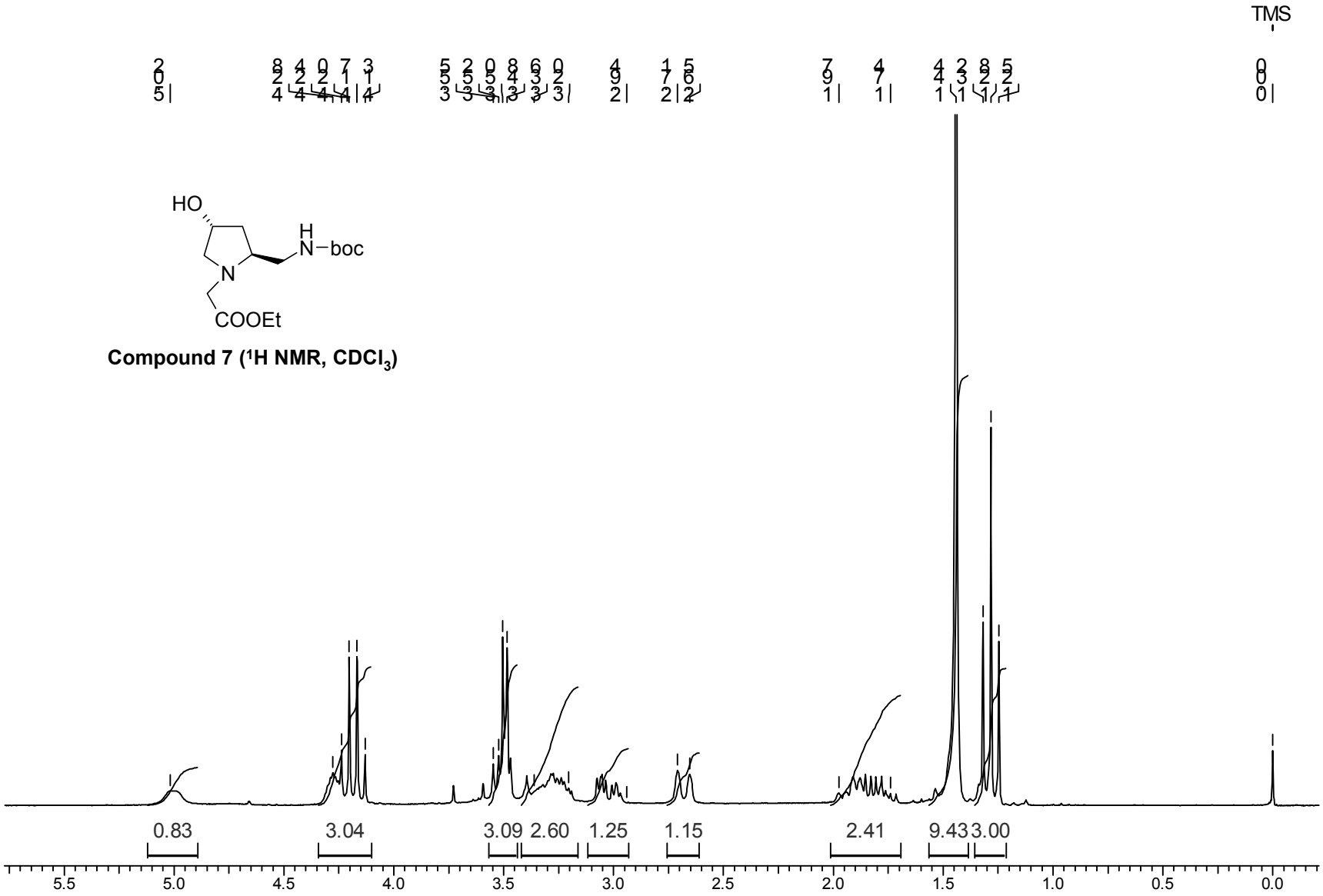

Compound 7 (^{1}H NMR, $CDCl_3$)

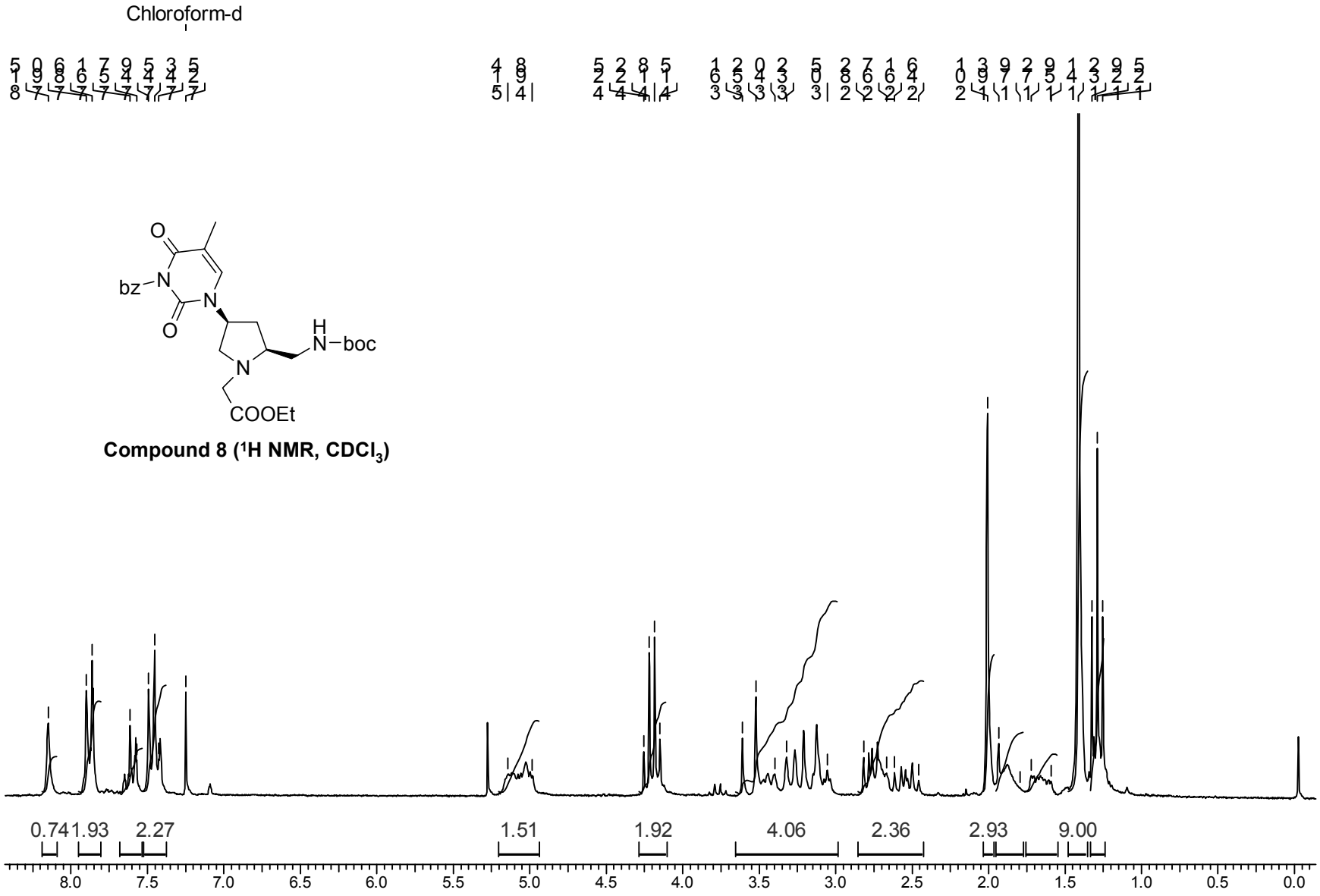

Compound 8 (^{1}H NMR, $CDCl_3$)

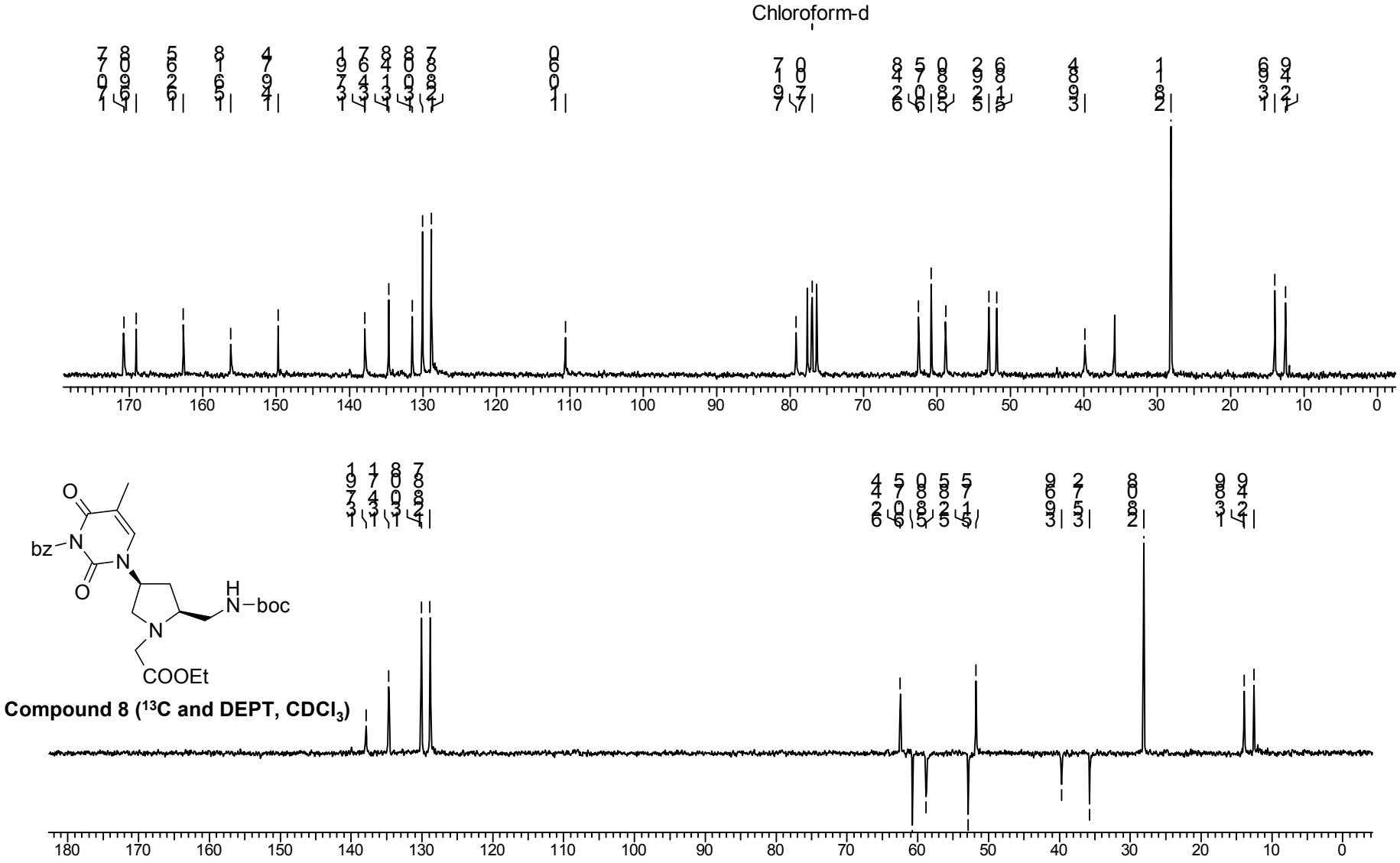

Compound 8 (^{13}C and DEPT, $CDCl_3$)

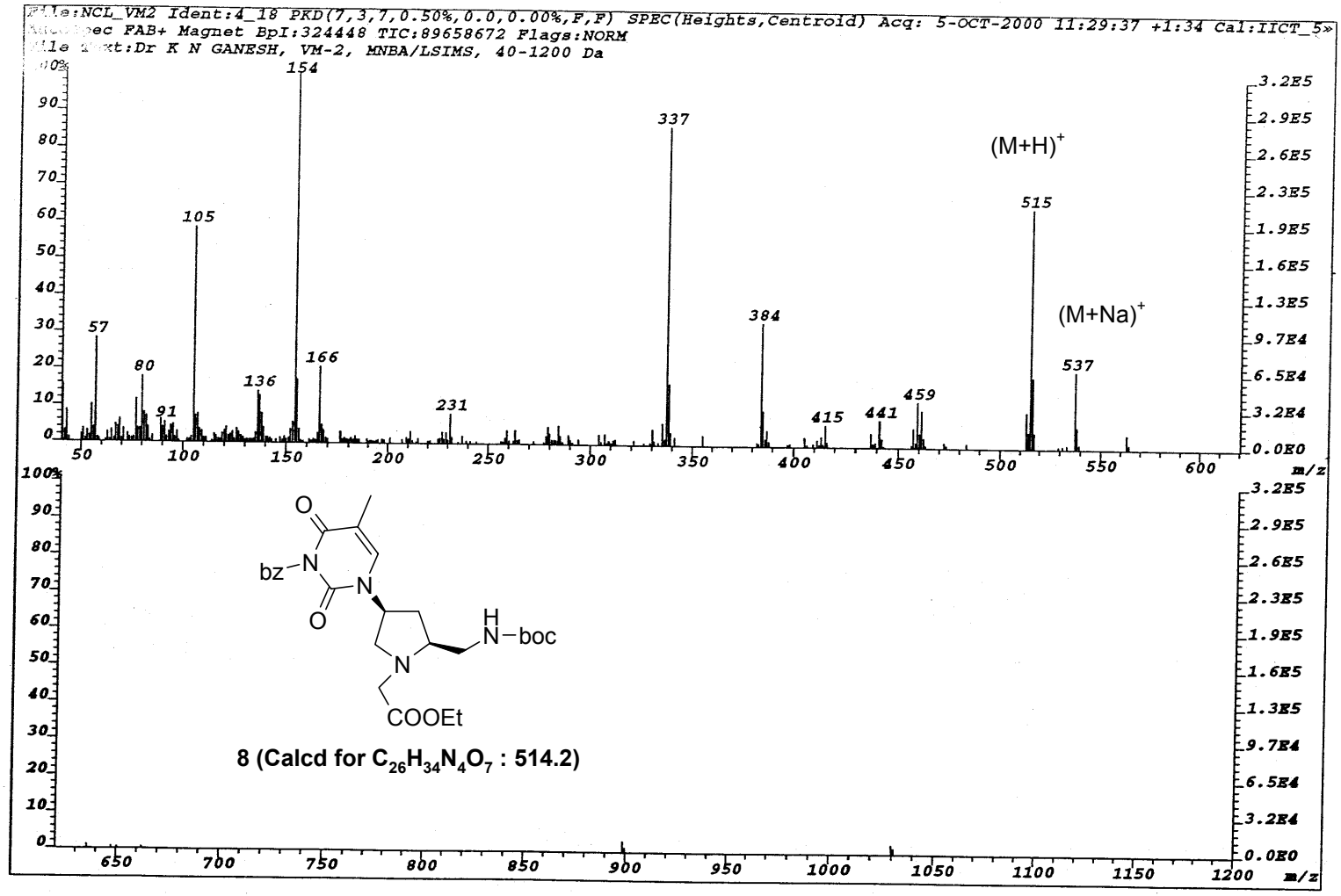

8 (Calcd for $C_{26}H_{34}N_4O_7$: 514.2)

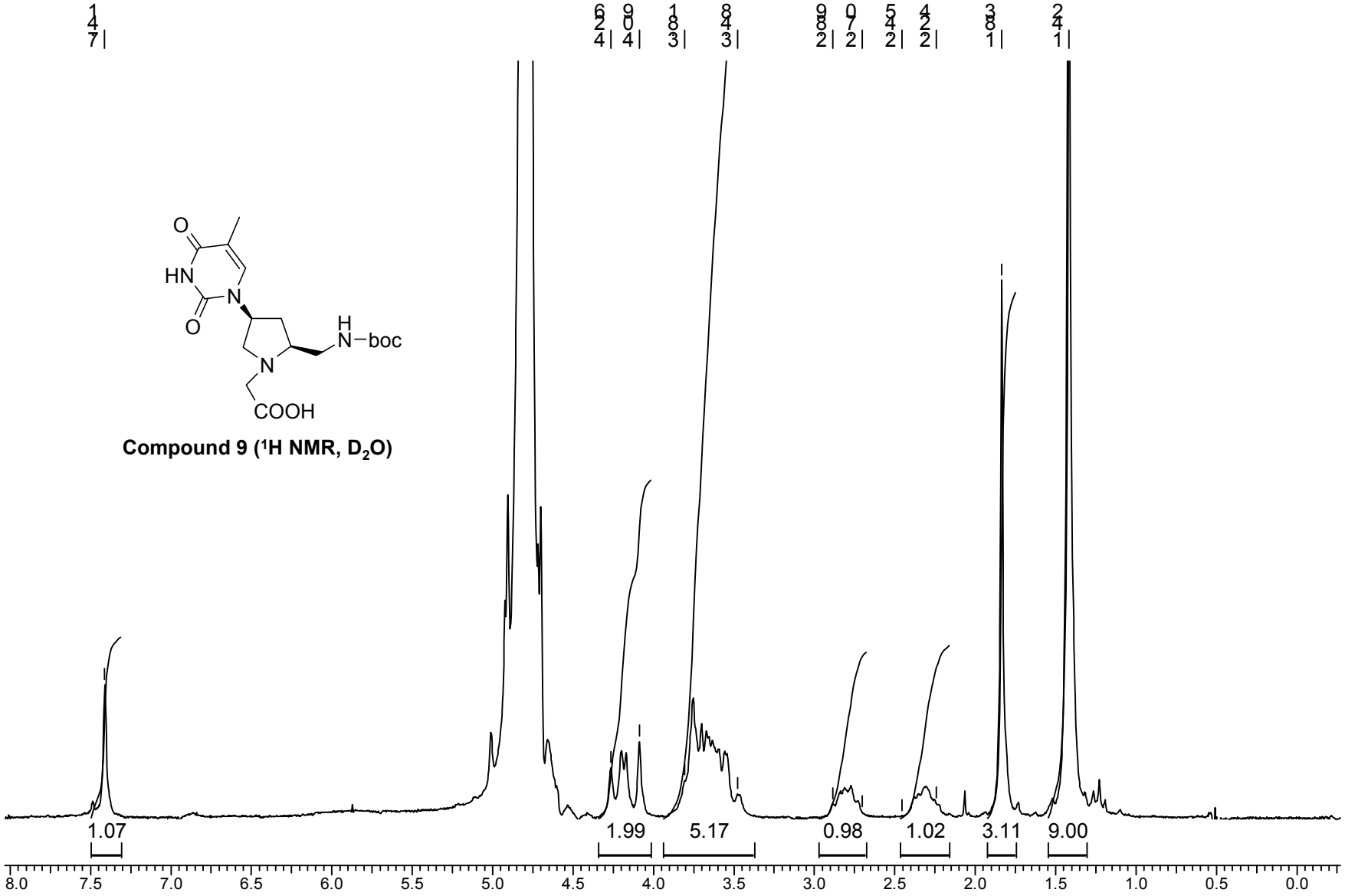

Compound 9 (^{1}H NMR, D_2O)

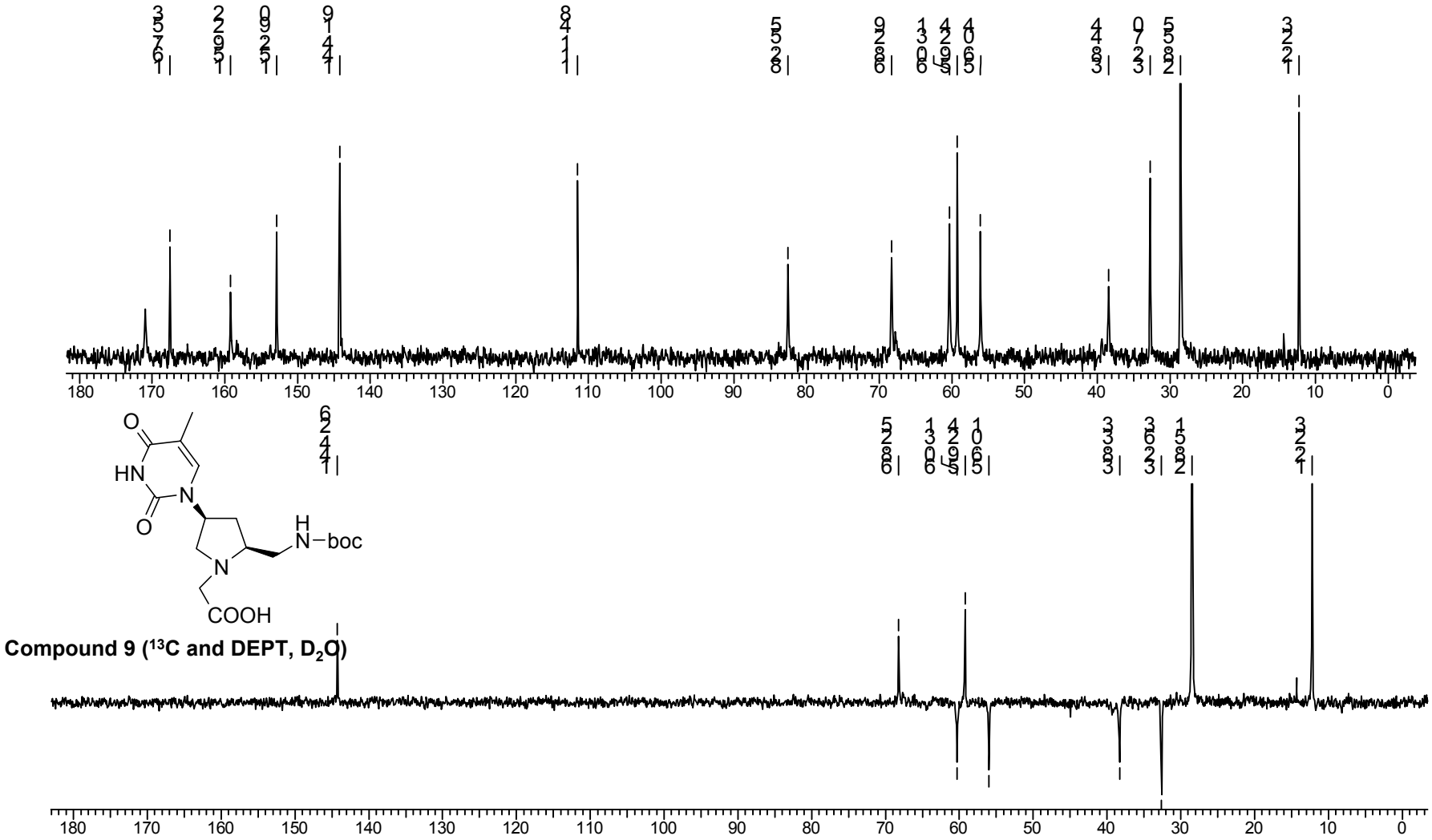

Compound 9 (^{13}C and DEPT, D_2O)

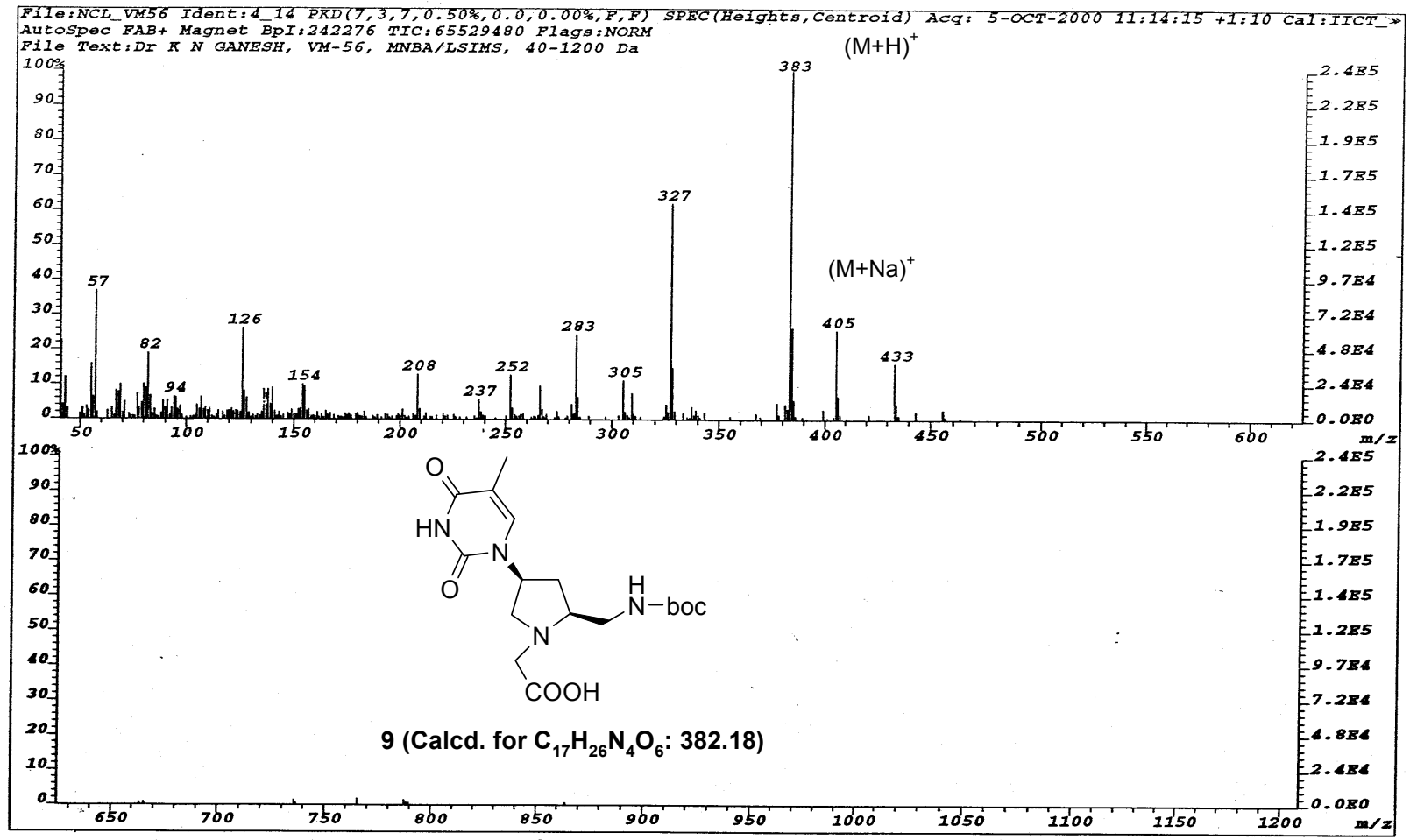

9 (Calcd. for $C_{17}H_{26}N_4O_6$: 382.18)

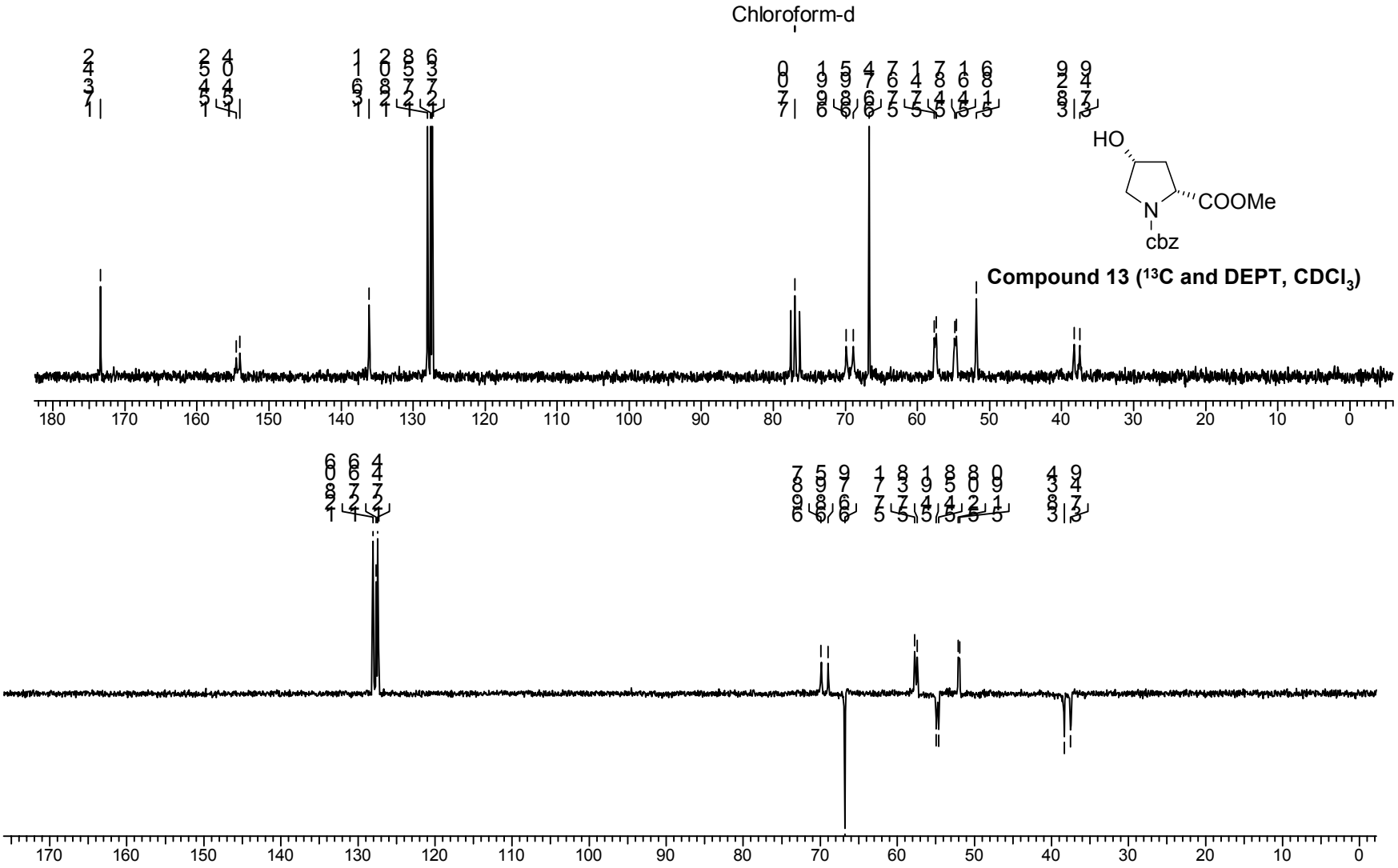
Chloroform-d
HO
COOMe
N
cbz
Compound 13 (13C and DEPT, CDCl3)

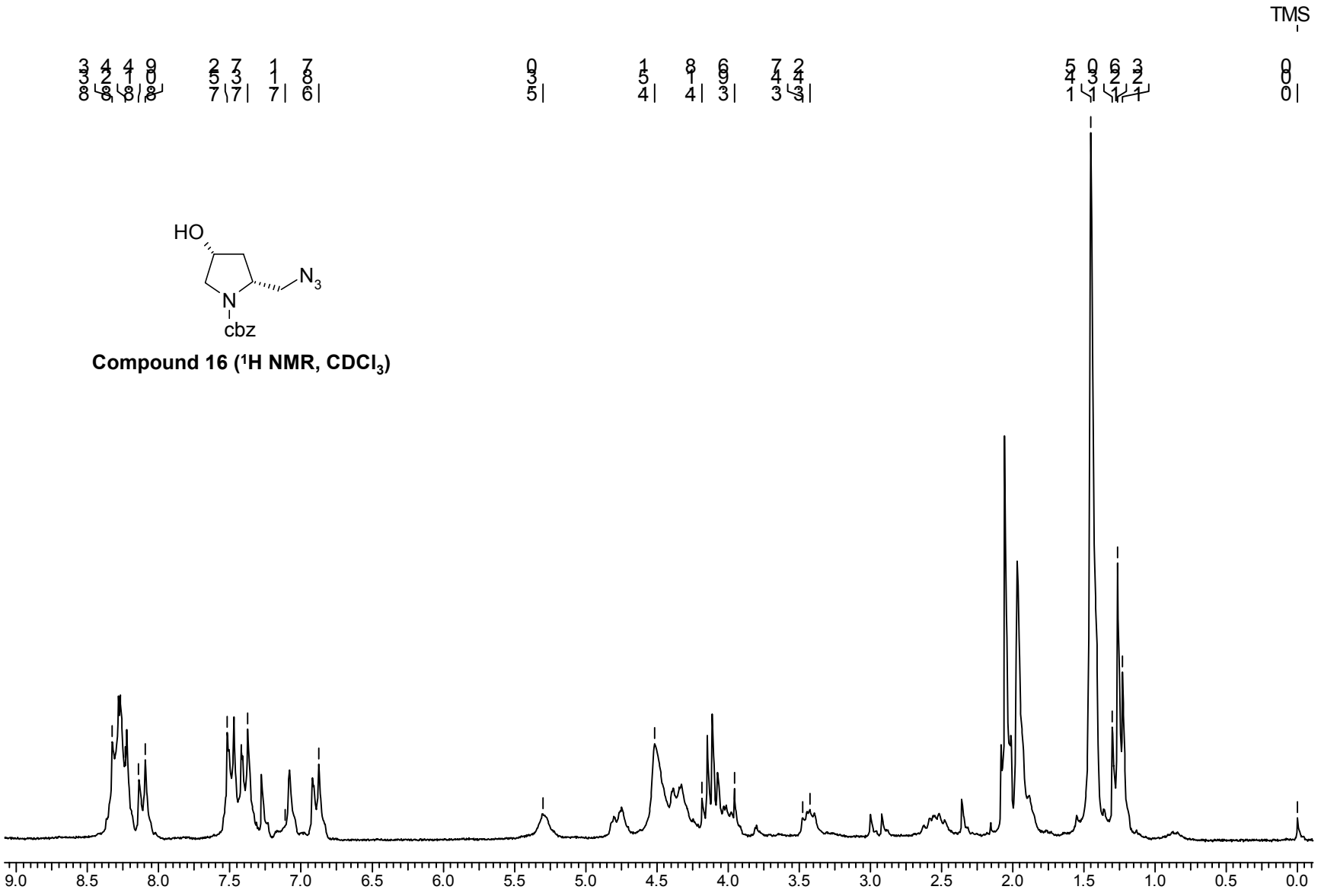

Compound 16 (^{1}H NMR, $CDCl_3$)

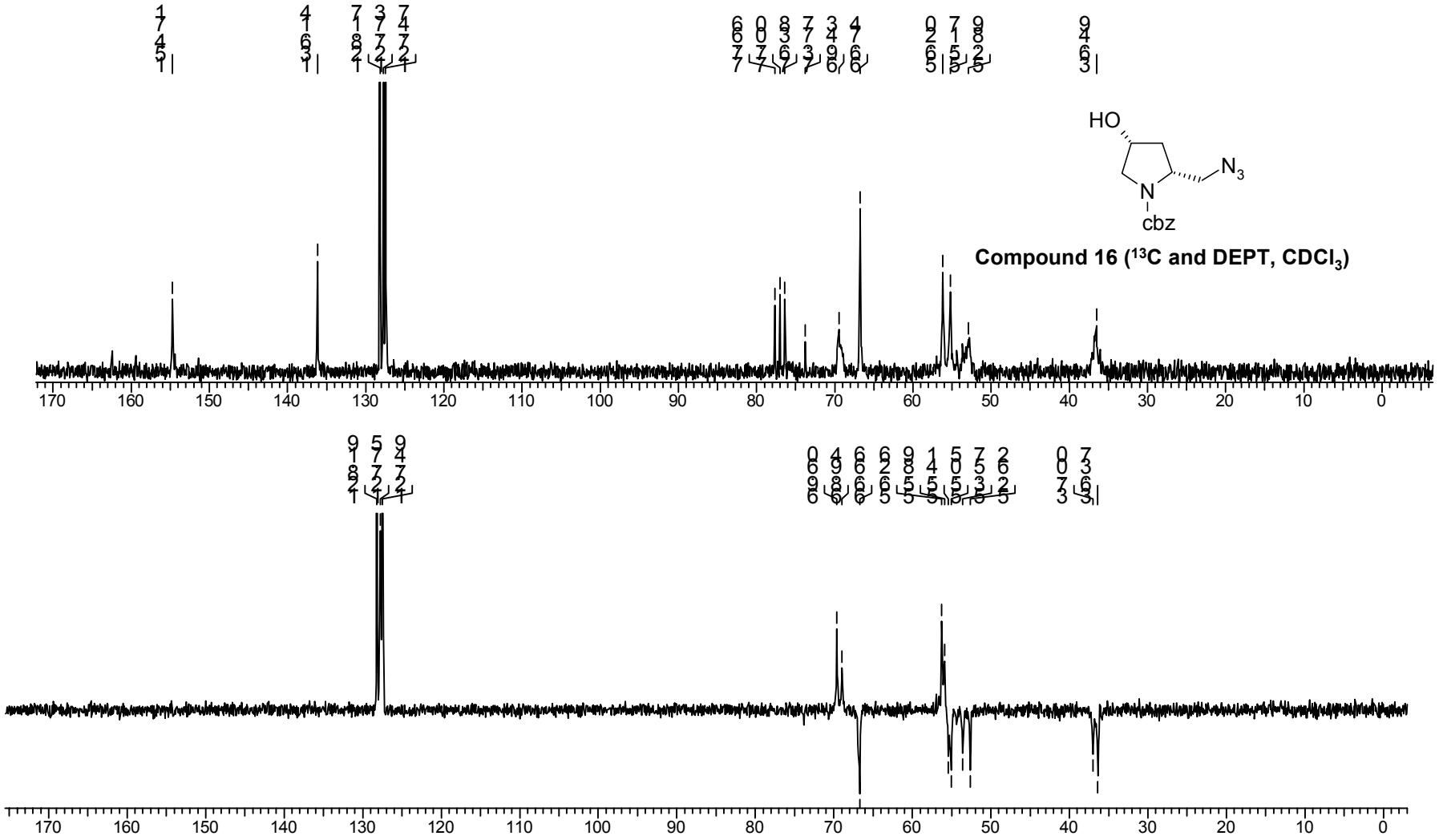

Compound 16 (^{13}C and DEPT, $CDCl_3$)

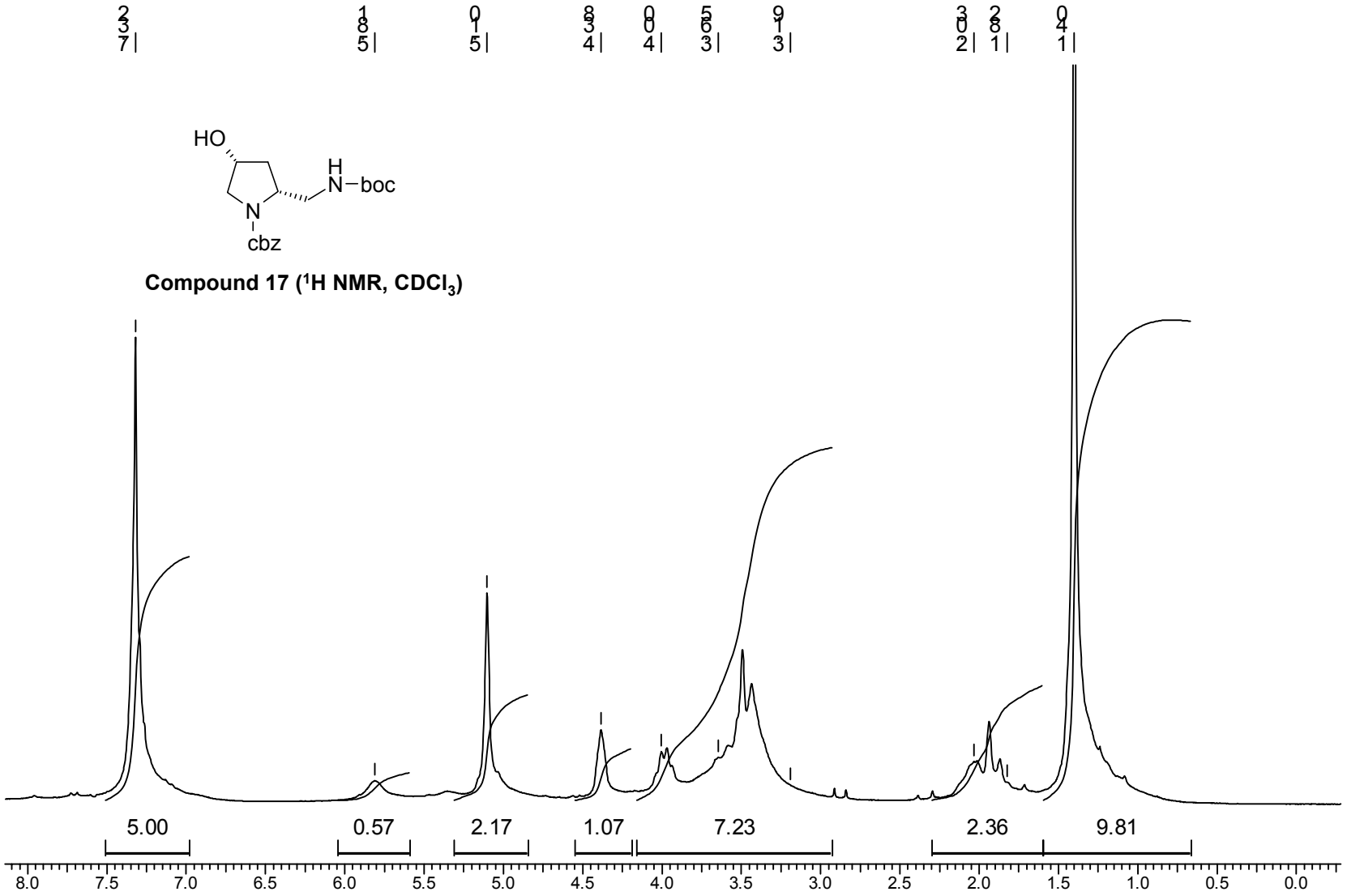

Compound 17 (^{1}H NMR, $CDCl_3$)

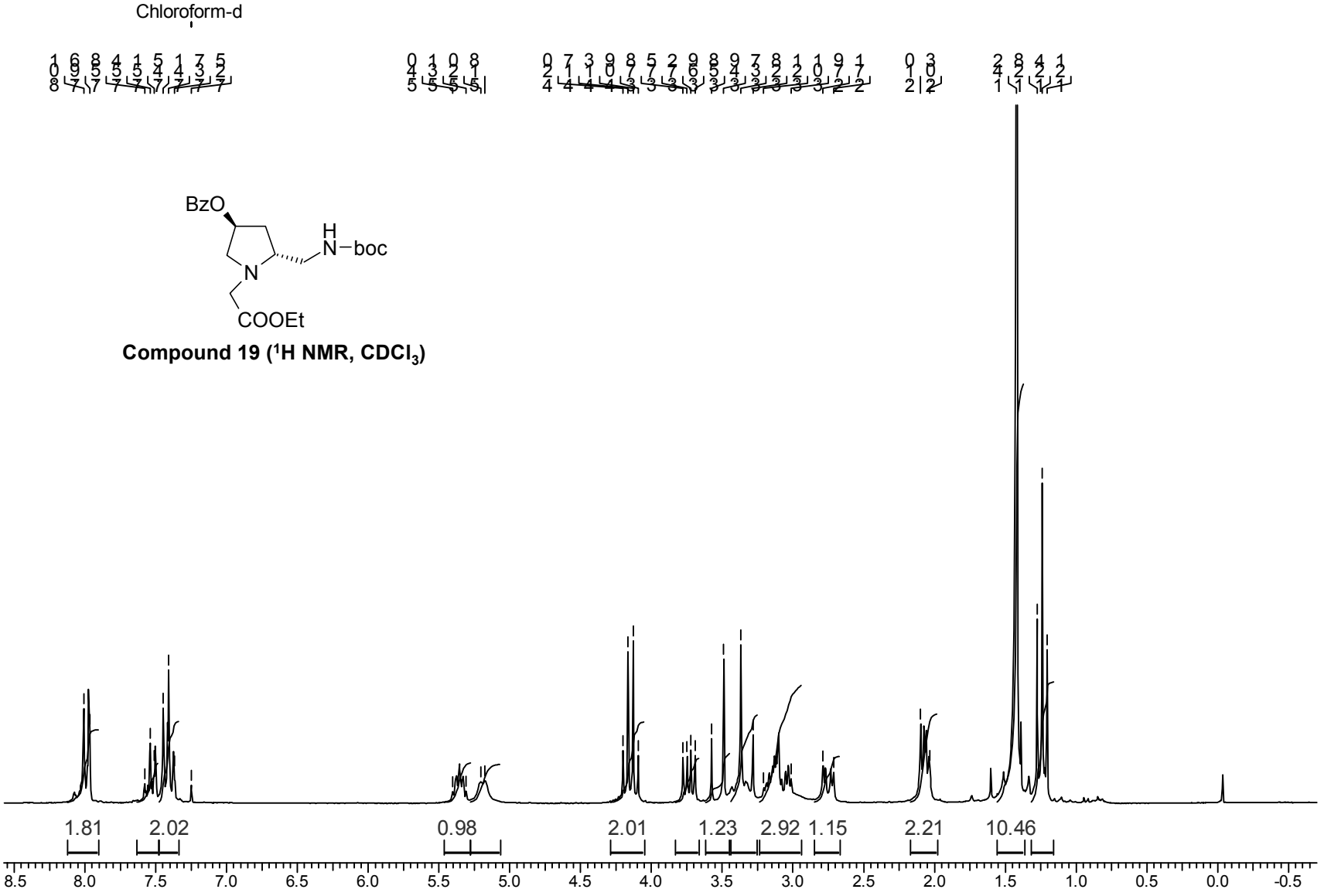

Compound 19 (^{1}H NMR, $CDCl_3$)

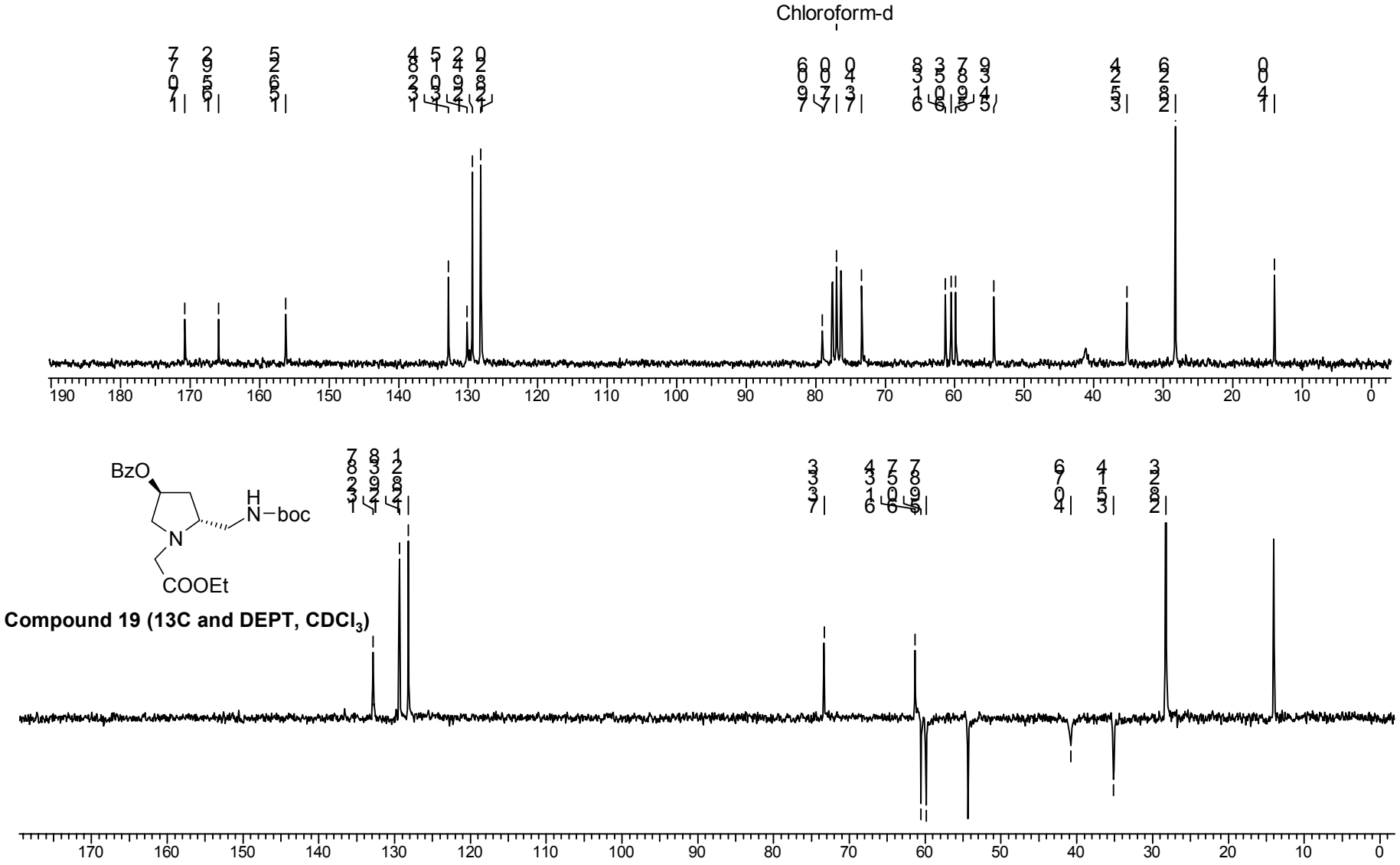

Compound 19 (13C and DEPT, $CDCl_3$)

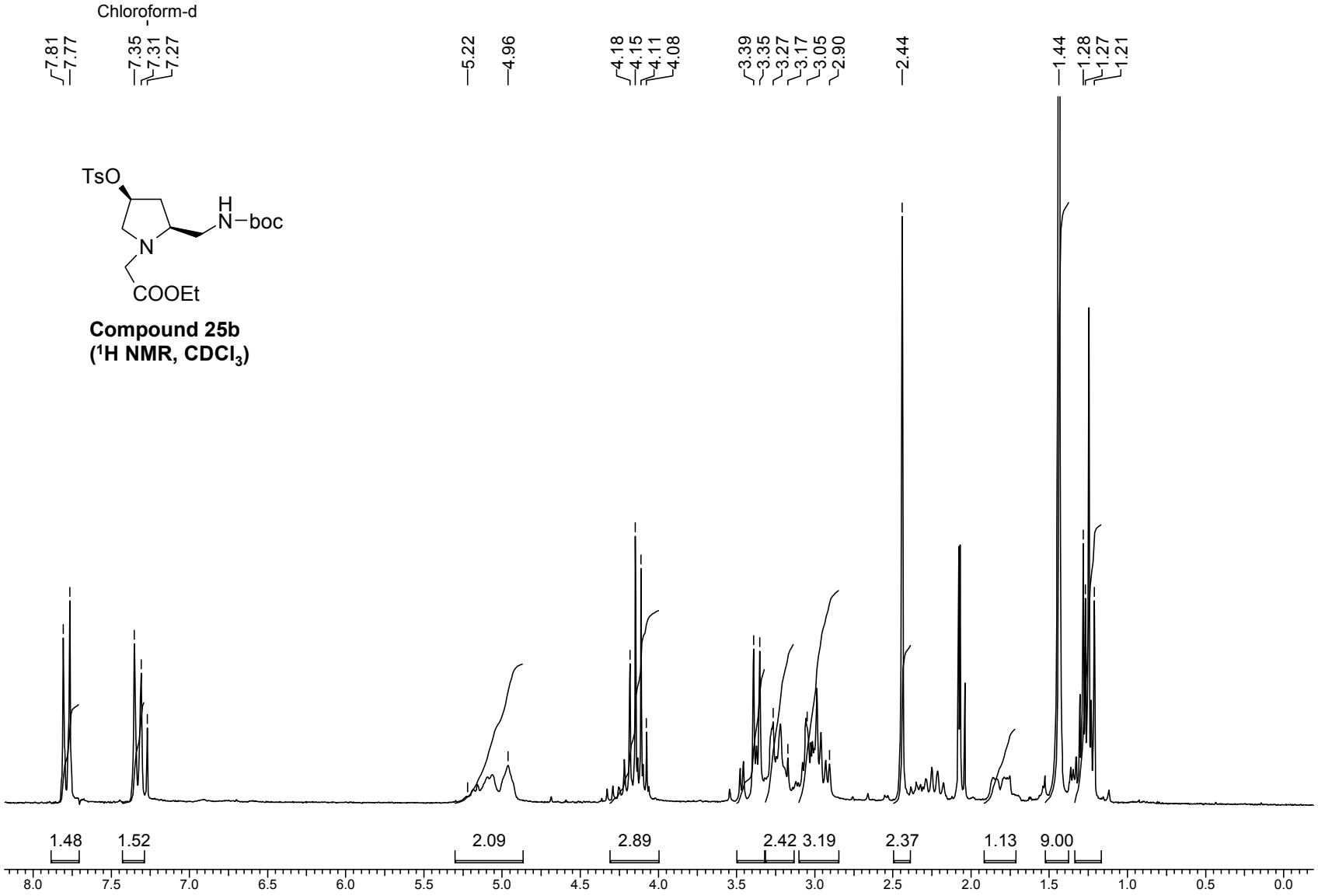

Compound 25b
(^{1}H NMR, $CDCl_3$)

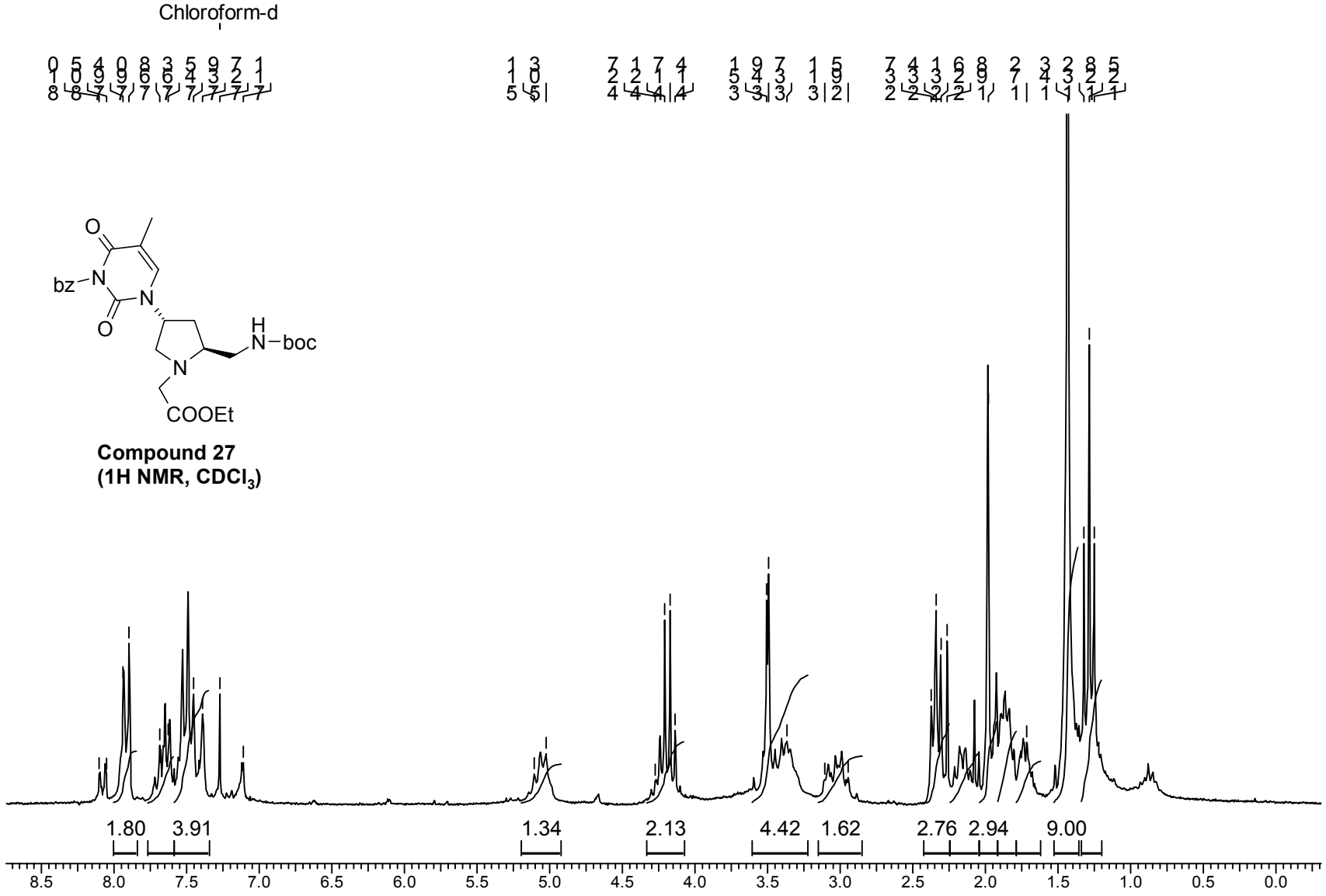

Compound 27
(1H NMR, $CDCl_3$)

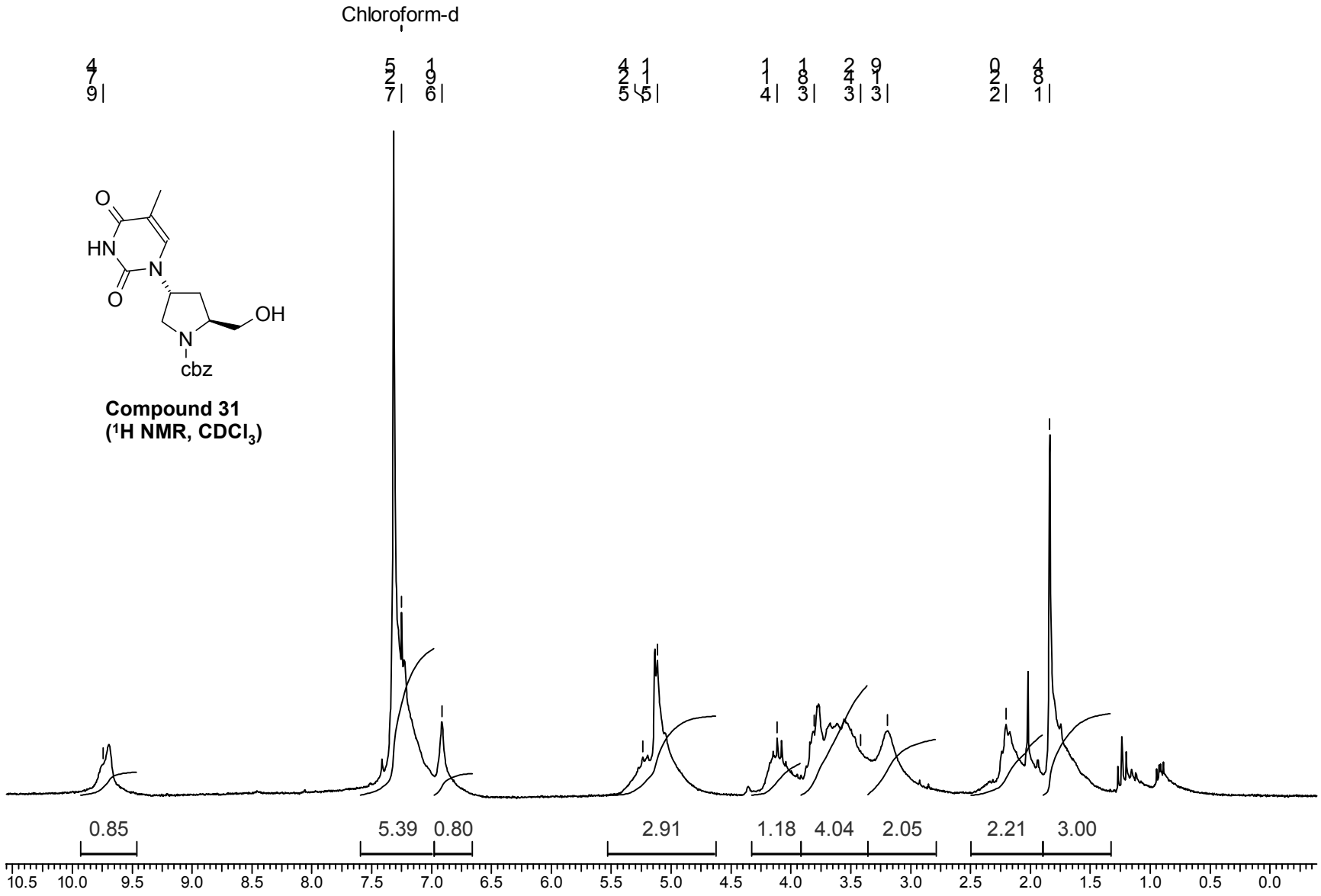

Compound 31
(^{1}H NMR, $CDCl_3$)

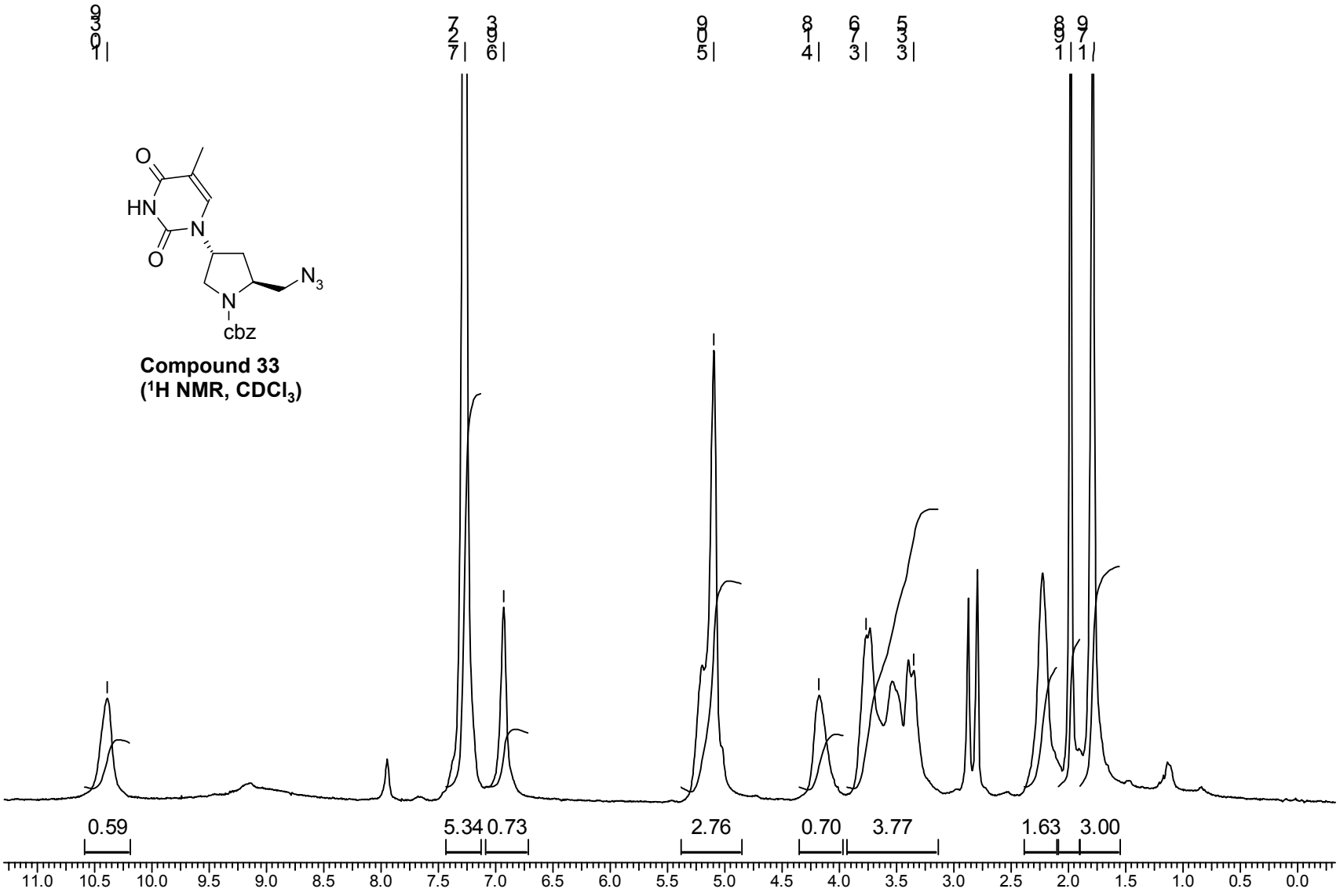
O
HN
N
O
N3
N
cbz
Compound 33
(1H NMR, CDCl3)
0.59
5.34
0.73
2.76
0.70
3.77
1.63
3.00
11.0
10.5
10.0
9.5
9.0
8.5
8.0
7.5
7.0
6.5
6.0
5.5
5.0
4.5
4.0
3.5
3.0
2.5
2.0
1.5
1.0
0.5
0.0

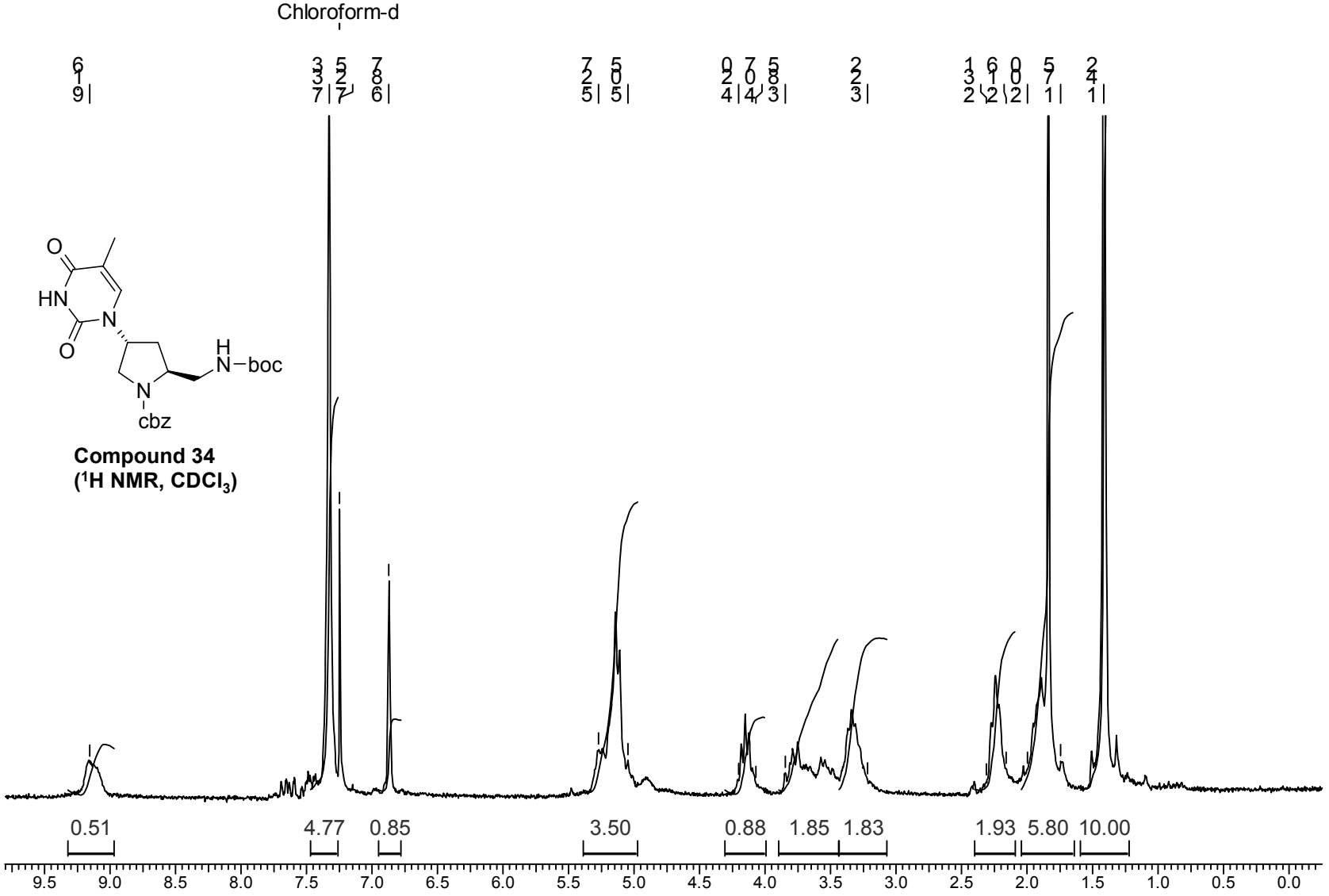

Compound 34
(^{1}H NMR, $CDCl_3$)

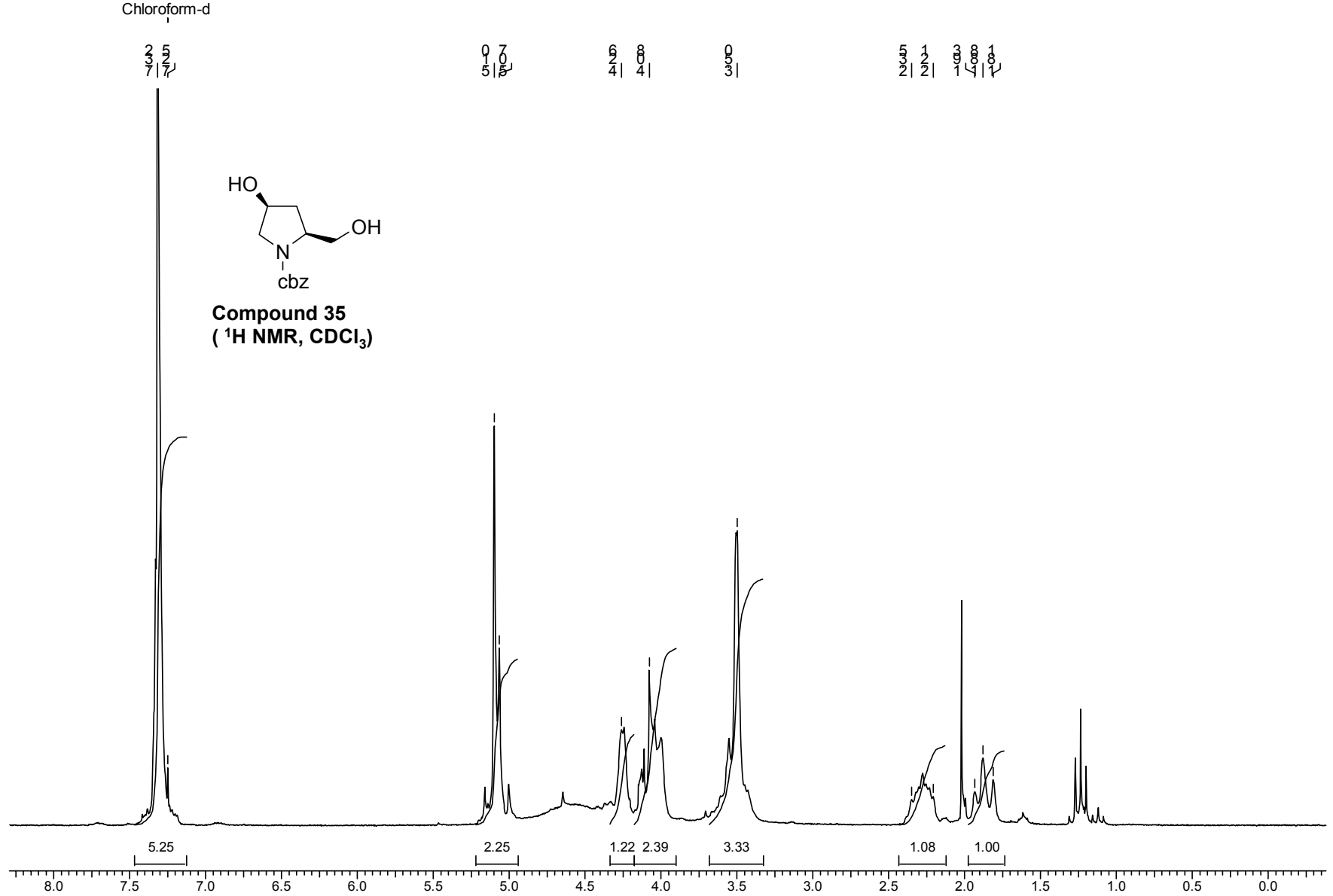

Compound 35
(^{1}H NMR, $CDCl_3$)

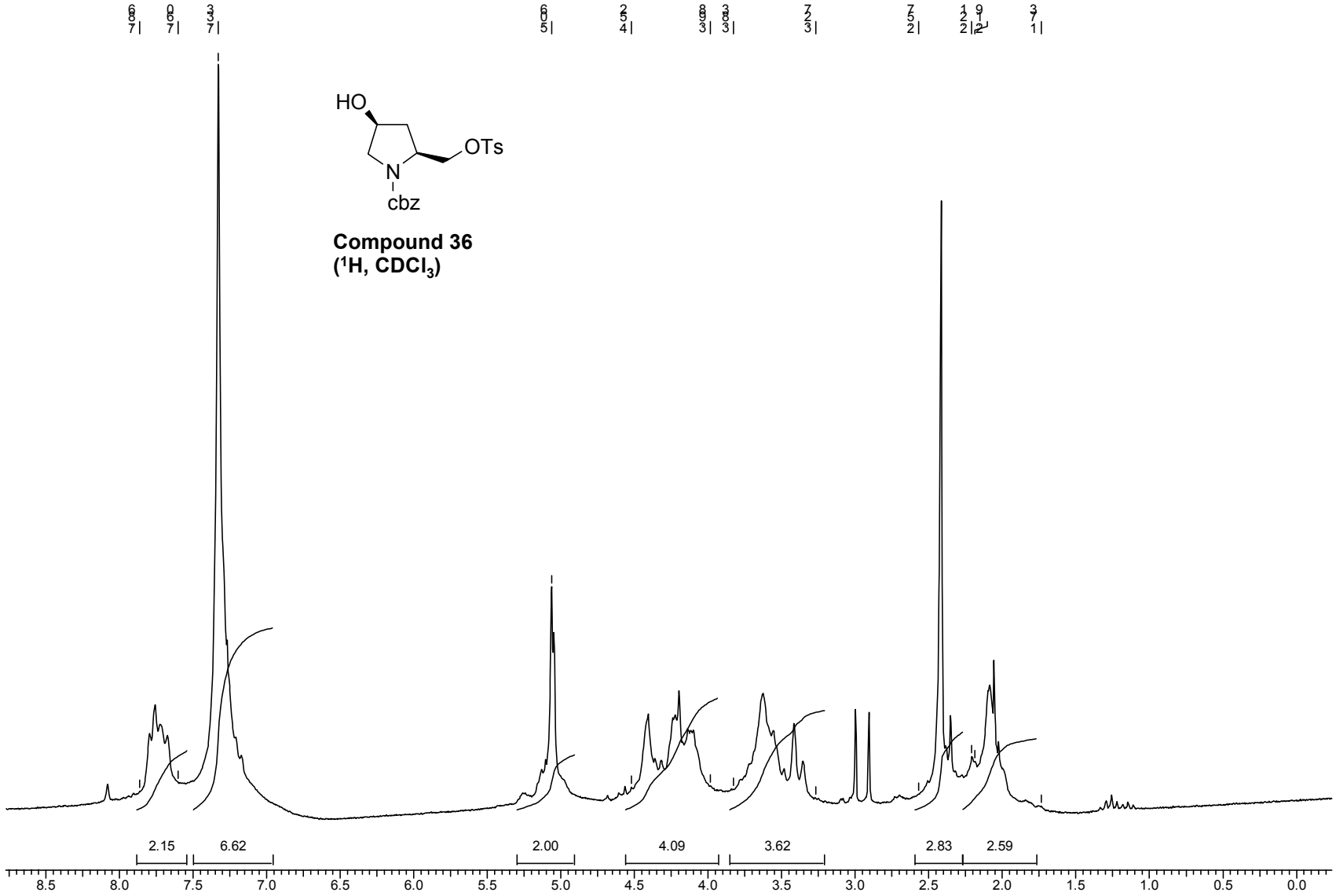

Compound 36
(^{1}H, $CDCl_3$)

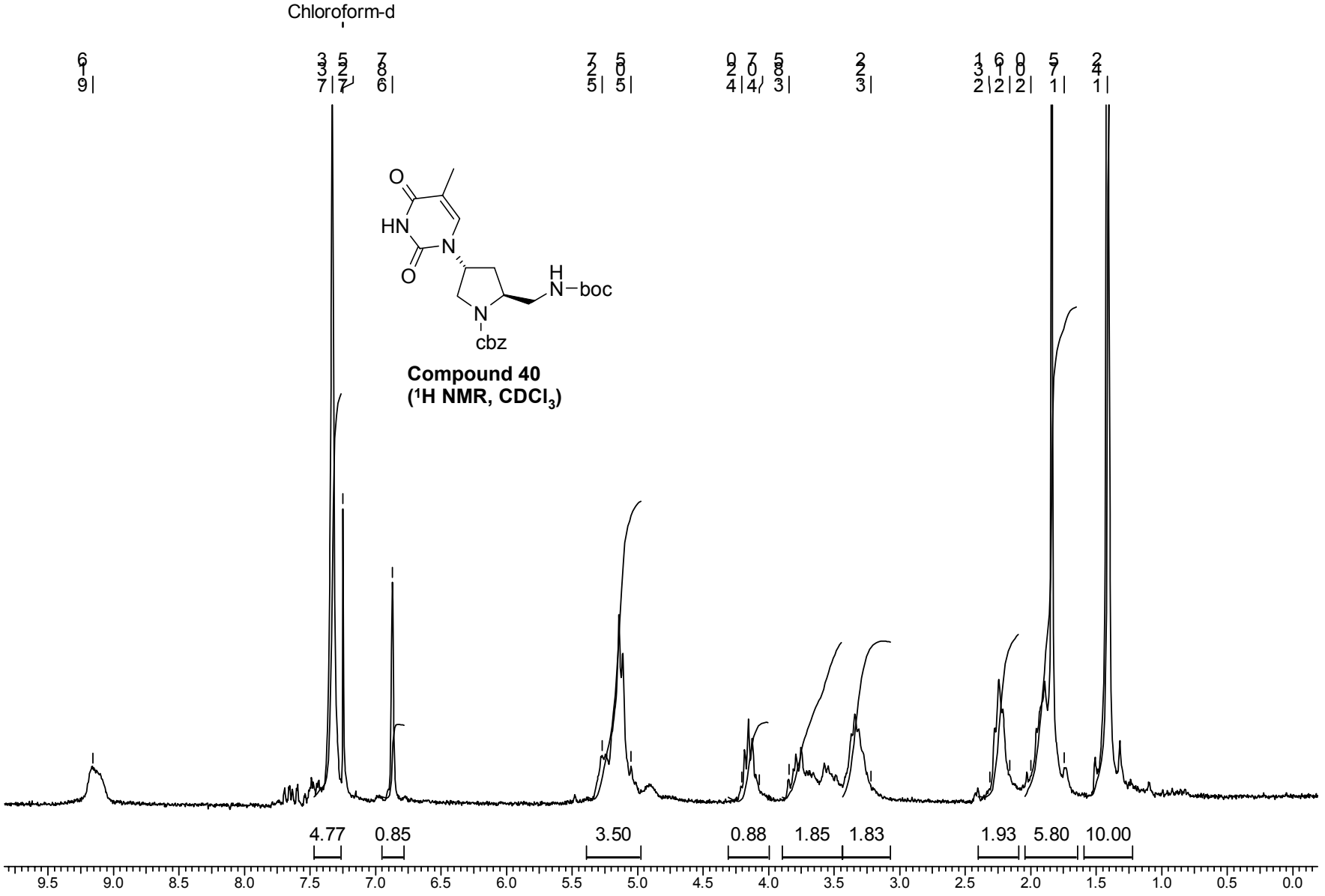

Compound 40
(^{1}H NMR, $CDCl_3$)

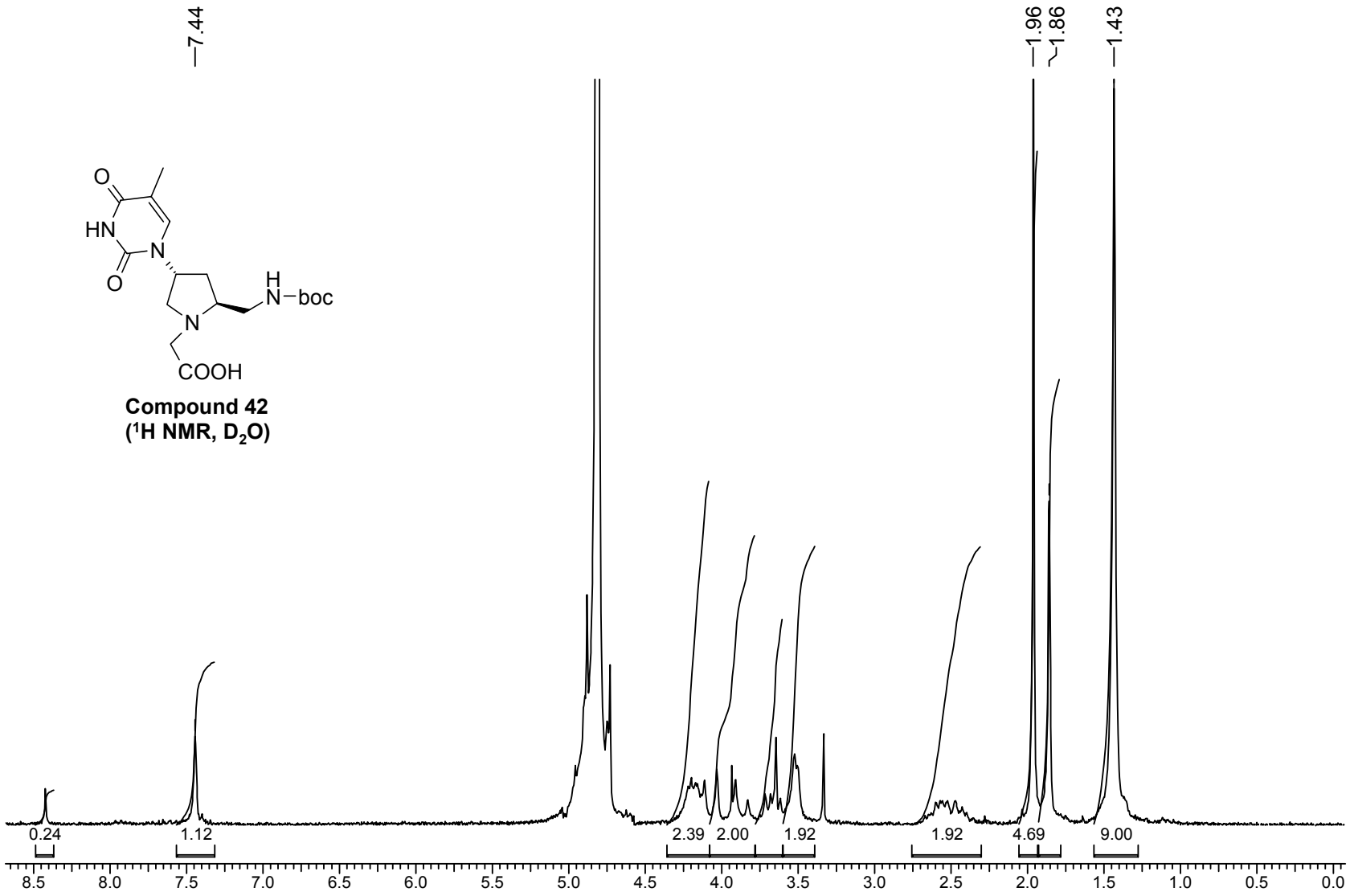

Compound 42
(^{1}H NMR, D_2O)

Table of bond lengths [A] and angles [deg] for compound 20.

C(2)-N(1)	1.467(5)
C(2)-C(6)	1.516(6)
C(2)-C(3)	1.522(6)
C(3)-C(4)	1.501(6)
C(4)-O(5)	1.432(5)
C(4)-C(5)	1.517(6)
C(5)-N(1)	1.459(5)
C(6)-N(2)	1.460(6)
C(7)-O(1)	1.206(5)
C(7)-N(2)	1.314(6)
C(7)-O(2)	1.365(6)
C(8)-O(2)	1.458(5)
C(8)-C(9)	1.487(8)
C(8)-C(11)	1.508(8)
C(8)-C(10)	1.525(8)
C(12)-N(1)	1.449(5)
C(12)-C(13)	1.499(6)
C(13)-O(3)	1.188(5)
C(13)-O(4)	1.329(5)
C(14)-O(4)	1.455(6)
C(14)-C(15)	1.484(10)
N(1)-C(2)-C(6)	113.3(4)
N(1)-C(2)-C(3)	102.5(3)
C(6)-C(2)-C(3)	115.4(4)
C(4)-C(3)-C(2)	106.0(3)
O(5)-C(4)-C(3)	112.7(4)
O(5)-C(4)-C(5)	107.3(4)
C(3)-C(4)-C(5)	104.9(4)
N(1)-C(5)-C(4)	105.6(3)
N(2)-C(6)-C(2)	112.7(4)
O(1)-C(7)-N(2)	125.7(5)
O(1)-C(7)-O(2)	125.0(4)
N(2)-C(7)-O(2)	109.3(4)
O(2)-C(8)-C(9)	111.0(5)
O(2)-C(8)-C(11)	110.5(4)
C(9)-C(8)-C(11)	112.9(5)
O(2)-C(8)-C(10)	101.2(4)
C(9)-C(8)-C(10)	110.5(5)
C(11)-C(8)-C(10)	110.2(5)
N(1)-C(12)-C(13)	112.3(4)
O(3)-C(13)-O(4)	124.5(4)
O(3)-C(13)-C(12)	125.6(4)
O(4)-C(13)-C(12)	109.8(4)
O(4)-C(14)-C(15)	107.5(5)
C(12)-N(1)-C(5)	112.8(3)
C(12)-N(1)-C(2)	114.6(3)
C(5)-N(1)-C(2)	104.9(3)
C(7)-N(2)-C(6)	121.7(4)
C(7)-O(2)-C(8)	120.1(4)
C(13)-O(4)-C(14)	117.3(4)

Table of torsion angles [deg] for compound 20.

N(1)-C(2)-C(3)-C(4)	29.4(4)
C(6)-C(2)-C(3)-C(4)	153.1(4)
C(2)-C(3)-C(4)-O(5)	108.3(4)
C(2)-C(3)-C(4)-C(5)	-8.1(5)
O(5)-C(4)-C(5)-N(1)	-136.6(4)
C(3)-C(4)-C(5)-N(1)	-16.6(5)
N(1)-C(2)-C(6)-N(2)	68.1(5)
C(3)-C(2)-C(6)-N(2)	-49.7(5)
N(1)-C(12)-C(13)-O(3)	15.2(6)
N(1)-C(12)-C(13)-O(4)	-168.0(4)
C(13)-C(12)-N(1)-C(5)	77.2(5)
C(13)-C(12)-N(1)-C(2)	-162.8(4)
C(4)-C(5)-N(1)-C(12)	161.3(3)
C(4)-C(5)-N(1)-C(2)	36.0(4)
C(6)-C(2)-N(1)-C(12)	70.4(4)
C(3)-C(2)-N(1)-C(12)	-164.6(4)
C(6)-C(2)-N(1)-C(5)	-165.3(4)
C(3)-C(2)-N(1)-C(5)	-40.3(4)
O(1)-C(7)-N(2)-C(6)	7.1(7)
O(2)-C(7)-N(2)-C(6)	-174.9(4)
C(2)-C(6)-N(2)-C(7)	118.2(5)
O(1)-C(7)-O(2)-C(8)	-4.9(7)
N(2)-C(7)-O(2)-C(8)	177.1(4)
C(9)-C(8)-O(2)-C(7)	65.3(6)
C(11)-C(8)-O(2)-C(7)	-60.7(6)
C(10)-C(8)-O(2)-C(7)	-177.4(5)
O(3)-C(13)-O(4)-C(14)	2.6(7)
C(12)-C(13)-O(4)-C(14)	-174.2(4)
C(15)-C(14)-O(4)-C(13)	161.2(5)

Chapter 3

Pyrrolidinyl Carbamate-Linked Nucleic Acids

3.1 Introduction

Of the many backbone modifications, those involving the replacement of phosphodiester group with neutral linkers form a major class. These lipophilic oligomers can pass into cells more efficiently and the absence of interstrand electrostatic repulsion with target nucleic acids improves their binding affinity. A variety of nucleic acid analogues containing wholly or substantially uncharged backbones have been shown to enter living animal cells and to be resistant to nucleolytic degradation therein. Amongst these non-ionic modifications, the carbamate linkage is stable under physiological conditions and is resistant to nuclease action (Mungall & Kaiser, 1977).

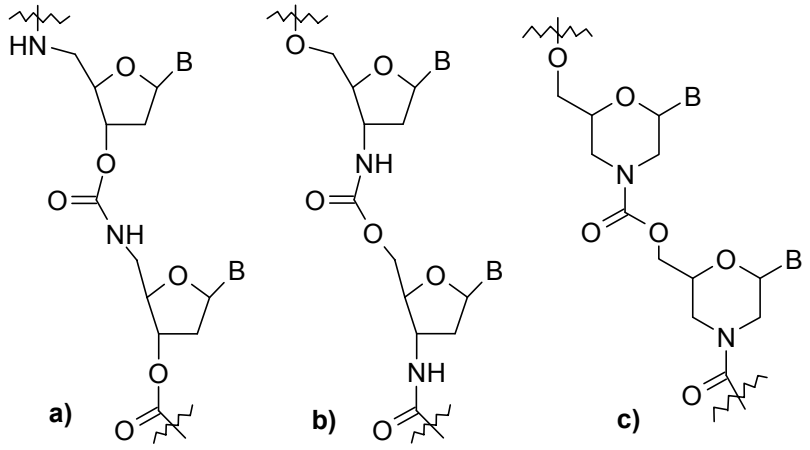

Figure 1. Carbamate-linked nucleic acid analogues. a) 3-'O-CO-NH-5' linked 2'-deoxyribose; b) 3'NH-CO-O-5' linked 2'-deoxyribose and c) carbamate-linked morpholine.

There are reports in the literature describing the synthesis and characterization of oligonucleotides with a 3'-O-CO-NH-5' (Figure 1a), 3'-NH-CO-O-5' (Figure 1b) linked 2'-deoxysugar or a carbamate linkage with morpholine subunit (Stirchak *et al.*, 1989) (Figure 1c). Coull *et al.* (1987) prepared a carbamate-linked (3'-O-5'-N-) oligomer containing *six thymidine units* in solution Hydrolytic and thermal denaturation studies did not indicate the presence of intramolecular base stacking. However, the experiments were inconclusive due to the low thermal stability of short A:T duplexes. Interestingly, Stirchak *et al.* (1987) have shown that cytosine containing oligonucleotides, with an identical backbone to that reported by Coull *et al.* (1987) forms stable complexes with their complementary DNA, $d(pG)_6$ and poly(dG), with Tm values higher than their corresponding DNA:DNA duplexes.

Habus *et al.* (1994) achieved synthesis of di-, T*T, tri-, T*T*T, and tetrameric, T*T*T*T, building blocks with carbamate internucleoside linkage-3'-NH-CO-O-5' was

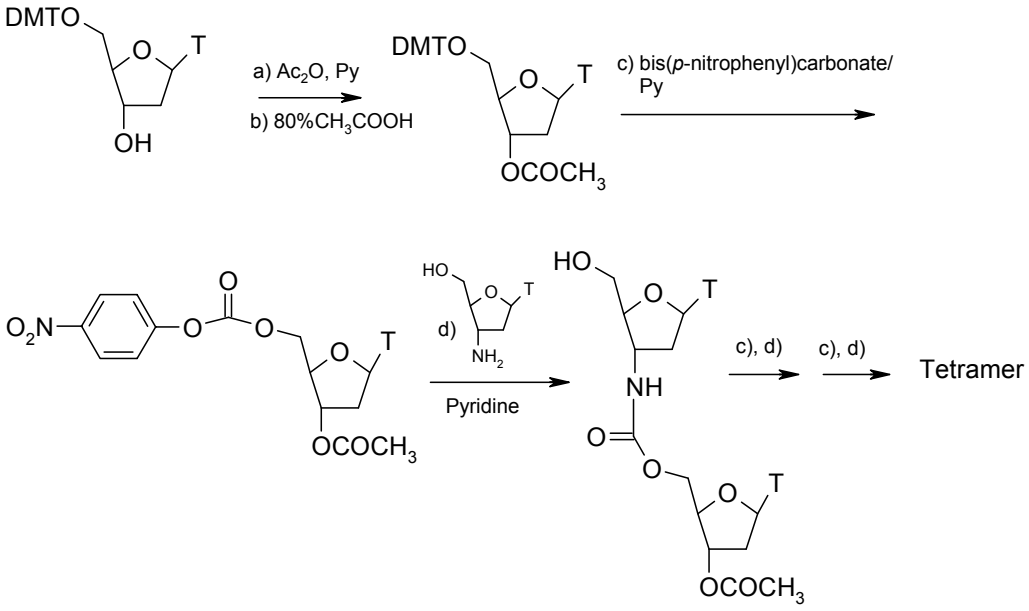

Figure 2. The synthesis of 3'-NH-CO-O-5' linked thymidine tetramer.

achieved by suitably protecting 5'-position and using these building blocks in the synthesis of chimeric oligonucleotides by standard phosphoramidite chemistry (Figure 2). The carbamate oligonucleotides, so derived, were studied for their binding-affinity to complementary nucleic acids and nuclease resistance. Oligonucleotides containing one, two, or three carbamate units at 3'-end, were found to have increased nuclease resistance but had no significant influence on the duplex thermal stability.

In another report, *chimeric carbamate-internucleoside dimer* of 2'-deoxy-2',3'-secothymidine (Figure 3) protected in the 5'-position, was incorporated into the oligonucleotides by phosphoramidite chemistry. These chimeric oligonucleotides

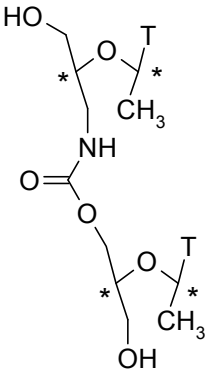

Figure 3. Carbamate-linked acyclic sugar unit

showed less affinity towards complementary DNA compared to unmodified strand (Habus & Agrawal, 1995).

Stirchak *et al.* (1989) developed an efficient methodology to prepare morpholine monomer of cytosine, which was used to synthesize carbamate-linked hexamer in solution. The solubility characteristics of the resulting oligomers were improved by conjugation with a terminal polyethylene glycol chain. Thermal denaturation studies with $p(dG)_6$ showed a Tm of 62.5°C as compared to the control $p(dC)_6$. The hypochromicity upon binding to DNA for these carbamate-linked oligomers was much higher than that observed for the control sequences.

3.2 Present Work: Rationale and Objectives

The hybridization of DNA and RNA double-helices is slowed down by the electrostatic repulsion between the negatively charged phosphodiester linkages on the adjacent chains. The tight binding of rigid achiral polyamide of PNA (peptide nucleic acid polymers) to DNA was attributed to the absence of charge repulsion and an entropic gain from the favourable preorganization of PNA. However, the prospects of PNA as a drug have limitations due to its poor cell membrane permeability, small rate constants for association with DNA and RNA, and the high thermal stability of helical PNA:DNA or PNA:RNA structure that lead to decreased sequence specificity at physiological temperature. Moreover, PNA shows little discrimination between the parallel and antiparallel modes of binding to DNA.

To overcome these problems, PNA structure is further modified in various ways; mixed sequences of positive and negative linkers, positive or neutral linkers with simultaneous introduction of chiral centers. Towards this, in this laboratory, chiral PNAs were designed by using 4-aminoproline having nucleobase attached to the ring nitrogen via acetyl linker (Gangamani *et al.*, 1999) (Figure 4). The homooligomers of 4-

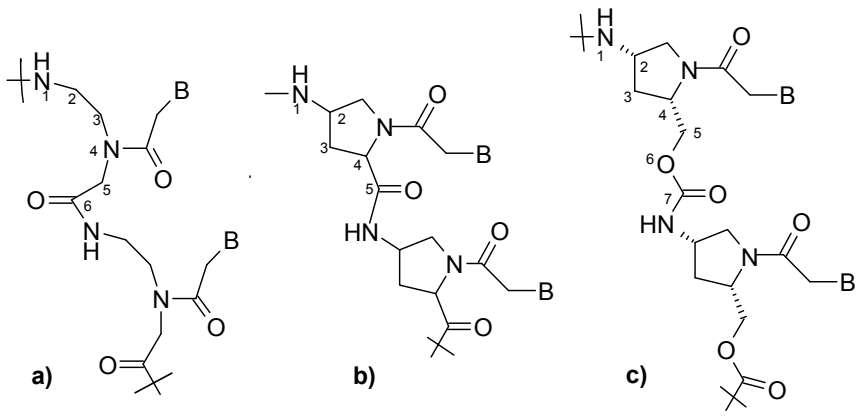

Figure 4. a) Aminoethyl glycyl nucleic acid b) prolyl nucleic acid c) Carbamate-linked pyrrolidinyl nucleic acid.

aminoprolyl peptide nucleic acids thus obtained did not bind to complementary DNA probably as a result of incompatible internucleobase distances arising from the introduction of backbone constraint. It was conceived that extending the backbone by replacing the peptide linkage with carbamate linkage may release some of the geometric constraints in the *prolyl*PNA. The carbamate-linkage, though longer than the amide linkage, is shorter by 0.32 Å than a phosphodiester linkage (Stirchak *et al.*, 1987). Thus, the incorporation of more atoms in the backbone is necessary to assume an internucleobase distance that is compatible with the duplex formation. To achieve this, this chapter aims at:

1. The synthesis (2*S*,4*S*)-4-amino-2-hydroxymethyl pyrrolidine carrying nucelobase (thymine and cytosine) attached to N1 via acetyl linker.
2. The activation of primary alcohol in the above monomer for synthesis of pyrrolidinyl Carbamate Nucleic Acids (pyCNA).
3. Synthesis of carbamate-linked dimer in solution to standardize and establish the necessary chemistry.
4. Synthesis of oligomers having mixed amide/carbamate backbone and carbamate-linked homooligomers
5. UV melting studies of these oligomers with complementary DNA.

3.3 Synthesis of Pyrrolidinyl Monomers

3.3.1 Synthesis of *t*-Boc Protected Aminoalcohol (62)

Compound **62** was synthesized from (2*S*,4*R*)-4-hydroxyproline according to Scheme 3.1. After stepwise protection of the ring nitrogen as benzylcarbamate and the 2*S*-carboxylic acid as methyl ester to obtain compound **3** (Chapter 2, Scheme 2.1a), whose 4*R*-hydroxy function was converted to the 4*R*-mesyl derivative **59** in 99% yield

Scheme 3.1

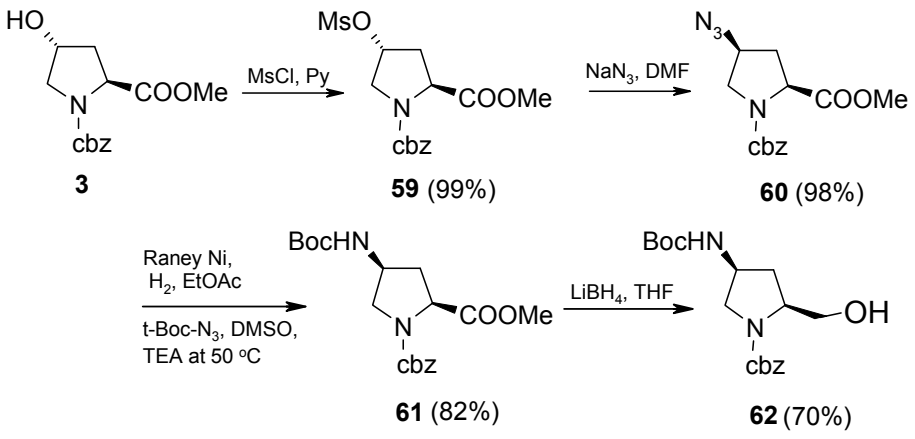

3 **59** (99%) **60** (98%)

61 (82%) **62** (70%)

by treatment with mesylchloride. The ^{1}H NMR spectrum of compound **59** showed a singlet at δ 3.00 for CH_3 of mesyl group. The 4*R*-mesyl derivative **59** was reacted with NaN_3 in DMF at 70^{o}C, which led to an inversion at C4 to give the 4*S*-azido compound **60** in 98% yield. A peak at 2106 cm^{-1} in the IR spectrum of compound **60** confirmed the presence of azide group. Catalytic hydrogenation using Raney Ni readily converted this azido component to 4*S*-amine without affecting Cbz group. The resulting 4*S*-amine without further isolation was directly treated with *t*-Boc azide in DMSO at 50^{o}C in the presence of TEA as base to give the 4*S*-*t*-butoxycarbonylamino compound **61** in 82% yield. Reacting with two equivalents of $LiBH_4$ in THF reduced the methyl ester in compound **61** to afford the 2*S*-hydroxymethyl compound **62** in 70% yield. The reaction was complete within 3.5h and longer reduction times resulted in the partial removal of Cbz group.

3.3.2 Methods for The Synthesis of Carbamate Linkage

General synthetic approaches for the formation of the carbamate linkage are mostly derived from active ester method used for polypeptide synthesis. A carbamate linkage can be synthesized by first activating the primary hydroxyl component of one unit, which is then condensed with the primary/secondary amine of the second unit. The activation of alcohol is achieved in two ways: (a) by preparation of its corresponding active carbamate or (b) by conversion to its corresponding reactive carbonate (Figure 4). A reactive carbamate can be prepared by treating the alcohol

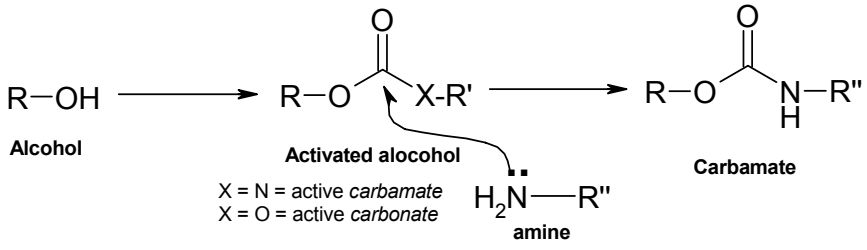

Figure 4. Schematic representation of carbamate synthesis by active carbamate and active carbonate methods

with 1,1'-carbonyldiimidazole (CDI) while reagents such as *p*-nitrophenylchloroformate, bis (*p*-nitrophenyloxy)carboyl (Wang & Weller, 1991) or dibenzotriazolyl carbonate (DBTC) can readily convert the alcohol to the active carbonate (Figure 5).

The first synthesis of a 3'-O-5'-N-carbamate-linked dimer of thymidine was reported using CDI as coupling reagent in 44% yield (Gait *et al.*, 1974). Using the same strategy, later, Coull *et al.*, (1987) prepared a carbamate-linked hexamer. In 1977,

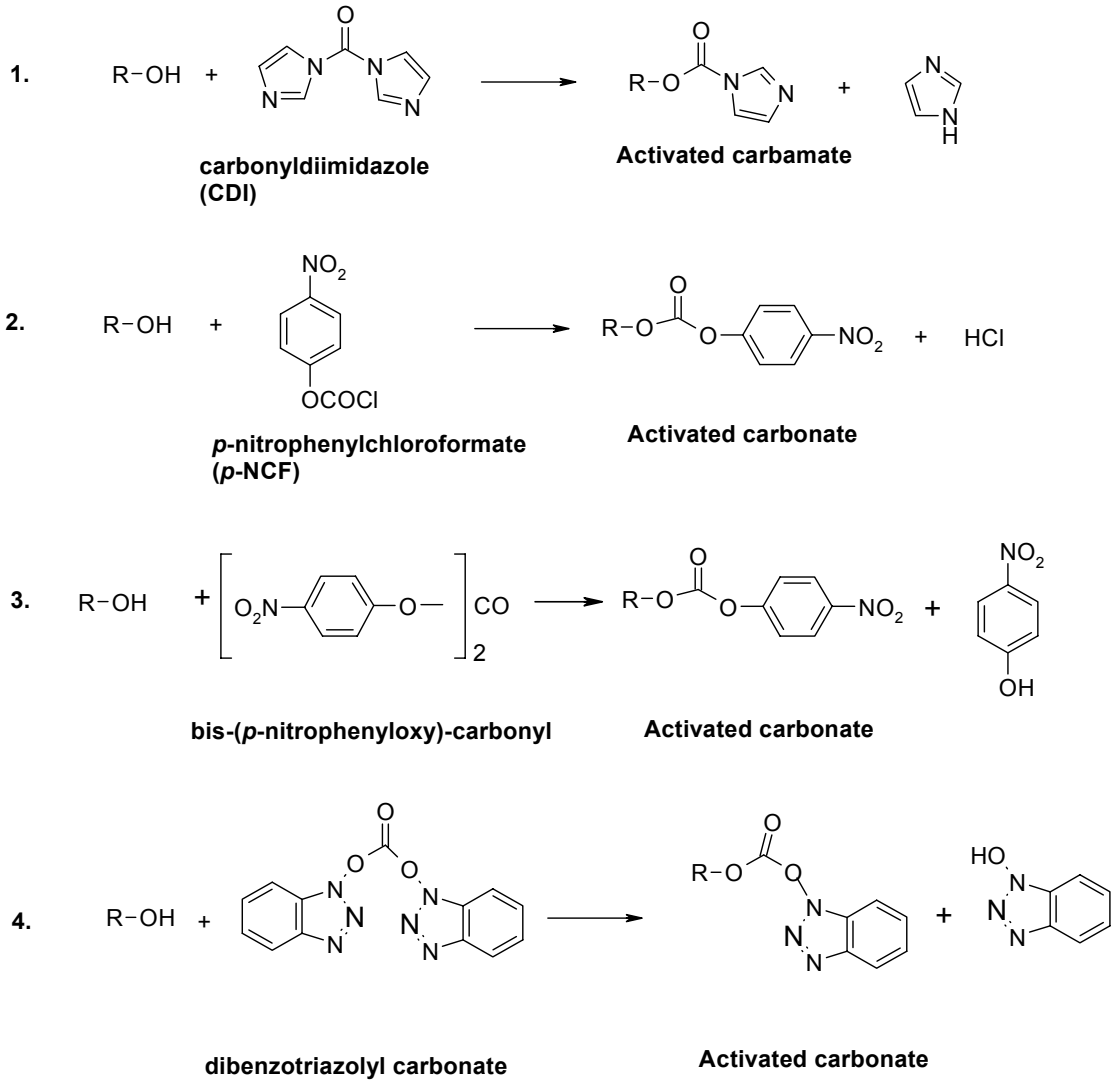

Figure 5. The activating reagents for alcohol

Mungall & Kaiser described the synthesis of a trimer where 3'-O-tritylthymidine was activated with *p*-nitrophenylchloroformate (86%yield) followed by coupling with 5'-amino-5'-deoxythymidine. Further activation of the dimer and repeat of condensation gave the trimer. Warrass & Jung (1998) used dibenzotriazolyl carbonate (DBTC) as an activating reagent, which gave excellent yields for the preparation of cyclic oligocarbamates on solid support

3.3.3 Activation of t-Boc Protected Aminoalcohol Monomers

Activation using Carbonyldiimidazole (CDI)

In the literature, for the solution phase synthesis of carbamates, N-protected aminoalcohols, after activation are reacted with *O*-protected aminoalcohol component

(Coull *et al.*, 1987). In the present work, it was decided to investigate the need for the hydroxyl protection in the synthesis of oligocarbamates. For this purpose, *t*-Boc protected amino alcohol **62** was activated to its imidazolyl carbamate **63** in 95% yield by the reaction of **62** with 1,1'-carbonyldiimidazole (CDI) (Scheme 3.2). The activated monomer was carefully chromatographed to remove unreacted amino alcohol. 1-

Scheme 3.2

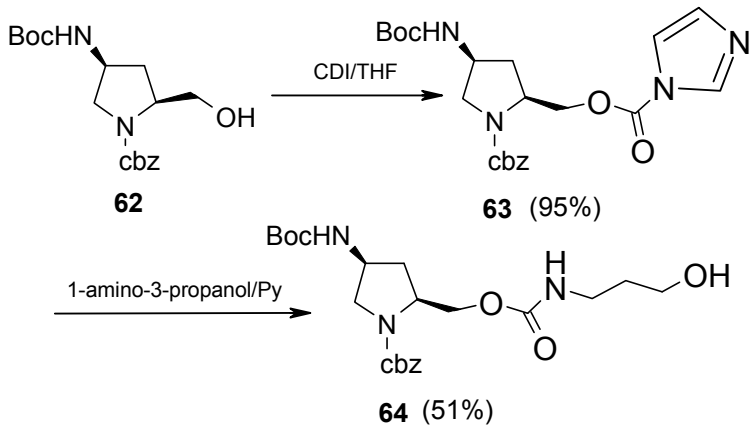

62

63 (95%)

64 (51%)

amino-3-propanol was coupled to the imidazolyl carbamate **63** in the presence of pyridine to obtain the carbamate linkage. The coupling reaction was very slow, giving only 51% yield of carbamate-linked moiety **64**. No undesired product resulting from the attack of the hydroxyl group of 3-aminopropanol on the activated carbonate was detected. This suggested that the protection at the hydroxyl group in aminoalcohol component might not be required to achieve a selective reaction with amine for the carbamate formation, when CDI is used as the activating reagent.

Synthesis of nucleobase acetic acids (**65** and **68**)

To attach a nucelobase to the N1 of the *t*-Boc protected amino alcohol **62**, N1-acetic acid of thymine (Rabinowitz & Gurin, 1953) and cytosine were prepared as shown in Scheme 3.3. Thymine was refluxed with chloroacetic acid in water in the presence of KOH, which gave the potassium salt of thymine acetic acid, which upon neutralization with HCl gave **65** in 71% yield (Scheme 3.3a). Cytosin-yl-acetic acid **68** was obtained in two steps, as shown in scheme 3.3b, starting from Cbz protected cytosine **58** (Chapter 2, Scheme 2.9b). Compound **58** was treated with ethylbromoacetate in DMF using K_2CO_3 as base to obtain **66** in 87% yield. After alkaline hydrolysis of N1-alkyated product **66** followed by neutralization with HCl, Cbz protected cytosine acetic acid (**68**) was obtained in 90% yield.

Under the above reaction conditions, substantial amount of a compound with an Rf value higher than **66** was formed. The ^{1}H NMR spectrum of this byproduct showed two sets of triplets and quartets corresponding to ethyl ester groups and also, the FAB-

Scheme 3.3

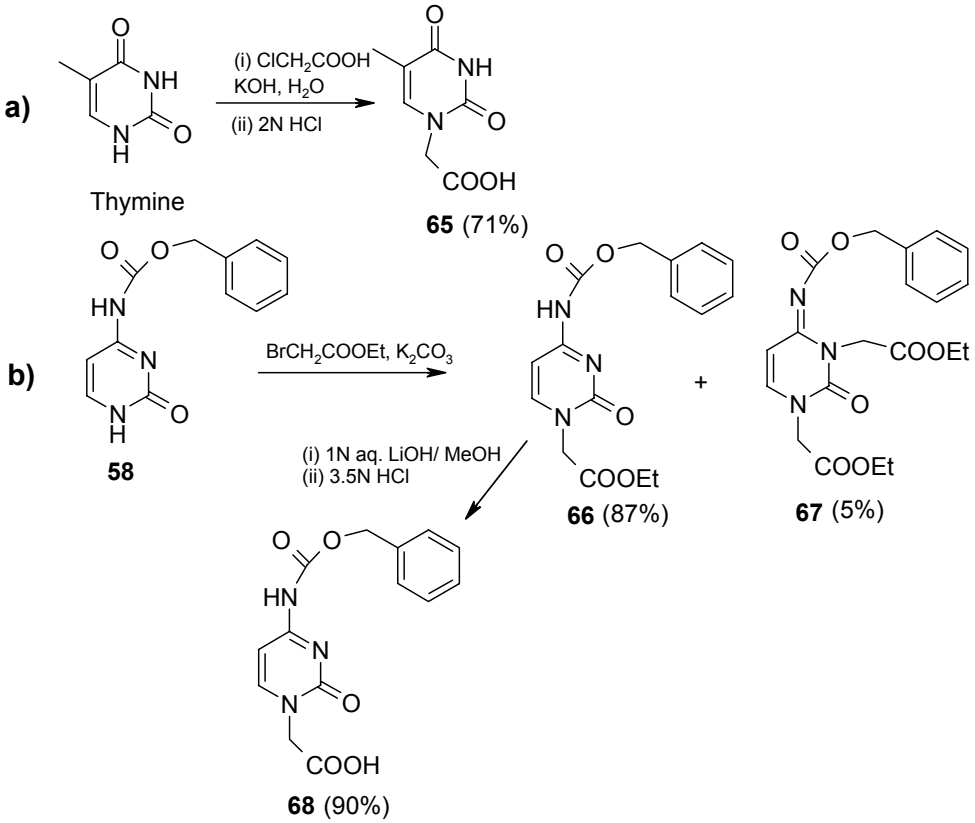

MS analysis showed peaks at 418 and 440 mass units [$(M+H)^+$ and $(M+Na)^+$ respectively, Calcd for $C_{20}H_{23}N_3O_7$: 417.1], which suggested the product to be dialkylated. The second alkyl group can either be on N3 or O2 of cytosine. However, ^{13}C NMR spectrum showed a signal at δ 153.3 corresponding to the 2-carboxo group and a signal at δ 45.9 for N3-CH_2 in addition to N1-CH_2 signal at δ 50.3, confirming the N3-alkylation, thus, assigning the structure as compound **67**. In case of alternative N1,O2-dialkylation, the 2-carboxo signal would be absent and the N3-CH_2 signal would have shifted downfield. The amount of the undesirable N1,N3-dialkylated product formed in this reaction could be lowered to < 5% by performing the reaction at 0^oC temperature with a slow addition of ethylbromoacetate.

Synthesis of activated thymine monomer 70 (Scheme 3.4)

The compound **69** was obtained in 85% yield by subjecting compound **62** to hydrogenation using Pd/C giving N1-amine followed by coupling with thymine acetic

Scheme 3.4

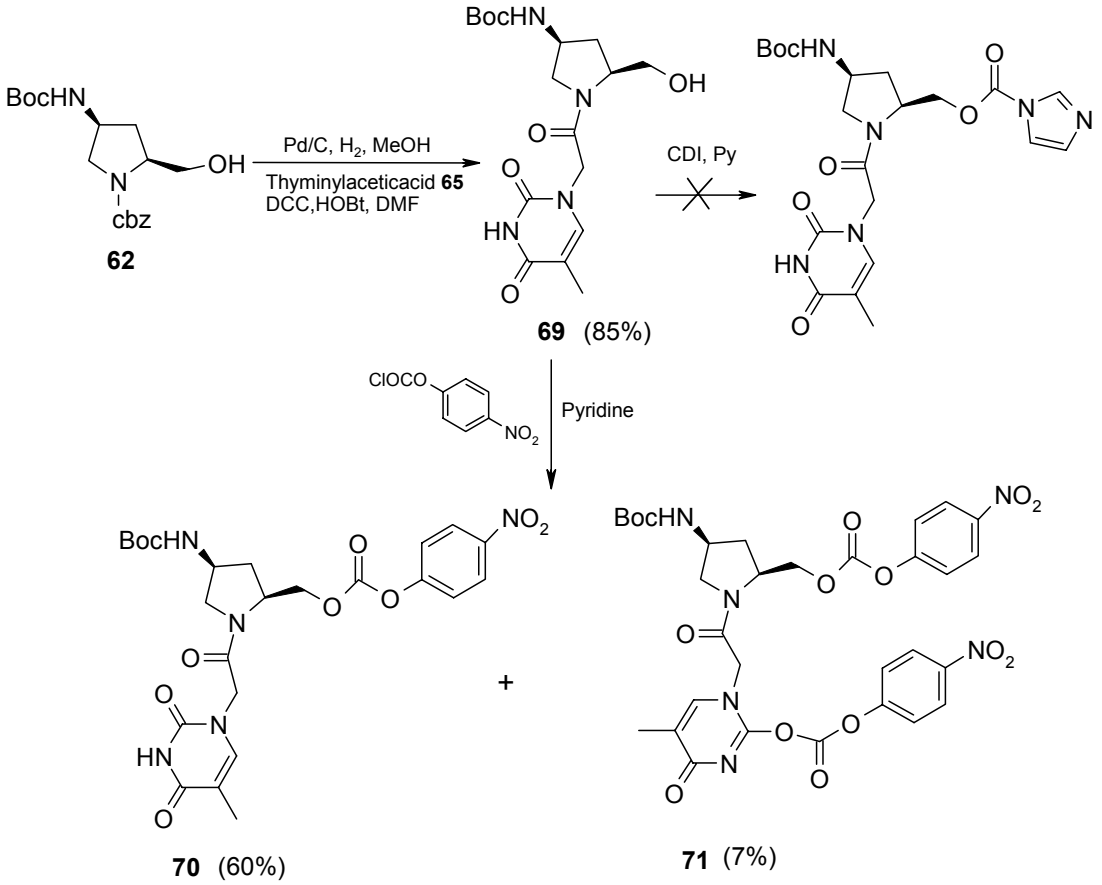

acid **65** using DCC/HOBt coupling conditions. Activation of the primary alcohol function in **69** could not be achieved using CDI even after prolonged reaction times and the starting material was recovered unchanged. Probably, the alcohol component **69** (N1-acetyl thymin-1-yl) is more hindered compared to **62** (N1-Cbz), in the later case, the CDI activation gave excellent yields (95%, Scheme 3.2). An attempt to activate the alcohol in thymine monomer **69** using *p*-nitrophenylchloroformate/Et_3N, provided exclusively the dicarbonate **71** whose structure was confirmed by ^1H NMR spectrum with signals in the aromatic region integrating for 8H and the FAB-MS analysis showing a peak at 735 $(M+Na)^+$ (calcd. for $C_{31}H_{32}N_6O_{14}$:712.19). It appears that the Et_3N is a sufficiently strong base to enolize thymine, the enol form of which reacts with *p*-nitrophenylchloroformate to give the dicarbonate. When this reaction was carried out using pyridine as both a base and solvent the desired product, **70** was obtained in very low yield (10%). With dioxane as solvent in the presence of one equivalent of pyridine as base, the reaction proceeded at a much faster rate to yield **70** in 70% yield. The activated monomer **70** was moderately stable at room temperature and decomposed to

give the parent alcohol **69** and *p*-nitrophenol. However, when stored at 4°C under argon atmosphere, this was stable for long periods.

Synthesis of activated cytosine monomer (73)

The common precursor **62**, after N1-deprotection using Pd/C in MeOH under H_2 pressure (60psi) followed by coupling with Cbz protected cytosine acetic acid **68** in the presence of DCC/HOBt afforded **72** in 91% yield (Scheme 3.5). Activation of the alcohol in compound **72** was effected in a manner similar to that described for the synthesis of thymine monomer **69** (Scheme 3.4) using Et_3N as base to obtain the *p*-nitrophenylcarbonate **73** in 53% yield.

Scheme 3.5

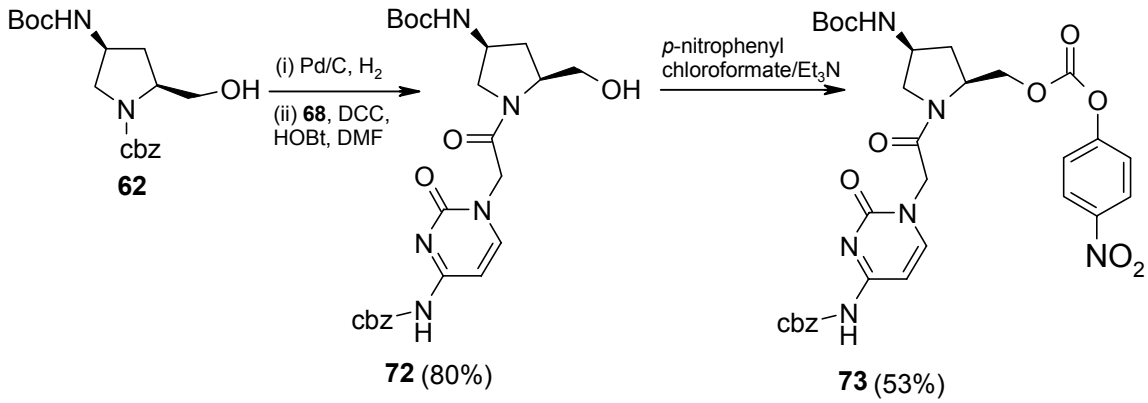

3.4 Solution Phase Synthesis Of The Dimer

The formation of carbamate linkage in pyrrolidine system was first investigated by preparation of carbamate linked dimer in solution. Carbamate linked pyrrolidinyl

Scheme 3.6

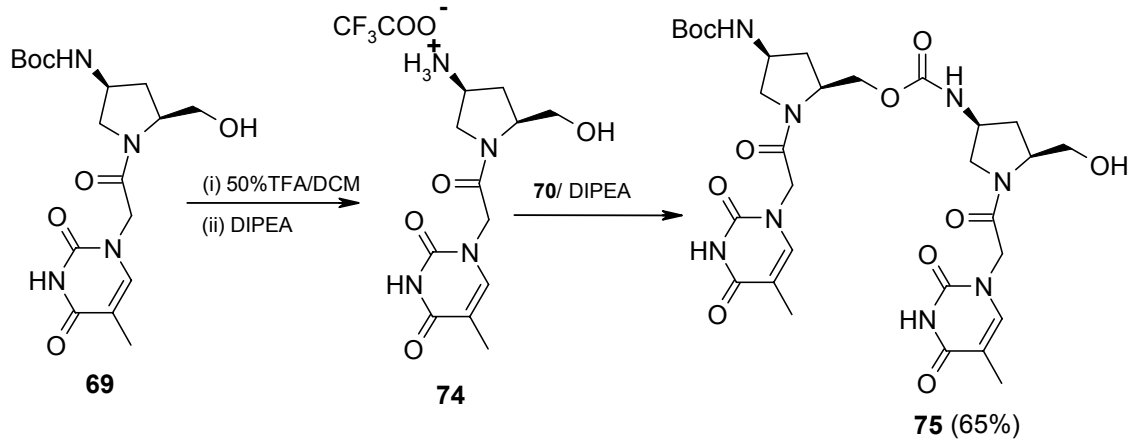

dimer was synthesized from the thymine monomer as shown in scheme 3.6. The deprotection of *t*-Butoxycarbonyl in **69** was achieved by treating it with 50%TFA/DCM to obtain the trifluoroacetate salt **74**. In the next step, amine salt **74** after neutralization was coupled with one equivalent of the activated monomer **70** at ambient temperature to furnish the dimer **75** in 65% yield. It was observed that the formation of carbamate is catalyzed by the addition of DIPEA with the reaction proceeding to completion in 3-6h. The amine functionality of **74** reacted to give the dimer **75** selectively and no undesirable carbonate product that could arise from the reaction of hydroxyl in the amino-alcohol **74** with the activated alcohol **70** was isolated. This confirmed that even when *p*-nitrophenylchloroformate is used as an activating reagent, the protection of hydroxyl group in aminoalcohol moiety is not necessary.

3.5 Solid Phase Synthesis of Oligocarbamates

The solid phase synthesis of carbamate-linked nucleic acids was carried out using the scheme outlined in Figure 6. The chloromethylated 1% DVB-cross-linked polystyrene resin (Merrifield resin) was functionalized with the first residue *t*-Boc-β-alanine by treating the resin with the cesium salt of *t*-Boc-β-alanine (Gisin, 1970). β-alanine [$H_2N(CH_2)_2COOH$] linker decreases the steric-hindrance between growing peptide chains and being achiral does not interfere with conformational/structural properties of the derived oligomer. The amount of the first residue loaded was estimated as 0.68mmol/g using picric acid assay (Merrifield & Stewart, 1966; Erickson & Merrifield, 1976). The amine of the β-alanine anchored to the resin was freed by deprotecting the *t*-Boc group with 1:1 TFA/DCM followed by neutralization with 5% DIPEA/DCM. The resin was partially capped using calculated amount of acetic anhydride in pyridine to decrease the loading value to approximately 0.3mmol/g. The resin with the free amine function was soaked in DMF and reacted with three equivalents of activated thymine monomer **70** in the presence of catalytic amount of DIPEA. The coupling reaction was complete in 2 h to give the resin bound monomer. This deprotection-coupling cycle was repeated twice to get the trimer. The deprotection of the *N*-*t*-Boc protecting group and the coupling reaction were monitored by Kaiser's test (Kaiser *et al.*, 1970).

Successful application of the chemistry for the synthesis of carbamate linkage on solid support requires the verification of the stability of the linkage towards the conditions used to cleave the oligomer from the resin. So far in literature, there are two reports for the synthesis of carbamate oligomers using solid-phase technique. Wang &

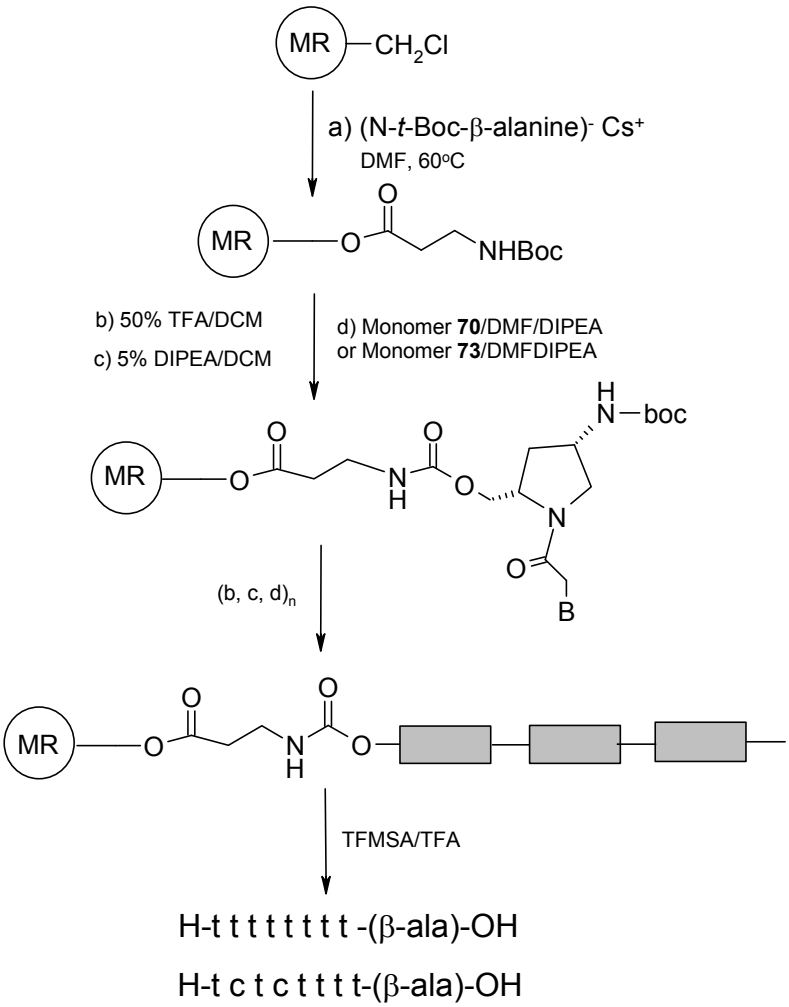

Figure 6. Schematic representation of solid phase synthesis of pyrrolidinyl carbamate nucleic acids

Weller (1991) using 1% cross-linked aminomethyl polystyrene resin developed an anchor for solid phase synthesis that allows the release of oligonucleotide analogues together with the base protective groups from the solid support. In their work, oligomer was cleaved with DBU/diethylmalonate in DMF to recover morpholine based carbamate-linked hexamer in 95% yield. In a second report, cyclic oligocarbamates were synthesized by using 2-chlorotrityl chloride resin where the ester linker is cleaved with hexafluoro-2-propanol (HFIP) at the end of the synthesis (Warrass et al., 1998).

In the present work, to extend the standard method of peptide-resin cleavage to the oligocarbamates, the resin-bound trimer **76** (H-t t t-β-alanine-MF) was subjected to two well-known methods of peptide-resin cleavage (Stewart & Young, 1984) (Figure 7). In the acidolysis method, the peptide linked via benzyl ester to the resin is cleaved by treatment with strong acids like trifluoromethanesulphonic acid (TFMSA) in trifluoroacetic acid (TFA) to yield the peptide with free carboxy-terminus (Fields &

Fields, 1991). In the ammonolysis method, the peptide-resin is treated with methanolic ammonia at 55°C for 16h to yield peptide-C-terminal amide.

To study the stability of the linkage to acidic as well as basic conditions, the resin bound trimer was first subjected to TFMSA/TFA treatment. After cleavage reaction, the trimer was precipitated from methanol with dry diethyl ether and the oligomer was subjected to gel-filtration on Sephadex G10. Another portion of resin

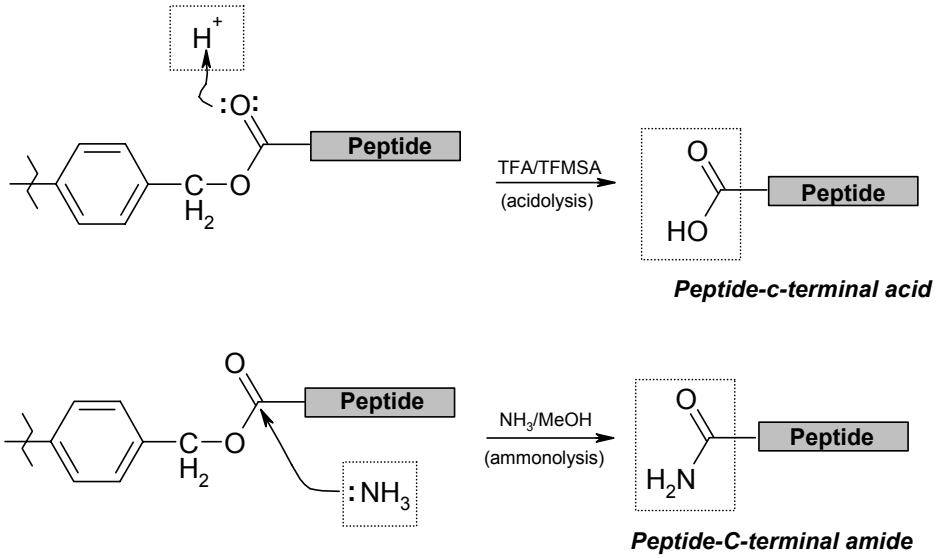

Figure 7. Schematic representation of acidolysis and ammonolysis of resin bound peptide giving *c*-terminal acid and *c*-terminal amide respectively.

containing the oligomer was treated with methanolic ammonia in a sealed vial at 55°C for 16h to liberate the C-terminal amide of the trimer. The trimer so liberated was further subjected to TFA/DCM (1:1) treatment for the removal N-terminal-*t*-Boc group.

HPLC and MALDI-TOF mass spectral analyses were performed on the crude products obtained from both TFMSA/TFA and NH_3/MeOH treatment. RP-18 HPLC profile of the acidolysis product showed a peak with a retention time of 21.36 min (Figure 8a), while in the case of ammonolysis product, there was only a minor peak (5%) at 21.4 min and a major peak at 5.9 min (Figure 8b) that may correspond to the degraded product. This shows that the carbamate linkage is stable in strong acidic conditions but not towards basic conditions. MALDI-TOF mass spectrum of the crude product from TFMSA/TFA cleavage reaction showed peaks at 1015.3 $(M+H)^+$, 1037.3 $(M+Na)^+$, 1057.5 $(M+K)^+$ [Calcd. for $C_{42}H_{55}N_{13}O_{17}$=1013.38] (Figure 9a), where as only a small peak at 1015.5 corresponding to the *C*-terminal amide was observed in the MALDI-TOF mass spectrum of the ammonolysis product of the carbamate trimer [Calcd. for $C_{42}H_{56}N_{14}O_{16}$=1012.34] (Figure 9b).

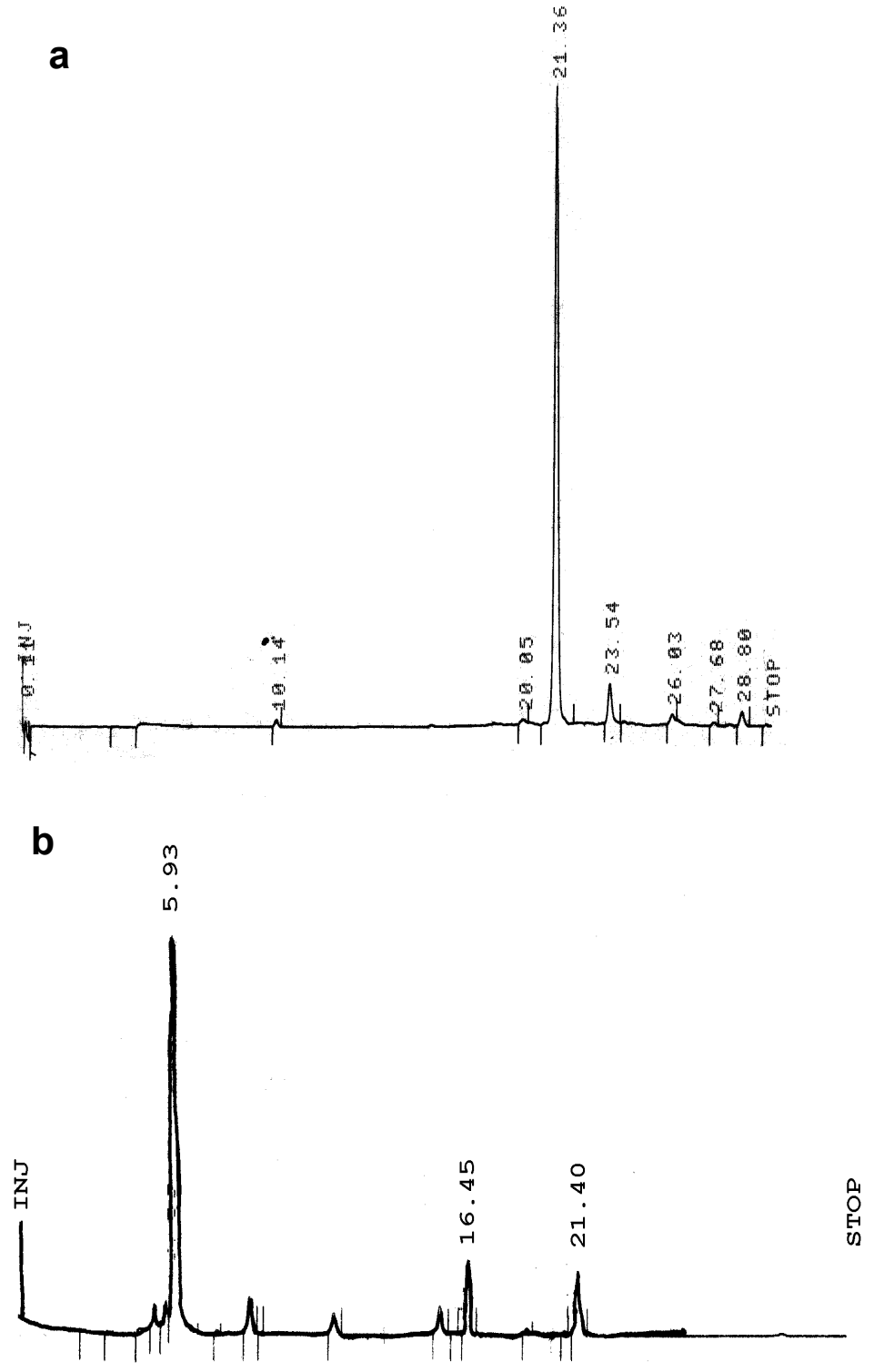

Figure 8. HPLC profiles of carbamate-linked trimer cleaved from the resin with a) TFMSA/TFA b) NH_3/MeOH analyzed on RP-C18 column, gradient A to 30%B in 30min where A = 0.1%TFA in H_2O and B = 0.1%TFA in CH_3CN:H_2O 1:1, flow rate 1ml/min.

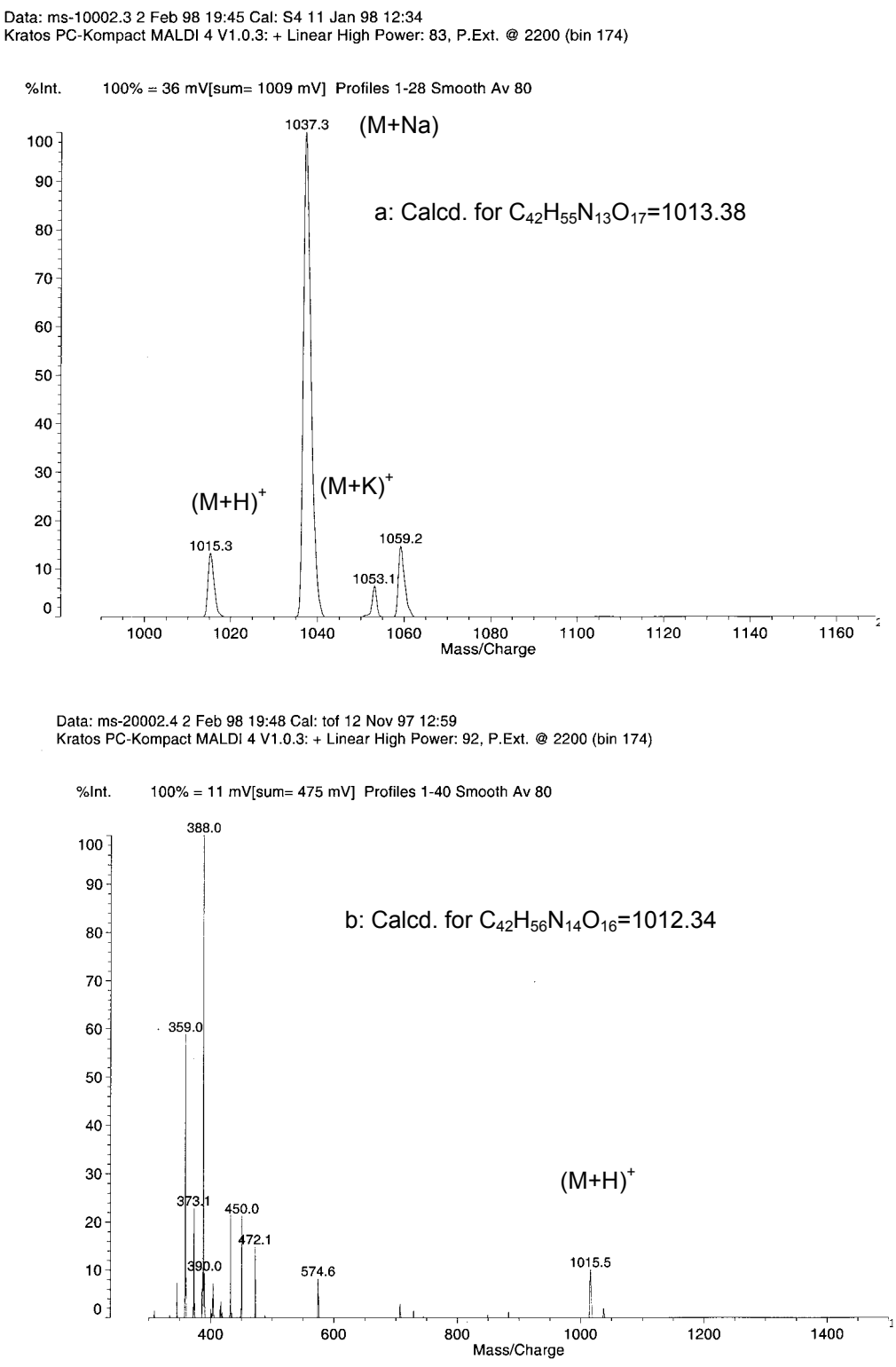

Figure 9. MALDI-TOF spectra of carbamate-linked trimer cleaved from resin with a) TFMSA/TFA b) NH_3/MeOH

Synthesis of pyrrolidinyl carbamate nucleic acids (pyCNA)

Various oligomers synthesized in the present study are shown in Table 1. The synthesis of the oligomers (CNA1-CNA3) incorporating the chiral conformationally constrained modified unit **70** [t = (2*S*,4*S*)-thymine monomer], at specific positions in the *aeg*PNA was done on the solid support using the procedures described above. In the present discussion, the oligomers with both mixed *aeg*/*pyrrolidine* as well as only *pyrrolidine* backbone will be represented as *py*CNA. Three sequences with mixed *aeg*/*pyrrolidine* backbone were prepared each having one pyrrolidine unit. the

Table 1. PNA/*py*CNA and DNA sequences used in the present study

Entry	Sequence
*aeg*PNA	H-T T T T T T T T-(β-ala)-OH
CNA1	H-T T T T T T t T-(β-ala)-OH
CNA2	H-T T T t T T T T-(β-ala)-OH
CNA3	H-t T T T T T T T-(β-ala)-OH
CNA4	H-t t t t t t t t-(β-ala)-OH
CNA5	H-t c t c t t t t-(β-ala)-OH
DNA1	5'-G C A A A A A A A A C G-3'
DNA2	5'- A A A A G A G A -3'

T denotes *aeg* monomer, **t** and **c** denote pyrrolidinyl monomer with thymine and cytosine nucleobase respectively

sequence CNA1 carries the modification at the position which is penultimate form C-terminal so that carbamate linkage comes in the sequence. CNA2 and CNA3 have the modification in the middle and N-terminal respectively. Two oligomers with stereoregular backbone (all carbamate) were also prepared. An octamer CNA4 (t_8) carries all pyrrolidinyl thymine monomers (**70**) and CNA5 is prepared using both **70** and cytosine monomer (**73**). The unmodified *aeg*PNA oligomer T_8 prepared in Chapter 2 was used as a control here.

Cleavage of the pyCNA from the solid support

The cleavage of the carbamate/peptide mixed as well as carbamate-linked homooligomers was carried out using TFMSA/TFA method (Fields & Fields, 1991) which yielded sequences bearing free *C*-termini of the β-alanine. As the deprotection of benzyloxycarbonyl group also occurs under these conditions (Stewart & Young, 1984), no further treatment was given to CNA5 to remove Cbz protection on the cytosine. After the cleavage reaction, the oligomers were precipitated from methanol with dry diethylether. While precipitation, it was observed that the homooligomers CNA4 and CNA5 had considerable solubility in diethylether.

Purification of pyCNA

The cleaved oligomers CNA1-CNA3 were subjected to an initial gel-filtration, using Sephadex G25 to remove truncated sequences and scavengers used during the cleavage reaction. Due to the poor water-solubility of CNA4 and CNA5 gel-filtration on Sephadex G25, which requires aqueous conditions, could not be performed. So, LH-20 was used for their purification using isopropanol as eluant. Sephadex LH-20 (Pharmacia) is a beaded, cross-linked dextran, which is hydroxypropylated to yield a chromatographic media with both hydrophilic and lipophilic character. Due to its dual character, Sephadex LH-20 swells in water and a number of organic solvents. The oligomers were further purified by reverse phase HPLC on a semi-preparative RP-C4 column. The purity of the oligomers thus obtained was rechecked by reverse phase HPLC on a RP-18 column and their structural integrity was confirmed by MALDI-TOF mass spectral analysis. Representative HPLC profiles and mass spectra are shown in Figures 10-13.

Synthesis of the complementary deoxyribonucleic acids (DNA)

The sequences DNA1 and DNA2 (Table 1) complementary to *aeg*PNA/*py*CNA sequences were synthesized on a Pharmacia Gene Assembler Plus DNA synthesizer using the standard β-cyanoethyl phosphoramidite chemistry. The oligomers were synthesized in the 3' → 5' direction on a *controlled pore glass* (CPG) solid support and were cleaved by treatment with aq. ammonia (Gait, 1984; Agrawal, 1993). The oligomers were de-salted by gel-filtration through Sephadex G25 and their purity as ascertained by RP-18 analytical HPLC was more than 98%. Thus these oligonucleotides were used without further purification in the biophysical studies.

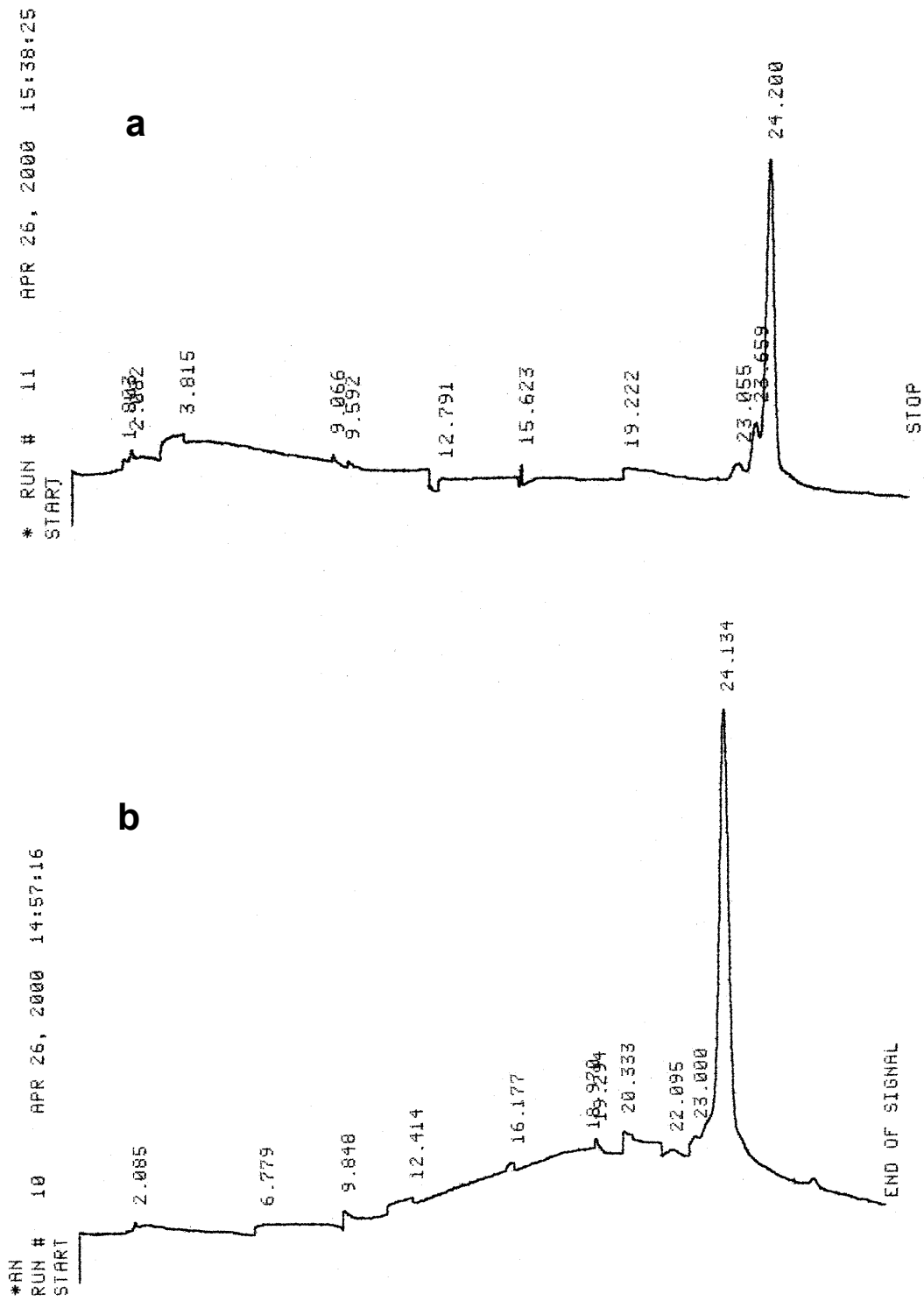

Figure 10. HPLC profiles of a) CNA1; *aeg*PNA octamer with modification at C-terminal b) CNA2; *aeg*PNA octamer with modification in the center analyzed on RP-C18 column, gradient A to 30%B in 30min where A = 0.1%TFA in H_2O and B = 0.1%TFA in CH_3CN:H_2O 1:1, flow rate 1ml/min.

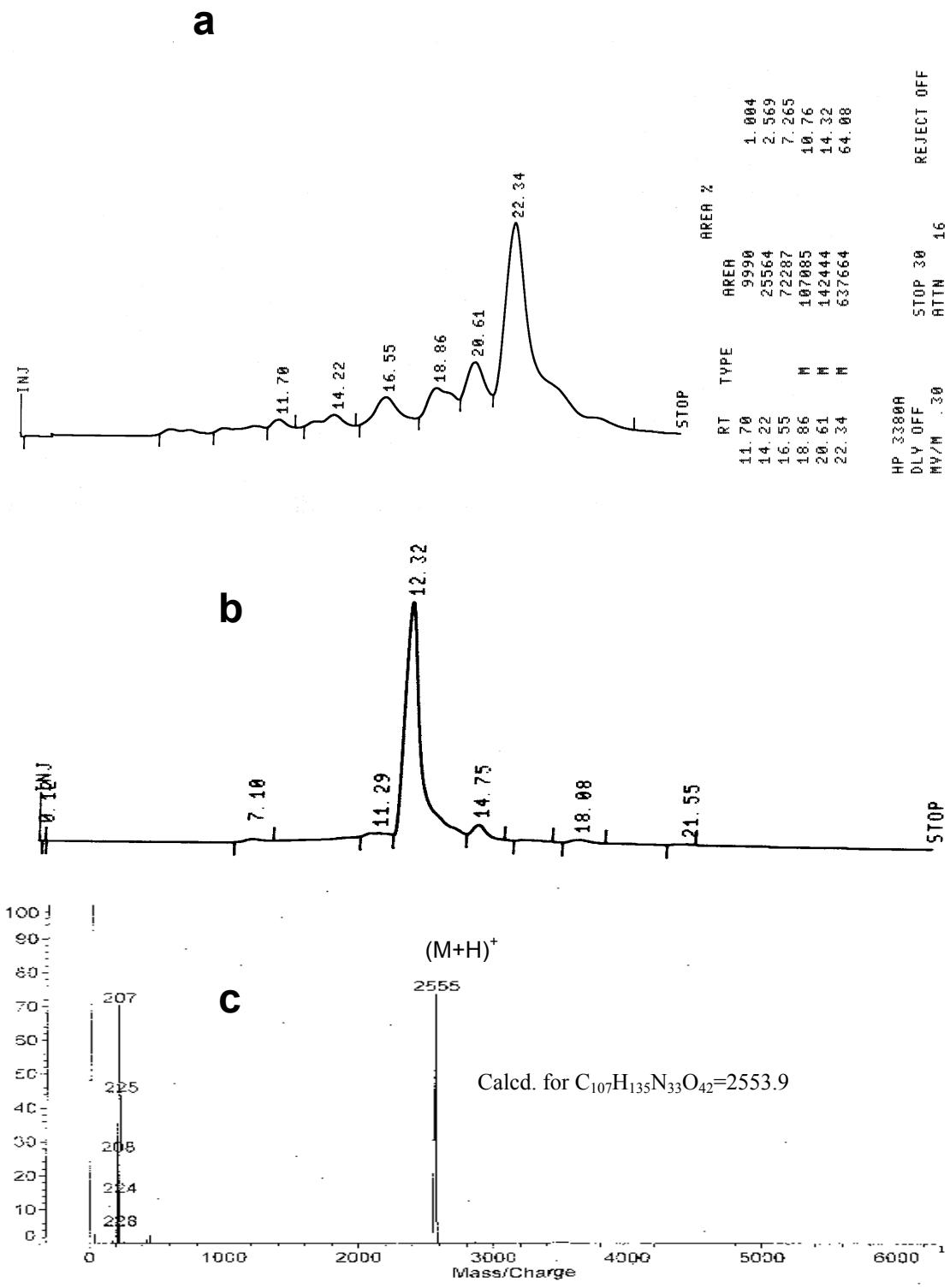

Figure 11. HPLC profiles **a)** of crude CNA4; octamer: with all t modified units on RP-C4-semipreparative column, isocratic 0.1%TFA in CH_3CN/H_2O 1:9 **b)** purified CNA4 on RP-C18 analytical column, gradient A to 50%B in 30min., flow rate 1ml/min. **c)** the MALDI-TOF mass spectrum of the purified CNA4.

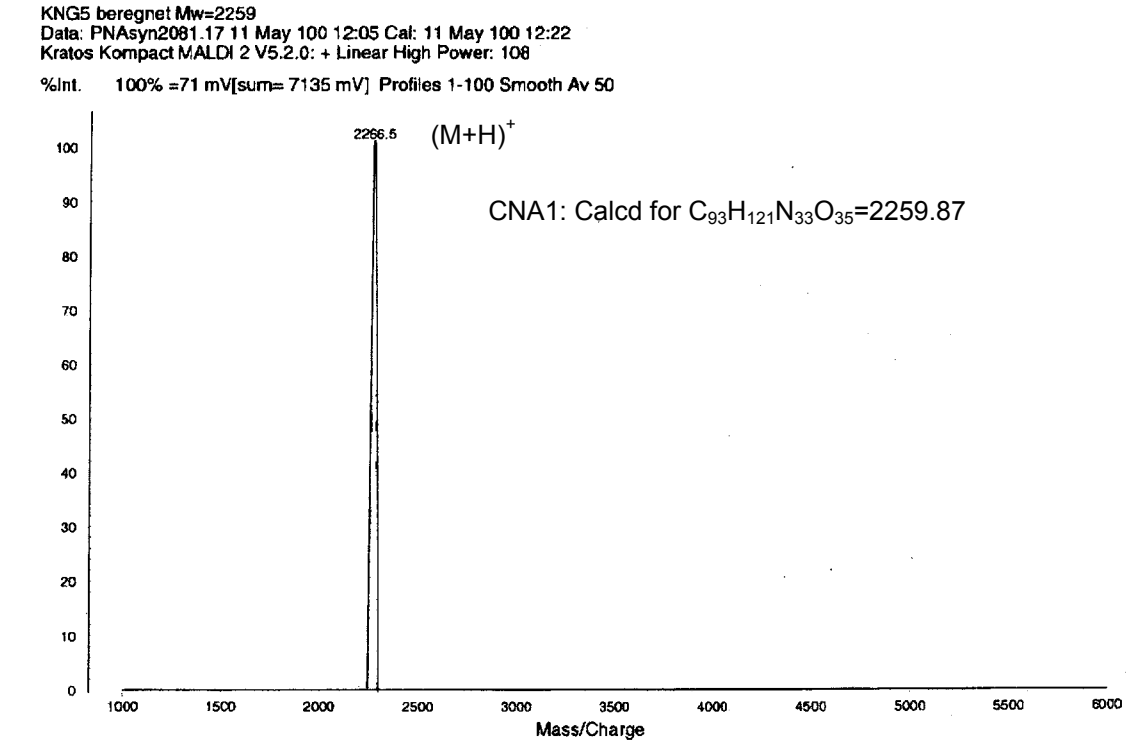

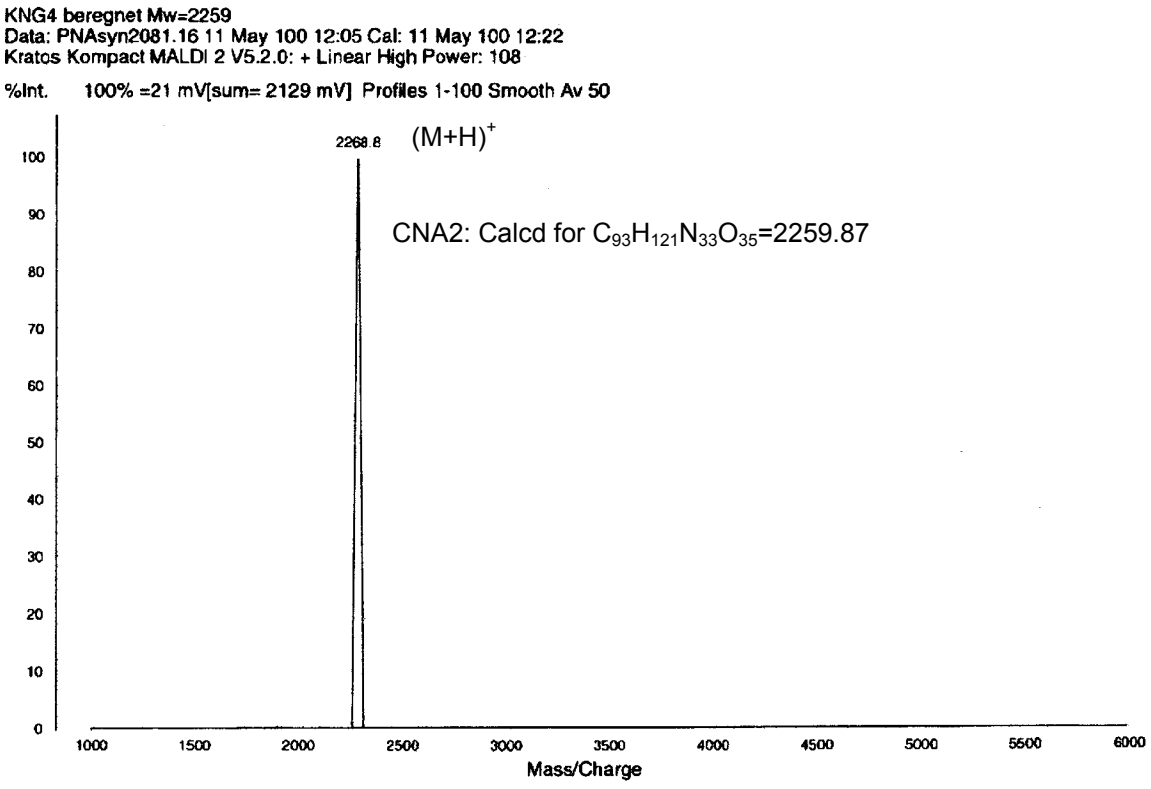

Figure 12. MALDI-TOF mass spectra CNA1 and CNA2

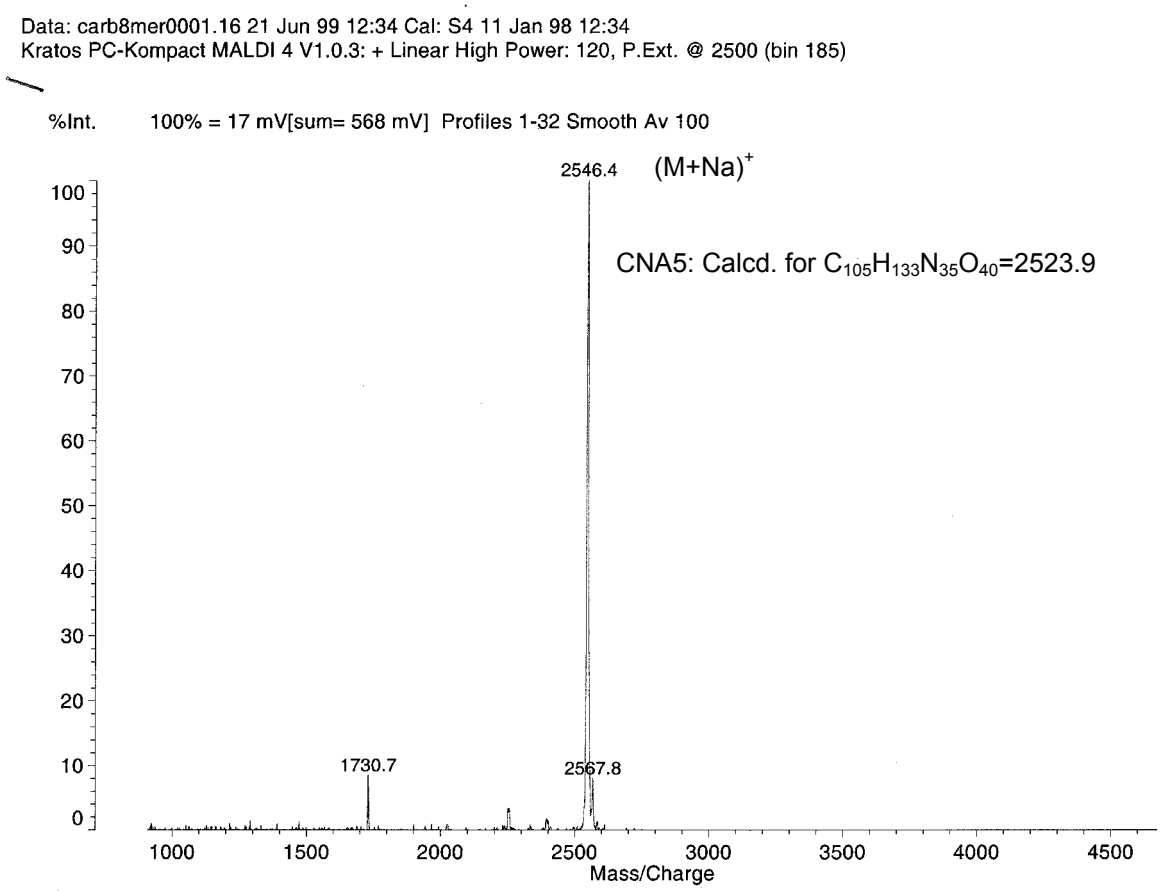

Figure 13. MALDI-TOF mass spectrum of CNA5

3.7 Biophysical Studies of *py*CNA:DNA Complexes

To investigate the binding ability of *py*CNA towards complementary DNA, first the stoichiometry of the *py*CNA:DNA was determined using Job's method (Job, 1928). The UV-melting studies were carried out with all the synthesized oligomers and the Tm data was compared with the reference *aeg*PNA T_8. To study the difference between the association and dissociation rates of *py*CNA:DNA complexes, the hysteresis experiment was carried out. The CD spectra were recorded for the sequences that were found to make complexes with complementary DNA strand.

3.7.1 Binding Stoichiometry

CD Mixing Curve

As described in the Chapter 2, a*eg*PNA is inherently achiral. However, upon complexation with complementary nucleic acids, it is rendered chiral and exhibits an induced CD signal. Chirality can be induced in the achiral PNA strand by linking chiral moieties like amino acids (Egholm *et al.*, 1993), peptides (Koch *et al.*, 1995), or

oligonucleotides (Petersen *et al.*, 1995; Petersen *et al.*, 1996; Uhlmann *et al.*, 1998) to the PNA termini. PNA has also been rendered chiral by the incorporation of chiral amino acids in its backbone (Gangamani *et al.*, 1999; Lowe *et al.*, 1997; Haaima *et al.*, 1996).

In order to determine the stoichiometry of binding of the *py*CNA/DNA complexes various stoichiometric mixtures of CNA3 and DNA1 were prepared with relative molar ratios of (DNA1:CNA3) strands in 9:1, 8:2, 7:3, 6:4, 5:5, 4:6, 3:7, 2:8, 1:9,

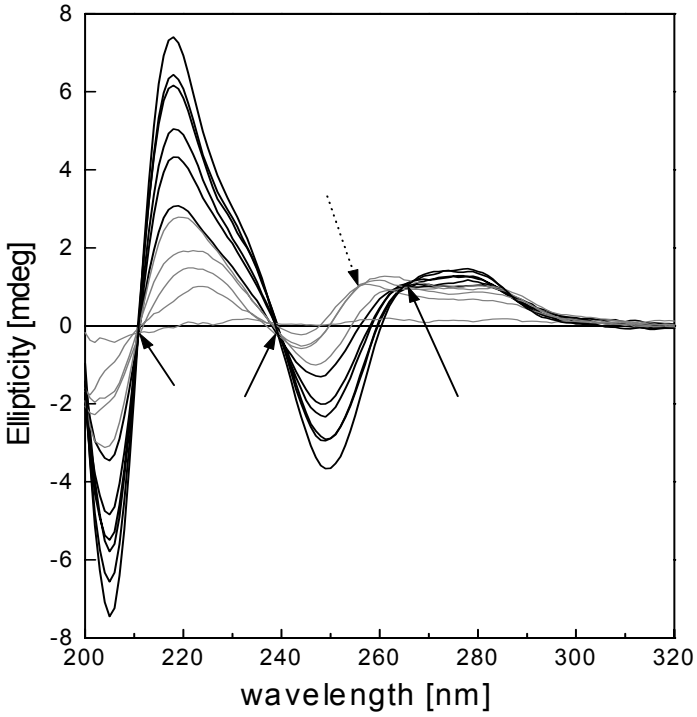

Figure 14. CD mixing spectra of CNA3:DNA1 in molar ratios; 10:0, 9:1, 8:2, 7:3, 6:4, 5:5, 4:6, 3:7, 2:8, 1:9, 0:10 in 10mM sodium phosphate buffer (pH= 7.3).

all at the identical total strand concentration of 2μM in sodium phosphate buffer (10mM, pH 7.3). The complexes were annealed before the CD spectra were recorded. Figure 14 shows the CD spectra of the various mixtures as measured at 15°C.

The CD spectrum of pure DNA shows a strong CD signal (220nm wavelength regions) where as, no detectable CD bands are observed in the CD spectrum of pure CNA3 at 2μM strand concentration. Such behavior is expected in an oligomer comprising largely achiral monmeric units (*aeg*PNA). Introduction of a single carbamate unit at the N-terminus does not seem to induce detectable CD signals. In the CD spectra of the mixtures, at all stoichiometries, two isodichroic points were seen at 211

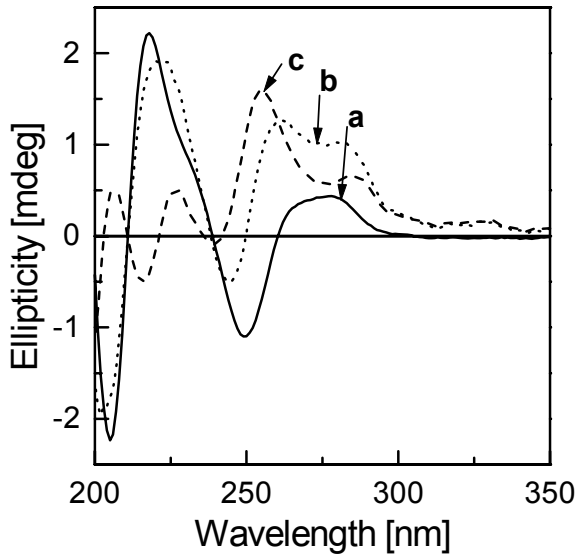

Figure 15. a) Calculated, b) recorded and c) difference, CD spectra of 7:3 mixture of CNA3 and DNA1 at 15^{o}C in 10mM phosphate buffer (pH 7.3).

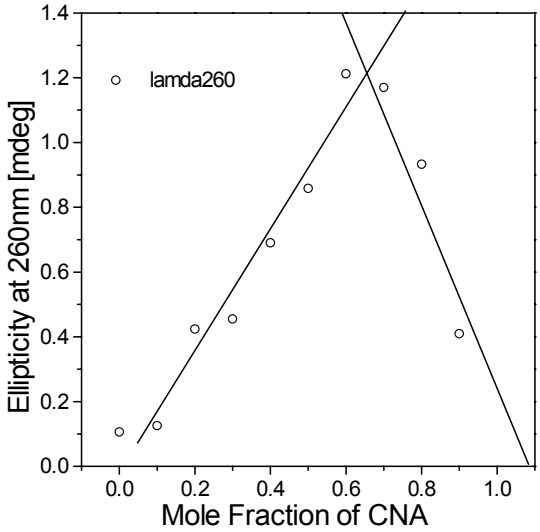

Figure 16 CD mixing curve for CNA3 and DNA1 mixtures in the molar proportions of 0:100, 20:80, 30:70, 40:60, 50:50, 60:40, 70:30, 80:20, 10:90. Solution conditions (10mM sodium phosphate buffer, pH 7.3)

and 239 nm (Figure 14). However, in DNA1:CNA3 in the stoichiometric range 10:0-4:6 a distinct isodichroic point is seen at 266nm which is shifted to 257nm for the mixtures with 3:7-1:9 molar ratio of DNA1:CNA3. Difference spectra for all the solutions were obtained by subtracting the calculated CD of each mixture (obtained by addition of pure CNA3 and DNA1 CD spectra in arithmetic proportions) from the recorded CD spectrum of the solution for that molar ratio. Upon investigation of the difference spectra of all the mixtures, it was found that the difference spectrum for the mixture of CNA3:DNA1 in molar ratio 7:3 deviated the most form the recorded one. Figure 15 shows the calculated, recorded and the difference spectra for the complex in 7:3 ratio with a distinct +ve band at 260nm. Thus mixing curve (Figure 16) was plotted using the CD data at 260nm obtained from the spectra in Figure 14. The data were fitted to two straight lines which intersected at 65:45 molar ratio of CNA3:DNA1 suggesting a 2:1 stoichiometry for their association forming the complex [$(PNA3)_2$:DNA1]. Moreover, in the difference spectrum, the positive band in the region of 260-265nm is more prominent compared to the positive band in the same region for the (aegPNA)$_2$:DNA1 complex, which is a characteristic band for the triplexes formed by *aeg* polypurines with complementary DNA (Kim *et al.*, 1993).

3.5.2. UV-Tm Studies of The Triplexes

UV-melting experiments with 2:1 stoichiometry for *aeg*PNA/*py*CNA:DNA were carried out in 10 mM phosphate buffer at pH 7.3. For experiments with *aeg*PNA T_8 and CNA1-CNA4, the polypurine sequence DNA1, A_8 with GC clamps on both sides was used as a complementary strand. The mixed base all-modified carbamate octamer CNA5 compring two cytosine bases and six thyminyl units was complexed with its complementary DNA2. Figure-17A shows the plot of hyperchromicity at 260 nm Vs the temperature of measurement. The Tm data was derived from the first derivative curves of the normalized A_{260} data (Figure 17B) and the corresponding Tm values are listed in Table 2. The control triplex (*aeg*PNA $T_8)_2$:DNA1 shows a Tm of 44.5°C. The CNA1 where the modified residue "t" is present in the penultimate position from the *C*-terminus of the *aeg*PNA sequence, shows a Tm of 31.5 °C, while $(CNA3)_2$:DNA1 with t

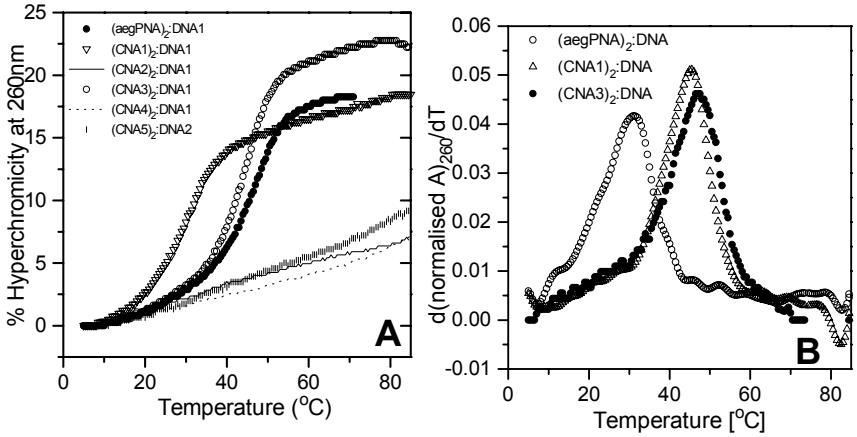

Figure 17. UV-Tm profiles of A) (*aeg*PNA/*py*CNA)$_2$:DNA complexes B) First derivative of normalized A_{260} for (*aeg*PNA/*py*CNA)$_2$:DNA complexes

at the N-terminus shows a Tm of 44°C. In contrast, the stereoregular carbamate-linked oligomers CNA4 and CNA5 in their respective complexes with DNA1 and DNA2 do not show a melting-transition. Also, the hyperchromicity chages observed for these complexes are among the lowest ($(CNA4)_2$:DNA1=7.1%; $(CNA5)_2$:DNA2=9.3%). The slopes of the sigmoidal curves and the widths of their correpsonding first derivative curves of both the (*py*CNA oligomers)$_2$:DNA1 complexes and the control triplex (*aeg*PNA)$_2$:DNA1 are very similar. Moreover the percentage hyperchromicity for the *py*CNA:DNA complexes was higher than that of *aeg*PNA:DNA triplexes, in the order CNA3>CNA1>*aeg*PNA.

Table 2. UV-Tm of *aeg*PNA/*py*CNA complexes.

PNA/*py*CNA:DNA	Complex	Tm ^{o}C (ΔTm)	%Hyperchromicity
H-T T T T T T T T-(β-ala)-OH 3'-G C A A A A A A A A C G-5'	(*aeg*PNA)$_2$:DNA1	44.5	13
H-T T T T T T t T-(β-ala)-OH 3'-G C A A A A A A A A C G-5'	(CNA1)$_2$:DNA1	31.5 (-13)	18.4
H-T T T t T T T T-(β-ala)-OH 3'-G C A A A A A A A A C G-5'	(CNA2)$_2$:DNA1	nt	6.8
H-t T T T T T T T-(β-ala)-OH 3'-G C A A A A A A A A C G-5'	(CNA3)$_2$:DNA	44 (-0.5)	22.2
H-t t t t t t t t-(β-ala)-OH 3'-G C A A A A A A A A C G-5'	(CNA4)$_2$:DNA	nt	7.1
H-t c t c t t t t-(β-ala)-OH 3'- A G A AGA A A A -3'	(CNA5)$_2$:DNA2	nt	9.3

Buffer: 10mM sodium phosphate, pH=7.3. Tm values are ± 0.5^{o}C. Experiments are repeated at least three times and the Tm values are obtained from the peaks of the first derivative plots of the A_{260}. The PNA/*py*CNA strand concentration in each case was taken as 2.5μM. nt represents no transition

These results show that a single carbamate-linked modification towards the C-terminus (the penultimate residue) of the *aeg*PNA i.e. CNA1, causes a larger destabilization (ΔTm= -13°C) as compared to an equivalent *N*-terminal modification (CNA3). The latter does not seem to affect the stability of the triplex significantly (ΔTm= -0.5°C). At the same time a single modification in the center (CNA2) results in no complex formation with its complementary DNA1.

For the DNA complexes of *aeg*PNA, CNA1 and CNA3, the UV-melting (by heating) and re-association (by cooling) studies were carried out. (Figure 18) shows the curves obtained from these studies and It is seen that the cooling curves and heating curves are displaced significantly indicating the presence of hysteresis. This suggests that like *aeg*PNA, the association and dissociation kinetics of the complexes formed by CNA1 and CNA3 with DNA are different.

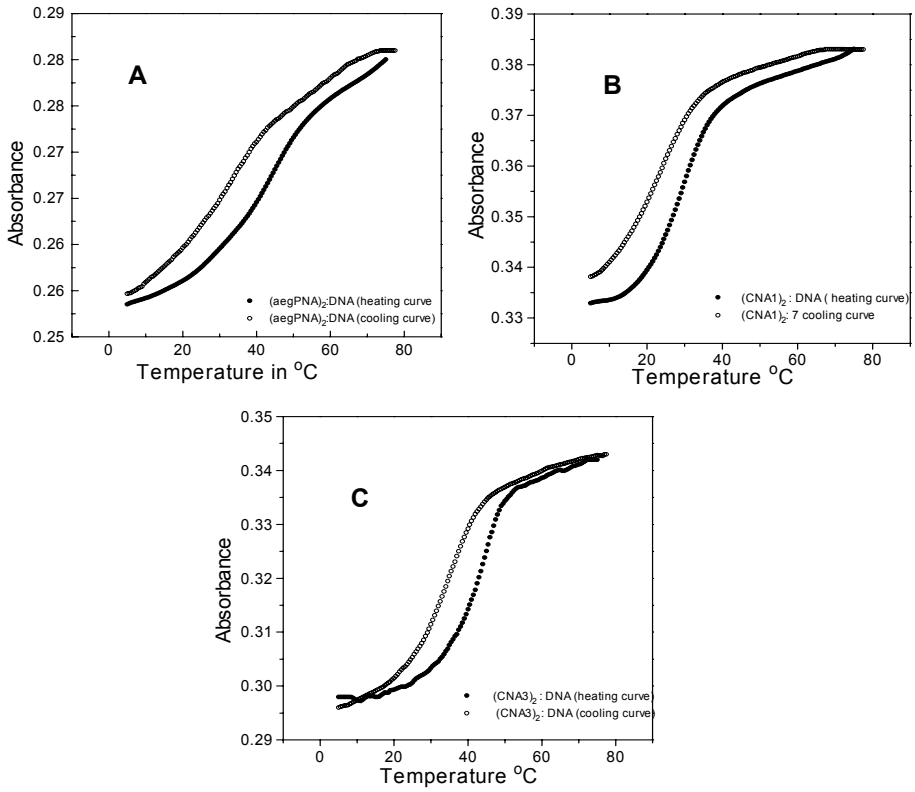

Figure 18. A_{260} measured during heating and cooling of complexes A) (*aeg*PNA)$_2$:DNA1 B) (CNA1)$_2$:DNA1 and C) (CNA3)$_2$:DNA1

3.7.3 CD Spectroscopic Studies

CD spectroscopy provides reliable information about the complex formation as the complex shows significantly different CD characteristics than the components. The CD spectra of the *aeg*PNA, CNA1 and CNA3 complexes with DNA1 were recorded under the condition described for UV-Tm experiments. These spectra together with the calculated spectra by addition of singles strand spectra in 2:1 molar ratio for triplex [(PNA/CNA)$_2$:DNA] are shown in Figure 19. For (*aeg*PNA)$_2$:DNA1 complex, the calculated spectrum shows a positive bands at 219nm and cross over points at 259 and 238nm. The measured CD spectrum for the same complex has an additional positive band at 260nm that is absent in the calculated spectrum. Moreover, the cross over points at 252nm to 238nm as seen in the calculated spectrum are also shifted by 8nm compared to that in measured CD spectrum of the (*aeg*PNA)$_2$:DNA1. Similarly the complex (CNA3)$_2$:DNA1 shows a shift in one of the cross over points from 260 to 252 and a positive band at 260nm. The CD spectrum of (CNA2)$_2$:DNA1 complex is found to

be different from the its corresponding calculated CD spectrum with a shift in both crossover points with the former showing cross over points 263 and 239nm and the latter with crossover points at 252 and 233nm. In addition, a positive band at 259nm is also observed in the CD spectrum of $(CNA2)_2$:DNA1 complex, which is absent in the calculated spectrum. The fact that the observed spectra differed from the addition spectra of the constituent strands and the presence of the additional positive band in the region of 260-259nm (characteristic of triplex, Chapter 2) in all cases confirms the existence of the triplex.

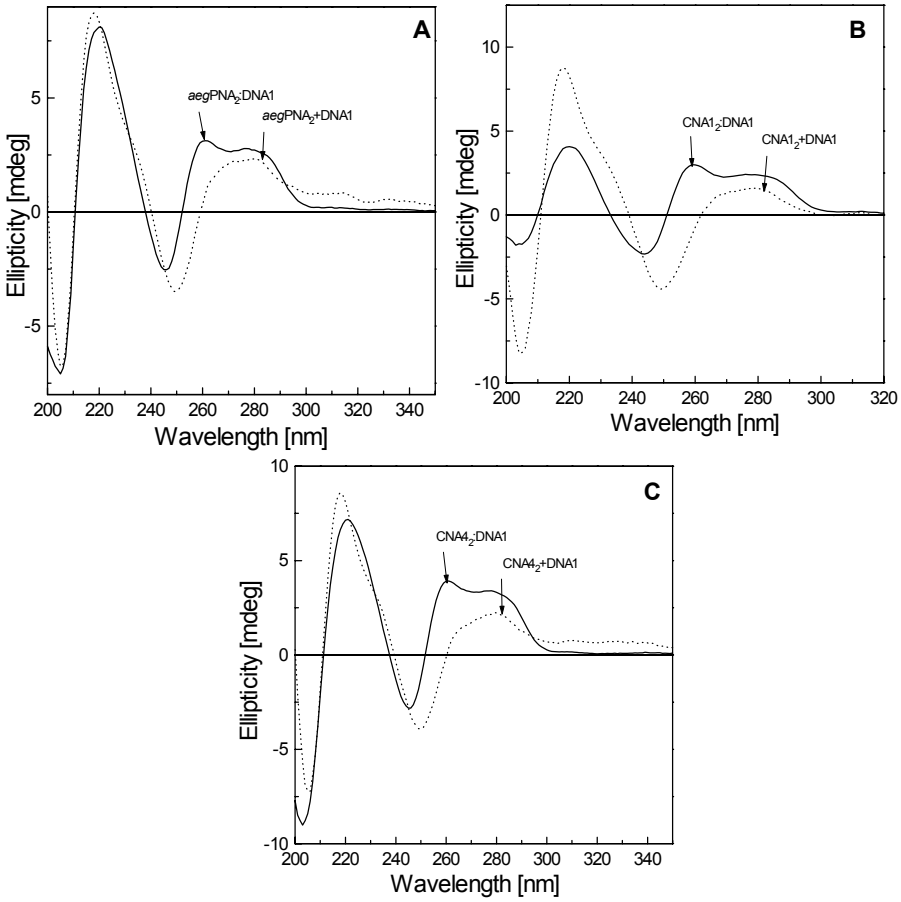

Figure 19. CD profiles of measured (——) and calculated (------) spectra of (*aeg*PNA/*py*CNA)$_2$:DNA complexes

The CD of the triplex is dominated by the CD signature of the DNA as is evident from the CD of various mixtures of CNA3:DNA1 in Figure 14. To see the characteristic band for triplex formed by the polypyrimidine T_8 with polypurine A_8 clearly, from the CD spectra of the complexes of *aeg*PNA, CNA1 and CNA3 individually hybridized with complementary DNA1 (Figure 20). The CD of DNA1 single strand was subtracted from the CD spectrum of each complex, and plotted. The plots showed a large amplification

in the positive band at 260nm for difference spectra of all the three complexes, which is characteristic of PNA_2:DNA triplexes. Thus, there is a little CD induced by the pyrrolidinyl unit in *aeg*PNA compared to the CD of *prolyl*PNA.

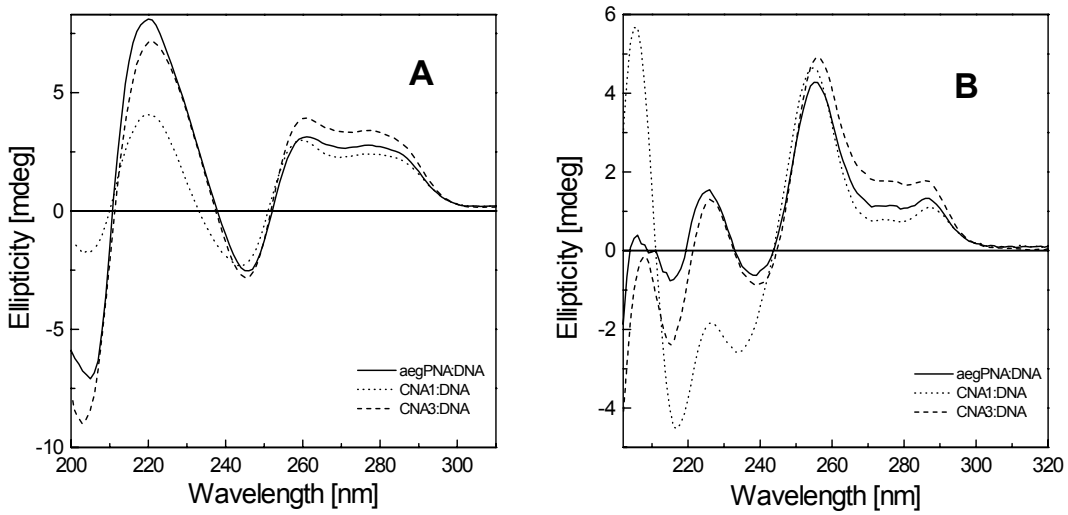

Figure 20. A) CD spectra of triplexes B) Difference spectra of triplexes taken by subtracting the CD signal of DNA from that of the complex

3.8 Conclusions

An efficient solid phase synthesis of pyrrolidinyl carbamate nucleic acids was developed. The pyrrolidinyl nucleic acids with 2*S*,4*S* strereochemistry having nucleobases thymine and cytosine were successfully incorporated in *aeg*PNA. Oligomers with all modified units were also prepared. The results from binding studies show that the (2*S*,4*S*) pyrrolidinyl carbamate-linked homooligomers stereochemistry do not bind to DNA. These hooligomers also have poor aqueous solubility. Though, the placement of carbamate linkage at C-terminus *aeg*PNA results in the destabilization of triplexes the modification at the N-terminus does not affect the stability of the complex significantly. One important finding in these studies is that the percentage hyperchromicity found in $(CNA1)_2$:DNA1 and $(CNA3)_2$:DNA1 was more than that for *aeg*PNA_2:DNA complexes which can be attributed to the better base-stacking in the case of CNA/DNA complexes.

These results emphasize that in addition to the monomer parts' length and possibility of hydrogen bond formation, other structural properties like sterically allowed constriction, which can be controlled by the right kind of the stereochemistry, of the oligomers are important as well. In this regard, the carbamate-linkage needs to be explored more with other three strereochemistries of the pyrrolidine unit.

3.8. Experimental Section

General Remarks

All the solvents used were purified according to the literature procedures (Perrin, 1989). Reactions were monitored by TLC. Usual work-up implies sequential washing of the organic extract with water and brine followed by drying over anhydrous sodium sulphate and evaporation under vacuum. Column chromatography was performed for purification of compounds on 100-200 mesh silica gel, except in case of activated monomers in which case purification was done by flash column using 200-400 mesh silica gel.

FAB-MS and MALDI-TOF mass spectral analysis is followed by the calculated M^+ and the molecular formula for this.

(2S,4R) 4-O-mesyl-N1-benzyloxycarbonylproline methylester **59**

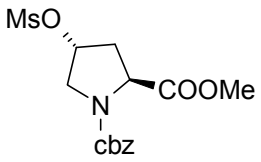

59

Compound **2** (Chapter 1, Scheme 2.1a) (9.7g, 34.6mmol) was taken in dry pyridine (75ml) and mesyl chloride (3.2ml, 41.5mmol) was added dropwise over a period of 30 min while maintaining the temperature of the flask at 0-5^{o}C. After stirring for 1h, the reaction mixture was kept in refrigerator overnight. Pyridine was removed under vacuum in a rotavapor and traces of pyridine were removed by coevaporation with toluene (2 x 20ml). EtOAc (200ml) was added to the residue and washed with water. The aqueous layer was further extracted with EtOAc (3x50ml) and the organic layers were pooled, washed sequentially with water, brine and dried over anhy. Na_2SO_4. Upon removal of EtOAc, 4*R*-mesyl-N1-benzyloxycarbonyl-proline methylester **59** was obtained (12.3g, Yield=99%, Rf=0.4, EtOAc:Petroleum ether 6:4).

^{1}H NMR ($CDCl_3$) δ 7.35-7.25 (2s 5H $C_6\underline{H}_5$), 5.3-5.0 (2m 3H C2$\underline{H}$, $C\underline{H}_2Ph$), 4.5 (dd 1H C4$\underline{H}$), 4.0-3.8 (m 2H C5$\underline{H}$), 3.75 & 3.5 (2s 3H $COOC\underline{H}_3$), 3.0 (2s 3H $SO_3C\underline{H}_3$), 2.7-2.2 (m 2H C3$\underline{H}$)

(2S,4S) 4-azido-N1-benzyloxycarbonyl proline methylester **60**

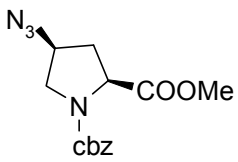

60

The 4*S* mesyl derivative **59** (12.3g 34.3mmol) was taken in dry DMF (100ml) and NaN_3 (17.8g, 0.27mol) was added into it. The reaction mixture stirred at 70^{o}C for 7-8h. DMF was removed under vacuum and the residue was taken in EtOAc

(200ml) and washed with water. The aqueous layer was washed with EtOAc (3x50ml) and all organic layers were pooled together and washed with water, brine and dried over anhy. Na_2SO_4. The solvent was removed to obtain the azido compound **60** (10.27g, yield=98.5%, Rf=0.36, EtOAc:Petroleum ether 4:6).

^{1}H NMR, ($CDCl_3$) δ 7.27-7.23 (m 1H $C_6\underline{H}_5$), 5.17-4.90 (m 2H -$C\underline{H}_2$Ph), 4.43-4.31 (dd J=8, 16, 1H C2$\underline{H}$), 4.16-4.04 (bm 1H C4$\underline{H}$), 3.70-3.45 (m 5H C5$\underline{H}$ -$OC\underline{H}_3$), 2.33-2.17 (m 1H C3$\underline{H}$), 2.15-2.02 (m 1H C3'$\underline{H}$).

IR (neat) cm^{-1} 2953, 2106, 1753, 1711, 1499, 1416

(2S,4S) 4-tert-butoxycarbonylamino-N1-benzyloxycarbonyl proline methyl ester **61**

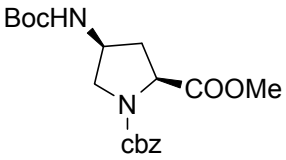

61

The azide **60** (3.11g, 10.2mmol) was dissolved in methanol (1.5 ml) and treated with suspension of Raney Nickel (4ml) in water. The mixture was subjected to reduction under hydrogen pressure (40psi) for 1.5h in a Parr hydrogen apparatus. Raney Ni was filtered through Celite and washed with methanol, which was then evaporated under vacuum to yield a pale yellow solid. This was dissolved in DMSO (20ml) and treated with *t*-Boc-N_3 (1.7ml, 12mmol) followed by addition of Et_3N (1.8ml, 13mmol). After stirring the reaction mixture for 8h, the contents were poured into a beaker containing ice-cold water (100ml), that led to the formation of a white precipitate. The precipitate was extracted in EtOAc and sequentially washed with water, aq. $KHSO_4$ (10%, w/v), water and brine. Upon evaporation of ethyl acetate layer, compound **61** was obtained (3.17g, yield= 82%, Rf=0.33, EtOAc: Petroleum ether 1:1).

^{1}H NMR ($CDCl_3$) δ 7.32-7.28 (m 5H $C_6\underline{H}_5$), 5.20-4.96 (m 2H -$C\underline{H}_2$Ph), 4.86-4.64 (bm 1H N$\underline{H}$), 4.46-4.34 (m 1H C2$\underline{H}$), 4.33-4.16 (bm 1H C4$\underline{H}$), 3.86-3.76 (m 1H C5$\underline{H}$), 3.71-3.54 (2s 3H -$OC\underline{H}_3$), 3.43-3.27 (m 1H C5$\underline{H}$), 2.28-2.09 (m 2H C3$\underline{H}$), 1.40 & 1.38 (2s 9H -$C(C\underline{H}_3)_3$ of *t*-Boc).

^{13}C NMR ($CDCl_3$) δ 172.4, 172.3 ($\underline{C}OOCH_3$), 155.0 (N1$\underline{C}$OO), 154.0 (NH$\underline{C}$OO), 136.1, 128.3, 127.9, 127.7 ($\underline{C}_6H_5$), 79.8 ($\underline{C}(Me)_3$), 67.1 ($O\underline{C}H_2$), 57.7, 57.5 ($\underline{C}$4), 52.2, 52.0 (C2), 51.7 ($O\underline{C}H_3$), 49.5, 48.9 ($\underline{C}$5), 36.7, 35.6 ($\underline{C}$3), 28.2 ($C(\underline{C}H_3)_3$).

(2S,4S) 4-tert-butoxycarbonylamino-N1-benzyloxycarbonyl 2(hydroxymethyl)-pyrrolidine **62**

The ester **61** (1g, 2.6mmol) was coevaporated with dry THF (2x10ml) and then dissolved in dry THF (20ml). The solution was cooled to 0°C and $LiBH_4$ (0.1g, 5.3mmol)

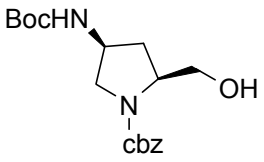

62

was added in two portions. After stirring it for 3.5 hrs, the reaction was quenched with saturated aq. NH_4Cl solution. The solvent was removed under vacuum, the residue was dissolved in EtOAc and the resulting solution was washed with water and brine. EtOAc layer was dried over anhy. Na_2SO_4, solvent was evaporated and the residue (0.83g) was purified by column chromatography to afford **66** (0.65g, yield=70%, Rf=0.25, EtOAc: Petroleum ether 1:1).

^{1}H NMR ($CDCl_3$) □7.45-7.3 (s 5H C_6H_5), 5.5 (bs 1H NH), 5.1 (s 2H OCH_2), 4.3-4.15 (m 1H C4H), 4.1-3.9 9m 2H C5H), 3.4 (bs 1H OH), 3.4-3.2 (m1H C2H), 2.5-2.3 (m 1H C3H), 1.7-1.5 (m 1H C3'H), 1.4 (s 1H $C(CH_3)_3$).

(2S,4S) (4-tert-butoxycarbonylamino-N1-benzyloxycarbonyl-pyrrolidin-2-yl) methyl 1H-imidazole-1-carboxylate **63**

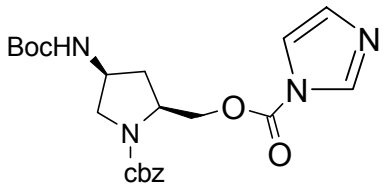

63

Compound **62** (100mg, 0.27mmol) was taken in dry THF (1ml) and freshly crystallized carbonyldiimidazole from dry THF (53mg, 0.33mmol) was added into it. After stirring the solution for 4h, THF was evaporated under *vacuo*, and EtOAc was added into it. The organic layer was sequentially washed with aq. NaH_2PO_4 (5%, w/v) solution, water, brine and dried over anhy. Na_2SO_4. Upon concentrating the EtOAc layer, crude product (150 mg), was obtained which was chromatographed over silica gel column to achieve pure product **63** (120mg, yield=95.3%, Rf=0.4, EtOAc)

^{1}H NMR ($CDCl_3$) δ 8.1 (s 1H Im), 7.5-7.3 (2s 6H C_6H_5, Im), 7.1 (s 1H Im), 5.1 (s 2H OCH_2), 4.8-4.5 (m 3H C4H, CH_2OCO), 4.5-4.0 (m 3H C5H, C2H), 2.6-2.4 (m 1H C3H), 2-1.8 (m 1H C3'H), 1.4 (s 9H $C(CH_3)_3$).

(2S,4S)-(4-tert-butoxycarbonylamino-N1-benzyloxycarbonyl-pyrrolidin-2-yl)methyl 3-hydroxypropylcarbamate **64**

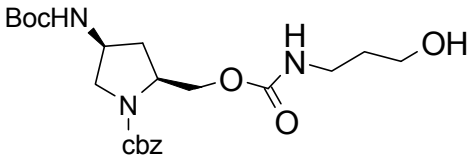

64

The imidazolylcarbamate **63** (120mg, 0.26mmol) was taken in dry pyridine (1ml) and 3-amino-1-propanol (22μl, 28.7mmol) was added into it. The reaction was stirred overnight and pyridine was evaporated under vacuum. EtOAc was added to the residue and washed with aq. NaH_2PO_4 (5%, w/v) solution, water and brine. EtOAc layer was concentrated to

dryness and purified by column chromatography to get pure **64** (60mg, yield=51%, Rf=0.16, EtOAc).

^{1}H NMR ($CDCl_3$) δ 7.4 (s 5H C_6H_5), 5.3 (bs 0.4H N<u>H</u>), 5.2 (s 2H O$C\underline{H}_2C_6H_5$), 4.1 (bs 1H O<u>H</u>), 3.9-3.6 (m 3H C4<u>H</u>, C5<u>H</u>), 3.5-3.3 (m 3H C2<u>H</u>, $C\underline{H}_2$OCO), 2.5-2.4 (m 1H C3<u>H</u>), 1.9-1.4 (m 7H C3'<u>H</u>, $((C\underline{H}_2)_3)$, 1.5 9s 9H $C(C\underline{H}_3)_3$) Rf = 0.15 (EtOAc) m/z = 452 (actual mass 451.5)

IR ($CHCl_3$) cm^{-1} 3447.49, 3018.92, 2924.53, 2401.38, 1703.15, 1495.68

N1-carboxymethylthymine **65** (Rabinowitz & Gurin, 1953)

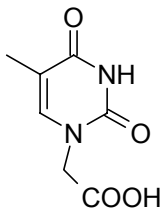

65

To a suspension of thymine (5g, 4mmol) and KOH (4.4g, 8mmol) in water (35 ml), chloroacetic acid (3.75g, 4mmol) solution in water (12ml) was added slowly. The pH of the solution was adjusted to ~10 by dropwise addition of a KOH solution. After refluxing for 2h, the solution was cooled and adjusted to pH 2 by addition of conc. HCl. The resulting precipitate was filtered, washed with a little cold water, dissolved in a saturated potassium bicarbonate solution and reprecipitated with HCl. The precipitate was filtered, partially dried and recrystalized out of hot water. Upon drying pure thymine acetic acid **65** (5.2g, yield=71%, Rf=0.2, MeOH:EtOAc 2:8) was obtained.

^{1}H-NMR (D_2O) δ 11.33 (s 1H N<u>H</u>), 7.49 (s 1H Thy-<u>H</u>6), 4.5 (s 2H $C\underline{H}_2$), 1.85 (s 3H Thy-$C\underline{H}_3$)

Ethyl(N^4-Benzyloxycarbonyl- cytosine-N^1-yl-)acetate **66**

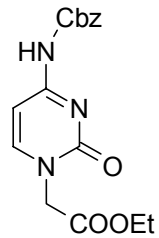

66

N^4-Cbz protected cytosine **58** (Chapter 1, Scheme 1.9b) (2g, 8.1mmol) was suspended in dry DMF (100 ml) and anhy. K_2CO_3 (1g, 7.2mmol) was added into it. The reaction mixture was cooled to 0-5^{o}C and ethylbromoacetate (0.8ml, 7.3mmol) was added. The mixture was stirred vigorously for 24 hrs, filtered, and evaporated to dryness in vacuum. After the addition of water (30 ml), the solution was brought to pH 5 with 1N HCl, stirred for 5 minutes, and then extracted with DCM. The organic layers were pooled, washed with water, brine and dried over anhy. Na_2SO_4. Upon removal of DCM an oil was obtained and was subjected to silica gel column chromatography to yield a white solid of compound **66** (2.06g, yield= 86.7%, Rf=0.3, MeOH:DCM 5:95, mp=130^{o}C).

^{1}H NMR ($CDCl_3$) δ7.74 (bs 1H NHCOO), 7.56-7.52 (d 1H J = 7.32Hz Cy-C6H), 7.38 (s 5H C_6H_5), 7.29-7.25 (d 1H J=7.32Hz Cy-C5H), 5.2 (s 2H OCH_2), 4.60 9s 2H NCH_2), 4.3-4.12 ((q 2H J=6.84Hz $COOCH_2CH_3$), 1.32-1.25 (t 3H J= 6.84 $COOCH_2CH_3$).

^{13}C NMR ($CDCl_3$) δ 167.35 (COOEt), 162.83 (NHCOO), 155 (Cyt-C4), 151.5 (Cyt-CO), 149.01 (Cyt-C6), 135.00, 128.3, 127.95, 127.87 (C_6H_5), 95.16 (Cyt-C5), 67.52 ($OCH_2C_6H_5$), 61.67 (OCH_2CH3), 50.61 (NCH_2), 13.74 ($COOCH_2CH_3$)

m/z = 331 (actual mass=331)

Benzyl -N1,N3-diethyl-2-oxo-2,3-dihydropyrimidin-4(1H)-ylidenecarbamate **67**

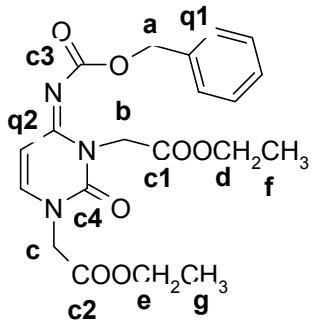

67

In the column purification of compound **66**, N1,N3-dialkylated product **67** (0.15g, yield=5%, Rf=0.5, MeOH:DCM 5:95) was also isolated.

^{1}H NMR ($CDCl_3$) δ7.52-7.48 (d 1H J=7.33 Cyt-C6H), 7.46-7.43 (d 1H J=7.33 Cyt-C5H), 7.36 (s 4H C_6H_5), 5.26 (s 2H $OCH_2C_6H_5$), 4.91 (s 2H N3-CH_2), 4.58 (s 2H N1-CH_2), 4.29-4.17 (q 2H J=7.32N1COOCH_2), 4.17-4.07 (q 2H J=6.84 N1-CH_2COOCH_2), 1.32-1.24 (t 3H J=7.32 N3-CH_2COOCH_3), 1.23-1.16 (t 3H J=6.84 N1-$CH_2COOCH_2CH_3$)

^{13}C NMR ($CDCl_3$) δ 168.4 (ester CO **c1**), 166.9 (ester CO **c2**), 163.6 (NCOO **c3**), 155.0 (CN **q2**), 153.3 (NCON **c4**), 147.6 (Cyt-C6), 134.5 (**q1**), 128.3, 127.8 (Ar), 97.7 (Cyt-C5), 68.6 (OCH_2 **a**), 61.6 (OCH_2CH_3 **e**), 61.0 (OCH_2CH_3 **d**), 50.3 (NCH_2 **c**), 45.9 (NCH_2 **b**), 13.7 (CH_3 **g,f**)

FAB-MS 418 $(M+H)^+$, 440 $(M+Na)^+$ (Calcd for $C_{20}H_{23}N_3O_7$: 417.1)

N^4-Benzyloxycarbonyl- cytosine- N1-acetic acid **68**

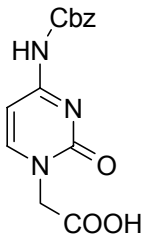

68

The ethyl ester **66** (1g, 3mmol) was treated with aq. NaOH (0.5N, 5ml) and stirred for 15 min. The reaction mixture was cooled, filtered, washed with chilled water and to the filtrate, aq. HCl (3.5N) was added till pH reached 5.0. The white precipitate obtained was filtered, washed with chilled water and ether. The white solid was partially dried in air and then boiled with ethanol. The suspension was filtered and vacuum dried to afford the compound **68** (0.82g, yield=90%, Rf=0.2, MeOH:DCM:CH_3COOH 2:8:0.1, mp=200°C).

^{1}H-NMR (DMSO-d_6): δ 10.21 (bs COOH), 8.05-8.01(d 1H J=7.33 Cyt-C6H), 7.38 (s 5H C_6H_5), 7.04-7.00 (d 1H J= 7.33 Cyt-C5H), 5.18 (s 2H OCH_2), 4.52 (s 2H NCH_2).

(2S,4S) {4-t-butoxycarbonylamino-2-hydroxymethyl-pyrrolidin-1-yl}-2-(oxoethyl-thymine) **69**

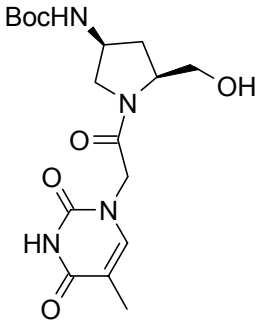

69

The alcohol **62** (3g, 8.57mmol) was dissolved in methanol and 10%Pd-C (0.3g) was added into it. This slurry was subjected to hydrogenation at 60 psi H_2 pressure for 7h. The catalyst was filtered off over Celite and filtrate was evaporated under vacuum to obtain the amine as yellow solid (~1.9g). The free amine was taken in dry DMF (30 ml) to which thymine acetic acid **65** (1.73g, 9.4mmol) and HOBt (0.578g, 4.28mmol) were added. After cooling the mixture in an ice bath, DCC (1.94g 9.4mmol) was added and stirred for 4h. The DCU that precipitated was removed by filtration through Celite and the solvent was removed under vacuum followed by purification of the residue by silica gel column to give **69** (2.78g, yield=85%, Rf=0.3, MeOH:DCM 1:9, $\alpha^{27}{}_D$= -67.5, mp=58-60^{o}C)

^{1}H NMR (CDCl$_3$ + D$_2$O) δ 10.2 (bs 0.4H Thy-NH), 7.0 (s 1H Thy-H6), 4.9-4.5 (m 1H C4H), 4.4-4.0 (m 4H C5H, NCOCH_2), 3.6-3.1 (m 1H C2H), 1.9 (s 3H Thy-CH_3), 3.1-2.8 (m 2H CH_2OH), 2.65-2.35 (m 2H C3H), 1.5 (2s 9H C(CH_3)$_3$)

^{13}C NMR (CD$_3$OD) δ 168.2, 167.9 (Thy-2CO), 166.8 (Thy-4CO), 157.6 (*t*-Boc CO), 153.1 (NCO), 111.2 (Thy-C6), 80.3 (C(CH$_3$)$_3$), 65.2 (NCOCH_2), 62.8 (Thy-C5), 60.4 (Pro-C4), 59.5 (Pro-C5), 53.6 (Pro-C2), 35.6 (CH_2OH), 33.8 (Pro-C3), 28.6 (C(CH_3)$_3$), 12.1 (Thy-CH_3))

(2S,4S) {4-tert-butoxycarbonylamino pyrrolidin-1-yl}-2-(oxoethyl-thymine) 2-methyl 4-nitrophenyl carbonate **70**

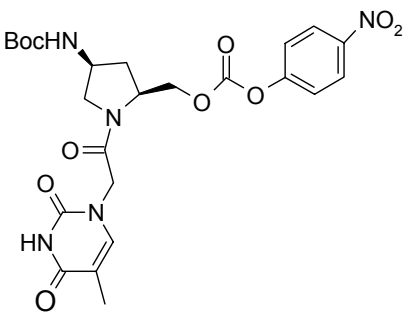

70

tert-Boc-protected thymine monomer **69** (0.53g, 1.38mmol) was dried by coevaporation with dry dioxane (3X5ml) under reduced pressure. The resulting solid was dissolved in dioxane:Py mixture (11ml; 10:1) and cooled to 10^{o}C. *p*-nitrophenylchloroformate (0.56g, 2.78mmol) was added to the reaction vessel in portions under anhydrous conditions and mixture was stirred for 4h after second addition. The solvent was evaporated, without heating, under reduced pressure to obtain a crude product (1.6g), which was purified by flash column chromatography using ethylacetate/petroleum ether (7:3) to

obtain the pure product **70** (0.46 g, yield=60%, Rf=0.34, EtOAc:Petroleum ether 7:3, $\alpha^{27}{}_D$= -71, mp=80°C)

^{1}H NMR ($CDCl_3$) δ 8.25 (d 2H Ar J=7Hz), 7.4 (d 2H Ar J=7Hz), 7 (s 1H Thy-H6), 5.2 (bs 1H NH), 4.8-4.1 (m 7H $NCOCH_2$, CH_2O, C4H, C5H), 4.05-3.7 (m 1H C2H), 2.6-2.2 (m 1H C3H), 2.15-1.95 (m 1H C3'H), 1.9 (s 3H Thy-CH_3), 1.4 (d 9H $C(CH_3)_3$)

((2S,4S) {4-tert-butoxycarbonylamino pyrrolidin-1-yl}-2-methyl,1-(2-oxoethyl-5-methyl-4-oxopyrimidin-2-yl)-bis (4-nitro-phenylcarbonate) **71**

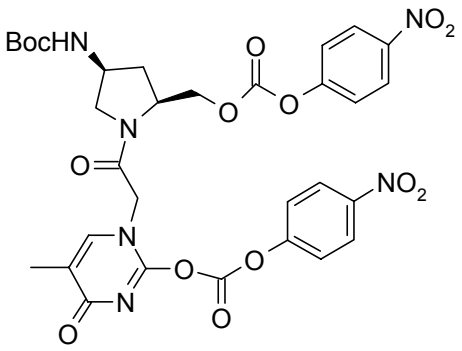

71

During the preparation of the activated thymine monomer **70**, a side product identified as product **71** (70mg, yield=7%, Rf =0.6, EtOAc:Petroleum ether 7:3) was also isolated.

^{1}H NMR ($CDCl_3$) δ 8.45-8.2 (2d 4H Ar), 7.65-7.4 (2d 4H Ar), 7.1 (Thy-H6), 5.2 9bs 1H NH), 4.9-4.8 (C4H), 4.6-4.3 (m 2H OCH_2), 4.2-4.0 (m 2H C5H), 3.5-3.4 (C2H), 3.0 (m NCH_2), 2.7-2.45 (C3H), 2.2-2.0 (m 1H C3'H, 1.4 (2s 9H $C(CH_3)_3$). **FAB-MS** 735 $(M+Na)^+$ (calcd. for $C_{31}H_{32}N_6O_{14}$: 712.19).

{(2S,4S) {4-tert-butoxycarbonylamino pyrrolidin-1-yl}-2-(oxoethyl-N^4-benzyloxycarbony-cytosine **72**

The cbz deprotection in **62** was achieved in an identical manner as for **69**. The Cbz group in *t*-Boc protected 4-amino alcohol **62** (1.62g, 4.63mmol) was deprotected to obtain the free amine (1g). To this amine (1g, 4.6mmol) in dry DMF (30ml), N^4-cbz protected N1-cytocine acetic acid **68** (1.54g, 5.09mmol) and HOBt (0.3g, 2.3 mmol) were added and cooled in an ice bath. DCC (1.1g, 5.1mmol) was added to this mixture and the reaction was stirred at room temperature for 6h. It was filtered over celite and the filtrate was evaporated to dryness under reduced pressure. The residue was purified by silica gel column chromatography using MeOH/DCM to afford pure **72** (1.85g, yield= 80%, Rf=0.2, MeOH:DCM 3:97, $\alpha^{27}{}_D$= -54, mp=70°C).

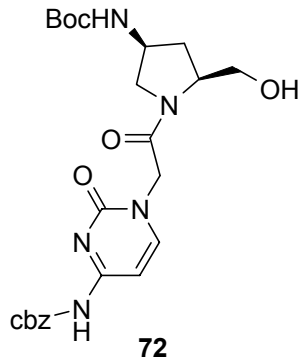

72

^{1}H NMR ($CDCl_3$) δ 7.6 (d 1H Cyt-C6H), 7.4-7.1 (s & d 6H C_6H_5, Cyt-C5H), 5.2 (s 2H $OCH_2C_6H_5$), 4.5-3.35 (m 7H $NCOCH_2$, CH_2OH, C5H, C2H), 2.5-2.25 (1H C3H), 1.95-1.65 (m 1H C3'H), 1.4 (s 9H $C(CH_3)_3$)

^{13}C NMR ($CDCl_3$) δ 165.7 (Cyt-2CO), 163.1 ($NHCOOCH_2C_6H_5$), 155.8 (Cty-C4), 155.5 (NHCOO *t*-Boc), 152.7 ($NCOCH_2$), 149.8 (Cyt-C6), 135.1, 128.3, 128.1, 127.8 (C_6H_5), 95.1 (Cyt-C5), 79.3 ($C(CH_3)_3$), 77.1 (Pro-C4), 67.3 ($CH_2C_6H_5$), 63.5, 62.6 (CH_2OH, $NCOCH_2$), 59.5(Pro-C2), 53.0, 51.2 (Pro-C5), 35.5, 33.6 (Pro-C3), 28.1 ($C(CH_3)_3$)
FAB-MS 502 $(M+H)^+$, 524 $(M+Na)^+$ (Calcd for $C_{24}H_{31}N_5O_7$: 501.2)

{(2S,4S) {4-tert-butoxycarbonylamino pyrrolidin-1-yl}-2-(oxoethyl-N^4-benzyloxycarbonyl-cytosine)-2-methyl 4-nitrophenyl carbonate **73**

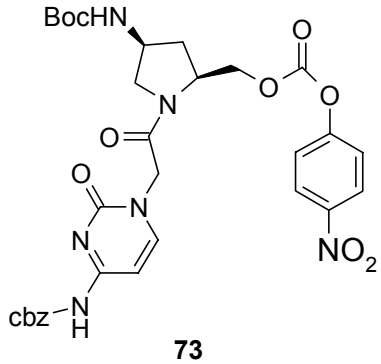

73

The cytosine monomer **72** (0.5g, 1mmol) was coevaporated with dry dioxane (2X10ml) and then treated with *p*-nitrophenylchloroformate (0.6g, 3mmol) and Et_3N (2.7ml, 20mmol) in dry dioxane (10ml). After stirring it overnight, solvent was evaporated under vacuum and residue was taken in EtOAc and subsequently washed with aq. NaOH (0.01N, 2X5ml), water and brine. The organic layer was dried over anhy. Na_2SO_4 and concentrated to get **73** (340mg, yield=53%, Rf=0.5, EtOAc, $\alpha^{27}{}_D$= -68, mp=94°C)

^{1}H NMR ($CDCl_3$) δ 8.25 (d 2H nitrophenyl J=7.0Hz), 7.1 (d 1H J=7.3 Hz Cyt-C6H), 7.5-7.1 (d, s & d 7H nitophenyl, C_6H_5, Cyt-C5H), 5.4 (bs 1H NH), 5.25 (s 2H $OCH_2C_6H_5$), 4.8-3.8 (m 7H CH_2O, $NCOCH_2$, C5H, C2H), 2.2-1.6 9m 2H C3H), 1.4 (s 9H $C(CH_3)_3$).
FAB-MS 667$(M+H)^+$, 689 $(M+Na)^+$ (Calcd for $C_{31}H_{34}N_6O_{11}$: 666.2)

Carbamate dimer **75**

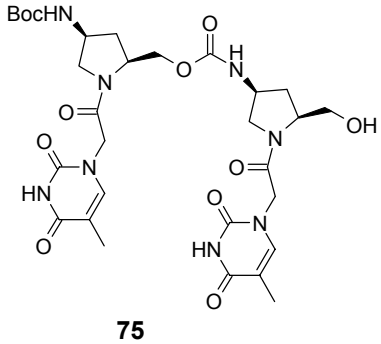

75

The thymine monomer **69** (100mg, 0.26mmol) was treated with 50%TFA/DCM (2ml) and stirred at room temperature for 30minutes. The solvent and acid were removed under reduced pressure and coevaporated twice with dry dichloromethane. To this amine salt (**74**), DIPEA (89μl, 0.52mmol), activated thymine monomer **70** (142mg, 0.26mmol) and dry DMF (5ml) were added. After stirring it for 3h at room temperature, solvent was removed under vacuum and the residue was purified by column to afford the dimer **75** (116 mg, yield=65%, Rf=0.3, MeOH:EtOAc 23:77).
FAB-MS 691 $(M+H)^+$, 713 $(M+Na)^+$, (Calcd for $C_{30}H_{42}N_8O_{11}$: 690.29)

High Performance Liquid Chromatography (HPLC) purification of oligomers

Peptide purifications were performed on an RPC-C4 semi-preparative column attached to HPLC system equipped with Jasco-UV970 variable-wavelength detector. An isocratic elution method was used and purification was carried out using 0.1%TFA in CH_3CN:H_2O 10:90, with flow rate 1.5ml/min. The purity of the oligomers was further assessed by RP-18 analytical HPLC column (25x0.2cm, 5μm) using gradient method: A→50%B in 30min., where buffer A=0.1%TFA /H_2O and buffer B= 0.1% TFA in Ch_3CN:H_2O 1:1 with flow rate 1ml/min and the eluant was monitored at 260nm Representative HPLC profiles (Figure 10 and 11) and mass spectra (Figure 12 and 13) are shown here.

Melting Experiments

The melting experiments were carried out in 10 mM phosphate buffer at pH 7.3. *aeg*PNA/*py*CNA oligomers and their complementary DNA oligonucleotide pairs were taken at concentrations of 2.5μM and 1.25μM respectively. In the case of CNA4 and CNA5, the stock solutions of the oligomers were prepared in DMSO and then 10-15μl of the solution was diluted with phosphate buffer to make up the required concentration and volume. The triplexes were formed by an annealing procedure as described in Chapter 2. Melting experiments were carried out at a heating rate of 0.5^oC/min, while the absorbance at 260 nm was monitored at every temperature. The Tm values were obtained from the first derivative curves of the A_{260} Vs temperature plots.

Binding stoichiometry determination **(Job, 1928)**

Nine mixtures of DNA/*py*CNA complementary pair were made with molar ratios of the strands in 9:1, 8:2, 7:3, 6:4, 5:5, 4:6, 3:7, 2:8, 1:9 relative ratios. Together with samples of the individual strands, this gave eleven samples, all of the same total strand concentration (2μM) in Sodium phosphate buffer (10mM, pH7.3). The samples including the individual strands were heated to 85^oC in water bath for 2.0 min, allowed to cool to room temperature upon standing and then cooled further to 15^oC. All CD spectra were recorded at 15^oC in the wavelength range 190-350nm with a scan speed of 100nm/min. Spectra are an average of 6 scans and were recorded with a response time of 4sec at 1nm bandwidth and 10mdeg sensitivity. CD cell used for the studies was of 10mm path length. Base line was subtracted from all the CD spectra.

Appendix II

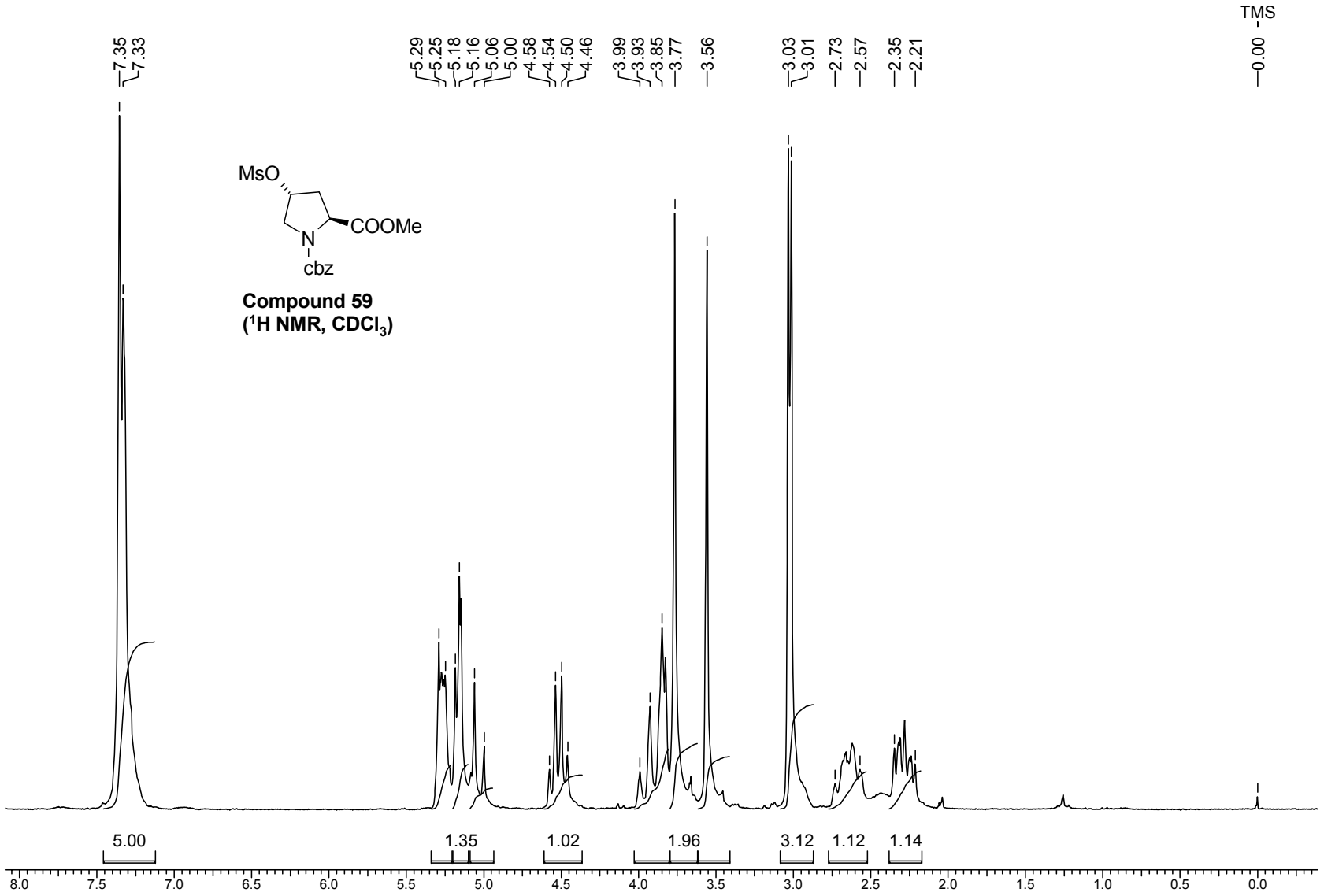

Compound 59
(^{1}H NMR, $CDCl_3$)

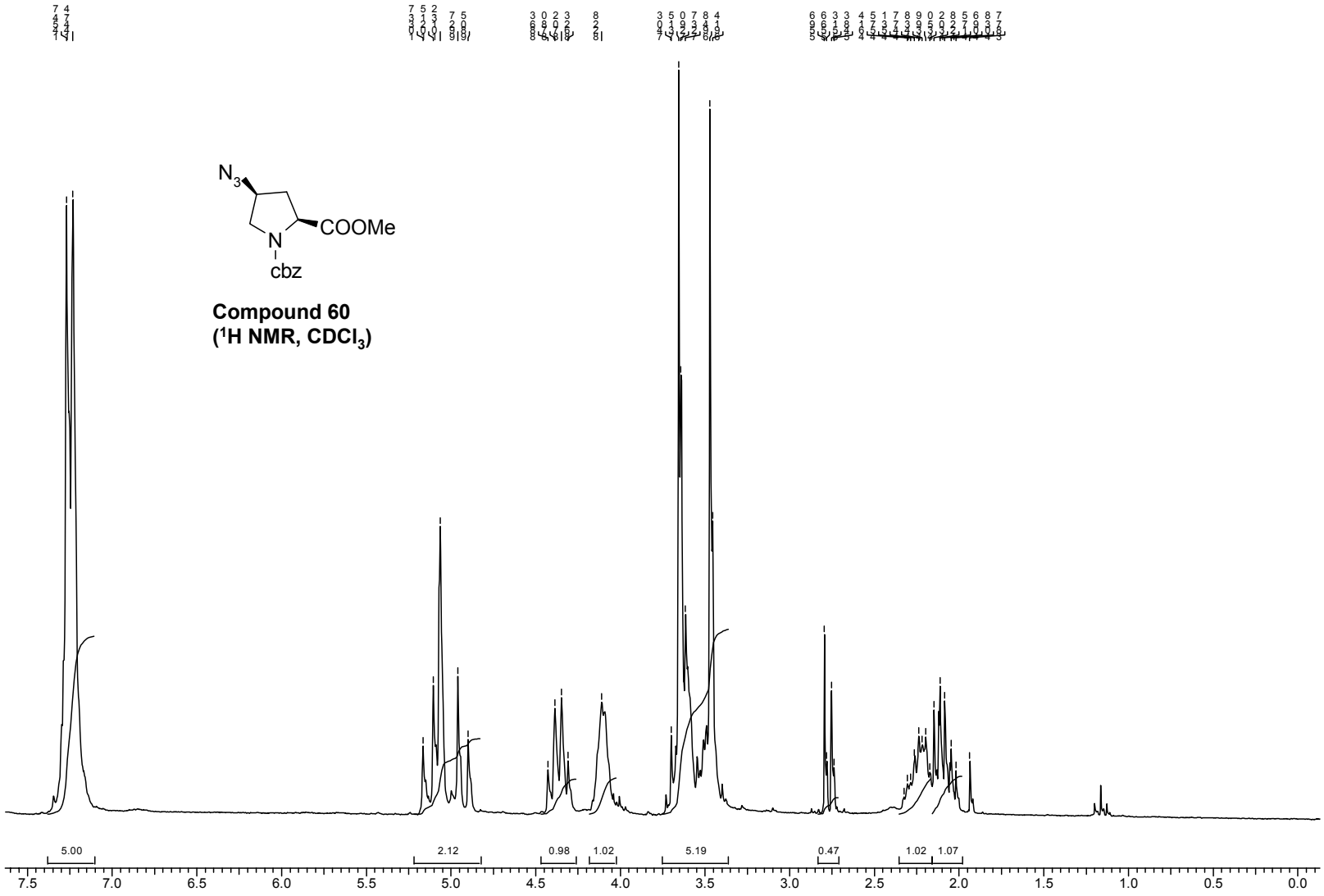

Compound 60
(^{1}H NMR, $CDCl_3$)

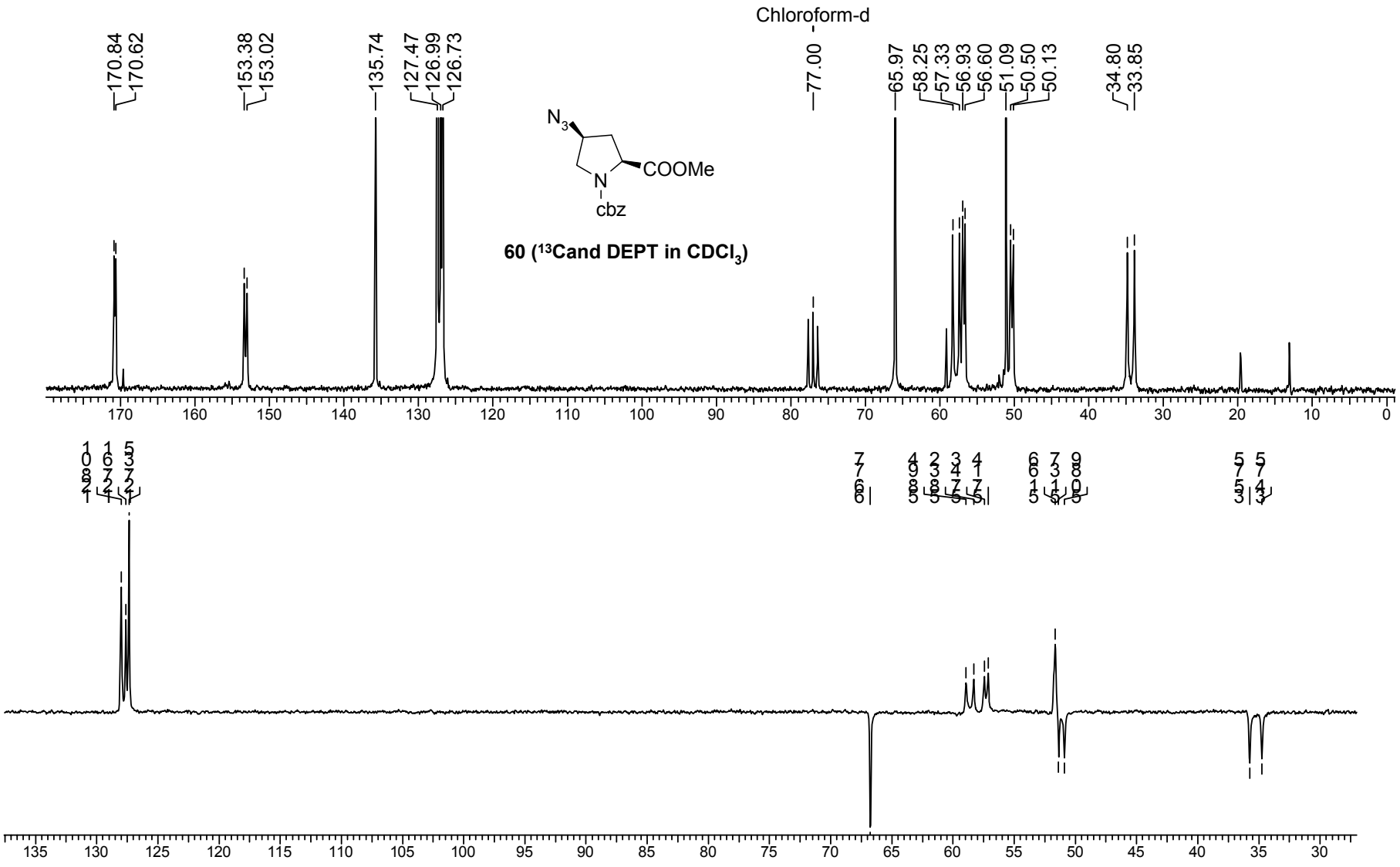
Chloroform-d
170.84
170.62
153.38
153.02
135.74
127.47
126.99
126.73
77.00
65.97
58.25
57.33
56.93
56.60
51.09
50.50
50.13
34.80
33.85
N3
COOMe
N
cbz
60 (13Cand DEPT in CDCl3)

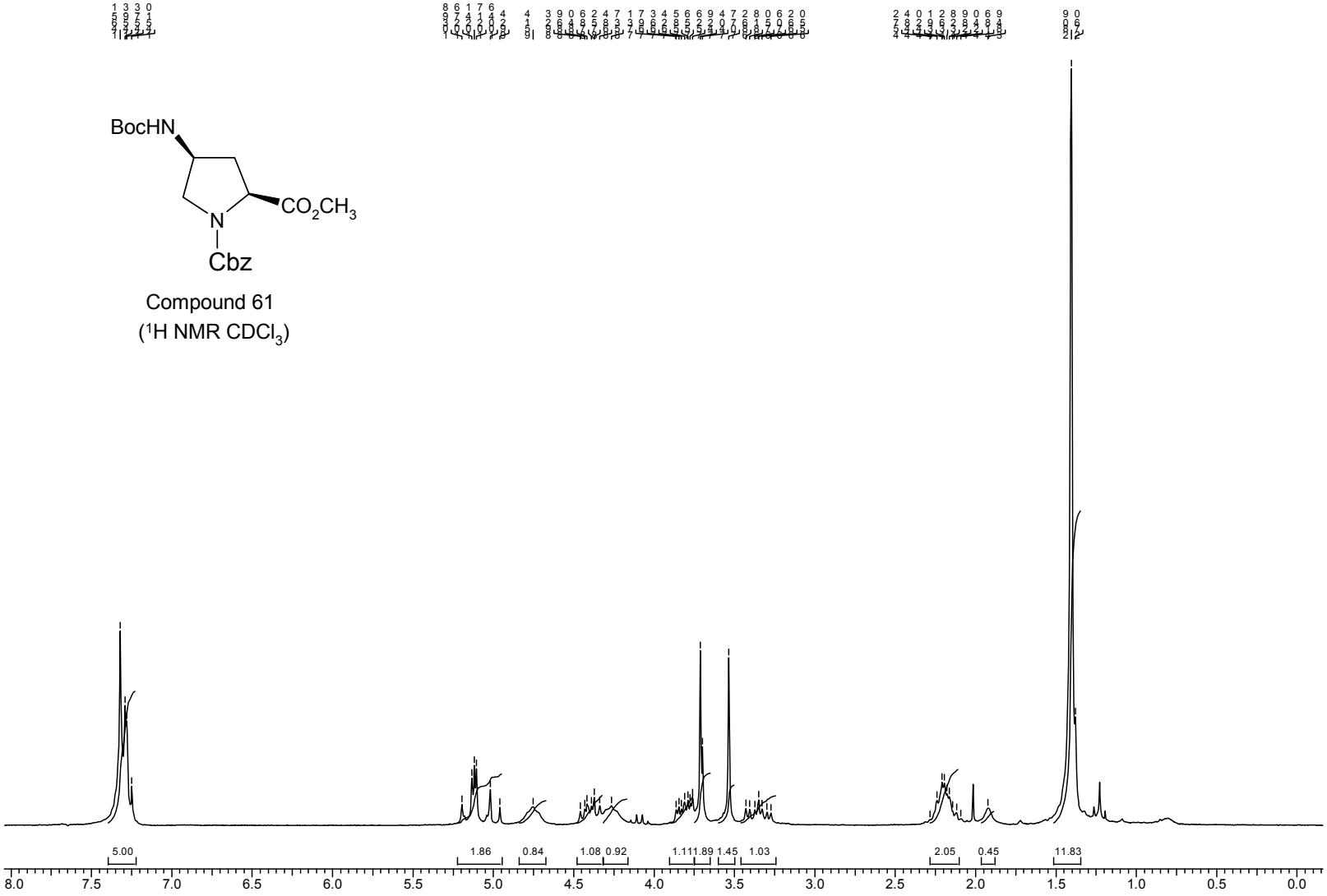

Compound 61
(^{1}H NMR $CDCl_3$)

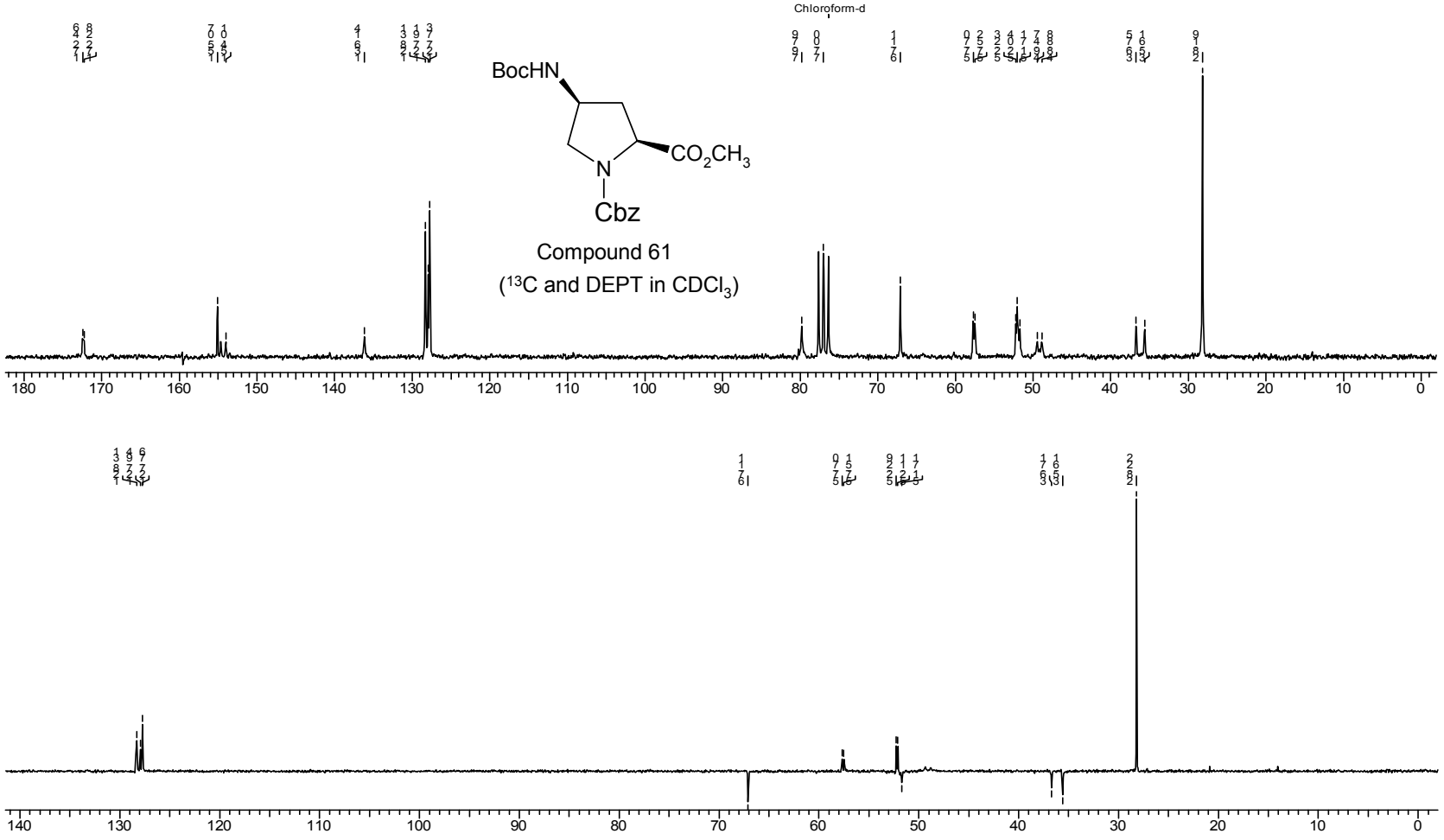
Chloroform-d
BocHN
CO2CH3
N
Cbz
Compound 61
(13C and DEPT in CDCl3)

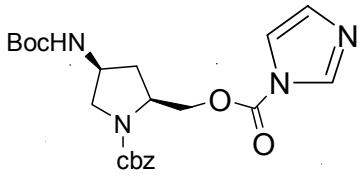

Compound 63
(^{1}H NMR, $CDCl_3$)

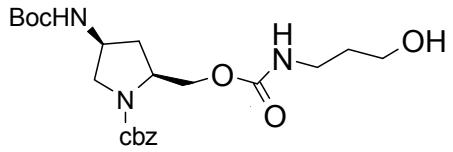

Compound 64
(^{1}H NMR, $CDCl_3$)

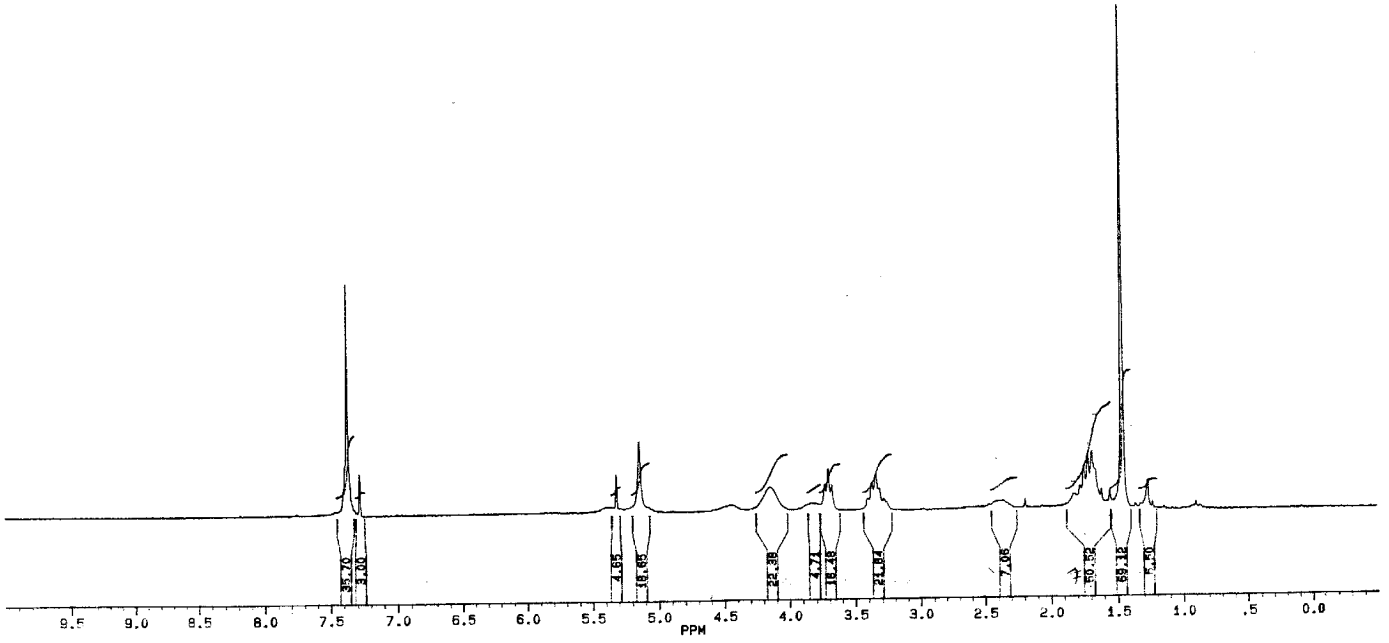

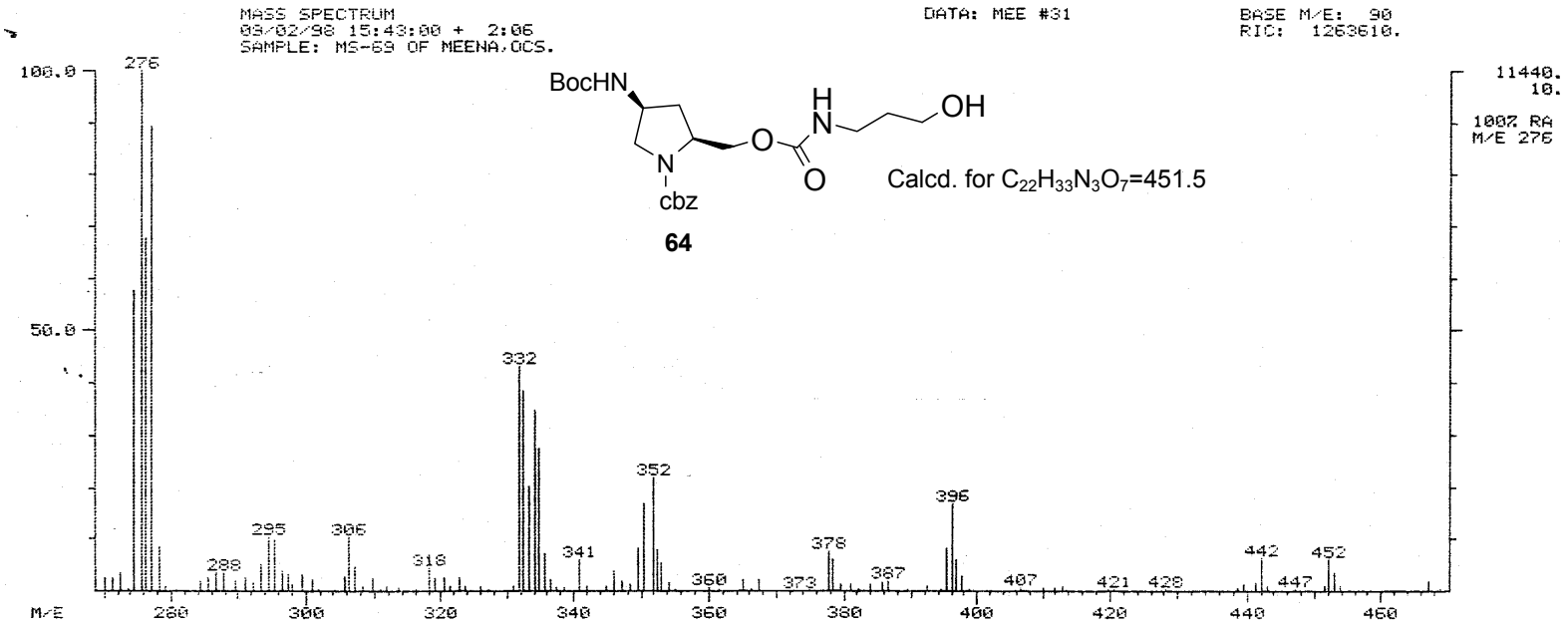
MASS SPECTRUM
09/02/98 15:43:00 + 2:06
SAMPLE: MS-69 OF MEENA/OCS.
DATA: MEE #31
BASE M/E: 90
RIC: 1263610.
100.0
50.0
M/E
11440.
10.
100% RA
M/E 276
276
288
295
306
318
332
341
352
360
373
378
387
396
407
421
428
442
447
452
280
300
320
340
360
380
400
420
440
460
BocHN
N
cbz
O
H
N
O
OH
64
Calcd. for $C_{22}H_{33}N_3O_7$=451.5

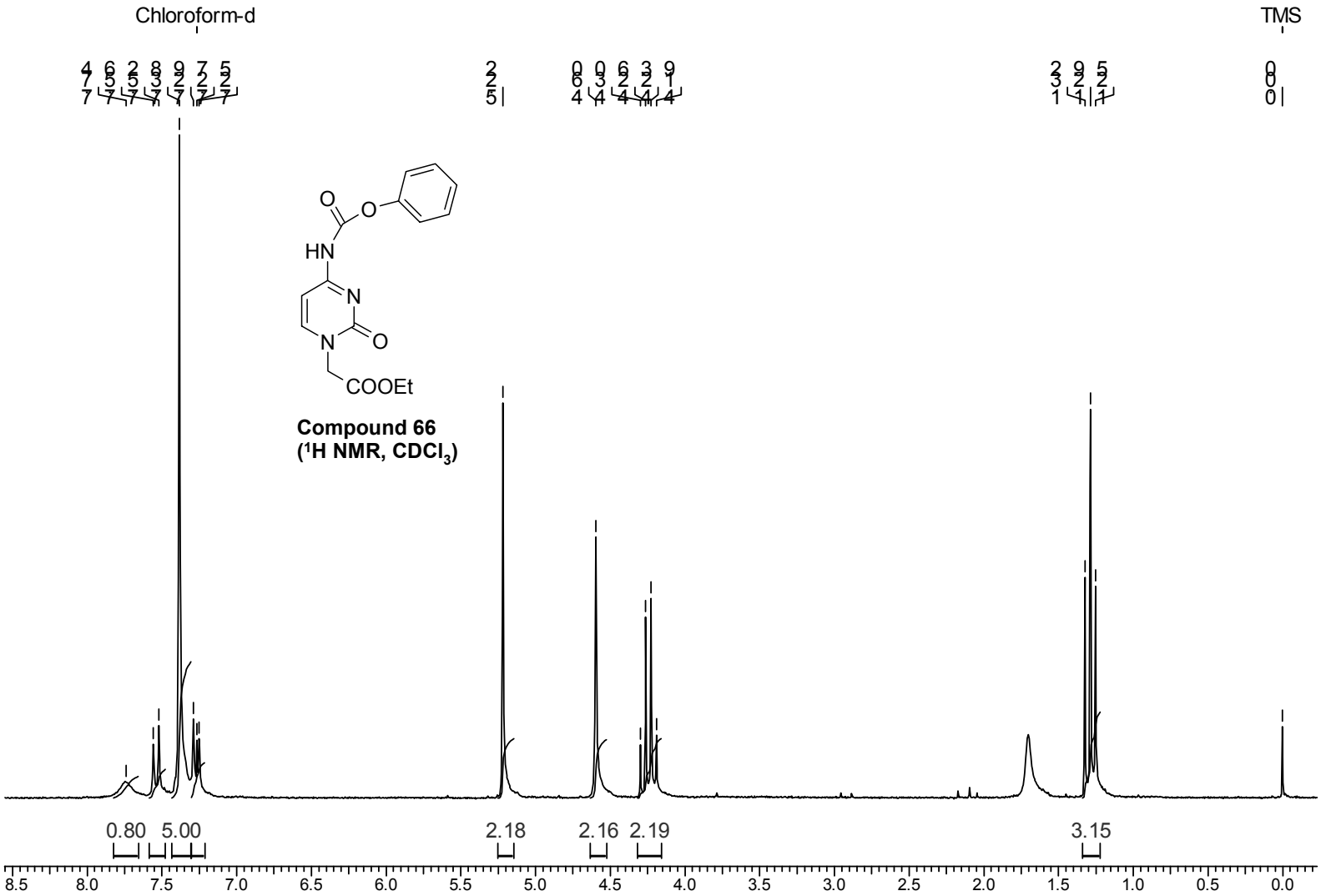

Compound 66
(^{1}H NMR, $CDCl_3$)

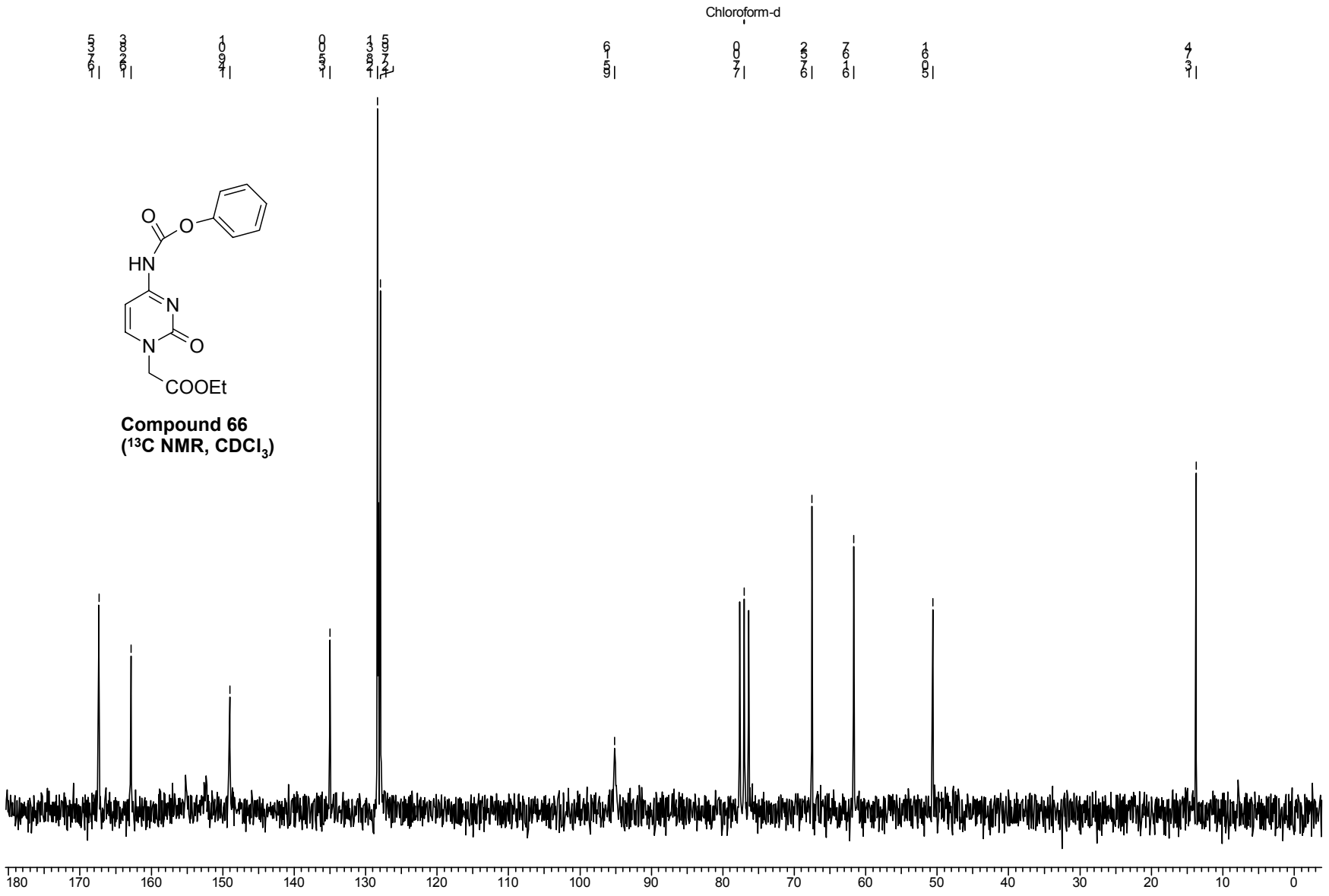

Compound 66
(^{13}C NMR, $CDCl_3$)

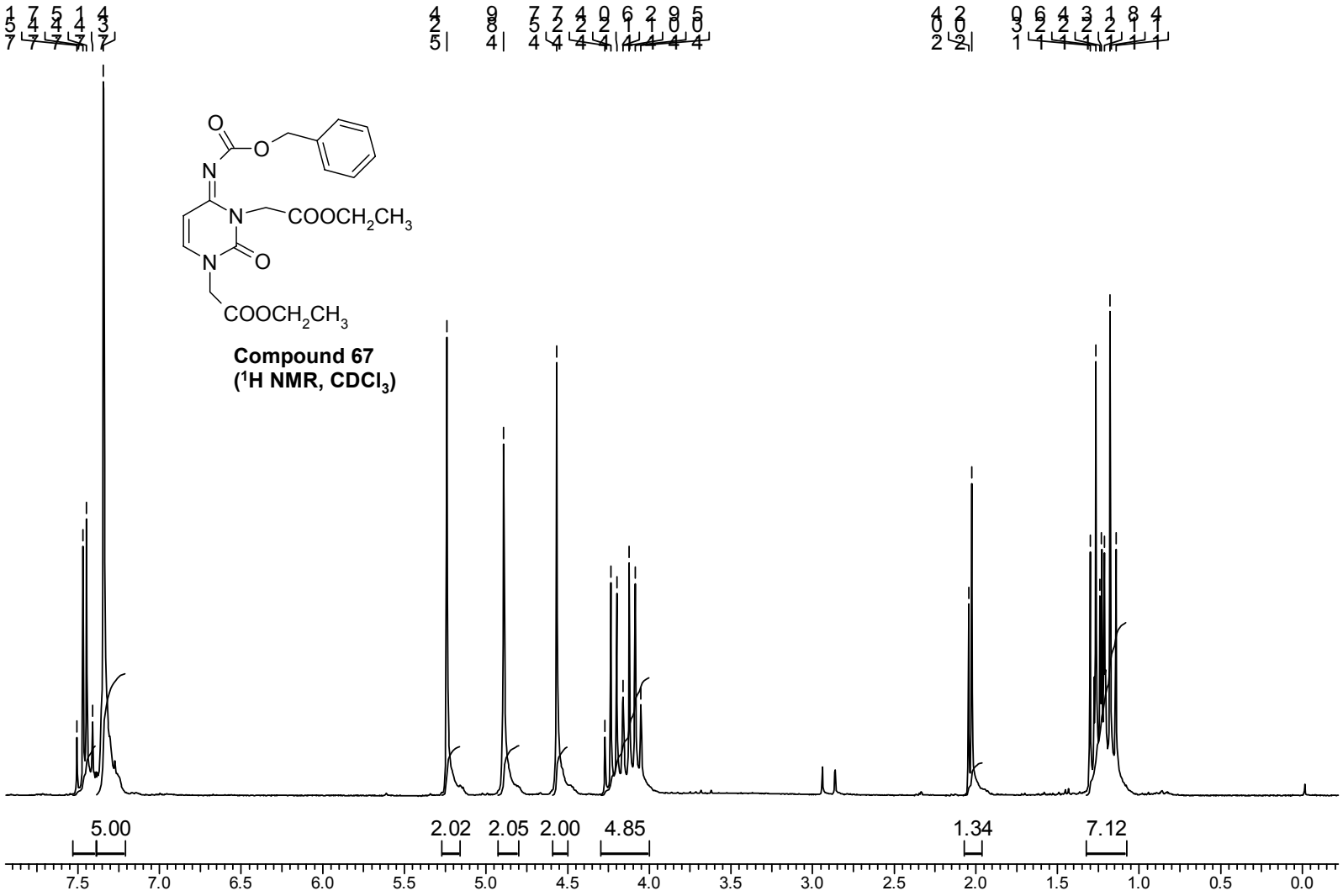
COOCH2CH3
COOCH2CH3
Compound 67
(1H NMR, CDCl3)
5.00
2.02
2.05
2.00
4.85
1.34
7.12
7.5
7.0
6.5
6.0
5.5
5.0
4.5
4.0
3.5
3.0
2.5
2.0
1.5
1.0
0.5
0.0

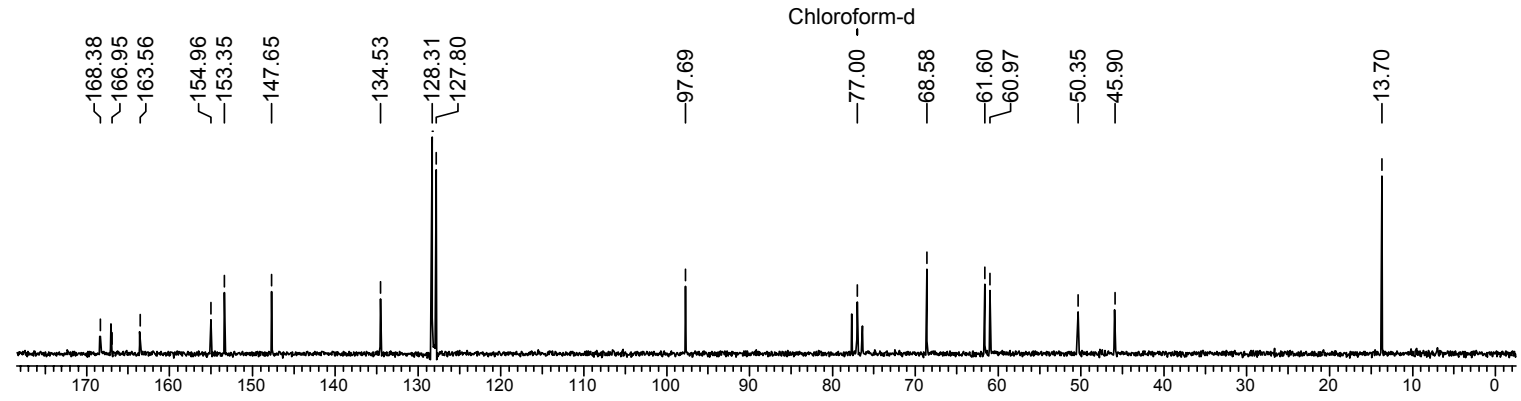

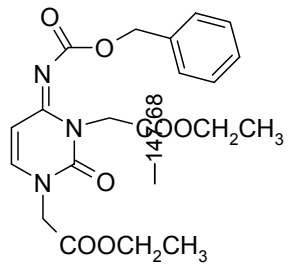

Compound 67
(^{13}C and DEPT, $CDCl_3$)

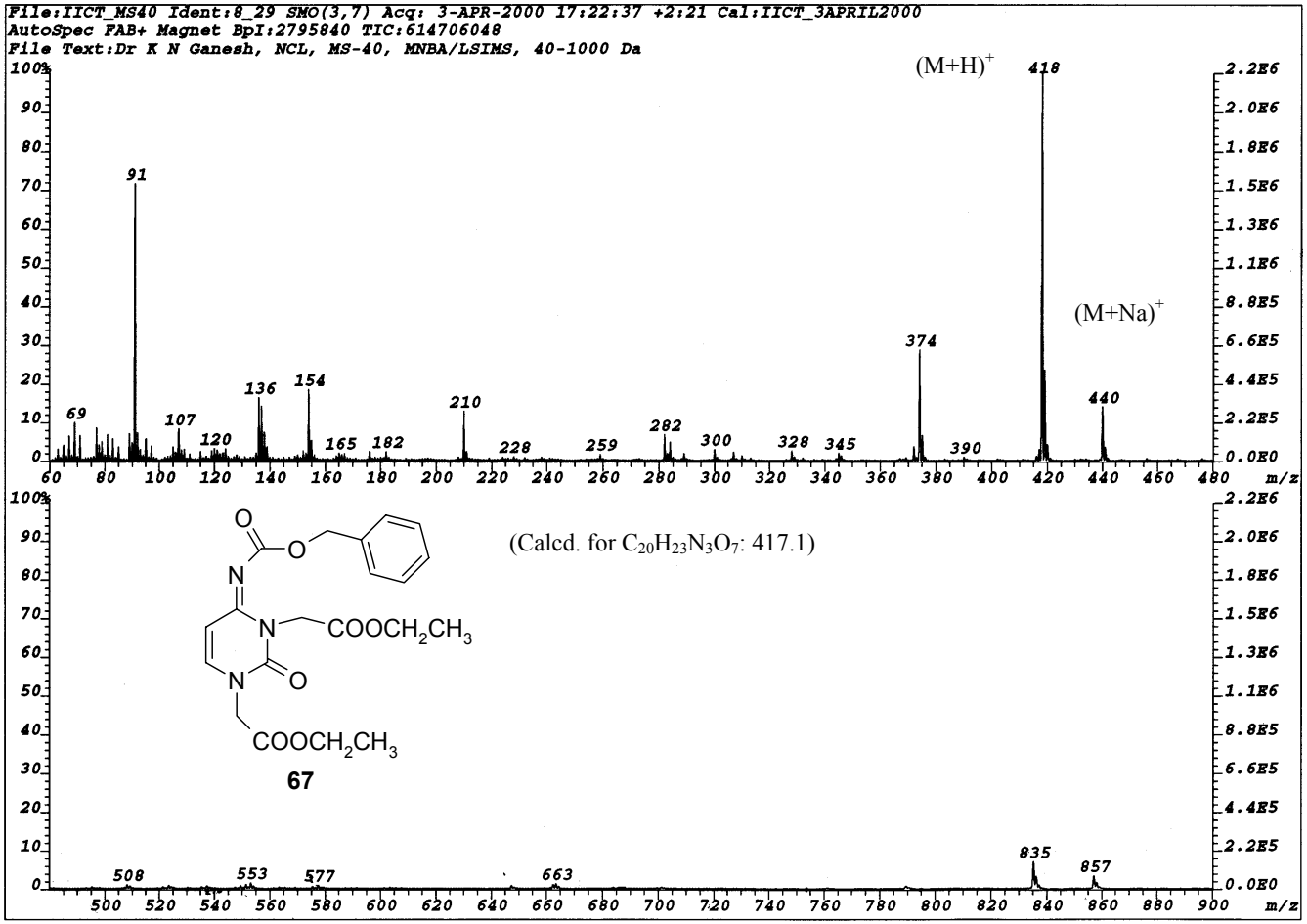

67

(Calcd. for $C_{20}H_{23}N_3O_7$: 417.1)

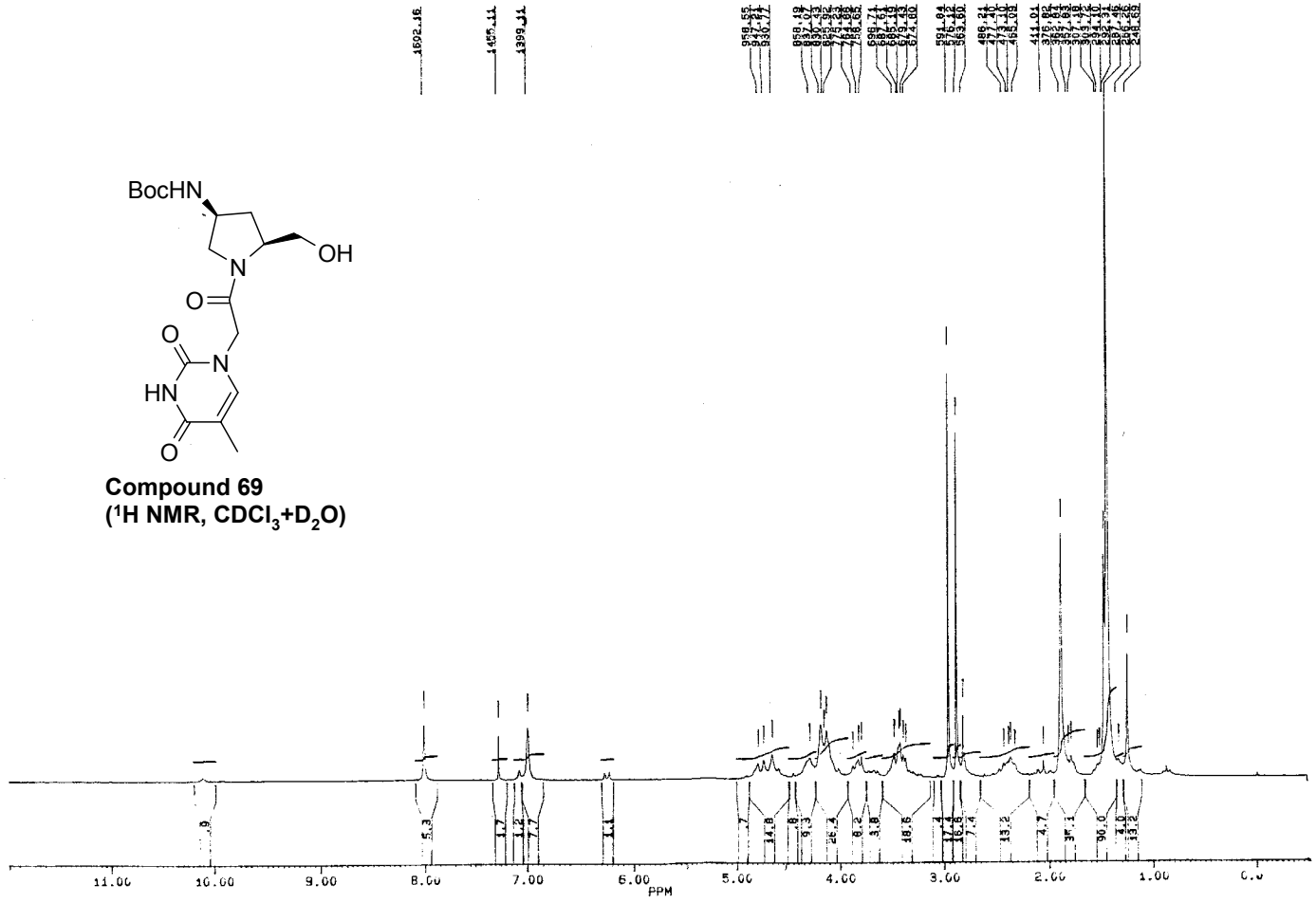

Compound 69
(^{1}H NMR, $CDCl_3$+D_2O)

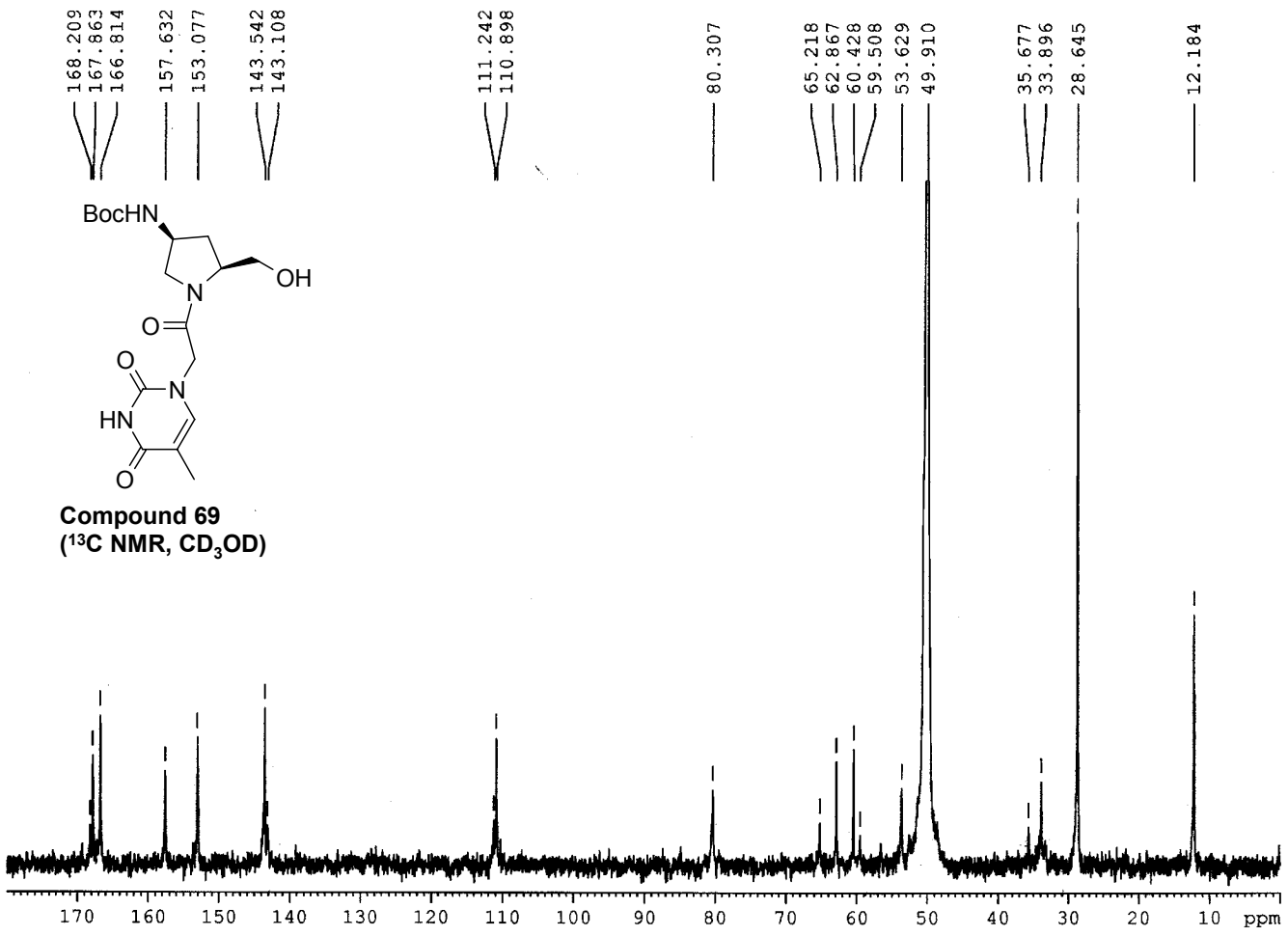

Compound 69
(^{13}C NMR, CD_3OD)

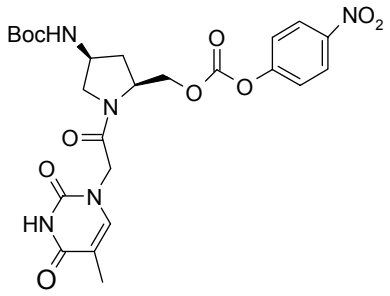

Compound 70
(^{1}H NMR, $CDCl_3$)

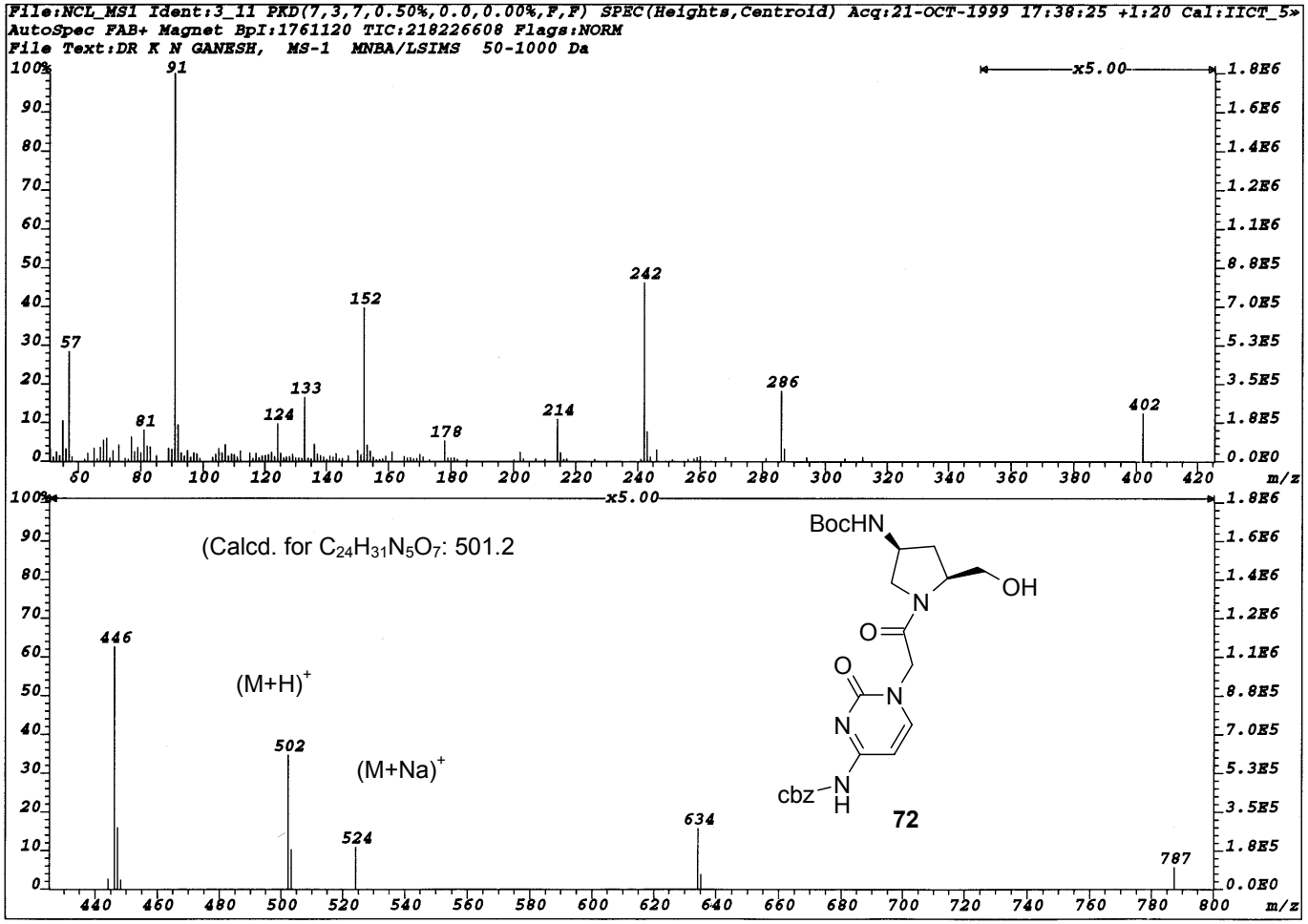
File:NCL_MS1 Ident:3_11 PKD(7,3,7,0.50%,0.0,0.00%,F,F) SPEC(Heights,Centroid) Acq:21-OCT-1999 17:38:25 +1:20 Cal:IICT_5»
AutoSpec FAB+ Magnet BpI:1761120 TIC:218226608 Flags:NORM
File Text:DR K N GANESH, MS-1 MNBA/LSIMS 50-1000 Da
x5.00
91
57
81
133
124
152
178
214
242
286
402
m/z
(Calcd. for C24H31N5O7: 501.2
(M+H)+
(M+Na)+
446
502
524
634
787
BocHN
OH
N
O
O
N
N
N
H
cbz
72

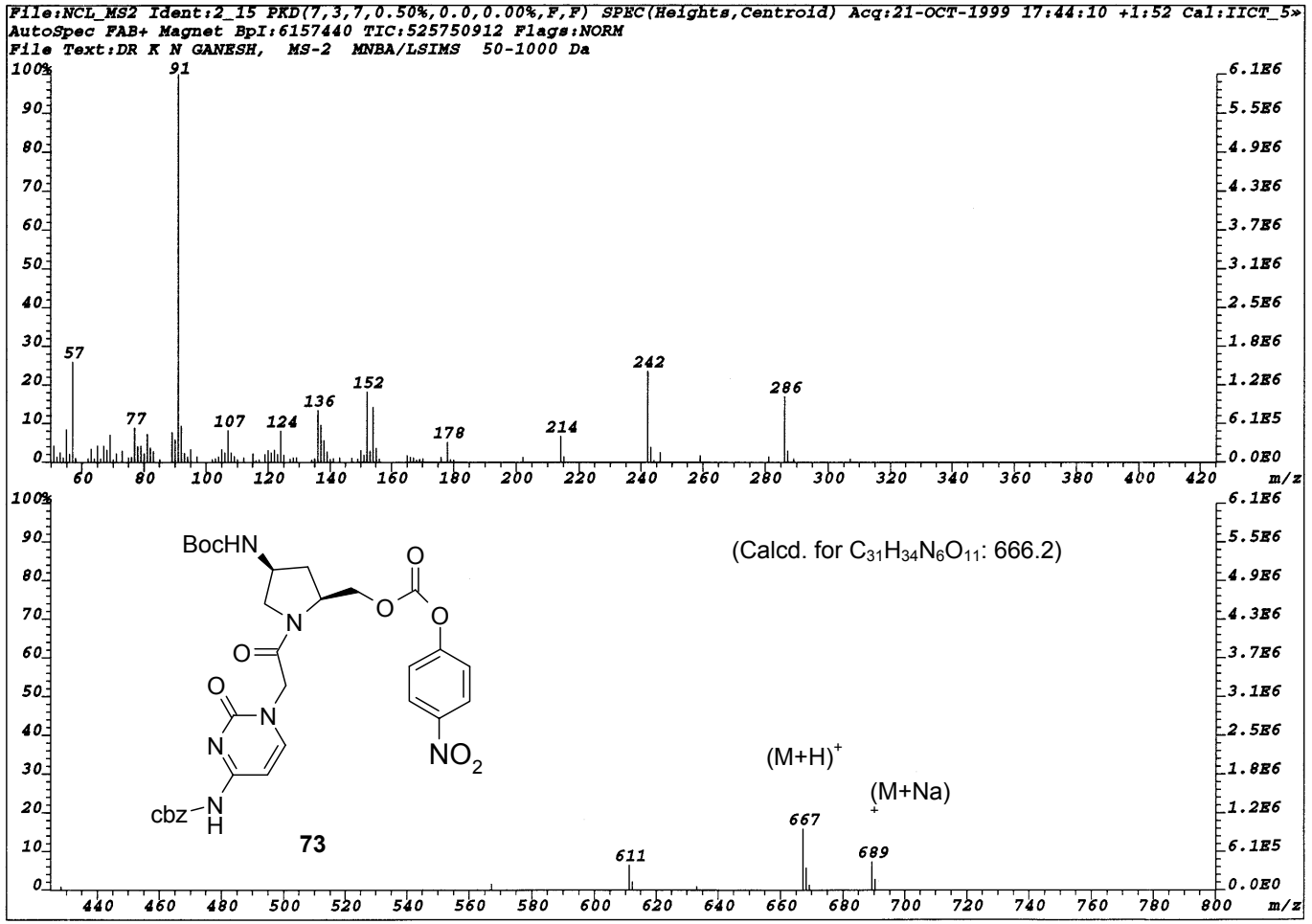
File:NCL_MS2 Ident:2_15 PKD(7,3,7,0.50%,0.0,0.00%,F,F) SPEC(Heights,Centroid) Acq:21-OCT-1999 17:44:10 +1:52 Cal:IICT_5»
AutoSpec FAB+ Magnet BpI:6157440 TIC:525750912 Flags:NORM
File Text:DR K N GANESH, MS-2 MNBA/LSIMS 50-1000 Da
91
57
77
107
124
136
152
178
214
242
286
m/z
BocHN
cbz
NO2
73
(Calcd. for C31H34N6O11: 666.2)
(M+H)+
(M+Na)+
611
667
689

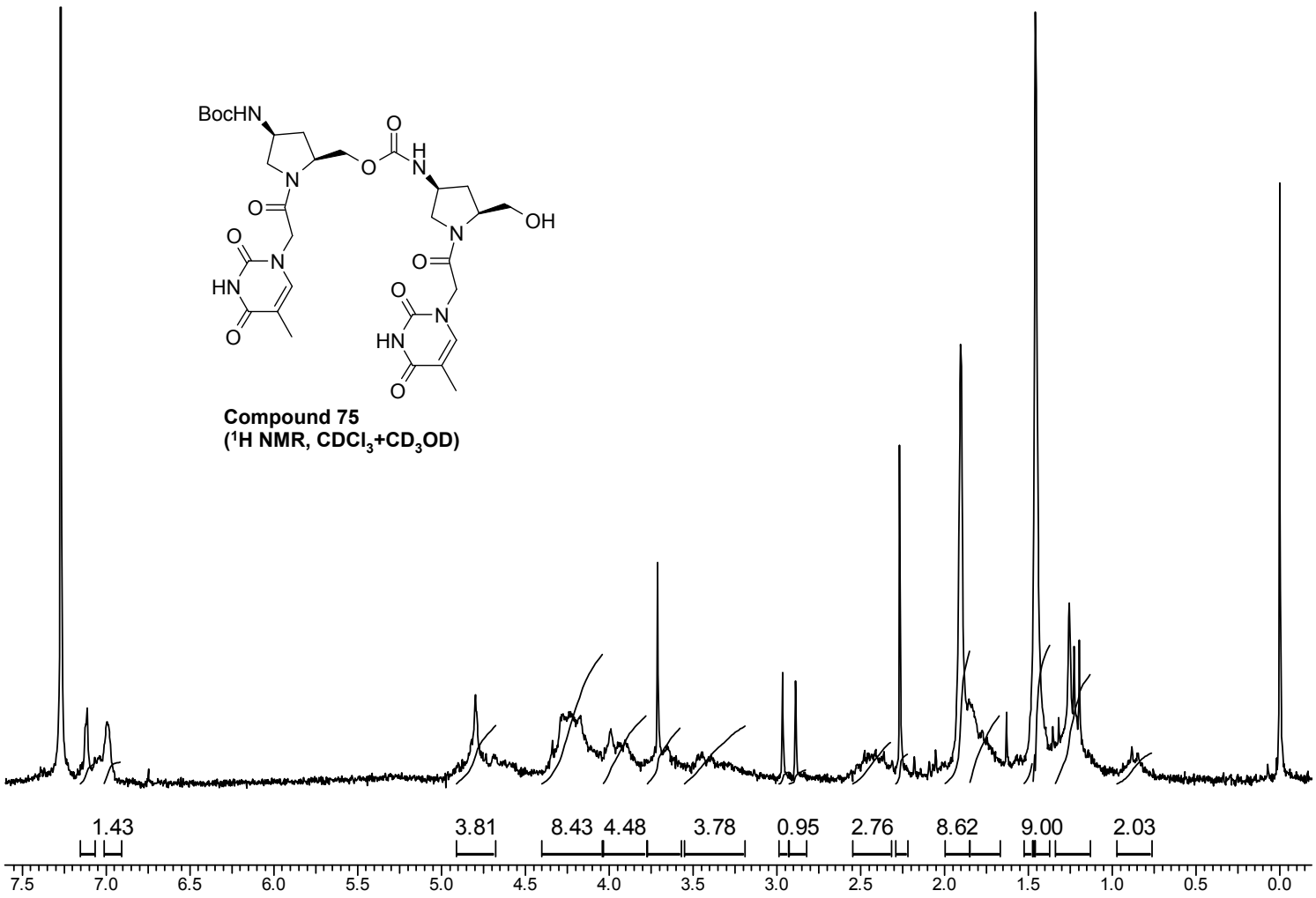

Compound 75
(^{1}H NMR, $CDCl_3$+CD_3OD)

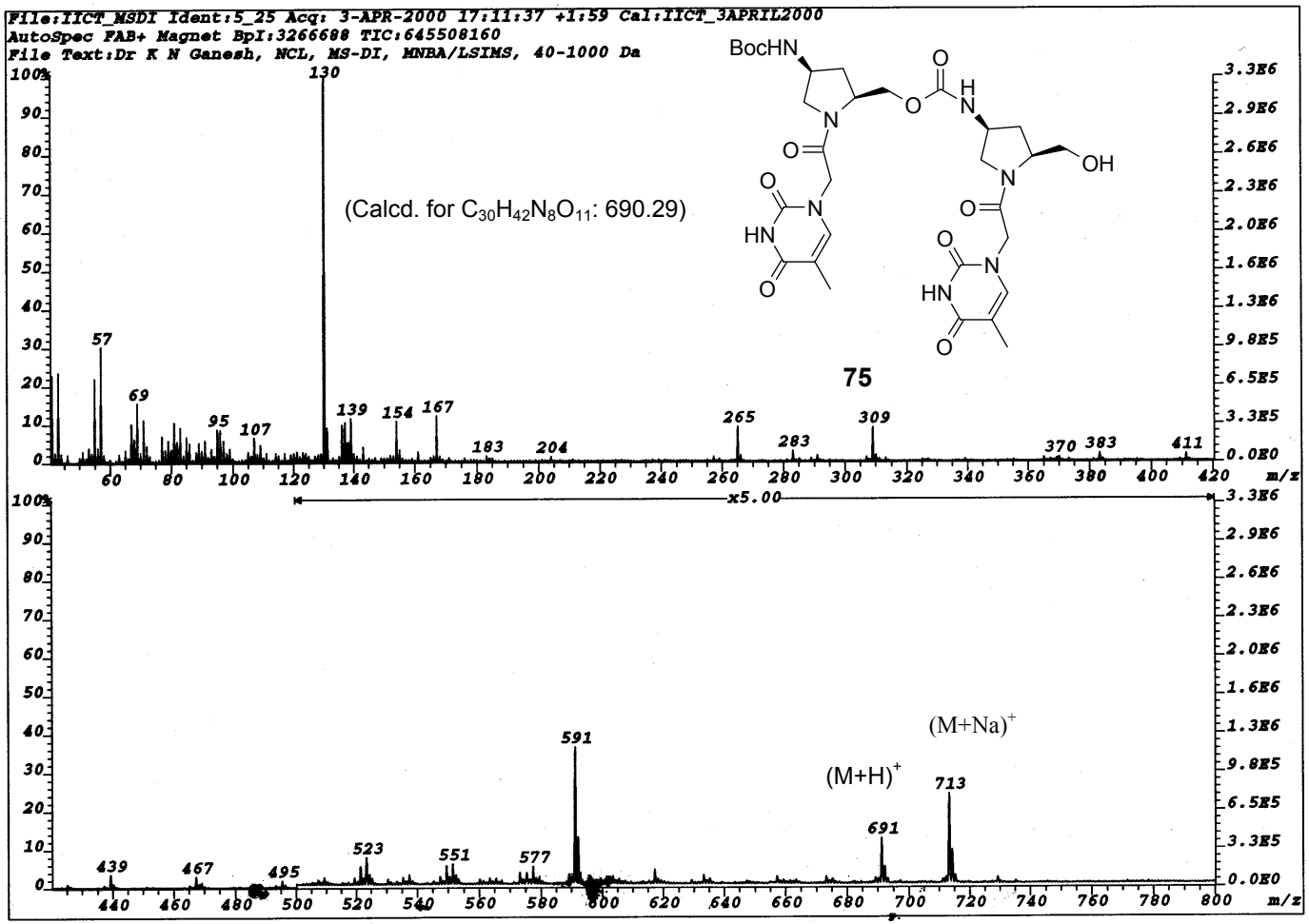
File:IICT_MSDI Ident:5_25 Acq: 3-APR-2000 17:11:37 +1:59 Cal:IICT_3APRIL2000
AutoSpec FAB+ Magnet BpI:3266688 TIC:645508160
File Text:Dr K N Ganesh, NCL, MS-DI, MNBA/LSIMS, 40-1000 Da
(Calcd. for C30H42N8O11: 690.29)
75
x5.00
(M+H)+
(M+Na)+
m/z

Chapter 4

Oxyamide Prolyl Nucleic Acids

4.1. Introduction

In the first chapter, structural modifications required to enable oligonucleotides for use as antisense therapeutic agents in biological systems were discussed. Chapter 2 discusses the various structural modifications to achieve preorganisation in *aeg*PNA, which includes incorporation of bridges in the flexible *aeg*PNA backbone. Chapter 3 has shown that the elongation of the amide backbone in prolyl PNA by one carbon atom in the form of a carbamate-linkage decreases the thermal stability of its complex with DNA. This probably arises from the elongated backbone having a lower degree of preorganisation in the geometry required for optimal hybridization. The preorganisation can also be engineered from stereoelectronic effects, the best example being hydroxylamine glycosidic linkage present in Calicheamicin. This linkage give rise to two conformers and it has been shown from NMR data that the major hydroxylamine conformer in solution is the one that binds to DNA (Walker *et al.*, 1994).

The structures of hydroxylamine and its various methylated derivatives have been studied (Riddell, 1981; Walker *et al.*, 1994). Both experimental and *ab initio* calculations have shown that hydroxylamine has a two fold rotational barrier and there is a significant energy difference between the two ground state conformers (Figure 1). In both conformers, the lone pairs on adjacent atoms are as close to orthogonal as permitted by the bond angles in order to avoid destabilizing interactions. The N- and O-

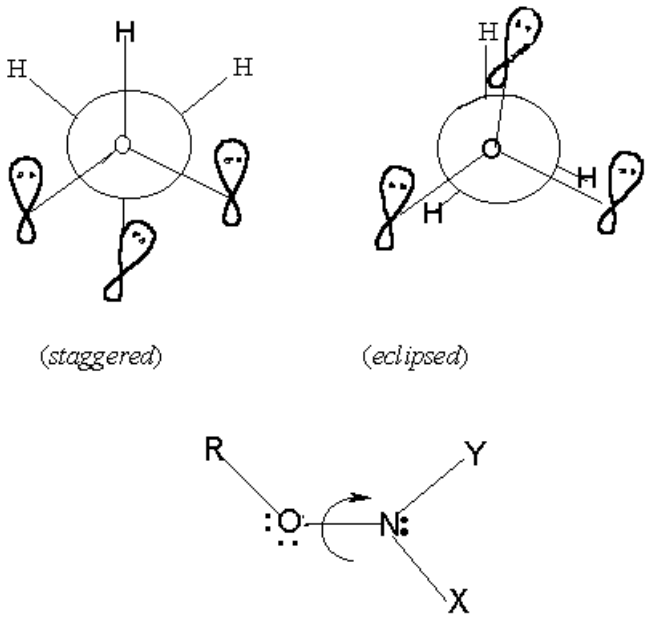

Figure 1. Conformers of hydroxylamine arising around N-O bond.

substituents have some effect on the energy differences between N-O bond conformers, but the eclipsed conformer with least repulsion between the lone pairs on N and O, is much lower in energy than the staggered conformer in all the cases.

Sanghvi and coworkers have investigated methylene(methylimino) (MMI) function as the internucleosidic linkage (Figure 2) (Perbost *et al.*, 1995). MMI/phosphodiester chimeras showed similar affinity for complementary RNA, with a change in Tm of -0.2 to +1.5^{o}C per modification as compared with native DNA (Figure

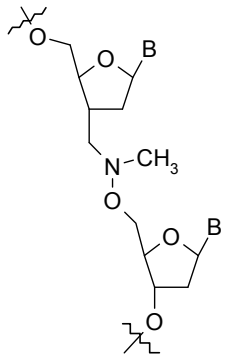

R=H, PO, PS

Figure 2. Methylene methylimino (MMI) linkage.

2). In addition, MMI/ phosphorothioate chimeras have also been prepared form oximes. NMR and modelling studies with MMI dimers revealed that the MMI linkages are restricted in conformation to either of the two low energy structures that differ in the orientation of the methyl group and both allow the bases to take up a stacked helical conformation for base pairing (Vasseur *et al.*, 1992; Debart *et al.*, 1992).

There is only one report in the literature, where a conformationally restricted oxyamide linkage replaces a phosphate linkage. Burgess *et al.* (1994) synthesized an oxyamide linked thymidine dimer (Figure 3a), which, when incorporated into an

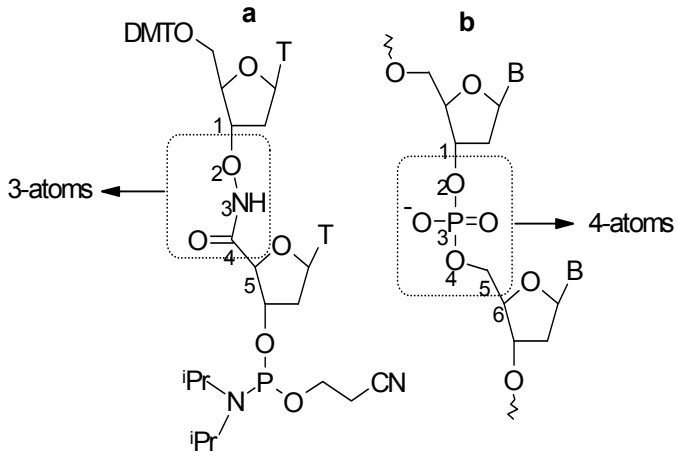

Figure 3. a) 5'-O-NH-CO-3' linked dinucleotide phosphoramidite b) DNA

oligodeoxyribonucleotide was shown to bind to complementary DNA with slightly less affinity as compared to the unmodified DNA. The oxyamide linked T*T dimers have one atom less than the natural TT phosphates in backbone. The planarity of the *trans* amide linkage was supposed to offset this shortening effect.

The introduction of the hydroxylamine functionality has been studied in ribozyme sequences. Incorporation of 2'-O-amino protected nucleosides into a hammerhead ribozyme resulted in a significant improvement in their catalytic rates. The presence of an O-amino group in an oligonucleotide provides a unique opportunity for introduction of post-synthetic modifications via oxime formation (Karpeisky *et al.*, 1998) (Figure 4).

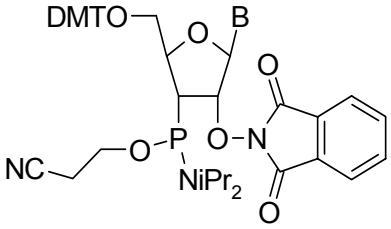

Figure 4. 2'-O-phthalimido nucleoside phosphoramidite

Recently, aminoxy chemistry has been applied to immobilize oligonucleotides (Salo *et al.*, 1999) (Figure 5). Phosphoroamidites bearing phthaloyl protected aminoxy tail were prepared and were used in automated oligonucleotide synthesis and after the chain assembly the phthaloyl protection was removed with

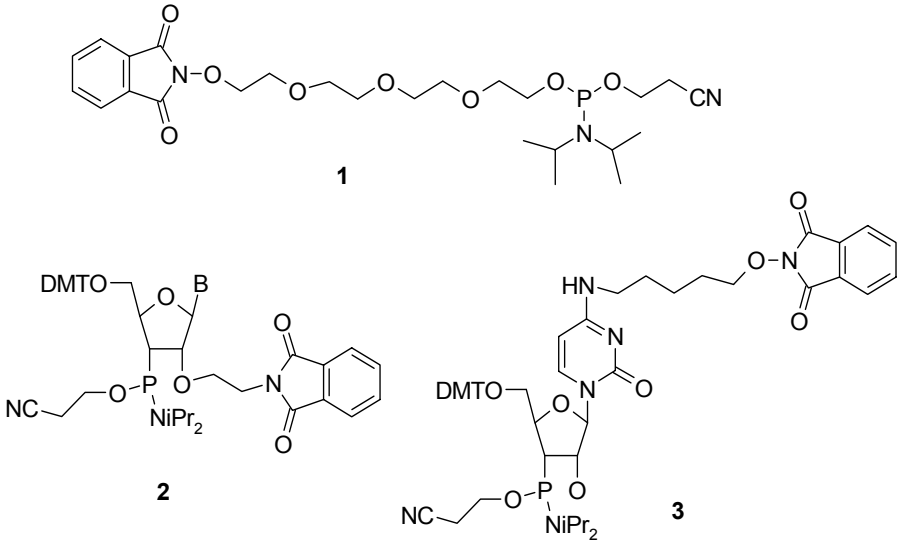

Figure 5. N-hydroxyphthalimide masked phosphoramidites

hydrazinium acetate. The support-bound oligonucleotides can be converted, when desired, to more stable oxime conjugates before the conventional base deprotection and release from the support.

Notably, α-aminoxy acids are under extensive studies since they induce a strong N-O turn in backbone, similar to the γ-turn found in normal peptides (Yang *et al.*, 1999; Peter *et al.*, 2000) (Figure 5a).

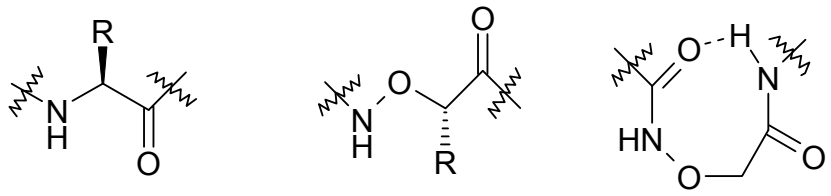

Figure 5a. α-aminoxyacids showing an N-O turn in contrast to α-aminoacids.

4.2. Rationale and objective

In light of the above mentioned reports using amino-oxy and oxyamide linkages, the present work is directed towards the introduction of chirality and conformational restriction via oxyamide linkage in the classical *aeg*PNA backbone. This was envisaged to control the orientation selectivity and specificity in binding by preorganization. The previous work from this laboratory on *prolyl*PNA (as discussed in chapter 3) has shown that the homooligomers based on 4-aminoproline backbone (Figure 6b; Gangamani *et al.*, 1999a) do not bind to complementary DNA due to incompatible internucleobase distances. There are five atoms in the backbone of *prolyl*PNA unlike six in natural DNA

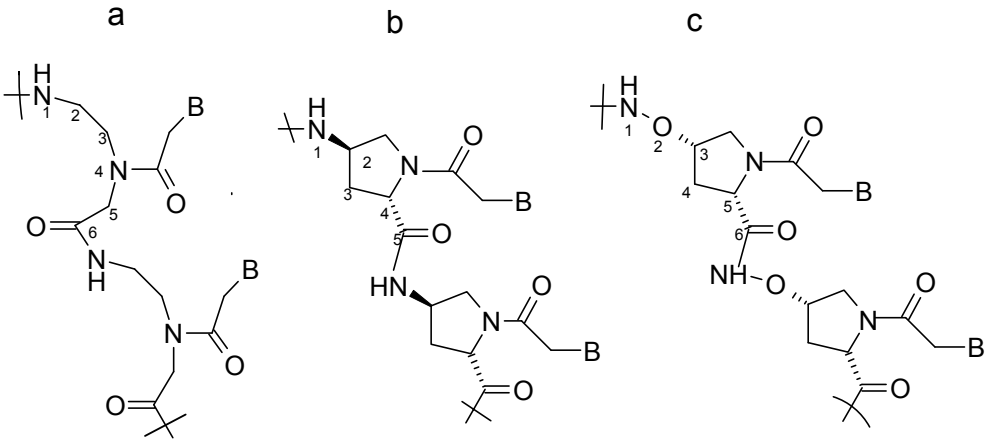

Figure 6. Comparison of backbones: a) *aeg*PNA b) Prolyl PNA c) Oxyamide linked nucleic acids.

and *aeg*PNA. To increase the internucleobase distance in *prolyl*PNA with simultaneous introduction of conformational restriction in the linkage, this chapter aims at:

1. The synthesis of pyrrolidine O-N monomer with suitable N-protecting group (PG) and free carboxylic acid, that can be used on solid support to synthesize oxyamide linked oligomers.

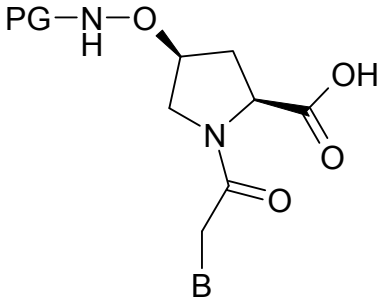

2. Incorporation of these monomers to generate oxyamide linkage in *aeg*PNA.
3. Cleavage of oligomers from the resin, their purification and DNA complementation studies.

4.3 Synthesis of The Protected Oxyamine monomer (86)

The substitution of *N*-(*t*-Boc)-hydroxylamine at the C-4 of (2*S*,4*R*)-*N*1-benzyloxycarbonyl proline methyl ester **3** under Mitsunobu conditions failed to give the required product **77** (Scheme 4.1a). Alternatively, the C4-hydroxyl of (2*S*,4*R*)-*N*1-benzyloxycarbonyl-4-(*O*-mesyl)proline methyl ester **59** was functionalised with *N*1-(*t*-Boc)-hydroxylamine via S_N2 reaction in K_2CO_3/DMF to obtain compound **77** in low yields (25%). When compound **77** was subjected to hydrogenation with Pd-C/H_2 to remove the *N*1-Cbz it was observed that the O-N bond was cleaved giving the 4*S*-hydroxy compound **78** (Gangamani *et al*., 1999). Hence, another route was adopted to generate oxy-amine function at the C-4 through the attachment of the nucleobase to ring nitrogen at the beginning itself (Scheme 4.1b). (2*S*,4*R*)-4-Hydroxyproline was treated with thionylchloride in methanol which gave the methyl ester. The methyl ester was coupled with thymine acetic acid **65** under DCC/HOBt conditions to give compound **79** in 78% yield. N-Hydroxyphthalimide was prepared from phthalic anhydride and hydroxylamine hydrochloride in Na_2CO_3/H_2O according to the literature procedure (Fieser & Fieser, 1967). Reacting N-hydroxyphthalimide with the 4*R*-hydroxy compound **79** under Mistunobu conditions yielded compound **80** with the required masked oxyamine functionality (Burgess *et al.*, 1994; Yang *et al.*, 1999). ^{1}H NMR of **80** showed a multiplet for four protons at δ 7.87-7.85 (phthaloyl group) and the FAB-MS showed peaks at 457 for $(M+H)^+$ and 479 for $(M+Na)^+$ (Calcd. $C_{21}H_{20}N_4O_8$=456.12),

Scheme 4.1a

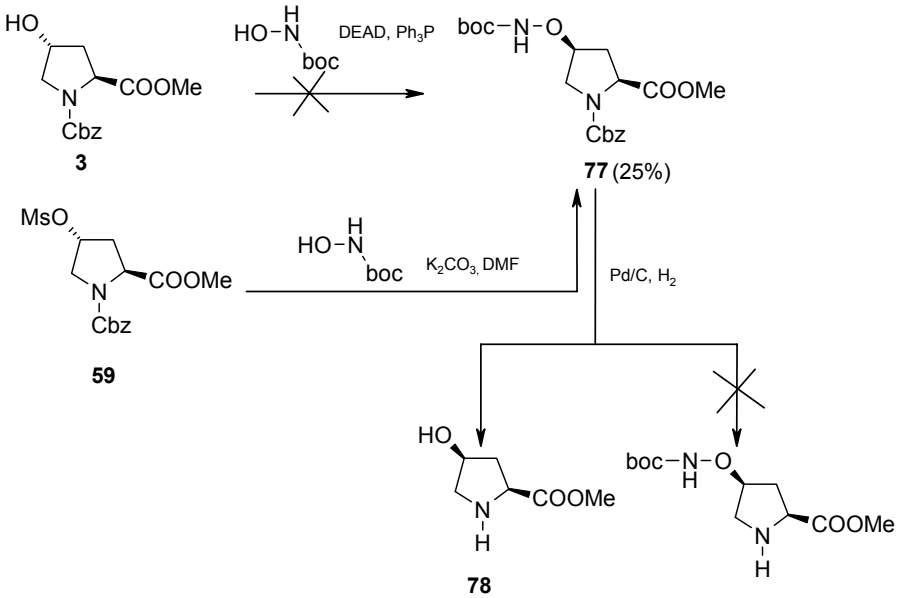

Scheme 4.1b

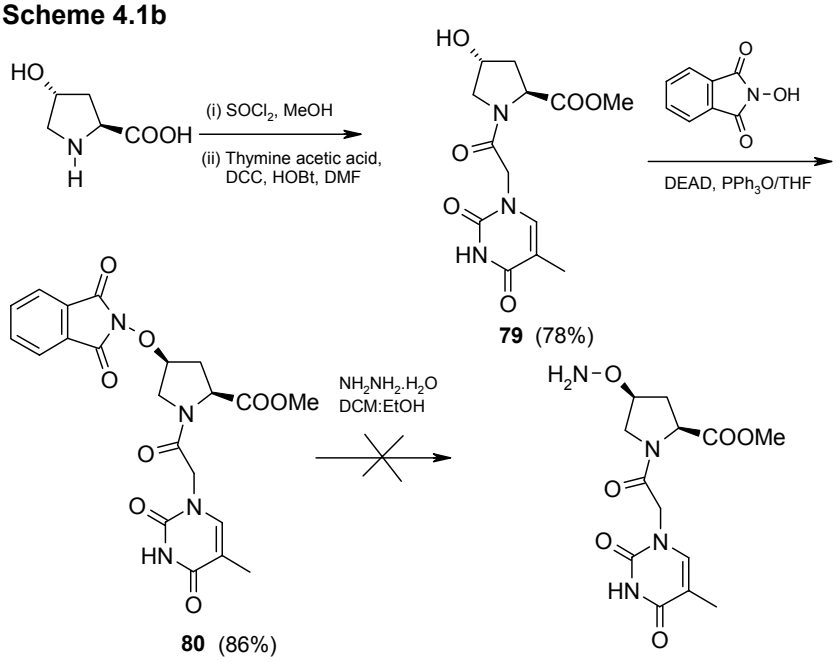

both confirming the identity of the product. However, the deprotection of phthalimide in **80** with hydrazine hydrate did not give the desired 4*S*-ONH_2 compound.

In view of the above-mentioned difficulties, it was decided to prepare an orthogonally protected monomer such as **86**, which makes it possible to attached the nuceobase to the proline unit on solidsupport. The monomer **86** was synthesized in five steps (Scheme 4.2). *trans*-4-Hydroxy-L-proline on treatment with thionyl chloride in ethanol gave hydroxyproline ethyl ester hydrochloride **81**. This was then reacted with *t*-butoxycarbonylazide to furnish (2*S*,4*R*)-*N*1-(*t*-butoxycarbonyl)hydroxyproline ethyl ester **82** in 96% overall yield (Kaname & Yoshifugi, 1992). The treatment of 4*R*-OH

Scheme 4.2

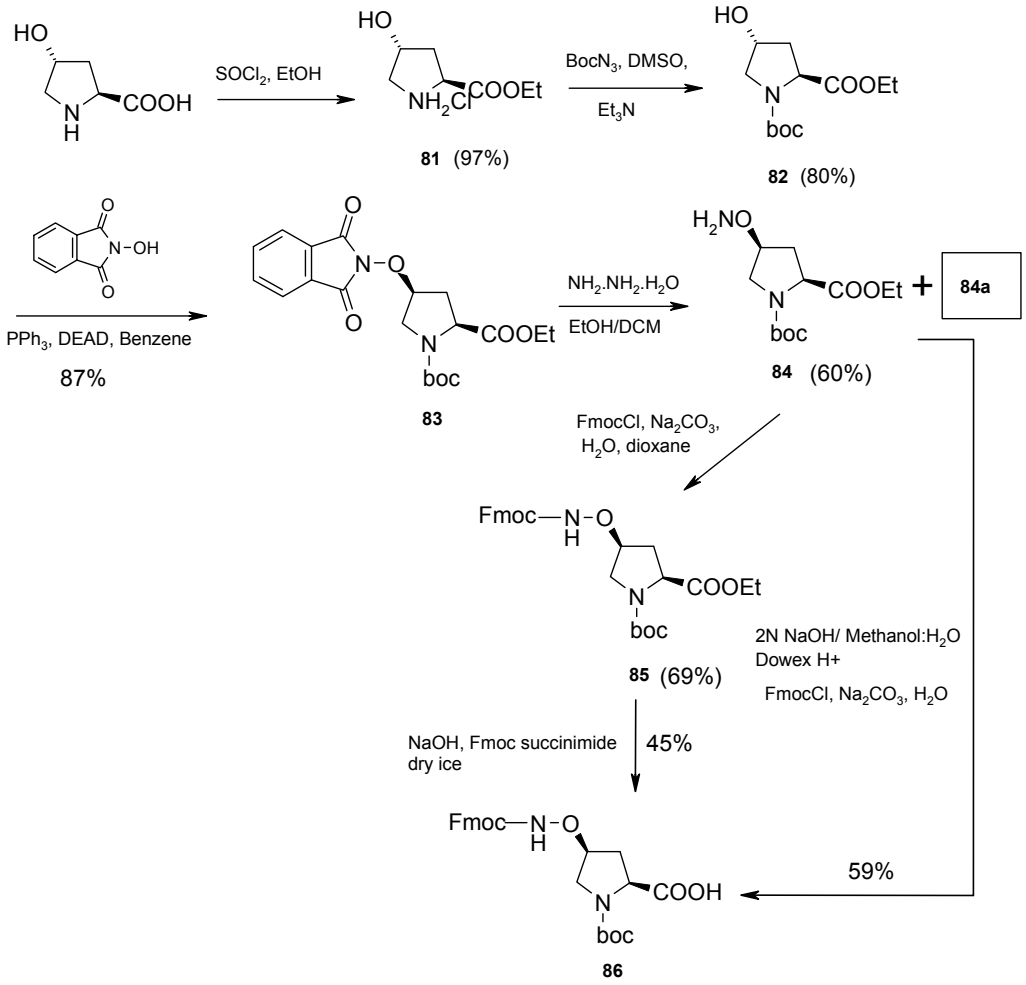

compound **82** with *N*-hydroxyphthalimide in the presence of DEAD and PPh_3P gave 4*S*-ONphthalimide compound **83** in 87% yield. ^{1}H NMR spectrum of **83** showed a multiplet at δ 8.0-7.7 for phthaloyl group with an expected downfield shift in C4H multiplet from δ 4.43-4.29 to 4.98-4.86. The removal of phthaloyl protection on the oxyamine function in **83** was achieved by treatment with a stoichiometric amount of hydrazine hydrate to give the free oxyamine **84** in 60% yield. ^{1}H NMR spectrum of compound **84** showed a sharp singlet integrating for two protons at δ 5.4 for 4-ONH_2 group with no peaks seen in the aromatic region. Further, an upfield shift in C4 carbon signals in ^{13}C NMR of **84** form δ 85.94 and 84.76 (in compound **83**) to 81.7 and 80.7 confirmed the removal of phthalimide group. FT-IR of compound **84** showed a sharp band at 3323 cm^{-1} for amine (ONH_2). The lower yield (60%) of the desired **84** in the deprotection step is presumably due to the instability of oxyamines and the formation of side product. The characterization of this side product is discussed in section 4.8. The

m/z for compound **84** in GC analysis did not show the M^+ peak, rather a peak at 241 was present which could be the elimination product with the elimination of fragment hydroxylamine. The treatment of oxyamine **84** with FmocCl in the presence of Na_2CO_3 as base gave the 4*S*-O-NH-Fmoc compound **85** in 69% yield. The saponification of ester **85** in aq. NaOH also resulted the complete removal of Fmoc group while the use of LiOH, a milder base, for the hydrolysis led to only 20% yield of the required acid **86**.

Breipohl *et al.* (1996) reported the base (aq. NaOH) catalyzed ester hydrolysis of Fmoc derivatives to retain the Fmoc group by simultaneous use of Fmoc-succinimide in the reaction mixture with dry ice as buffer. Application of this method gave the acid **86** in 45% yield. In order to further improve the yield of the acid **86**, hydrolysis of the ester prior to Fmoc protection was attempted. The oxyamine **84** was hydrolyzed with aq. NaOH followed by the amine protection with FmocCl giving **86** in 70% overall yield. Compound **86** was characterized by ^{1}H NMR showing peaks in aromatic region δ 8-7 for nine protons (Fmoc) and FAB-MS having peaks at 469 $(M+H)^+$ and 491 $(M+Na)^+$ (Calcd. for $C_{25}H_{28}N_2O_7$=468.189).

4.4.1. Oligomer Synthesis

The synthesis of the mixed base *aeg*PNA 10-mer **1** (Entry 1, Table 1) was carried out using standard *t*-Boc chemistry and *aeg*PNA monomers **54**-**57**, the synthesis of which has been described in chapter 2. The incorporation of the oxyamide pyrrolidine moiety in the middle of mixed base *aeg*PNA (Entry 2, Table 1)was achieved according to the scheme outlined in Figure 7. *aeg*PNA monomers were coupled to the Merrifield resin, preloaded with β-alanine, using diisopropylcarbodiimide/HOBt reagent. After the chain extension using normal procedure and the coupling of monomer **86**, *N*1-*t*-Boc of the oxyamine unit was removed by deprotection with TFA/DCM, which was monitored by isatin test (Kaiser *et al.*, 1980). After the neutralization of the trifloroacetate salt with 5% DIPEA in DCM, thymine acetic acid **65** (Chapter 3) was coupled to the N1 of the pyrrolidine ring using

Table 1. PNA and DNA sequences

Entry	Sequence
1	H-G T A G A T C A C T-βala-OH
2	H -G T A G A t C A C T -βala-OH
3	5' -A G T G A T C T A C- 3'

t indicates oxyamide linked prolyl thymine

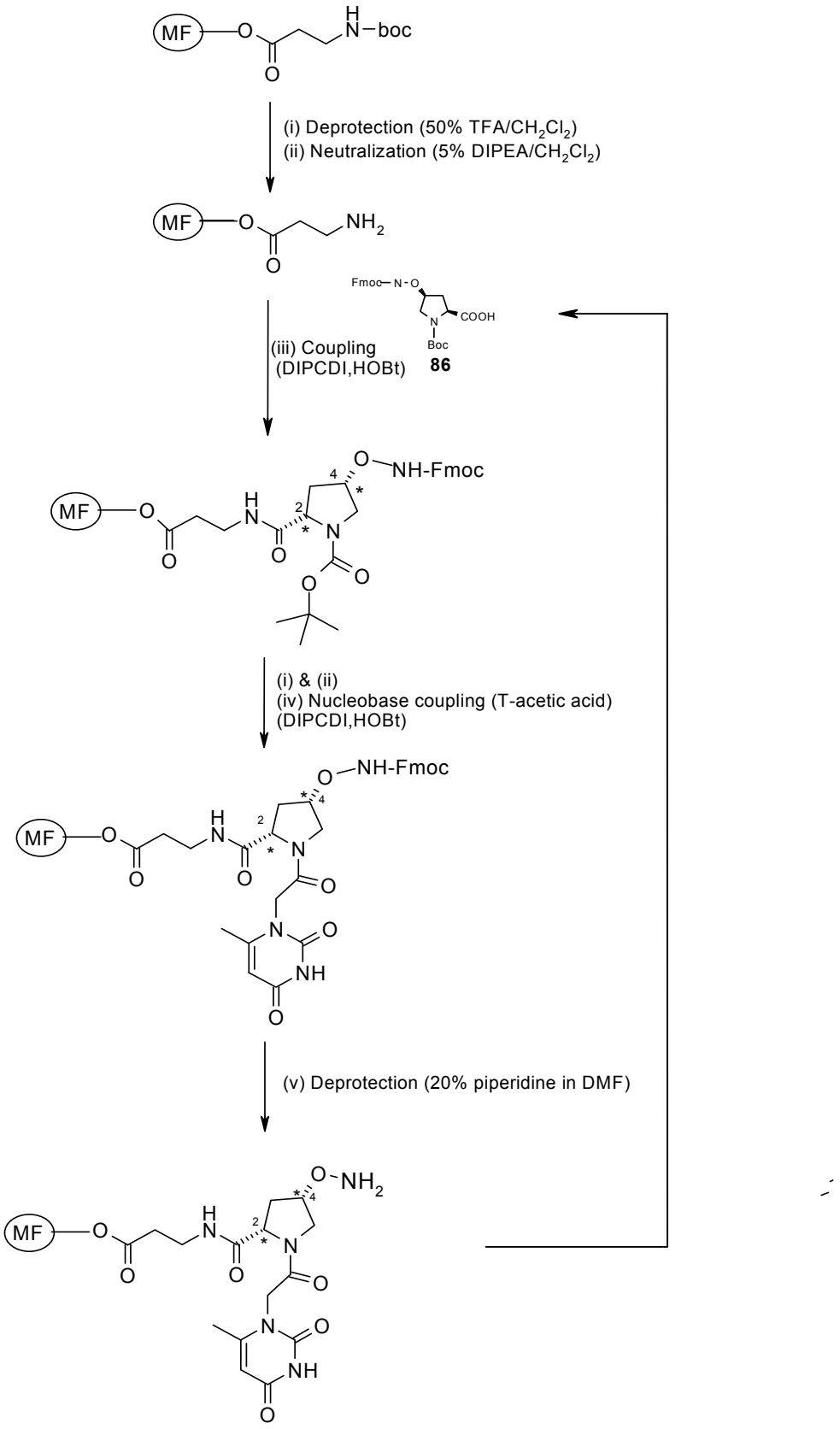

Figure 7. Solid phase synthesis of oxyamide nucleic acids using orthogonally protected monomer.

4.4.2. Cleavage and Purification of Oligomers

The oligomers **1** and **2** were cleaved by TFMSA/TFA method which resulted in simultaneous removal of exocyclic Cbz group on cytosine. The peptides were precipitated from their methanolic solutions with dry diethyl ether, were desalted by Gel Filtration and subsequently purified by RP-4 semipreaprative HPLC with isocratic elution. The HPLC profiles of the purified peptides are shown in Figure 8.

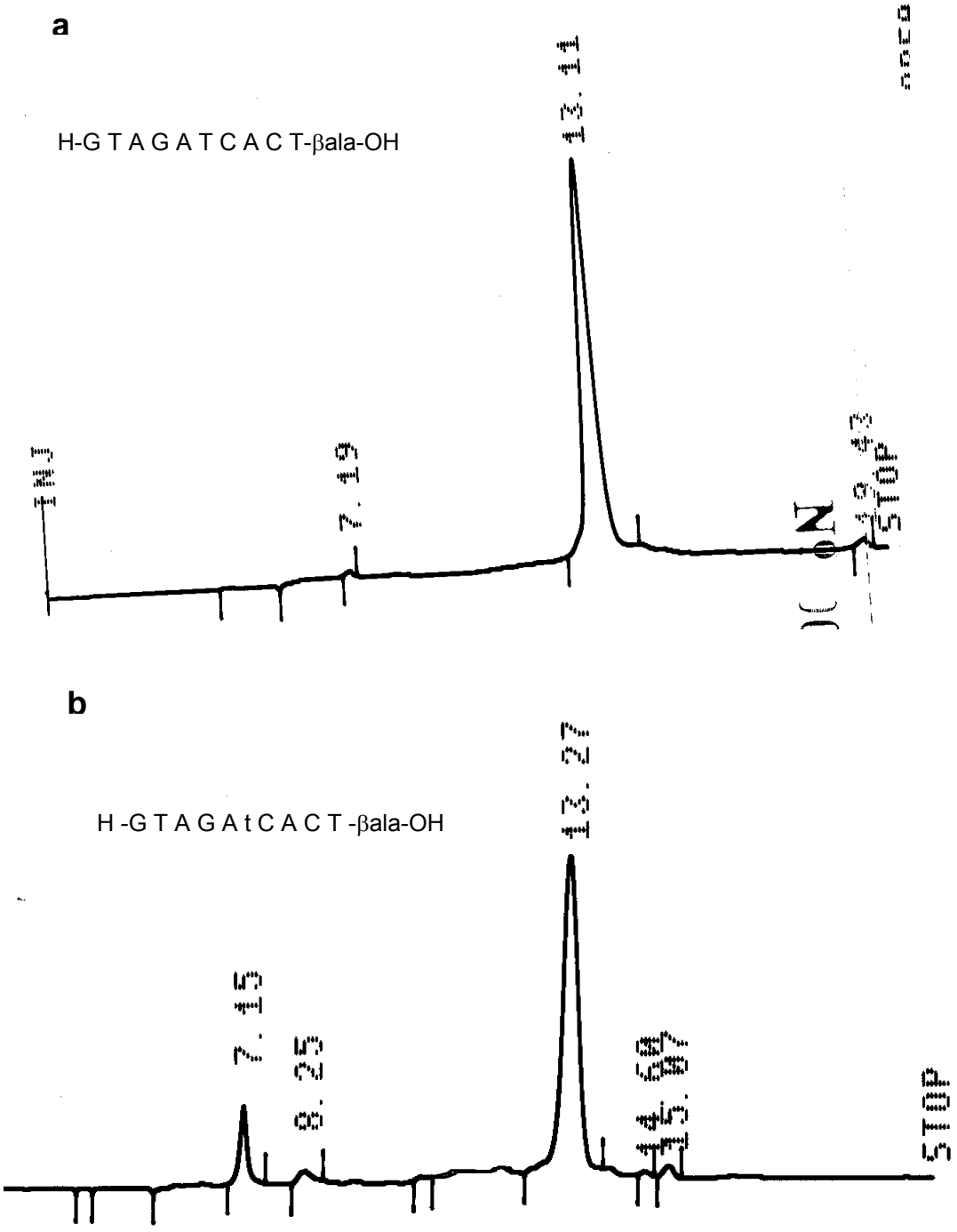

Figure 8. HPLC profiles of PNA oligomers a) mixed base *aeg*PNA b) mixed base *aeg*PNA with proline oxyamide unit in the center.

4.5. Synthesis of The Complementary DNA 3

DNA sequence **3** complementary to the PNA sequences was synthesized on a Pharmacia GA Plus DNA synthesizer using the standard β-cyanoethyl phosphoramidite chemistry as described before (Section 2.7.4, page 58). The oligonucleotide **3** was de-salted by gel filtration and the purity as ascertained by RP-18 analytical HPLC was more than 98% (Figure 9). Thus, this DNA 3 was used without further purification in the biophysical studies.

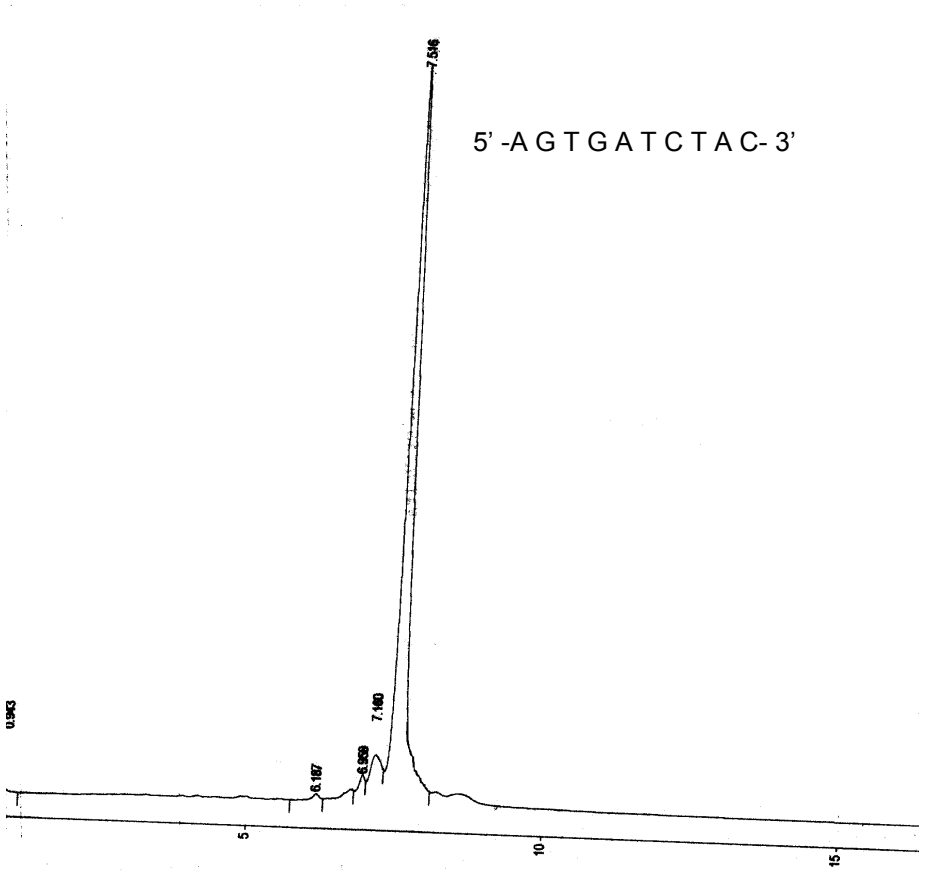

Figure 9. HPLC profile of the crude DNA oligomer **3**.

4.6. UV-melting experiments

PNA sequences composed of mixed purine and pyrimidine nucleobases bind to DNA to form duplexes. The melting experiments were carried out using PNA sequences **1** and **2** in 1:1 stoichiometry. The first derivative plots of the Tm data are shown in Figure 10 and the corresponding Tm values are listed in Table 2. The control duplex of *aeg*PNA **1**:DNA **3** showed a Tm of 56.7^{o}C (entry 1, Table 2). Incorporation oxyamide linked proline-T (**86**) in the middle of the sequence destabilized the duplex by

6.5°C (Tm=50.2°C) (entry 2, Table 2). Thus the introduction of single oxyamide-linked proline unit in the *aeg*PNA seems to be incompatible for hybridization.

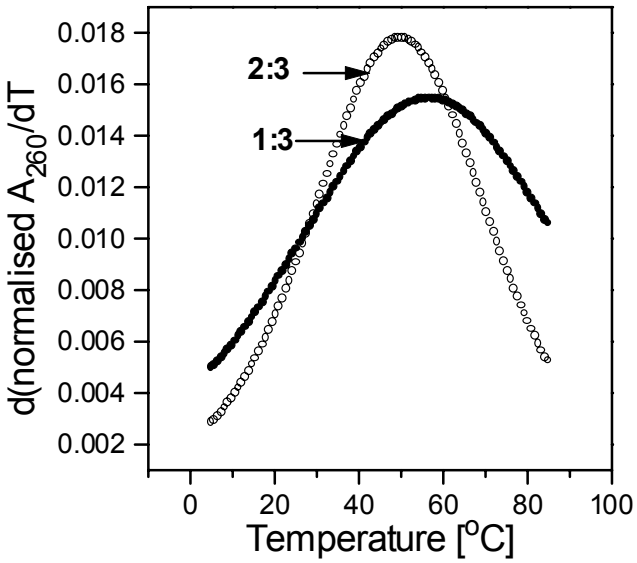

Figure 10. First derivative plots of UV-Tm of duplexes **1:3** and **2:3**. Buffer: 10mM sodium phosphate pH~7.3

Table 2. UV-Tm values of PNA:DNA duplexes

Entry	Complex	Tm (°C) ΔTm
1	H-G T A G A T C A C T-βala-OH 3'-C A T C T A G T G A-5'	56.7
2	H -G T A G A t C A C T -βala-OH 3'-C A T C T A G T G A-5'	50.2 (-6.5)

t indicates the oxyamide linked prolyl thymine

4.7. Conclusion

Orthogonally protected (2*S*,4*S*)-4-aminoxy proline monomer **86** is synthesized and is introduced into *aeg*PNA by solid phase method. The use of orthogonal protecting groups on 4-oxyamine (Fmoc) and N1 (*t*-Boc) circumvent the problem of pre-synthesis of monomers with each nucleobase. This chemistry is particularly useful in the generation of oxyamide-linked oligonuleotide mimetics by solid phase synthesis. The incorporation of (2*S*,4*S*)-oxyamide proline unit in mixed base *aeg*PNA resulted in the destabilization of the duplex. From the results of chapter 3 where carbamate linked (2*S*,4*S*)-pyrrolidine unit also caused destabilization of the triplexes compared to *aeg*PNA, it may be concluded that while extending the backbone of 4-aminoproline

PNA *cis* streochemistries are not suitable. The *cis* configuration as in (2*S*,4S) and (2*R*,4*R*) 4-aminoproline and 4-aminopyrrolidine may induce turn-like structures which inhibit the formation of the extended helical structure as required for hybridization with DNA.

Thus the chemistry developed in the present chapter can be employed in exploring other stereoisomers of proline based oxyamide linked nucleic acid analogues.

4.8. Characterization of The Byproduct 84a

During the deprotection of phthalimide group in compound **83** with hydrazine hydrate (Scheme 4.2), an unusual product **84a** was formed having the following characteristics:

1. Higher Rf value than the oxyamine product **84.**
   *It suggests that **84a** is less polar than **84**.*
2. Compound **84a** starts to appear in the reaction mixture even before the complete disappearance of starting material as monitored by TLC.
   The rate of byproduct formation is competing and is more than the deprotection rate.
3. Compound **84a** also formed during the column chromatography and the amount of which varied with the solvents used for elution with EtOAc giving greater yield than DCM.
   Hence, polar solvents catalyze the formation of byproduct.
4. Use of methanol instead of ethanol as a solvent in the deprotection step also resulted in the formation of this product.
   The nature of product formed is independent of the solvent used for deprotection.
5. A change of deprotecting reagent from hydrazine hydrate to 40% aq. methylamine gave the same product **84a**.
   *The deprotecting reagent is not involved in the formation of **84a**.*
6. Even after purification of compound **84**, upon standing it was spontaneously converted to compound **84a**.
   *Compound **84a** is a result of either intermolecular or intramolecular rearrangement of **84**.*
7. The complete conversion **84** to **84a** in $CDCl_3$ took 3-4 months as was followed by NMR spectroscopy.

The rate of formation of 84a is slow in the absence of basic medium.

8. Interestingly, no other product was isolated in the conversion of **84** to **84a**.
   The rearrangement does not involve any fragment elimination.
9. The ^{1}H NMR spectrum of **84a** showed peaks at δ 1.79 and 1.71, each integrating for three protons, with the characteristic peak sets for t-Boc (δ 1.36, 1.42), ethyl ester (δ 1.28-1.15) and proline signals (^{1}H NMR of compound **84** and **84a** are shown in Figure 11).
   Two methyl groups are present in addition retention of t-Boc and ethyl ester with intact proline core.
10. ^{13}C NMR spectrum of **84a** showed peaks at δ 21.3 and 15.2 respectively, with one signal at δ 155, which was absent in DEPT (^{13}C and DEPT of compound **84a** are shown in Figure 12).
    in addition to extra methyl groups,one quaternary carbon is present.
11. The FT-IR spectrum of compound **84a** revealed that the characteristic band for --ONH_2 (present in the FT-IR spectrum of compound **84**) at 3323 cm^{-1} was absent (FT-IR of compounds **84** and **84a** are shown in Figure 13).
    Free -ONH_2 group is absent in 84a.
12. The compound **84a** did not react with Ac_2O/Pyridine.
    The absence of free –ONH_2 group is confirmed.
13. Elemental analysis: C, 57.27; H, 8.37; N, 8.91.
    The empirical formula of the compound 84a is $C_{15}H_{26}N_2O_5$
14. The GC-MS of **84a** showed m/z =241 (Figure 14 shows GC-MS of compounds **84** and **84a**). This could be the same fragment ion peak as seen in GC-MS of compound **84** also.
15. FAB-MS shows a peak at 315 (Figure 15).
    *If this is considered as $(M+H)^+$ then the molecular mass of **84a** should be 314, which indicates that the molecular formula of side chain should be $C_3H_6N_1O_1$ (72.0). These results suggest the structure of the side chain as ($Me_2C=NO$).*

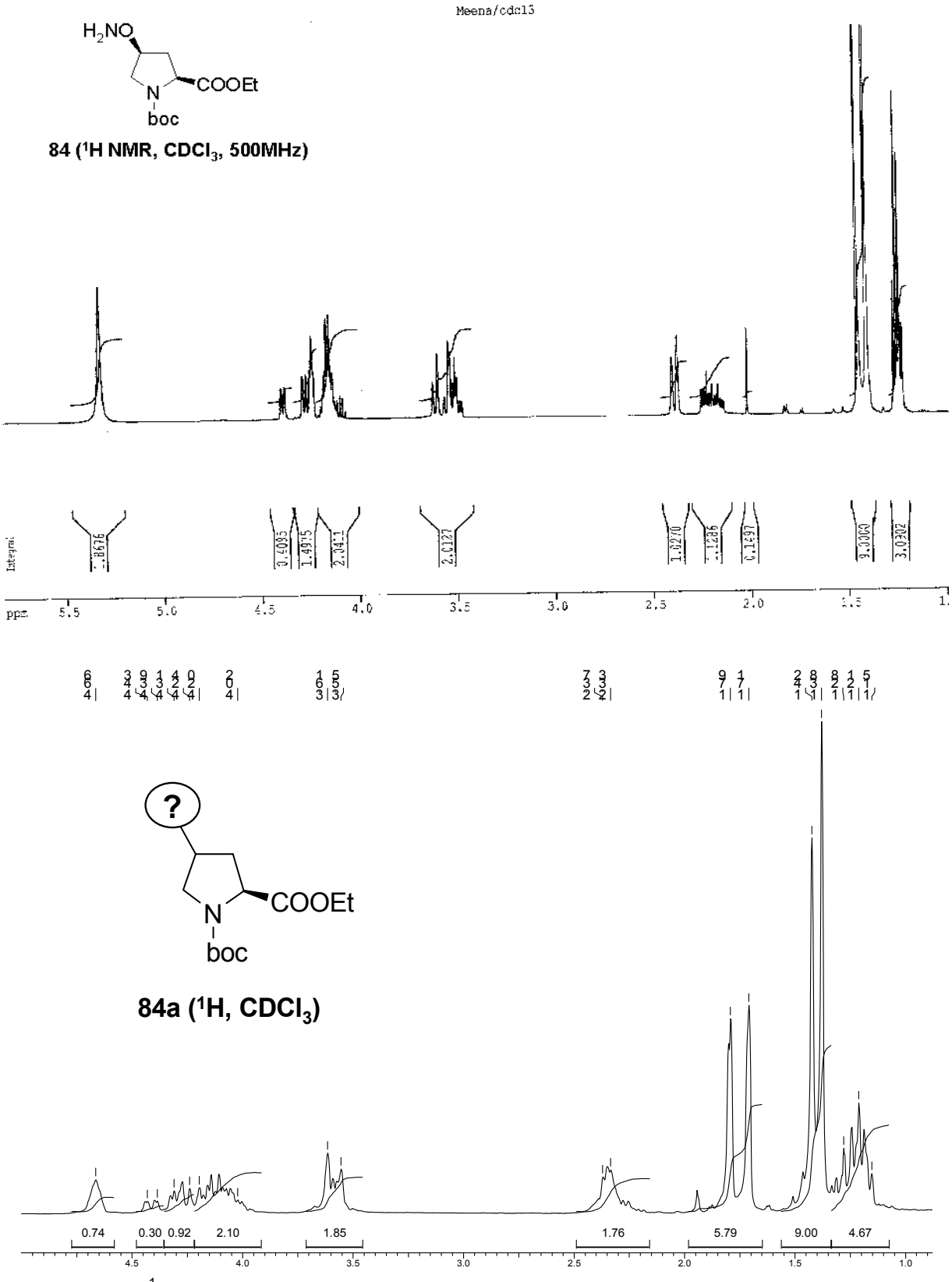

Figure 11.[1]H NMR spectra of compound **84** and **84a**.

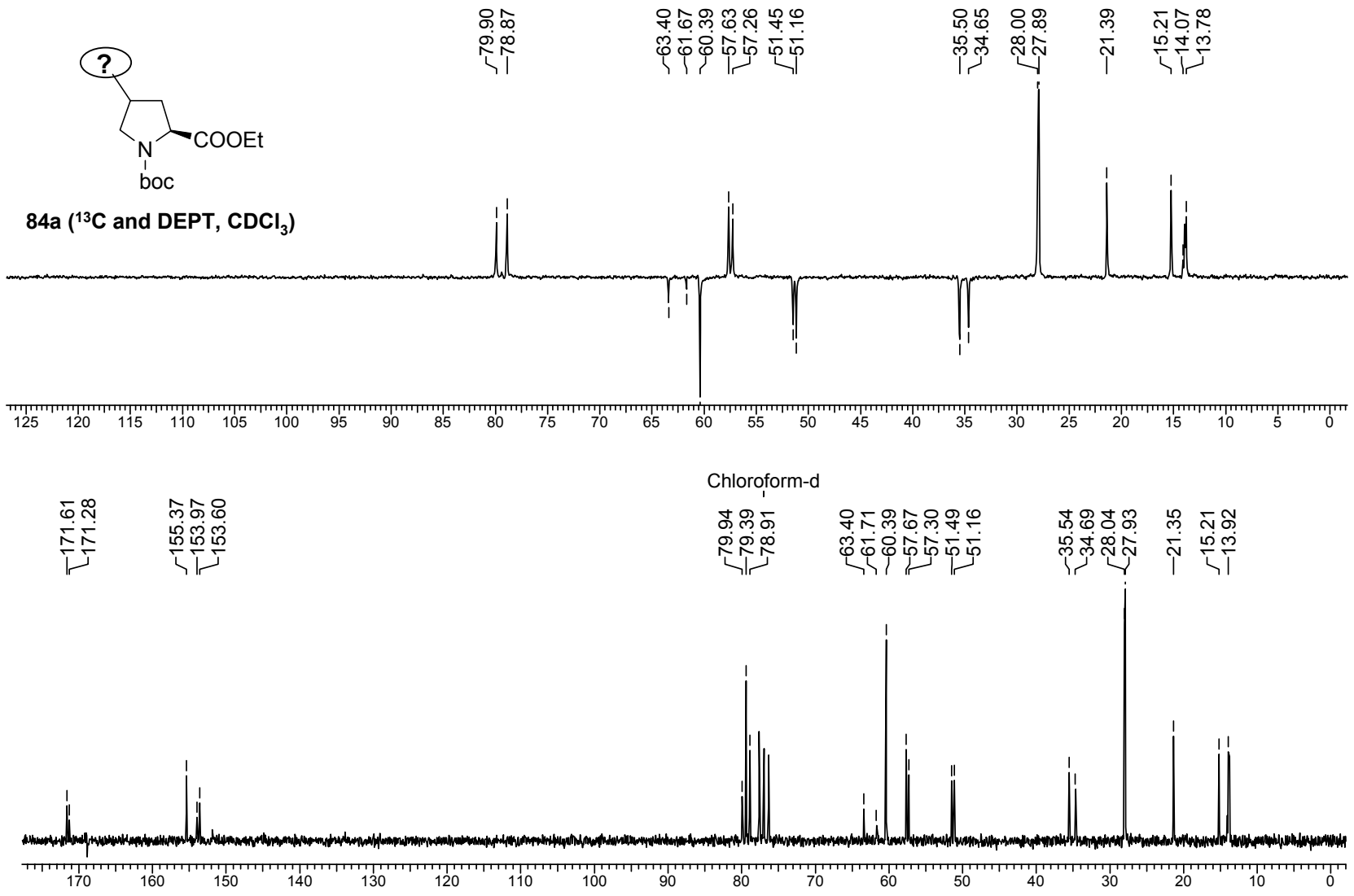

Figure 12. ^{13}C and DEPT spectra of compound **84a**.

15.

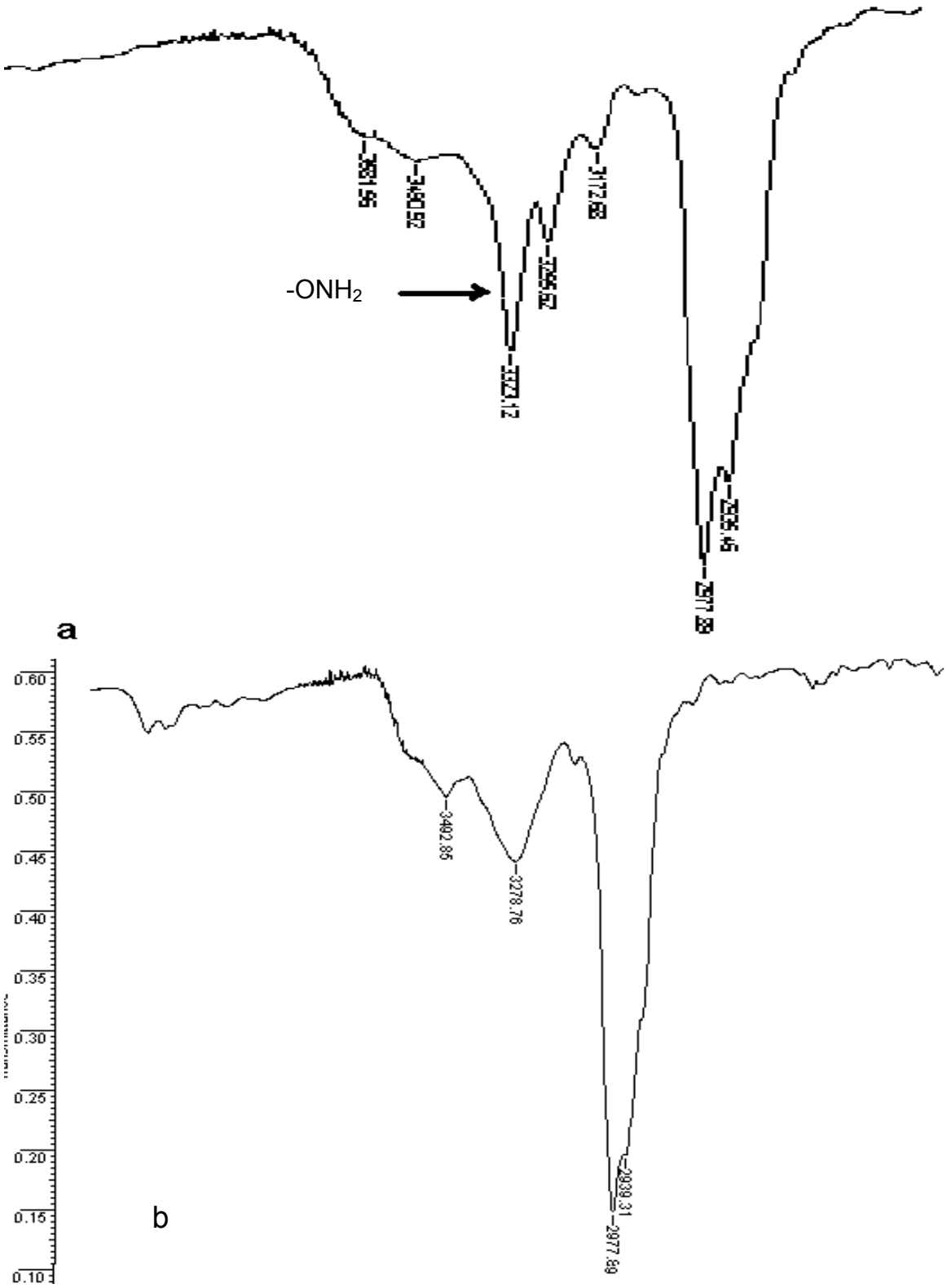

Figure 13. FT-IR spectra of a) compounds **84** b) compound **84a**.

16.

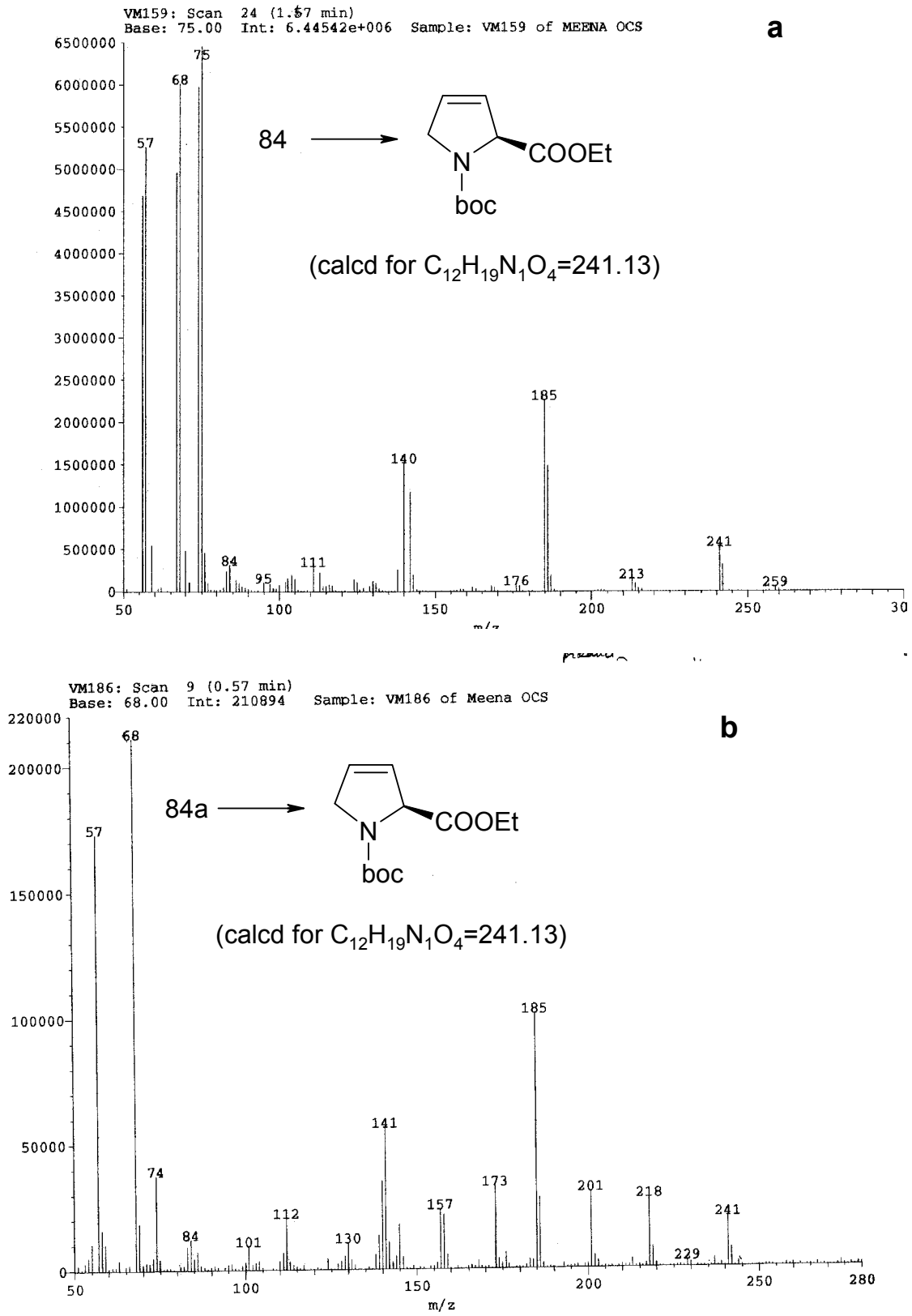

Figure 14. GC-MS spectra of a) compound **84** and b) compound **84a** both showing the peak for elimination product.

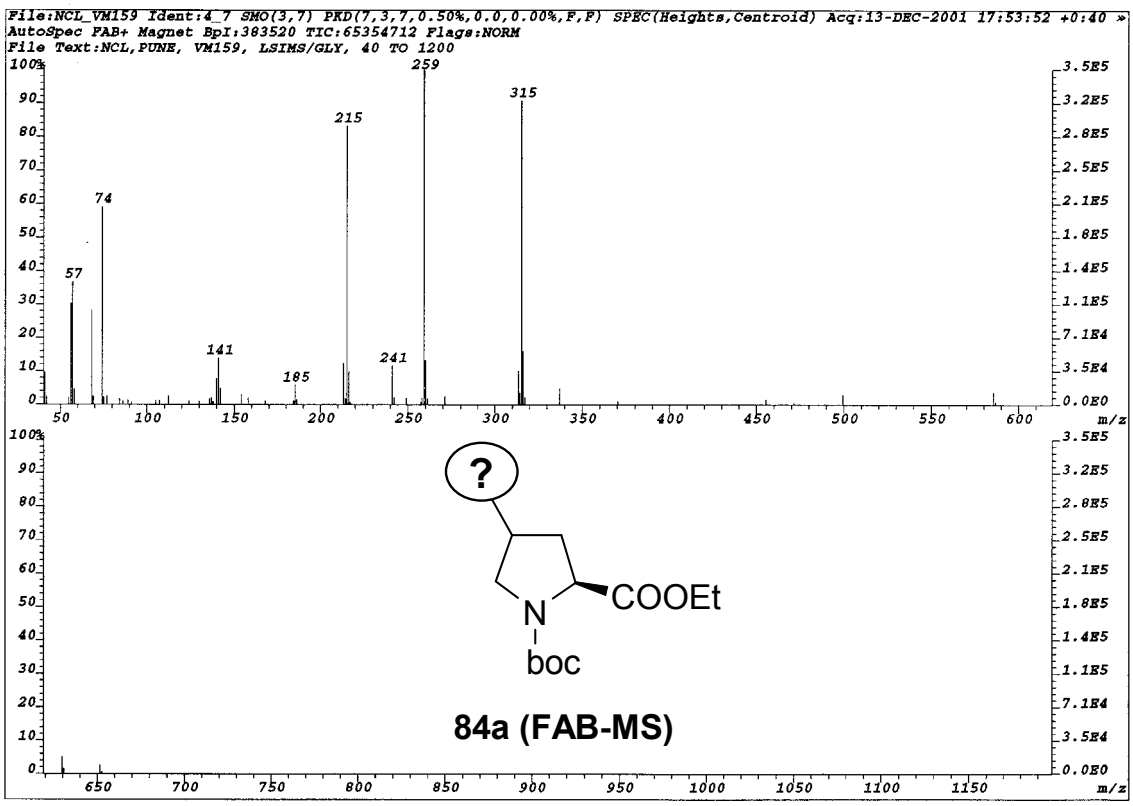

Figure 15. FAB-Mass spectrum of compound **84a**.

To unambiguously assign the structure of **84a**, attempts were made to derivatize **84a** to a crystalline compound. The N1-*t*-Boc in compound **84a** was deprotected with 1:1 TFA/DCM and the resulting trifloroacetate salt was coupled to *p*-nitrophenyl acetic acid under DCC/HOBt/DIPEA to obtain the derivative **84b** which was characterized by ^{1}H, ^{13}C and FAB-MS (Figure 16, 17 and 18).

1. ^{1}H NMR of derivative **84b** showed signals for methyl groups, which were well dispersed each with rotameric population 2:1 (Figure 16).

   Other than the ring nitrogen amide, which is the cause of rotamers, there is some conjugation in the side chain, which resulted in further splitting of methyl signals. The dispersion of the –CH_3 signals became more prominent when t-Boc was replaced with more bulky p-nitrophenylacetyl group. This is perhaps a result of differential ring current effects in methyl group.

2. The FAB-MS of the **84b** compound showed $(M+H)^{+}$ peak at 378 (Figure 18).

   The Molecular formula of the side chain is confirmed as $C_3H_6N_1O_1$.

Unfortunately diffraction quality crystals of compound **84b** could not be obtained.

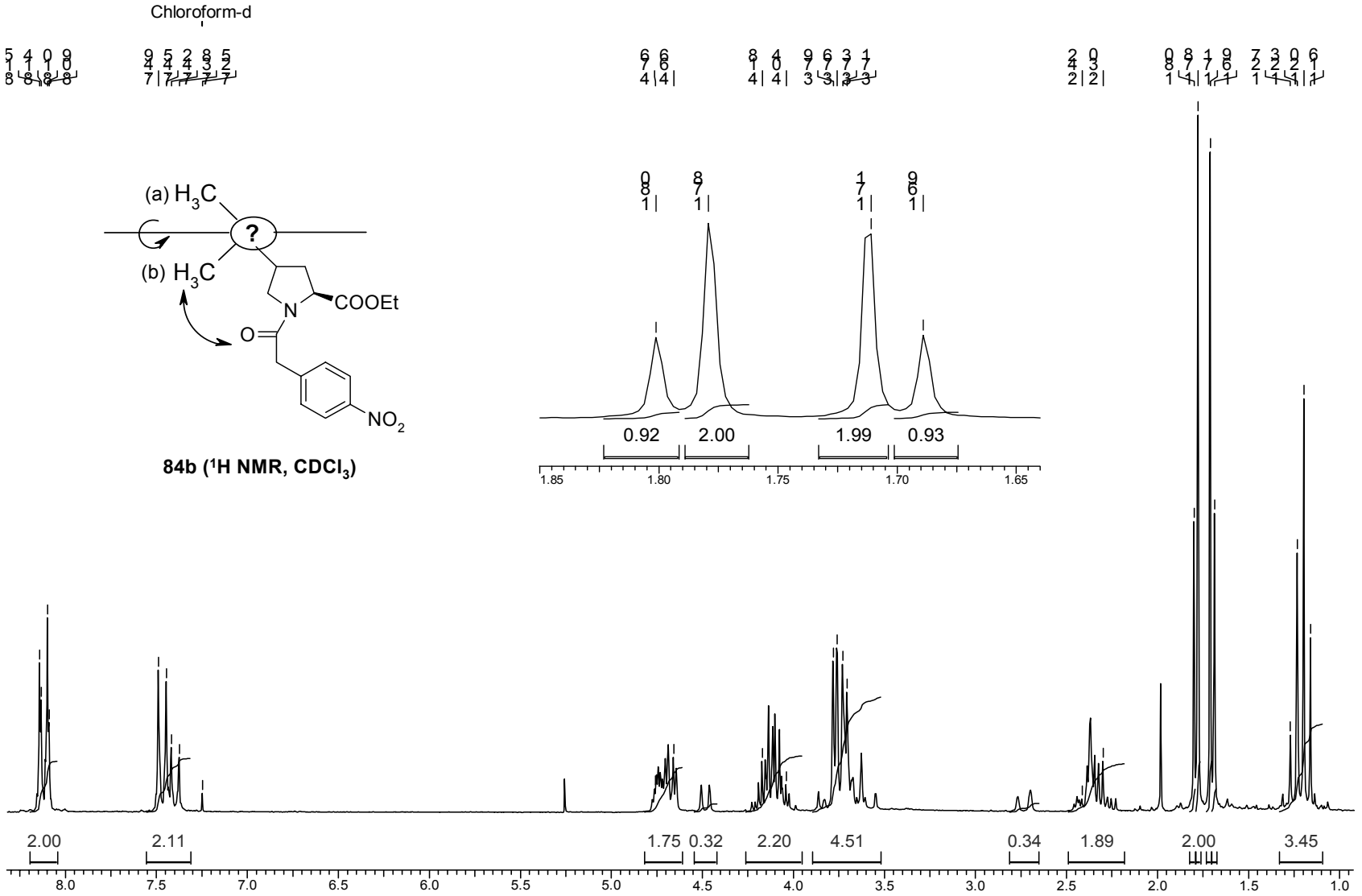

Figure 16. ^{1}H NMR spectrum of compound **84b** in $CDCl_3$.

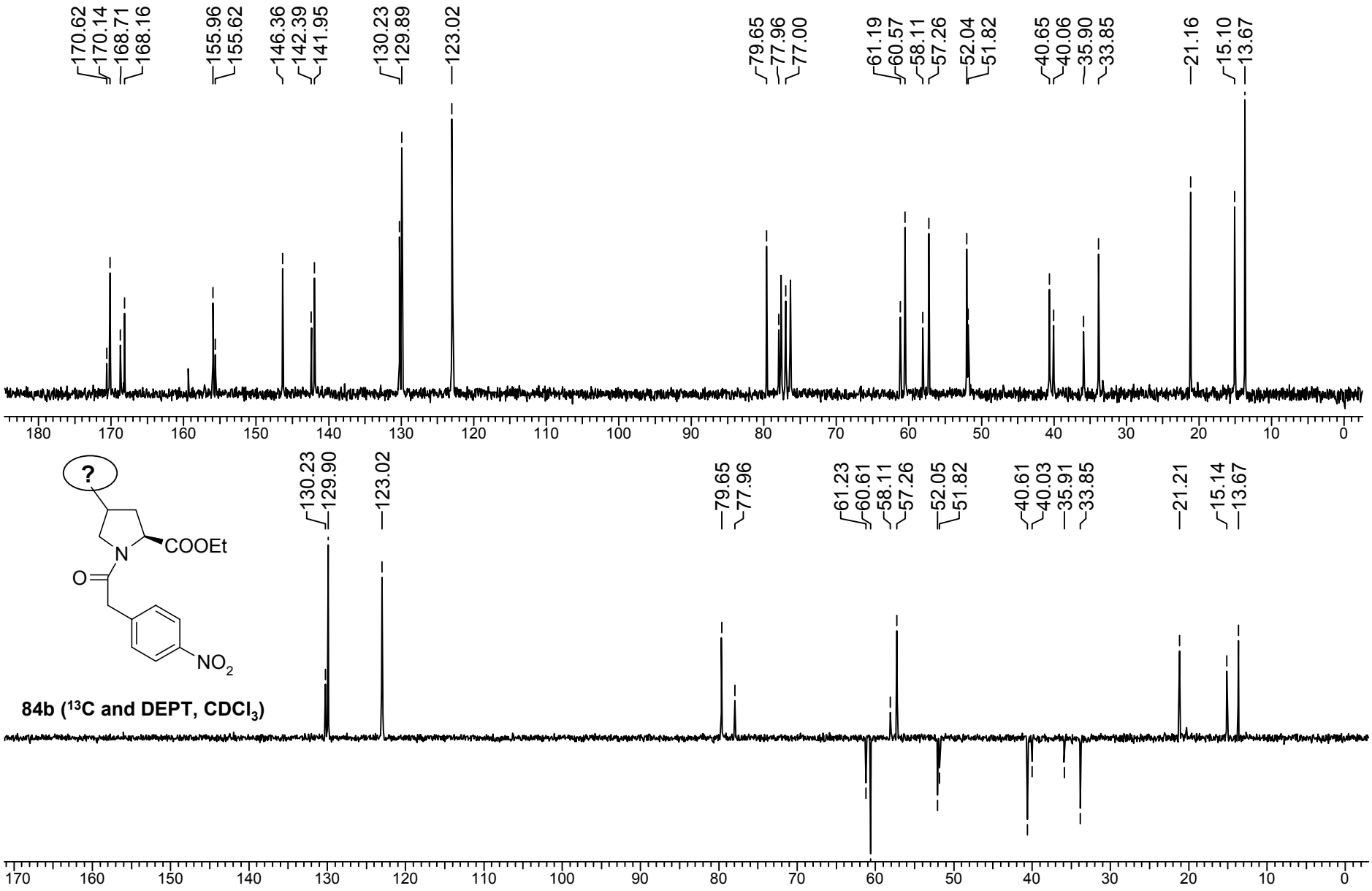

Figure 17. ^{13}C and DEPT spectra of compound **84b**.

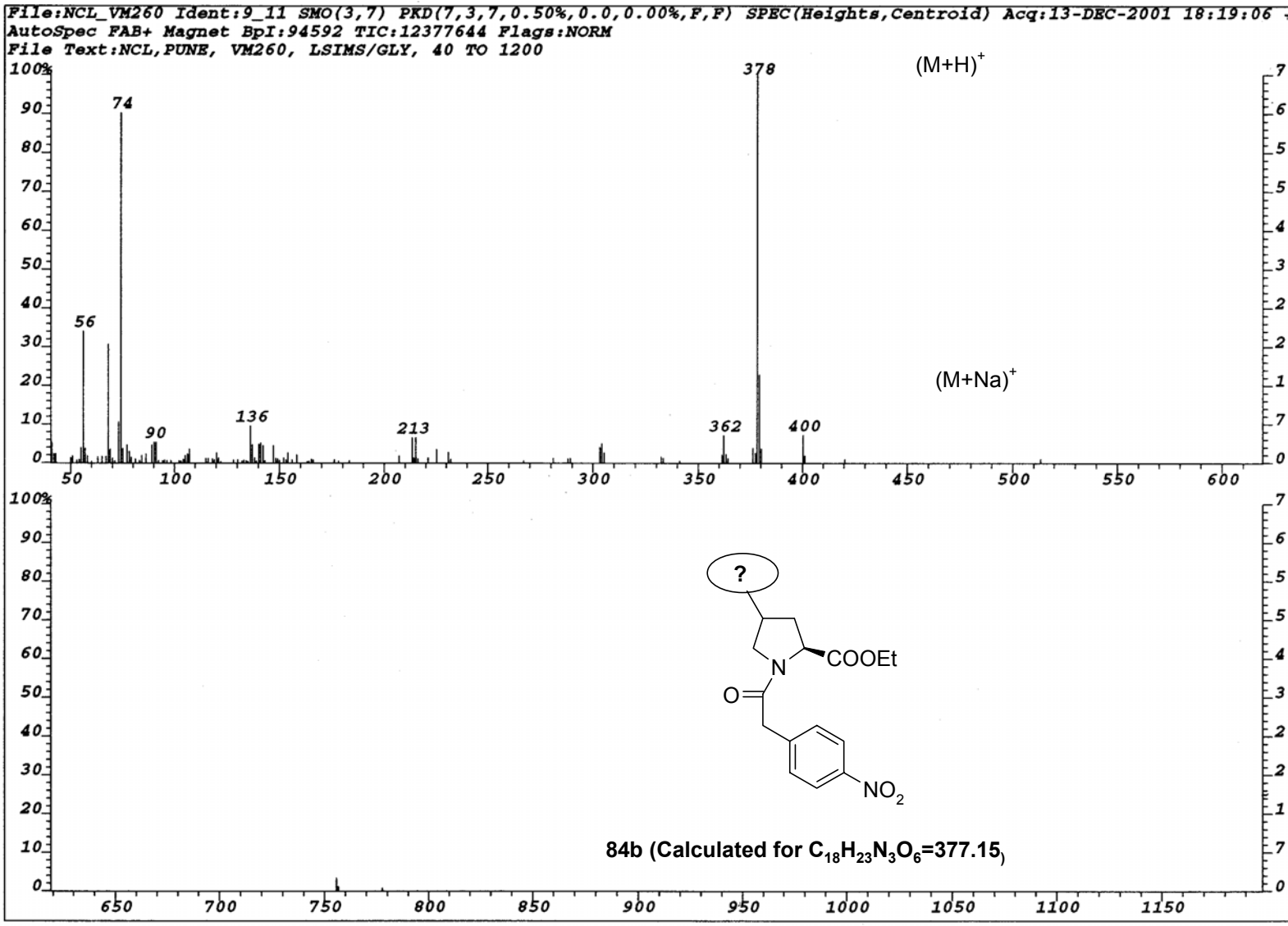

Figure 18. FAB-MS spectrum of compound **84b**.

Hence, an N1-*m*-dinitrobenzoyl derivative **84c** was prepared which yielded diffraction quality crystals. X-ray crystal data of **84c** revealed a structure (Figure 19) where the methyl groups are attached to proline through an oxyimine carbon. ^{1}H NMR and FAB-MS [409 $(M+H)^+$ and 431 $(M+Na)^+$ when calcd. for $C_{18}H_{23}N_{42}O_6$=377.158] of **84c** (Figure 20 and 21) fully agreed with the crystal structure.

The aminoxy group, -ONH_2, is more nucleophilic than the primary amino group, with its enhanced nucleophilicity attributed to the so-called α-effect (Isaacs, 1995). It is well known that the *O*-alkyloximes, formed upon the reaction of O-alkylhydroxylamines with carbonyl compounds are much more stable than the corresponding imines derived from their primary amines counterparts (Jencks, 1964). In the present case, carbonyl source in the reaction mixture is either ethyl ester or the *t*-Boc group. To investigate the role of ethyl ester, the ester hydrolysis in compound **83** was carried out before phthalimide deprotection and Fmoc protection (scheme 4.3). The change in sequence of steps gave the compound **86** with the similar side product having two extra methyl

Scheme 4.3

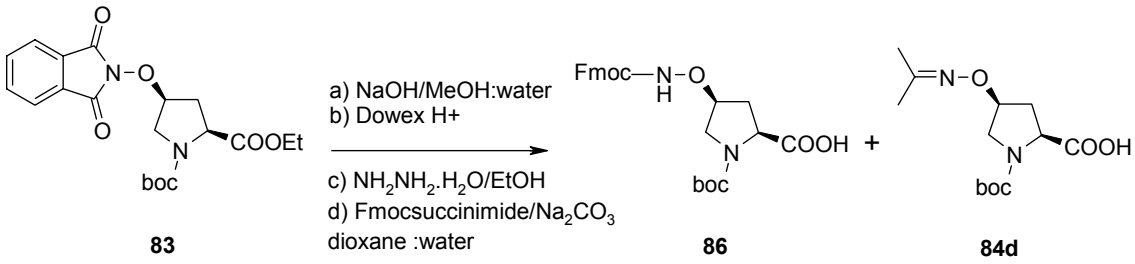

groups, but now with free carboxylic acid (Figure 22). This test ruled out the possibility of ester involvement in the side reaction. But the fact, that there is no other observable byproduct isolated in the mixture excludes the possibility of intermolecular reaction. On these grounds at present, no satisfactory mechanism for the formation of this product could be formulated.

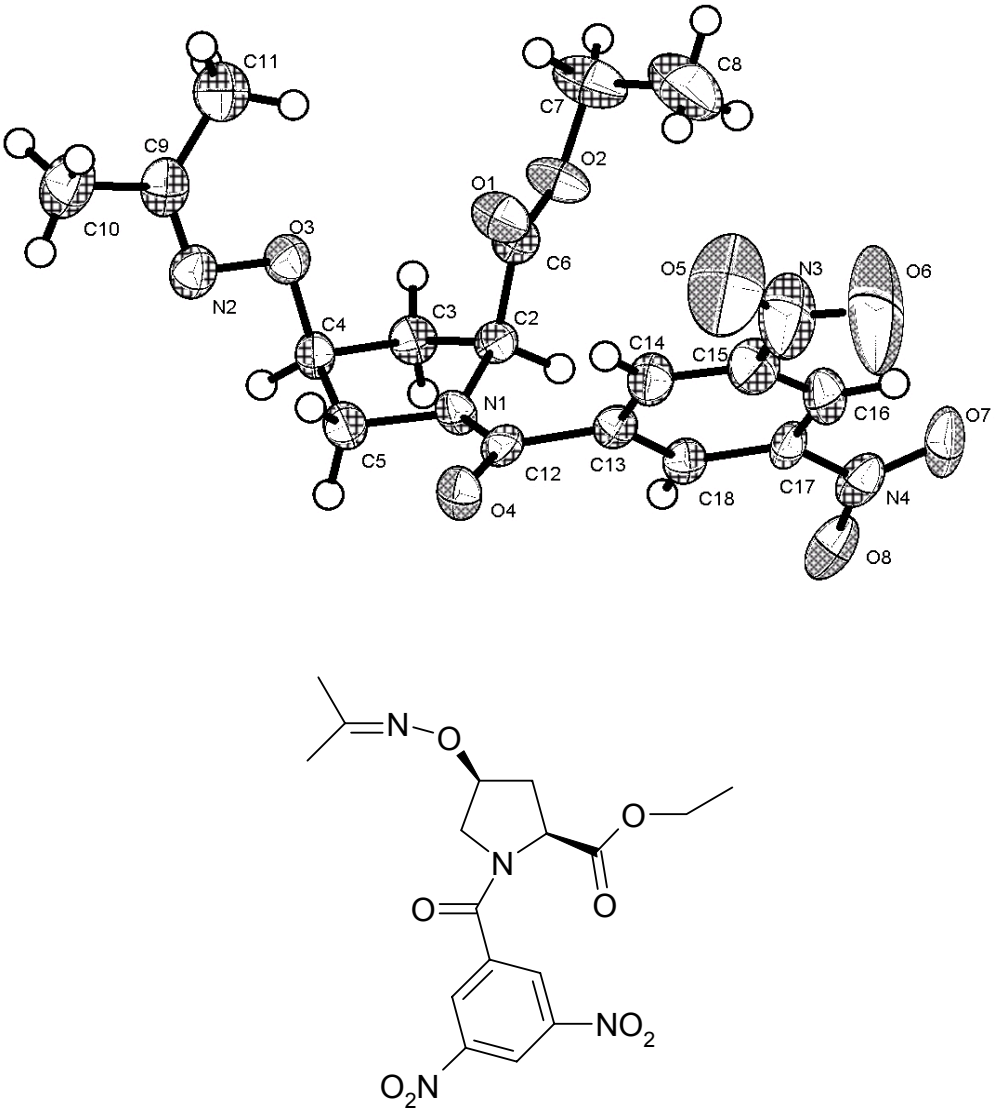

Figure 19. Crystal structure and chemical structure of compound **84c**.

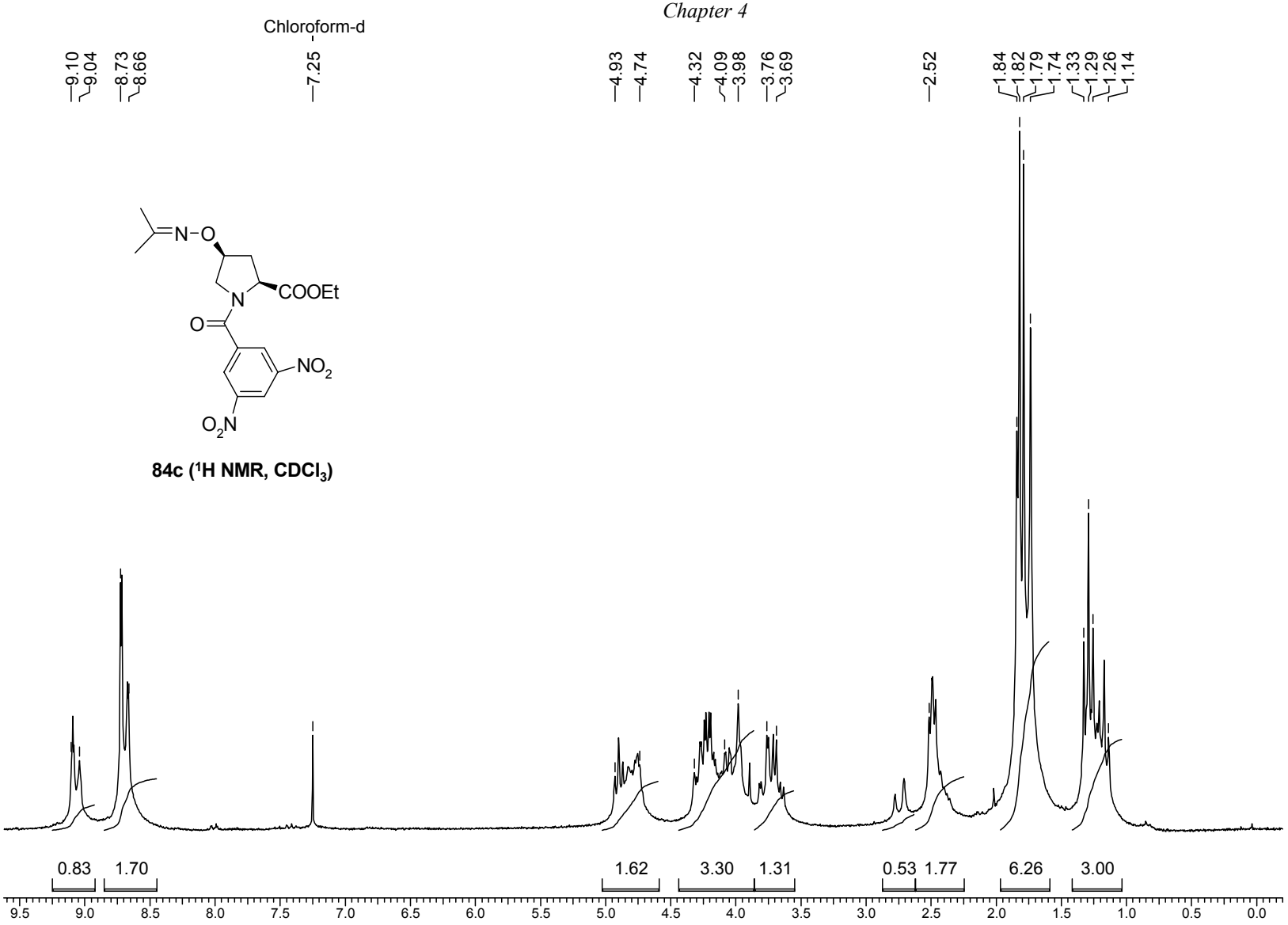

Figure 20. ^{1}H NMR spectrum of compound **84c**.

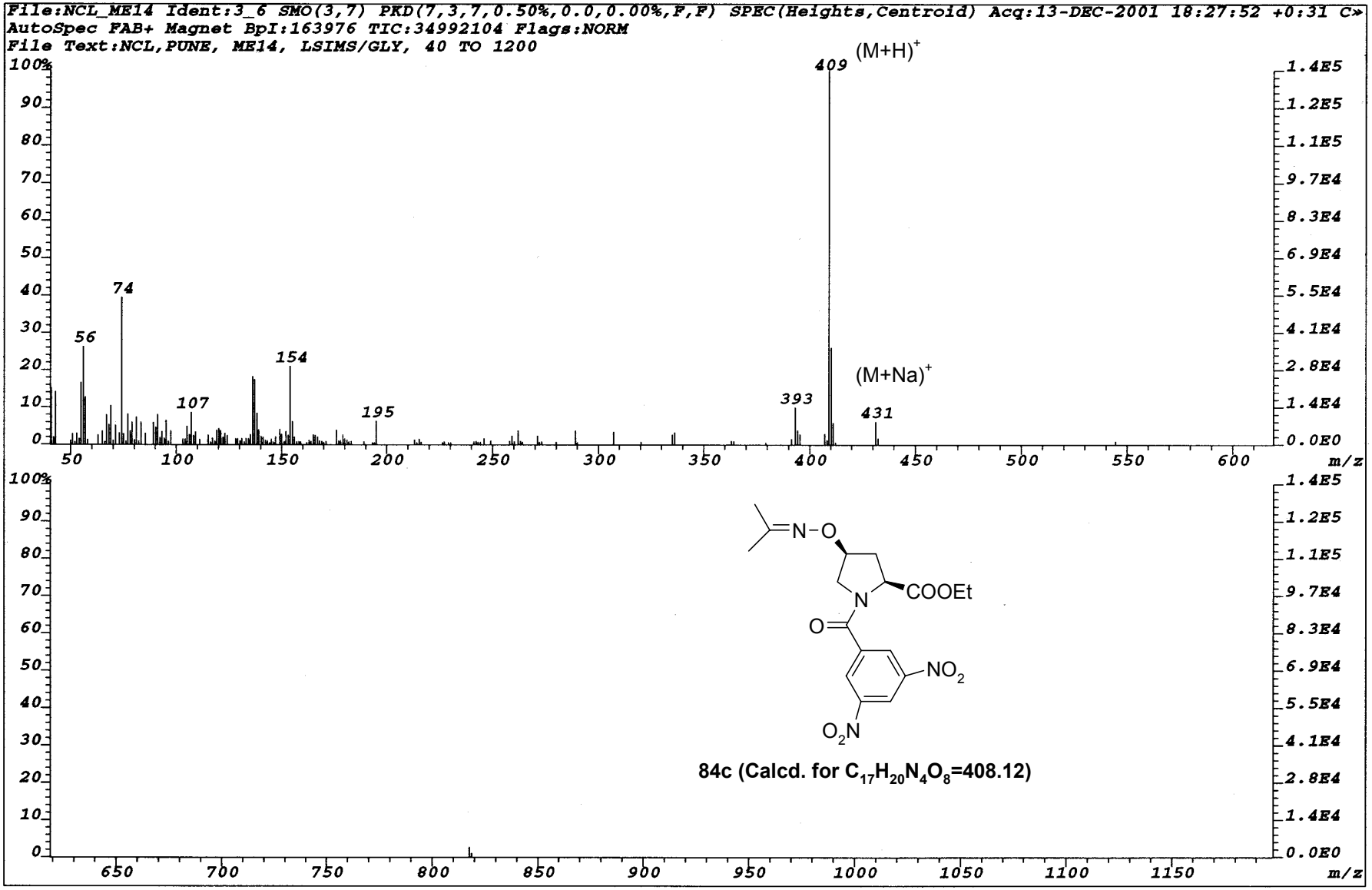

Figure 21. FAB-MS spectrum of compound **84c**.

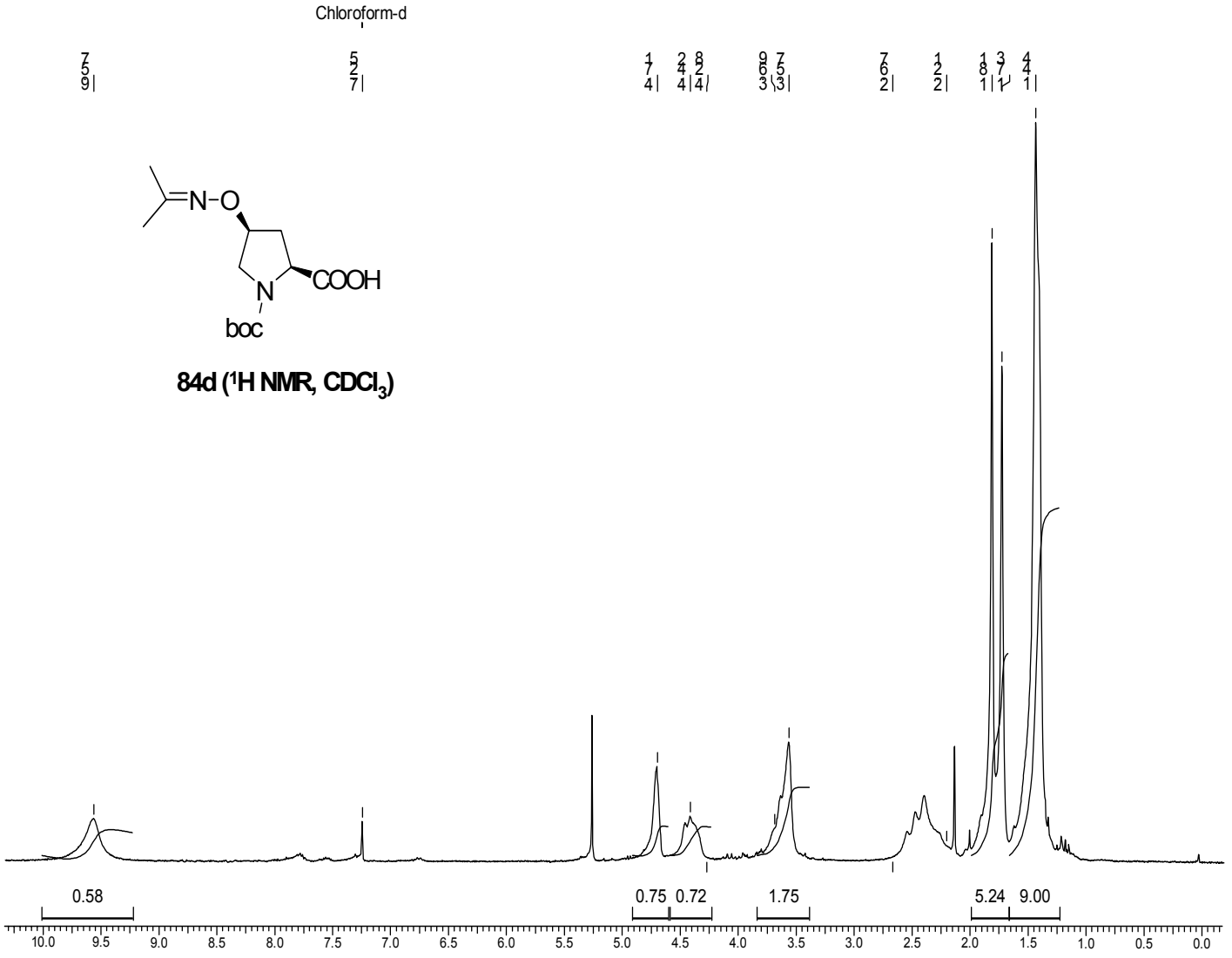

Figure 22. ^{1}H NMR spectrum of compound **84d**.

4.9 4-Oxyamino-prolyl-2-carboxamide as a β-turn mimetic

Introduction

At the molecular level almost, all important physiological and pathophysiological processes in human organism are modulated by peptide-protein and protein-protein interactions. Consequently for pharmaceutical research these recognition phenomena represent attractive target systems for therapeutic intervention in a broad spectrum of disease states (Beddell, 1992). Studies have suggested that many peptide hormones when bound to their protein receptors adopt turn conformations (Smith & Pease, 1980; Richardson, 1977). Also, turns have been identified as sites for posttranslational modification of proteins; this is particularly true with respect to phosphorylation and glycosylation. Additionally, formation of β- or γ-turns may initiate formation of β-sheets in protein folding (Rose *et al.*, 1985). Because of their biochemical importance a number of peptide and non-peptides that confer a β- or γ-turn conformations, called β-turn mimetics, have been described (Ramesh & Balaram, 1999; Fink *et al.*, 1998; MacDonald *et al.*, 2000; Das *et al.*, 1999). From the view point of structural chemistry, β-turns have been attributed a special importance as carriers of molecular recognition since, within the context of pharmacophore arrangement they allow a sterically controlled presentation of two or four interaction mediated amino acid side chains.

A turn is defined as a site where the polypeptide chain reverses its overall direction. The terms γ- and β-turn have more restricted definitions and describe turns of three or four consecutive residues, respectively (Perczal & Fasman, 1992). These turns may or may not be stabilized by an intramolecular hydrogen bond (Muller *et al.*, 2000). In γ- turns, the C=O of the first residue (i) may be hydrogen bonded to the NH of the

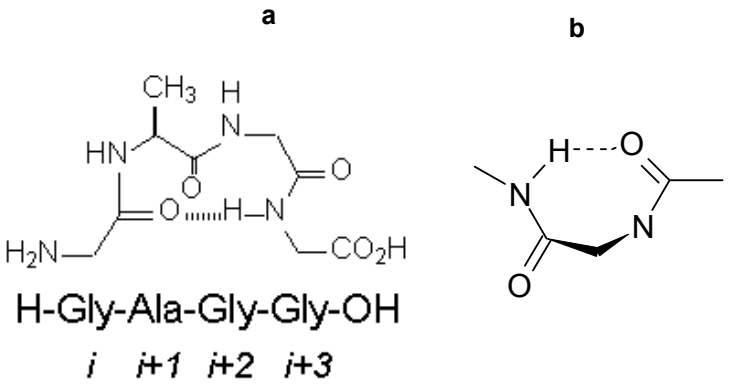

Figure 23. Structures of β-turn (a) and γ-turn (b)

third residue (i+2), giving rise to a seven membered ring. In β- turns, the C=O of the first residue (i) may be hydrogen bonded to the NH of the fourth residue (i+3), forming a ten membered ring (Madalengoitia, 2000; kolde *et al.*, 2000) (Figure 23). Further classification into specific γ-turn or β- turn classes is based upon the geometry of the peptide backbone, as described by ϕ and ψ backbone torsion angles in residues i+1 and i+2 (β- turn) or in i+1 (γ- turn).

Present work:

From an examination of the structure of (2*S*,4*S*)-4-amidoxy-proline-2-amide, it appeared that this moiety, depending upon the location of intramolecular hydrogen bond, may adopt either a β- or γ-turn like conformation (Figure 24). To determine

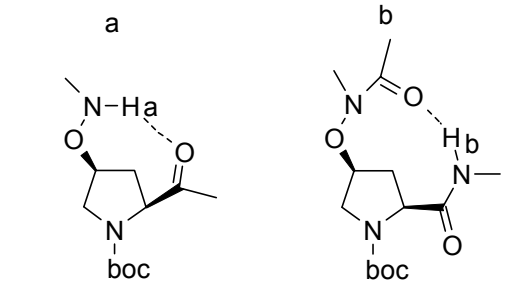

Figure 24. Two possibilities of intramolecular hydrogen bonding

whether (2*S*,4S)-4-amidoxy-proline-2-ester/amide directs the formation of γ/β-turn, compound **84** was used as the starting material to functionalize the C-4 oxyamine and C-2 carbonyl group (Scheme 4.4). Compound **84** on treatment with Ac_2O in pyridine gave a mixture of diacetylated **87** and monoacetylated **88** compounds. The 4*S*-oxyamine diacetylate was characterized by ^{1}H NMR showing a singlet for six protons in the region δ 2.8-2.5 (two $-CH_3$ groups). Even the use of equivalent amounts of Ac_2O provided the mixture of compound **87** and **88** and the starting material. Hence, the excess amount of Ac_2O was used to ensure the complete conversion to compound **87** which upon saponification followed by neutralization with cation exchange resin (Dowex H+) gave the 4*S*-monooxyacylated free acid **89** in **96%** overall yield. Complete ester hydrolysis was ensured from the ^{1}H NMR of free carboxylic acid **89** where characteristic peaks of ethyl ester were absent. To prepare a crystalline derivative, the compound **89** was coupled with *p*-anisidine in the presence of DCC and HOBt to obtain compound **90** in 45% yield. The compound **90** was characterized by ^{1}H NMR displaying

three sets of doublets in the aromatic region (2 x d 2H δ 7.6-7.4 and 1 x d 2H 6.9) and one singlet at δ 3.8 for three protons characteristic of *p*-anisidine and GC-MS showing m/z=393 (Calcd. for $C_{19}H_{27}N_3O_6$=393.18).

Scheme 4.4

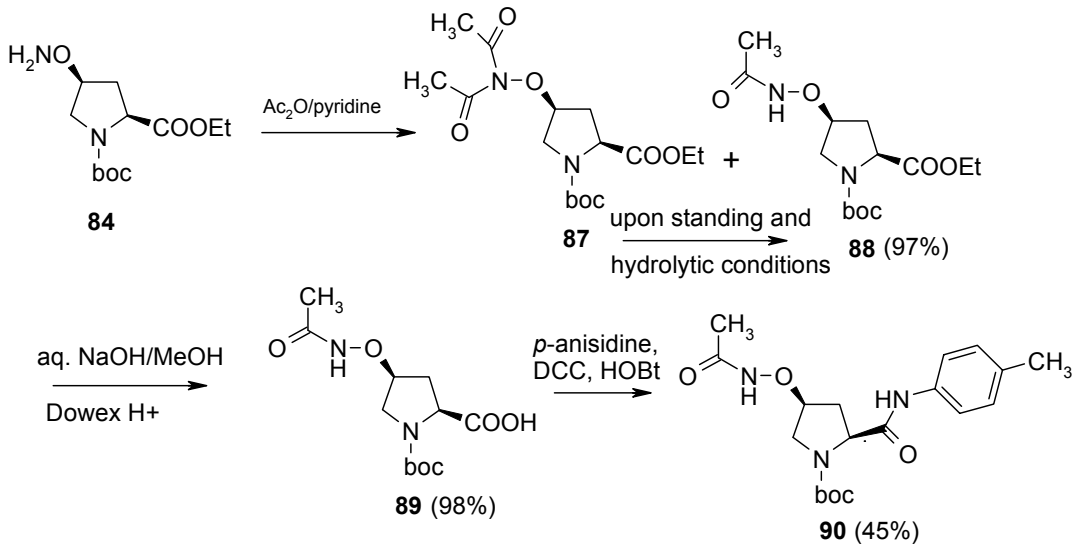

The compound **88**, which has only one amide hydrogen, shows a set of two peaks at δ 9.2 and 9.04 as a result of the *cis-trans* isomerization of peptidyl-prolyl bond. The two amide hydrogens (Ha and Hb) in compound **90**, appear as a set of two peaks for each proton in ^{1}H NMR in $CDCl_3$ (conc. 38μMoles in 0.6ml $CDCl_3$). Four peaks ascribed to N<u>H</u> are δ 9.9, 9.5 and 9.4 and 9.0, perhaps correspond to four species present in the solution (*cis* and *trans* conformer form each NH). These hydrogens can participate in either intermolecular or intramolecular hydrogen bonding (8-membered ring or 10- membered ring as shown in Figure 24).

For the assignment of amide hydrogens, 2D-NOESY (Nuclear Overhauser Effect Spectroscopy) was carried out for compound **90** at two concentrations; 38μMoles in 0.6ml $CDCl_3$ and 51μMoles in 0.6ml $CDCl_3$). In the NOESY spectrum of **90** at conc. 38μMoles in 0.6ml $CDCl_3$, cross peaks for amide hydrogens at δ 9.8 and 9.6 were seen with the *ortho* hydrogen of *p*-anisidine as a set of two peaks at δ 7.6 and 7.5, which indicates that this set should correspond to Hb as shown the NOE between Hb and *ortho*-Hydrogen of *p*-anisidine (Figure 27, 28). Consequently, the N-H peaks at upfield δ 9.4 and 9.0 correspond to the Ha protons and did not show any cross peak with anisidine protons. The presence of a set of two peaks for each N<u>H</u>, could also be arising form the hydrogen bonded and nonhydrogen bonded species for each N<u>H</u>. The

^{1}H NMR recorded at higher conc. i.e. 51μmol in 0.6ml $CDCl_3$ showed a downfield shift in the minor peak of the set corresponding to Ha, leading to collapse of the signals whereas the there is no change in the chemical shift of the major peak. Since the

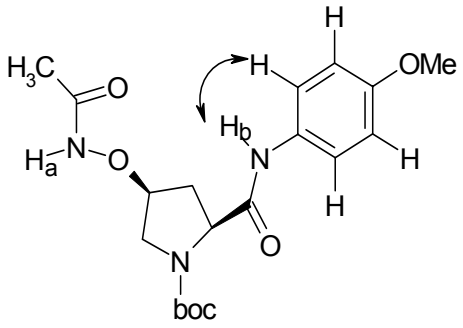

Figure 27. Chemical structure of compound **90** showing possible NOE between amide proton Hb and *ortho*-H of anisidine.

intramolecular hydrogen bonding is not affected by compound concentration, this also suggests that Hb and Ha are involved in intramolecular and intermolecular hydrogen bonding respectively.

The NOE of **90** at higher concentration (51μMoles in 0.6ml $CDCl_3$) too, shows the cross peak for a set of two peaks at δ 9.8, 9.6 and the *ortho* hydrogen of *p*-anisidine. The 2D-NOESY of compound **90** at higher concentration is shown in Figure 29.

The data clearly confirms the structural assignments of Ha and Hb, with downfield Hb signal corresponding to the C-2 carboxamide NH while the highfield Ha signal corresponds to C4-oxyamide NH.

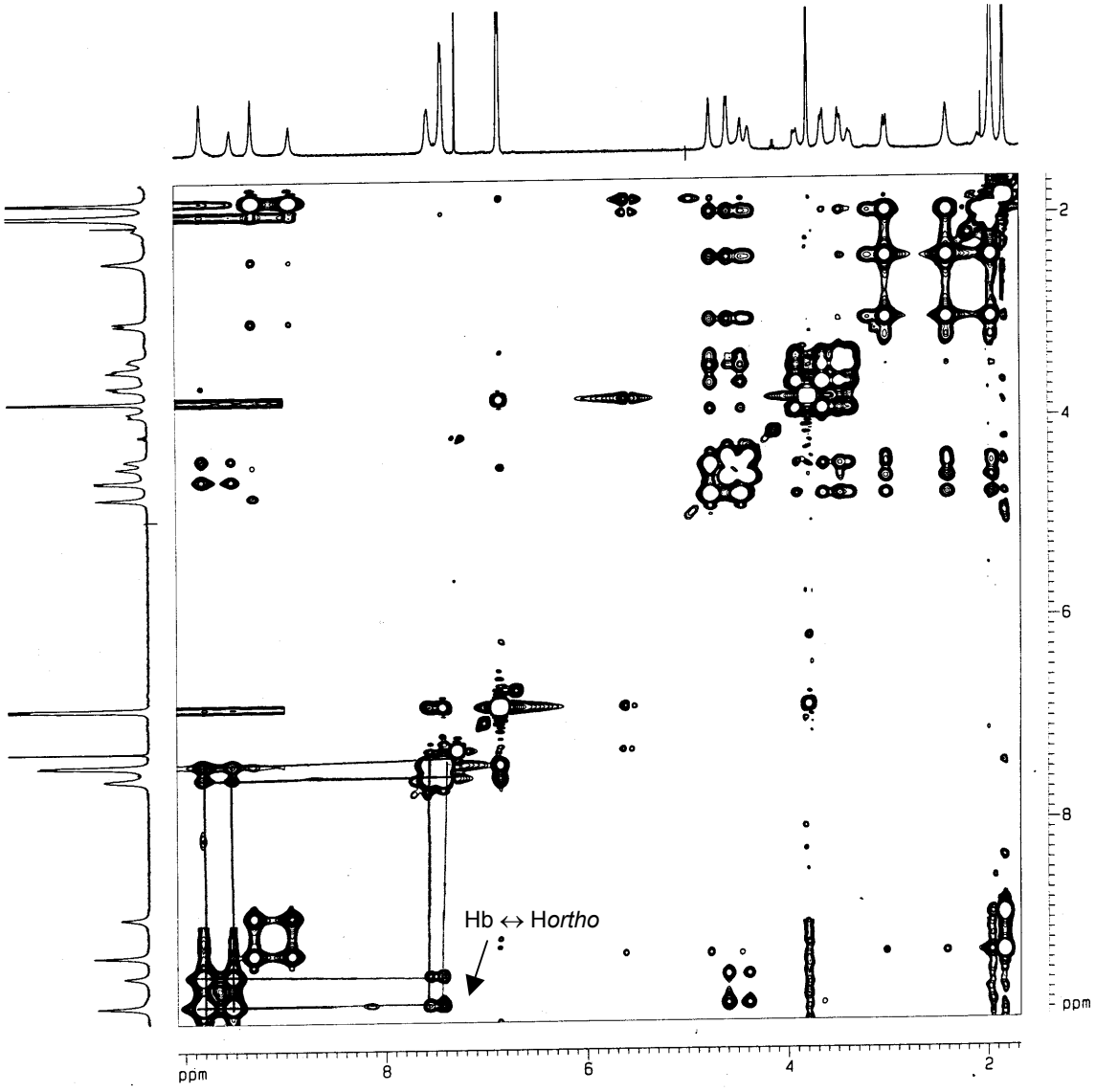

Figure 28. NOESY of compound **90** (conc. 38μMoles in 0.6 ml $CDCl_3$)

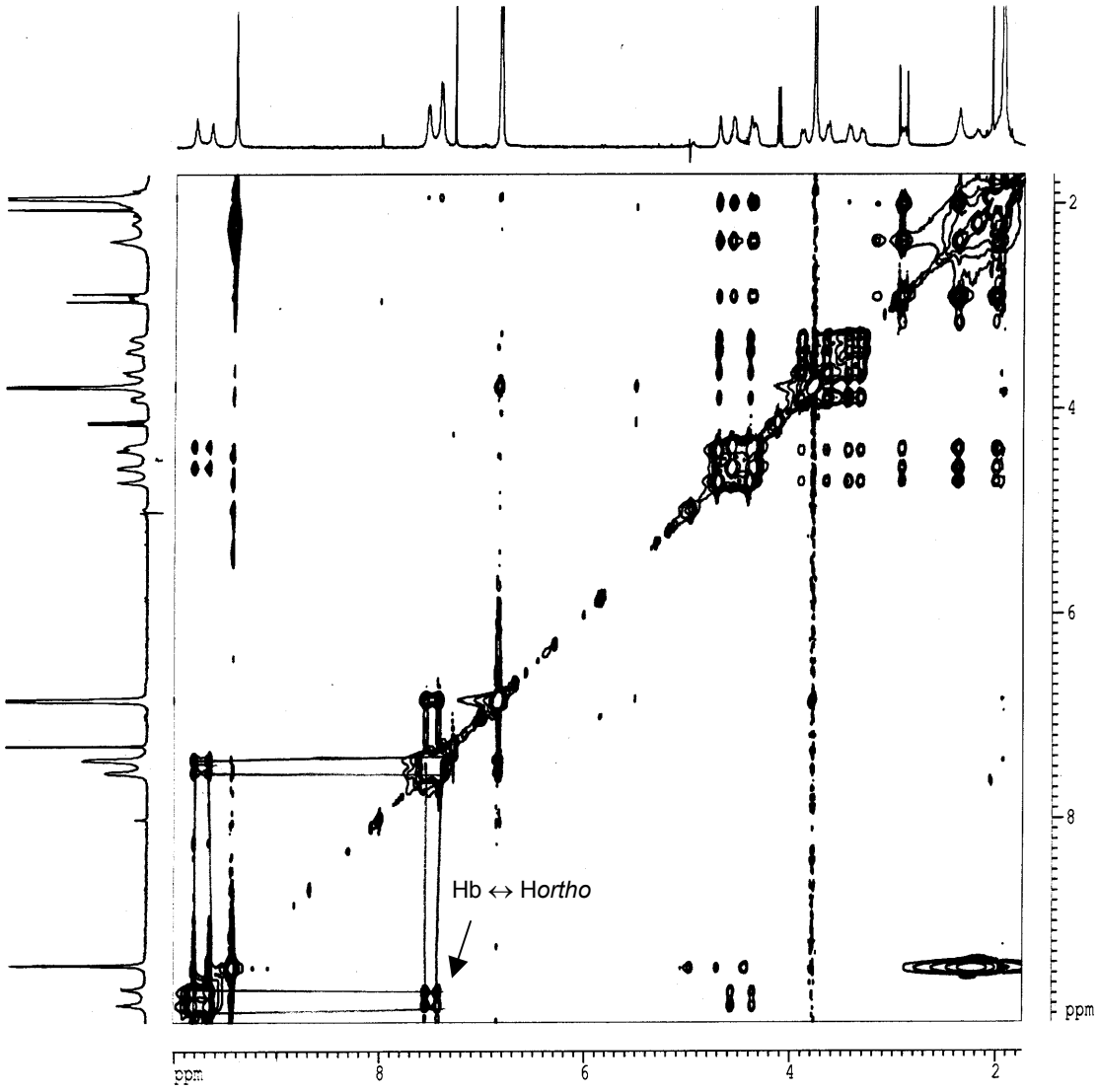

Figure 29. NOESY of compound 90 (conc. 51μMoles in 0.6 ml $CDCl_3$)

DMSO-d_6 NMR titration

After the assignment of amide hydrogens, to find out their involvement in intramolecular hydrogen bonding, addition NMR titration with DMSO-d_6 was carried out. To the $CDCl_3$ solution of compound **90** (15mg, 38 μmol in 0.6ml $CDCl_3$). DMSO-d_6 was

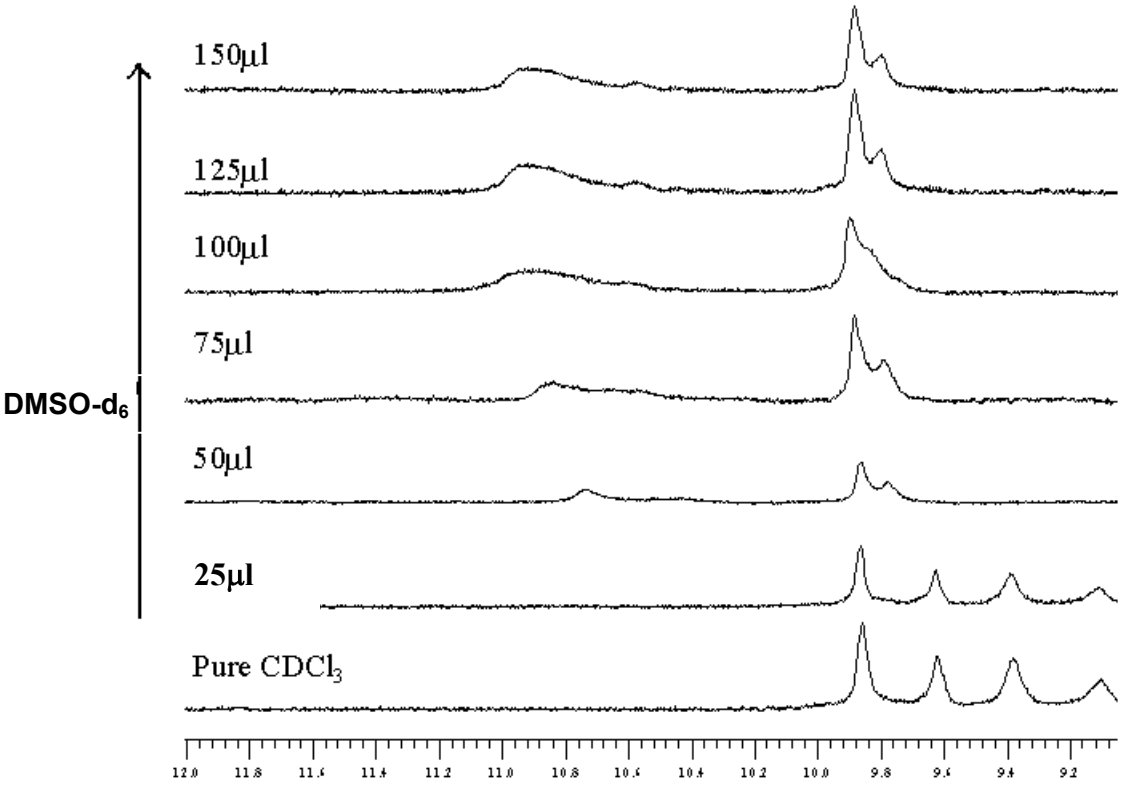

Figure 30. Shift in amide proton Ha in compound **90** (15mg, 38μM in 0.6ml $CDCl_3$ with increasing amount of DMSO-d_6

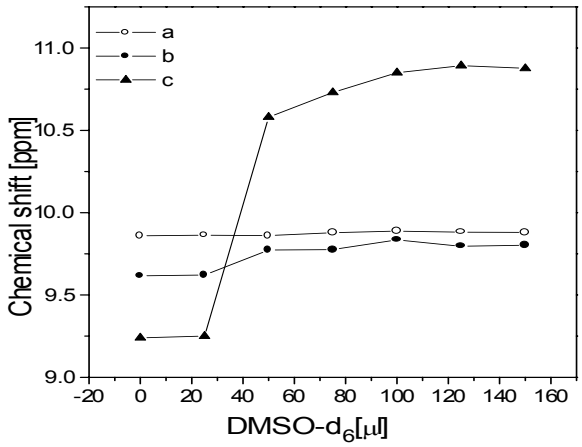

Figure 31. ^1H NMR chemical shifts of amide protons of **90** in $CDCl_3$ at 15^0C. (a) and (b) set of two peaks for Hb. (c) Ha when increasing amount od DMSO-d_6 were added.

added in increments of 25μl. Figure 30 shows the ^{1}H spectra of compound **90** after each addition of DMSO-d_6. ^{1}H NMR studies showed that Ha at the N-terminus had a dramatic downfied shift (δ 9.38-10.7), whereas Hb at the C-terminus showed little change upon addition of DMSO-d_6. This suggests that Ha is solvent accessible whereas Hb is intramolecularly hydrogen-bonded. Upon further addition of DMSO-d_6 there was a marginal change in the chemical shift in one of the isomer (minor) of Hb, whereas the major isomer peak position remained stationary. This shows that the Hb amide proton is involved in intramolecular hydrogen bonding. Further, the slight shift in one of the peaks for Hb corresponding to minor isomer with DMSO-d_6 addition indicates that the major isomer (*trans* in conformation) is involved in intramolecular hydrogen bonding. The ^{1}H NMR of compound **90** in pure DMSO-d_6 (conc. 38μmoles in 0.6 DMSO-d_6) shows peaks at δ 11.2 (Ha) and 9.86 (Hb) indicating that the intramolecular hydrogen bonding is significantly strong and is not affected even in pure DMSO-d_6.

Crystal Structure of compound 90

Crystal structure data (Figure 32) shows that the oxyamide and carboxamide are oriented in such a way that the oxyamide CO and the carboxamide NH are oriented towards each other with O-H bond distance of 2.3Å, which is in the range of hydrogen bond distances, thus making a ten membered ring.

4.10. Conclusion

NMR data and the crystal structure of a tripeptide analogue containing (2*S*,4*S*) N1-*t*-Boc-4-oxyamino-proline is shown to induce an N-O turn which makes ten membered ring similar to β-turns. Further studies to explore the conformational behavior of **90** in long peptides in order to gain a β-sheet structure are required. Also the role of N1 substituent (*tert*-amide, alkyl or free amine) in changing the ring conformation which may further affect the turn has to be studied.

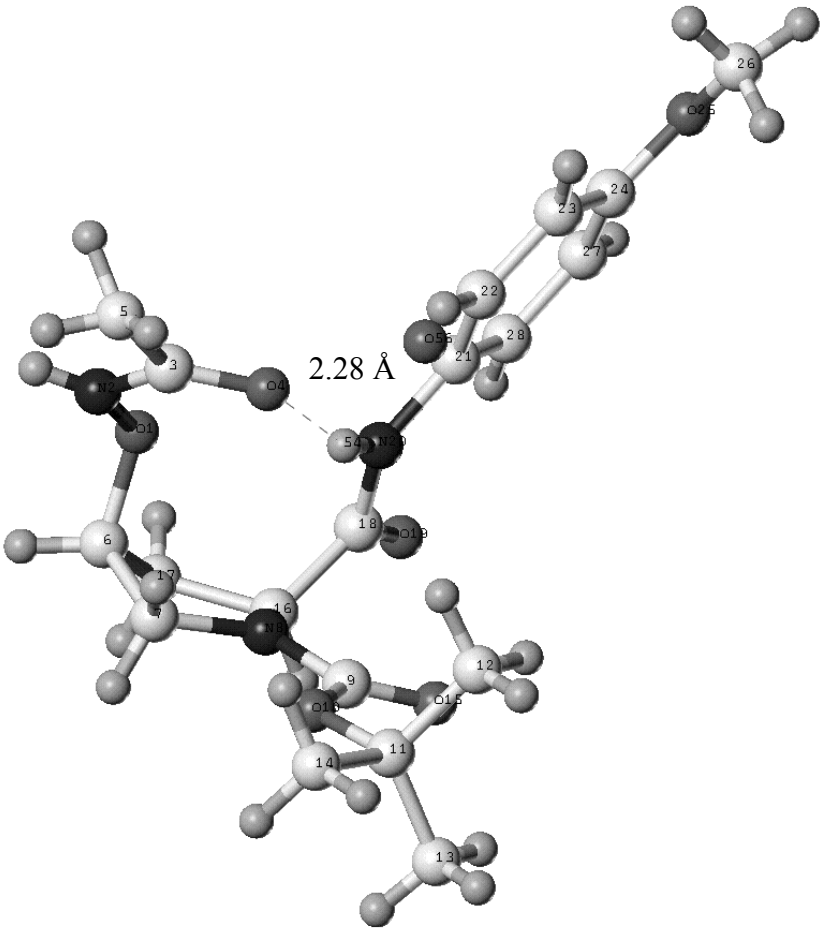

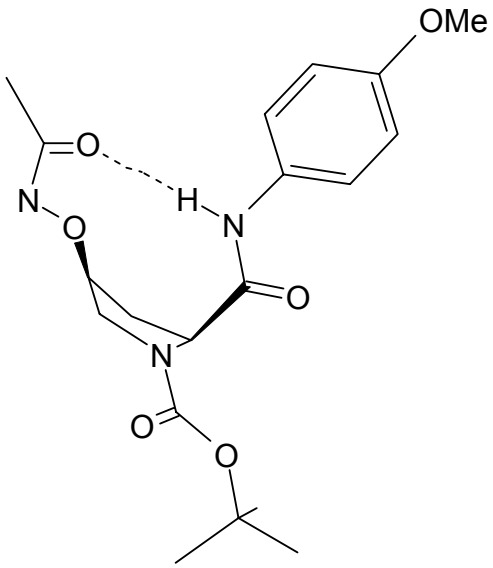

Figure 32. X-ray crystal structure and the chemical structure of compound **90**.

4.9. Experimental procedures

(*2S,4S)1-Benzyloxycarbonyl-4-(tert-butoxycarbonyl-aminooxy)-proline methyl ester* **77**

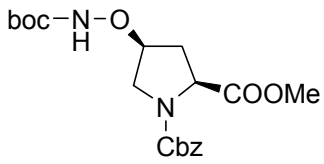

77

To a solution of mesyl derivative Compound **59** (page 129) (2g, 5.6mmol) in dry DMF (20ml), K_2CO_3 (1.45g, 11.2mmol) and N-*t*-Boc hydroxylamine (1.5g, 11.2mmol) were added and stirred at 60°C. After 16h, the reaction mixture was cooled to room temperature and poured into a beaker containing 1N HCl (100ml). The product was extracted in diethylether from DMF/water mixture and ether layer was dried over anhy. Na_2SO_4. The ether layer was concentrated and after silica gel column chromatography, compound **77** was obtained in very poor yield (0.55, yield=25%, Rf=0.5 EtOAc:Petroleum ether 1:1)

^{1}H NMR ($CDCl_3$) δ 7.45,7.3 (2s 5H $C_6\underline{H}_5$ major, minor), 7.2 (bs 1H CON<u>H</u>O exchangeable), 5.25-5 (m 2H O$C\underline{H}_2C_6H_5$), 4.75-4.5 (m 1H C4<u>H</u>), 4.5-4.3 (m 1H C2<u>H</u>), 3.8,3.75 (2s 3H O$C\underline{H}_3$ major, minor), 3.7-3.5 (m 2H C5<u>H</u>), 2.6-2.2 (m 2H C3<u>H</u>), 1.5 (s 9H C($C\underline{H}_3$)$_3$)

(2S,4R) 4-hydroxy-1-(thymin-1-acetyl)proline methyl ester **79**

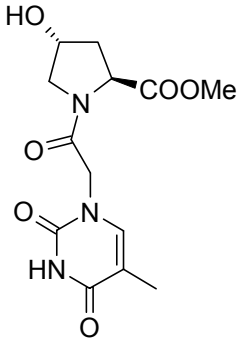

79

To a solution of trans-L-hydroxyproline methyl ester hydrochloride (6g, 33mmol) in DMF (50ml), thyminyl-1-acetic acid (6.67g, 36.3mmol) (Compound **65** in chapter 3), DCC (7.4g, 36.3mmol), HOBt (2.2g, 16.5mmol), DMAP (2g, 16.5mmol) and *DEPEA* (5.66ml, 33mmol) were added sequentially. The mixture was stirred for 3h, solvent evaporated and the residue was purified by silica gel column chromatography to obtain the pure thyminyl derivative **79** (8g, yield=78%, Rf=0.3 MeOH:EtOAc 2:8).

^{1}H NMR (D_2O) δ 7.37 (s 1H <u>H</u>6-Thy), 4.68-4.56 (m 4H C4<u>H</u>, C2<u>H</u>, N$C\underline{H}_2$), 3.82-3.64 (m 5H O$C\underline{H}_3$, C5<u>H</u>), 2.6-2.3 (m 1H C3<u>H</u>), 2.25-2.0 (m 1H C3'<u>H</u>), 1.84 (s 3H $C\underline{H}_3$-Thy)

^{13}C NMR (D_2O) δ 176.6 (<u>C</u>OOCH_3), 170.1 (<u>C</u>4-Thy), 169.2 (N$^{\alpha}$<u>C</u>O), 154.5 (<u>C</u>2-Thy), 145.6 (<u>C</u>5-Thy), 113.29 (<u>C</u>6-Thy), 72.4 (OO$C\underline{H}_3$), 60.9 (<u>C</u>4), 56.7 ($C\underline{H}_2$-Thy), 52.1, 51.5 (<u>C</u>5), 39.1 (<u>C</u>3), 13.9 (Thy-<u>C</u>H3)

(2S,4S)4-O-phthalimide-1-(thymine-1-acetyl)proline methyl ester **80**

Compound **79** (2g, 6.43mmol) was dissolved in dry THF (20ml) and N-hydroxyphthalimide (1.5g, 9.64mmol) and PPh_3P (2.5g, 9.64mmol) were added sequentially. The mixture was cooled in an ice bath and DEAD (1.5ml, 9.64mmol) was added drop-wise. The mixture was stirred for 8h and concentrated under *vacuo*. The residue was partitioned between water and ethylacetate and the later was washed with 5% aq. Na_2CO_3, water and brine. The organic layer was dried over Na_2SO_4 and removal of solvent gave crude product which was purified by column chromatography to achieve product **80** (2.5g, yield=86%, Rf=0.2 EtOAc).

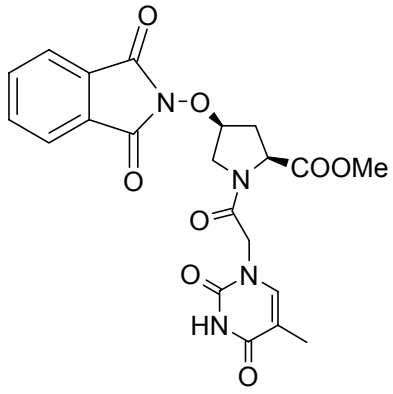

80

^{1}H NMR (DMSO-d6) δ 11.33 (s 1H NH-Thy), 7.87- 7.85 (m 4H Ar), 7.6-7.33 (d 1H H6-THy), 5.1-5.0 (m 1H C4H), 4.7-4.57 (m 2H C5H), 3.8-3.6 (m 5H C2H, $COOCH_3$), 2.7-2.25 (m 2H C3H), 1.75 (s 3H CH_3-Thy).

FAB-MS $(M+H)^+$=457, $(M+Na)^+$=479 (Calcd. $C_{21}H_{20}N_4O_8$=456.12)

trans-4-Hydroxy-L-proline ethyl ester hydrochloride **81**

A suspension of trans-4-hydroxy-L-proline (10g, 76.3mm0l) in absolute ethanol (60ml) was stirred at 0°C. To this was added thionylchloride (6.1ml, 10g, 83.6mm0l) dropwise in 10 min. The stirring was continued at 0°C for 4h and then at ambient temperature until the reaction mixture became homogeneous (6h). Removal of ethanol under vacuum and washing the precipitate with EtOAc and then with diethylether followed by drying under vacuum over phosphorus pentoxide yielded ethyl ester hydrochloride **81** (14.5g, yield=97.4%) as a white solid. The solid was used for the following experiment without further purification.

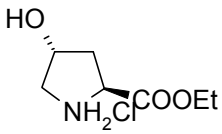

81

^{1}H NMR (D_2O) δ 4.33-4.22 (q 2H OCH_2CH_3 J=7.32Hz), 3.54-3.34 (m 2H C5H), 2.57-2.41 (m 1H C3H), 2.3-2.19 (m 1H C3'H), 1.26 (t 3H OCH_2CH_3 J=7.32Hz)

trans-4-Hydroxy-N1-(tert-Butoxycarbonyl)-L-proline ethyl ester **82**

A mixture of the ester **81** (10g, 51.1mmol), tert-butoxycarbazide (8.7ml, 61.3mmol), Et_3N (15.6ml, 0.11mol) and DMSO (75ml) was stirred under argon atmosphere at 50°C for 8h. The reaction mixture was cooled to room temperature and poured into a beaker containing ice cold water (500ml). The precipitate thus obtained was extracted with

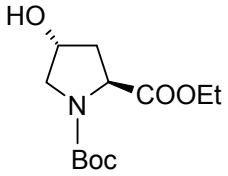

82

diethylether and the ether layer was washed with water, brine and dried over anhy. Na_2SO_4. The solvent was evaporated on rotary evaporator to obtain a pale yellow oil (10.6g, yield=80%, Rf=0.5, EtOAc:Petroleum ether 3:7).

^{1}H NMR ($CDCl_3$) δ 4.43-4.29 (m 2H C4H, C2H), 4.13 (q 2H OCH_2CH_3 J=6.83), 3.62-3.38 (m 2H C5H), 2.95-2.71 (m 3H C2H, OH), 2.33-2.17 (m 1H C3H), 2.07-1.94 (m 1H C3'H), 1.47, 1.37 (2s 9H $C(CH_3)_3$ major, minor), 1.24 (t 3H OCH_2CH_3)

(2S,4S)N1-tert-butoxycarbonyl-4- {oxyphthalimide}-proline-ethyl ester **83**

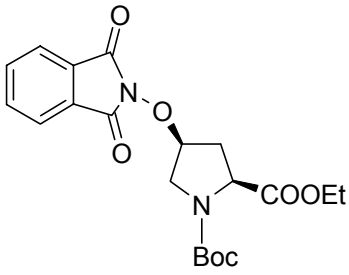

83

Compound **82** (2g, 7mmol), PPh_3 (3g, 11.5 mmol) and N-hydroxyphthalimide (1.88g, 11.5mmol) were taken in dry benzene (50 ml). The mixture was cooled to 5-10^{o}C and DEAD (1.8ml 11.5mmol) was added dropwise into it. The reaction was further stirred for 5h at ambient temperature. Benzene was evaporated and the residue was dissolved in EtOAc (25ml). EtOAc layer was washed sequentially washed with aqueous $NaHCO_3$ solution (5% w/v), water and brine. The organic layer was dried over anhy. Na_2SO_4 and concentrated under vacuum. Diethylether (10ml) was added to dissolve the crude residue, and most of the PPh_3O was precipitated with the help of petroleum ether. PPh_3O was filtered and the filtrate concentrated to obtain crude product, which was purified by silica gel column chromatography using petroleum ether/EtOAc to obtain pure a pale yellow crystalline compound (3.27g, yield=87%, Rf = 0.5 EtOAc: Petroleum ether, 4:6)

$\alpha^{27}{}_D$= -5.06

^{1}H NMR ($CDCl_3$) δ 7.9-7.7 (m 4H C_6H_4), 4.4 (m C4H), 4.5-4.1(m 3H C2H, OCH_2CH_3), 4-3.75 (m 2H C5H), 2.7-2.35 (m 2H C3H), 1.5 (m 9H $C(CH_3)_3$), 1.4-1.2 (m 3H OCH_2CH_3)

^{13}C NMR ($CDCl_3$) δ 171.3, 170.9 (COOCH3), 163.4 ($(CO)_2N$), 153.6, 153.2 (NCOO), 134.4, 128.4, 123.2 (C6H5), 86, 84.8 (C4), 79.8 ($C(CH_3)_3$), 60.9 (OCH_2CH_3), 57.6, 57.2 (C2), 51, 50.6 (C5), 35.1, 34.4 (C3), 27.9 ($C(CH_3)_3$), 13.7 (OCH_2CH_3)

IR ($CHCl_3$) cm^{-1} 3016, 2978, 2399, 2361, 1736, 1697

(2S,4S)N1-tert-butoxycarbonyl-4- aminooxy-proline-ethyl ester **84**

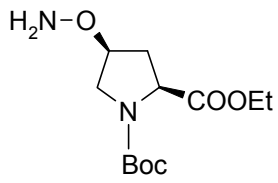

84

Compound **83** (2g, 4.9 mmol) was dissolved in DCM:EtOH mixture (20ml, 1:1) and 99% hydrazine hydrate (0.24ml, 4.9mmol) was added into it. The mixture was kept undisturbed for 8h and the precipitated phthalahydrazide was filtered and washed with DCM:ethanol (1:1) mixture. The filtrate thus obtained was evaporated to dryness *in vacuo* to obtain the oily residue which was immediately purified by flash chromatography using DCM to achieve pure **84** (0.8 g, yield=60%, Rf=0.2, EtOAc:Petroleum ether 1:1)

^{1}H NMR ($CDCl_3$) δ 5.4 (s 2H ONH_2), 4.45-4.33 (m 1H C4H), 4.3 (m 2H C2H) 4.3-4.15 (m 2H OCH_2CH_3), 3.6-3.45 (m 2H C5H), 2.4 (m 1H C3H), 2.25-2.15 (m 1H C3'H), 1.4 (d 9H $(CH_3)_3$), 1.2 (m 3H OCH_2CH_3)

^{13}C NMR ($CDCl_3$) δ 172.1, 171.8 ($COOCH_2CH_3$), 154.0, 153.7 ($NCOO$), 81.7, 80.7 (C4), 79.5 ($C(CH_3)_3$), 60.6, 60.5 (OCH_2CH_3), 57.6, 57.1 (C2), 50.8, 50.4 (C5), 34.8, 33.9 (C3), 28.1, 28.0 ($C(CH_3)_3$), 14.0 (OCH_2CH_3)

IR (neat) cm^{-1} 3323, 3256, 2978, 2935, 1753, 1697, 1593

(2S,4S)N1-tert-butoxycarbonyl-4- [flourenylmethoxycarbonyaminooxy]proline ethyl ester **85**

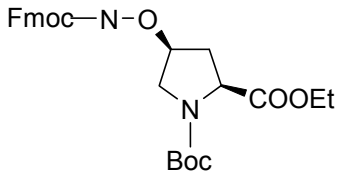

85

Oxyamine **84** (1.45g, 5.3mmol) was taken in dioxane:water mixture (20ml, 1:1) and Na_2CO_3 (0.67g, 6.4mmol) was added into it. The mixture was cooled in an ice bath and while stirring FmocCl (1.64g, 6.4mmol) was added in three portions in 30 min. The reaction was stirred further at room temperature for 4h and the pH ~9 was maintained throughout the reaction with 5% Na_2CO_3 aq. solution. The solvent was evaporated under *vacuo* and the residue was purified by silica gel column chromatography to obtain compound **85** (1.8g, yield=69%, Rf=0.5, EtOAc:Petroleum ether 1:1)

^{1}H NMR $CDCl_3$ 7.8-7.29 (m 9H Ar), 4.5-4.48 (m 4H $OC\underline{H}_2$, N<u>H</u>, C4<u>H</u>), 3.81-3.65 (C5<u>H</u>), 3.59-3.5 (C5'<u>H</u>), 4.27-4.21 (m 3H $OC\underline{H}_2CH_3$, C2<u>H</u>), 2.5-2.22 (C3<u>H</u>, C3'<u>H</u>), 1.54, 1.46 (2s major, minor 9H $C(C\underline{H}_3)_3$), 1.28 (t 3H $OCH_2C\underline{H}_3$)

^{13}C NMR ($CDCl_3$) δ 17.8 (COOEt), 159.57, 157.2 (<u>C</u>ONHO), 153.6 (N<u>C</u>O), 143.3, 141.0, 127.5, 126.8, 124.7, 119.6 (Ar), 79.8 ($\underline{C}(CH_3)_3$), 67.0 ($O\underline{C}H_2$-Fmoc), 60.89 ($O\underline{C}H_2CH_3$), 50.2, 50.0 (<u>C</u>5), 46.7 (<u>C</u>2), 34.5, 33.6 (<u>C</u>3), 28.0 ($C(\underline{C}H_3)_3$), 13.81 ($OCH_2\underline{C}H_3$)

(2S,4S)N1-tert-butoxycarbonyl-4- [flourenylmethoxycarbonyaminooxy]-proline **86**

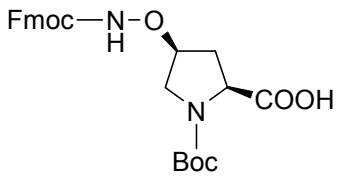

86

a) To the solution of compound **84** (1g, 3.64mmol) in methanol (5ml), 1N NaOH (1ml) was added and after stirring for 1h the solution was brought to pH~7 with 5% aq. $KHSO_4$. The methanol was evaporated under *vacuo* and to it dioxane (ml) and Na_2CO_3 (0.46g, 4.4mmol) were added. The mixture was cooled in an ice bath and while stirring FmocCl (1.13g, 4.4mmol) was added in two portions in 30 min. The pH~9 was maintained with addition of 5% aq. Na_2CO_3 and after 4h dioxane was evaporated under vacuo. The aq. layer was extracted with diethylether and ether layers were discarded. The aq. layer was brought to pH~7 and extracted with ethylacetate (5x50ml). The combined organic layers were washed with brine, dried over Na_2SO_4, filtered and evaporated to give a residue. Purification of the residue by silica gel column chromatography gave the title compound **86** (1g, yield=59%, Rf=0.2 MeOH:DCM 3:97).

b) Fmoc protected monomer compound **85** (1g, 2mmol) was dissolved in dioxane:water (5ml, 3:2) and saponified at 0^{o}C by portion wise addition of 1N NaOH and dioxane. After the reaction was complete, the mixture was buffered by adding a little solid CO_2. Fmoc-elimination, during hydrolysis was reversed by addition of Fmoc-ONSu (0.34g, 1mmol) and stirred for 45min. The pH was adjusted to 6.5 with 2M $KHSO_4$. Dioxane was removed under *vacuo*, and solution was diluted with water, acidified to pH 5 with $KHSO_4$ and extracted three times with ether. The combined organic phases were dried over sodium sulfate and concentrated under *vacuo*. The residue was purified by column chromatography to obtain (0.42g, yield=45%) compound **86**.

$\alpha^{27}{}_D$= -22, mp=79^{o}C

IR ($CHCl_3$) cm^{-1} 4214, 3325 (bd), 3098, 1733, 1716, 1701

FAB-MS 469$(M+H)^+$, 491 $(M+Na)^+$ (Calcd. for $C_{25}H_{28}N_2O_7$=468.189)

(2S,4S)1-tert-butoxycarbonyl-4-{[(1-methylethylidene)amino]oxy}proline ethyl ester **84a**

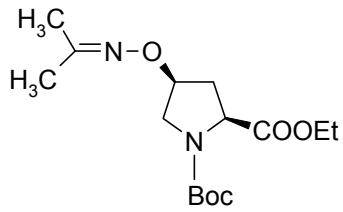

84a

^{1}H NMR CDCl$_3$ δ 4.66 (m 1H C4H), 4.44-4.2 (m 3H C2H, OCH$_2$CH$_3$), 3.61-3.55 (m 2H C5H), 2.37-2.33 (m 2H C3H), 1.79 (s 3H NCHCH$_3$), 1.71 (s 3H NCHCH$_3$), 1.42-1.38 (d 9H C(CH$_3$)$_3$), 1.28-1.15 (m 3H OCH$_2$CH$_3$)

^{13}C NMR (CDCL$_3$) 171.6, 171.3 (COOCH$_2$CH$_3$), 155.4 (NC(CH$_3$)$_2$), 154, 153.6 (NCOO), 79.9, 79.4 (C4), 79.4 (C(CH$_3$)$_3$), 60.4 (OCH$_2$CH$_3$), 57.7, 57.3 (C2), 51.5, 51.2 (C3), 28.0, 34.7 (C3), 28.0, 27.9 (C(CH$_3$)$_3$), 21.3, 15.2 (NC(CH$_3$)$_2$), 13.9, 13.8 (OCH$_2$CH$_3$)

IR (neat) cm^{-1} 3279, 2978, 2939, 1803, 1765, 1699

Anal. Found: C, 57.27; H, 8.37; N, 8.91 Calcd. for $C_{15}H_{26}N_2O_5$; C, 57.31; H, 8.34; N, 9.06.

FAB-MASS 315 $(M+H)^+$ (Calcd. for $C_{15}H_{26}N_2O_5$=314.18)

(2S,4S) N-(p-nitrophenyacetyl)-4-{[(1-methylethylidene)amino]oxy}proline ethyl ester **84b**

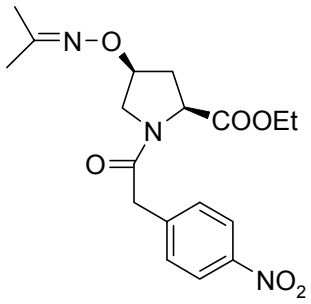

84b

Compound **84a** (0.3g, 0.95mmol) was stirred with 50%TFA/DCM (2ml) for 30 min. and dried under vacuum. Added DIPEA (2X0.5ml) and evaporated each time. Resulting free amine was taken in dry DMF (2ml) and subsequently *p*-nitrophenyl acetic acid (0.19g, 1mmol), DCC (0.21g, 1mmol) and HOBt (0.14g, 1mmol) were added into it. After stirring the mixture for 4h, DCU was filtered through Celite and was washed with DCM (5ml). The filtrate was concentrated to obtain a yellow residue which was purified by column chromatography to obtain pure compound **84b** (0.2g, 60% yield Rf=0.6 EtOAc)

^{1}H NMR CDCl$_3$ δ 8.15, 8.10 and 8.14, 8.09 (2d major, minor 2H J=8.79, Ar), 7.49, 7.42 and 7.45, 7.38 (2d major, minor 2H J=8.79, Ar), 4.76-4.65 (m 2H C4H, C2H), 4.39-4.03 (dq 2H J=7.32 OCH$_2$CH$_3$), 3.79-3.63 (m 4H, C5H, C5'H, CH$_2$Ph), 2.39-2.3 (m 2H C3H, C3'H), 1.8, 1.78 9d 3H J=4.39, C=CH$_3$), 1.71, 1.69 (d 2H J=4.39, C=CH$_3$), 1.35-1.15 (dt 3H J=7.32 OCH$_2$CH$_3$)

^{13}C NMR ($CDCl_3$) δ (170.6, 170.1 (COOEt), 168.5, 168.2 (NCO), 156, 155.6 ($C(CH_3)_2$), 146.4, 146 (qua. Ar), 142.4, 141.9 (qua. Ar), 130.2, 129.9, 123.0, 122.9 (Ar), 79.6, 79.9 (C4), 61.1, 60.6 (OCH_2CH_3), 58.1, 57.2 (C2), 52.0, 51.8 (C5), 40.65, 40.06 (CH_2Ph), 35.9, 33.8 (C3), 21.16 and 15.1 ($C(CH_3)_2$), 13.67 (OCH_2CH_3)
FAB-MAS 378$(M+H)^+$, 400 $(M+Na)^+$ (calcd. for $C_{18}H_{23}N_3O_6$=377.15)

(2S,4S) N1-(m-dinitrobenzoyl)-4-{[(1-methylethylidene)amino]oxy}proline ethyl ester **84c**

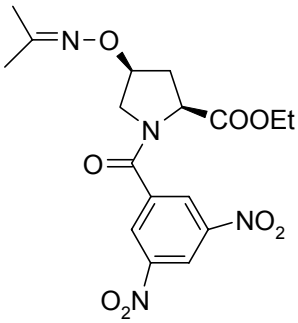

84c

The free amine obtained as above from **84a** was taken in dry pyridine and freshly crystallized *m*-dinitrobenzoylchloride (0.24g, 1mmol) was added into it. After stirring for 1h, pyridine was evaporated under reduced pressure. The residue was taken in DCM (10ml) and washed with 5% $KHSO_4$, water and then with brine. The organic layer was dried *in vacuo* affording crude solid that was purified by column to give yellow needles of pure compound **84c** (0.3g, yield=79%).

^{1}H NMR ($CDCl_3$) δ 9.10-9.0 (m 1H C_6H_3), 8.73-8.67 (m 2H C_6H_3), 4.95-4.74 (m 2H C4H, C2H), 4.32-3.96 (m 2H OCH_2CH_3), 3.82-3.63 (m 2H C5H), 2.78-2.36 (m 2H C3H), 1.93-1.74 (m 6H $C(CH_3)_2$), 1.33-1.14 (m 3H OCH_2CH_3)
^{13}C NMR ($CDCl_3$) δ 170.5, 169.8 (COOEt), 165.8, 165 (NCO), 156.62, 156.2 ($C=(CH_3)_2$), 148.3, 139.4, 127.28, 119.7, 119.5 (Ar), 79.6, 78.3 (C4), 61.9, 61.4 (OCH_2CH_3), 60.2, 58.1 (C2), 54.3, 52.4 (C5), 36.5, 34.1 (C3), 21.6 and15.54 ($C=(CH_3)_2$), 13.4 (OCH_2CH_3)
FAB-MASS 409$(M+H)^+$, 431$(M+Na)^+$ (Calcd. for $C_{17}H_{20}N_4O_8$=408.12)

(2S,4S)1-tert-butoxycarbonyl-4-{[(1-methylethylidene)amino]oxy}proline **84d**

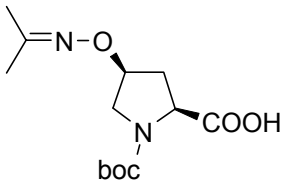

84d

Compound **83** (1g, 2.47mmol) was taken in methanol (2ml) and 0.5N NaOH (2ml) was added into it. After stirring for 30 min, the mixture was brought to pH~7.0 with cation exchange resin (Dowex H+). Resin was filtered, solvent evaporated and to the residue ethanol (5ml) and 99% hydrazine hydrate (12.5μl) were added. After 7h, ethanol was evaporated, residue was taken in water and extracted in EtOAc to remove phthalahydrazide. To the aq. layer, Na_2CO_3 (0.52g, 4.95mmol) was added and the mixture was cooled in an ice bath. Fmoc-ONSu (1g, 2.96mmol) was added in portions in 30min. After the completion of reaction, work

up was done following the procedure (a) as mentioned for the compound **86**. Purification by silica gel column chromatography achieved compound **86** (0.46g, yield=40%) and compound **84d** (0.1g, yield=15% Rf=0.25 MeOH/DCM 3:97).

^{1}H NMR ($CDCl_3$) δ 9.57 (bs 1H COOH), 4.8-4.6 (m 1H C4H), 4.42-4.28 (m 1H C2H), 3.9-3.4 (m 2H C5H), 2.67-2.21 (m 2H C3H), 1.18, 1.73 (2s $NC(CH_3)_2$), 1.44 (s 9H $C(CH_3)_3$).

(2S,4S)-4-[(diacetylamino)oxy]-1-tert-butoxycarbonyl-proline ethyl ester **87**

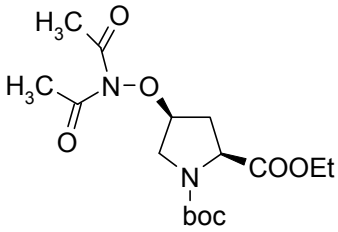

87

The Oxyamine **84** (0.8g, 2.92mmol), acetic anhydride (0.56ml, 5.84mmol) and pyridine (0.5ml 5.84mmol) were stirred for two h at room temperature. The pyridine was evaporated under reduced pressure and the residue was washed with water yielding (1g) of a mixture of **87** (1g, Rf=0.4 EOAc:Petroleum ether 1:1) and **88** Rf=0.6 EtOAc:Petroleum ether 1:1) and a part of it was purified by column for characterization.

1H NMR $CDCl_3$ δ 4.75 (m 1H C4H), 4.5-4.0 (m 3H C5H, OCH_2CH_3), 2.8-2.25 (m 8H C3H, $C(CH_3)_2$), 1.7-1.4 (m 9H $C(CH_3)_3$), 1.3 (m 3H OCH_2CH_3)

(2S,4S)-4-[(acetylamino)oxy]-1-tert-butoxycarbonyl-proline ethyl ester **88**

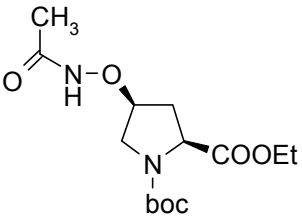

88

^{1}H NMR $CDCl_3$ δ 9.2, 9.1 (1H NHCO major, minor), 4.55 (m 1H C4H), 4.5-4.0 (m 2H C5H), 3.9-3.6 (m 2H OCH_2CH_3), 3.5 (m 1H C2H), 2.5-2.2 (m 2H C3H), 1.9 (s 3H $COCH_3$), 1.5 (m 9H $(CH_3)_3$), 1.3 (m 3H OCH_2CH_3)

(2S,4S)-1-(tert-butoxycarbonyl)-4-[(acetylamino)oxy]proline **89**

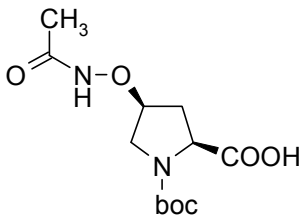

89

The ester (mixture of **87** and **88**) was stirred with 2N NaOH/water: MeOH (1:1) for 1h at room temperature. The methanol was evaporated from reaction mixture and the aqueous solution was adjusted to pH 2.0 with cation exchange resin (Dowex H^+). The crude title compound was isolated by concentrating the aqueous layer giving white powder (0.83g, yield=98% Rf=0.3 MeOH:EtOAc 5:95).

^{1}H NMR $CDCl_3$ δ 4.6 (m 1H C4H), 4.35 (m 1H C5H), 3.75 (m 1H C5'H), 3.5 (m 1H C2H), 2.72-2.5 (C3H), 2.4-1.9 (m 1H C3'H), 1.95 (s 3H $COCH_3$), 1.4 (s 9H $C(CH_3)_3$)

*(2S,4S)-4-[(acetylamino)oxy]-1-(tert-butoxycarbonyl)-N-(4-methoxyphenyl)pyrrolidine-2-carboxamid***e 90**

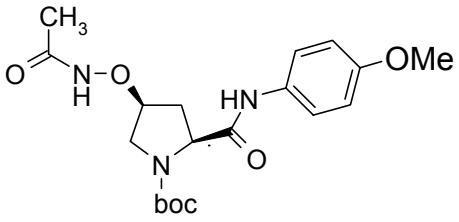

90

To a solution of **89** (0.8g, 2.77 mmol) in dry DMF (10ml), freshly crystallized *p*-anisidine (0.37g, 3mmol) and HOBt (0.18g, 1.3mmol) was added. The solution was cooled to 0°C and DCC (0.63g, 3mmol) was added into it. The ice bath was removed after 1h and stirring was continued for another 2h. The precipitated DCU was removed by filtration and washed with DCM (2X10ml). To the filtrate, more DCM (20ml) was added and the solution was washed successively with dilute aqueous $NaHCO_3$ (2X 5ml), dilute aqueous $KHSO_4$ (2X5ml), and finally brine (1X5ml). The precipitate in the organic phase was removed by filtration, whereupon the organic phase was dried and evaporated to dryness i*n vacuo.* The solid residue was further purified by column using MeOH/DCM to obtain compound **90** (0.5g, yield=45% Rf= 0.23 EtOAc)

^{1}H NMR ($CDCl_3$) δ 9.9, 9.5 (2s1H NHC_6H_4 major, minor), 9.4, 9.0 (2s 1H $NHCOCH_3$ major, minor), 7.6-7.4 (m 2H C_6H_4), 6.9 (m 2H C_6H_4), 4.5-4.3 (m 1H C4H), 4.25-4.0 (m 1H C2H), 3.9-3.68 (m 5H OCH_3, C5H, C5'H), 2.25-1.8 (m 5H $COCH_3$, C3H, C3'H), 1.4 (2s 9H $C(CH_3)_3$).

GC-MS m/z=393 (Calcd. for $C_{19}H_{27}N_3O_6$=393.18)

Peptide Cleavage, purification and UV-melting experiments

In the present chapter, the peptides were cleaved and purified using same conditions as mentioned in experimental section of chapter 2. For UV-melting experiments, the strand concentration taken for PNA and DNA was 1μM each. The preparation of the samples and the melting experiments were carried out following the same protocol as given in chapter 2.

Appendix III

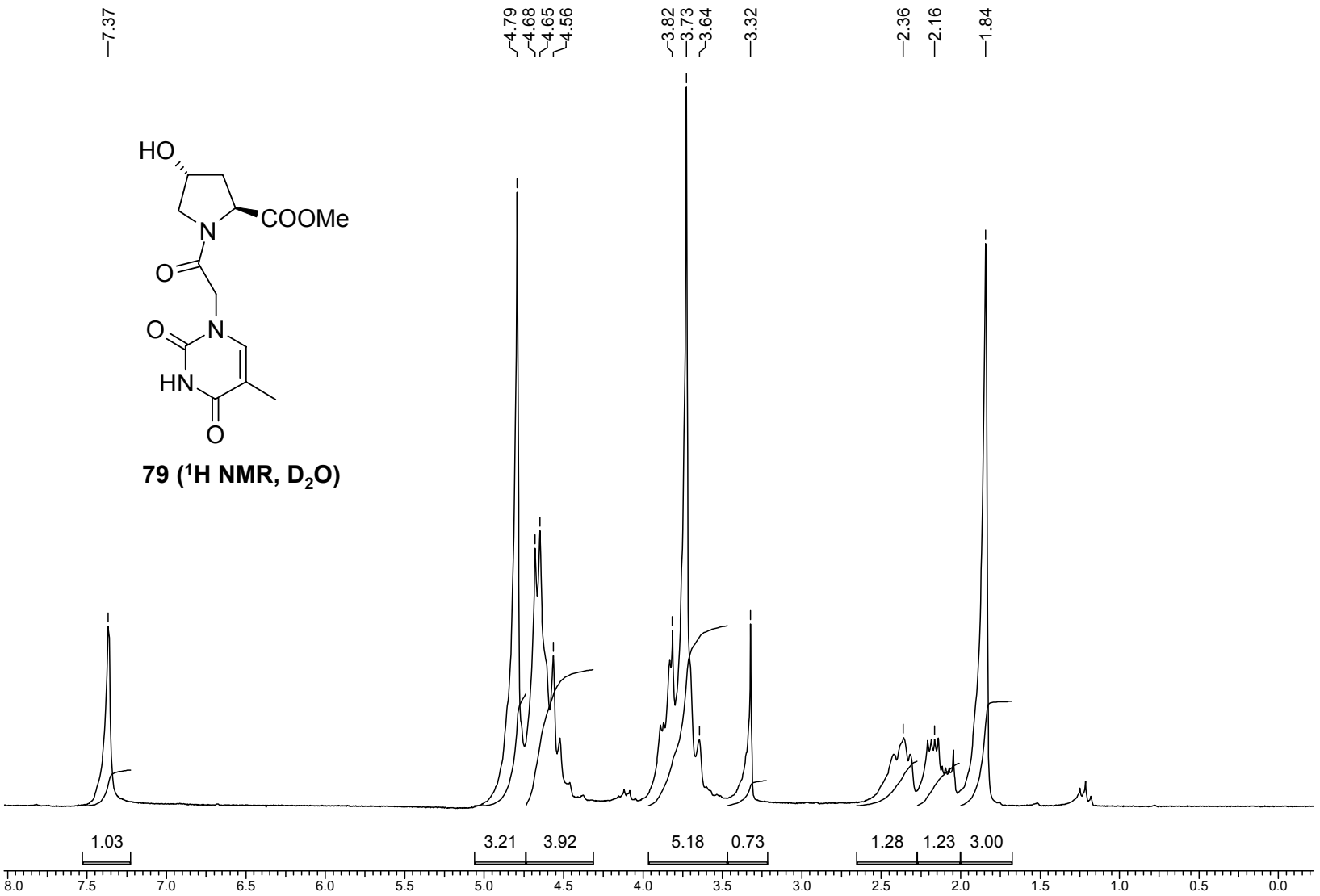
7.37
4.79
4.68
4.65
4.56
3.82
3.73
3.64
3.32
2.36
2.16
1.84
HO
COOMe
N
O
O
N
HN
O
1.03
3.21
3.92
5.18
0.73
1.28
1.23
3.00
8.0
7.5
7.0
6.5
6.0
5.5
5.0
4.5
4.0
3.5
3.0
2.5
2.0
1.5
1.0
0.5
0.0

79 (^{1}H NMR, D_2O)

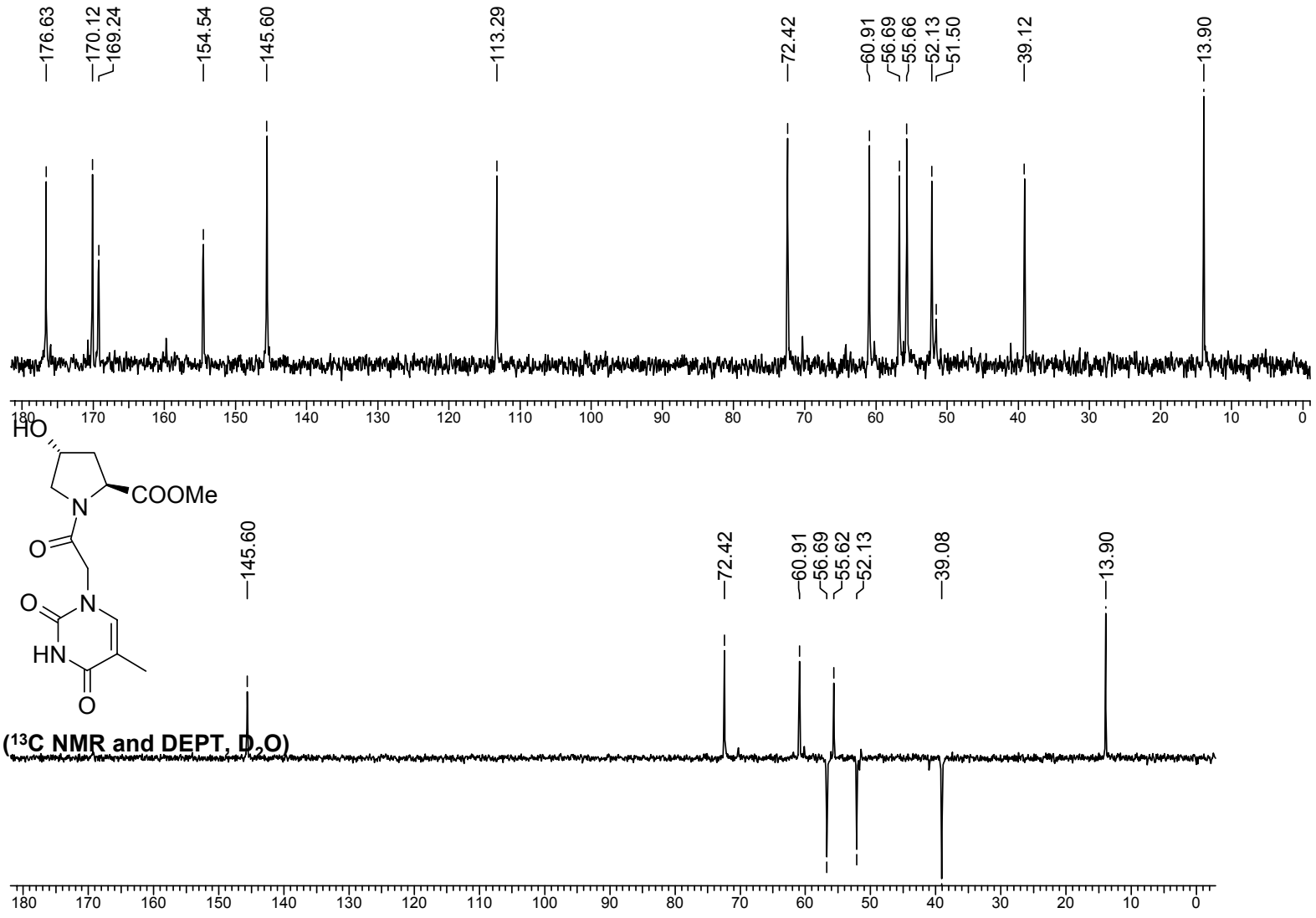

79 (^{13}C NMR and DEPT, D_2O)

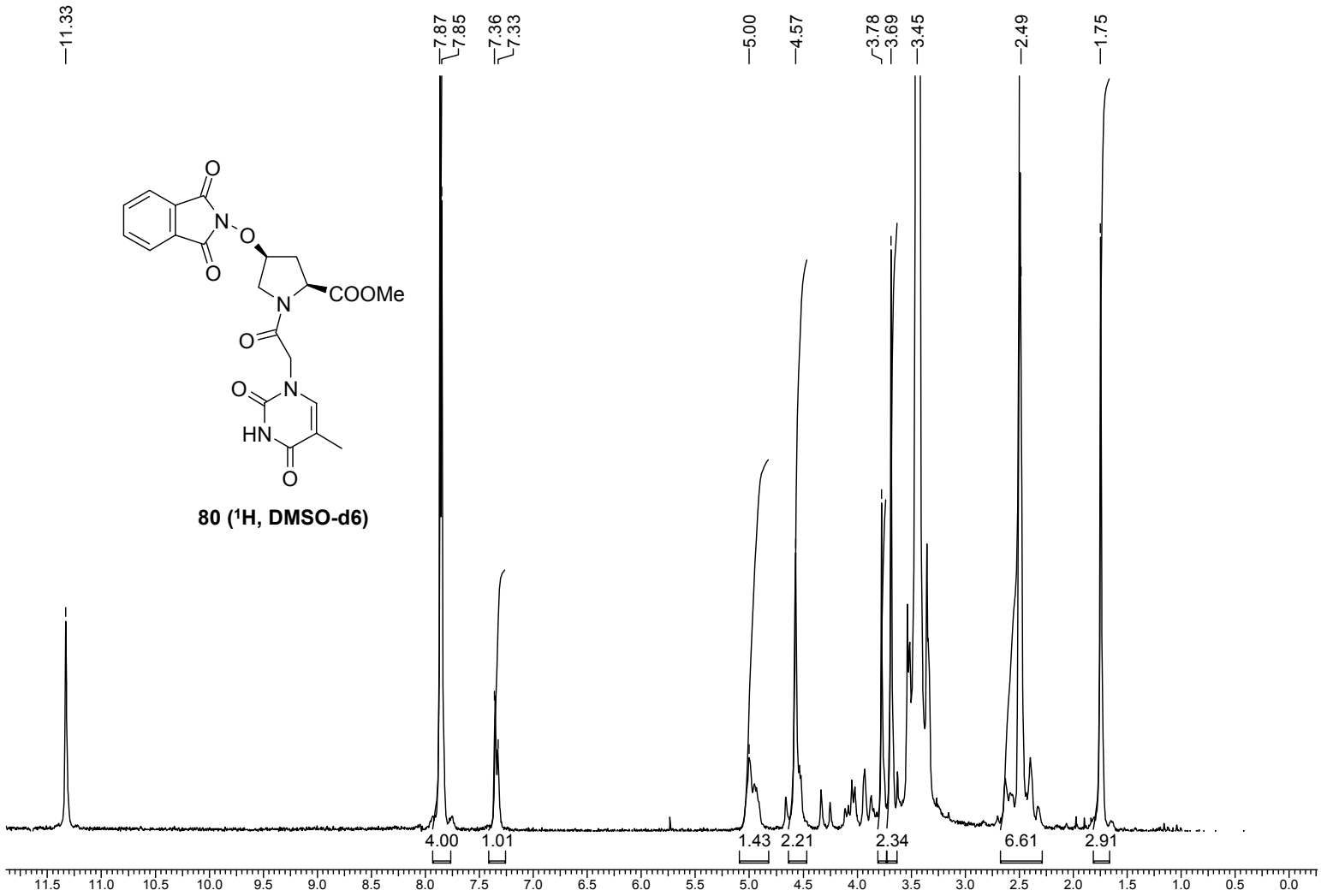
11.33
7.87
7.85
7.36
7.33
5.00
4.57
3.78
3.69
3.45
2.49
1.75
COOMe
4.00
1.01
1.43
2.21
2.34
6.61
2.91

80 (^{1}H, DMSO-d6)

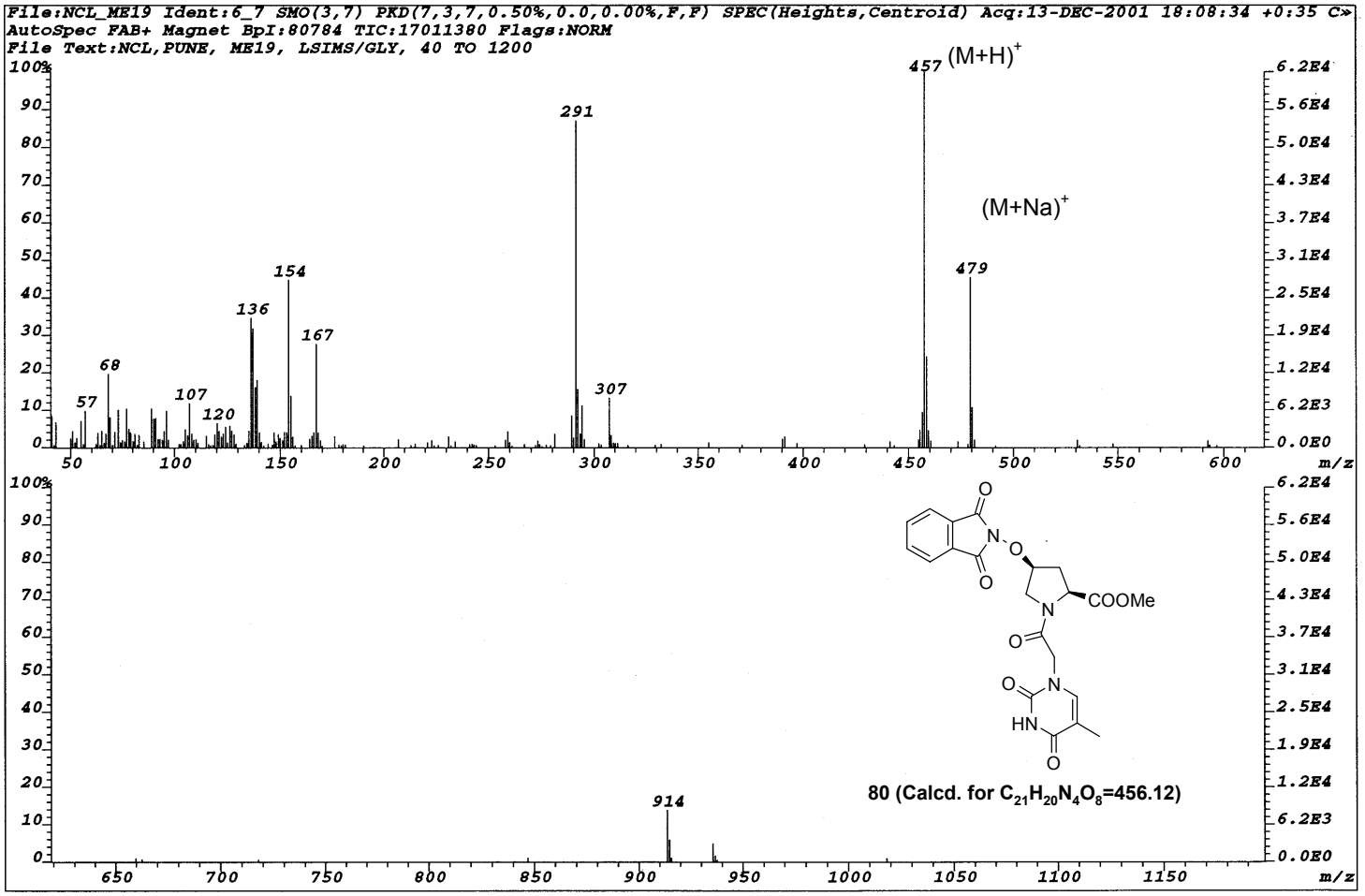
File:NCL_ME19 Ident:6_7 SMO(3,7) PKD(7,3,7,0.50%,0.0,0.00%,F,F) SPEC(Heights,Centroid) Acq:13-DEC-2001 18:08:34 +0:35 C
AutoSpec FAB+ Magnet BpI:80784 TIC:17011380 Flags:NORM
File Text:NCL,PUNE, ME19, LSIMS/GLY, 40 TO 1200
457 (M+H)+
291
(M+Na)+
479
154
136
167
68
57
107
120
307
914
m/z
COOMe
80 (Calcd. for C21H20N4O8=456.12)

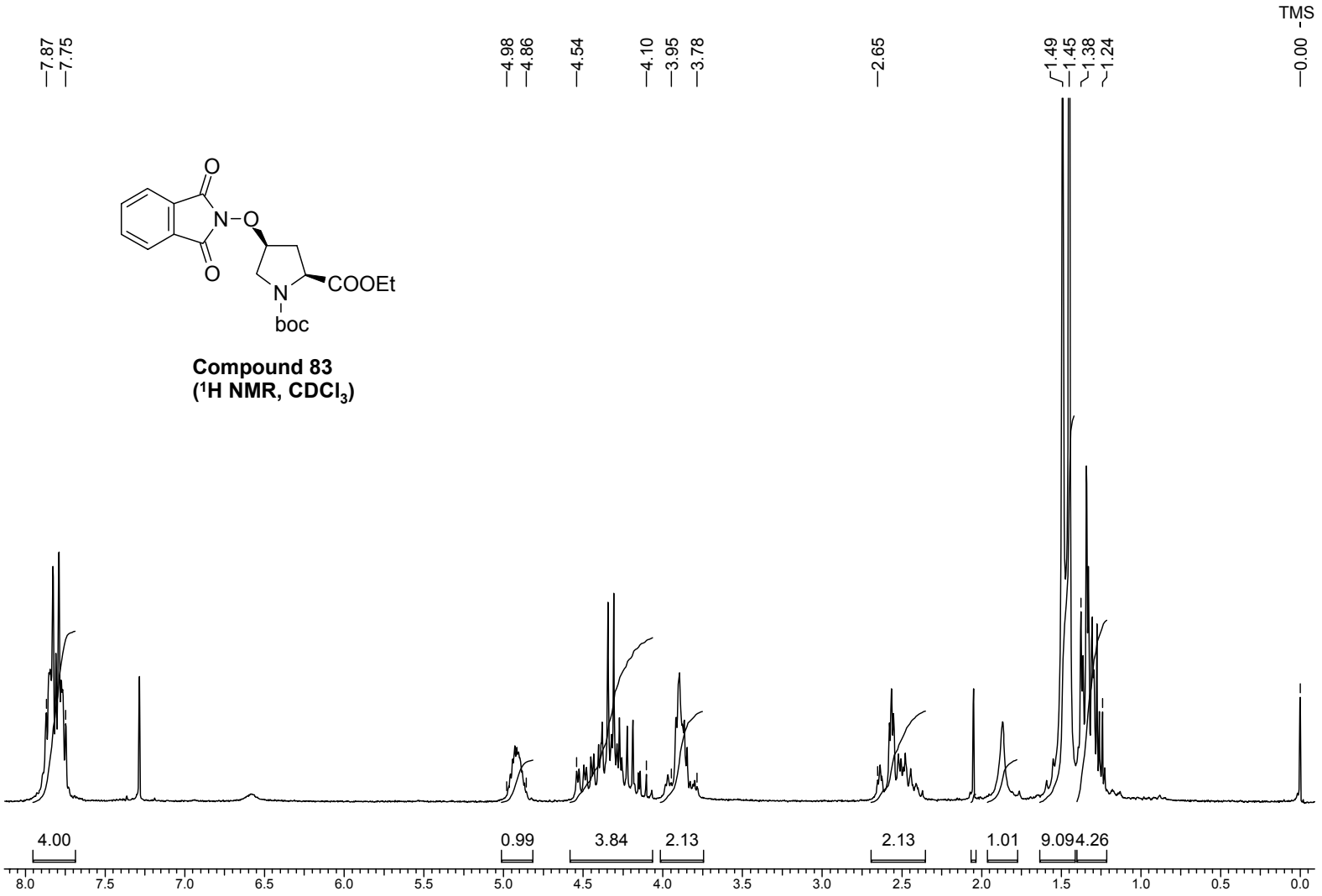

Compound 83
(^{1}H NMR, $CDCl_3$)

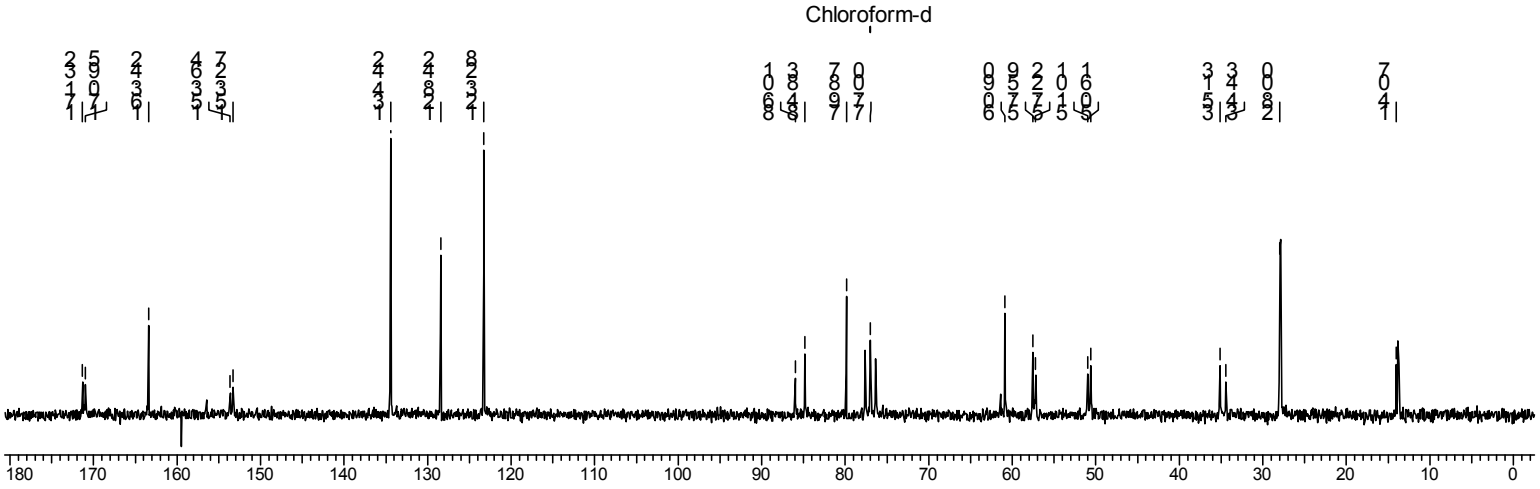

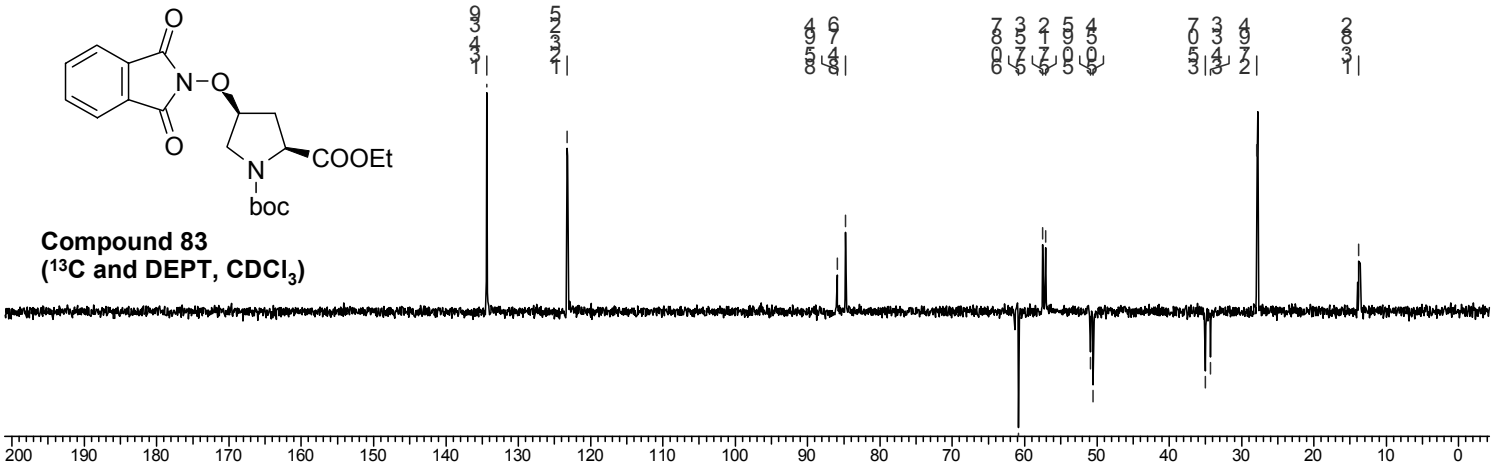

Compound 83
(^{13}C and DEPT, $CDCl_3$)

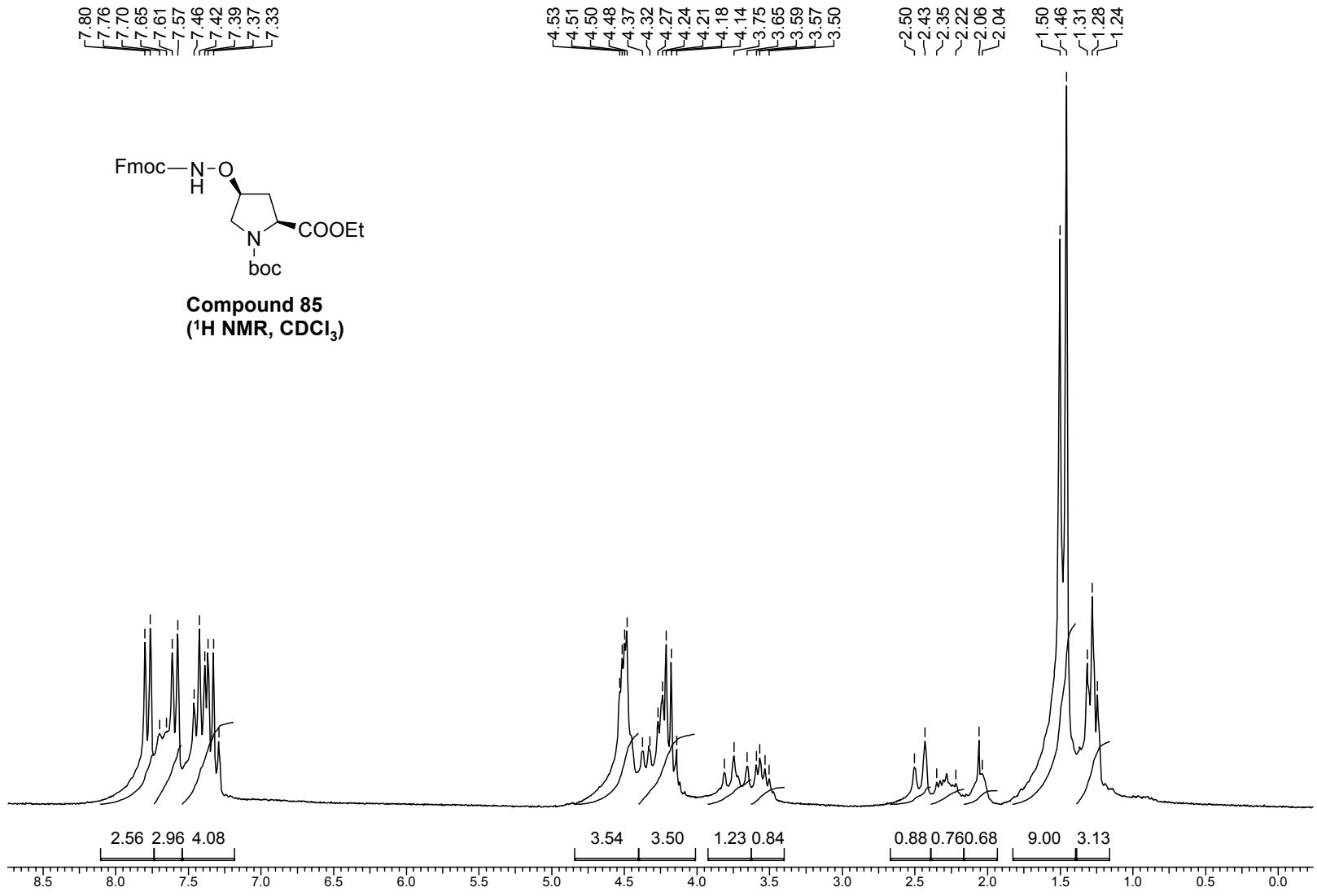

Compound 85
(^{1}H NMR, $CDCl_3$)

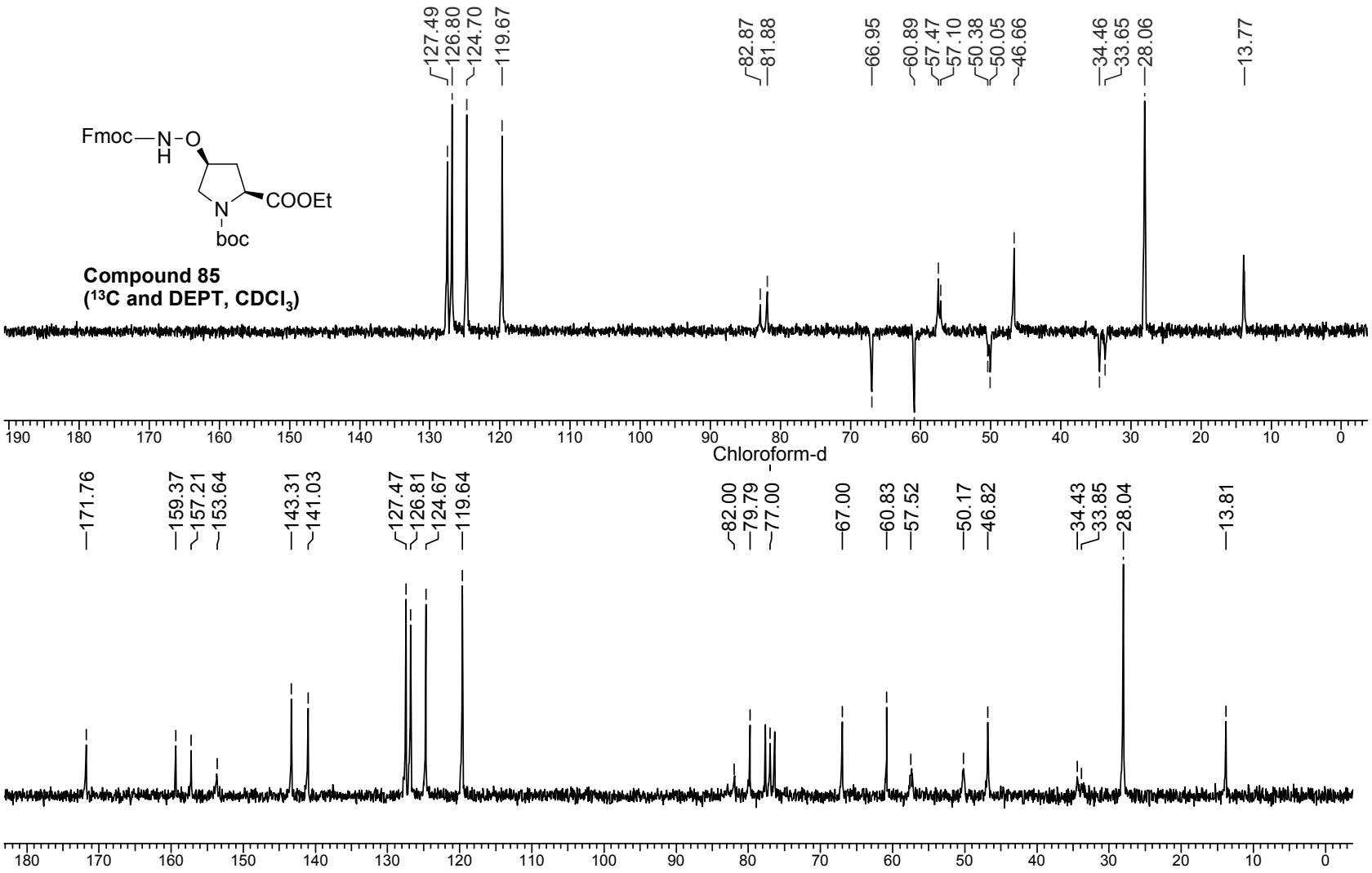
Fmoc—N—O
H
COOEt
N
boc
Compound 85
(13C and DEPT, CDCl3)
127.49
126.80
124.70
119.67
82.87
81.88
66.95
60.89
57.47
57.10
50.38
50.05
46.66
34.46
33.65
28.06
13.77
Chloroform-d
171.76
159.37
157.21
153.64
143.31
141.03
127.47
126.81
124.67
119.64
82.00
79.79
77.00
67.00
60.83
57.52
50.17
46.82
34.43
33.85
28.04
13.81

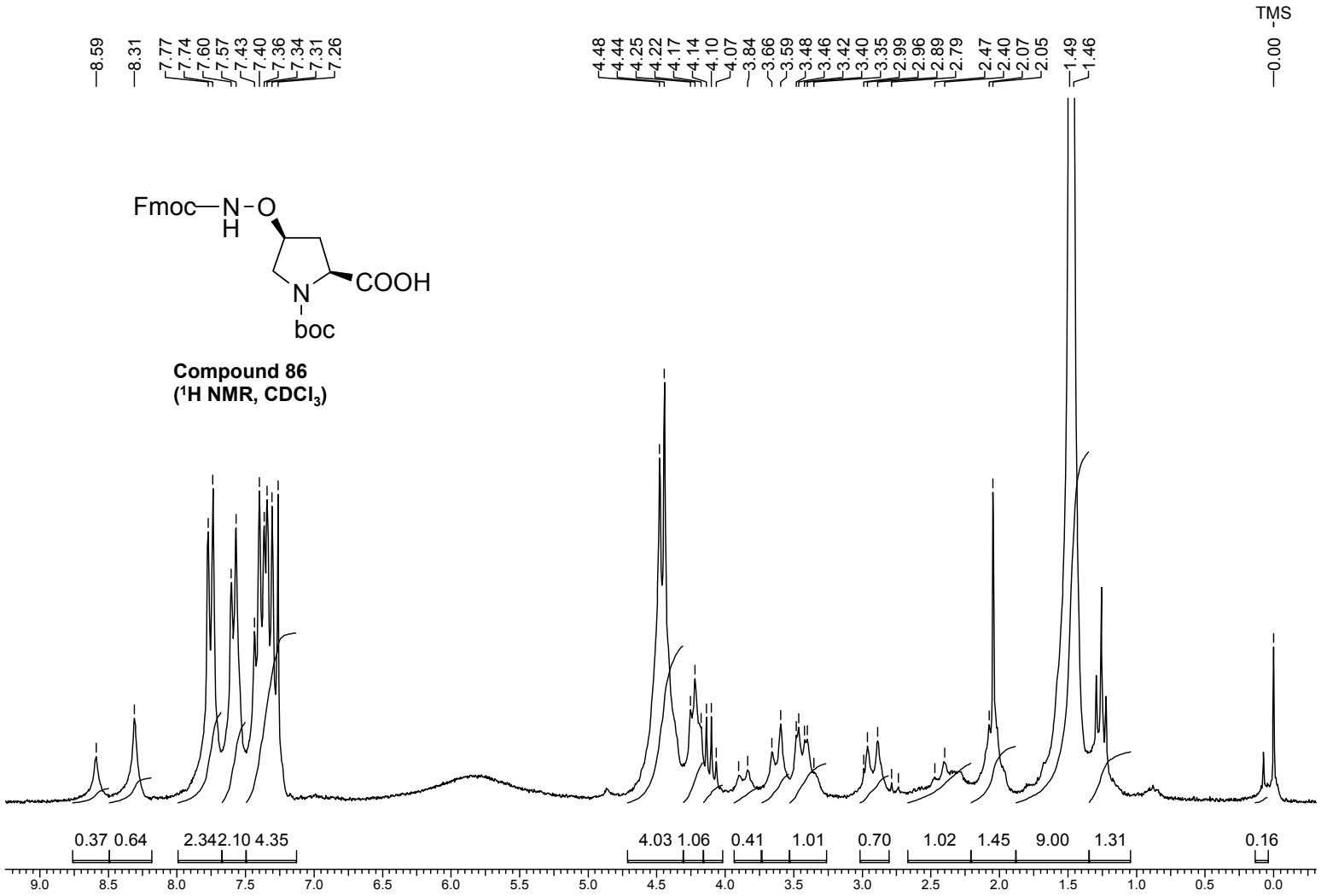

Compound 86
(^{1}H NMR, $CDCl_3$)

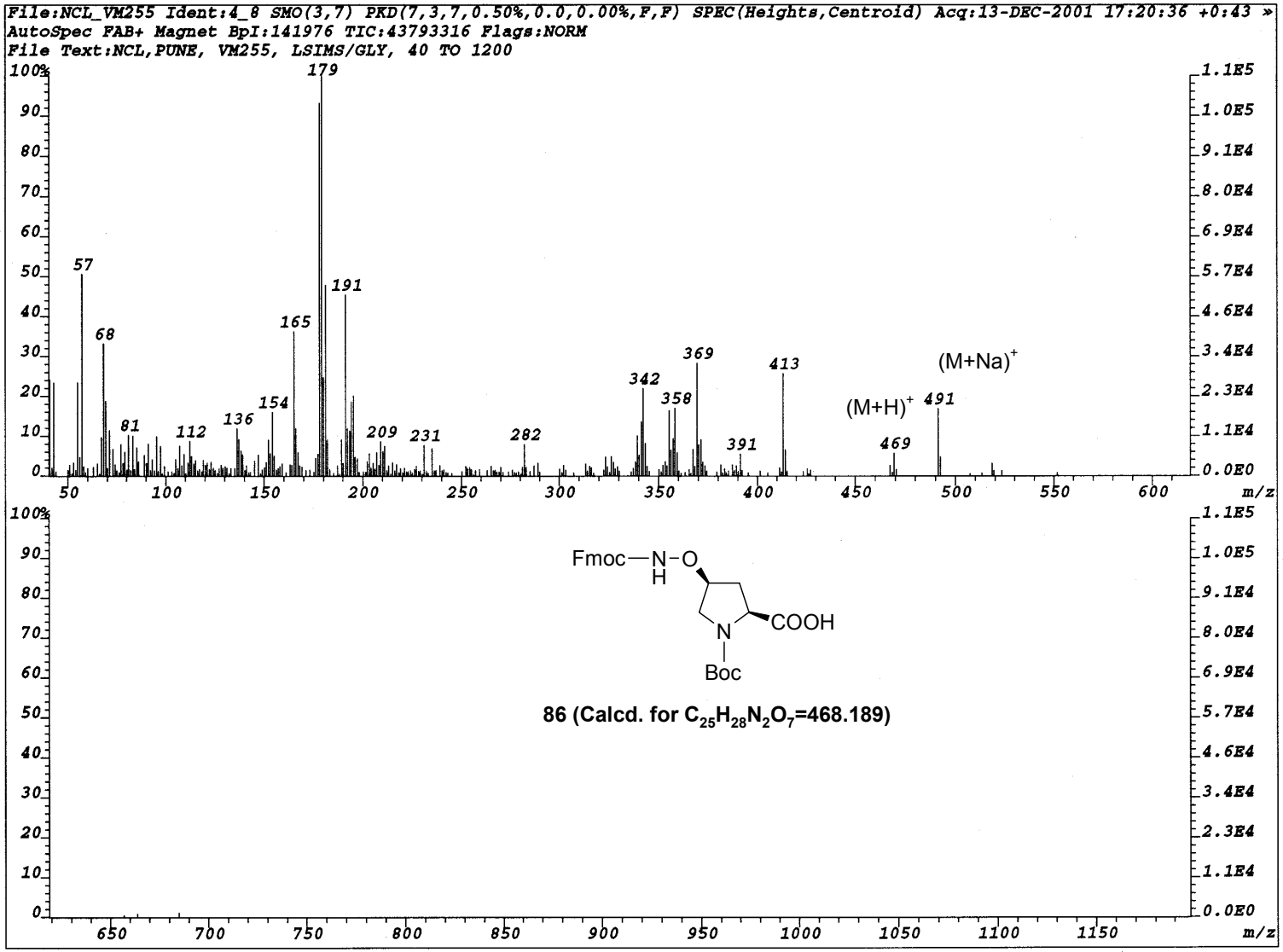
File:NCL_VM255 Ident:4_8 SMO(3,7) PKD(7,3,7,0.50%,0.0,0.00%,F,F) SPEC(Heights,Centroid) Acq:13-DEC-2001 17:20:36 +0:43 »
AutoSpec FAB+ Magnet BpI:141976 TIC:43793316 Flags:NORM
File Text:NCL,PUNE, VM255, LSIMS/GLY, 40 TO 1200
179
57
191
165
68
369
413
(M+Na)+
342
358
154
136
(M+H)+
491
81
112
209
231
282
391
469
m/z
Fmoc—N—O
H
COOH
N
Boc
86 (Calcd. for C25H28N2O7=468.189)

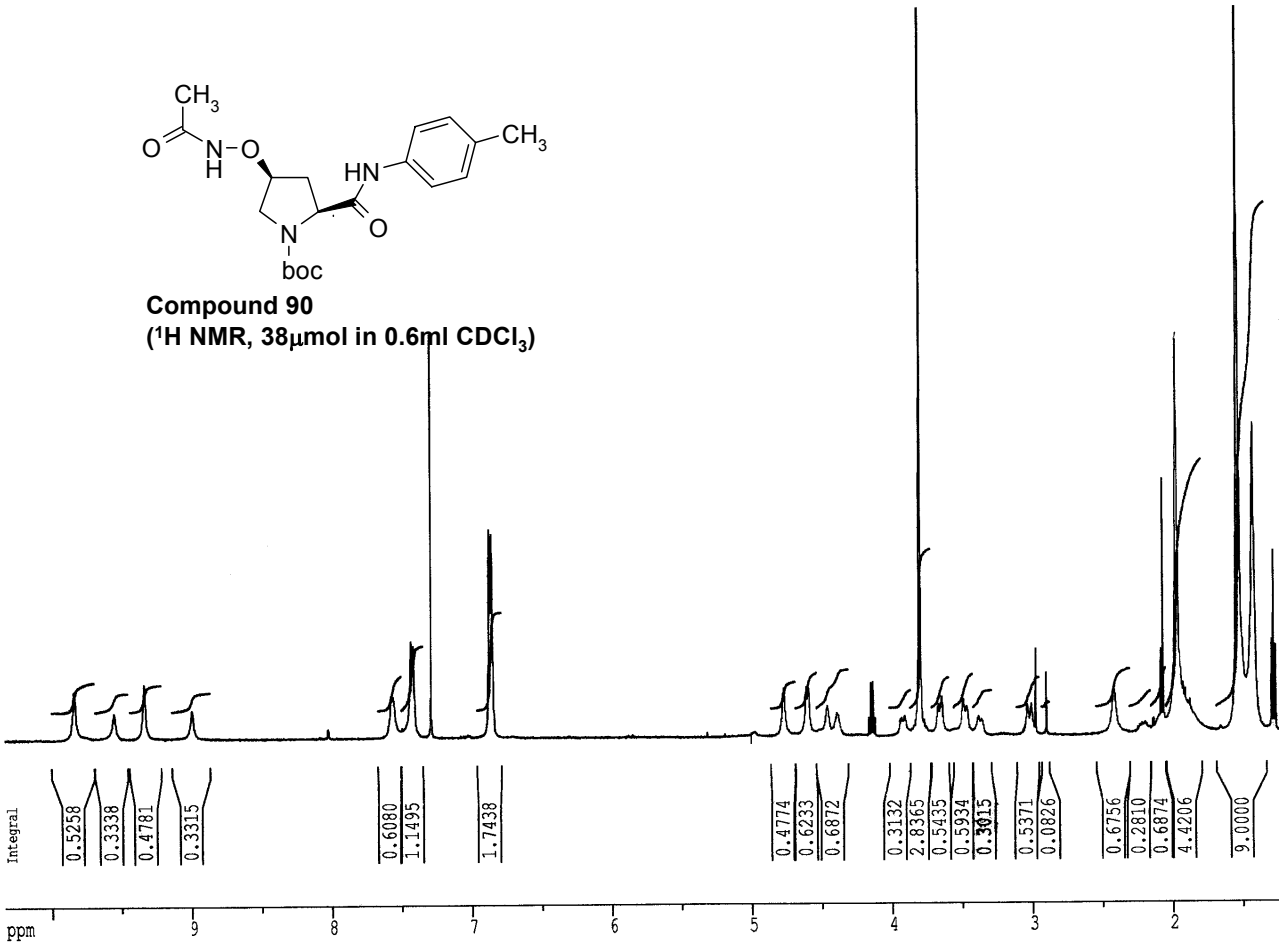

Compound 90
(^{1}H NMR, 38μmol in 0.6ml $CDCl_3$)

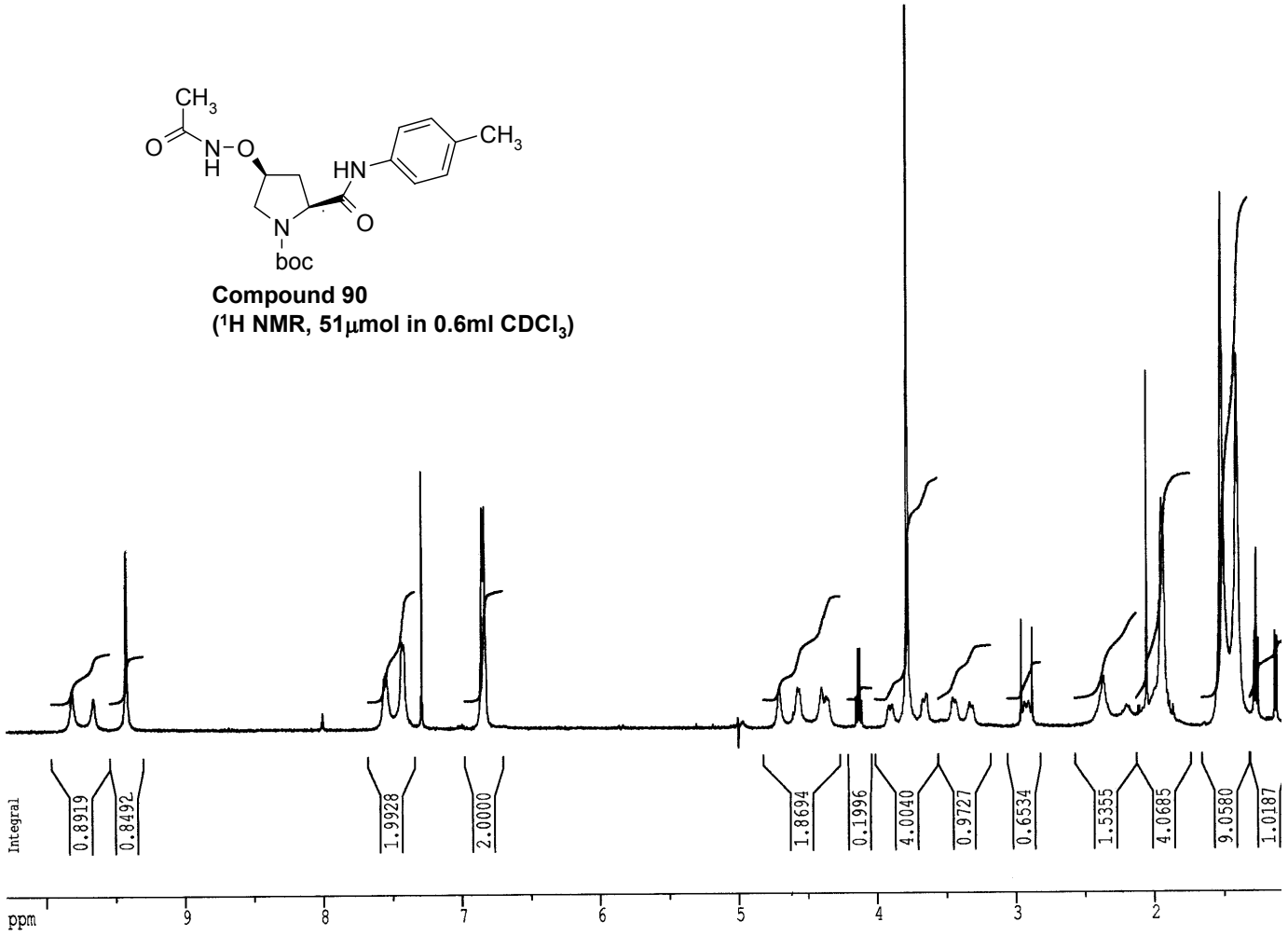

Compound 90
(^{1}H NMR, 51μmol in 0.6ml $CDCl_3$)

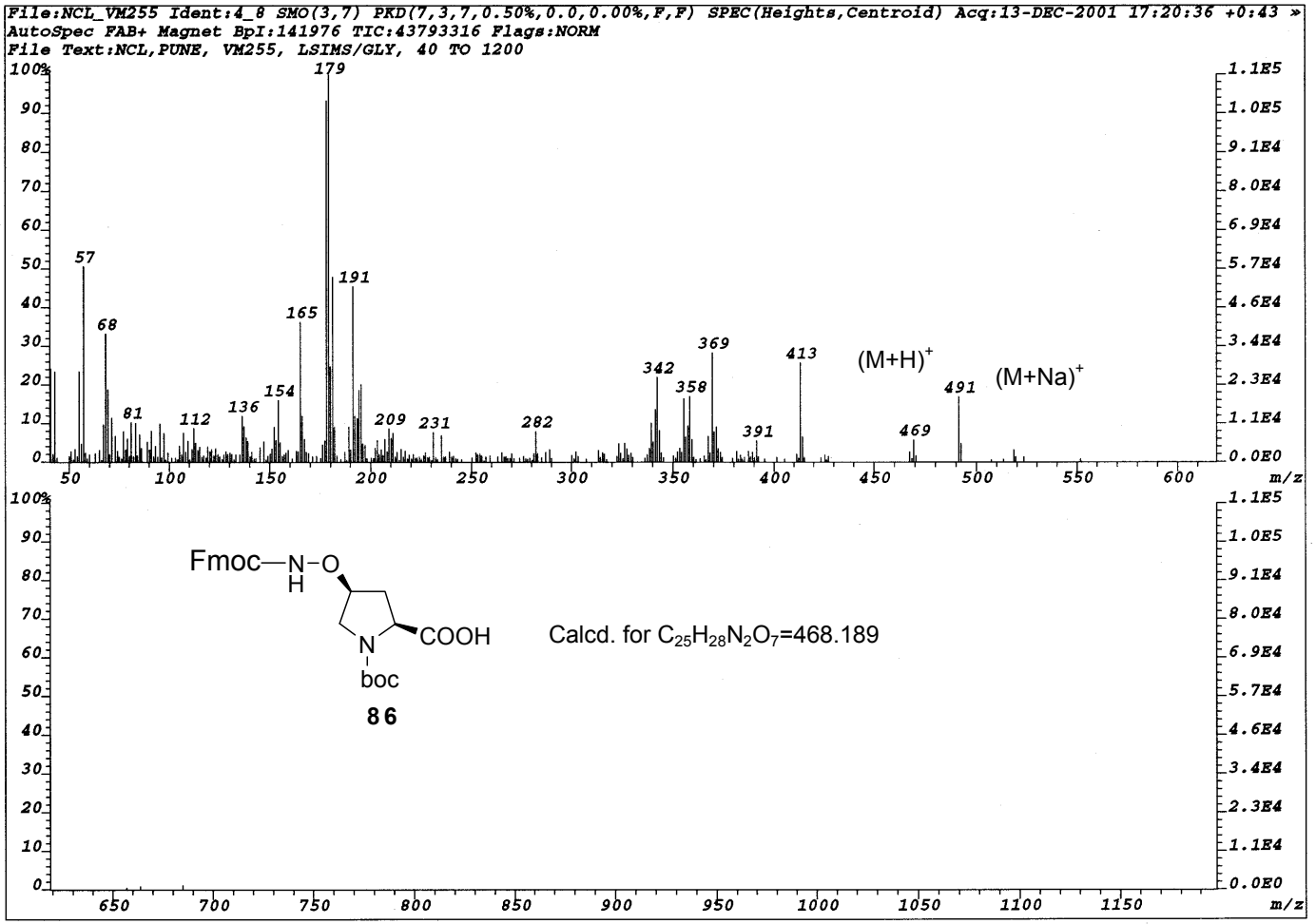
File:NCL_VM255 Ident:4_8 SMO(3,7) PKD(7,3,7,0.50%,0.0,0.00%,F,F) SPEC(Heights,Centroid) Acq:13-DEC-2001 17:20:36 +0:43 »
AutoSpec FAB+ Magnet BpI:141976 TIC:43793316 Flags:NORM
File Text:NCL,PUNE, VM255, LSIMS/GLY, 40 TO 1200
(M+H)+
(M+Na)+
m/z
Fmoc—N–O
H
COOH
N
boc
Calcd. for C25H28N2O7=468.189

86

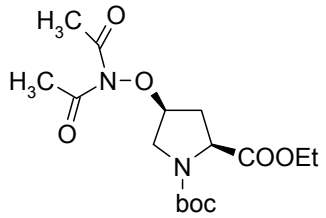

Compound 87
(^{1}H NMR, $CDCl_3$)

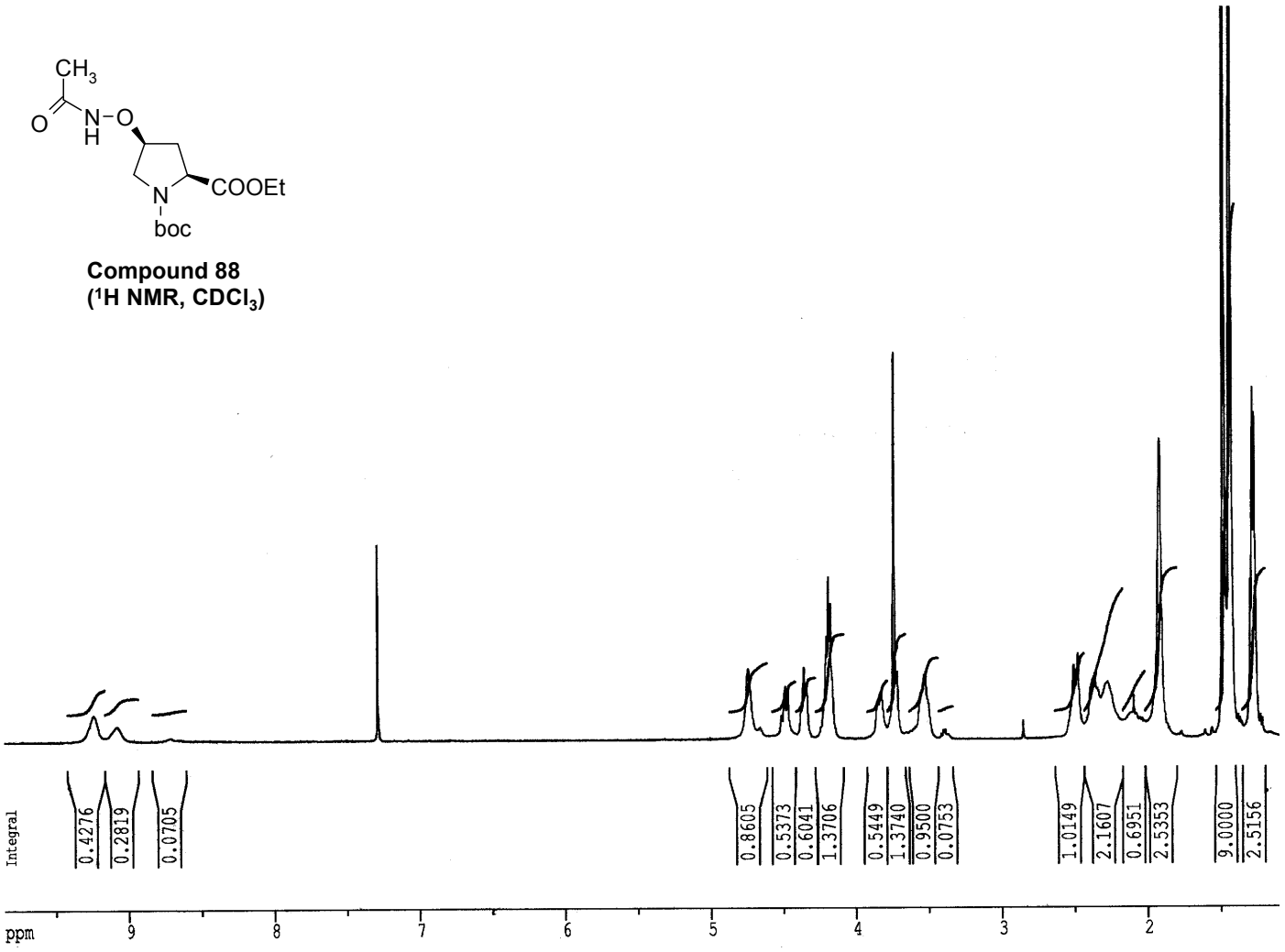

Compound 88
(^{1}H NMR, $CDCl_3$)

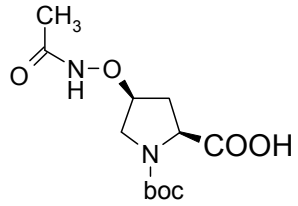

Compound 89
(^{1}H NMR, $CDCl_3$)

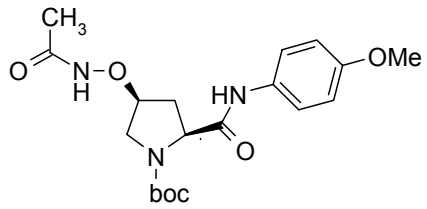

90 (^{1}H NMR with 38μmol in 0.6ml $CDCl_3$)

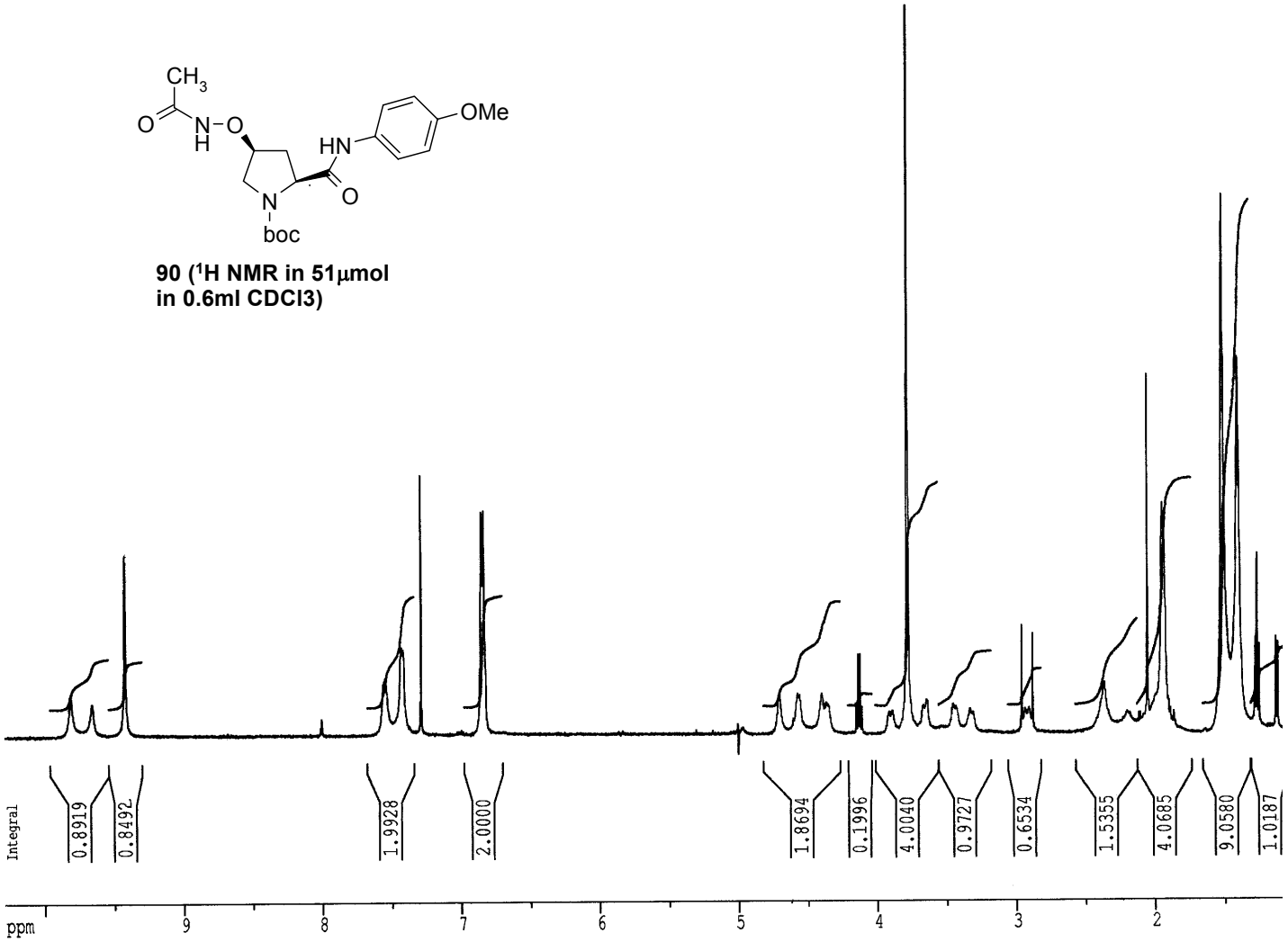

90 (^{1}H NMR in 51μmol in 0.6ml CDCl3)

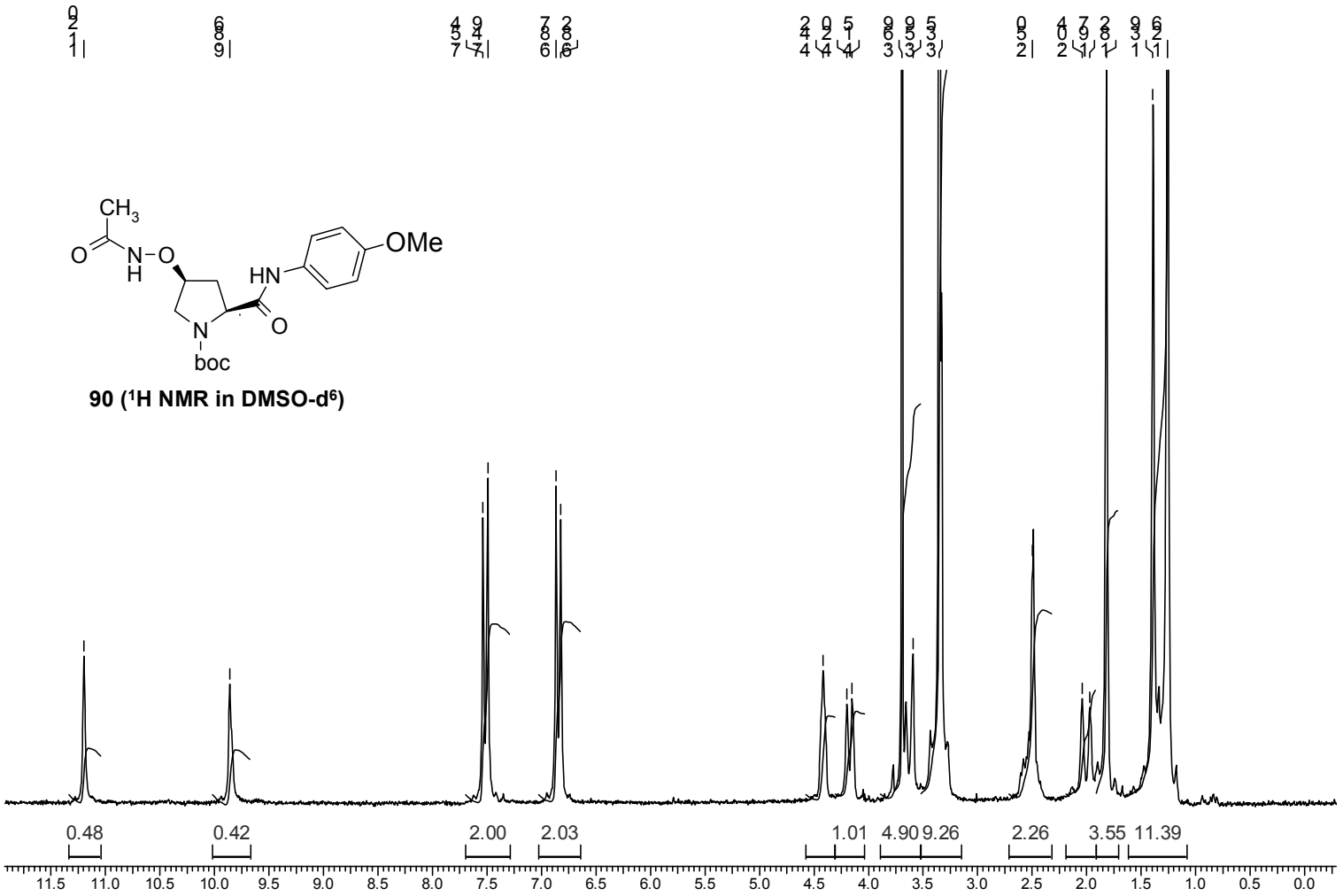

90 (^{1}H NMR in DMSO-d^6)

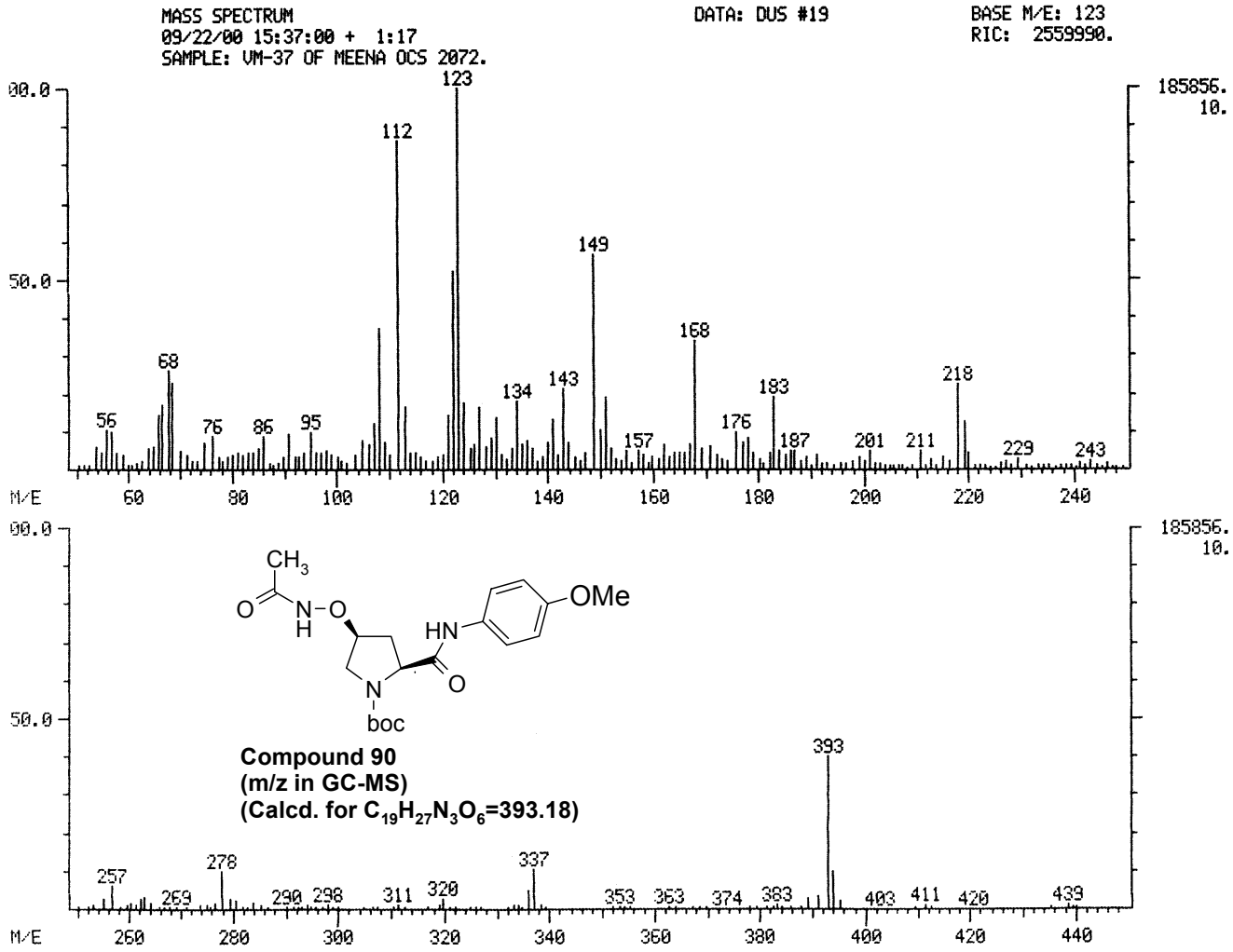
MASS SPECTRUM
09/22/00 15:37:00 + 1:17
SAMPLE: VM-37 OF MEENA OCS 2072.
DATA: DUS #19
BASE M/E: 123
RIC: 2559990.
185856.
10.
M/E
CH3
O
N
H
O
HN
OMe
N
boc
O
Compound 90
(m/z in GC-MS)
(Calcd. for C19H27N3O6=393.18)

Crystal data and structure refinement for compound 84c

Identification code	meena1
Empirical formula	C25.50 H30 N6 O12
Formula weight	612.55
Temperature	293(2) K
Wavelength	0.71073 A
Crystal system, space group	Orthorhombic, P212121
Unit cell dimensions	a = 5.9963(15) A alpha = 90 deg. b = 23.924(6) A beta = 90 deg. c = 41.980(11) A gamma = 90 deg.
Volume	6022(3) A^3
Z, Calculated density	8, 1.351 Mg/m^3
Absorption coefficient	0.109 mm^-1
F(000)	2568
Crystal size	? x ? x ? mm
Theta range for data collection	0.97 to 25.00 deg.
Limiting indices	-6<=h<=7, -22<=k<=28, -48<=l<=49
Reflections collected / unique	30242 / 10554 [R(int) = 0.0979]
Completeness to theta = 25.00	99.7 %
Refinement method	Full-matrix least-squares on F^2
Data / restraints / parameters	10554 / 0 / 793
Goodness-of-fit on F^2	0.945
Final R indices [I>2sigma(I)]	R1 = 0.0672, wR2 = 0.0980
R indices (all data)	R1 = 0.1978, wR2 = 0.1306
Absolute structure parameter	0.4(14)
Largest diff. peak and hole	0.168 and -0.133 e.A^-3

Chapter 5

Pyrrolidine Based Chimeric Antisense Nucleic Acids

5.1. Introduction

The unique property of PNA as antisense/antigene therapeutic agent arises from its ability to displace one strand of a DNA double-helix. This strand displacement process, which is more efficient than DNA, is due to the formation of an unusually stable $(PNA)_2$:DNA triple helix. The sequence specific and faster strand invasion of PNA may extend the potential utility of PNA in diagnostics and as biomolecular probes. To improve the properties of PNA, the covalent combination of PNA and DNA in a single molecule, resulting in PNA/DNA chimeras, have been studied. These may have PNA moiety conjugated to the 3' end of DNA (A), at the 5'-end of the DNA (B), at both 3' and 5'-ends of DNA (C) or may be within a DNA oligomer (D) (Figure 1). Compared

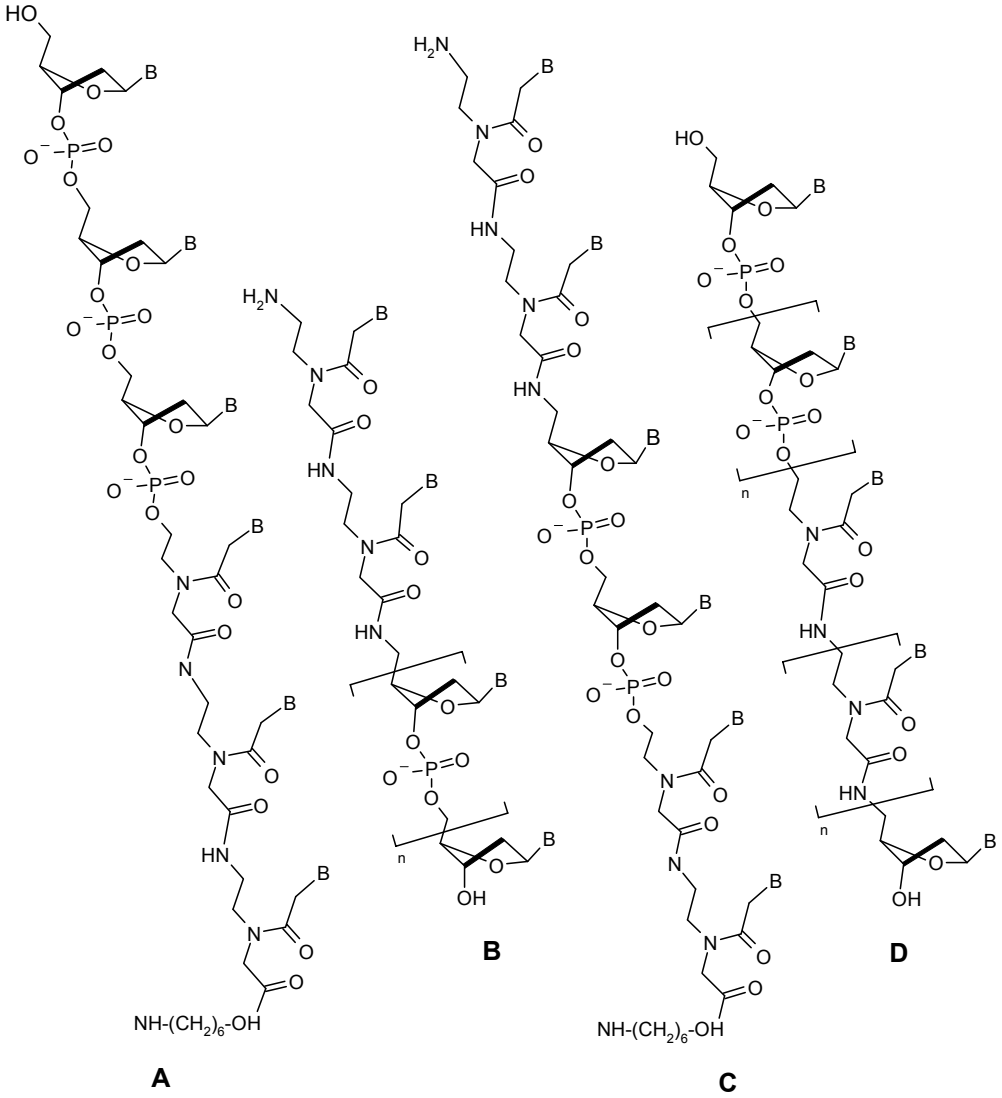

Figure 1. Different types of PNA-DNA chimeras. (A) 5'-DNA-3'-PNA (B) H-PNA-5'-DNA-3' (C) H-PNA-5'-DNA-3'-PNA (D) 5'-DNA-3'-PNA-5'-DNA-3'.

to homooligomer PNAs, the chimeras show improved aqueous solubility due to their negative charged structure and a better cellular uptake. Uhlmann *et al*., (1996) developed a fully automated synthesis of DNA/PNA chimeras compatible with the standard DNA synthesis methods. The binding affinity of DNA-PNA chimeras was found to be higher to that of the equivalent DNA-phosphorothioate chimeras or natural oligonucleotides, the strength of binding strongly dependent on the PNA:DNA ratio. Unlike homooligomeric PNAs, the DNA-PNA chimeras bind only in the antiparallel orientation to their complementary nucleic acids under physiological conditions (Uhlmann *et al*., 1999; Breipohl *et al*., 1997). Further, PNA cannot induce RNase H cleavage of target RNA, which is a desirable biological efficacy of antisense agents. DNA-PNA chimeras are able to stimulate the cleavage of target RNA by RNase H through formation of an RNA chimera duplex (Uhlmann *et al*, 1996; Uhlmann, 1998).

To prevent the nonsequence-specific effects of antisense oligonucleotides induced by their binding to the proteins, the uncharged analogues of DNA have been extensively evaluated. An important outcome of these is methylphosphonates, which are nonionic and therefore less soluble than other commonly available analogues. In addition, RNase H, the cellular enzyme responsible for mRNA cleavage, is not activated by methylphosphonates (Quartin *et al*., 1989).

To address the insolubility and RNase H susceptibility Tidd and colleagues constructed chimeric oligomers such that the central part of the oligonucleotide was left unmodified (or alternatively thioLated) while 3' and 5' termini were synthesized as methylphosphonates (Figure 2). The length of the central portion was varied, and the effects of the oligonucleotides on the cleavage of mRNA in *vivo* and in *vitro* were studied. It was shown that such hybrid oligonucleotides can cleave mRNA in the presence of RNase H with impressive specificity (Giles & Tidd, 1992; Giles et al., 1993). Amongst the chimeric oligomers studied so far, the ones comprising

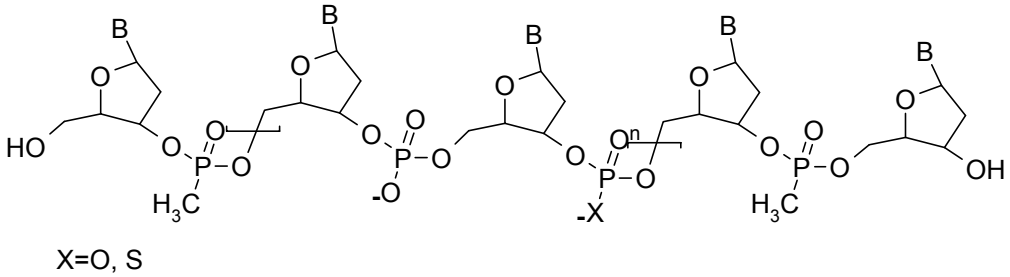

X=O, S

Figure 2. Chimeric oligodeoxynucleotides comprised of internal phosphodiester/phosphorothioate and terminal methylphosphonodiester sections

methylphosphonate and PS/PO linkages the most specific and effective antisense molecules.

Barawkar et al., 2000 obtained DNG/PNA chimeras (Figure 3) by incorporation of positively charged guanidinium linkages into PNA sequences which formed $(DNG/PNA)_2$:DNA triplexes upon binding to single strand or duplex DNA. The $(DNG/PNA)_2$:DNA triplexes of DNG/PNA T_{10}, with DNA dA_{10}, were found to be more

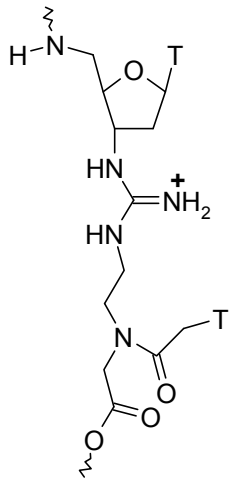

Figure 3. Deoxyribonucleic guanidine (DNG)/aegPNA chimera

stable than DNA:DNA triplexes $(T_{10})_2 \times dA_{10}$. The binding of DNG/PNA chimera with guanidinium linkages to complementary DNA was sequence specific. The association process of DNG/PNA chimera with single strand DNA and strand invasion of longer doble stranded DNA was faster than the association rate of PNA, with the same DNA targets, as evident by thermal hysteresis and gel retardation under isothermal conditions. In contrast to PNA, the chimeras bind exclusively in the antiparallel orientation under physiological conditions.

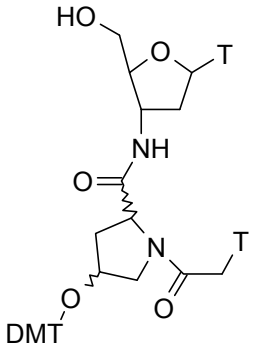

Figure 4. 4-Dimethoxytrityl-N-(thymin-1-yl)acetyl proline/DNA-3' chimera

The study of DNA-(3')-PNA chimeras containing rigid linkers based on (*R*/*S*)-4-hydroxy-D/L-proline) showed that installation of the *trans*-L-linker using the tetrabutylammonium salt of (R)-4-(4,4'-dimethoxytrityloxy)-N-(thymin-1-yl)acetyl-L-proline leads to a DNA-(3')-PNA chimera which hybridizes efficiently with complementary RNA (Verheijen *et al*., 1999) (Figure 4).

Peyman et al., 1998 synthesized an oligomer containing peptide nucleic acid (PNA) and (aminomethyl)phosphonic acid backbones and the melting temperatures (Tm) of complexes with complementary DNA were found to be similar to those of PNAs, but the chimera had a much better water solubility (Figure 5).

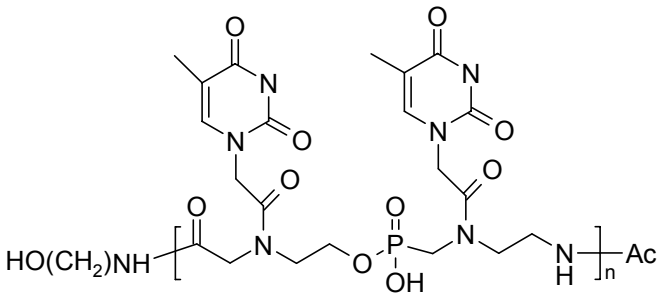

Figure 5.Chimera containing peptide nucleic acid and (aminomethyl)phosphonic acid backbone

To study the effect of Influence of the type of junction in DNA-3'-peptide nucleic acid (PNA) chimeras on their binding affinity to DNA and RNA, Greiner *et al*., (1999) developed an automated online synthesis of a series of three DNA-3'-PNA chimeras in which the 3'-terminus of the oligonucleotide was linked to the amino terminus of the PNA via an N-(2-mercaptoethyl)- (X=S), N-(2-hydroxyethyl)- (X=O), or N-(2-aminoethyl)- (X=NH) N-[(thymin-1-yl)acetyl]glycine unit (Figure 6). In addition, the DNA-3'-PNA chimera without nucleobase at the linking unit was prepared The binding

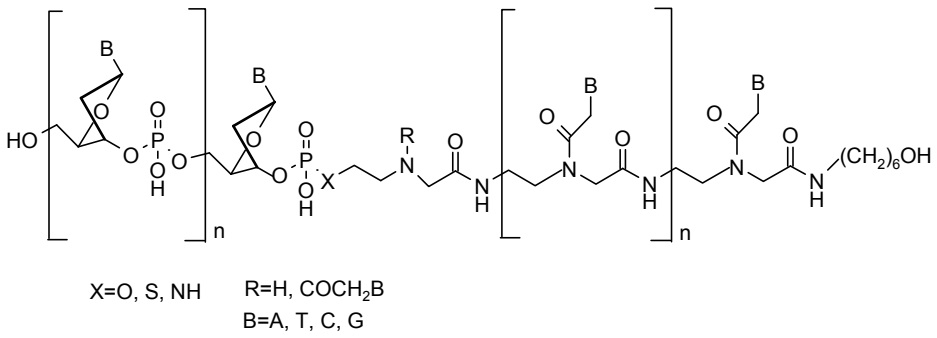

X=O, S, NH R=H, $COCH_2B$
B=A, T, C, G

Figure 6. DNA-3'-PNA chimera with mercaptoethyl (X=S), hydroxyethyl (X=O) aminoethyl (X=O)

affinities of all chimeras were directly compared by determining their Tm values in duplexes with complementary DNA and RNA. It was found that all chimeras in this study that had a nucleobase at the junction were able to form more stable duplexes with complementary DNA and RNA than the corresponding unmodified DNA. The influence of X on duplex stabilization was determined to be O > S > NH, thus demonstrating the phosphodiester bridge to be the most favored linkage at the DNA/PNA junction.

The replacement of one phosphodiester linkage by an amide unit in oligonucleotides (Figure 7) has been considered superior in terms of the thermal

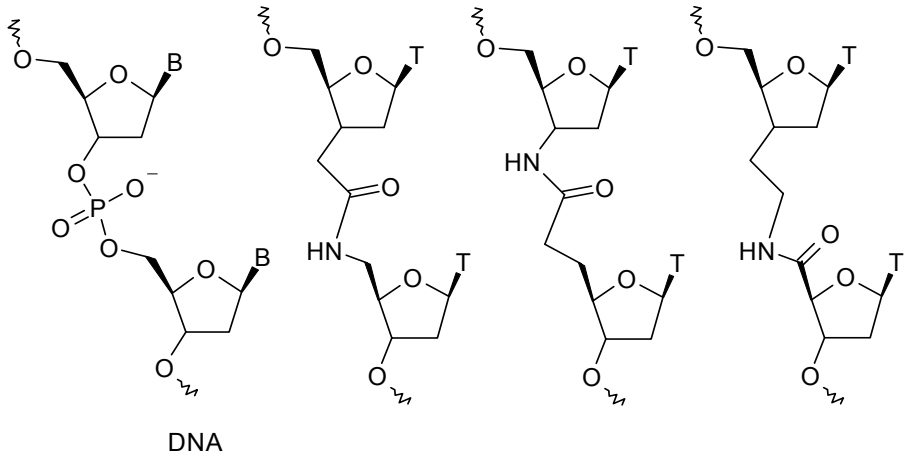

Figure 7. DNA and analogues of DNA having amide linkages.

stability of their complexes with complementary nucleic acids (De Mesmaeker et al., 1994a).

Figure 8 depicts the modifications to alter the conformational flexibility of the backbone (De Mesmaeker *et al*., 1994b) as in **b-e**, which were incorporated into ODN sequences and their binding with complementary ODNs studied. The alkane linkage '**b'** containing hybrids did not lead to duplex formation with its DNA complement. On the other hand, changing the hybridization of one carbon atom from sp^3 to sp^2, and thereby restricting the flexibility of the linkage as in '**c'** led to an increased thermal stability of the duplexes compared to the very flexible modification '**b'**. The instability of PNA:DNA chimera is attributed to the flexibility at the junction of these chimeric ODNs (Kuimelis et al., 1999).

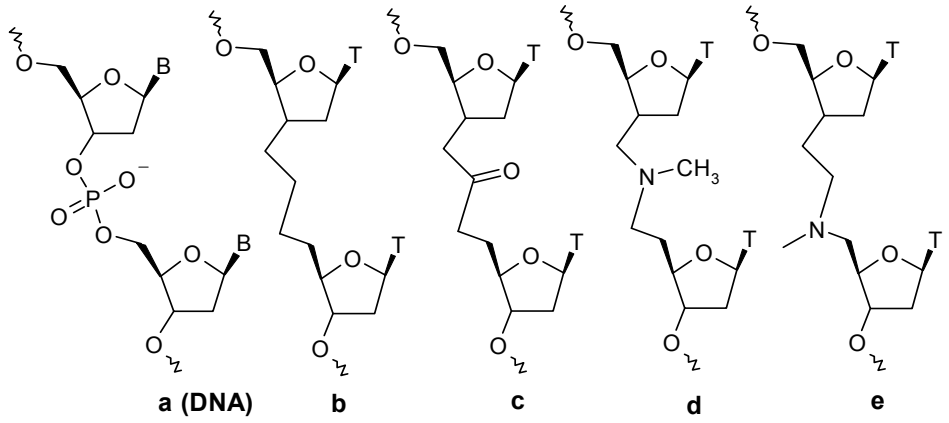

Figure 8. DNA and its modifications involving conformational flexibility.

5.2. Rationale and Objective

This chapter targets the synthesis of chimeric ODNs containing a pyrrolidine ring. A positively charged pyrrolidine ring carrying the HN^{+}-CH_2-CO-NH-5' linkage for replacement of the sugar phosphate backbone in DNA has been studied earlier (Kumar et al., 2000). The replacement of the acyclic PNA junction in the PNA-DNA chimera, by a pyrrolidine ring, was expected to have advantages over the PNA-DNA chimeras due to geometric and/or entropic attributes exerted by the rigid cyclic-PNA-DNA junction. The dimeric unit (Figure 9a) was chosen to have configurational equivalence to natural DNA which corresponds to a (2*R*,4*R)* configuration (Hickman et al., 2000) for the pyrrolidine unit. Further, the design of the dimer was such as to enable its introduction into oligonucleotides using the standard 2-cyanoethyl-phosphoramidite methodology.

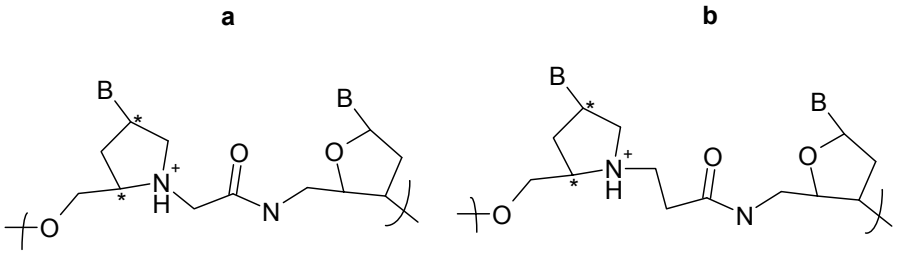

Figure 9. PNA-DNA chimera a) with four atoms in the linker b) with an extra atom in the linker

Incorporation of the peptide linked pyrrolidine (2*R*,4*R*)/sugar dimer in DNA resulted in decrease in thermal stability of duplexes and triplexes. Since the phosphodiester linkage is longer than C-C, C-N or C-C bonds, it is perhaps essential to have a five-atom linker for the replacement of phosphodiester linkage. Gilbert et al., (1995) studied the effect of 4 Vs 5 atom chimeric internucleoside linkages and found

that five atom secondary amine linker inserted in the center of a 10-mer (T_5-L-T_5) stabilized the duplexes formed with *poly*(dA) and *poly*(A) compared to the corresponding four atom linker. In the present case, replacement of phosphodiester linkage with amide linkage may require the insertion of an extra atom in the backbone to complement the internucleotide distances. With this idea, study of PNA-DNA chimera where pyrrolidine unit having one extra carbon atom in the backbone as compared to phosphodiester linkage was attempted. The present work aims at:

1. Synthesis of amide linked (2*R*,4*R*) pyrrollidine/sugar dimer phosphoraamidite **100** (Figure 10).
2. Incoporation of dimer in polypyrimidine and mixed control DNA sequences.
3. Study of duplex and triplex stability by UV-Tm experiments.

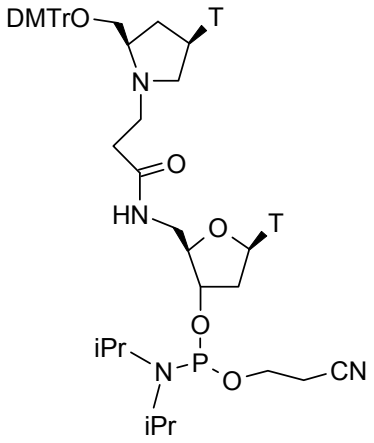

100

Figure 10. (2*R*,4*R*) pyrrolidine/sugar dimer phophoramidite

5.3. Synthesis of The Dimer Block (100)

The phosphoramidite **100** was derived form (2*R*,4*R*) N1-benzyloxycarbnyl 4-hydroxyproline methyl ester in ten steps (Scheme 5.1). Compound **13** was treated with benzoic acid under Mitsunobu conditions to obtain the benzoyl derivative **91** with inversion at C4. The O-benzoylation resulted in a downfield shift of C4 proton form δ 4.5-4.2 to δ 5.24-4.98. Solvolysis of compound **91** gave (2*R*,4*S*) 4-OH **92** in 77% yield and the complete benzoyl deprotection was indicated by disappearance of benzoyl protons in aromatic region and the upfield shift of C4-H to 4.6-4.4. Also, the specific rotation of the compound (α^{27}_D= -4.96) was exactly opposite to its enantiomer (compound **3** in chapter 2) indicating the enantiopurity of the compound. Compound **92**

Scheme 5.1

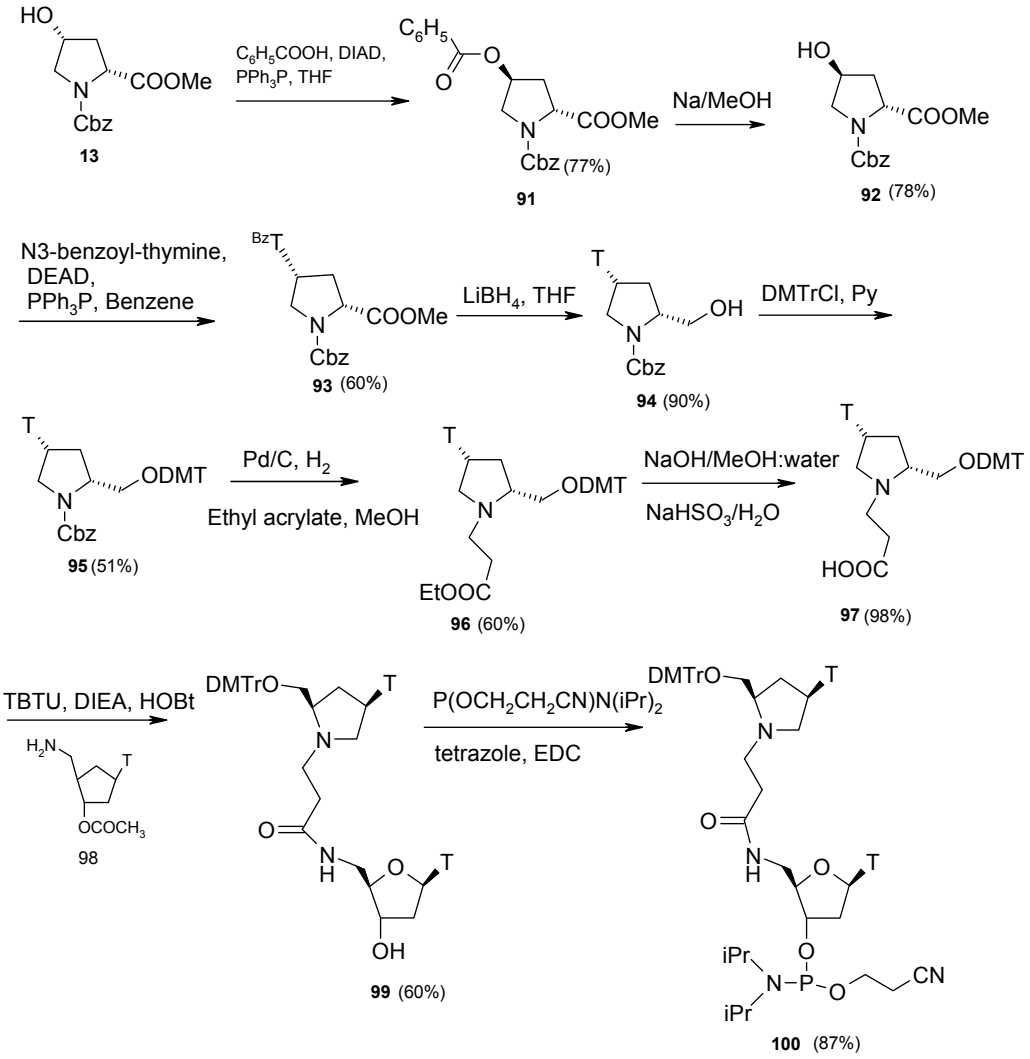

on treatment with N3-benzoylthymine under Mitsunobu conditions gave (2*R*,4*R*)-4-(N3-benzoylthymin-1-yl)-proline methyl ester **93** with inversion of configuration at C4 center. A downfield shift of the H4 multiplet in ^{1}H NMR from δ 4.6-4.4 to δ 5.40-5.10 and the appearance of a characteristic peak at δ2.0 due to CH_3 of thymine confirmed the identity of the Mitsunobu product. The mass spectral analysis gave the expected $(M+H)^+$ ion peak at 491 in support of the structure. The reduction of the ester **93** with excess $LiBH_4$ afforded the alcohol **94** with simultaneous removal of the N3-benzoyl group of thymine. In the ^{1}H NMR spectrum of **94**, the upfield shift of C2H from δ 3.4-3.25 to δ 3.9-3.6 and the appearance of HO-CH_2 at δ 3.80-3.50 indicated the successful reduction of the ester. The IR spectrum exhibited a broad band at 3390 cm^{-1} due to OH, while the disappearance of the ester stretching band at 1740 cm^{-1} was observed. The primary hydroxyl function in **94** was protected by treatment with

dimethoxytritylchloride in pyridine to get the dimethoxytrityl ether, **95** the structure of which was confirmed by ^{1}H and ^{13}C NMR spectroscopy. Compound **95** on hydrogenation over Pd-C for removal of N-benzyloxycarbonyl followed by alkylation of the deprotected pyrrolidine ring nitrogen with ethylacrylate provided the N-alkylated ester **96**. The ^{1}H NMR spectrum of **96** exhibited the methylene protons of N-CH_2CH_2 at δ 2.59-2.53 and the ethyl ester quartet and triplet at δ 4.10 and 1.190 respectively. In the ^{13}C NMR, the N-alkylated group appeared as a set of distinct signals at δ 49.2 (N-C$\underline{H}_2$), 60.4 (COOC$\underline{H}_2CH_3$), 33.74 ($NCH_2C\underline{H}_2$) and 13.85 (-COO-CH_2-CH_3). The MALDI-TOF spectrum of **96** showed $(M)^+$, $(M+Na)^+$ and $(M+K)^+$ signals at 627.8, 649.7 and 665.6 respectively. The ethyl ester in **96** was hydrolyzed in 1N aq. NaOH and the resulting salt was neutralized with aq. $NaHSO_3$ to obtain free acid **97**. The compound **97** was characterized by MALDI-TOF (Figure 12). 3'-O-acetyl-5'-amino-thymidine **98** was prepared according the literature procedure (Lin & Prusoff, 1977) from commercially available thymidine. The condensation of free carboxylic acid **97** with the amine component **98** in the presence of *O*-(1H-benzotriazol-1-yl)-N,N,N',N'-tetramethyluronium tetrafluoroborate (TBTU), 1-hydroxybenzotriazole (HOBt) and diisopropylethylamine (DIPEA) yielded the dimer **99**, that was characterized by ^{1}H , ^{13}C NMR and mass spectroscopy. ^{1}H NMR of **94** did not have a signal for 3'-O-acetyl, which shows that 3'-O-acetyl got hydrolysed during coupling reaction. Also the H4' signal was upfield shifted by δ 4.32 indicating the loss of acetyl group. The C3-OH group of sugar in 94 was phosphorylated with 2-cyanoethyl-N,N,N',N'-tetraisopropyl-phosphorodiamidite in EDC in the presence of tetrazole to yield phosphoramidite **100** in 87% yield.

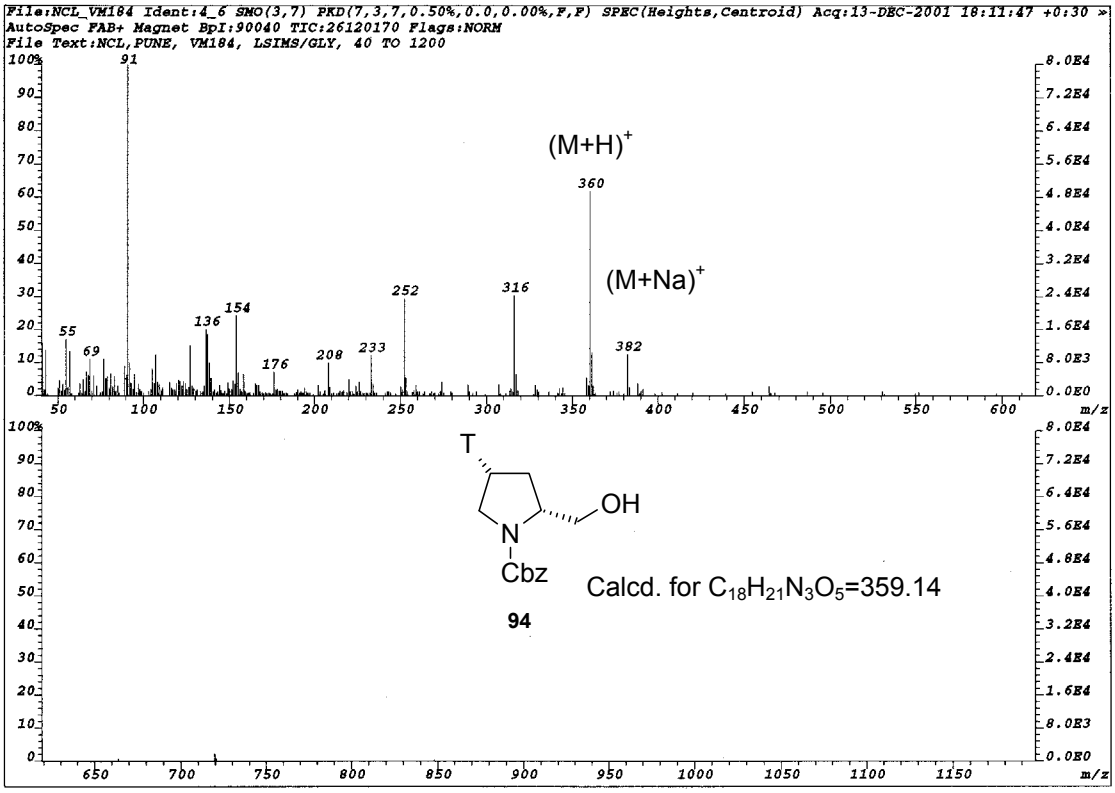

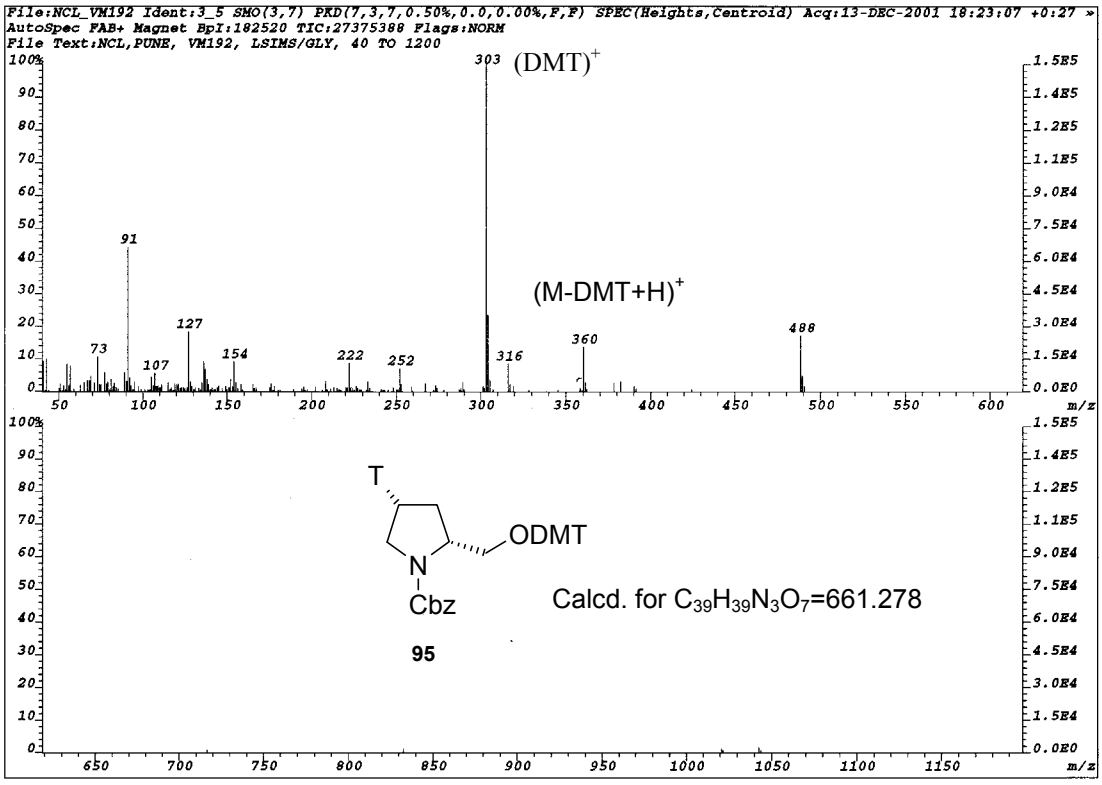

Figure 11. FAB-MS of compound **94** and **95**.

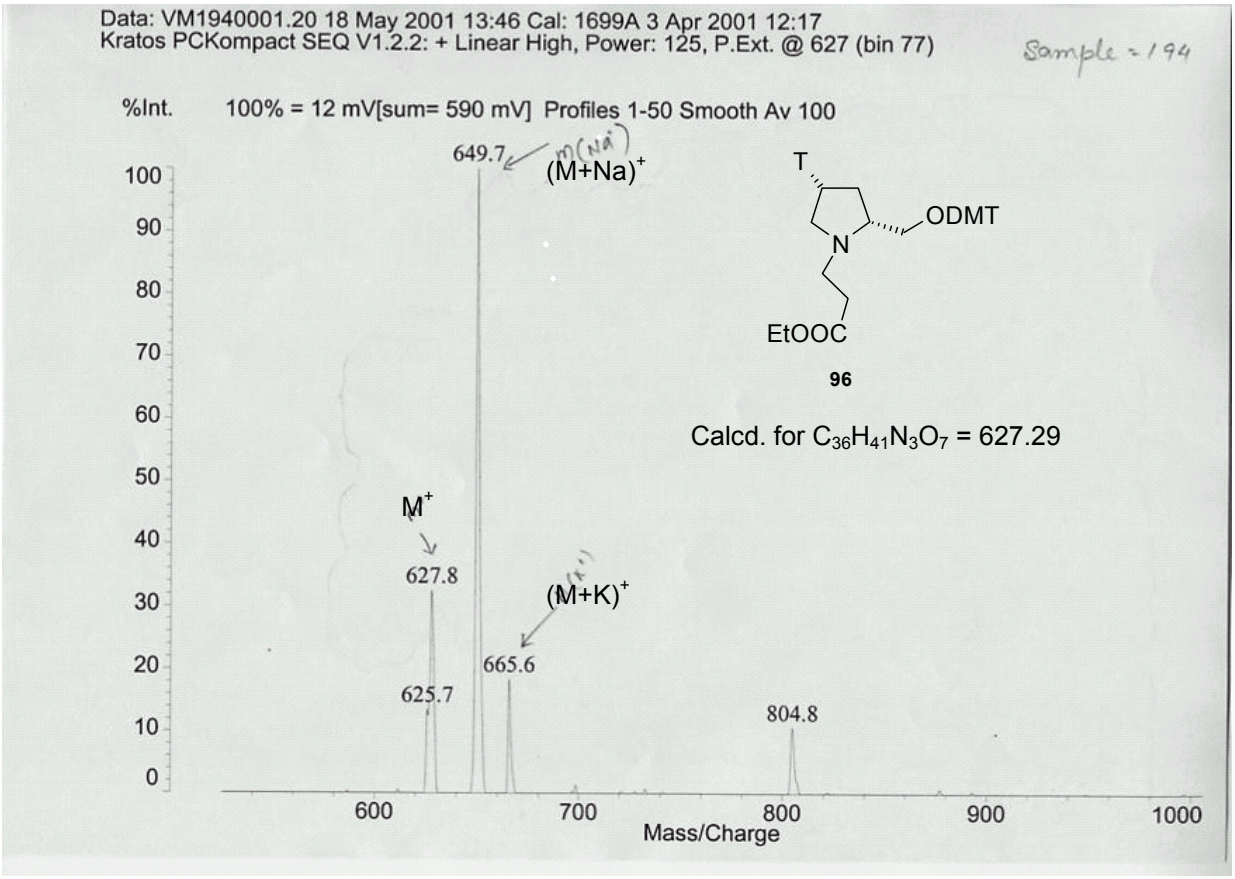

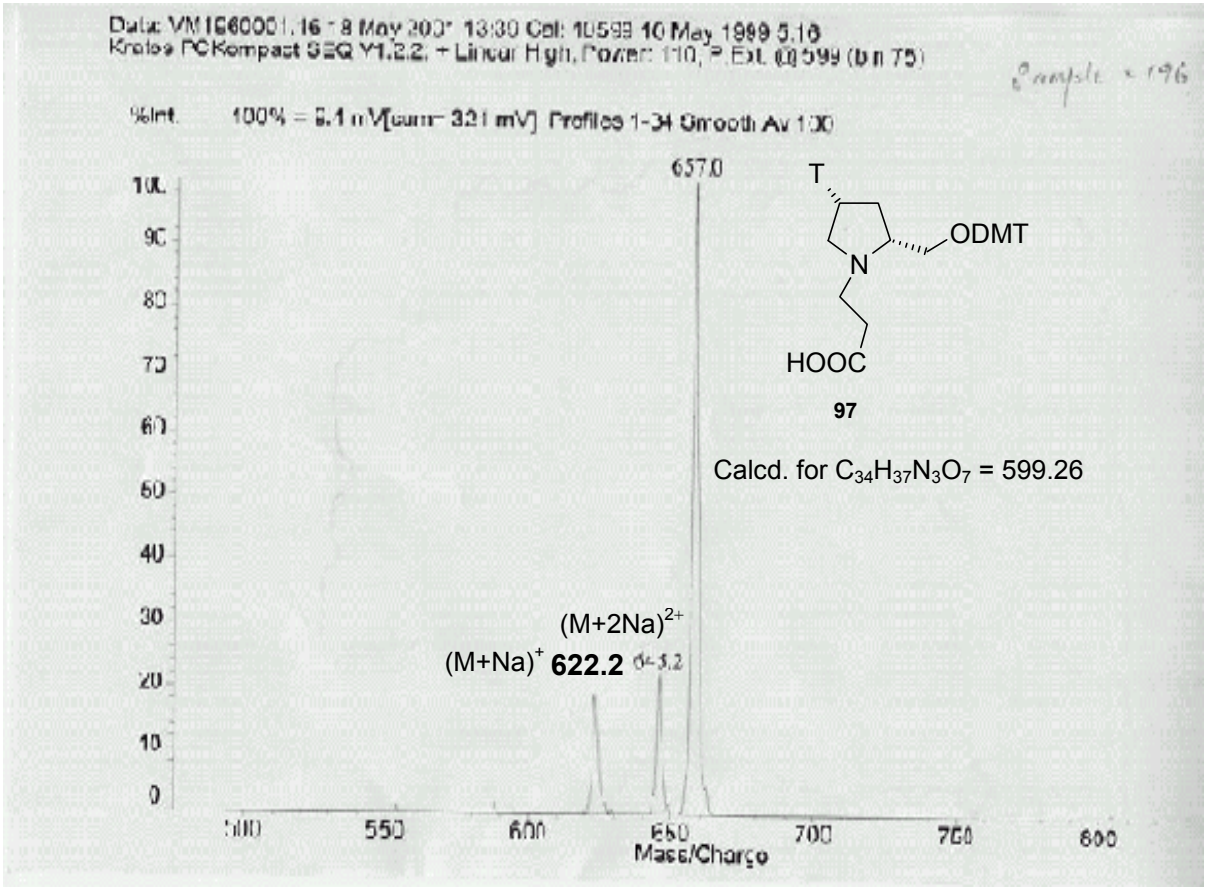

Figure 12. MALDI-TOF spectra of compound **96** and **97**

The phosphoramidite **100** was used for incorporation of the dimer block into oligonucleotides at the desired positions in control DNA by automated solid phase DNA synthesis using N^4-phenoxyacetyl (PAC) 3'-O- phosphoramidites that protected regular amidites on Gene assembler plus synthesizer. The chimeric oligonucleotides were individually hybridized with complementary DNA strand and the Tm of the resulting complexes determined by the temperature dependent change in UV absorbance will be presented here

5.4 Synthesis of Oligonucleotide Sequences

General Method of Oligonucleotide Synthesis and base protected β-cyanoethylphosphoramidites were used for the synthesis of unmodified ODN (1, 3, 4, 6-8 Table 1) and these were prepared on an automated DNA synthesizer using the standard oligonucleotide synthesis protocol (Figure 13). The crude oligonucleotides obtained after deprotection with NH_4OH were desalted and the purity of ODNs was checked by RP-HPLC which showed >95% purity. Therefore, they were used without further purification for biophysical studies.

Synthesis of Chimeric Oligonucleotide Sequences

The dimer was subjected to aq. NH_3 treatment for 16h at 55^oC to check the stability of amide linkage towards the standard cleavage conditions. TLC of the resulting product showed the degradation of the product. Thus, for chimeric oligomers DNA synthesis protocol employed N^4- phenoxyacetyl (PAC) 3'-O-phosphoramidites that could be cleaved under milder NH_4OH conditions. The deoxyribonucleoside phosphoramidites having the PAC group (Schulhof et al., 1987) for protection of the exocyclic amino function of adenine and guanine, and the isobutryl group for that of cytosine, were necessary to ensure rapid ODN deprotection with conc. NH_4OH at room temperature without affecting the amide linkage. The dimer phosphoramidite was incorporated into ODN sequences at the desired positions by automated DNA synthesis to yield the chimeric ODNs **2** and **5** (Table 1). The coupling yields of the chimeric ODNs were >93% as quantified by the released DMT cation. The synthesized ODNs after on-column detritylation were cleaved form the solid support with conc. NH_4OH, lyophilized and desalted to get the crude ODNs. The purity of these crude ODNs were checked by RP-HPLC and found to be more than >95%.

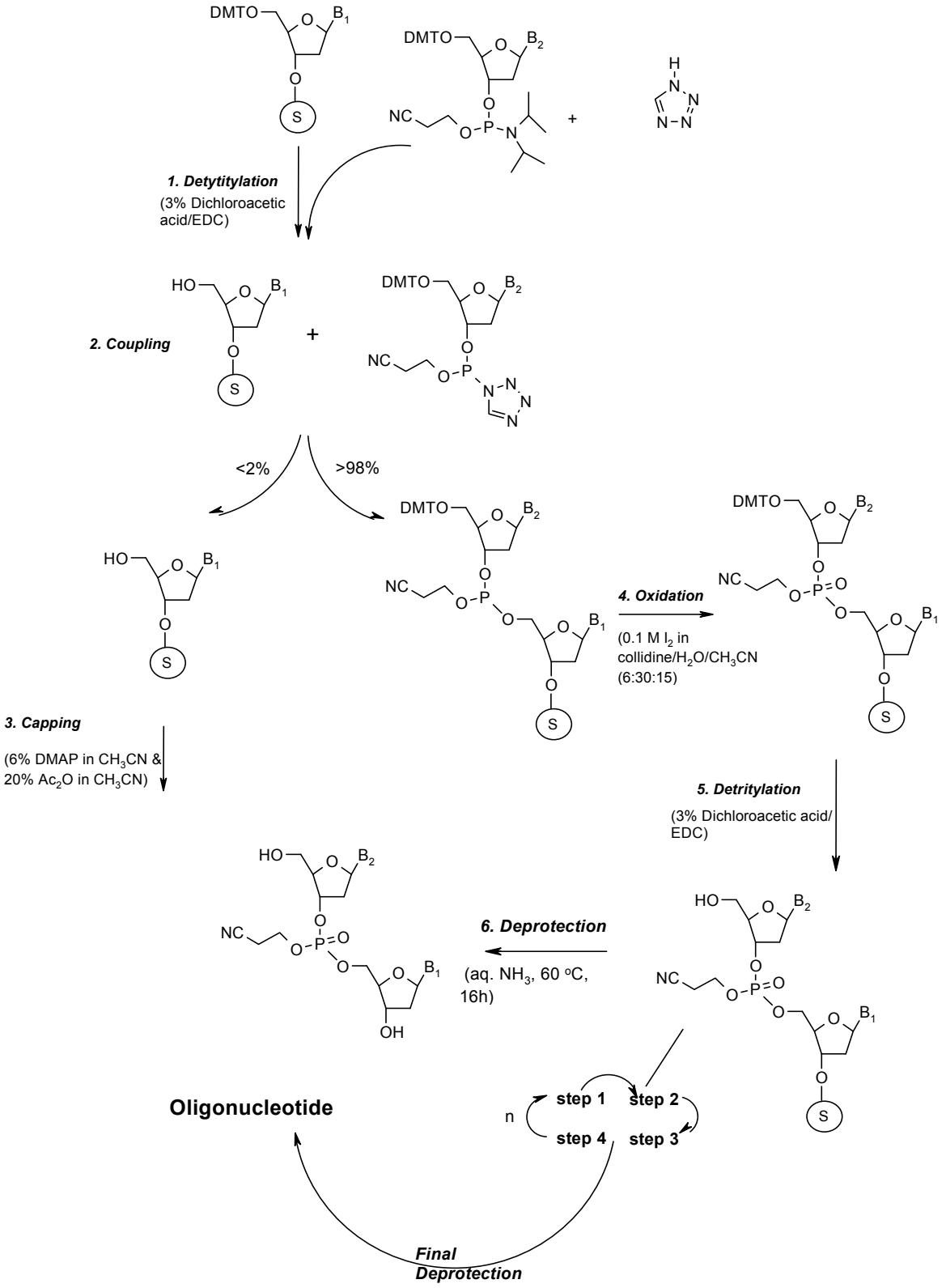

Figure 13. Solid phase chemical synthesis of oligodeoxynucleotides

Table 1. DNA and chimeric DNA sequences

Entry	**Sequence**
1	TTC TTC TTC TTT TCT TTT
2	TTC TTC TTC **t*T**T TCT TTT
3	AAA AGA AAA GAA GAA GAA
4	CTT GTA CTT TTC CGG TTT
5	CTT GTA CT**t*T**TC CGG TTT
6	AAA CGG GAA AAG TAC AAG
7	TCC AAG AAG AAG AAA AGA AAA TAT
8	ATA TTT TCT TTT CTT CTT CTT GGA

t*T = pyrrolidinamide dimer block

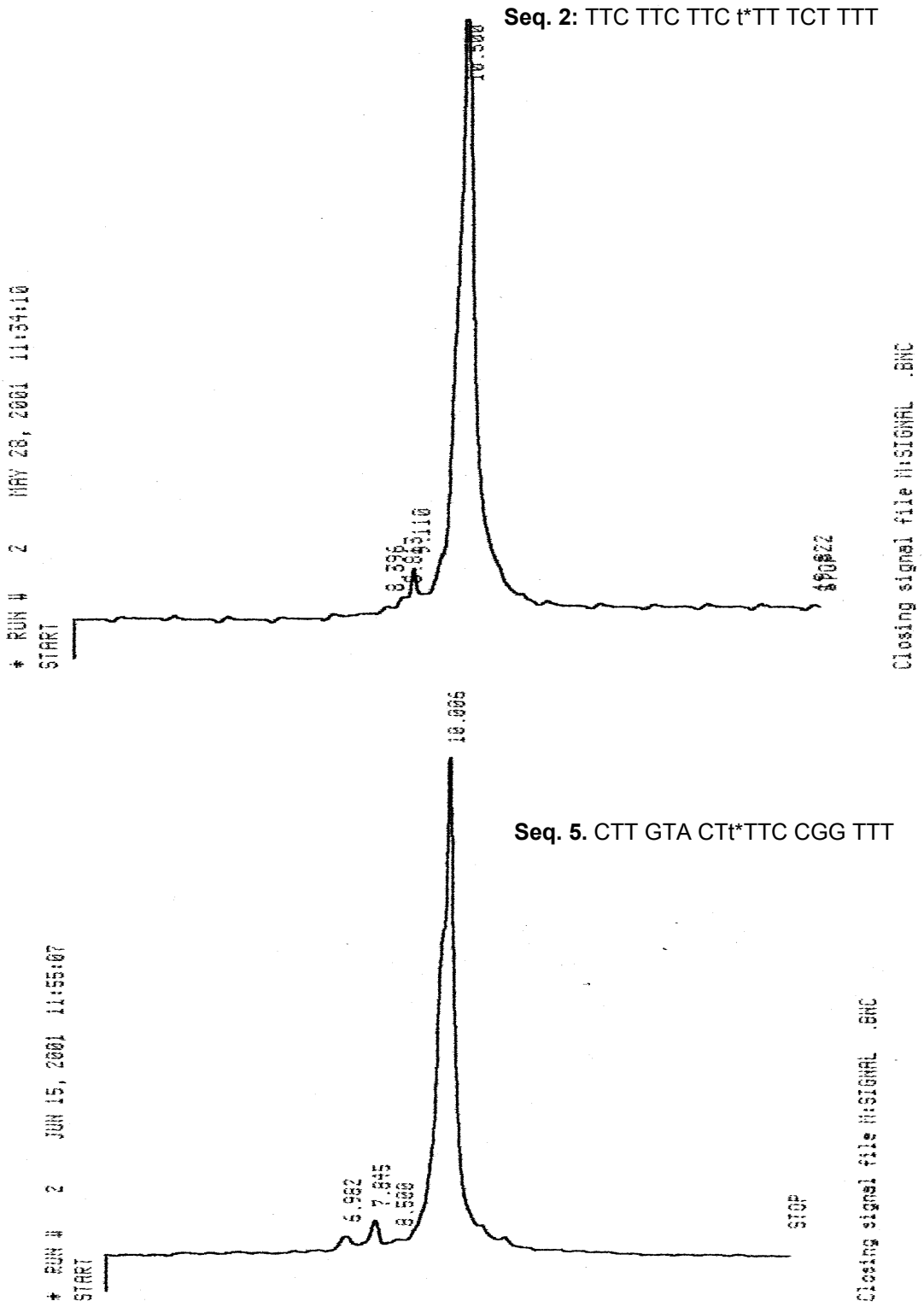

Figure 14. HPLC profiles of crude chimeric oligomers

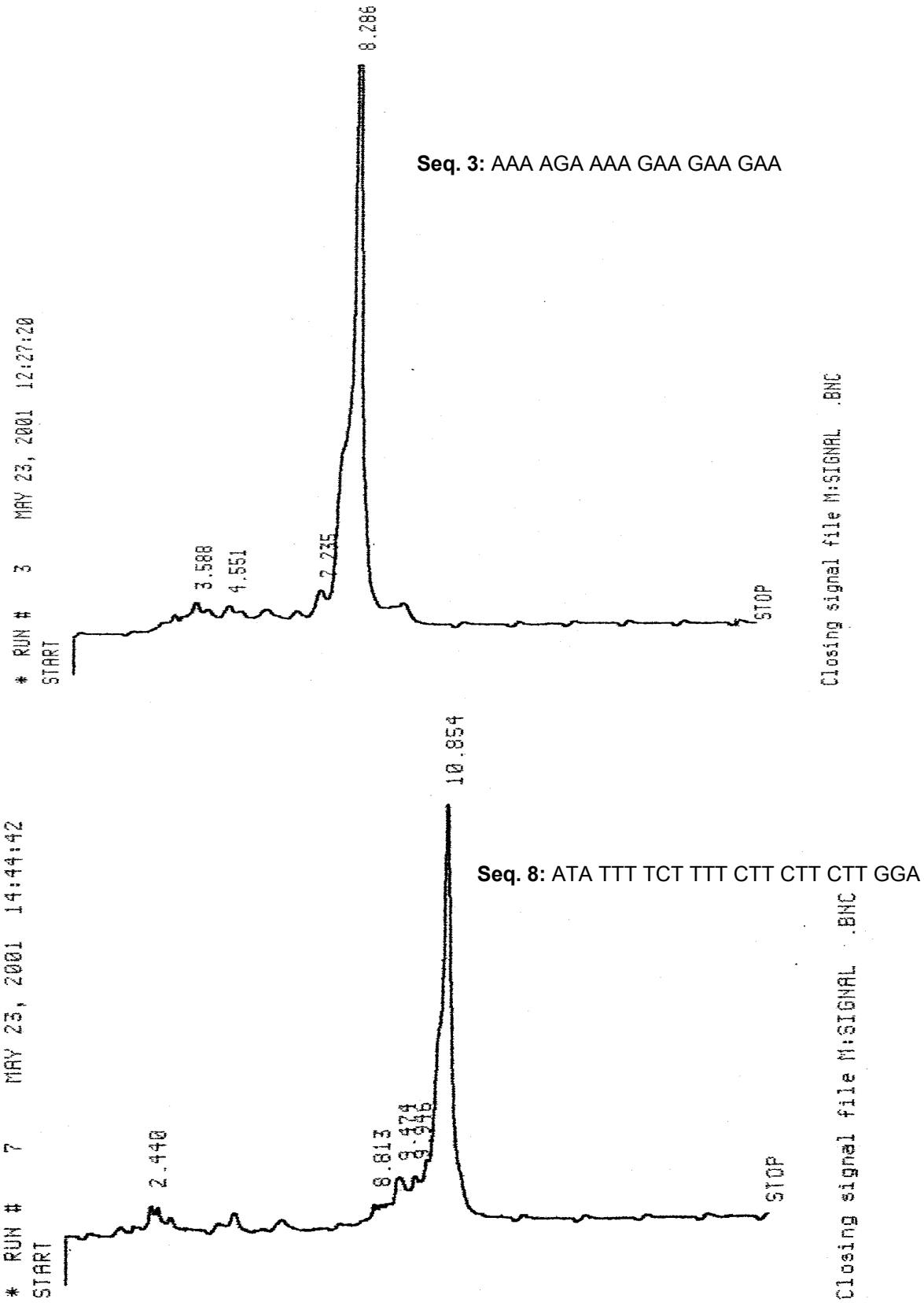

Seq. 3: AAA AGA AAA GAA GAA GAA

Seq. 8: ATA TTT TCT TTT CTT CTT CTT GGA

Figure 15. HPLC profiles of crude oligomers

5.5 UV-Melting Studies of Chimeric Oligonucleotides

The binding affinity of the chimeric oligonucleotides (**2** and **5**) to their complementary nucleic acid sequences was investigated by measuring the melting

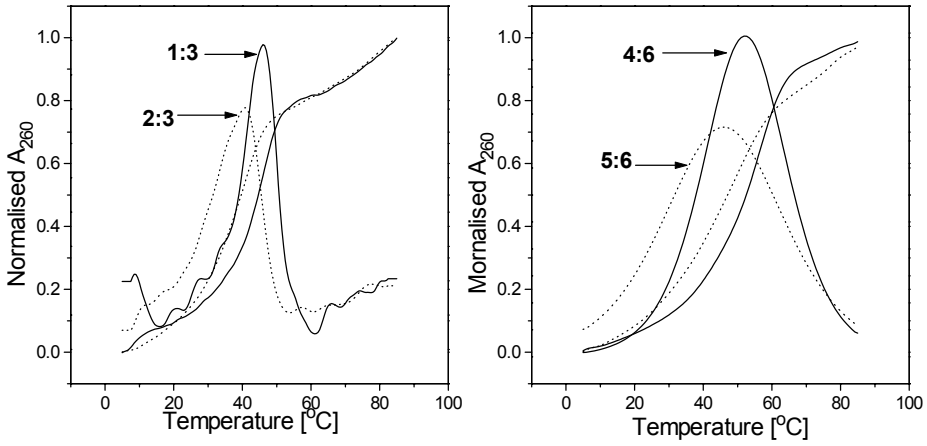

Figure 15. UV-melting profiles of duplex DNA in the 10mM phosphate buffer pH=7.3 and 100mM NaCl

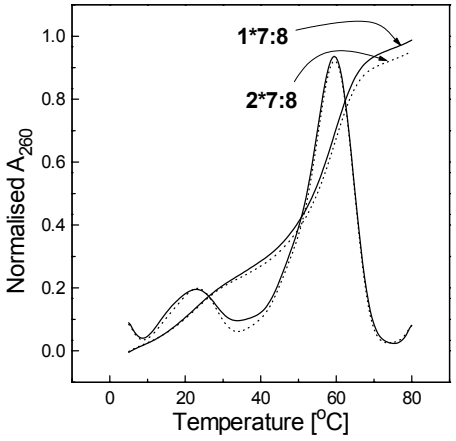

Figure 16. UV-melting profile of the DNA truplexes. Buffer: 10mM phosphate pH=7.3, 200mM NaCl

temperatures (Tms) of the duplexes and triplexes. The Tm experiments of duplexes were carried out in phosphate buffer (pH 7.0) containing 100 mM NaCl. The chimeric ODN **2** and **5** were individually hybridized with the complementary DNA strands **3** and **6** respectively, to obtain duplexes while all DNA duplexes **1:3** and **4:6** served as the references. The observed sigmoidal transitions (Figure 15) indicated successful formation of duplexes. The reference polypyrimidine/ polypurine duplex **1**:**3** exhibited a

Tm of 46°C (entry 1, table 2). The incorporation of the chimera in the middle of the polypyrimidine sequence as in the complex **2**:**3** led to the destabilization over the control by 5°C (T_m=41°C) (entry 2). The mixed pyrimidine-purine DNA sequence **4** showed a Tm of 51.8°C (entry 3) when complexed with complementary strand **6**, whereas the chimeric sequence **5** with the amide linkage at the center destabilised the complex **5**:**6** by 5.6°C (entry 4).

Table 2. UV-Tm of chimeric DNA duplexes and triplexes

Entry	**Sequences**	**Complex**	**Tm (°C)**	**Δ Tm (°C) (Lit.)**
1	5'-TTC TTC TTC TTT TCT TTT 3'-AAG AAG AAG AAA AGA AAA	1:3	46.0	
2	5'-TTC TTC TTC t*TT TCT TTT 3'-AAG AAG AAG AAA AGA AAA	2:3	41.0	-5 (-7)
3	5'-CTT GTA CTT TTC CGG TTT 3'-GAA CAT GAA AAG GCC AAA	4:6	51.8	
4	5'-CTT GTA CTt*TTC CGG TTT 3'-GAA CAT GAA AAG GCC AAA	5:6	46.2	-5.6 (-6)
5	5'-TTC TTC TTC TTT TCT TTT 5'-TCC AAG AAG AAG AAA AGA AAA TAT 3'-AGG TTC TTC TTC TTT TCT TTT ATA	1*7:8	23.5	
6	5'-TTC TTC TTC t*TT TCT TTT 5'-TCC AAG AAG AAG AAA AGA AAA TAT 3'-AGG TTC TTC TTC TTT TCT TTT ATA	2*7:8	23.5	0 (-4)

Tm values in parentheses indicate the melting temperatures of the oligomers derived from modification **6a** in above sequences at same positions. Experiments were repeated thrice and the Tm values are obtained from the peaks in the first derivative plots.

When the chimeric DNA **2** was used as a third strand to complex with the duplex **7***8, in phosphate buffer containing 200mM NaCl the triplex formed (**2**:**7***8) showed the same Tm as that with the reference 1:7*8.

The duplex melting studies show that when modification is present in polypyrimidine sequence, the complex was stabilised by 2°C compared to the similar complex formed by the 4-atom linker (Figure 9a). The complex **2**:**3** exhibited a Tm of

41^0C, whereas the reference duplex for this complex showed a Tm of 46^0C indicating a destabilization compared to unmodified DNA. However, when the modification is present in the mixed purine/pyrimidine sequence, it showed marginal stabilization compared of the duplex formed compared to the duplex formed by its analogue 4-atom linker.

The introduction of the dimer block in a polypyrimidine sequence when studied for triplex formation **2**:**7*8** showed 4^0C compared to the triplex formed by 4-atom linker, and showed the same Tm as exhibited by the unmodified DNA **1**:**7*8**. This indicates that the amide linked five-atom backbone is tolerated more for triplex studies.

5.6. Conclusions

A fully automated solid-phase synthetic procedure for the incorporation of amide linked pyrrolidine/sugar dimer block into DNA sequences has been developed. Although both duplexes (**2**:**3** and **5**:**6**) resulted in a decreased binding to a complementary native sequence, these results show that, 5 atom linker resulted in a better binding than a 4 atom linker. In the triplex too, the 5-atom linker is completely tolerated when present in the center unlike the 4- that destabilised it by 4^oC. Thus, it is proved here that 5-atom nonphosphorous replacements (in particular amides) have merits compared to universally used 4-atom linker. The presence of positive charge on pyrrolidine PNA may also favour cell permeation as seen in the case of cationic peptide-PNA conjugates (Simmons et al., 1997).

The (2*R*,4*R*) stereochemistry used for the pyrrolidine-sugar thymine dimer unit was expected to be compatible with DNA geometry (Hickman et al., 2000), the nucleobase being *cis* to the aminomethyl segment of the backbone, as the *cis*-hydroxymethyl in the DNA sugar. However, the pyrrolidine ring nitrogen being positively charged, might adopt a ring pucker that results in a nucleobase orientation detrimental to duplex formation with the complementary DNA as seen in the crystal structure of the pyrolidine monomer (2*R*,4*S*) in Chapter 2 where *trans*-pyrrolidine (2*S*,4*R*) is found to be the optimal strereochemistry to be introduced. Thus, further studies on the effective stereochemical preferences exerted by these units on the DNA/RNA binding properties are necessary.

5.7 Experimental Section

(2R,4S) N1-benzyloxycarbonyl-4-O-benzoyl proline methyl ester **91**

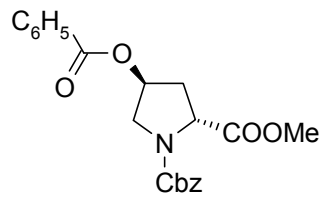

91

To a solution of N-Cbz proline methyl ester **13** (10 g, 35.8 mmol), benzoic acid (5.22 g, 42.8 mmol) and triphenyl phosphine (11.2g, 42.8mmol) in dry THF (100ml), DIAD (8.4ml, 42.8mmol) was added dropwise at 0^{o}C. The reaction mixture was stirred at room temperature for 4h and the solvent was removed in vacuum to obtain an oily residue. Diethylether (20ml) was added to this residue and PPh_3O was precipitated by addition of petroleum ether. PPh_3O precipitate was filtered off, filtrate was concentrated and purified by silica gel column chromatography to get the pure benzoyl ester **87** (10.6 g, yield=77.3%).

^{1}H CDCl$_3$ δ: 7.97-7.93 (m 2H Bz), 7.57-7.5 (m 1H Bz), 7.42-7.35 (m 2H Bz), 7.29 9s 5H $C_6\underline{H}_5$), 5.24-4.98 (m 3H O$C\underline{H}_2$, C4$\underline{H}$), 4.62-4.47 (m 1H C2$\underline{H}$), 3.92-3.82 (m 2H C5$\underline{H}$), 3.74-3.53 (m 3H O$C\underline{H}_3$), 2.65-2.49 (m 1H C3$\underline{H}$), 2.38-2.23 (m 1H C3'$\underline{H}$)

(2R,4S) N1-benzyloxycarbonyl-4-hydroxy proline methyl ester **92**

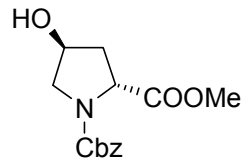

92

To compound **91** (10.5 g, 27.3 mmol) in dry methanol (100 ml), Na metal (50mg, 2mmol) was added and the mixture was stirred at room temperature for 1h. Solid $KHSO_4$ was added to the reaction mixture till the pH reached 7.0. The solution was filtered and the solvent was removed under *vacuo*. After silica gel column chromatography using EtOAc/Pet ether compound **92** was obtained. (5.92 g, yield=77.8 %).

^{1}H (CDCl$_3$) δ 7.45-7.2 (m 5H $C_6\underline{H}_5$), 5.2-4.8 (m 2H O$C\underline{H}_2$), 4.6-4.4 (m 2H C4$\underline{H}$), 3.8-3.4 (m 6H O$C\underline{H}_3$, C5$\underline{H}$, C2$\underline{H}$), 2.4-2.2 (m 1H C3$\underline{H}$), 2.1-2.95 (m 1H C3'$\underline{H}$)

$\alpha^{27}{}_D$= -4.96

(2R,4R) N1-benzyloxycarbonyl-4(N3-benzoyl-thymin-1-yl) proline methyl ester **93**

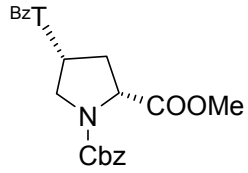

93

N3-benzoylthymine (9.4g, 40.8mmol) and PPh_3P (10.7g, 40.8mmol) were added to compound **92** (5.92g, 20.4mmol) in dry benzene (100ml). The contents were cooled to 5^{o}C in an ice bath and DEAD (1.6ml, 40.8mmol) was added dropwise into it. After completion of the reaction as indicated by TLC (4h), the solvent was removed in vacuum and the residue was purified by silica

gel column chromatography to get the pure product **93** (6g, yield=60%, Rf=0.3 EtOAc:Pet ether 1:1).

^{1}H ($CDCl_3$) δ: 8.0-7.3 (m 10H ArH), 5.4-5.1 (m 3H C4H, OCH_2), 4.6-4.4 (m 1H C5H), 4.15-3.9 (m 1H C5'H), 3.9-3.6 (m 4H OCH_3, C2H), 2.3-2.1 (m 1H C3'H), 2.0 (s 3H CH_3-Thy).

(2R,4R)N1-benzyloxycarbonyl-4(N3-benzoyl-thymin-1-yl)2-hydroxymethyl pyrrolidine **94**

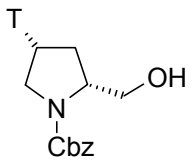

94

To a solution of **93** (5g, 10.1 mmol) in dry THF (100 ml) at 0°C, $LiBH_4$ (o.44g, 20.2 mmol) was added in two portions and stirred at room temperature. After 8h, the reaction mixture was brought to pH 2.0 with saturated aq. NH_4Cl, concentrated to obtain a white solid, to which water (30ml) was added and was extracted with EtOAc:MeOH (8:2). Upon concentration of the organic layer followed by silica gel (100-200mesh) column chromatography with EtOAc:Pet ether, compound **94** (3.2g, yield= 90%) was obtained.

^{1}H $CDCl_3$ δ: 7.5-7.3 (s 5H Ar<u>H</u>), 5.2-5.0 (m 3H O<u>CH</u>$_2$Ph, C4<u>H</u>), 4.2-3.9 (m 1H C5<u>H</u>), 3.8-3.6 (m 1H C5'<u>H</u>), 3.4-3.25 (m 1H C2<u>H</u>), 2.35-2.1 (m 2H C3<u>H</u>), 1.9 (s 3H Thy-C<u>H</u>$_3$)

FAB-MS $(M+H)^+$=360, $(M+Na)^+$ =382 (Calcd for $C_{18}H_{21}N_3O_5$)=359.14

(2R,4R)N1-benzyloxycarbonyl-4(N3-benzoyl-thymin-1-yl)2-(4,4'-dimethoxytrityl)oxymethyl pyrrolidine **95**

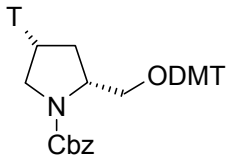

95

The compound **94** (1g, 2.78mmol) was dried by co-evaporation with dry pyridine (2x10 ml), dissolved in dry pyridine (10ml) and DMTrCl (1.6g, 4.7mmol) was added to the above solution. After stirring at room temperature for 8h, the reaction mixture was concentrated, dissolved in dichloromethane (30ml) and washed with $NaHCO_3$ solution. Concentration of the organic fraction gave the crude product which after silica gel column chromatography afforded the compound **95** (0.92g, yield=51%, Rf= 0.2, MeOH:CH_2Cl_2:Py 1:99:0.05) as a light yellowish foam.

^{1}H NMR ($CDCl_3$) δ 8.6 (m 1H <u>H</u>6-Thy), 8.5-8.4 (bs 1H N<u>H</u>), 7.5-7.1 (m 14 H Ar<u>H</u>), 6.9-6.7 (d 4H Ar<u>H</u>), 5.3-5.0 (m, 3H C<u>H</u>$_2$-Ph, C4<u>H</u>), 4.25-4.0 (m 2H OC<u>H</u>$_2$), 3.8 (s 6H OC<u>H</u>$_3$), 3.6-3.35 (m 2H C5<u>H</u>), 3.2-3.0 (m 1H C2<u>H</u>), 2.6-2.4 (m 1H C3<u>H</u>), 2.2-2.0 (m 1H C3'H), 1.7 (s C<u>H</u>$_3$-Thy)

(2R,4R)N1-carbethoxymethyl-4(N3-benzoyl-thymin-1-yl)2-(4,4'-dimethoxytrityl)oxymethyl pyrrolidine **96**

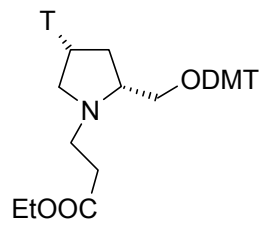

96

Compound **91** (0.9g, 1.36mmol) was taken in MeOH (10ml) and 10% Pd-C (0.15g) was added into it. After the addition of pyridine (0.2ml) the slurry was subjected to hydrogenation at 55psi H_2 for 10h. The catalyst was filtered off through celite and to this filtrate ethylacrylate (0.3ml, 3mmol) was added. The reaction mixture was stirred at room temperature for 2h and concentrated to get the crude product which was purified by silica gel column chromatography to get pure **96** (0.52 g, yield=60%, Rf=0.2 MeOH:DCM:Py 2:98:0.05).

^{1}H NMR ($CDCl_3$) δ 9.6 (bd 1H N<u>H</u>-Thy), 8.65 (d 1H Thy-<u>H</u>6), 7.78-7.21 (m 9H Ar), 6.85-6.81 (d 2H Ar J=8.79Hz), 5.18-5.1 (m 1H C4<u>H</u>), 4.1 (q 2H OCH_2CH_3, J=7.33Hz), 3.79 (s 6H $OC\underline{H}_3$), 3.28-3.14 (m 4H $OC\underline{H}_2$, C5<u>H</u>), 2.59-2.35 (m 6H C2<u>H</u>, C3<u>H</u>, $NC\underline{H}_2C\underline{H}_2$), 1.78 (4H C3'H, $C\underline{H}_3$-Thy), 1.19 (t 3H $OCH_2C\underline{H}_3$ J=7.33Hz)

^{13}C NMR ($CDCl_3$) δ 171.7 (<u>C</u>OOEt), 164 (C4-Thy), 158.2 (C2-Thy), 149.3 (C6-Thy), 151.2, 144.6, 137.7, 135.7, 129.8, 127.6, 127.4, 126.5, 123.4, 112.8 (Ar-DMT), 110.70 (Thy-C5), 85.9 ($C\underline{C}Ph_3$), 63.7 (<u>C</u>4), 60.02 ($COO\underline{C}H_2CH_3$), 58.7 (O-$C\underline{H}_2$-DMT), 54.7 (OCH_3-DMT), 51.34 (C2), 49.2 (($\underline{C}$5, $N\underline{C}H_2$), 33.74 ($NCH_2\underline{C}H_2$), 33.7 (<u>C</u>3), 13.8 ($OCH_2\underline{C}H_3$), 12.1 (Thy-$\underline{C}H_3$).

MALDI-TOF $(M)^+$=627.8, $(M+Na)^+$=649.7, $(M+K)^+$=665.6 (Calcd. for $C_{36}H_{41}N_3O_7$=627.29)

(2R,4R) N1- carboxymethyl -4(N3-benzoyl-thymin-1-yl) 2-(4,4'-dimethoxytrityl)oxymethyl pyrrolidine **97**

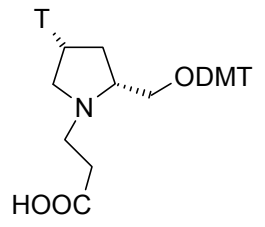

97

The ethyl ester **96** (0.5 g, 0.79 mmol) was taken in methanol (2ml) and 2N aq. NaOH (3ml) was added. Stirring was continued for 2h, after which, the excess alkali was neutralized with $NaHSO_3$ solution, and the resulting mixture was concentrated and extracted with chloroform. Upon concentration of the organic layer under vacuum, the product **93** was obtained in good yields (0.47 g, yield=98.5%, Rf=0.3, MeOH:DCM:Py 9:98:0.05).

MALDI-TOF $(M+Na)^+$=622.2, $(M+2Na)^{2+}$=645.2 (Calcd. for $C_{34}H_{37}N_3O_7$=599.26)

3'-Hydroxy-T,T-Dimer **99**

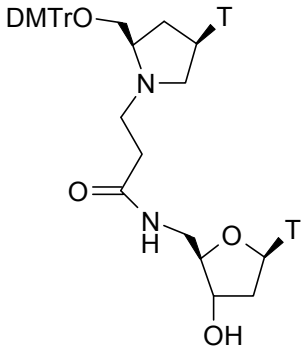

99

To compound **97** (0.45g, 0.75mmol) in dry DMF (2ml), TBTU (0.26g, 0.83mmol), DIEA (0.14 ml, 0.83 mmol) and HOBt (0.112g, 0.83mmol) were added and stirred for 15min. 3'-O-acetyl-5'-amino-5'-deoxythymidine **98** (0.21g, 0.75mmol) was then added into the reaction mixture and further stirred at room temperature for 1.5h. The reaction mixture was concentrated to dryness, dissolved in $CHCl_3$ (30ml) and washed with 5% $NaHCO_3$ solution (10ml). The organic layer was dried over anhy. Na_2SO_4 and concentrated to get the crude product. This was purified by column chromatography using $CHCl_3$/MeOH to get pure product **99**.

^{1}H NMR ($CDCl_3$) δ 10.22 (bs 1H N<u>H</u>-Thy), 8.62 (d 2H J=4.39 Ar-DMT), 7.75-7.65 (m 2H <u>H</u>6-Thy X 2), 7.45-7.13 (m 7H Ar-DMT), 6.8 (d 4H J=7.32, Ar-DMT), 6.05 (m 1H C'1<u>H</u>), 5.03 (m 1H C4<u>H</u>-Py), 4.3 (m 1H C3'<u>H</u>), 3.9 (m 1H C'5<u>H</u>), 3.76 (s 6H OCH_3-DMT), 3.58-3.04 (m 7H C<u>H</u>$_2$ODMT, C5<u>H</u>, C5'<u>H</u>, C'2<u>H</u>, C2<u>H</u>, O<u>H</u>), 2.71-2.2 (m 8H NC<u>H</u>$_2$C<u>H</u>$_2$, C'5-C<u>H</u>$_2$NH, C3<u>H</u>, C3'<u>H</u>), 1.84, 1.64 (2s 6H CH_3-Thyx2)

3'-O-(2-cyanoethyl-N,N-diisoprpylphosphoramido)-5'-O-(4,4'-dimethoxy) trityl-dimer **100**

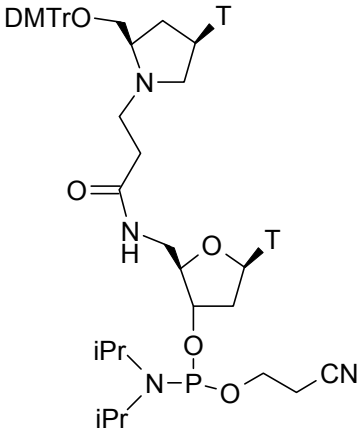

100

Compound **99** (0.12g, 0.14mmol) was dissolved in dry EDC (1ml) followed by the addition of tetrazole (13mg, 0.18mmol) and 2-cyanoethyl-N,N,N',N'-tetraisopropyl-phosphorodiamidite (66mg, 0.22mmol) and the reaction mixture was stirred at room temperature for 3h. The contents were then diluted with dry dichloromethane and washed with 5% $NaHCO_3$ solution. The organic phase was dried over anhy. Na_2SO_4 and concentrated to a foam. The residue was dissolved in DCM and precipitated with hexane to obtain **100** (0.13g, yield=87%). The phosphoramidite was dried overnight over P_2O_5 and KOH in a desiccator before using on DNA synthesizer. TLC shows two close moving spots for two diastreomers (Rf=0.5, EtOAc).

^{31}P NMR ($CDCl_3$) δ 148.37, 147.82.

Oligonucleotide synthesis

Base protected standard nucleoside phosphoramidites (A,T,C,G) and nucleoside derivatised controlled pore glass supports from Cruachem were used. The DNA synthesis was carried out on Pharmacia LKB Gene Assembler Plus. Dry solvents

were used for synthesis. The commercially available amidites (0.1M) were dissolved in dry acetonitrile while 0.15M solution was prepared for dimer phosphoramidite and 4A molecular sieves were added to it to remove traces of moisture. Acetonitrile was distilled over P_2O_5 and then twice over CaH_2 immediately before use. Dichloroethane was dried by distilling twice over P_2O_5. For oxidation, after each coupling, 0.1M iodine in collidine, water and acetonitrile, while for capping, 20% acetic anhydride in acetonitrile was used. The solid phase synthesis protocol is summarized in Figure 13.

HPLC Analysis

To check the purity of unmodified and chimeric oligonucleotides, Merck-Lichrosphere Lichrocart 100RP-18 (250x4mm) endcapped (5μm) column was used. A gradient elution method with A to B in 20 min. was used, where buffer A was 5%CH_3CN in 0.1M TEAA and buffer B was 30%CH_3CN in 0.1M TEAA with flow rate 1.5ml/min. The HP 1050 multiwavelength UV detector was used which was set at 254nm.

UV-Tm Studies

Oligonucleotide duplexes were constituted by mixing together stoichiometric quantities (1μmol) of the corresponding complementary strands in 10mM phosphate buffer containing 100 mM NaCl and 0.1 mM EDTA at pH 7.3. The samples were annealed and UV-Tm experiments carried out.

The various triplexes containing the respective triads (Table 2) were individually constituted by taking 1 μM each of the appropriate single strands based on the UV absorbance at 260 nm. The three constituents were taken in 10 mM sodium phosphate buffer containing 200 mM NaCl at pH 7.3 and were annealed. The thermal stability of triplexes was measured by following UV-Tm experiments.

Appendix IV

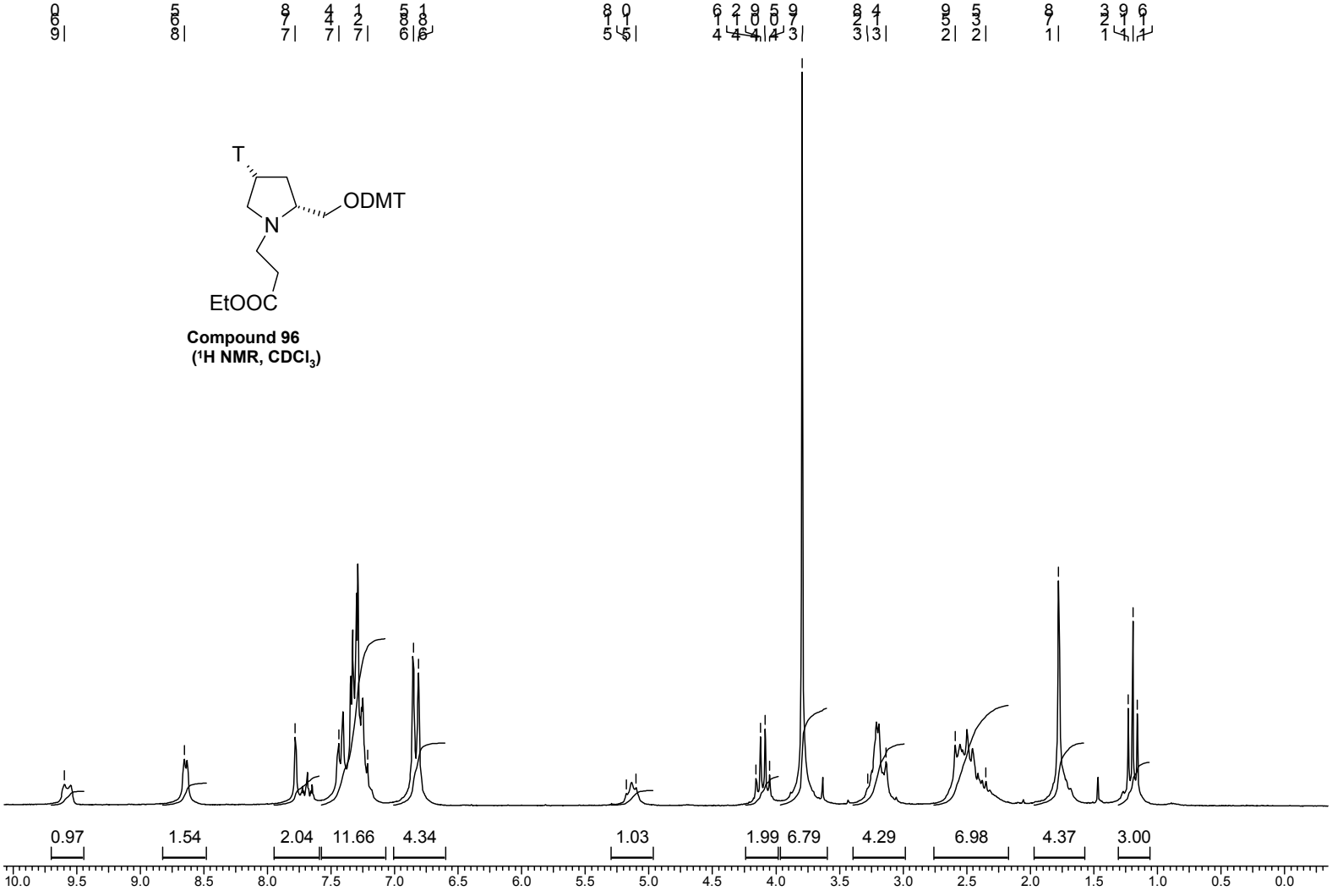

Compound 96
(^{1}H NMR, $CDCl_3$)

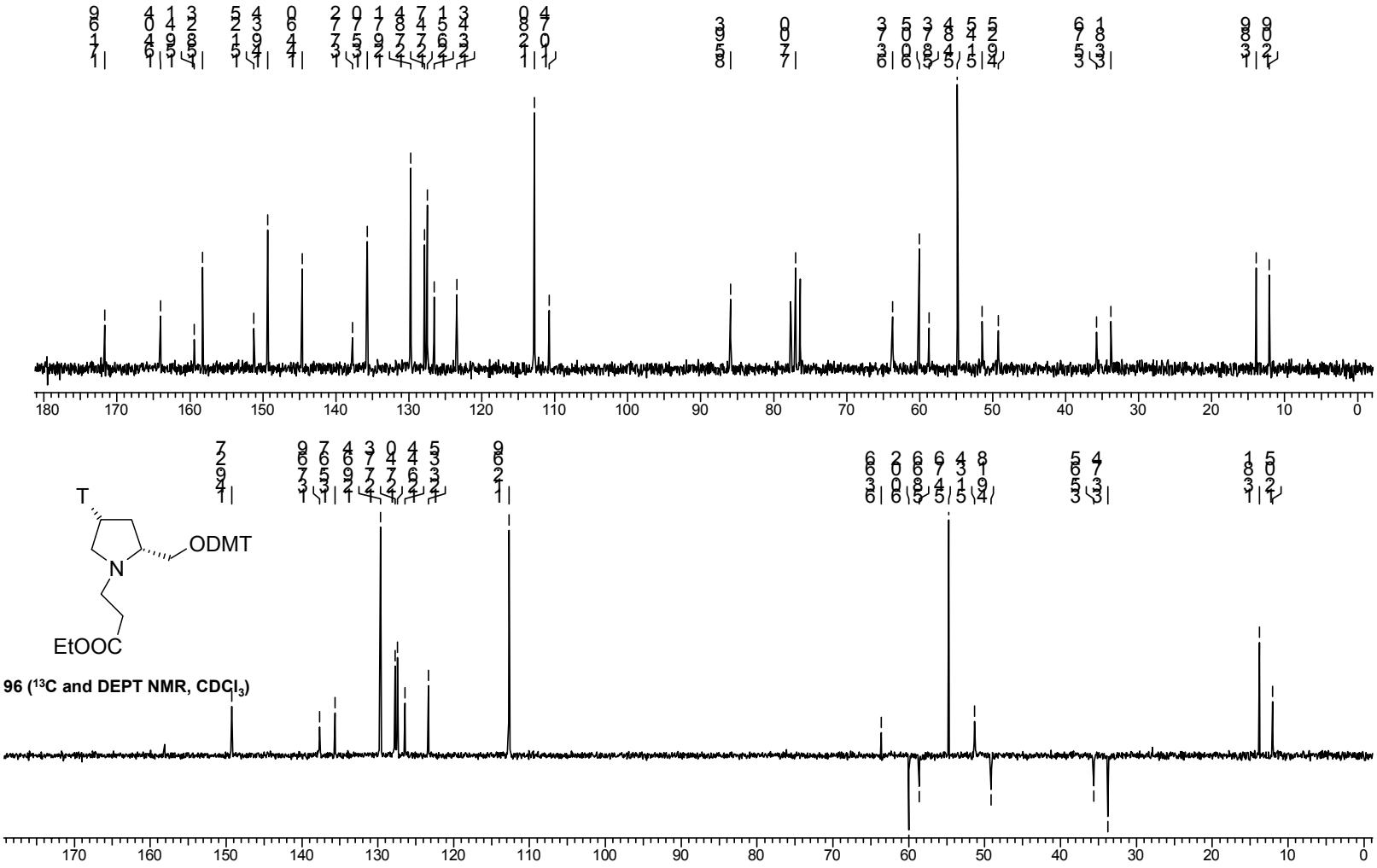

96 (^{13}C and DEPT NMR, $CDCl_3$)

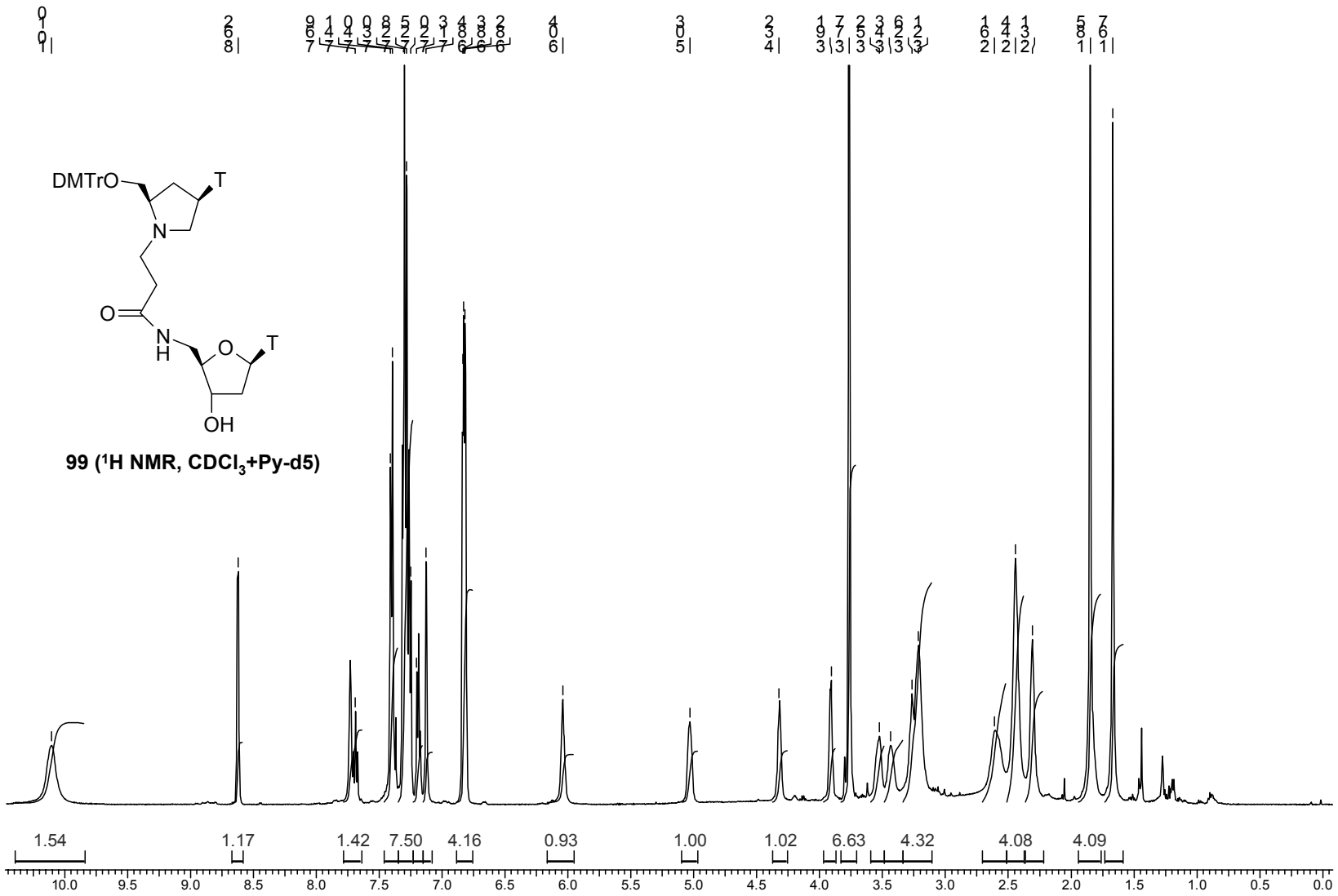

99 (^{1}H NMR, $CDCl_3$+Py-d5)

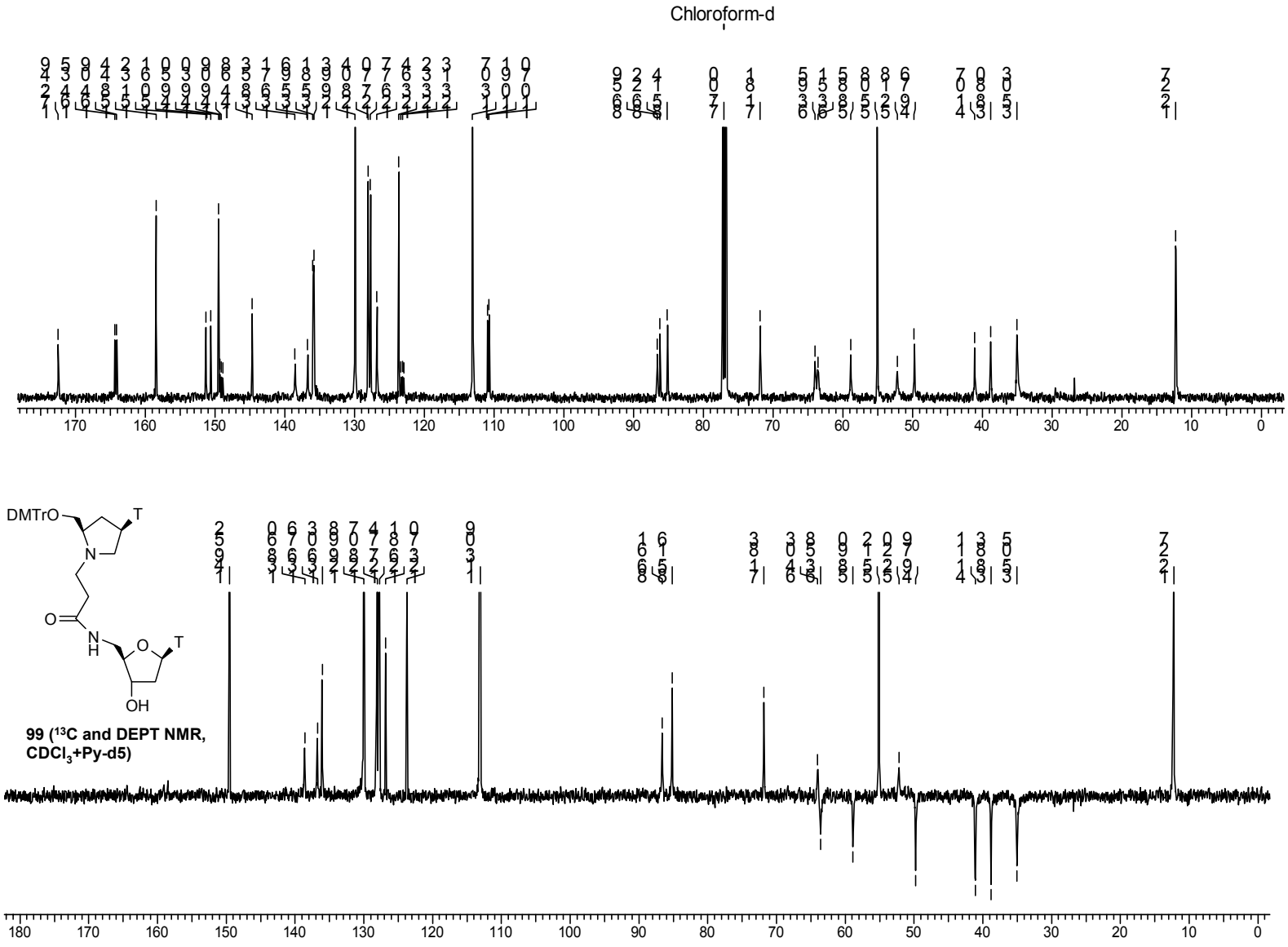
Chloroform-d
DMTrO
T
N
O
N
H
O
T
OH
99 (13C and DEPT NMR, CDCl3+Py-d5)

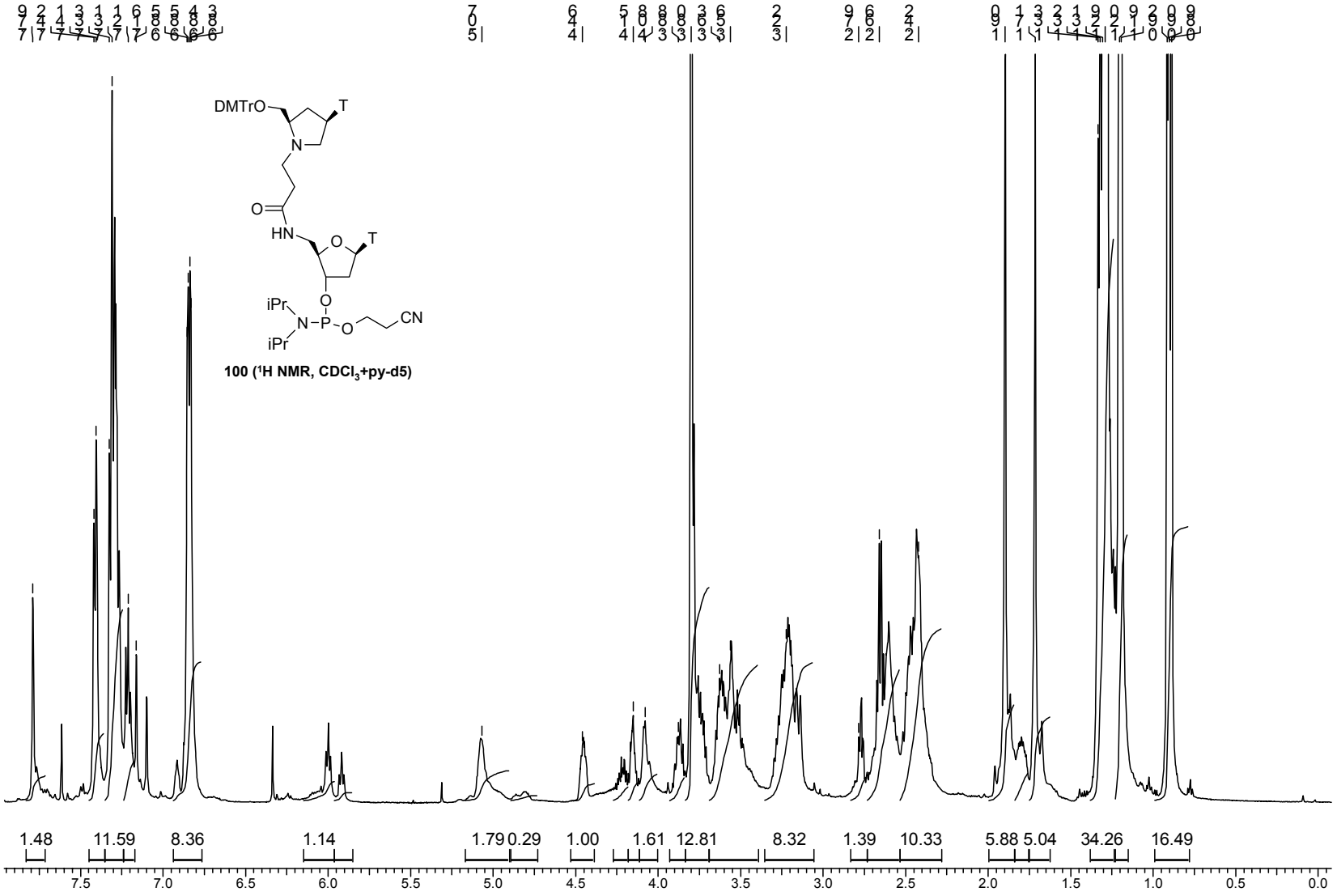
DMTrO
T
N
O
HN
O
T
O
iPr
N
P
O
CN
iPr
100 (1H NMR, CDCl3+py-d5)
1.48
11.59
8.36
1.14
1.79
0.29
1.00
1.61
12.81
8.32
1.39
10.33
5.88
5.04
34.26
16.49
7.5
7.0
6.5
6.0
5.5
5.0
4.5
4.0
3.5
3.0
2.5
2.0
1.5
1.0
0.5
0.0

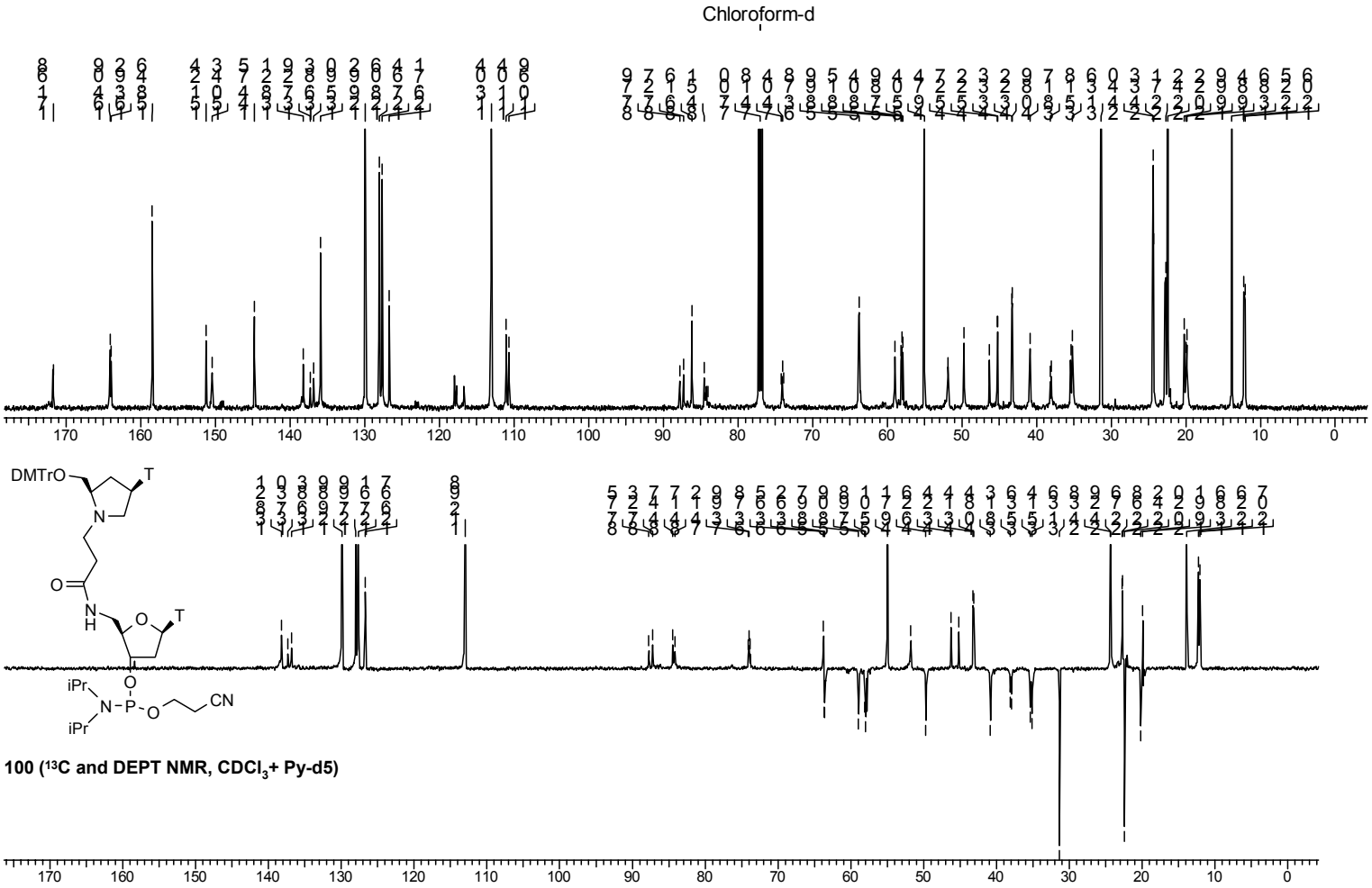

100 (^{13}C and DEPT NMR, $CDCl_3$+ Py-d5)

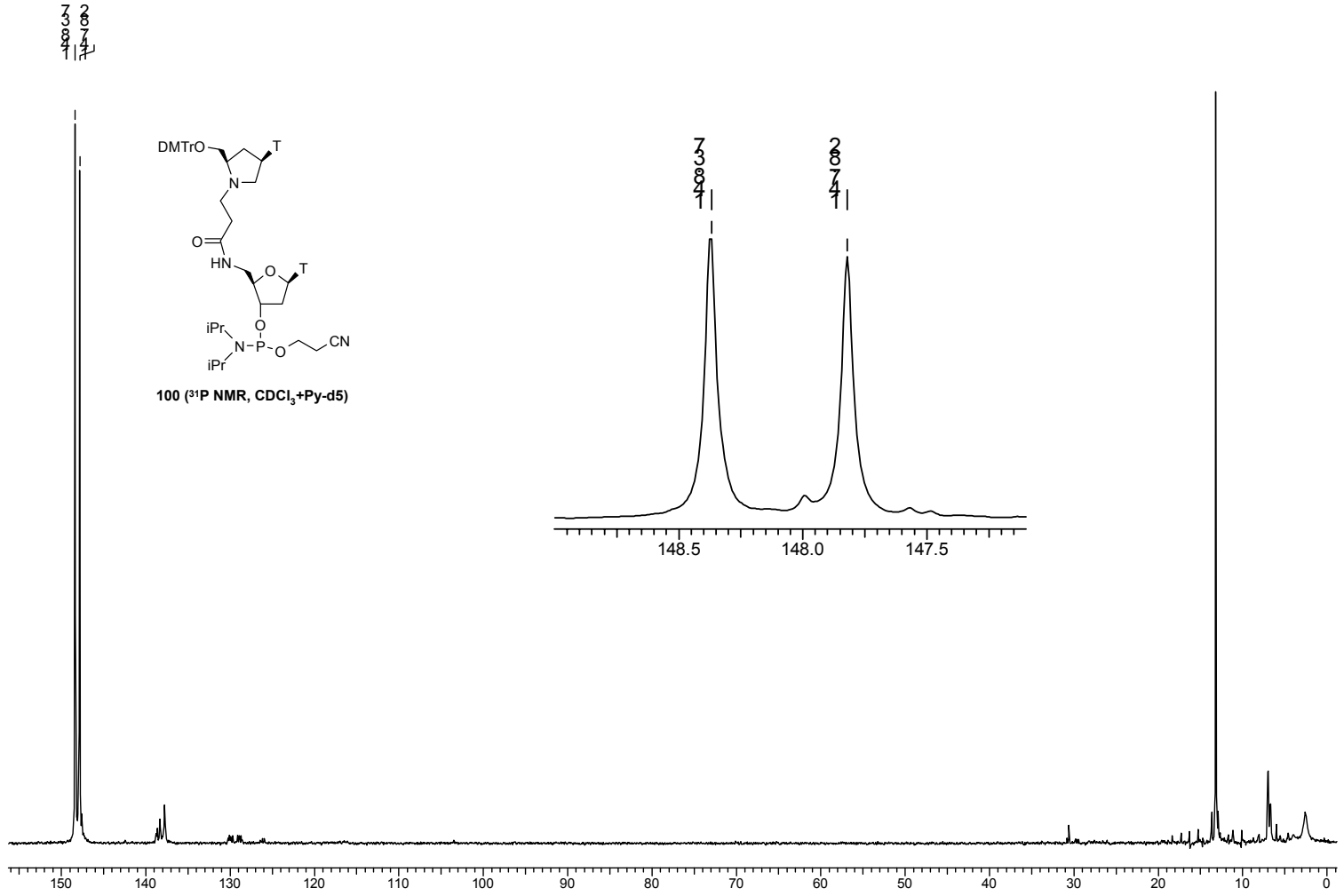

100 (^{31}P NMR, $CDCl_3$+Py-d5)

References

Agrawal, S. (1992) **Antisense oligonucleotides as antiviral agents**. *Trends in Biotech*. 10, 152-158.

Agrawal, S. (1993) **Protocols for Oligonucleotides and Analogs: Synthesis and Properties**. *Methods Mol. Biol.* 20.

Almarsson, O., Bruice, T. C. (1993) **Peptide nucleic acid (PNA) conformation and polymorphism in PNA-DNA and PNA-RNA hybrids**. *Proc. Natl. Acad. Sci*. 90, 9542-9546.

Anderson, P., Bauer, W. (1978) Supercoiling in closed circular DNA: dependence upon ion type and concentration. *Biochemistry* 17, 594-601.

Ando, T., Yamawaki, J. (1979) **Potassium fluoride on Celite. A versatile reagent for C-, N-, O-, and S-alkylations**. *Chem. Lett*. 1, 45-46.

Augustyns, K., Vandendriessche, F., Van A. A., Busson, R., Urbanke, C., Heredewijn, P. (1992) **Incorporation of hexose nucleoside analogs into oligonucleotides: synthesis, base-pairing properties and enzymatic stability**. *Nucleic Acids Res*. 20, 4711-4716.

Baase, W. A., Johnson, Jr. W. C. (1979) **Circular dichroism and DNA secondary structure**. *Nucleic Acids Res*. 6, 797-814.

Baker, Gl L., Scott, J. F., Stille, J. R., Stille, J. K. (1981) **Transition-metal-catalyzed asymmetric organic synthesis via polymer-attached optically active phosphine ligands. 5.Preparation of amino acids in high optical yield via catalytic hydrogenation**. *J. Org. Chem*. 46, 2954-2960.

Barawkar, D. A., Kwok, Y., Bruice, Thomas, W., Bruice, T. C. (2000) **Deoxynucleic Guanidine/Peptide Nucleic Acid Chimeras: Synthesis, Binding and Invasion Studies with DNA.** *J. Am. Chem. Soc*. 122, 5244-5250.

Barawkar, D. A., Rajeev, K. G., Kumar, V. A., Ganesh, K. N. (1996) **Triplex formation at physiological pH by 5-Me-dC-N4-(spermine) [X] oligodeoxynucleotides: non protonation of N3 in X and X*G:C triad and effect of base mismatch/ionic strength on triplex stabilities.** *Nucleic Acids Res*. 24, 1229-1237.

Barn, D. R., Richard, M. J. and David, C. R. (1996) **Synthesis of an Array of Amides by Aluminium Chloride Assisted Cleavage of Resin-Bound Esters**. *Tetrahedron Lett*. 37, 3213-3216.

Barsky, D., Colvin, M. E., Zon, G., Gryaznov, S. M. (1997) **Hydration effects on the duplex stability of phosphoramidate DNA-RNA oligomers**. *Nucleic Acids Res*. 25, 830-835.

Beddell, C. R. (1992) *The Design of Drugs to Macromolecular Targets*. Wiley, Chichester.

Breipohl, G., Knolle, J., Langner, D., O'Malley, G., Uhlmann E. (1996) **Synthesis of Polyamide Nucleic Acids (PNAs) using a Novel Fmoc/Mmt Protecting-Group combination**. *Bioorg. Med. Chem. Lett*. 6, 665-670.

Breipohl, G., Will, D. W., Peyman, A., Uhlmann, E. (1997) **Novel synthetic routes to PNA monomers and PNA-DNA linker molecules**. *Tetrahedron* 53, 14671-14686.

Burgess, K., Gibbs, R. A., Metzker, M. L., Raghavachari, R. (1994) **Synthesis of an oxyamide linked nucleotide dimer and incorporation into antisense oligonucleotide sequences**. *J. Chem. Soc. Chem. Commun*. 8, 915-916.

Butler, J. M., Jiang-B, P., Huang, M., Belgrader, P., Girard, J. (1996) **Peptide Nucleic Acid Characterization by MALDI-TOF Mass Spectrometry**. *J. Anal. Chem***.** 68, 3283-3287.

Callis, P. R. (1983) **Electronic states and luminescence of nucleic acid systems**. *Annu. Rev. Phys. Chem*., 34, 329-357.

Cantor, C. R., Schimmel, P. R. (1980) **The behaviour of biological molecules**. *Biophysical chemistry part III* 624pp.

Ceulemans, G., Aerschot, A. V., Rozenski, J., Herdewijn, P. (1997) **Oligonucleotides with 3-hydroxy-N-acetylprolinol as sugar substitute**. *Tetrahedron* 53, 14957-14974.

Christensen, L., Fitzpatrick, R., Gildea, B., Petersen, K., Hansen, H. F., Koch, C., Egholm, M., Buchardt, O., Nielsen, P. E., Coull, J., Berg, R. H. (1995) **Solid-phase synthesis of peptide nucleic acids**. *J. Peptide Sci*. 3, 175-183.

Chur, A., Holst, B., Hahl, O., Valentin-H, P., Pedersen, E. B. (1993) **Synthesis of a carboxamide linked T*T dimmer and its incorporation in oligonucleotides**. *Nucleic Acids Res*. 21, 5179-5183.

Coull, J. M., Carlson, D. V., Weith, M. L. (1987) **Synthesis and characterization of a carbamate linked oligonucleoside**. *Tetrahedron Lett*. 28, 745-748.

Crick, F. H. C. (1966) **Codon-Anticodon pairing**. **The Wobble Hypothesis**. *J. Mol. Biol*. 19, 548-555.

Cruickshank, K. A., Jiricny, J., Reese, C. B. (1984) **The benzoylation of uracil and thymine**. *Tetrahedron Lett. 25*, 681-684.

D'Costa, M. Kumar, V. A., Ganesh, K. N. (1999) **Aminoethylprolyl Peptide Nucleic Acids (aepPNA): Chiral PNA Analogues That Form Highly Stable DNA:aepPNA$_2$ Triplexes**. *Org. Lett*. 1, 1513-1516.

Das, C., Raghothama, s., Balaram, P. (1999) **A four stranded β-sheet structure in a designed, synthetic polypeptide**. *Chem. Com*. 967-968.

D'Costa, M., Kumar, V. A., Ganesh, K. N. (2001) **Aminoethylprolyl (aep) PNA: Mixed Purine/Pyrimidine Oligomers and Binding Orientation Preferences for PNA:DNA Duplex Formation**. *Org. Lett*. 3, 1281-1284.

De Mesmaeker, A., Haener, R., Martin, P., Moser, H. E. (1995) **Antisense Oligonucleotides**. *Acc. Chem. Res*. 28, 366-374.

De Mesmaeker, A., Waldner, A., Lebreton, J., Hoffmann, P., Fritsch, V., Wolf, R. M., Freier, S. M. (1994a) **Amide bridging, a new type of modification of oligonucleotide backbones**. *Angew. Chem*., 106, 237-240.

De Mesmaeker, A., Waldner, A., Sanghvi, Y. S., Lebreton, J. (1994b) **Comparison of rigid and flexible backbones in antisense oligonucleotides**. *Bioorg. Med. Chem. Lett. 4*, 395-398.

De Mesmaeker, A., Waldner, A., Wendeborn, S., Wolf, R. M. (1997) **Backbone modifications for antisense oligonucleotides**. *Pure Appl. Chem*. 69, 437-440.

De Mesmaeker, Al., Waldner, A., Fritsch, V., Wolf, R. M. (1995) **Improvement of antisense oligonucleotides by synthetic modifications**. *Eur. J. Med. Chem*. 30 (Suppl., Proceedings of the 13th International Symposium on Medicinal Chemistry, 1994), 479s-484s.

Debart, F., Vasseur, J. J., Sanghvi, Y. S., Cook, P. D. (1992) **Synthesis and incorporation of methyleneoxy(methylimino)-linked thymidine dimer into antisense oligonucleotides**. *Bioorg. Med. Chem. Lett*. 2, 1479-1482.

Dormoy, J.-R. (1982) **Synthesis of L-3,4-didehydroproline: favored orientation in the key-step elimination reaction**. *Synthesis* 9, 753-756.

Dormoy, J.-R., Castro, B. (1986) **Synthesis of N-tert-butoxycarbonyl-4,4-dideuterio-L-proline**. *Synthesis* 1, 81-82.

Dueholm, K. L., Petersen, K. H., Jensen, D. K., Egholm, M., Nielsen, P. E., Buchardt, O. (1994) **Peptide nucleic acid (PNA) with a chiral backbone based on alanine**. *Bioorg. Med. Chem. Lett*. 4, 1077-1080.

Dueholm, K. L., Egholm, M., Behrens, C., Christensen, L., Hansen, H. F., Vulpius, T., Petersen, K. H., Berg, R. H., Nielsen, P. E.; Buchardt, O. (1994) **Synthesis of Peptide Nucleic Acid Monomers Containing the Four Natural Nucleobases: Thymine, Cytosine, Adenine, and Guanine and Their Oligomerization**. *J. Org. Chem.* 59, 5767-5773.

Dueholm, K. L., Egholm, M., Behrens, C., Christensen, L., Hansen, H. F., Vulpius, T., Petersen, K. H., Berg, R. H., Nielsen, P. E., Buchardt, O. (1994) **Synthesis of Peptide Nucleic Acid Monomers Containing the Four Natural Nucleobases: Thymine, Cytosine, Adenine, and Guanine and Their Oligomerization**. *J. Org. Chem*. 59, 5767-5773.

Dueholm, K. L., Petersen, K. H., Jensen, D. K., Egholm, M., Nielsen, P. E., Buchardt, O. (1994) **Peptide nucleic acid (PNA) with a chiral backbone based on alanine**. *Bioorg. Medicinal Chem. Lett*. 4, 1077-1080.

Dueholm, K.L, Nielsen, P.E. (1997) **Chemistry, properties and applications of PNA (peptide nucleic acid)**. *New J. Chem.* 21,19-31.

Egholm, M., Buchardt, O., Christensen, L., Behrens, C., Freier, S. M., Driver, D. A., Berg, R. H., Kim, S. K., Norden, B., Nielsen, P. E. (1993) **PNA hybridizes to complementary oligonucleotides obeying the Watson-Crick hydrogen-bonding rules**. *Nature* 365, 566-568.

Egholm, M., Buchardt, O., Nielsen, P. E. (1992) **Peptide nucleic acids (PNA). Oligonucleotide analogs with an achiral peptide backbone**. *J. Am. Chem. Soc*. 114, 1895-1897.

Egholm, M., Nielsen, P., E Buchardt, O., Berg, R. H. (1992) **Recognition of guanine and adenine in DNA by cytosine and thymine containing peptide nucleic acids (PNA)**. *J. Am. Chem. Soc*. 114, 9677-9678.

Endo, M., Komiyama, M. (1996) **Novel Phosphoramidite Monomer for the Site-Selective Incorporation of a Diastereochemically Pure Phosphoramidate to Oligonucleotide**. *J. Org. Chem*. 61, 1994-2000.

Erickson, B. W., Merrifield, R. B. (1976) in **Solid Phase Peptide Synthesis**. In the *Proteins* Vol. II, 3rd ed.; Neurath, H. and Hill, R. L. eds., Academic Press, New York, pp 255.

Eschenmoser, A., Loewenthal, E. (1992) **Chemistry of potentially prebiological natural products**. *Chem. Soc. Rev*. 21, 1-16.

Fields, G. B., Fields, C. G. (1991) **Solvation effects in solid-phase peptide synthesis**. *J.Am. Chem. Soc.* 113, 4202-4207.

Fieser, M. & Fieser, L. F. *Reagents for Organic synthesis* (1967) Vol I, 485, 7, 177

Fink, B. E., Kym, P. R., Katzenellenbogen, J. A. (1998) **Design, Synthesis, and conformational analysis of a proposed Type I β-Turn Mimic**. *J. Am. Chem. Soc*. 120, 4334-4344.

Froehler, B., Ng, P., Matteucci, M. (1988) **Phosphoramidate analogs of DNA: synthesis and thermal stability of heteroduplexes**. *Nucleic Acids Res*. 16, 4831-4839.

Froehler, B., Ng, P., Matteucci, M. (1998) **Phosphoramidate analogs of DNA: synthesis and thermal stability of heteroduplexes**. *Nucleic Acids Res*. 16, 4831-4839.

Furuya, T., Iwanami, S., Takenaka, A., Sasada, Y. (1986) **Structure of N-[(3*RS*,5*SR)*- l-Benzyl-5-methyl-3-pyrrolidinyl]-5-chloro-2-methoxy-4-methylaminobenzamide Hydrochloride**. *Acta Crystallogr. Sect. C*: *Cryst. Struct. Commun*. C42, 1345-1347.

Gait, J. M., Jones, A. S., Walker, R. T. (1974) **Synthetic analogs of polynucleotides. Part 15. The synthesis and properties of poly (5'-amino-3'-O-carboxymethyl-2',5'-dideoxy-erythro-pentonucleosides) containing 3'(O) →5'(C) acetamidate linkages**. *J. Chem. Soc. Perkin I*, 1684-1686.

Gait, M. J. (1984) *Oligonucleotide Synthesis: A Practical Approach* IRL Press Oxford, UK 217 pp.

Ganesh, K. N., Kumar, V. A., Barawkar, D. A. *in Perspective in Supramolecular Chemistry* 1996, (vol3), p. 263.

Gangamani, B. P., De Costa, M., Kumar, V. A., Ganesh, K. N. (1999b) **Conformationally restrained chiral PNA conjugates: synthesis and DNA complementation studies.** *Nucleosides Nucleotides*, 18, 1409-1411.

Gangamani, B. P., Kumar, V. A., Ganesh, K. N. (1996) **Synthesis of Na-(purinyl/pyrimidinyl acetyl)-4-aminoproline diastereomers with potential use in PNA synthesis.** *Tetrahedron*, 52, 15017-15030.

Gangamani, B. P., Kumar, V. A., Ganesh, K. N. (1999a) **Chiral analogs of peptide nucleic acids: synthesis of 4-aminoprolyl nucleic acids and DNA complementation studies using UV/CD spectroscopy**. *Tetrahedron* 55, 177-192.

Gilbert, S., Chengzhi, Z., Sergei, G., Ronald, S. (1995) **Modified Oligonucleotides. Effect of 4 Vs 5-atom chimeric internucleoside linkages on duplex stability**. *Tetrahedron Lett*. 36, 6387-6790

Giles, R. V., Spiller D. G., Tidd, D. M. (1993) **Chimeric oligodeoxynucleotide analogues: enhanced cell uptake of structures which direct ribonuclease H with high specificity**. *Anti-Cancer. Drug. Des*. 8, 33-51.

Giles, R. V., Tidd, D. M. (1992) **Increased specificity for antisense oligodeoxynucleotide targetting of RNA cleavage by RNase H using chimeric methylphosphonodiester/phosphodiester structures**. *Nucleic Acids res*. 20, 763-770.

Giles, R.V., Spiller, D. G., Tidd, D. M. (1995) **Detection of ribonuclease H-generated mRNA fragments in human leukemia cells following reversible membrane permeabilization in the presence of antisense oligodeoxynucleotides**. *Antisense Research and Development* 5,

23-31.

Gisin, B. F. (1970) **The preparation of Merrifield Resins through total esterification with cesium salts**. *Helv. Chim. Acta.* 56, 1476-1482.

Gray, D. M., Hung, S. -H., Johnson, K. H. (1995) *Method. In Enzymol.* 246, 19-34.

Green, E. A., Rosenstein, R. D., Shiono, R., Abraham, D. J., Trus, B. L., Marsh, R. E. (1975) **The crystal structure of uridine.** *Acta Crystallogr. Sect. B*: 31, 102-107.

Greiner, B., Breipohl, G., Uhlmann, E. (1999) **Influence of the type of junction in DNA-3'-peptide nucleic acid (PNA) chimeras on their binding affinity to DNA and RNA**. *Helv. Chim. Acta*. 82, 2151-2159.

Gryaznov, S. M., Chen, J-K. (1994) **Oligodeoxyribonucleotide N3'→P5' Phosphoramidates: synthesis and Hybridization Properties**. *J. Am. Chem. Soc*. 116, 3143-3144.

Gryaznov, S. M., Lloyd, D. H., Chen, J-K., Schultz, R. G., De Dionisio, L. A., Ratmeyer, L., Wilson, W. D. (1995) **Oligonucleotide N3'→P5' phosphoramidates**. *Proc. Natl. Acad. Sci*. 92, 5798-5802.

Gryaznov, S. M., Skorski, T., Cucco, C., Nieborowska, S. M., Chiu, C-Y, Lloyd, D., Chen J.-K., Koziolkiewicz, M., Calabretta, B. (1996) **Oligonucleotide N3'→P5' phosphoramidates as antisense agents**. *Nucleic Acid Res.* 24, 1508-1514.

Haaima, G., Lohse, A., Buchardt, O., Nielsen, P. E. (1996) **Peptide nucleic acids (PNAs) containing thymine monomers derived from chiral amino acids: hybridization and solubility properties of D-lysine PNA**. *Angew. Chem. Int. Ed. Eng*. 35, 1939-1941.

Habus, I., Agrawal, S. (1995) **Oligonucleotides containing acyclic nucleoside analogs with carbamate inter-nucleoside linkages**. *Nucleosides Nucleotides* 14, 1853-1859.

Habus, I., Temsamani, J., Agrawal, S. (1994) **Synthesis of di-, tri-, and tetrameric building blocks with novel carbamate internucleoside linkages and their incorporation into oligonucleotides**. *Bioorg. Med. Chem. Lett*. 4, 1065-1070.

Heidenreich, O., Gryznov, S., Nerenberg, M. (1997) **RNase H-independent antisense activity of oligonucleotide N3'→P5' phosphoramidates**. *Nuceic Acids Res*. 25, 776-780.

Hickman, D. T., King, P. M., Cooper, M. A., Slater, J. M., Mickelfield, J. (2000) **Unusual RNA and DNA binding properties of a novel pyrrolidine-amide oligonucleotide mimic (POM)**. *Chem. Commun*. 2251-2252.

Higson, A. P, Sierzchala, A., Brummel, H., Zhao, Z., Caruthers, M. H. (1998) **Synthesis of an oligothymidylate containing boranophosphate linkages**. *Tetrahedron Lett*. 39, 3899-3902.

Ho, P. S.; Zhou, G.; Clark, L. B. (1990) **Polarized electronic spectra of Z-DNA single crystals**. *Biopolymers* 30, 151-163.

Hodges, R. S., Merrifield, R. B. (1975) **Monitoring of Solid Phase Peptide Synthesis by an Automated Spectrophotometric Picrate Method**. *Anal. Biochem*. 65, 241-272.

Hoogsteen, K. (1963) **The crystal and molecular structure of a Hydrogen-bonded complex between 1-Methyl thymine and 9-methyl adenine**. *Acta. Crystal.* 16, 907.

Hyrup, B., Egholm, M., Buchardt, O., Nielsen, P. E. (1996) **A flexible and positively charged PNA analog with an ethylene-linker to the nucleobase: synthesis and hybridization**

properties. *Bioorg. Med. Chem. Lett*. 6, 1083-1088.

Hyrup, B., Egholm, M., Nielsen, P. E., Wittung, P., Norden, B., Buchardt, O. (1994) **Structure-Activity Studies of the Binding of Modified Peptide Nucleic Acids (PNAs) to DNA**. *J. Am. Chem. Soc*. 116, 7964-7970.

Hyrup, B., Egholm, M., Rolland, M., Nielsen, P. E., Berg, R. H., Buchardt, O. (1993) **Modification of the binding affinity of peptide nucleic acids (PNA). PNA with extended backbones consisting of 2-aminoethyl-β 6 t-alanine or 3-aminopropylglycine units.** *J. Chem. Soc. Chem. Commu*. 6, 518-519.

Idziak, I., Just, G., Damha, M. J., Giannaris, P. A. (1993) **Synthesis and hybridization properties of amide-linked thymidine dimers incorporated into oligodeoxynucleotides**. *Tetrahedron Lett*. 34, 5417-5420.

Isaacs, N. (1995) *Physical Organic Chemistry*, 2nd ed., Longman, Essex, pp 276-277.

Jencks, W. P. (1964) **Mechanism and catalysis of simple carbonyl group reactions**. *Prog. Phys. Org. chem.* 2, 63-128.

Job, P. *Ann. Chim. (*1928) 9, 113-203.

Jones, R. J., Lin, K. –Y., Miligan, J. F., Wadwani, S., Matteucci, M. D. (1993) **Synthesis and binding properties of pyrimidine oligodeoxynucleoside analogs containing neutral phosphodiester replacements: the formacetal and 3'-thioformacetal internucleoside linkages**. *J. Org. Chem*. 58, 2983-2991.

Jordan, S., Schwemler, C., Kosch, W., Kretschmer, A., Schwenner, E., Milke, B. (1997) **New hetero-oligomeric peptide nucleic acids with improved binding properties to complementary DNA**. *Bioorg. Med. Chem Lett*. 7, 687-692.

Jordan, S., Schwemler, C., Kosch, W., Kretschmer, A., Stropp, U., Schwenner, E., Milke, B. (1997) **Synthesis of new building blocks for peptide nucleic acids containing monomers with variations in the backbone**. *Bioorg. Med. Chem Lett*. 7, 681-686.

Jung, P. M., Histand, G., Letsinger, R. L. (1994) **Hybridisation of alternating cationic/anionic oligonucleotides to RNA segments**. *Nucleosides Nucleotides* 13, 1597-1605.

Kaiser, E., Bossinger, C. D., Colescott, R. L., Olsen, D. B. (1980) **Color test for terminal prolyl residues in the solid phase synthesis of peptides**. *Anal. Chim. Acta*. 118, 149-151.

Kaiser, E., Colescott, R. L., Bossinger, C. D., Cook, P. I. (1970) **Color test for the detection of free terminal amino groups in the solid phase sythesis of peptides**. *Anal. Biochem*. 34, 595-598.

Kaname, M.; Yoshifugi, S. (1992) **First synthesis of lycoperdic acid.** *Tetrahedron Lett*. 33, 8103-8104.

Karpeisky, A., Gonzalez, C., Burgin, A. B., Beigelman, L. (1998) **Highly efficient synthesis of 2'-O-amino nucleosides and their incorporation in hammerhead ribozymes**. *Tetrahedron Lett*. 39, 1131-1134.

kaul, R., Balaram, P. (1999) **Stereochemical control of peptide folding**. *Biorg. Med. Chem. Lett.* 7, 105-117.

Kean, J. M., Kipp, S. A., Miller, P. S., Kulka, M., Aurelian, L. (1995) **Inhibition of herpes simplex virus replication by antisense oligo-2'-O-methylribonucleoside**

methylphosphonates. *Biochemistry* 34, 14617-14620.

Kim, S. K., Nielsen, P. E., Egholm, M., Buchardt, O., Berg, R. H., Norden, B. (1993) **Right-handed triplex formed between peptide nucleic acid PNA-T8 and poly(dA) shown by linear and circular dichroism spectroscopy**. *J. Am. Chem. Soc*. 115, 6477-6481.

Knudsen, H., Nielsen, P. E. (1996) **Antisense properties of duplex- and triplex-forming PNAs.** *Nucleic Acids Res*. 24, 494-500.

Koch, T., Naesby, M., Jørgensen, M., Larsson, C., Buchardt, O., Stanley, C. J., Nielsen, P. E., Ørum, H., Wittung, P., Nordén, B. (1995) **PNA-Peptide Chimerae**. *Tetrahedron Lett. 36*, 6933-6936.

kolde, S.,Huang, X., link, K., kolde, a., Bu, Z., engelman, D. M. (2000) **Design of single layer β-sheets without a hydrophobic core**. *Nature* 403, 456-460**.**

Krotz, A. H., Buchardt, O., Nielsen, P. E. (1995a) **Synthesis of 'retro-inverso' peptide nucleic acids. 1. Characterization of the monomers**. *Tetrahedron Lett*. 36, 6937-6940.

Krotz, A. H., Buchardt, O., Nielsen, P. E. (1995b) **Synthesis of 'retro-inverso' peptide nucleic acids. 2. Oligomerization and stability**. *Tetrahedron Lett*. 36, 6941-6944.

Krotz, A. H., Larsen, S., Buchardt, O., Nielsen, P. E. (1998) **A "retro-inverso" PNA: structural implications for DNA and RNA binding**. *Bioorg. Med. Chem*. 6, 1983-1992.

Kuimelis, R. G., van der Laan, A. C., Vinayak, R. (1999) **Thermal melting studies with PNA and PNA-DNA chimera**. *Tetrahedron Lett. 40*, 7671-7674.

Kumar, V. A. Pallan, P.S., Meena, Ganesh, K. N. (2001) **Pyrrolidine Nucleic Acids: DNA/PNA Oligomers with 2-Hydroxy/Aminomethyl- 4-(thymin-1-yl) pyrrolidine-N-acetic acid**. *Org. Lett*. 3, 1269-1272.

Lagriffoul, P. H., Egholm, M. E., Nielsen, P. E., Berg, R. H., Buchardt, O. (1994) **The synthesis, co-oligomerization and hybridization of a thymine-thymine heterodimer containing PNA**. *Bioorg. Med. Chem. Lett*. 4, 1081-1082.

Lagriffoule, P., Wittung, P., Eriksson, M., Jensen, K. K., Norden, B., Buchardt, O., Nielsen, P. E. (1997) **Peptide nucleic acids with a conformationally constrained chiral cyclohexyl-derived backbone**. *Chem. Eur. J*. 3, 912-919.

Lebreton, J., Waldner, A., Fritsch, V., Wolf, R. M., De Mesmaeker, A. (1994) **Comparison of two amides as backbone replacement of the phosphodiester linkage in oligodeoxynucleotides**. *Tetrahedron Lett*. 35, 5225-5228.

Lebreton, J., Waldner, A., Lesueur, C., De Mesmaeker, A. (1994) **Antisense oligonucleotides with alternating phosphodiester-amide-3 linkages**. *Synlett*. 137-140.

Lescrinier, E., Esnouf, R., Schraml, J., Busson, R., Heus, H. A., Hilbers, C. W., Herdewijn, P. (2000) **Solution structure of a HNA-RNA hybrid**. *Chem. Biol*. 7, 719-731.

Letsinger, R. L., Singman, C. N., Histand, G., Salunkhe, M. (1988) **Cationic oligonucleotides**. *J. Am chem. Soc*.110, 4470-4471.

Li H, Huang F, Shaw BR. (1997) **Conformational studies of dithymidine boranomonophosphate diastereoisomers**. *Bioorg. Med. Chem*. 5, 787-795.

Liebhaber, S. A., Cash, F. E., Shakin, S. H. (1984) **Translationally associated helix-**

destabilizing activity in rabbit reticulocyte lysate. *J. Biol. Chem*. 259, 15597-15602.

Lin, K. –Y., Pudlo, J. S., Jones, R. J., Bischofberger, N., Matteucci, M. D., Froehler, B. C. (1994) **Oligodeoxynucleotides containing 5-(1-propynyl)-2'-deoxyuridine formacetal and thioformacetal dimer synthons**. *Bioorg. Med. Chem. Lett*. 4, 1061-1064.

Lin, T. -S., Prusoff, W. H. (1977) **Synthesis and biological activity of several amino analogs of thymidine**. J. Med. Chem. 21, 109-112.

Lowe, G., Vilaivan, T. (1997a) **Amino acids bearing nucleobases for the synthesis of novel peptide nucleic acids**. *J. Chem Soc. Perkin Trans. 1*, 539-546.

Lowe, G., Vilaivan, T. (1997b). **Solid-phase synthesis of novel peptide nucleic acids**. *J. Chem Soc. Perkin Trans. 1*, 555-560.

MacDonald, M., Velde, D. V., Aube, J. (2000) **Synthesis and conformation of Gly-Gly dipeptides constrained with phenylalanine-like aminocaproic acid linkers.** *Org. Lett* 2, 1653-1655.

Madalengoitia, J. S. (2000) **A Novel Peptide Fold: A Repeating βII' Turn Secondary Structure**. *J. Am. Chem. Soc.*, 122, 4986-4987.

Maison, W., Schlemminger, I., Westerhoff, O., Martens, J. (1999) **Modified PNAs: a simple method for the synthesis of monomeric building blocks**. *Bioorg. Med. Chem. Lett*. 9, 581-584.

Merrifield, R. B., Stewart, J. M., Jernberg, N. (1966) **Instrument for automated synthesis of peptides**. *Anal. Chem*. 38, 1905-1914.

Merrifield, R.B. (1963) **Solid Phase Peptide Synthesis. I. The Synthesis of a Tetrapeptide**[1]. *J. Am. Chem. Soc.* 85, 2149-2154.

Mesmaeker, A. D., Lebreton, J., Walder, A., Fritsch, V., Wolf, R. M. (1994) **Replacement of the phosphodiester linkage in oligonucleotides: comparison of two structural amide isomers**. *Biorg. Med. Chem. Lett*. 4, 873-878.

Mesmaeker, A. D., Walder, A., Lebreton, J., Hoffmann, P., Fritsch, V., Wolf, R. M., Frier, S. M. (1994) **Amide bridging, a new type of modification of oligonucleotide backbones**. *Angew. Chem. Int. Ed. Eng*. 33, 226-229.

Mesmaeker, A. De, Waldner, A., Sanghvi, Y. S., Lebreton, J. (1994) **Comparison of rigid and flexible backbones in antisense oligonucleotides**. *Bioorg. Med. Chem. Lett*. 4, 395-398.

Metteuci., M. D. (1990) **Deoxunucleotide analogues based on formacetal linkages**. *Tetrahedron Lett*. 31, 2385-2388.

Miller, P. S., Yano, J., Yano, E., Carroll, C., Jayaraman, K., Ts'O, P. O. P. (1979) **Nonionic nucleic acid analogs**. **Synthesis and characterization of dideoxyribonucleoside methylphosphonates**. *Biochemistry* 18, 5134-5143.

Milligan, J. F., Matteucci, M. D., Martin, J. C. (1993) **Current concepts in antisense drug design**. *J. Med. Chem*. 36, 1923-1927.

Mitsunobu, O. (1981) **The use of diethyl azodicarboxylate and triphenylphosphine in synthesis and transformation of natural products**. *Synthesis* 1, 1-28.

Muller, G., Hessler, G., Decornez, H. Y. (2000) **Are β-turn Mimetics Mimics of β-turns**.

Angew. Chem. Int. Ed. 108, 2941-2943.

Mungall, W. S., Kaiser, J. K. (1977) **Carbamate Analogues of Oligonucleotides**. *J. Org. Chem*. 42, 703-706.

Nielsen, P. E, Haaima, G. (1997) **Peptide nucleic acid (PNA)**. **A DNA mimic with a pseudopeptide backbone**. *Chem. Soc. Rev*. 26, 73-78.

Nielsen, P. E., Egholm, M., Berg, R. H., Buchardt, O. (1991) **Sequence-selective recognition of DNA by strand displacement with a thymine-substituted polyamide**. *Science* 254, 1497-1500.

Nielsen, P. E., Egholm, M., Buchardt, O. (1994) **Evidence for $(PNA)_2$/DNA Triplex Structure upon Binding of PNA to dsDNA by Strand Displacement**. *J. Molecular Recognition* 7, 165-170.

Nielsen, P. E., Egholm, M., Buchardt, O. (1994) **Peptide nucleic acid (PNA)**. **A DNA mimic with a peptide backbone**. *Bioconj. Chem. 5*, 3-7.

Papaioannou, D., Stavropoulos, G., Karagiannis, K., Francis, G. W., Brekke, T., Aksnes, D. W. (1990) **Simple synthesis of cis-4-hydroxy-L-proline and derivatives suitable for use as intermediates in peptide synthesis**. *Acta Chem. Scand*. 44, 243-251.

Peffer, N. J., Hanvey, J. C., Bisi, J. E., Thomson, S. A., Hassman, C. F., Noble, S. A., Babiss, L. E. (1993) **Strand-invasion of duplex DNA by peptide nucleic acid oligomers.** *Proc. Natl. Acad. Sci. U.S.A.* 90, 10648-10652.

Perbost, M., Hoshiko, T., Morvan, F., Swayze, E., Griffey, R. H., Sanghvi, Y. S. (1995) **Synthesis of 5'-O-Amino-2'-Deoxypyrimidine and Purine Nucleosides: Building-Blocks for Antisense Oligonucleotides**. *J. Org. Chem.* 60(16), 5150-5156.

Perbost, M., Lucas, M., Chavis, C., Pompon, A., Baumgartner, H. (1989) **Sugar modified oligonucleotides. I Carbo-oligodeoxynucleotides as potential antisense agents**. *Biochem. Biophys. Res. Commun*. 165, 742-747.

Perczal, A., Fasman, G. D. (1992) **Quantitative analysis of cyclic β-turn models**. *Protein Science* 1, 378-395.

Perrin, D. D., Amarego, W. L. F. (1989) *Purification of Laboratory Chemicals, 3rd edition,* Pergamon Press.

Peter, C., Daura, X., Gunsteren, W. F. (2000) **Peptides of Aminoxy Acids: Molecular Dynamics Simulation stusy of Conformational Equilibria under various Conditions**. *J. Am. Chem. Soc*. 122, 7461-7466.

Petersen, K. H., Buchardt, O., Nielsen, P. E. (1996) **Synthesis and oligomerization of N^{δ}-Boc-N^{α}-(thymin-1-ylacetyl)ornithine**. *Bioorg. Med. Chem. Lett. 6*, 793-796.

Petersen, K. H., Jensen, K. D., Buchardt, O., Nielsen, P. E., Buchardt, O. (1995) **A PNA-DNA linker synthesis of N-((4,4`-dimethoxytrityloxy)ethyl)-N-(thymin-1-ylacetyl)glycine**. *Bioorg. Med. Chem. Lett.* 5, 1119-1124.

Peterson, M. L., Robert, V. (1991) **Synthesis and Biological evaluation of 4-purinylpyrrolidine nucleosides**. *J. Med. Chem*. 34, 2787-2797.

Peyman, A., Uhlmann, E., Wagner, K., Augustin, S., Weiser, C., Will, D. W., Breipohl, G. (1998) **PHONA - PNA co-oligomers: nucleic acid mimetics with interesting properties**. *Angew.*

Chem., Int. Ed. Engl. 36, 2809-2812.

Peyrottes, S., Vasseur, J-J., Imbach, J. L., Rayner, B. (1996) **Oligodeoxynucleoside phosphoramidates (P-NH2): synthesis and thermal stability of duplexes with DNA and RNA targets**. *Nucleic Acids Res*. 24, 1841-1848.

Puschl, A., Boesen, T., Zuccarello, G., Dahl, O., Pitsch, S., Nielsen, P. E. (2001) **Synthesis of Pyrrolidinone PNA: A Novel Conformationally Restricted PNA Analogue**. *J. Org. Chem*. 66, 707-712.

Puschl, A., Sforza, S., Haaima, G., Dahl, O., Nielsen, P. E. (1998) **Peptide nucleic acids (PNAs) with a functional backbone**. *Tetrahedron Lett*. 39, 4707-4710.

Puschl, A., Tedeschi, T., Nielsen, P. E. (2000) **Pyrrolidine PNA: a novel conformationally restricted PNA analogue.** *Org. lett*. 2, 4161-4163.

Puschl, A., Thomas, B., Guido, Z., Otto, D., Stefan, P., Nielsen, P. E. (2001) **Synthesis of Pyrrolidinone PNA: A Novel Conformationally Restricted PNA Analogue**. *J. Org. Chem*. 66, 707-712.

Quartin, R. S., Brakel, C. L., Wetmur, J. G. (1989) **Number and distribution of methylphosphonate linkages in oligodeoxynucleotides affects exo- and endonuclease sensitivity and ability to form RNase H substrates**. *Nucleic Acids Res*. 17, 7253-7262.

Rabinowitz, J. L., Gurin, S. (1953) **Some pyrimidine derivatives**. *J. Am. Chem. Soc*. 75, 5758-5759.

Rait, V. K., Shaw, B. R. (1999) **Boranophosphates support the RNase H cleavage of polyribonucleotides**. *Antisense Nucleic Acid Drug Dev*. 9, 53-60.

Rasmussen, H., Kastrup, J. S., Nielsen, J. N., Nielsen, Jesper M., Nielsen, P. E. (1997) **Crystal structure of a peptide nucleic acid (PNA) duplex at 1.7 Å resolution**. Nat. *Struct. Biol*. 4, 98-101.

Rein, R., Ornstein, R. L., Macelroy, R**.** D. (1978) **Nucleic acid constituent interactions**. *Proc. - Indian Acad. Sci.* Sect. B, 87B, 135-145.

Remuzon, P. (1996) **Trans-4-Hydroxy-L-Proline, a useful and versatile Chiral Starting Block**. *Tetrahedron* 52, 13803-13835.

Riazance, J. H., Baase, W. A, Johnson, Jr., W. C., Hall, K., Cruz, P., Tinoco, Jr., I. (1985) **Evidence for Z-form RNA by vacuum UV circular dichroism***.* Nucleic Acids Res. 13, 4983-4989.

Richardson, J. S. (1977) **Beta-Sheet topology and the relatedness of proteins**. *Nature* 268, 495-500.

Riddell, F. G. (1981) **The conformations of hydroxylamine derivatives**. *Tetrahedron* 37, 849-858.

Robinson, D. S., Greenstein, J. P. (1952) **Stereoisomers of hydroxyproline**. *J. Biol. Chem*. 195, 383-388.

Rose. G. D.; Gierasch, L. M.; Smith, J. A. (1985) **Turns in peptides and proteins**. *Adv. Prot. Chem.* 37, 1-109.

Rueger, H.; Benn, M. H. (1982) **A synthesis of (+)-2-oxa-6-azabicyclo[3.3.0]octan-3-one (the**

Geissman-Waiss lactone): a synthon for some necines. *Heterocycles* 19, 23-25.

Saenger, W. (1984) *Principles of Nucleic Acids Structure* Springer Verlag, New York

Salo, H., Virta, P., Hakala, H., Prakash, T. T., Kawasaki, A. M., Manoharan, M., Lonnberg, H. **Aminoxy fuctionalized oligonucleotides: preparation, on-support derivatization, and postsynthetic attachment to polymer support**. *Biocnjugate Chem*. 10, 815-823.

Sanghvi, Y. S., Cook, P. D. (1995) **Synthesis of a new hydroxylamino linked thymidine dimer via a radical C-C bond formation**. *Nucleosides Nucleotides* 14, 859-62.

Schlatter, J. M., Mazur, R. H., Goodmonson, O. (1977) **Hydrogenation in solid phase peptide synthesis. I. Removal of product from the resin**. *Tetrahedron Lett*. 2851-2852.

Schmit, C., Bevierre, M., De Mesmaeker, A., Altmann, K. (1994) **The effects of 2'- and 3'-alkyl substituents on oligonucleotide hybridization and stability**. *Bioorg. Med. Chem. Lett*. 4, 1969-1974.

Schulhof, J. C., Molko, D., Teoule, R. (1987) **The final deprotection step in oligonucleotide synthesis is reduced to a mild and rapid ammonia treatment by using labile base-protecting groups**. *Nucleic Acids Res*. 15, 397-416.

Seeman, N. C., Rosenberg, J. M., Rich, A. (1976) **Sequence specific recognition of double helical nucleic acids by proteins**. *Proc. Natl. Acad. Sci. USA*. 73, 804-807.

Seki, M., Matsumoto, K. (1995) **Synthesis of amino acids and related compounds. 43. A convenient synthesis of (2S,4S)-4-hydroxyproline**. *Biosci. Biotech. Biochem*. 59, 1161-1162.

Sergueev D. S, Shaw B. R. (1998) **H-Phosphonate Approach for Solid-Phase Synthesis of Oligodeoxyribonucleoside Boranophosphates and Their Characterization**. *J. Am. Chem. Soc*. 120, 9417-9427.

Shakin, S. H., & Liebhaber, S. A. (1986) **Destabilization of messenger RNA/complementary DNA duplexes by the elongating 80 S ribosome**. *J. Biol. Chem*. 261, 16018-16025.

Simmons, C. G., Pitts, A. E., Mayfield, L. D., Shay, J. W., Corey, D. R. (1997) **Synthesis and membrane permeability of PNA-peptide conjugates**. *Bioorg. Med. Chem. Lett*. *7*, 3001-3006.

Skorski, T., Perrotti, D., Nieborowska-Skorska, M., Gryaznov, S. M., Calabretta, B. (1997) **Antileukemia effect of c-myc N3'→P5' phosphoramidate antisense oligonucleotides in vivo**. *Proc. Natl. Acad. Sci*. 94, 3966-3971.

Smith, J. A., Pease, L. G. (1980) **Reverse turns in peptides and proteins**. *CRC Criti. Rev. Biochem*. 8, 315-399.

Soll, D., Cherayil, J. D., Bock, R. M. (1966) *J. Mol. Biol*. 19, 97.

Sood, A, Shaw, B. R., Spielvogel, B. F. (1990). **Boron-containing nucleic acids. 2. Synthesis of oligodeoxynucleoside boranophosphates**. *J. Am. Chem. Soc*. 112, 9000-9001.

Spielvogel, B.F., Sood, A., Shaw, B. R., Hall, I. H. (1991) **From boron analogs of amino acids to boronated DNA: potential new pharmaceuticals and neutron capture agents**. *Pure & Appl. Chem*. 63, 415-418.

Sprecher, C. A., Baase, W. A., Johnson, W. C. Jr., (1979) **Conformation and circular dichroism of DNA**. *Biopolymers* 8, 1009-1019.

Stec, W. J., Zon, G. (1984a) **Synthesis, separation and strereochemistry of diastereomeric oligodeoxyribonucleotides having a 5'-terminal internucleotide phosphorothioate linkage**. *Tetrahedron Lett.* 25, 5275-7578.

Stec, W. J., Zon, G. (1984b) **Stereochemical studies of the formation of chiral internucleotide linkages by phosphoaramidite coupling in the synthesis of oligodeoxyribonucleotides**. *Tetrahedron Lett.* 25, 5279-5282.

Stein, C. A. (1995) **Does antisense exist?** *Nat. Med*. 1, 1119-1121.

Stein, D., Foster, E., Huang, S., Weller, D., Summerton, J. (1997) **A specificity comparison of four antisense types: morpholino, 2'-O-methyl RNA, DNA, and phosphorothioate DNA**. *Antisense Nucleic Acid Drug Dev*. 7, 151-157.

Stephenson, M. L., Zamecnik, P.C. (1978) **Inhibition of Rous sarcoma viral RNA translation by a specific oligodeoxyribonucleotide**. *Proc. Natl. Acad. Sci*. 75, 285-288.

Stewart, J. M., Young, J. D. (1984) *Solid phase peptide synthesis*.

Stirchak, E. P., Summerton, J. E., Weller, D. D. (1987) **Uncharged stereoregular nucleic acid analogs. 1. Synthesis of a cytosine-containing oligomer with carbamate internucleoside linkages**. *J. Org. Chem*. 52, 4202-4206.

Stirchak, E. P., Summerton, J. E., Weller, D. D. (1989) **Uncharged stereoregular nucleic acid analogs: 2. Morpholino nucleoside oligomers with carbamate internucleoside linkages**. *Nucleic Acids Res*. 17, 6129-6141.

Stork, G., Zhang, C., Cryaznov, S., Schultz, R., (1995) **Modified oligonucleotides. Effect of 4 vs 5-atom chimeric internucleoside linkages on duplex stability**. *Tetrahedron Lett*. 36, 6387-6390.

Summers, M. F., Powell, C., Egan, W., Byrd, R. A., Wilson, W. D., Zon, G. (1986) **Alkyl phosphotriester modified oligodeoxynucleotides. VI. NMR and UV spectroscopic studies of ethyl phosphotriester (et) modified R_p-R_p and S_p-S_p duplexes, $(d(GGAA(Et)TTCC))_2$**. *Nucleic. Acids Res*. 14, 7421-7437.

Summerton, J., Stein, D., Huang, S. B., Matthews, P., Weller, S., Partridge, M. (1997). **Morpholino and phosphorothioate antisense oligomers compared in cell-free and in-cell systems**. *Antisense Nucleic Acid Drug Dev*., 7, 63-70.

Summerton, J., Weller, D. (1997a). **Morpholino antisense oligomers: design, preparation, and properties**. *Antisense Nucleic Acid Drug Dev*. 7, 187-195.

Summerton, J., Weller, D. (1997b) **Antisense properties of morpholino oligomers Nucleosides & Nucleotides**. 16, 889-898.

Taylor, M. F., Paulauskis, J. D., Weller, D. D., Kobzic, L. (1996) **In vitro efficacy of morpholino-modified antisense oligomers directed against tumor necrosis factor-a mRNA**. *J. Biol. Chem*. 271, 17445-17452.

Taylor, M. F., Weller, D. D., Kobzic, L. (1998) **Effect of TNF-a antisense oligomers on cytokine production by primary murine alveolar macrophages**. *Antisense Nucleic Acid Drug Dev*. 8, 199-205.

Tong, B. Y., Leung, M. L. C. (1977) **Correlation between percentage guanine-cytosine content and melting temperature of deoxyribonucleic acid**. *Biopolymers* 16, 1223-1231.

Uhlmann, E. (1998) **Peptide nucleic acids (PNA) and PNA-DNA chimeras. From high binding affinity towards biological function**. *Biol. Chem*. 379, 1045-1052.

Uhlmann, E., Greiner, B., Breipohl, G. (1999) **PNA/DNA chimeras**. *Pept. Nucleic Acids* 51-70.

Uhlmann, E., Peyman, A. (1990) **Antisense oligonucleotides: a new therapeutic principle**. *Chem. Rev*. 90, 543-584.

Uhlmann, E., Peyman, A., Breipohl, G., Will, D. W. (1998) **PNA: synthetic polyamide nucleic acids with unusual binding properties**. *Angew. Chem. Int. Ed. Engl.*, 37, 2796-2823.

Uhlmann, E., Will, D. W., Breipohl, G., Langner, D., Ryte, A. (1996) **Synthesis and properties of PNA/DNA chimeras**. *Angew. Chem., Int. Ed. Engl*. 35, 2632-2635.

Uhlmann, E., Will, D. W., Breipohl, G., Langner, D., Ryte, A. (1996) **Synthesis and properties of PNA/DNA chimeras**. *Angew. Chem., Int. Ed. Engl*. 35, 2632-2635.

Vasseur, J. J., Debart, F., Sanghvi, Y. S., Cook, P. D. (1992) **Oligonucleosides: synthesis of a novel methylhydroxylamine-linked nucleoside dimer and its incorporation into antisense sequences**. *J. Am. Chem. Soc.*, 114, 4006-4007.

Vasseur, J. J., Debart, F., Sanghvi, Y. S., Cook, P. D. (1992) **Oligonucleosides: synthesis of a novel methylhydroxylamine-linked nucleoside dimer and its incorporation into antisense sequences**. *J. Am. Chem. Soc*. 114, 4006-4007.

Verheijen, J. C., Anne-Marie M. van R., Meeuwenoord, N. J., Stuivenberg, H. R., Bayly, S. F., Chen, L., van der Marel, G. A., Torrence, P. F., van Boom, J. H. (2000). **Incorporation of a 4-hydroxy-N-acetylprolinol nucleotide analogue improves the 3'-exonuclease stability of 2'-5'-oligoadenylate-antisense conjugates**. *Bioorg. Med. Chem Lett*. 10, 801-804.

Verheijen, J. C., Van Roon, Anne-Marie M., Van der Laan, Alexander C., Van der Marel, Gijsbert A., Van Boom, Jacques H. (1999) **Synthesis of DNA-(3')-PNA chimeras with conformationally restricted linkers based on 4-hydroxyproline**. *Nucleosides Nucleotides* 18, 493-508.

Vilaivan, T., Khongdeesameor, C., Harnyuttanakorn, P., Westwell, M. S., Lowe, G. (2000) **Synthesis and properties of chiral peptide nucleic acids with a N-aminoethyl-D-proline backbone**. *Bioorg. Med. Chem. Lett*. 10, 2541-2545.

Vilaivan, T., Khongdeesameor, C., Harnyuttanokam, P., Lowe, G. (2001) **Synthesis and properties of novel pyrrolidinyl PNA carrying b-amino acid spacers**. *Tetrahedron Lett*. 42, 5533-5536.

Wagner, R. W. (1994) **Gene inhibition using antisense oligodeoxynucleotides**. *Nature* 372, 333-335.

Wagner, R. W. (1995) **The state of the art in antisense research**. *Nat. Med*. 1, 1116-1118.

Wagner, R. W., Matteucci, M. D., Lewis, J. G., Gutierrez, A. J., Moulds, C., Froehler, B. C. (1993) **Antisense gene inhibition by oligonucleotides containing C-5 propyne pyrimidines**. *Science* 260, 1510-1513.

Waldner, A., Mesmaeker, A. D., Lebreton, J. (1994) **Synthesis of oligodeoxyribonucleotides containing dimers with carbamate moieties as replacement of the natural phosphodiester linkage**. *Bioorg. Med. Chem. Lett*. 4, 405-408.

Walker, S., Gange, D., Gupta, V., Kahne, D. (1994) **Analysis of Hydroxylamine Glycosidic**

Linkages: Structural Consequences of NO Bond in Calicheamicin. *J. Am. Chem. Soc*. 116, 3197-3206.

Wang, A. H. J., Quigley, G. J., Kolpak, F. J., Van der M. G., Van Boom, J. H., Rich, A. (1981) **Left-handed double helical DNA: variations in the backbone conformation**. *Science* 211, 171-176.

Wang, H., Weller, D. D. (1991) **Solid phase synthesis of neutral oligonucleotide analogues**. *Tetrahedron Lett*. 32, 7385-7388.

Warrass, R., Wiesmuller, K. -H., Jung, G. (1998) **Cyclic Oligocarbamates**. *Tetrahedron Lett*. 39, 2715-2716.

Watson, J. D., and Crick, F.H.C. (1953) **Molecular structure of nucleic acid. A structure for deoxyribose nucleic acid**. *Nature*, 171, 737-738.

Webb, T. R., Eigenbrot, C. (1991) **Conformationally Restricted Arginine Analogues**. *J. Org. Chem*. 56, 3009-3016.

Wengel, J. (1999) **Synthesis of 3'-C- and 4'-C-Branched Oligodeoxynucleotides and the Development of Locked Nucleic Acid (LNA)**. *Acc. Chem. Res*. 32, 301-310.

Williams M. A., Rapoport H. (1994) *J. Org. Chem.* **Synthesis of Conformationally Constrained DTPA Analogs. Incorporation of the Ethylenediamine Units as Aminopyrrolidines**. 59, 3616-3625.

Wittung, P., Nielsen, P. E., Buchardt, O., Egholm, M., Norden, B. (1994) **DNA-like double helix formed by peptide nucleic acid**. **DNA-like double helix formed by peptide nucleic acid**. *Nature*, 368, 561-563.

Wittung, P., Nielsen, P. E., Buchardt, O., Egholm, M., Norden, B. (1994) **DNA-like double helix formed by peptide nucleic acid**. *Nature 368*, 561-563.

Wright, D. E., Agarwal, N. S., Hruby, Victor, J. (1980) **Synthesis of protected secretin16-27 on a Merrifield resin. Examination of ammonolysis conditions of preparing carboxamide terminal protected peptides suitable for fragment condensation**. *Int. J. Pept. Protein Res*. 15, 271-278.

Yang, D., Qu, J., Li, B., Ng, F-F., Wang, X-C., Cheung, K-K., Wang, D-P., Wu, Y-D. (1999) **Novel Turns and Helices in Peptides of Chiral a-Aminoxy Acids**. *J. Am. Chem. Soc*. 121, 589-590.

Ying, L., Tao, J., and Keliang, L. (2001) **Synthesis and Binding Affinity of a Chiral PNA Analogue**. *Nucleosides, Nucleotides & Nucleic acids***.** 20, 1705-1721.

Zamecnik, P. C., Stephenson, M. L. (1978) **Inhibition of Rous sarcoma virus replication and cell transformation by a specific oligodeoxynucleotide**. *Proc. Natl. Acad. Sci*. 75, 280-284.